EMERGING INFECTIOUS DISEASES®

CDC
SAFER • HEALTHIER • PEOPLE™

Central Nervous System Infections

June 2017

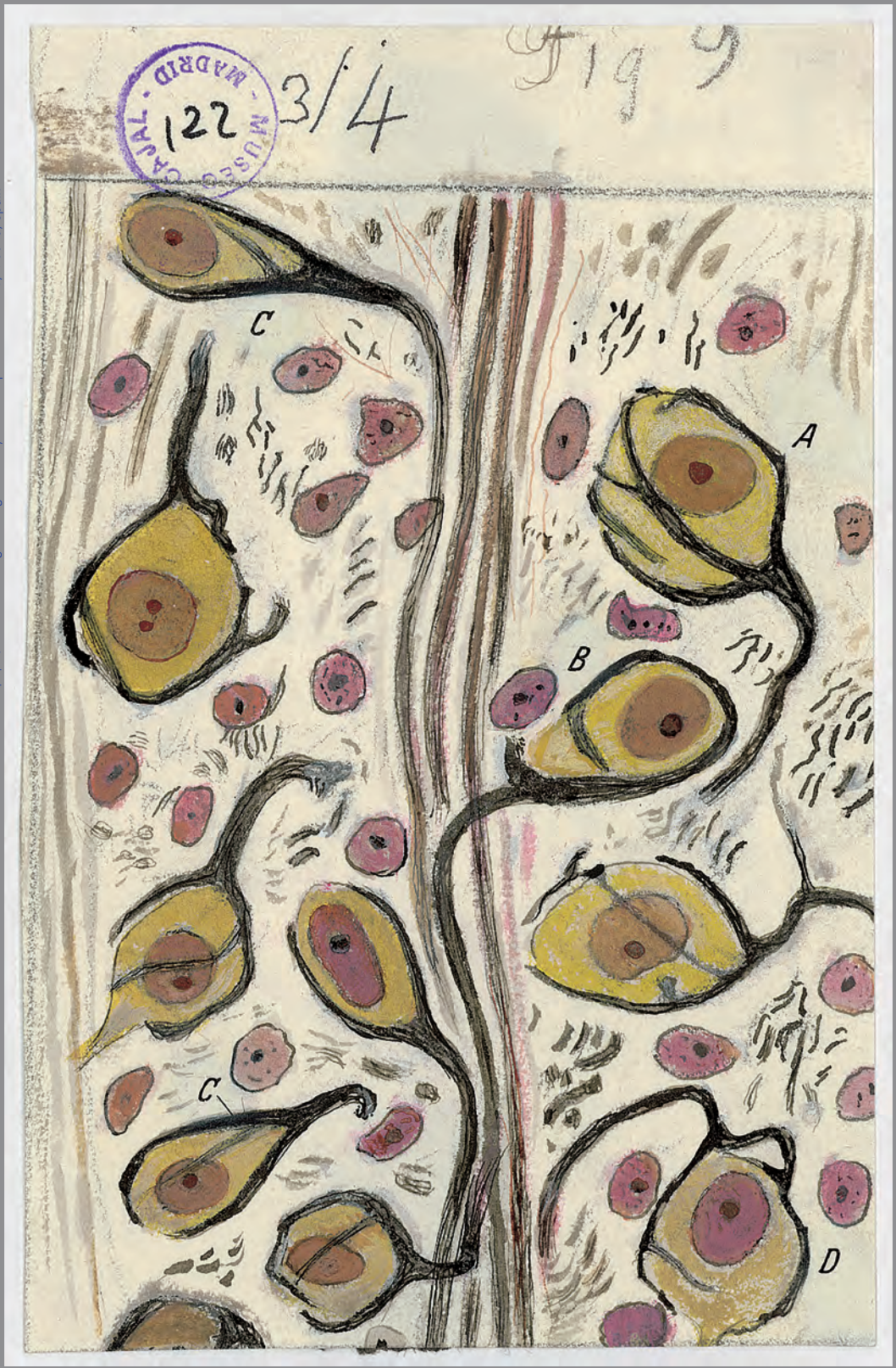

Ramón y Cajal (1852–1934). Calyx of Held (3676) (date unknown). Pencil, India ink, ink washes on cardboard or paper, circa 1920. Digital image courtesy of the Cajal Institute-CSIC, Madrid, Spain

EMERGING INFECTIOUS DISEASES®

EDITOR-IN-CHIEF
D. Peter Drotman

Associate Editors
Paul Arguin, Atlanta, Georgia, USA
Charles Ben Beard, Fort Collins, Colorado, USA
Ermias Belay, Atlanta, Georgia, USA
David Bell, Atlanta, Georgia, USA
Sharon Bloom, Atlanta, GA, USA
Mary Brandt, Atlanta, Georgia, USA
Corrie Brown, Athens, Georgia, USA
Charles Calisher, Fort Collins, Colorado, USA
Michel Drancourt, Marseille, France
Paul V. Effler, Perth, Australia
Anthony Fiore, Atlanta, Georgia, USA
David Freedman, Birmingham, Alabama, USA
Peter Gerner-Smidt, Atlanta, Georgia, USA
Stephen Hadler, Atlanta, Georgia, USA
Matthew Kuehnert, Atlanta, Georgia, USA
Nina Marano, Atlanta, Georgia, USA
Martin I. Meltzer, Atlanta, Georgia, USA
David Morens, Bethesda, Maryland, USA
J. Glenn Morris, Gainesville, Florida, USA
Patrice Nordmann, Fribourg, Switzerland
Didier Raoult, Marseille, France
Pierre Rollin, Atlanta, Georgia, USA
Frank Sorvillo, Los Angeles, California, USA
David Walker, Galveston, Texas, USA

Senior Associate Editor, Emeritus
Brian W.J. Mahy, Bury St. Edmunds, Suffolk, UK

Managing Editor
Byron Breedlove, Atlanta, Georgia, USA

Copy Editors Claudia Chesley, Kristina Clark, Karen Foster, Thomas Gryczan, Shannon O'Connor, Jude Rutledge, Carol Snarey, P. Lynne Stockton, Deborah Wenger

Production Thomas Eheman, William Hale, Barbara Segal, Reginald Tucker

Editorial Assistants Kristine Phillips, Susan Richardson

Communications/Social Media Sarah Logan Gregory

Founding Editor
Joseph E. McDade, Rome, Georgia, USA

Emerging Infectious Diseases is published monthly by the Centers for Disease Control and Prevention, 1600 Clifton Road, Mailstop D61, Atlanta, GA 30329-4027, USA. Telephone 404-639-1960, fax 404-639-1954, email eideditor@cdc.gov.

EDITORIAL BOARD
Timothy Barrett, Atlanta, Georgia, USA
Barry J. Beaty, Ft. Collins, Colorado, USA
Martin J. Blaser, New York, New York, USA
Richard Bradbury, Atlanta, Georgia, USA
Christopher Braden, Atlanta, Georgia, USA
Arturo Casadevall, New York, New York, USA
Kenneth C. Castro, Atlanta, Georgia, USA
Louisa Chapman, Atlanta, Georgia, USA
Benjamin J. Cowling, Hong Kong, China
Vincent Deubel, Shanghai, China
Isaac Chun-Hai Fung, Statesboro, Georgia, USA
Kathleen Gensheimer, College Park, Maryland, USA
Duane J. Gubler, Singapore
Richard L. Guerrant, Charlottesville, Virginia, USA
Scott Halstead, Arlington, Virginia, USA
Katrina Hedberg, Portland, Oregon, USA
David L. Heymann, London, UK
Keith Klugman, Seattle, Washington, USA
Takeshi Kurata, Tokyo, Japan
S.K. Lam, Kuala Lumpur, Malaysia
Stuart Levy, Boston, Massachusetts, USA
John S. MacKenzie, Perth, Australia
John E. McGowan, Jr., Atlanta, Georgia, USA
Jennifer H. McQuiston, Atlanta, Georgia, USA
Tom Marrie, Halifax, Nova Scotia, Canada
Nkuchia M. M'ikanatha, Harrisburg, Pennsylvania, USA
Frederick A. Murphy, Bethesda, Maryland, USA
Barbara E. Murray, Houston, Texas, USA
Stephen M. Ostroff, Silver Spring, Maryland, USA
Marguerite Pappaioanou, Seattle, Washington, USA
Johann D. Pitout, Calgary, Alberta, Canada
Ann Powers, Fort Collins, Colorado, USA
Mario Raviglione, Geneva, Switzerland
David Relman, Palo Alto, California, USA
Guenael R. Rodier, Geneva, Switzerland
Connie Schmaljohn, Frederick, Maryland, USA
Tom Schwan, Hamilton, Montana, USA
Ira Schwartz, Valhalla, New York, USA
Bonnie Smoak, Bethesda, Maryland, USA
Rosemary Soave, New York, New York, USA
P. Frederick Sparling, Chapel Hill, North Carolina, USA
Robert Swanepoel, Pretoria, South Africa
Phillip Tarr, St. Louis, Missouri, USA
John Ward, Atlanta, Georgia, USA
J. Todd Weber, Atlanta, Georgia, USA
Jeffrey Scott Weese, Guelph, Ontario, Canada
Mary E. Wilson, Cambridge, Massachusetts, USA

The conclusions, findings, and opinions expressed by authors contributing to this journal do not necessarily reflect the official position of the U.S. Department of Health and Human Services, the Public Health Service, the Centers for Disease Control and Prevention, or the authors' affiliated institutions. Use of trade names is for identification only and does not imply endorsement by any of the groups named above.

All material published in Emerging Infectious Diseases is in the public domain and may be used and reprinted without special permission; proper citation, however, is required.

Use of trade names is for identification only and does not imply endorsement by the Public Health Service or by the U.S. Department of Health and Human Services.

EMERGING INFECTIOUS DISEASES is a registered service mark of the U.S. Department of Health & Human Services (HHS).

∞ Emerging Infectious Diseases is printed on acid-free paper that meets the requirements of ANSI/NISO 239.48-1992 (Permanence of Paper)

EMERGING INFECTIOUS DISEASES®

June 2017

On the Cover

Ramón y Cajal (1852–1934), Calyx of Held (3676) (detail), circa 1920. Pencil, India ink, ink washes on cardboard or paper. Digital image courtesy of the Cajal Institute-CSIC, Madrid, Spain

About the Cover p. 1052

Synopsis

Medscape EDUCATION ACTIVITY

Sporadic Creutzfeldt-Jakob Disease in 2 Plasma Product Recipients, United Kingdom
P. Urwin et al. **893**
Two cases of sporadic CJD with clotting disorders have been identified, but this may represent a chance event.

Genomic Analysis of *Salmonella enterica* Serovar Typhimurium DT160 Associated with a 14-Year Outbreak, New Zealand, 1998–2012
S.J. Bloomfield et al. **906**
Related material available online: http://wwwnc.cdc.gov/eid/article/23/6/16-1934_article

Stockpiling Ventilators for Influenza Pandemics
H.-C. Huang et al. **914**
Related material available online: http://wwwnc.cdc.gov/eid/article/23/6/16-1417_article

Invasive Serotype 35B Pneumococci Including an Expanding Serotype Switch Lineage, United States, 2015–2016
S. Chochua et al. **922**
Related material available online: http://wwwnc.cdc.gov/eid/article/23/6/17-0071_article

Serologic and Molecular Evidence of Vaccinia Virus Circulation among Small Mammals from Different Biomes, Brazil
J.B. Miranda et al. **931**
Related material available online: http://wwwnc.cdc.gov/eid/article/23/6/16-1643_article

Medscape EDUCATION ACTIVITY

Relative Risk for Ehrlichiosis and Lyme Disease in an Area Where Vectors for Both Are Sympatric, New Jersey, USA
A. Egizi et al. **939**
Vector tick infection and encounter rates suggest gross underreporting or misreporting of ehrlichiosis in the northeast United States.

Distribution and Quantitative Estimates of Variant Creutzfeldt-Jakob Disease Prions in Tissues of Clinical and Asymptomatic Patients
J.Y. Douet et al. **946**

Research

Hospital Outbreaks of Middle East Respiratory Syndrome, Daejeon, South Korea, 2015
J.W. Park et al. **898**
Related material available online: http://wwwnc.cdc.gov/eid/article/23/6/16-0120_article

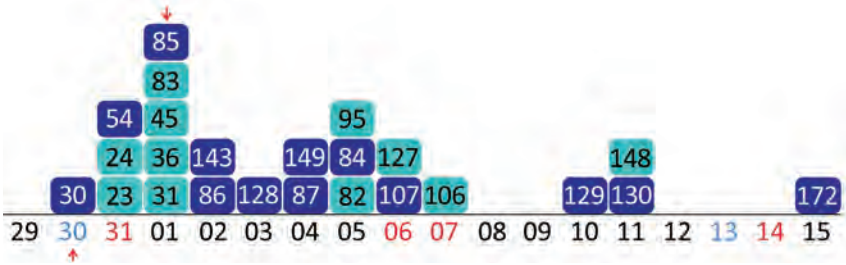

EMERGING INFECTIOUS DISEASES®
June 2017

Outbreak-Related Disease Burden Associated with Consumption of Unpasteurized Cow's Milk and Cheese, United States, 2009–2014
S. Costard et al. **957**

Related material available online: http://wwwnc.cdc.gov/eid/article/23/6/15-1603_article

Dispatches

Sustainability of High-Level Isolation Capabilities among US Ebola Treatment Centers
J.J. Herstein et al. **965**

Clinical and Molecular Characteristics of Human Rotavirus G8P[8] Outbreak Strain, Japan, 2014
K. Kondo et al. **968**

Related material available online: http://wwwnc.cdc.gov/eid/article/23/6/16-0038_article

Seoul Virus Infection In Humans, France, 2014–2016
J.-M. Reynes et al. **973**

Central Nervous System Brucellosis Granuloma and White Matter Disease in Immunocompromised Patient
M. Alqwaifly et al. **978**

Severe Neurologic Disorders in 2 Fetuses with Zika Virus Infection, Colombia
J. Acosta-Reyes et al. **982**

Related material available online: http://wwwnc.cdc.gov/eid/article/23/6/16-1702_article

Domestic Pig Unlikely Reservoir for MERS-CoV
E. de Wit et al. **985**

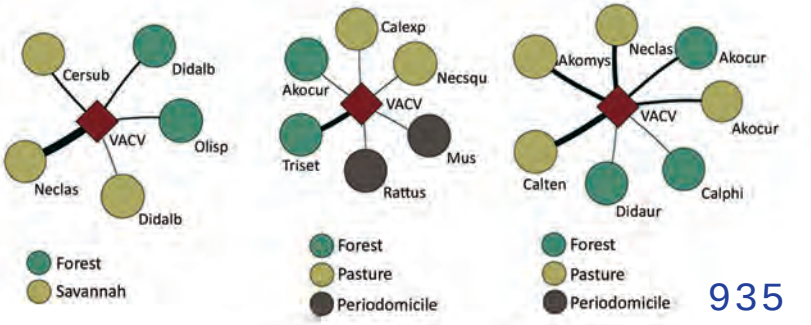

935

High Rates of Neutralizing Antibodies to Toscana and Sandfly Fever Sicilian Viruses in Livestock, Kosovo
N. Ayhan et al. **989**

Congenital Malformations of Calves Infected with Shamonda Virus, Southern Japan
Y. Hirashima et al. **993**

***Brucella neotomae* Infection in Humans, Costa Rica**
M. Suárez-Esquivel et al. **997**

Related material available online: http://wwwnc.cdc.gov/eid/article/23/6/16-2018_article

Isolated Case of Marburg Virus Disease, Kampala, Uganda, 2014
L. Nyakarahuka et al. **1001**

Crimean-Congo Hemorrhagic Fever in Migrant Worker Returning from Oman to India, 2016
P.D. Yadav et al. **1005**

Rise in Group W Meningococcal Carriage in University Students, United Kingdom
N.J. Oldfield et al. **1009**

Related material available online: http://wwwnc.cdc.gov/eid/article/23/6/16-1768_article

Penicillin Resistance of Nonvaccine Type Pneumococcus before and after PCV13 Introduction, United States
C.P. Andam et al. **1012**

Related material available online: http://wwwnc.cdc.gov/eid/article/23/6/16-1331_article

979

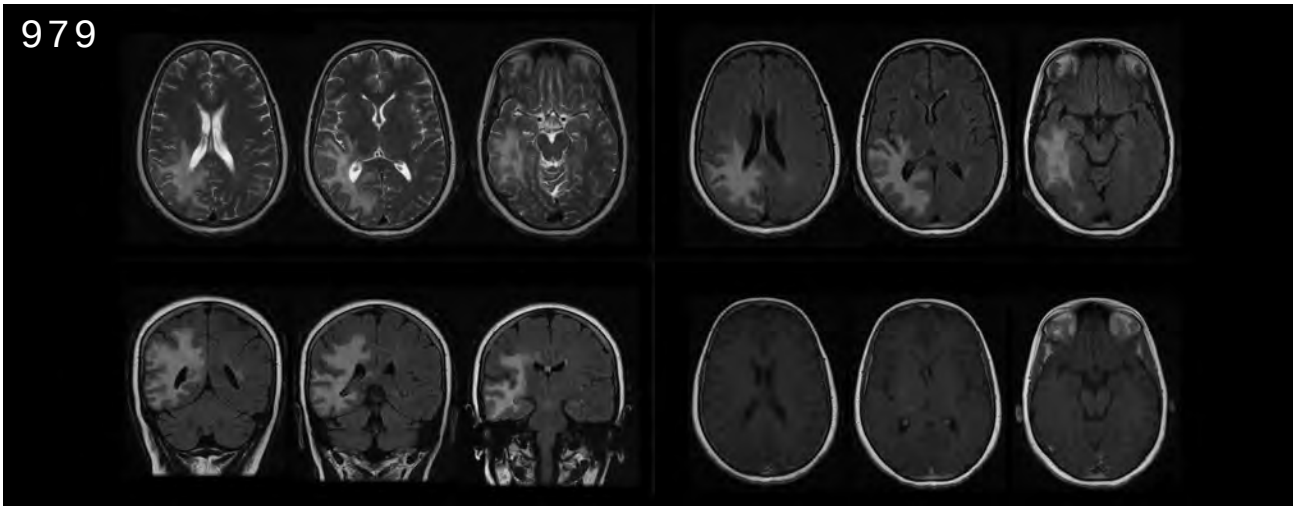

EMERGING INFECTIOUS DISEASES®

June 2017

Febrile Respiratory Illness Associated with Human Adenovirus Type 55 in South Korean Military, 2014–2016
H. Yoo et al. **1016**

Related material available online: http://wwwnc.cdc.gov/eid/article/23/6/16-1848_article

Commentary

Stockpiling Ventilators for Influenza Pandemics
M.I. Meltzer, A. Patel **1021**

Letters

Epidemiologic Survey of Japanese Encephalitis Virus Infection, Tibet, China, 2015
H. Zhang et al. **1023**

High Frequency of Mayaro Virus IgM among Febrile Patients, Central Brazil
S.Brunini et al. **1025**

Related material available online: http://wwwnc.cdc.gov/eid/article/23/6/16-0929_article

Ebola Virus Imported from Guinea to Senegal, 2014
D. Ka et al. **1026**

Tick-Borne Encephalitis Virus in Ticks and Roe Deer, the Netherlands
S. Jahfari et al. **1028**

Outbreaks of Tilapia Lake Virus Infection, Thailand, 2015–2016
W. Surachetpong et al. **1031**

Related material available online: http://wwwnc.cdc.gov/eid/article/23/6/16-1278_article

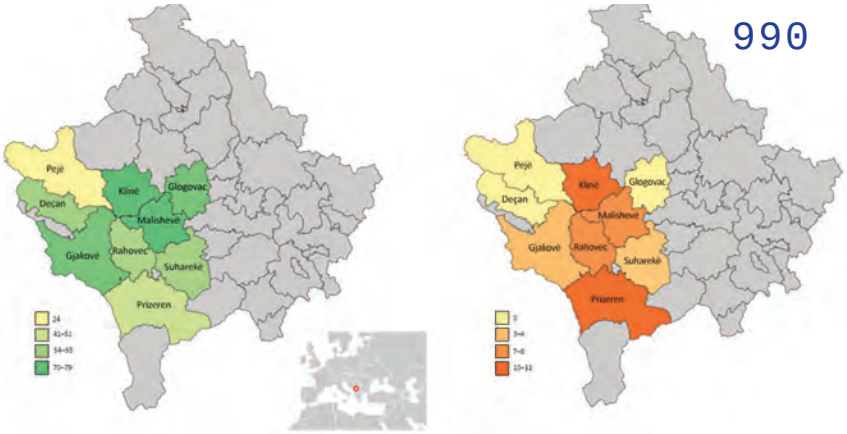

Endemic Hantavirus in Field Voles, Northern England
A.G. Thomason et al. **1033**

Related material available online: http://wwwnc.cdc.gov/eid/article/23/6/16-1607_article

Measles Cases during Ebola Outbreak, West Africa, 2013–2016
F. Colavita et al. **1035**

***Angiostrongylus cantonensis* Meningitis and Myelitis, Texas, USA**
R. Al Hammoud et al. **1037**

***Enterocytozoon bieneusi* Microsporidiosis in Stem Cell Transplant Recipients Treated with Fumagillin**
I. Bukreyeva et al. **1039**

Influenza A(H9N2) Virus, Myanmar 2014–2015
T.N. Lin et al. **1041**

Related material available online: http://wwwnc.cdc.gov/eid/article/23/6/16-1902_article

PCR Detection of Mimivirus
D. Raoult et al. **1043**

Autochthonous Case of Eosinophilic Meningitis Caused by *Angiostrongylus cantonensis*, France, 2016
Y. Nguyen et al. **1045**

Zika Virus–Associated Cognitive Impairment in Adolescent, 2016
J. Zucker et al. **1047**

Related material available online: http://wwwnc.cdc.gov/eid/article/23/6/16-2029_article

Highly Pathogenic Avian Influenza Virus (H5N8) Clade 2.3.4.4 Infection in Migratory Birds, Egypt
A.A. Selim et al. **1048**

Related material available online: http://wwwnc.cdc.gov/eid/article/23/6/16-2056_article

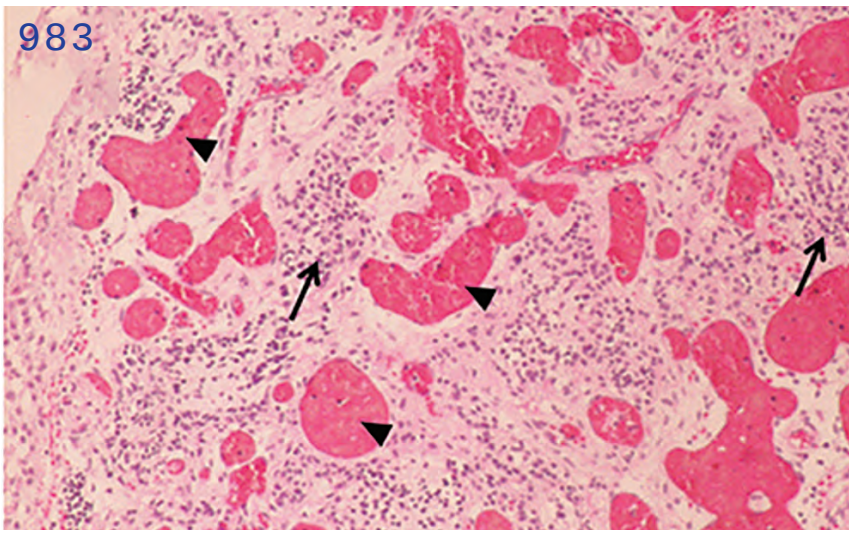

About the Cover

"Unexplored Continents and Great Stretches of Unknown Territory"
B. Breedlove **1052**

Etymologia

Creutzfeldt-Jakob Disease
R. Henry, F.A. Murphy **956**

EID *SPOTLIGHT*

These spotlights highlight the latest articles and information on emerging infectious disease topics in our global community.

Antimicrobial Resistance

Food Safety

Ebola

HIV/AIDS

Lyme Disease

Influenza

MERS

Pneumonia

Rabies

Tuberculosis

Ticks

Zika

EMERGING INFECTIOUS DISEASES®

http://wwwnc.cdc.gov/eid/page/spotlight-topics

Sporadic Creutzfeldt-Jakob Disease in 2 Plasma Product Recipients, United Kingdom

Patrick Urwin, Kumar Thanigaikumar, James W. Ironside, Anna Molesworth, Richard S. Knight, Patricia E. Hewitt, Charlotte Llewelyn, Jan Mackenzie, Robert G. Will

Medscape EDUCATION ACTIVITY

JOINTLY ACCREDITED PROVIDER™
INTERPROFESSIONAL CONTINUING EDUCATION

In support of improving patient care, this activity has been planned and implemented by Medscape, LLC and Emerging Infectious Diseases. Medscape, LLC is jointly accredited by the Accreditation Council for Continuing Medical Education (ACCME), the Accreditation Council for Pharmacy Education (ACPE), and the American Nurses Credentialing Center (ANCC), to provide continuing education for the healthcare team.

Medscape, LLC designates this Journal-based CME activity for a maximum of 1.00 ***AMA PRA Category 1 Credit(s)™***. Physicians should claim only the credit commensurate with the extent of their participation in the activity.

All other clinicians completing this activity will be issued a certificate of participation. To participate in this journal CME activity: (1) review the learning objectives and author disclosures; (2) study the education content; (3) take the post-test with a 75% minimum passing score and complete the evaluation at http://www.medscape.org/journal/eid; and (4) view/print certificate. For CME questions, see page 1,055.

Release date: May 12, 2017; Expiration date: May 12, 2018

Learning Objectives

Upon completion of this activity, participants will be able to:

- Recognize the clinical features of 2 cases of sporadic Creutzfeldt-Jakob disease (sCJD) reported in patients with clotting disorders treated with fractionated plasma products.
- Identify the laboratory and pathology findings of 2 cases of sCJD reported in patients with clotting disorders treated with fractionated plasma product.
- Determine the clinical implications of 2 cases of sCJD reported in patients with clotting disorders treated with fractionated plasma products.

CME Editor
Jude Rutledge, BA, Technical Writer/Editor, Emerging Infectious Diseases. *Disclosure: Jude Rutledge has disclosed no relevant financial relationships.*

CME Author
Laurie Barclay, MD, freelance writer and reviewer, Medscape, LLC. *Disclosure: Laurie Barclay, MD, has disclosed the following relevant financial relationships: owns stock, stock options, or bonds from Alnylam; Biogen; Pfizer.*

Authors
Disclosures: ***Patrick Urwin, MBBS, MA (CANTAB); Kumar Thanigaikumar, MBBS, MRCP, FRCPATH; James W. Ironside, MD; Anna Molesworth, PhD; Patricia E. Hewitt, MD, FRCPATH; Charlotte A. Llewelyn, PhD;*** *and* ***Jan Mackenzie, PG Cert Epidemiology,*** *have disclosed no relevant financial relationships.* ***Richard S. Knight, BMBCh, FRCP (E),*** *has disclosed the following relevant financial relationships: served as a speaker or a member of a speakers bureau for Pfizer Inc.* ***Robert G. Will, MD,*** *has disclosed the following relevant financial relationships: served as an advisor or consultant for LFB (Paris); Ferring Pharmaceuticals.*

Author affiliations: University of Edinburgh Western General Hospital, Edinburgh, Scotland, UK (P. Urwin, J.W. Ironside, A. Molesworth, R.S. Knight, J. Mackenzie, R.G. Will); University Hospital Lewisham, London, UK (K. Thanigaikumar); National Health Service Blood and Transplant, London (P.E. Hewitt); National Health Service Blood and Transplant/Public Health England Epidemiology Unit, Cambridge, UK (C. Llewelyn)

DOI: https://dx.doi.org/10.3201/eid2306.161884

Sporadic Creutzfeldt-Jakob disease (sCJD) has not been previously reported in patients with clotting disorders treated with fractionated plasma products. We report 2 cases of sCJD identified in the United Kingdom in patients with a history of extended treatment for clotting disorders; 1 patient had hemophilia B and the other von Willebrand disease. Both patients had been informed previously that they were at increased risk for variant CJD because of past treatment with fractionated plasma products sourced in the United

Kingdom. However, both cases had clinical and investigative features suggestive of sCJD. This diagnosis was confirmed in both cases on neuropathologic and biochemical analysis of the brain. A causal link between the treatment with plasma products and the development of sCJD has not been established, and the occurrence of these cases may simply reflect a chance event in the context of systematic surveillance for CJD in large populations.

Human prion diseases are a group of rare and fatal neurodegenerative diseases that include idiopathic (sporadic), genetic (inherited), and acquired (infectious) disorders (*1*). All are associated with the accumulation of an abnormal isoform of the prion protein (PrP^{Sc}) in the central nervous system (*1*). The most common human prion disease is the sporadic form of Creutzfeldt-Jakob disease (sCJD), which occurs worldwide with a relatively uniform incidence of 1–2 cases per million population per year, a peak incidence in the 7th decade of life, and a median duration of illness of 4 months. The relatively consistent mortality rates associated with sCJD, the overall random spatial and temporal distribution of cases, and the absence of any confirmed environmental risk factor have led to the hypothesis that sCJD occurs because of the spontaneous generation of PrP^{Sc} in the brain (*1*). In contrast, variant Creutzfeldt-Jakob disease (vCJD) is an acquired disorder that is most likely caused by the consumption of meat or meat products contaminated with the bovine spongiform encephalopathy agent. The median age at death in vCJD is 30 years, with a median duration of illness of 14 months. Most cases of vCJD have occurred in the United Kingdom, which has had the largest epizootic of bovine spongiform encephalopathy in the world. Of the 178 UK vCJD cases, 3 have been identified as cases of secondary transmission caused by the transfusion of nonleukodepleted red blood cell components from vCJD-infected blood donors.

Lookback studies have shown no evidence of transmission through blood transfusion in sCJD (*2*,*3*), despite the identification of PrP^{Sc} in some peripheral tissues (*4*) and experimental evidence, which demonstrated infectivity in blood (*5*) by using intracerebral inoculation of highly sensitive transgenic mice. The absence of clinical cases causally linked to past treatment with fractionated plasma products has been used as evidence of the safety of these products in relation to sCJD (*6*). These products are generally manufactured from the pooled plasma from several thousand donors; production using UK plasma was discontinued in 1999.

We describe 2 cases of sCJD in patients who had previously received treatment with UK plasma–sourced plasma products; both patients had been informed that they were at increased risk for vCJD because of that treatment. The clinical features and investigations in these cases were typical of sCJD; the neuropathologic diagnosis in both cases was sCJD (subtype MM1).

The Investigation

The UK National CJD Research and Surveillance Unit has been carrying out systematic epidemiologic study of CJD since 1990. The methodology of this study has been published previously (*7*). In brief, patients with suspected CJD are referred by clinicians and visited by a research registrar, who obtains details of the clinical history and investigations, information on a range of possible risk factors, and past medical history. The Transfusion Medicine Epidemiology Review study investigates potential links between donors and recipients of labile blood components and, in cases of sCJD, investigates patients who have a history of blood donation or having received a blood transfusion.

Coordinated surveillance of CJD has been undertaken in the European Union since 1993 (*8*). National surveillance programs for CJD also are in place in several other countries, including Australia, Canada, Japan, and the United States.

Case 1

In 2014, a 64-year-old woman suffered a rapidly progressive dementia with deterioration in driving skills and balance disturbance, then limb coordination deficits with handwriting impairment. In the second month, her gait deteriorated, becoming shuffling and unsteady, she struggled to dress herself, and she had onset of daytime hypersomnolence. She became distractible, had visual misperceptions, emotional lability, and spatial memory problems. She was hospitalized at the beginning of the third month of her illness and had onset of cortical blindness, myoclonus, and akinetic mutism. She experienced rapid decline and died after a total illness duration of 3 months.

An electroencephalogram performed during the final stages of illness showed background slowing and runs of periodic complexes, and a magnetic resonance imaging (MRI) brain scan showed high signal in the caudate heads with posterior cortical ribboning. A cerebral spinal fluid (CSF) 14–3–3 assay and real-time quaking-induced conversion test for PrP^{Sc} both were positive. Prion protein gene (*PRNP*) sequencing showed no mutations with methionine homozygosity at codon 129.

Postmortem examination of the brain showed widespread spongiform encephalopathy of predominantly microvacuolar type. Immunocytochemistry for prion protein gave a widespread positive reaction in a granular/synaptic pattern (Figure). No plaques or plaque-like structures were identified. Results of immunocytochemistry for disease-associated prion protein were negative in peripheral nerve, liver, lymph node, appendix, and spleen. Western blot analysis of frontal cortex and cerebellum confirmed

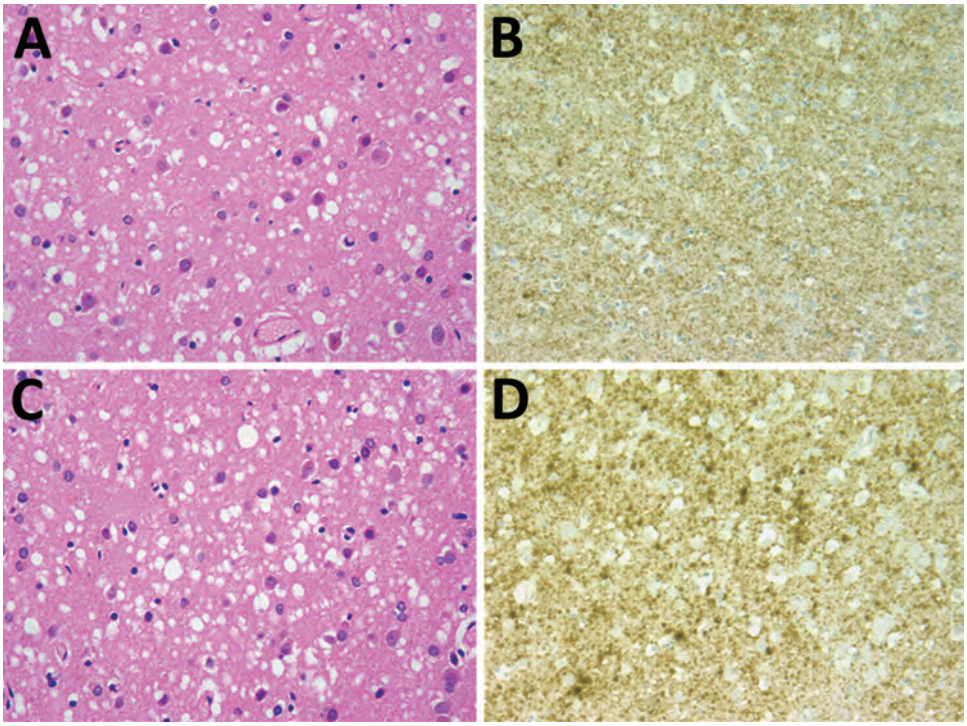

Figure. Results of neuropathologic examinations of the brains of the 2 patients with sporadic Creutzfeldt-Jakob disease, United Kingdom, 2014. A) Microvacuolar spongiform change in the frontal cortex (case 1). Hematoxylin and eosin stain; original magnification ×400. B) Fine granular/synaptic accumulation of abnormal prion protein in the cerebral cortex (case 1). 12F10 antiprion protein antibody; original magnification ×400. C) Microvacuolar spongiform change with neuronal loss and gliosis in the frontal cortex (case 2). Hematoxylin and eosin stain; original magnification ×400. D) Focally intense granular/synaptic accumulation of abnormal prion protein in the cerebral cortex (case 2). 12F10 antiprion protein antibody; original magnification ×400.

the presence of protease-resistant prion protein with a type 1A isoform.

The patient had been diagnosed with von Willebrand disease in childhood. Her early therapies include numerous transfusions of red blood cells and platelets; in more recent years, she received plasma-derived and recombinant factor VIII and additional blood component transfusions at times of hemorrhage. Factor VIII was administered on 4 occasions in the 1990s and during 2000–2004 and von Willebrand factor/factor VIII (Haemate-P) during 2001–2013. Because of her history of exposure to UK-sourced plasma products, for public health purposes she had been informed that she was at risk for vCJD, although she was not known to have been exposed to factor VIII derived from a batch including a vCJD donation. She had no history of potential iatrogenic exposure to CJD and no family history of CJD.

Donors for all blood or platelet transfusions since 2001 have been identified. Of the 107 donors, 106 are still alive, with a median age of 55 years (range 27–80 years). (Table 1). One donor of leukodepleted platelets, which were transfused 12 years before clinical onset in the recipient, died in 2013 at 76 years of age, and the diagnoses on the death certificate were vascular dementia and bladder cancer. Identification of donors for transfusions before 2001 has not been possible.

Case 2

In 2014, a 64-year-old woman reported day/night reversal of sleep patterns and, 3 months later, excessive tearfulness, for which she was started on antidepressants. She then had onset of writing problems, followed during the next few days by increasing language problems that led to expressive dysphasia. She deteriorated rapidly thereafter, requiring assistance with her activities of daily living and having coordination and memory problems, jerking movements suggestive of myoclonus, and itching in both arms. She was admitted to the hospital and experienced a probable focal seizure with secondary generalization. She had onset of a homonymous hemianopia and limb rigidity and then became bedbound and mute, dying 7 months after the onset of symptoms.

Table 1. Selected characteristics of blood donors to the patient with sporadic Creutzfeldt-Jakob disease described in case 1, United Kingdom, 2014*

Interval from transfusion to onset, y	Component	No. donors	No. donors alive	No. donors dead
3	RBC LD	4	4	0
6	RBC LD	6	6	0
7	RBC LD	19	19	0
9	RBC LD	3	3	0
10	RBC LD	4	4	0
12	Whole blood LD; RBC LD; platelets LD	2; 27; 42	2; 27; 41	0; 0; 1

*LD, leukodepleted; RBC, red blood cells. Median age of donors, 56 years (range 27–80 years).

An electroencephalogram performed during the final stages of illness showed widespread slowing, more evident on the left. An MRI brain scan showed left-sided caudate head and anterior putaminal high signal. Diffusion weighted imaging showed areas of cortical high signal. Results of a CSF 14–3–3 assay and real-time quaking-induced conversion tests were positive. Consent for full sequencing of the *PRNP* was not obtained; methionine homozygosity at codon 129 was identified.

Postmortem neuropathologic examination of the brain showed a widespread spongiform encephalopathy with microvacuolar spongiform change, neuronal loss, and gliosis. Immunostaining for prion protein showed widespread positivity with a granular/synaptic pattern (Figure). No amyloid plaques were identified. Western blot analysis confirmed the presence of protease resistant prion protein with a type 1A isoform. There was no evidence of abnormal prion protein accumulation in spleen and appendix either on immunocytochemistry or high sensitivity Western blot analysis.

The patient was known to have hemophilia B since 1964 and had received plasma-derived and recombinant factor IX during 1984–2012. For public health purposes, she had been informed that she was at risk for vCJD and in 1991 had received factor IX derived from a pool containing plasma from a donor who subsequently had vCJD. She had no history of potential iatrogenic exposure to CJD and no family history of CJD.

In 1985, the patient received 6 units of fresh frozen plasma (FFP). Tracing of donors has not been possible.

Discussion

This report describes 2 cases of sCJD in patients with a history of treatment with UK-sourced plasma products, 1 with a history of hemophilia B and 1 with von Willebrand's disease. To our knowledge, no previous case of sCJD in a person with a history of extended exposure to plasma products has been reported. It is clearly of concern that there have been 2 such cases in a relatively short period in the UK, where many plasma product recipients have been informed that they are at increased risk for vCJD. However, a causal link between the treatment with plasma products and the onset of sCJD has not been established, and the occurrence of these cases may simply reflect a chance event in the context of systematic surveillance of CJD in large populations.

Both patients had been informed that they were at increased risk for vCJD, and considering the evidence for the type of CJD in the 2 cases is important. Both patients had a clinical phenotype suggestive of sCJD, including a short duration of illness, typical early symptoms, a suggestive MRI scan, and, in 1 patient, a typical EEG. Notably, both patients had a positive real-time quaking-induced conversion test result for PrP^{Sc} in CSF; previously this test had not been positive in any case of vCJD evaluated in our laboratory (Table 2) (*9*). However, neuropathological examination was critical; it showed appearances typical of sCJD in both patients and no evidence of peripheral pathogenesis on immunostaining of lymphoreticular tissues, a feature that is observed in all tested specimens of vCJD patients to date (*10*). Furthermore, both patients had a type 1A isoform PrP^{Sc} on Western blot consistent with a diagnosis of sCJD subtype MM1 (*11*). Neither patient had a history of potential iatrogenic exposure or a family history of CJD, and for the case for which sequencing of the *PRNP* was performed, no mutations were detected. In both cases, an MM genotype occurred at codon 129 of *PRNP*, which does not distinguish between sCJD and vCJD. Laboratory transmission studies to provide evidence of agent strain in the cases have not been possible.

One patient had received multiple transfusions of blood components over an extended period, and the other had received 6 units of FFP 19 years before clinical onset, raising the possibility that these cases could have resulted from secondary transmission through blood components. In the case of the patient with von Willebrand disease, 107 donors have been traced, and none appear in the register of cases of CJD kept at the National CJD Research and Surveillance Unit. However, it has not been possible to obtain information on blood transfusions for this patient before 2001 nor on the FFP transfusions for the patient with hemophilia B. Lookback studies in the United States and United Kingdom have provided no evidence of transfusion-transmission of sCJD (*2*,*3*), and although 1 study suggested an increase in risk after a lag period of 10 years (*12*), this finding was not confirmed in another study (*13*). The balance of evidence

Table 2. Selected characteristics and clinical features of the 2 patients with sCJD described in cases 1 and 2, United Kingdom, 2014*

Characteristic/clinical feature	Case 1	Case 2
Patient age, y/sex	64/F	64/F
Symptoms/signs	Ataxia, cognitive impairment, visual impairment, myoclonus	Somnolence/depression, dysphasia, cognitive impairment, myoclonus/ataxia
Magnetic resonance imaging	+	+
Electroencephalogram	+	Slow activity
Cerebrospinal fluid 14–3–3 assay	+	+
RT-QuIC	+	+
Genotype	MM	MM
Diagnosis	Definite sCJD	Definite sCJD
Duration	3 mo	7 mo

*RT-QuIC, real-time quaking-induced conversion; sCJD, sporadic Creutzfeldt-Jakob disease.

indicates that, if sCJD is transmitted by blood transfusion, it must be a rare event, if it happens at all, and transfusion transmission is probably not the explanation for the 2 cases we describe.

Systematic surveillance for CJD, including a coordinated study in Europe (*14*), has been carried out in many countries over the past 25 years and is continuing. Many of these studies obtain information on potential risk factors, including details of past medical history. To date, no case of sCJD has been reported in a person who has received treatment for a clotting disorder. In fact, the absence of such a case has been used to argue against the possibility that plasma-derived products pose a risk for sCJD transmission (*6*). CJD surveillance centers are aware of the relevance of this issue, and sCJD patients with a history of treatment with plasma products probably would have been identified and reported if they occurred. Although it is surprising that 2 cases of sCJD have been identified among a population of 4,000–5,000 patients in the UK who have been treated for clotting disorders with fractionated plasma products, the total population under surveillance for CJD in Europe and internationally exceeds 500 million. Assuming an annual incidence rate of sCJD of 1.5–2.0 per million population (*15*), the occurrence of 2 cases of sCJD in this total population may not imply a causal link between the treatment and the occurrence of the disease. The 2 cases were identified over a period of months, and no further cases have been found since 2014; however, continuing to search for such cases through CJD surveillance programs is essential.

Acknowledgment

We thank Mark W. Head for the Western blot data.

The National CJD Research and Surveillance Unit is supported by the Policy Research Program of the Department of Health and the Government of Scotland (grant no. PR-ST-0614-00008). This report is independent research in part funded by the Department of Health Policy Research Programme and the Government of Scotland. The views expressed in this publication are those of the authors and not necessarily those of the Department of Health or the Government of Scotland.

Dr. Urwin worked as a research registrar at the National CJD Research and Surveillance Unit and is currently training in neurology. His primary research interests include human prion diseases.

References

1. Prusiner SB. Molecular biology of prion diseases. Science. 1991;252:1515–22. http://dx.doi.org/10.1126/science.1675487
2. Dorsey K, Zou S, Schonberger LB, Sullivan M, Kessler D, Notari E IV, et al. Lack of evidence of transfusion transmission of Creutzfeldt-Jakob disease in a US surveillance study. Transfusion. 2009;49:977–84. http://dx.doi.org/10.1111/j.1537-2995.2008.02056.x
3. Urwin PJ, Mackenzie JM, Llewelyn CA, Will RG, Hewitt PE. Creutzfeldt-Jakob disease and blood transfusion: updated results of the UK Transfusion Medicine Epidemiology Review Study. Vox Sang. 2016;110:310–6. http://dx.doi.org/10.1111/vox.12371
4. Glatzel M, Abela E, Maissen M, Aguzzi A. Extraneural pathologic prion protein in sporadic Creutzfeldt-Jakob disease. N Engl J Med. 2003;349:1812–20. http://dx.doi.org/10.1056/NEJMoa030351
5. Douet JY, Zafar S, Perret-Liaudet A, Lacroux C, Lugan S, Aron N, et al. Detection of infectivity in blood of persons with variant and sporadic Creutzfeldt-Jakob disease. Emerg Infect Dis. 2014;20:114–7. http://dx.doi.org/10.3201/eid2001.130353
6. European Medicines Agency. CHMP position statement on Creutzfeldt-Jakob disease and plasma-derived and urine-derived medicinal products. London, 23 June 2011 [cited 2015 May 1]. http://www.ema.europa.eu/docs/en_GB/document_library/Position_statement/2011/06/WC500108071.pdf
7. Cousens SN, Zeidler M, Esmonde TF, De Silva R, Wilesmith JW, Smith PG, et al. Sporadic Creutzfeldt-Jakob disease in the United Kingdom: analysis of epidemiological surveillance data for 1970–96. BMJ. 1997;315:389–95. http://dx.doi.org/10.1136/bmj.315.7105.389
8. Wientjens DPWM, Will RG, Hofman A. Creutzfeldt-Jakob disease: a collaborative study in Europe. J Neurol Neurosurg Psychiatry. 1994;57:1285–99.
9. McGuire LI, Peden AH, Orrú CD, Wilham JM, Appleford NE, Mallinson G, et al. Real time quaking-induced conversion analysis of cerebrospinal fluid in sporadic Creutzfeldt-Jakob disease. Ann Neurol. 2012;72:278–85. http://dx.doi.org/10.1002/ana.23589
10. Head MW, Ritchie D, Smith N, McLoughlin V, Nailon W, Samad S, et al. Peripheral tissue involvement in sporadic, iatrogenic, and variant Creutzfeldt-Jakob disease: an immunohistochemical, quantitative, and biochemical study. Am J Pathol. 2004;164:143–53. http://dx.doi.org/10.1016/S0002-9440(10)63105-7
11. Head MW, Bunn TJR, Bishop MT, McLoughlin V, Lowrie S, McKimmie CS, et al. Prion protein heterogeneity in sporadic but not variant Creutzfeldt-Jakob disease: UK cases 1991–2002. Ann Neurol. 2004;55:851–9. http://dx.doi.org/10.1002/ana.20127
12. Puopolo M, Ladogana A, Vetrugno V, Pocchiari M. Transmission of sporadic Creutzfeldt-Jakob disease by blood transfusion: risk factor or possible biases. Transfusion. 2011;51:1556–66. http://dx.doi.org/10.1111/j.1537-2995.2010.03004.x
13. Molesworth AM, Mackenzie J, Everington D, Knight RSG, Will RG. Sporadic Creutzfeldt-Jakob disease and risk of blood transfusion in the United Kingdom. Transfusion 2011;51:1872–3. https://doi.org/10.1111/j.1537-2995.2011.03198.x
14. Ladogana A, Puopolo M, Croes EA, Budka H, Jarius C, Collins S, et al. Mortality from Creutzfeldt-Jakob disease and related disorders in Europe, Australia, and Canada. Neurology. 2005;64:1586–91. http://dx.doi.org/10.1212/01.WNL.0000160117.56690.B2
15. Minikel EV, Vallabh SM, Lek M, Estrada K, Samocha KE, Sathirapongsasuti JF, et al.; Exome Aggregation Consortium (ExAC). Quantifying prion disease penetrance using large population control cohorts. Sci Transl Med. 2016;8:322ra9. http://dx.doi.org/10.1126/scitranslmed.aad5169

Address for correspondence: R.G. Will, National CJD Research and Surveillance Unit, Western General Hospital, Edinburgh, Scotland EH4 2XU, UK; email: r.g.will@ed.ac.uk

RESEARCH

Hospital Outbreaks of Middle East Respiratory Syndrome, Daejeon, South Korea, 2015

Jung Wan Park, Keon Joo Lee, Kang Hyoung Lee, Sang Hyup Lee, Jung Rae Cho, Jin Won Mo, Soo Young Choi, Geun Yong Kwon, Ji-Yeon Shin, Jee Young Hong, Jin Kim, Mi-Yeon Yeon, Jong Seok Oh, Hae-Sung Nam

From May through July 2015, a total of 26 cases of Middle East Respiratory Syndrome were reported from 2 hospitals in Daejeon, South Korea, including 1 index case and 25 new cases. We examined the epidemiologic features of these cases and found an estimated median incubation period of 6.1 days (8.8 days in hospital A and 4.6 days in hospital B). The overall attack rate was 3.7% (4.7% in hospital A and 3.0% in hospital B), and the attack rates among inpatients and caregivers in the same ward were 12.3% and 22.5%, respectively. The overall case-fatality rate was 44.0% (28.6% in hospital A and 63.6% in hospital B). The use of cohort quarantine may have played a role in preventing community spread, but additional transmission occurred among members of the hospital cohort quarantined together. Caregivers may have contributed in part to the transmission.

A few respiratory viruses constitute emerging threats to global health security (*1*); among them are Middle East respiratory syndrome (MERS) coronavirus (MERS-CoV), which has caused outbreaks in Saudi Arabia (*2*,*3*). The major MERS outbreaks that occurred during 2012–2015 have been in or near the Arabian Peninsula. However, information on the epidemiologic features of MERS is insufficient, especially for different environmental and cultural settings. The 2015 MERS outbreak in South Korea could provide more information about the epidemiology of MERS because it was the largest outbreak outside the Middle East (*4*).

Author affiliations: Korea Centers for Disease Control and Prevention, Cheongju, South Korea (J.W. Park, K.J. Lee); Sokcho Medical Center, Sokcho, South Korea (K.H. Lee); Ulsan Metropolitan City Hall, Ulsan, South Korea (S.H. Lee); Daejeon Provincial Government, Daejeon, South Korea (J.R. Cho); Chuncheongbukdo Provincial Government, Cheongju (J.W. Mo); DaeChung Hospital, Daejeon (S.Y. Choi); Ministry of Health and Welfare, Sejong, South Korea (G.Y. Kwon); Eulji University School of Medicine, Daejeon (J.-Y. Shin); Konyang University College of Medicine, Daejeon (J.Y. Hong); Chungnam National University School of Medicine, Daejeon (J. Kim, M.-Y. Yeon, H.-S. Nam); Gwanggyo Ean Pediatric Clinic, Suwon, South Korea (J.S. Oh)

DOI: http://dx.doi.org/10.3201/eid2306.160120

The first case of MERS in South Korea was reported on May 20, 2015. The patient had flown among several countries in the Middle East (Bahrein, the United Arab Emirates, Saudi Arabia, and Qatar) and became the source of consecutive hospital-to-hospital transmissions after his return to South Korea, which led to 186 laboratory-confirmed cases (*5*) and 38 deaths. Hospital-to-hospital transmission involved 17 hospitals and originated from 1 hospital (hospital P) (*5*,*6*). This transmission was attributable to "hospital shopping" by some MERS patients (*4*,*5*) and was particularly evident in Daejeon, which is the fifth largest city in South Korea. The index case-patient for nosocomial transmission in Daejeon had initially traveled from his home city of Daejeon to Pyeongtaek, South Korea, seeking healthcare at hospital P, after which he returned to Daejeon. Subsequently, 2 hospitals in Daejeon experienced MERS cases attributable to this patient. This index case-patient in Daejeon was consecutively hospitalized at hospital A in Daejeon during May 22–28, 2015, and at hospital B during May 28–30, 2015. Thereafter, an additional 25 MERS cases (14 in hospital A, 11 in hospital B) were reported.

After the South Korea government recognized the outbreak of MERS in Daejeon, cohort quarantine (isolation of persons who had been in contact with patients with confirmed cases in the hospital ward) was applied. This quarantine seems to have played a useful role in preventing the spread of MERS-CoV to the local community. We describe the MERS case-patients, the epidemiologic features of the disease, and the quarantine policy used to prevent additional transmission.

Methods

Setting

Hospital A is a 300-bed general hospital in Daejeon. The outbreak occurred in ward 51 on the fifth floor, where 13 rooms (5 with 7 beds, 6 with 4 beds, 1 with 2 beds, and 1 with 1 bed) are located. Hospital B is an 800-bed university hospital in Daejeon. The main outbreak occurred in ward

101 on the ninth floor, where 16 rooms (7 with 6 beds, 1 with 4 beds, 1 with 2 beds, and 7 with 1 bed) are located.

Data Collection and Exposure Assessment

Epidemiologic investigators of the Korea Centers for Disease Control and Prevention started their outbreak investigation with face-to-face interviews of the index case-patient in Daejeon and the 25 additional case-patients with confirmed MERS-CoV infection. We collected data on the demographic characteristics and the clinical, contact, and MERS-CoV exposure histories and thoroughly reviewed the medical records of the case-patients to identify symptoms, underlying concurrent medical conditions, laboratory findings, and clinical courses of illness. Clinical outcome was classified as recovery or death, and the ambulation status of the inpatients at the time of admission was clarified.

We collected the names of inpatients, their room numbers, medical staff, and caregivers (family members or professionals hired by the family or hospital) exposed to MERS-CoV in each hospital. The duration and route of exposure were further determined by reviewing recordings from closed-circuit televisions placed in the hospitals. Moreover, we used the floor plan of each hospital to estimate the spatial distributions and transmission routes of the virus within the hospitals. These estimates enabled us to identify a possible location of exposure and a transmission route for each confirmed case. When a patient with a confirmed case had experienced several possible exposures, we determined the most probable exposure by author consensus. Persons who had had face-to-face contact with patients with confirmed cases were considered the closest contacts. When the data were ambiguous, the following were reviewed independently by the Korea Centers for Disease Control and Prevention and the Daejeon In-Depth team: all potential exposures by symptom onset; disease duration; physical distance from a patient with a confirmed case; and infector factors including ambulation status, symptoms (including a productive cough), and sharing of caregivers. When a patient with a confirmed case had been subjected to several potential exposures, the most probable exposure was determined by consensus of the 2 teams. An expert member of the Korean Society of Epidemiology reviewed all decisions. The process was repeated until a final consensus was obtained.

Laboratory Diagnoses

Sputum samples from the persons suspected of having MERS were collected in sterile cups and sent to qualified local or national laboratories for confirmation. As a confirmatory test, a real-time reverse transcription PCR of nucleic acid extracted from sputum specimens was performed (*5*). Cycle threshold values were also measured to quantify viral loads. For each patient with a confirmed case, the Korea Centers for Disease Control and Prevention assigned a case number according to the order of confirmation during the 2015 MERS outbreak in South Korea. For example, the case number of the index case-patient in Daejeon was 16.

Data and Statistical Analyses

The cases were described in case-series form. Attack rates were calculated as the number of cases per number of exposed persons (defined as persons who had experienced face-to-face contact with a symptomatic MERS case-patient in either hospital or as persons who had been in the same hospital ward as the symptomatic case-patients). Such persons were identified from the outbreak investigation reports and the lists of those undergoing cohort or home quarantine. To assess differences in attack rates and case-fatality rates according to independent variables, we performed χ^2 and Fisher exact tests by using SAS software version 9.3 (SAS Institute, Inc., Cary, NC, USA). Comparisons were considered significant at $p<0.05$ and marginally significant at $p<0.1$ (both p values were 2-tailed).

We defined the incubation period as the time from exposure to onset of MERS-associated symptoms, including nonspecific signs and symptoms such as fever, chills, cough, sore throat, sputum production, dyspnea, myalgia, headache, nausea, vomiting, diarrhea, and abdominal discomfort. If the exposure period was >2 days, a single interval-censored estimate of the incubation period was computed by using the earliest and latest dates of exposure and the date of symptom onset for each case-patient (coarseDataTools package in R statistical software version 3.2.2) (*7*). To construct cumulative fraction curves of all cases by incubation period, we calculated the log-normal density function by fitting the interval-censored data on incubation periods. To do this, we used the maximum-likelihood method and calculated the medians and 5th and 95th percentiles of the incubation periods.

Results

Description of the Daejeon Index Case-Patient

The Daejeon index case-patient (case-patient 16), a 41-year-old man, lived in Daejeon and was a former smoker (10 to 20 pack-years). He had undergone colon surgery in August 2014 at hospital P. The index case-patient of the MERS outbreak in South Korea (case-patient 1) was in hospital P during May 15–17, 2015. The Daejeon index case-patient was admitted to hospital P at the same time (May 15–18, 2015) for a follow-up colonoscopy. After discharge on May 20, the Daejeon index case-patient felt feverish and had chills, cough, general weakness, and diarrhea. Because of these symptoms, he was hospitalized in hospital A in Daejeon during May 22–28; the room was shared by 3

Table 1. Quarantine policy to prevent additional transmission of MERS, Daejeon, South Korea*

Action
• The cohort quarantine applied to admitted patients and their caregivers (professional or family) exposed to the MERS case-patients.
• Inpatients admitted to the same hospital room before quarantine were quarantined in the same room because their degree of exposure was probably the same. Their caregivers were also quarantined in the same room because of the need for caregiving.
• The medical staff (physicians, nurses, and medical technologists) exposed to the MERS case-patients were subjected to home quarantine. However, members of the households of medical staff were not subjected to home quarantine until and unless that medical staff member exhibited any symptoms. Contact between household members and the medical staff member was severely restricted.
• The wards under cohort quarantine were controlled by unexposed medical staff using level D protectors (Microguard 2000; 3M, Bracknell, UK). Each protector included an N95 mask, protective glasses, a whole-body protective gown, gloves, and boots.
• The body temperature of persons (including inpatients and caregivers) and medical staff admitted to cohort or home quarantine was checked, and these persons were clinically interviewed twice daily. If they reported any symptoms (including a febrile sensation or chills) or if they were asymptomatic but with a body temperature >37.5C°, they were immediately placed in a quarantined area at each hospital. The KCDC performed laboratory tests at this stage; the results were available 3 d later. If the doctor in charge strongly suspected MERS, that patient could be transferred, with careful precautions, to a national isolation hospital within 1 d.
• All wards were disinfected by use of sodium hydrosulfite, 80% (vol/vol) alcohol, and 2% (vol/vol) chlorhexidine twice during each shift, thus 6 times/d.
• South Korea operates a nationwide medical insurance scheme; all costs incurred by MERS patients were covered.
• Persons with confirmed MERS were transferred to another quarantine room that had negative-pressure equipment.
Strategies for caregivers
• The infection control team carefully explained the risk for MERS and the need for cohort quarantine to all caregivers. Some caregivers did not wish to remain in hospital wards with inpatients. They were taken home and placed in in-home quarantine and used the same MERS quarantine strategy applicable to medical staff in close contact with the patients.
• Caregivers attended only noninfected inpatients who required total care. If an inpatient was confirmed to have MERS, nursing care was provided by professional nurses wearing protectors.
• The infection control team continuously educated caregivers on how MERS was transmitted and how to prevent infection. Caregivers were told to wear protectors (N95 masks, vinyl gowns, and gloves) and to not touch each other. However, during the first week of quarantine, checks of closed-circuit television footage showed that the protector and contact rules were sometimes not obeyed in hospital A.
• Hospital A designated 2 rooms for caregivers in the quarantine ward. The caregivers could use these rooms when they were not actively engaged in patient care.

*KCDC, Korea Centers for Disease Control and Prevention; MERS, Middle East respiratory syndrome.

inpatients and 1 caregiver. Because his symptoms did not improve, he was transferred to the emergency department at hospital B. After hospitalization in ward 101 in hospital B, he was suspected of having MERS and was isolated in a negative-pressure room on May 30. Ultimately, he became the 16th confirmed MERS patient of 186 total case-patients during the 2015 outbreak.

Before the Daejeon case-patient was isolated, those around him did not use protective equipment. Therefore, virus was spread from him during his first 10 days of illness, before MERS diagnosis and isolation. When we checked the closed-circuit television recordings from hospital A to estimate how many persons could have been in contact with the Daejeon index case-patient, we found that he had been in several sections of the hospital ward, in particular those located on the left side of the nurse station. These sections included his admission room, a restroom, the nurse station, the foyer, and the hall in front of the elevators. The Daejeon index case-patient had potentially contacted every inpatient in the same hospital ward. Therefore, we classified all patients and caregivers in that ward as possible contacts.

Description of Patients with Confirmed Cases

A total of 26 cases (including the index case) were confirmed in the 2 hospitals, and 11 case-patients died of MERS (4 in hospital A and 7 in hospital B) (online Technical Appendix, https://wwwnc.cdc.gov/EID/article/23/6/16-0120-Techapp1.pdf). Other than the index case, 14 cases occurred in hospital A and 11 in hospital B. Case-patients 30, 38, and 128 were admitted to the same room in hospital A as the Daejeon index case-patient. Case-patient 85 was a caregiver hired by case-patient 128, so she was in the same hospital room in hospital A during May 22–28. Case-patients 23, 24, 31, 36, and 95 were admitted to the same room in hospital B as the Daejeon index case-patient. Case-patient 82 was the wife of case-patient 36; case-patient 106 was a caregiver hired by case-patient 36; and case-patient 127 was the wife of case-patient 24. Therefore, when caregiving, they were in the same room as the Daejeon index case-patient.

The median age of the case-patients was 71 (interquartile range 38–86) years; 13 (52.0%) were male; 6 (24.0%) were commercial caregivers; and 3 (12.0%) were family caregivers. A total of 18 (72.0%) case-patients had underlying diseases; 7 (28.0%) had pulmonary diseases, such as asthma, chronic obstructive pulmonary disease, idiopathic pulmonary disease, lung cancer, and pulmonary tuberculosis.

All patients reported fever. Other signs and symptoms included chills (10 patients, 38.5%), cough (8, 30.8%), sputum (6, 23.1%), myalgia (9, 34.6%), headache (4, 15.4%), dyspnea (6, 23.1%), nausea (3, 11.5%), diarrhea (6, 23.1%),

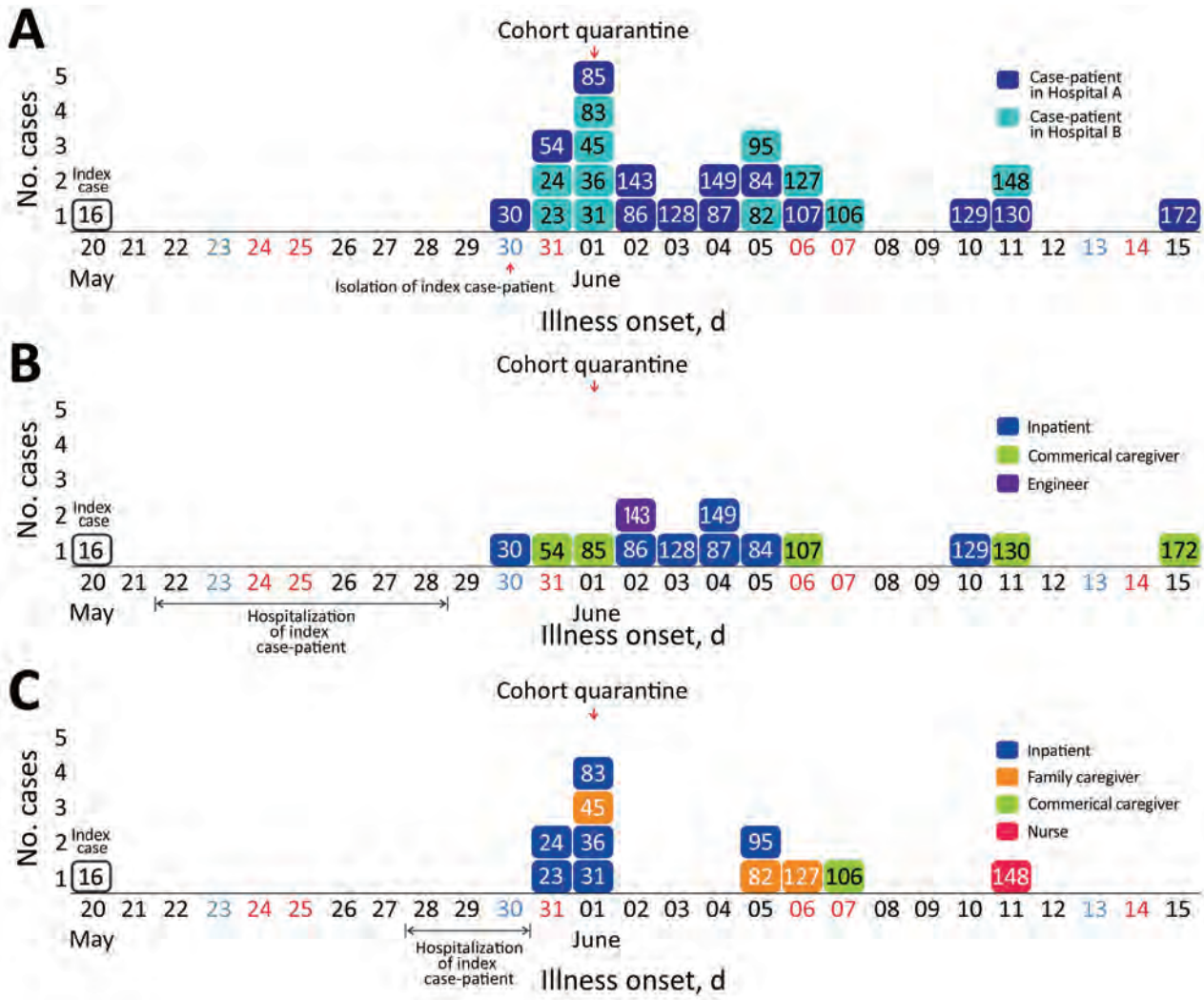

Figure 1. Epidemic curves for the Middle East respiratory syndrome outbreak in Daejeon, South Korea, 2015. The cases are numbered in the order in which they were confirmed in the context of all cases reported during the outbreak. A) Hospitals A and B; B) Hospital A; C) Hospital B. Case-patient 38 is not included because date of illness onset is unknown. Black, weekday; blue, Saturday; red, Sunday or holiday.

sore throat (3, 11.5%), rhinorrhea (2, 7.7%), hemoptysis (1, 3.8%), and abdominal discomfort (1, 3.8%)

Quarantine

To prevent the spread of MERS-CoV to the local community, on June 1, 2015, the government of South Korea ordered cohort quarantine, which hospitals A and B followed (Table 1). Persons with a history of exposure to patients with confirmed MERS were isolated in the same hospital ward.

Epidemic Curve

After the index case-patient in Daejeon spread MERS-CoV in Daejeon, the first case occurred on May 30, 2015, and the last on June 15, 2015 (total outbreak duration 17 days) (Figure 1). The epidemic curve for hospital A suggested a relatively sporadic pattern compared with that for hospital B. The peak in hospital B comprised mostly patients who shared a hospital room with the index case-patient. Most MERS cases appeared later in professional or family caregivers rather than in inpatients.

The estimated median incubation period for confirmed cases was 6.1 (95% CI 4.7–7.5) days (Figure 2). Incubation periods were 8.8 (95% CI 7.2–10.4) days for hospital A and 4.6 (95% CI 2.9–6.2) days for hospital B.

In hospital A, the index case-patient was admitted to room 5101, in sector A (Figure 3). Thereafter, 12 case-patients were in sector A, and 1 was in sector B. However, the case-patient in sector B had a history of contact with case-patient 85, who was transferred to sector B from sector A for quarantine. Most case-patients were presumed to have been infected by the Daejeon index case-patient

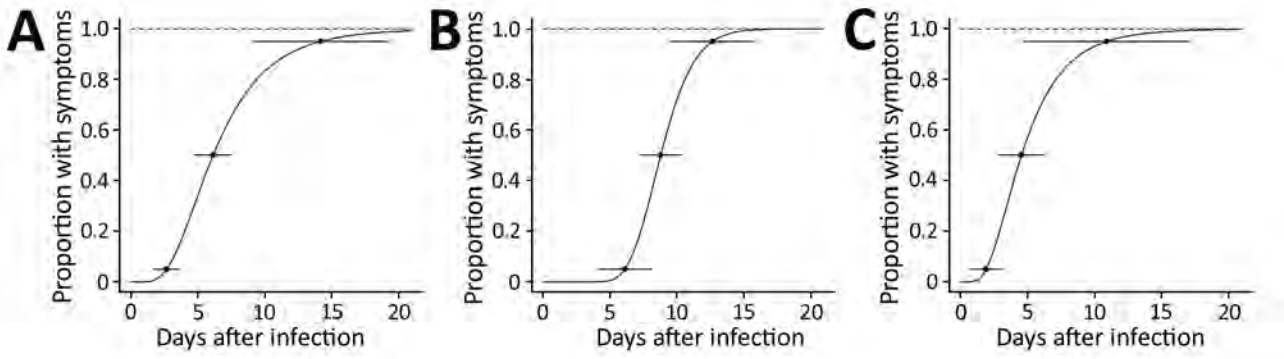

Figure 2. Estimated incubation periods for the Middle East respiratory syndrome outbreak in Daejeon, South Korea, 2015. Curves indicate estimated cumulative fractions of cases corresponding to the incubation periods, estimated by creating log-normal density functions fitting the observed data. Horizontal lines indicate 95% CIs for the 5th, 50th, and 95th percentiles of the estimated incubation periods. A) Total; estimated median incubation period was 6.1 (95% CI 4.7–7.5) days. B) Hospital A; estimated median incubation period was 8.8 (95% CI 7.2–10.4) days. C) Hospital B; estimated median incubation period was 4.6 (95% CI 2.9–6.2) days.

(case-patient 16). However, 3 instances of other transmission were noted: case-patient 85 to case-patient 130, case-patient 54 to case-patient 172, and several case-patients to case-patient 129. For this last instance of transmission, we could not identify the most probable source, because many possible exposures were evident (case-patients 54, 84, 86, 87, 107, and 149).

In hospital B, the index case-patient was admitted to room 1007, located on the upper side of ward 101 (sector C). Eight case-patients were in sector C. Case-patient 83 was in room 1013 on the opposite side of ward 101 (sector D). Case-patient 45 was in the emergency room and ward 101 with the index case-patient. Case-patient 148 was presumed to have been infected by case-patient 36 during performance of cardiopulmonary resuscitation in the intensive care unit.

Attack Rate and Case-Fatality Rate

A total of 14 cases developed among 301 persons exposed in hospital A (attack rate 4.7%) and 11 among 371 persons exposed in hospital B (attack rate 3.0%) (Table 2). The attack rates for the sectors hosting the index case-patients (sector A of hospital A, sector C of hospital B; Figure 3) were higher than those for other sectors (sector B of hospital A, sector D of hospital B; Figure 3) (31.6% vs. 2.4% in hospital A, $p<0.05$; 18.2% vs. 6.5% in hospital B; Table 3). The probability of infection for a person admitted to the same rooms as the index case-patient was 75.0%. In both hospitals, attack rates were somewhat higher for caregivers (22.5%) than for inpatients (12.3%), although statistical significance was not attained.

The overall case-fatality rate was 44% (Table 4). This rate was higher for patients in hospital B (63.6%) than for those in hospital A (28.6%), although statistical significance was not attained.

Discussion

During the MERS outbreak in South Korea, 25 confirmed cases (including 11 deaths) occurred in Daejeon, all associated with the same index case-patient. Two hospitals were affected. The incubation periods and case-fatality rates for the 2 hospitals differed.

Under the South Korea healthcare system, patients can visit secondary hospitals and the emergency rooms of tertiary hospitals without limitation (*5*), which probably facilitated nosocomial transmission of MERS-CoV. Indeed, the outbreak in Daejeon accounted for 1 of the 3 major MERS-CoV outbreaks in South Korea. These observations underscored the importance of the outbreak in Daejeon, leading the South Korea government to focus resources on controlling transmission of the virus.

The estimated median incubation period for MERS during the outbreak we report was similar to that for outbreaks in the eastern province of Saudi Arabia in 2013 (*1*). Incubation period estimates may differ, depending on the method used to select exposure: the most probable exposure versus overlapping exposures. In our study, the incubation periods estimated by using both methods were similar. The incubation period estimated by using the most probable exposure method was 6.1 (95% CI 4.7–7.5) days, and that estimated by using the overlapping exposures method was 5.6 (95% CI 4.2–6.9) days. The overall attack rate among all exposed persons in Daejeon was similar to that for Pyeongtaek (*5*). The case-fatality rate of the outbreak in Daejeon was lower than that in the eastern province of Saudi Arabia in 2013 (*1*) but similar to that in Jeddah, Saudi Arabia, in 2014 (*3*).

Our results indicate various epidemiologic characteristics of MERS-CoV. All persons acquired infection in a hospital setting, which is consistent with the previous outbreak in Saudi Arabia, in which nosocomial spread

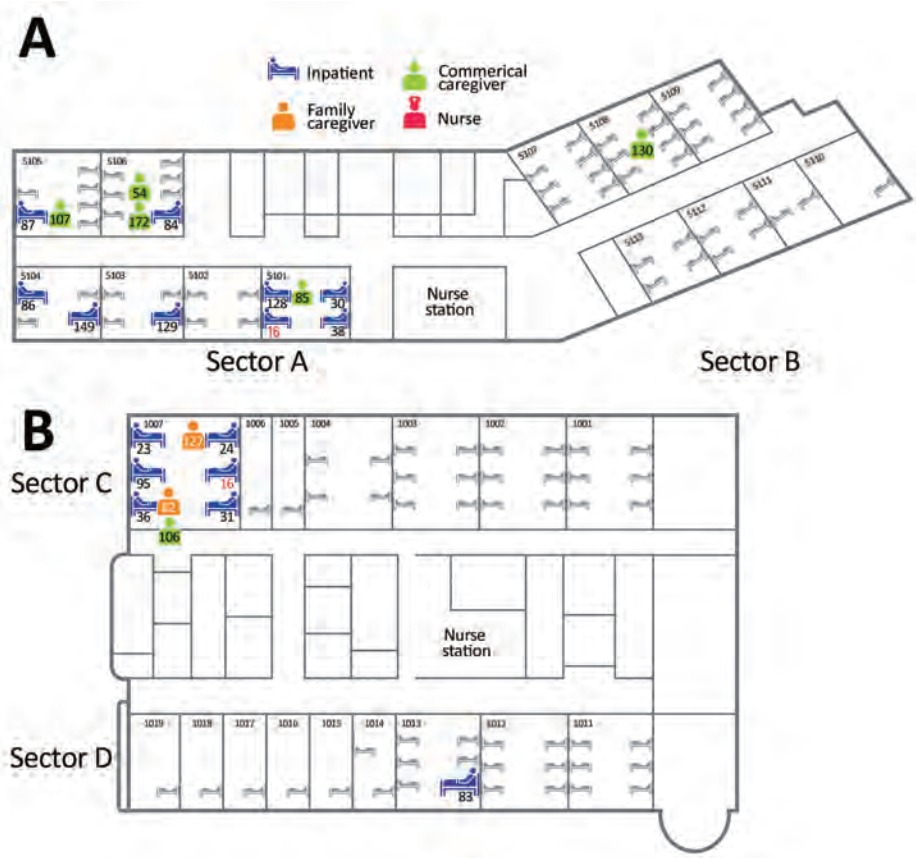

Figure 3. Locations of Middle East respiratory syndrome case-patients in hospitals A and B, Daejeon, South Korea, 2015, showing where case-patients were exposed to presumed infectors. Not shown are case-patient 143, an engineer working in hospital A, because the location of his exposure is unclear; case-patient 45, a family caregiver in either the emergency department or room 1015; and case-patient 148, a nurse in the intensive care unit.

was a major route of MERS-CoV transmission (*1*). The characteristics of the specific hospital seemed to affect attack rates and case-fatality rates. The index case-patient in Daejeon was consecutively admitted to 2 hospitals. The fifth floor of hospital A specializes in senile patients, most of whom have chronic illnesses, including Parkinson's disease, paraplegia attributable to old infarctions, or amyotrophic lateral sclerosis. Most beds on the fifth floor are occupied by bedridden patients. The attack rate among caregivers was higher in hospital A than in hospital B. Because immobile patients require personal caregiving, their caregivers were required to be in prolonged close contact with patients, which might have resulted in a higher attack rate. Hospital B is a university hospital and thus contained more severely ill patients than hospital A. Ward 101, to which the Daejeon

Table 2. Middle East respiratory syndrome attack rates among all exposed persons, Daejeon, South Korea, 2015

	Hospital A		Hospital B		Total	
Exposure	No. exposed /no. with confirmed case	Attack rate, %	No. exposed/no. with confirmed case	Attack rate, %	No. exposed/no. with confirmed case	Attack rate, %
Total	301/14	4.7	371/11	3.0	672/25	3.7
Inpatients	227/8	3.5	122/6	4.9	349/14	4.0
Same ward as index case-patient	62/8	12.9*	52/6	11.5*	114/14	12.3*
Other wards	165/0	0	70/0	0	235/0	0
Caregivers†	29/5	17.2*	32/4	12.5	61/9	14.8*
Same ward as index case-patient	17/5	29.4‡	23/4	17.4	40/9	22.5*
Other wards	12/0	0	9/0	0	21/0	0
Nurses	20/0	0	78/1	1.3	98/1	1.0
Doctors	8/0	0	35/0	0	43/0	0
Others§	17/1	5.9	104/0	0	121/1	0.8

*p<0.05
†Family or professional.
‡p<0.1.
§Paramedics, students, engineers, and visitors.

Table 3. Attack rates for Middle East respiratory syndrome among inpatients and caregivers in the same wards as the index case-patient, Daejeon, South Korea, 2015

Person	Hospital A		Hospital B		Total	
	No. exposed/no. with confirmed case	Attack rate, %	No. exposed/no. with confirmed case	Attack rate, %	No. exposed/no. with confirmed case	Attack rate, %
Total	79/13	16.5	75/10	13.3	154/23	14.9
Sex						
M	20/5	25.0	36/7	19.4	56/12	21.4*
F	59/8	13.6	39/3	7.7	98/11	11.2
Age, y						
30–64	28/5	17.9	28/3	10.7	56/8	14.3
≥65	51/8	15.7	47/7	14.9	98/15	15.3
Role						
Inpatient	62/8	12.9	52/6	11.5	114/14	12.3
Caregiver†	17/5	29.4	23/4	17.4	40/9	22.5
Hospital or room						
Same sector‡	38/12	31.6§	44/8	18.2	82/20	24.4§
Same room	4/4	100¶	12/8	66.7¶	16/12	75.0¶
Other room	34/8	23.5	32/0	0	66/8	12.1
Different sector#	41/1	2.4	31/2	6.5	72/3	4.2
Ambulatory						
Yes	32/10	31.3	41/7	17.1	73/17	23.3
No	23/3	13.0	13/3	23.1	36/6	16.7
Not known	24/0	0	21/0	0	45/0	0

*p<0.1.
†Family or professional.
‡Sector A of hospital A or sector C of hospital B, as described in Figure 3.
§p<0.05 when compared with attack rates in a different sector.
¶p<0.05 when compared with attack rates in other rooms.
#Sector B of hospital A or sector D of hospital B (Figure 3).

index case-patient was admitted, is the main ward of the pulmonary medicine department. We presumed that the case-fatality rate was higher for hospital B than hospital A because of underlying pulmonary disease, which has been reported to be a risk factor for development of more severe diseases (*8*).

Generally, cohort quarantine may be useful as an infection-control tool to limit virus transmission in hospitals in which susceptible inpatients are gathered or to more effectively detect infected patients (*9*). Hospitals A and B applied cohort quarantine. In this situation, cohort quarantine had several advantages and disadvantages. The primary purpose was to prevent the spread of MERS-CoV to the local community. After applying cohort quarantine, no further spread of MERS-CoV occurred other than within hospitals A and B. This result may have been achieved by quarantining all persons who had been in contact with MERS-CoV–infected patients and by refusing hospital entry to all susceptible persons. In addition, more cases were diagnosed promptly by active surveillance of the cohort. However, this policy had a limitation. One cohort accommodated inpatients and caregivers in the same hospital room; thus, if 1 person in the cohort was infected by MERS-CoV, others were exposed, increasing the probability of MERS-CoV transmission. This practice raises an ethical issue in terms of whether letting persons stay in the same room with potential MERS patients is justified by the purpose of preventing transmission of the virus to the community. Some caregivers at hospital A may have had difficulty complying with the quarantine policy (the protector and contact rules) because they cared for immobile patients. Thus, this practice may have increased transmission within the hospital.

We identified several cases with uncommon routes of transmission. Case-patient 148 was the head nurse of the intensive care unit to which case-patient 36 was admitted. When case-patient 36 experienced cardiac arrest, that nurse performed cardiopulmonary resuscitation while wearing a level D protector. However, afterward, she may have been exposed to MERS-CoV when she wiped sweat with her bare arm. Case-patient 143 was an employee of hospital A; he worked in information technology. He was employed by hospital A during January–May 30, 2015, and his bedroom was located on the

Table 4. Case-fatality rates among all Middle East respiratory syndrome case-patients, Daejeon, South Korea, 2015

Concurrent condition	Hospital A		Hospital B		Total	
	No. incident cases/ no. fatal cases	Case-fatality rate, %	No. incident cases/ no. fatal cases	Case-fatality rate, %	No. incident cases/ no. fatal cases	Case-fatality rate, %
Total	14/4	28.6	11/7	63.6	25/11	44.0
Pulmonary	1/0	0	6/5	83.3	7/5	71.4
None or nonpulmonary	13/4	30.8	5/2	40	18/6	33.3

seventh floor. His routine work routes, shown on closed-circuit television, did not reveal any close contact with case-patients; thus, the transmission route was unclear. We presume that he was infected by fomites in an elevator or exposed to a patient in a place lacking closed-circuit television coverage.

The transmission route for case-patient 83 was also unidentified. It is possible that some medical staff and caregiver, contaminated with MERS-CoV after visiting room 1007, may have visited case-patient 83 in room 1013. Of note, when case-patient 83 was exposed to MERS-CoV, the outbreak in Daejeon had not yet been recognized and hospital B had not yet implemented infection control strategies (e.g., handwashing; wearing gloves, masks, and vinyl gowns).

This study had several limitations. First, we cannot be certain that all chains of infection between case-patients have been identified. We did not perform serologic analyses to seek cases that were potentially missed; such missed cases may have affected the incubation period estimates and case-fatality rate. Second, closed-circuit television may not have captured all relevant movements.

In conclusion, in 2015, Daejeon experienced a hospital-associated outbreak of MERS-CoV. Two hospitals experienced nosocomial outbreaks, and virus transmission was evident among mostly inpatients and caregivers. To prevent the spread of the virus to the local community, we developed a unique and successful cohort quarantine policy. However, ethical issues associated with this policy require thorough discussion by policy makers.

Dr. Park is a medical specialist in infectious diseases and an epidemiologist at the Korea Centers for Disease Control and Prevention, in Cheongju, South Korea. His research interest is MERS-CoV infection.

References

1. Assiri A, McGeer A, Perl TM, Price CS, Al Rabeeah AA, Cummings DA, et al.; KSA MERS-CoV Investigation Team. Hospital outbreak of Middle East respiratory syndrome coronavirus. N Engl J Med. 2013;369:407–16. http://dx.doi.org/10.1056/NEJMoa1306742
2. Al-Tawfiq JA, Memish ZA. Middle East respiratory syndrome coronavirus: epidemiology and disease control measures. Infect Drug Resist. 2014;7:281–7.
3. Oboho IK, Tomczyk SM, Al-Asmari AM, Banjar AA, Al-Mugti H, Aloraini MS, et al. 2014 MERS-CoV outbreak in Jeddah—a link to health care facilities. N Engl J Med. 2015;372:846–54. http://dx.doi.org/10.1056/NEJMoa1408636
4. Kim SW, Yang TU, Jeong Y, Park JW, Lee K-J, Kim KM, et al. Middle East respiratory syndrome coronavirus outbreak in the Republic of Korea. Osong Public Health and Research Perspectives. 2015;6:269–78. http://dx.doi.org/10.1016/j.phrp.2015.08.006
5. Ki M. 2015 MERS outbreak in Korea: hospital-to-hospital transmission. Epidemiol Health. 2015;37:e2015033. http://dx.doi.org/10.4178/epih/e2015033
6. Kim KM, Ki M, Cho SI, Sung M, Hong JK, Cheong HK, et al.. Epidemiologic features of the first MERS outbreak in Korea: focus on Pyeongtaek St. Mary's Hospital. Epidemiol Health. 2015;37:e2015041. http://dx.doi.org/10.4178/epih/e2015041
7. Reich NG, Lessler J, Cummings DA, Brookmeyer R. Estimating incubation period distributions with coarse data. Stat Med. 2009;28:2769–84. http://dx.doi.org/10.1002/sim.3659
8. Assiri A, Al-Tawfiq JA, Al-Rabeeah AA, Al-Rabiah FA, Al-Hajjar S, Al-Barrak A, et al. Epidemiological, demographic, and clinical characteristics of 47 cases of Middle East respiratory syndrome coronavirus disease from Saudi Arabia: a descriptive study. Lancet Infect Dis. 2013;13:752–61. http://dx.doi.org/10.1016/S1473-3099(13)70204-4
9. Reynolds DL, Garay JR, Deamond SL, Moran MK, Gold W, Styra R. Understanding, compliance and psychological impact of the SARS quarantine experience. Epidemiol Infect. 2008;136:997–1007. http://dx.doi.org/10.1017/S0950268807009156

Address for correspondence: Hae-Sung Nam, Department of Preventive Medicine and Public Health, Chungnam National University School of Medicine, 266 Munhwa-ro, Jung-gu, Daejeon, 301-747, South Korea; email: hsnam88@gmail.com

EID Podcast: Unraveling the Mysteries of Middle East Respiratory Syndrome Coronavirus

Middle East respiratory syndrome coronavirus (MERS-CoV) is a novel CoV known to cause severe acute respiratory illness in humans; approximately 40% of confirmed cases have been fatal. Human-to-human transmission and multiple outbreaks of respiratory illness have been attributed to MERS-CoV, and severe respiratory illness caused by this virus continues to be identified. As of February 23, 2014, the World Health Organization has reported 182 laboratory-confirmed cases of MERS-CoV infection, including 79 deaths, indicating an ongoing risk for transmission to humans in the Arabian Peninsula.

Visit our website to listen:
https://www2c.cdc.gov/podcasts/player.asp?f=8631627

EMERGING INFECTIOUS DISEASES

Genomic Analysis of *Salmonella enterica* Serovar Typhimurium DT160 Associated with a 14-Year Outbreak, New Zealand, 1998–2012

Samuel J. Bloomfield, Jackie Benschop, Patrick J. Biggs,[1] Jonathan C. Marshall,[1] David T.S. Hayman,[1] Philip E. Carter,[1] Anne C. Midwinter, Alison E. Mather, Nigel P. French

During 1998–2012, an extended outbreak of *Salmonella enterica* serovar Typhimurium definitive type 160 (DT160) affected >3,000 humans and killed wild birds in New Zealand. However, the relationship between DT160 within these 2 host groups and the origin of the outbreak are unknown. Whole-genome sequencing was used to compare 109 *Salmonella* Typhimurium DT160 isolates from sources throughout New Zealand. We provide evidence that DT160 was introduced into New Zealand around 1997 and rapidly propagated throughout the country, becoming more genetically diverse over time. The genetic heterogeneity was evenly distributed across multiple predicted functional protein groups, and we found no evidence of host group differentiation between isolates collected from human, poultry, bovid, and wild bird sources, indicating ongoing transmission between these host groups. Our findings demonstrate how a comparative genomic approach can be used to gain insight into outbreaks, disease transmission, and the evolution of a multihost pathogen after a probable point-source introduction.

Nontyphoidal serovars of *Salmonella enterica* subsp. *enterica*, which cause salmonellosis, are responsible for an estimated 93.8 million illnesses and 155,000 deaths among humans worldwide each year (*1*). In New Zealand, these serovars are the second largest cause of bacterial gastroenteritis, annually causing 21 cases per 100,000 population (*2*). Nontyphoidal *Salmonella* spp. strains vary in host specificity and are usually transmitted to humans via direct contact or consumption of foods originating from animals (*3*,*4*). In New Zealand, salmonellosis incidence among humans peaks in the warm summer months, probably in association with increased multiplication of *Salmonella* in animal and food sources and with increased participation in higher risk outdoor activities (e.g., activities that increase contact with wild-life) (*5*). Climate change is expected to increase summer temperatures, potentially increasing salmonellosis incidence in New Zealand (*6*).

During 1998–2012, an extended outbreak of *Salmonella* Typhimurium definitive type 160 (DT160) occurred in New Zealand (*7*). During the outbreak, DT160 was the predominant *Salmonella* spp. subtype isolated from human salmonellosis patients and sick wild birds. DT160 was also isolated from other animals and the environment, but it was not the main *Salmonella* subtype isolated from these sources (*8*–*10*). DT160 has been isolated from animals and environments worldwide (*11*,*12*) and is usually associated with moribund birds (*13*,*14*). However, before the 1998–2012 outbreak, DT160 had not been reported in New Zealand. In 2009, an outbreak of DT160 involving humans and wild birds was reported in Tasmania, Australia (*15*); however, as with the outbreak in New Zealand, the relationship between DT160 within the bird and human host groups of Tasmania was unknown. We used genomic epidemiologic approaches to characterize the origin, evolution, and transmission of *Salmonella* Typhimurium DT160 in New Zealand.

Methods

Whole-Genome Sequencing

After stratifying the *Salmonella* strain collection at the Enteric Reference Laboratory of the Institute of Environmental Science and Research Ltd. (Wallaceville, New Zealand) by age and host, we randomly selected 35 human, 25 wild bird, 25 poultry, and 24 bovine DT160 isolates from 1998–2012. We extracted genomic DNA from these isolates

Author affiliations: Massey University, Palmerston North, New Zealand (S.J. Bloomfield, J. Benschop, P.J. Biggs, J.C. Marshall, D.T.S. Hayman, A.C. Midwinter, N.P. French); Institute of Environmental Science and Research, Wellington, New Zealand (P.E. Carter); University of Cambridge, Cambridge, UK (A.E. Mather)

DOI: https://dx.doi.org/10.3201/eid2306.161934

[1]These authors contributed equally to this article.

using a QIAamp DNA Mini Kit (QIAGEN, Hilden, Germany) (*16*). New Zealand Genomics Limited (NZGL) at Massey Genome Service, Massey University, Palmerston North, New Zealand, performed whole-genome sequencing of the extracts. NZGL also prepared a library for each isolate by using a TruSeq DNA PCR-Free Library Preparation Kit (Illumina, Scorsby, Victoria, Australia) and sequenced the libraries by using MiSeq (Illumina, San Diego, CA, USA) as 2 × 250 bp paired-end runs (≈120–150 genome coverage). After sequencing and standard barcode demultiplexing, NZGL used FASTQ-MCF (*17*) to perform quality control procedures to remove any PhiX control library reads and adaptor sequences. The raw reads for the 109 DT160 isolates are available in the European Nucleotide Archive (http://www.ebi.ac.uk/ena; accession no. PRJEB18077).

Genomic Assembly

Each isolate's genome was assembled de novo. We used an in-house Perl script to trim reads at an error probability of 0.01 and generate random subsets of paired reads from 750,000 to 1.2 million paired reads in increments of 150,000, varying the average coverage. We assembled each of the random sets by using the de novo assembler Velvet version 1.1 (*18*) at a variety of k-mers (from 55 to 245) in increments of 10. De novo assembly resulted in multiple genome assemblies for each isolate. We ranked the metrics for each of 4 parameters (longest genome length, fewest number of contigs, largest N_{50} value, and longest contig length) in numeric order and calculated an overall equally summed ranking score for each assembly. We used the assemblies with the lowest total rank for further analyses. We used QUAST (*19*), a quality assessment tool for evaluating and comparing genome assemblies, to analyze the DT160 de novo assemblies and determine their GC content (i.e., the percentage of a DNA sequence made up of guanine and cytosine bases).

Single-Nucleotide Polymorphism Identification

We used Snippy version 2.6 (https://github.com/tseemann/snippy) and kSNP version 3.0 (*20*) to identify core single-nucleotide polymorphisms (SNPs). Snippy is a pipeline that uses the Burrows-Wheelers Aligner (*21*) and SAMtools version 1.3.1 (*22*) to align reads from different isolates to a sequence and uses FreeBayes (*23*) to identify variants among the alignments. We used kSNP to analyze de novo assembled genomes, along with the reference genome, *S. enterica* serovar Typhimurium 14028S (GenBank accession no. NC_016856). We used an in-house Python script to determine the read coverage of all the SNPs identified via kSNP. We used Snippy to align reads from each isolate to the reference genome (GenBank accession no. NC_016856) before identifying SNPs. SNPs were accepted if they had a >10 read depth and a >90% consensus for each isolate. The position of the SNP on the reference genome was used to determine if both methods identified the SNP or if they were unique to the method (online Technical Appendix, https://wwwnc.cdc.gov/EID/article/23/6/16-1934-Techapp1.pdf). This method identified 793 core SNPs shared by the 109 New Zealand DT160 isolates.

Global DT160 Strains

Using the genomic assembly and SNP identification methods as we described, we compared 2 DT160 strains from the United Kingdom with the 109 DT160 isolates from New Zealand: 1,521 core SNPs were identified. We downloaded the UK strains, which were previously published by Petrovska et al. (*24*), from the European Nucleotide Archive (accession nos. ERS015626 and ERS015627).

Phylogenetic Inference and Distances

We used RAxML version 8.2.4 (*25*) to construct a maximum-likelihood tree based on the 793 core SNPs of the 109 DT160 isolates; we used EvolView version 2 (*26*) to visualize and edit the tree. We used SplitsTree (*27*) to form a NeighborNet tree of the 109 New Zealand DT160 isolates based on the 793 core SNPs that they share and to compare the New Zealand and UK isolates based on the 1,521 core SNPs that they share. We used MEGA6 (*28*) and the maximum composite likelihood model (29) to predict the pairwise distance between the 109 New Zealand DT160 isolates, based on the 793 core SNPs they share, and the 109 New Zealand and 2 UK isolates, based on the 1,521 core SNPs that they share.

Phylogenetic Analysis

We used an in-house Perl script to split the 793 codons into 5 groups: those associated with the first, second, or third codon; those contained in overlapping coding regions; and those found in intergenic regions. We also used the in-house Perl script to determine whether the SNPs were synonymous or nonsynonymous. We then exported the partitioned SNPs into BEAUti to create an XML file for BEAST 1.8.3 (*30*).

To allow for variation in base substitution among codon positions, we used separate Hasegawa Kishino Yano models to estimate the 5 SNP groups (*31*); to allow for and estimate changes in the effective population size, we used the Gaussian Markov random field Bayesian skyride model (*32*); to allow for variation in mutation rates among lineages, we used an uncorrelated relaxed molecular clock (*33*), which was calibrated by the tip dates. We ran the XML file in BEAST for 40 million steps a total of 3 times with different starting seeds before using LogCombiner (http://beast.bio.ed.ac.uk/LogCombiner) to combine the runs with a 10% burn-in. To visualize the results and the relative change in effective population size, we used Tracer version 1.6 (*34*).

To determine the mutation rate for the DT160 genome, we multiplied the mutation rate estimated by BEAST by the number of analyzed core SNPs (793 bp) and then divided the product by the mean genome size of the analyzed isolates (4,884,485 bp). We used the discrete phylogeographic model (*35*) to predict ancestral migrations between host groups over the course of the outbreak.

Protein Coding Gene Analysis

We used Prokka (*36*) to annotate de novo assembled genomes, and we used Roary (*37*) to cluster proteins and identify those that were found only in a subset of isolates and those that differed in length between the isolates. We used ClustalW version 2.1 (*38*) to align amino acid sequences, and we used an in-house Perl script to determine if these alignments contained mismatches. The nucleotide sequence of all proteins that differed were extracted from the assembled genomes, along with 500-bp flanks on either side of the sequence, by using an in-house Perl script. We could not obtain 500-bp flanks for some genes because they were located at the end of contigs. For those genes, the flank was cut short, but their length was annotated. We extracted flanks to help with read alignment. This extraction left a pool of nucleotide sequences from each isolate, for every protein that potentially differed in sequence. For each protein, we extracted all nucleotide variants from the pool by using an in-house Perl script. We used SRST2 version 2, a read mapping–based tool (*39*), to align reads from each isolate to the sequence variants, and we used SAMtools version 1.3.1 (*22*) to form a consensus sequence from the aligned reads. We set the consensus cutoff at a read depth of ≥8 and a consensus of ≥80%. The flanks were removed from the consensus sequences, and the sequence variants were translated into amino acid sequences by using an in-house Perl script. We identified protein differences by comparing the amino acid sequences from each isolate and combined the differences with the nonsynonymous SNPs identified by SNP analysis. The position of nonsynonymous SNPs within proteins was used to prevent repeats.

We used the Clusters of Orthologous Groups of proteins (COGs) database (*40*) to predict protein functions. For each functional group, we calculated the proportion of proteins that differed in sequence, and we used a Fisher exact test, computed via Monte Carlo Markov Chains of $\approx 10^9$ iterations, to determine if there were any differences between these proportions.

We used an in-house Perl script to form a presence–absence matrix of all the protein differences. We used PrimerE version 6 (*41*) to predict the Euclidian distance between the isolates based on the presence–absence matrix. The centroid is the arithmetic mean for a group of data points in an n-dimensional space. To assess differences in centroids among isolates collected from different sources or time periods, we applied PERMANOVA (http://www.primer-e.com/permanova.htm). To assess differences in dispersions between different groups, we computed dispersions (z-values) by using PermDisp (*42*) and then modeled them using a regression model with date of collection and source as the explanatory variables.

Scripts

The in-house scripts used for genomic analyses in this study were specifically designed for this dataset. The scripts are available from GitHub (https://github.com/samuelbloomfield/Scripts-for-genomic-analyses).

Results

During the 1998–2012 human outbreak of *Salmonella* Typhimurium DT160 in New Zealand, disease incidence displayed a typical epidemic curve: prevalence increased from 1999 to 2000, before peaking at 791 cases in 2001, and then slowly decreased from 2002 through 2012 (Figure 1). At the same time, numerous isolates were reported from nonhuman hosts (wild birds, poultry, bovids), and disease incidence among these host groups displayed epidemic curves similar to those for humans (online Technical Appendix).

Genomic DT160 Comparison

The genomes we assembled were 4.8–4.9 Mb in length and had a GC content of 52.11%–52.16% (reference value for *S. enterica* 50%–53%) (*43*). We identified 793 core SNPs shared by the 109 DT160 isolates from New Zealand.

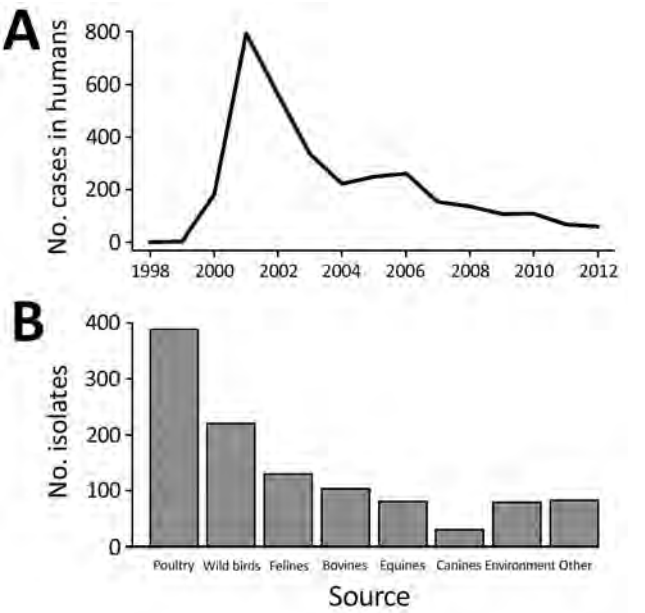

Figure 1. Number of *Salmonella enterica* serovar Typhimurium DT160 cases and isolates reported during an outbreak in New Zealand, 1998–2012. A) Cases in humans (*8*,*9*). B) Isolates from nonhuman sources (*8*,*10*).

DT160 Introduction Date

Ancestral date reconstruction analysis predicted that the 109 New Zealand DT160 isolates shared a date of common ancestor in approximately August 1997 (95% highest posterior density interval June 1996–August 1998). Comparative analysis indicated that the 2 DT160 isolates collected from the United Kingdom were genetically distinct from the 109 New Zealand DT160 isolates (online Technical Appendix). The average pairwise SNP distance between the 2 UK DT160 isolates and the New Zealand isolates was 0.0287, compared with an average pairwise distance of 0.0151 between New Zealand isolates.

In New Zealand, DT160 was first reported in Christchurch in 1998 from a human with salmonellosis (*44*) (an isolate from this case was included as part of this study). The New Zealand DT160 isolates we analyzed were estimated to share a common ancestor 0–2 years before this case and were distinct from the UK isolates analyzed, suggesting that DT160 was probably introduced into New Zealand as a single incursion within this time period. However, worldwide comparative studies are required to track DT160 migration and validate this hypothesis.

DT160 Evolution

Our phylogenetic analysis also predicted that the 109 DT160 isolates mutated at a rate of 3.3–4.3 × 10^{-7} substitutions/site/year (95% highest posterior density interval) and that the effective population size for DT160 increased from 1998 to 2003 (Figure 2). Over the course of the outbreak, DT160 also increased in genetic diversity (Figure 3).

The mutation rate estimated for the DT160 outbreak is similar to rates reported by Mather et al. (*45*) for an outbreak of *Salmonella* Typhimurium DT104 in Scotland during 1990–2012 and by Okoro et al. (*46*) for invasive *Salmonella* Typhimurium strains in sub-Saharan Africa. The similarity of these mutation rates suggests consistency between outbreaks caused by *S. enterica* serovar Typhimurium and has implications for modeling the evolution of future outbreaks caused by this serovar.

In bacteriology, the effective population size is the number of bacteria that contribute to the next generation. The increase in the DT160 effective population size during 1998–2003 coincided with an increased prevalence of DT160 among human and nonhuman hosts during this time. However, the subsequent levelling-off of the effective DT160 population size is probably an artifact because we calculated the effective population size from the timing of coalescent events for randomly sampled bacteria (*32*), and as the outbreak proceeded, fewer coalescent points were available for estimation.

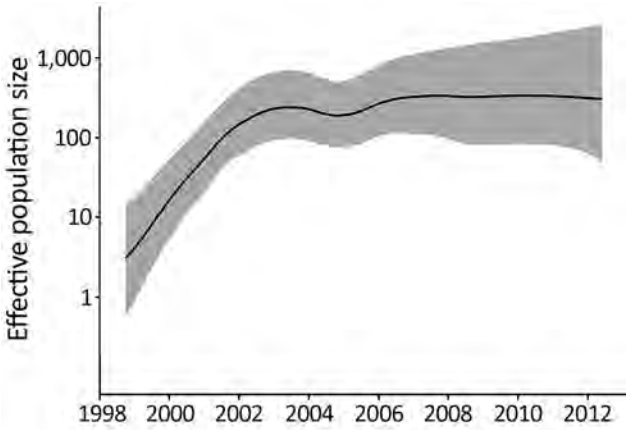

Figure 2. Relative effective population size (log scale) of *Salmonella enterica* serovar Typhimurium DT160 during an outbreak in New Zealand, 1998–2012. Population parameters were estimated using the Gaussian Markov random field Bayesian skyride model. The black line represents the median effective population size estimate; gray shading represents the 95% highest posterior density interval.

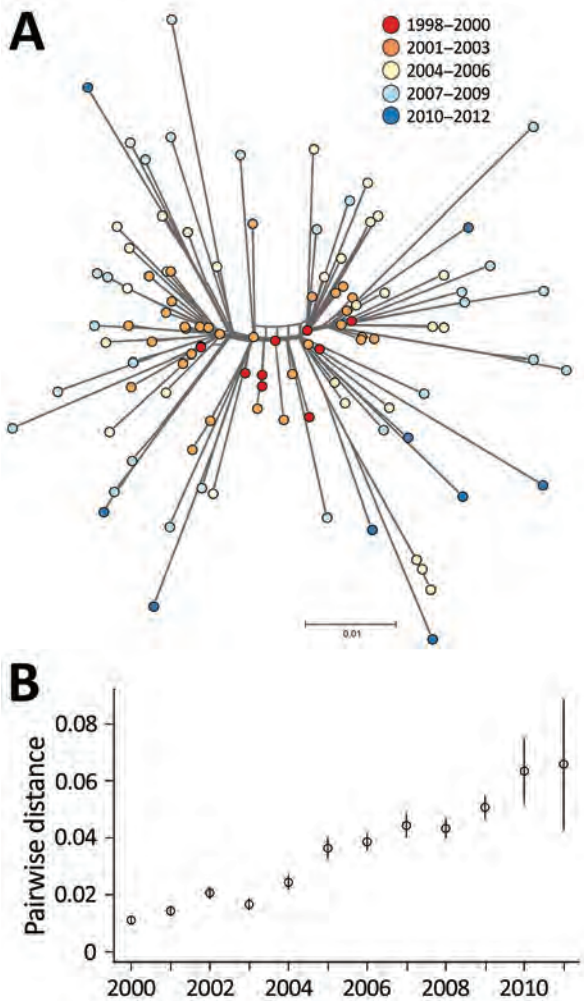

Figure 3. A) NeighborNet tree of 109 *Salmonella enterica* serovar Typhimurium DT160 isolates collected during an outbreak in New Zealand, 1998–2012. The tree was based on 793 core single-nucleotide polymorphisms. Colors indicate date of isolate collection. The scale bar represents the number of nucleotide substitutions per site. B) Scatterplot of the mean pairwise distance of 106 DT160 isolates from 2000–2011. Error bars represent 95% CIs.

Overall, our phylogenetic analyses suggest that the DT160 population increased dramatically in the first few years following introduction. As the DT160 population increased, it acquired multiple SNPs, resulting in a progressive increase in diversity over time.

DT160 Sources

PFGE (pulsed-field gel electrophoresis) was previously used to compare New Zealand DT160 isolates from humans, poultry, and wild birds (S. Omar, master's thesis, 2011; http://mro.massey.ac.nz/handle/10179/2681?show=full); however, PFGE could not distinguish DT160 from the separate sources. In our study, we were able to use whole-genome sequencing to distinguish DT160 at the isolate level. However, we did not find any distinct DT160 clades associated with any one source (Figure 4).

Identifying the source of a salmonellosis outbreak can be difficult because multiple potential sources must

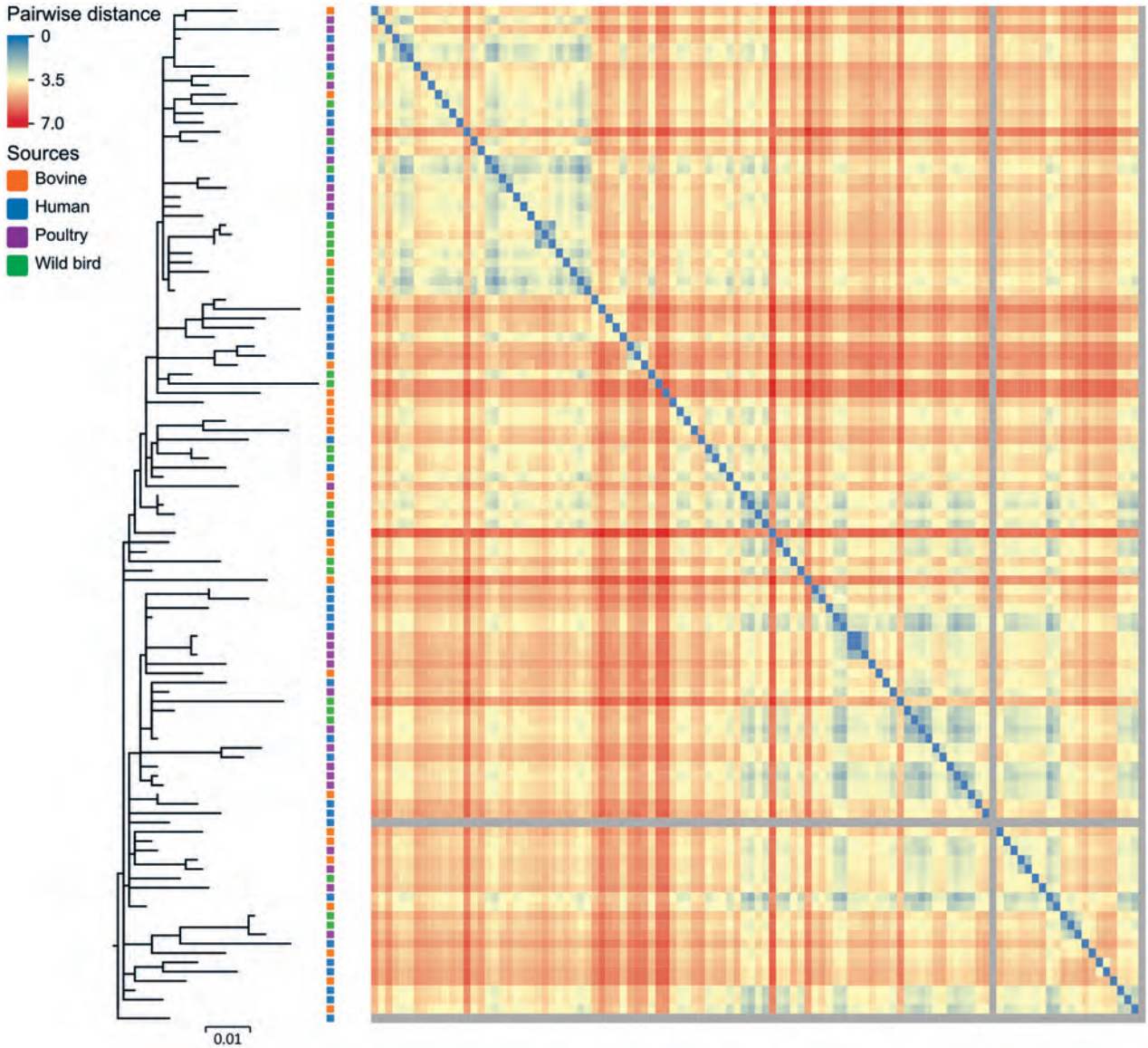

Figure 4. Maximum-likelihood tree of 109 *Salmonella enterica* serovar Typhimurium DT160 isolates collected during an outbreak in New Zealand, 1998–2012. The tree was based on 793 core single-nucleotide polymorphisms. Colored squares to the right of the branches indicate the source of isolates. The scale bar represents number of nucleotide substitutions per site. The heat map represents the Euclidean pairwise distance between isolates (based on the presence of 684 protein differences). Isolates that shared a small number of protein differences contained small Euclidean distances and are closer to blue in color on the heat map; isolates that shared a large number of protein differences contained large Euclidean distances and are closer to red in color. The gray squares represent the 2 outliers missing a large number of genes. The diagonal array of blue squares represents the pairwise distance for the same isolates.

be considered (*47*). Probable sources of *Salmonella* can be identified by comparing isolates from infected humans with those from other human, nonhuman, and environmental sources (*48*). We did not find distinct DT160 clades associated with any 1 source, suggesting that after its introduction into New Zealand, DT160 was transmitted between multiple hosts, resulting in large epidemics among humans and wild birds. Our results also suggest that humans obtained DT160 from multiple sources over the course of the outbreak. This finding is consistent with that in a case-control study performed by Thornley et al. (*44*), which found that human DT160 cases were associated with multiple risk factors involving different sources: handling dead wild birds, contact with persons with diarrhea, and consumption of fast food.

Ancestral Migration between Hosts

We used the discrete phylogeographic model to predict ancestral migration of DT160 between the animal and human host groups, similar to Mather et al. (*45*). However, we were unable to detect a signal that could not be attributed to different sampling fractions in the host groups (online Technical Appendix). Therefore, an alternate method, larger sample size, or both are required to predict these ancestral migrations.

Protein and Gene Analysis

Protein annotation identified 5,096 coding DNA sequences, of which 4,983 (98%) were found in all of the isolates, 108 (2%) were found in 95%–99% of isolates, and 3 (<1%) were found in 1%–5% of the isolates. Protein coding gene analysis also identified 477 nonsynonymous SNPs, of which 27 were nonsense mutations and 96 were INDELs (insertions/deletions). The nonsense SNPs and INDELs were responsible for 123 proteins that differed in length. Overall, we identified 684 differences in 604 protein sequences among the 109 DT160 isolates. We excluded 2 isolates from protein coding gene analysis because they were missing a large number of proteins (online Technical Appendix).

By using PERMANOVA, we found that centroids based on the 684 protein differences were indistinguishable among groups of DT160 isolates collected from different sources and time periods (online Technical Appendix). PERMANOVA's inability to distinguish centroids appears to be due to the fact that DT160 isolates radiated out from a point source. The z-value is the distance from an isolate to the centroid of a group of isolates; we calculated the z-value for 107 DT160 isolates on the basis of 684 protein differences. Our regression modeling results showed that the z-value was associated with the date, but not source, of collection (Figure 5).

The 684 protein differences shared by the DT160 isolates were associated with a large number of COG functional groups. The proportion of proteins that contained sequence differences differed between functional groups ($p = 0.00002$). The proportions varied from 0.06 to 0.18, although most were between 0.09 and 0.13 (online Technical Appendix). In addition, our data were insufficient to model the effects of source or date of collection on the number of protein differences associated with each group (online Technical Appendix).

Bacteria often adapt to new environments by altering (changing or losing) genes that are not essential for colonizing that environment (*49*). Gene loss can result in an increase in bacterial fitness, as fewer genes and processes need to be maintained within the bacteria (*50*). We

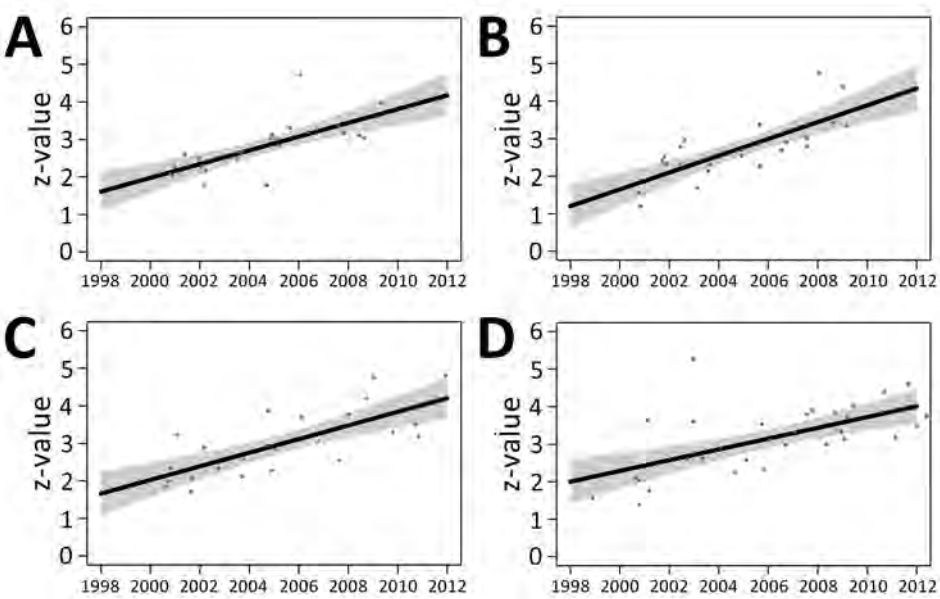

Figure 5. Scatter plots of year of collection versus z-values for 107 Salmonella enterica serovar Typhimurium DT160 isolates collected during an outbreak in New Zealand, 1998–2012. Of the 107 isolates, 25 were from poultry (A), 25 from wild birds (B), 24 from bovids (C), and 33 from humans (D). Black lines represent the regression equation; gray shading represents SE for this equation. Date of collection was significantly associated with z-values in this model ($p<2-16$). There was insufficient evidence to suggest that source was associated with z-values ($p = 0.558$), and the interaction between source and date of collection was not significant ($p = 0.458$).

identified multiple protein changes among the DT160 isolates, and these changes occurred in multiple COG functional groups as the epidemic progressed. However, we found no evidence of host group differentiation, suggesting that most of the evolution was due to random genetic drift rather than adaptive evolution.

Discussion

Using genomic analysis, we described the evolution and emergence of *Salmonella* Typhimurium DT160 within New Zealand. Our results suggest that DT160 was introduced into New Zealand on a single occasion from 1996 through 1998, before propagating throughout the country and becoming more genetically diverse over time. In addition, we found that DT160 isolates collected from human, poultry, bovine and wild bird sources were highly similar, indicating a large number of transmission episodes between these host groups.

Acknowledgments

We thank the staff at the Massey Genome Service (part of New Zealand Genomics Ltd), Massey University, Palmerston North, New Zealand, for their help and advice with the genome sequencing for this study; Tim G. Vaughan for his help with phylogenetic analyses; and the Enteric Reference Laboratory, Environmental Science and Research, Wallaceville, New Zealand for supplying *Salmonella* isolates.

This study was funded by the Allan Wilson Centre for Molecular Ecology and Evolution, Massey University; the Biotechnology and Biological Sciences Research Council (BB/M014088/1 to A.E.M); and the Royal Society of New Zealand Marsden Fund (MAU1503 to D.T.S.H.).

Mr. Bloomfield is a PhD student at Massey University, Palmerston North, New Zealand. His research interests include infectious diseases and genomics, particularly how infectious diseases are transmitted and evolve over the course of outbreaks.

References

1. Majowicz SE, Musto J, Scallan E, Angulo FJ, Kirk M, O'Brien SJ, et al.; International Collaboration on Enteric Disease 'Burden of Illness' Studies. The global burden of nontyphoidal *Salmonella* gastroenteritis. Clin Infect Dis. 2010;50:882–9. http://dx.doi.org/10.1086/650733
2. Institute of Environmental Science and Research Ltd. (ESR). Notifiable diseases. New Zealand public health observatory. 2014 [cited 2016 Feb 2]. http://www.nzpho.org.nz/NotifiableDisease.aspx
3. King N, Lake R, Campbell D. Source attribution of nontyphoid salmonellosis in New Zealand using outbreak surveillance data. J Food Prot. 2011;74:438–45. http://dx.doi.org/10.4315/0362-028X.JFP-10-323
4. Eswarappa SM, Janice J, Nagarajan AG, Balasundaram SV, Karnam G, Dixit NM, et al. Differentially evolved genes of *Salmonella* pathogenicity islands: insights into the mechanism of host specificity in *Salmonella.* PLoS One. 2008;3:e3829. http://dx.doi.org/10.1371/journal.pone.0003829
5. Lal A, Baker MG, French NP, Dufour M, Hales S. The epidemiology of human salmonellosis in New Zealand, 1997–2008. Epidemiol Infect. 2012;140:1685–94. http://dx.doi.org/10.1017/S0950268811002470
6. Lal A, Ikeda T, French N, Baker MG, Hales S. Climate variability, weather and enteric disease incidence in New Zealand: time series analysis. PLoS One. 2013;8:e83484. http://dx.doi.org/10.1371/journal.pone.0083484
7. Alley MR, Connolly JH, Fenwick SG, Mackereth GF, Leyland MJ, Rogers LE, et al. An epidemic of salmonellosis caused by *Salmonella* Typhimurium DT160 in wild birds and humans in New Zealand. N Z Vet J. 2002;50:170–6. http://dx.doi.org/10.1080/00480169.2002.36306
8. Institute of Environmental Science and Research Ltd (ESR). ESR LabLink. Quarterly surveillance summaries for New Zealand, March 2000–March 2003 [cited 2016 Nov 25]. https://surv.esr.cri.nz/PDF_surveillance/Lablink/
9. Institute of Environmental Science and Research Ltd (ESR). Public Health Surveillance; Information for New Zealand public health action. 2003–2012 human *Salmonella* isolates [cited 2016 Nov 25]. https://surv.esr.cri.nz/enteric_reference/human_salmonella.php
10. Institute of Environmental Science and Research Ltd (ESR). Public Health Surveillance; Information for New Zealand public health action. Non-human *Salmonella* isolates, 2003–2012 [cited 2016 Nov 25]. https://surv.esr.cri.nz/enteric_reference/nonhuman_salmonella.php
11. Penfold JB, Amery HC, Peet PJ. Gastroenteritis associated with wild birds in a hospital kitchen. Br Med J. 1979;2:802.
12. Tizard IR, Fish NA, Harmeson J. Free flying sparrows as carriers of salmonellosis. Can Vet J. 1979;20:143–4.
13. Lawson B, Howard T, Kirkwood JK, Macgregor SK, Perkins M, Robinson RA, et al. Epidemiology of salmonellosis in garden birds in England and Wales, 1993 to 2003. EcoHealth. 2010;7:294–306. http://dx.doi.org/10.1007/s10393-010-0349-3
14. Piccirillo A, Mazzariol S, Caliari D, Menandro ML. *Salmonella* Typhimurium phage type DT160 infection in two Moluccan cockatoos (*Cacatua moluccensis*): clinical presentation and pathology. Avian Dis. 2010;54:131–5. http://dx.doi.org/10.1637/8969-062509-Case.1
15. Grillo T, Post L. *Salmonella* Typhimurium DT160 outbreak in Tasmania. Animal Health Surveillance Quarterly Reports. 2010;14:8–8. http://www.sciquest.org.nz/node/72986
16. QIAGEN. QIAamp DNA mini and blood mini handbook. Third edition. 2012 [cited 2015 Feb 12]. https://moodle.ufsc.br/pluginfile.php/1379318/mod_resource/content/0/QIAamp_DNA_Mini_Blood.pdf
17. Aronesty E. Comparison of sequencing utility programs. The Open Bioinformatics Journal. 2013;7:1–8. http://dx.doi.org/10.2174/1875036201307010001
18 Zerbino DR, Birney E. Velvet: algorithms for de novo short read assembly using de Bruijn graphs. Genome Res. 2008;18:821–9. http://dx.doi.org/10.1101/gr.074492.107
19. Gurevich A, Saveliev V, Vyahhi N, Tesler G. QUAST: quality assessment tool for genome assemblies. Bioinformatics. 2013;29:1072–5. http://dx.doi.org/10.1093/bioinformatics/btt086
20. Gardner SN, Slezak T, Hall BG. kSNP3.0: SNP detection and phylogenetic analysis of genomes without genome alignment or reference genome. Bioinformatics. 2015;31:2877–8. http://dx.doi.org/10.1093/bioinformatics/btv271
21. Li H, Durbin R. Fast and accurate short read alignment with Burrows-Wheeler transform. Bioinformatics. 2009;25:1754–60. http://dx.doi.org/10.1093/bioinformatics/btp324
22. Li H. A statistical framework for SNP calling, mutation discovery, association mapping and population genetical parameter estimation from sequencing data. Bioinformatics. 2011;27:2987–93. http://dx.doi.org/10.1093/bioinformatics/btr509

23. Garrison E, Marth G. Haplotype-based variant detection from short-read sequencing. 2012 [cited 2017 Feb 2]. https://arxiv.org/abs/1207.3907
24. Petrovska L, Mather AE, AbuOun M, Branchu P, Harris SR, Connor T, et al. Microevolution of monophasic *Salmonella* Typhimurium during epidemic, United Kingdom, 2005–2010. Emerg Infect Dis. 2016;22:617–24. http://dx.doi.org/10.3201/eid2204.150531
25. Stamatakis A. RAxML version 8: a tool for phylogenetic analysis and post-analysis of large phylogenies. Bioinformatics. 2014;30:1312–3. http://dx.doi.org/10.1093/bioinformatics/btu033
26. He Z, Zhang H, Gao S, Lercher MJ, Chen WH, Hu S. Evolview v2: an online visualization and management tool for customized and annotated phylogenetic trees. Nucleic Acids Res. 2016;44: W236-41. http://dx.doi.org/10.1093/nar/gkw370
27. Huson DH, Bryant D. Application of phylogenetic networks in evolutionary studies. Mol Biol Evol. 2006;23:254–67. http://dx.doi.org/10.1093/molbev/msj030
28. Tamura K, Stecher G, Peterson D, Filipski A, Kumar S. MEGA6: Molecular Evolutionary Genetics Analysis version 6.0. Mol Biol Evol. 2013;30:2725–9. http://dx.doi.org/10.1093/molbev/mst197
29. Tamura K, Nei M, Kumar S. Prospects for inferring very large phylogenies by using the neighbor-joining method. Proc Natl Acad Sci U S A. 2004;101:11030–5. http://dx.doi.org/10.1073/pnas.0404206101
30. Drummond AJ, Suchard MA, Xie D, Rambaut A. Bayesian phylogenetics with BEAUti and the BEAST 1.7. Mol Biol Evol. 2012;29:1969–73. http://dx.doi.org/10.1093/molbev/mss075
31. Hasegawa M, Kishino H, Yano T. Dating of the human–ape splitting by a molecular clock of mitochondrial DNA. J Mol Evol. 1985;22:160–74. http://dx.doi.org/10.1007/BF02101694
32. Minin VN, Bloomquist EW, Suchard MA. Smooth skyride through a rough skyline: Bayesian coalescent-based inference of population dynamics. Mol Biol Evol. 2008;25:1459–71. http://dx.doi.org/10.1093/molbev/msn090
33. Drummond AJ, Ho SYW, Phillips MJ, Rambaut A. Relaxed phylogenetics and dating with confidence. PLoS Biol. 2006;4:e88. http://dx.doi.org/10.1371/journal.pbio.0040088
34. Rambaut A, Suchard MA, Xie D, Drummond AJ. Beast. Tracer 1.6 2014 [cited 2016 Sep 27]. http://beast.bio.ed.ac.uk/Tracer
35. Lemey P, Rambaut A, Drummond AJ, Suchard MA. Bayesian phylogeography finds its roots. PLOS Comput Biol. 2009; 5:e1000520. http://dx.doi.org/10.1371/journal.pcbi.1000520
36. Seemann T. Prokka: rapid prokaryotic genome annotation. Bioinformatics. 2014;30:2068–9. http://dx.doi.org/10.1093/bioinformatics/btu153
37. Page AJ, Cummins CA, Hunt M, Wong VK, Reuter S, Holden MTG, et al. Roary: rapid large-scale prokaryote pan genome analysis. Bioinformatics. 2015;31:3691–3. http://dx.doi.org/10.1093/bioinformatics/btv421
38. Thompson JD, Higgins DG, Gibson TJ. CLUSTAL W: improving the sensitivity of progressive multiple sequence alignment through sequence weighting, position-specific gap penalties and weight matrix choice. Nucleic Acids Res. 1994;22:4673–80. http://dx.doi.org/10.1093/nar/22.22.4673
39. Inouye M, Dashnow H, Raven LA, Schultz MB, Pope BJ, Tomita T, et al. SRST2: rapid genomic surveillance for public health and hospital microbiology labs. Genome Med. 2014;6:90. http://dx.doi.org/10.1186/s13073-014-0090-6
40. Tatusov RL, Galperin MY, Natale DA, Koonin EV. The COG database: a tool for genome-scale analysis of protein functions and evolution. Nucleic Acids Res. 2000;28:33–6. http://dx.doi.org/10.1093/nar/28.1.33
41. Clark KR, Gorle RN. PRIMER v6: user manual/tutorial. Plymouth (UK): PRIMER-E; 2006. p. 296.
42. Anderson MJ. Distance-based tests for homogeneity of multivariate dispersions. Biometrics. 2006;62:245–53. http://dx.doi.org/10.1111/j.1541-0420.2005.00440.x
43. Popoff MY, Le Minor LE. Genus XXXIII. *Salmonella*. In: Brenner DJ, Staley JT, editors. Bergey's manual of systematic bacteriology. New York: Springer; 2005. p. 764–99.
44. Thornley CN, Simmons GC, Callaghan ML, Nicol CM, Baker MG, Gilmore KS, et al. First incursion of *Salmonella enterica* serotype Typhimurium DT160 into New Zealand. Emerg Infect Dis. 2003;9:493–5. http://dx.doi.org/10.3201/eid0904.020439
45. Mather AE, Reid SWJ, Maskell DJ, Parkhill J, Fookes MC, Harris SR, et al. Distinguishable epidemics of multidrug-resistant *Salmonella* Typhimurium DT104 in different hosts. Science. 2013;341:1514–7. http://dx.doi.org/10.1126/science.1240578
46. Okoro CK, Kingsley RA, Connor TR, Harris SR, Parry CM, Al-Mashhadani MN, et al. Intracontinental spread of human invasive *Salmonella* Typhimurium pathovariants in sub-Saharan Africa. Nat Genet. 2012;44:1215–21. http://dx.doi.org/10.1038/ng.2423
47. Gieraltowski L, Julian E, Pringle J, Macdonald K, Quilliam D, Marsden-Haug N, et al. Nationwide outbreak of *Salmonella* Montevideo infections associated with contaminated imported black and red pepper: warehouse membership cards provide critical clues to identify the source. Epidemiol Infect. 2013;141:1244–52. http://dx.doi.org/10.1017/S0950268812001859
48. Byrne L, Fisher I, Peters T, Mather A, Thomson N, Rosner B, et al.; International Outbreak Control Team. A multi-country outbreak of *Salmonella* Newport gastroenteritis in Europe associated with watermelon from Brazil, confirmed by whole genome sequencing: October 2011 to January 2012. Euro Surveill. 2014;19: 20866. http://dx.doi.org/10.2807/1560-7917.ES2014.19.31.20866
49. Hottes AK, Freddolino PL, Khare A, Donnell ZN, Liu JC, Tavazoie S. Bacterial adaptation through loss of function. PLoS Genet. 2013;9:e1003617. http://dx.doi.org/10.1371/journal.pgen.1003617
50. Koskiniemi S, Sun S, Berg OG, Andersson DI. Selection-driven gene loss in bacteria. PLoS Genet. 2012;8:e1002787. http://dx.doi.org/10.1371/journal.pgen.1002787

Address for correspondence: Samuel J. Bloomfield, Massey University, Palmerston North, New Zealand; email: s.bloomfield@massey.ac.nz

Stockpiling Ventilators for Influenza Pandemics

Hsin-Chan Huang,[1] Ozgur M. Araz, David P. Morton, Gregory P. Johnson, Paul Damien, Bruce Clements, Lauren Ancel Meyers

In preparing for influenza pandemics, public health agencies stockpile critical medical resources. Determining appropriate quantities and locations for such resources can be challenging, given the considerable uncertainty in the timing and severity of future pandemics. We introduce a method for optimizing stockpiles of mechanical ventilators, which are critical for treating hospitalized influenza patients in respiratory failure. As a case study, we consider the US state of Texas during mild, moderate, and severe pandemics. Optimal allocations prioritize local over central storage, even though the latter can be deployed adaptively, on the basis of real-time needs. This prioritization stems from high geographic correlations and the slightly lower treatment success assumed for centrally stockpiled ventilators. We developed our model and analysis in collaboration with academic researchers and a state public health agency and incorporated it into a Web-based decision-support tool for pandemic preparedness and response.

Diligent preparation and effective countermeasures are critical to mitigating future influenza pandemics. The 1918 influenza pandemic, the most severe in recent history, resulted in ≈50 million deaths globally, of which nearly 675,000 occurred in the United States (*1*). The 1957 and 2009 pandemics were less severe, causing ≈70,000 and 9,000–18,000 US deaths, respectively (*1*). The US Department of Health and Human Services (HHS) estimated (*2*) that 865,000 US residents would be hospitalized during a moderate pandemic (as in 1957 and 1968) and 9.9 million during a severe pandemic (as in 1918).

When severe influenza outbreaks cause high rates of hospitalization, a surge of medical resources is required, including critical care supplies, antiviral medications, and personal protection equipment. Given uncertainty in the timing and severity of the next pandemic, as well as the time required to manufacture medical countermeasures, stockpiling is central to influenza preparedness (*3*). However, difficulty in forecasting and limited public health budgets often constrain decisions about sizes, locations, and deployment of such stockpiles.

Mechanical ventilators are essential for treating influenza patients in severe acute respiratory failure. Substantial concern exists that intensive care units (ICUs) might have insufficient resources to treat all persons requiring ventilator support. Prior studies argue that current capacities are insufficient to handle even moderately severe pandemics and that sentinel reporting and model-based decision-making are critical for managing limited resources (*4*–*6*). For this reason, the United States has stockpiled mechanical ventilators in strategically located warehouses for use in public health emergencies, such as an influenza pandemic. The Centers for Disease Control and Prevention (CDC) manages this Strategic National Stockpile (SNS) and has plans for rapid deployment to states during critical events (*7*).

However, SNS ventilators might not suffice to meet demand during a severe public health emergency. In 2002, the SNS included ≈4,400 ventilators (*8*,*9*), and 4,500 SNS ventilators were added during 2009 and 2010. The American Association for Respiratory Care suggested the SNS inventory should increase to at least 11,000–16,000 ventilators in preparation for a severe influenza pandemic (*10*). The American Association for Respiratory Care and CDC (*11*) provide training on 3 types of SNS ventilators—LP10 (Covidien, Boulder, CO, USA); LTV1200 (CareFusion, Yorba Linda, CA, USA); and Uni-vent Eagle 754 (Impact Instrumentation, Inc., West Caldwell, NJ, USA)—to ensure proper use nationwide. In addition to the nationally held SNS, some US states maintain their own stockpiles.

Successful deployment of central ventilator stockpiles, whether federal or state, requires rapid distribution to healthcare facilities with patients in need, along with adequate bed space, requisite supplies, and trained personnel

Author affiliations: The University of Texas at Austin, Austin, Texas, USA (H.-C. Huang, G.P. Johnson, P. Damien, L.A. Meyers); University of Nebraska, Lincoln, Nebraska, USA (O.M. Araz); University of Nebraska Medical Center, Omaha, Nebraska, USA (O.M. Araz); Northwestern University, Evanston, Illinois, USA (D.P. Morton); Department of State Health Services, Austin (B. Clements); Santa Fe Institute, Santa Fe, New Mexico, USA (L.A. Meyers)

DOI: http://dx.doi.org/10.3201/eid2306.161417

[1]Current affiliation: Precima, LoyaltyOne US, Inc., Chicago, IL, USA.

(*12–14*). Robust methods for sizing and locating ventilator stockpiles have not yet been developed (*15*). Wilgis (*16*) discussed the relative merits of central stockpiling of ventilators to be distributed during an emergency versus distributing ventilators to hospitals a priori. Centralized stockpiles benefit from better inventory tracking, more timely repairs, and superior allocation of a limited resource, but hospital-based supplies facilitate staff training, enable immediate use, and avoid the cost and logistical challenges of central storage and deployment.

We developed an optimization framework for allocating mechanical ventilators to central and local stockpiles to ensure adequate surge capacity during a future pandemic. This data-driven method considers the trade-off between risk and stockpiling cost, where risk is measured 2 ways: expected value of unmet demand (EUD; number of influenza patients not receiving required ventilation) and probability of unmet demand (PUD; probability at least 1 patient does not receive required ventilation). For a given set of healthcare providers in a region, we determined the optimal number of mechanical ventilators to stockpile centrally and at each provider site.

As a case study, we considered the US state of Texas under mild, moderate, and severe influenza pandemic scenarios. Based on the Texas Department of State Health Services (DSHS) response to the 2009 influenza A(H1N1) pandemic and planning efforts for future pandemics, we considered stockpiling across 9 sites: a centrally held state stockpile and local stockpiles in each of Texas' 8 health service regions (HSRs; online Technical Appendix Figure 1, https://wwwnc.cdc.gov/EID/article/23/6/16-1417-Techapp1.pdf). We implemented this model in a Web-based decision-support tool for DSHS (*17*).

Methods

Our approach had 3 stages (Figure 1). First, we estimated the weekly influenza-related hospitalizations at each site using an adaptive time-dynamic forecasting model. Second, we estimated the number of patients requiring ventilation at each site during the peak week on the basis of published estimates of the proportion of hospitalized influenza patients requiring mechanical ventilation. Finally, we allocated ventilators at minimum cost to achieve a specified level of preparedness through a mathematical optimization model. That model assumed centrally stockpiled ventilators have slightly lower treatment rates than locally held ventilators. In the Texas case study, we estimated hospitalizations under a mild scenario by fitting the forecasting model to data from the 2009 influenza A(H1N1) pandemic, and then we scaled the estimates to simulate moderate and severe pandemics. We summarize our optimization model and forecasting methods and provide details in the online Technical Appendix.

Optimization Model for Ventilator Stockpiling

Using a 2-stage model, we optimized the allocation of ventilators to a central stockpile and several local stockpiles (at healthcare facilities) to ensure that all sites had sufficient surge capacity to manage the peak of an influenza pandemic. We considered the trade-off between unmet ventilator demand (risk) and the cost of stockpiling ventilators (assuming cost is proportional to number of ventilators) and minimized cost while limiting risk to a specified threshold. We analyzed the risk–cost trade-off by solving a family of optimization models, across a range of risk thresholds.

We assumed the following: each stockpiled ventilator is both child- and adult-capable, will be used to treat at most 1 patient during peak demand, and will not be used for

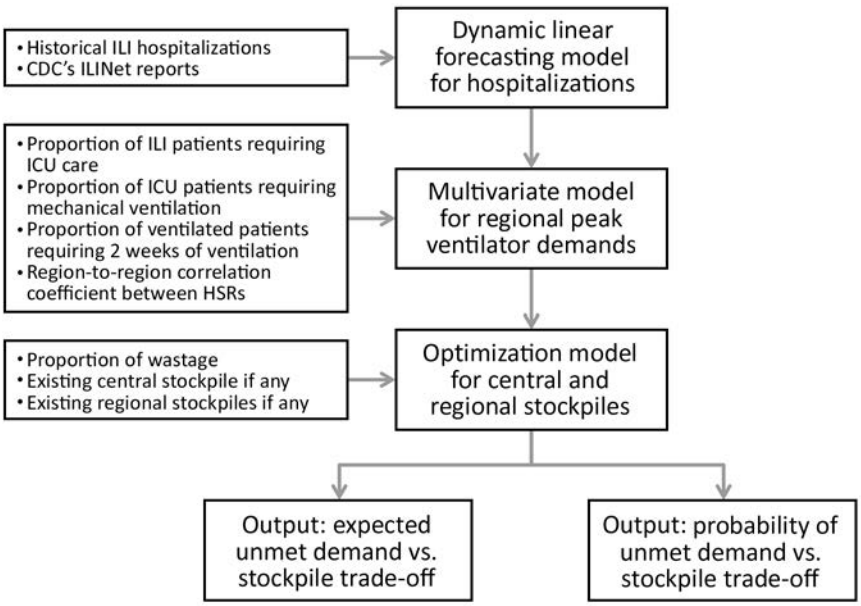

Figure 1. Overview of methods for projecting the need to stockpile ventilators for an influenza pandemic, Texas, USA. First, a forecasting model was used to estimate weekly hospitalizations at each site on the basis of historical ILI hospitalization data and CDC ILINet reports. Second, 3 additional factors, along with a spatial correlation coefficient, were used to form a probability distribution for peak-week ventilator demand at each site. Third, an optimization model was solved to determine local and central stockpile allocations and generate trade-off curves between the expected unmet demand and total stockpile and between the probability of unmet demand and total stockpile. CDC, Centers for Disease Control and Prevention; HSR, health service region; ICU, intensive care unit; ILI, influenza-like illness.

noninfluenza patients; stockpiles were established before the pandemic, and centrally held ventilators can be deployed only once to a site with excess demand (i.e., no redeployment is allowed, even though influenza peaks might be asynchronous across sites); patients requiring ventilatory support cannot move between sites; locally held ventilators are immediately and successfully administered to on-site patients requiring care, and centrally held ventilators incur wastage (i.e., a reduced fraction are successfully deployed to healthcare sites upon demand); patients at all sites have equal priority; and consumable ventilator supplies, requisite staffing, and space are in sufficient supply. The optimization model considers expected unmet demand, and we calculated the probability of unmet demand post hoc, as a secondary risk measure.

Texas Case Study

We assumed that ventilators can be stockpiled centrally by the Texas DSHS or locally by hospitals in Texas' 8 HSRs (online Technical Appendix Figure 1). We further assumed that local stockpiles within an HSR are available throughout the HSR by movement of either ventilators or patients among healthcare facilities; that is, any patient within an HSR requiring ventilatory support has access to available ventilators within that HSR. To model peak ventilator demand across Texas' 8 HSRs under different pandemic scenarios, we 1) estimated the region-to-region (HSR-to-HSR) correlation in peak-week ventilator demand on the basis of 2003–2008 seasonal influenza hospitalization data and 2009 pandemic hospitalization data; 2) generated probabilistic estimates of peak-week influenza-related hospitalizations by fitting our forecasting model to a baseline (mild) pandemic scenario estimated from 2009 pandemic data; 3) used the estimates derived in steps 1 and 2 to estimate the numbers of influenza patients requiring mechanical ventilation at the pandemic peak in each HSR; and 4) generated moderate and severe pandemic scenarios by scaling the peak demand estimates of the mild scenario. We summarize the parameters we used to estimate peak ventilator demand under different pandemic scenarios (Table 1) and outline the data and methods used to estimate these parameters.

Texas Influenza Data

We obtained weekly Texas hospital discharge data for 2003–2009, filtered for International Classification of Diseases, Ninth Revision, codes 487 and 488, corresponding to influenza-like-illness (ILI), and aggregated by HSR. These data comprised all Texas hospitals except those in counties with populations <35,000, those with <100 hospital beds, and those that do not accept insurance or government reimbursement. The number of ILI-related hospital discharges during the 2009 pandemic (April–December 2009) totaled 29,459. We assessed the validity of this International Classification of Diseases, Ninth Revision–based filter for influenza through comparison with CDC (*18*) and Texas DSHS (*19*) reports.

We also analyzed data from the CDC ILINet, which tracks weekly outpatient visits related to ILI. CDC guidelines define ILI as fever of at least 100°F and cough and/or sore throat in the absence of a known cause other than influenza. A network of 2,400 sites (health departments, laboratories, vital statistics offices, healthcare providers, and emergency departments) in the 50 states reports to ILINet, and we obtained weekly reports during the 2009 H1N1 pandemic for Texas, aggregated by HSR. Finally, Texas DSHS provided data on the 3,730 ventilators stockpiled in Texas in 2009 (online Technical Appendix Table 1).

Region-to-Region Correlation in Peak Hospitalizations

For each of the 6 influenza seasons in years starting 2003–2008 and the 2009 pandemic, we calculated peak-week ILI hospitalizations requiring ventilation in each HSR. Across all 28 pairs of HSRs, the average correlation in peak ventilator demand was 0.72 ± SD 0.23 (range 0.22–0.98). One HSR, with <3% of total hospitalizations during 2009, had pairwise correlations as low as 0.22, but all other pairs of HSRs had coefficients >0.50. We found similar spatiotemporal correlations in hospitalizations when we estimated pairwise HSR-to-HSR correlations for various values of the proportion of ventilated patients requiring 2 weeks (rather than 1 week) of ventilation, and weekly numbers of ILI hospitalizations requiring ventilation, throughout the 2003–2008 influenza seasons and the 2009 pandemic. Given this consistent statewide synchrony in epidemic intensity, we made the simplifying assumption that peak hospitalizations in all HSRs were correlated at a pairwise level of 0.70.

Forecasting Model for Hospitalizations

We used a dynamic linear forecasting model (online Technical Appendix), which provides a powerful method for

Table 1. Parameters for estimating peak-week ventilator demand in mild, moderate, and severe influenza pandemics, Texas, USA*

Parameter	Mild (2009-like)	Moderate (1957- and 1968-like)	Severe (1918-like)	Source
Hospitalization scaling over mild	1	3.14	36	(*2*,*21*)
Proportion of hospitalized ILI patients requiring ICU care	0.2	0.25	0.25	(*2*,*19*,*21*,*22*,*23*)
Proportion of ICU patients requiring ventilation	0.5	0.5	0.5	(*2*,*21*,*22*)
Proportion of ventilated patients requiring 2 weeks of ventilation	0.4	0.4	0.4	(*22*)
Region-to-region correlation for peak-week demand	0.7	0.7	0.7	Estimated

*ICU, intensive care unit; ILI, influenza-like illness.

capturing system uncertainty when numerous dynamic factors influence a system (*20*). Although hospitalizations could be forecast only on the basis of historical ILI data, our approach can incorporate additional predictors, such as the most recent ILINet reports, to better represent demand uncertainty. Our forecasting method estimated weekly influenza-related hospitalizations in the 8 HSRs for 2009 pandemic–like scenarios, using CDC ILINet influenza A(H1N1)pdm09 weekly reports as a predictor, from the week ending April 4, 2009, through the week ending December 26, 2009. To account for seasonality, we assumed 5 distinct time periods (September–October, November–December, January–February, March–April, and May–August). We also considered other candidate variables, such as school calendars, humidity, and Google Flu Trends, but these did not substantially improve peak estimates.

Estimating Regional Ventilator Demand

To estimate regional ventilator peak-week demand, we integrated our weekly forecasts of influenza hospitalizations in each region, the spatial correlation in peak-week demand for ventilators, and 3 additional factors: 1) the proportion of hospitalized ILI patients requiring ICU care, 2) the proportion of ICU patients requiring ventilation, and 3) the proportion of ventilated patients requiring 2 weeks of ventilation (rather than 1). To model "spillover" demand of patients requiring 2 weeks of ventilation, we used week-to-week correlations in influenza hospitalization (online Technical Appendix Table 2).

Proportion of Hospitalized ILI Patients Requiring ICU Care

From 2009 influenza hospital discharge data, we estimated that 18% of patients required ICU care during the peak week. Texas DSHS reported that 23% of the 2,030 confirmed influenza A(H1N1)pdm09 patients requiring hospitalization in Texas during October–December 2009 required ICU care (*19*). For moderate and severe planning scenarios, the US Homeland Security Council (HSC) (*21*) uses an ICU proportion of 15% for the overall pandemic and 25.7% for the peak week. For seasonal influenza, CDC's FluSurge 2.0 (*22*,*23*) assumes that a baseline of 15% of admitted influenza patients require ICU care; HHS makes similar assumptions (*2*) (online Technical Appendix Table 3). On the basis of these data and reports, we assumed peak-week ICU proportions of 20% during a mild pandemic and 25% during moderate and severe pandemics.

Proportion of ICU Patients Requiring Ventilation

FluSurge 2.0 assumes 50% of patients with seasonal influenza admitted to the ICU require ventilation (*22*). HSC assumes 50% throughout a pandemic (*21*), and HHS uses 50.4% for a moderate scenario and 50% for a severe scenario (*2*) (online Technical Appendix Table 3). We assumed that 50% of patients in the ICU who have pandemic influenza require ventilation across all scenarios.

Proportion of Ventilated Patients Requiring 2 Weeks of Ventilation

FluSurge 2.0 (*22*) assumes that ventilatory support of ILI patients lasts 10 days. We have weekly time resolution and assumed 60% of patients receiving ventilatory support require only 1 week, and the remaining 40% require a second week.

Simulating Pandemic Scenarios

We generated a mild scenario by fitting our forecasting model to hospital discharge data for the 2009 pandemic. Because comparable data are not available from 1957 and 1968 (moderate) and 1918 (severe), we scaled the 2009 estimates to model these scenarios. HHS (*2*) and HSC (*21*) use similar pandemic scaling factors, except HSC rates for hospitalization, ICU care, and mechanical ventilation are ≈17% and 14% lower than HHS rates for moderate and severe scenarios, respectively. (See [*24*] for scaling methods for an emerging pandemic.) CDC's median estimate of hospitalizations for influenza A(H1N1)pdm09 (April 2009–April 2010) is 275,000. Combining this with the HHS scenario (online Technical Appendix Table 3), we scaled our mild pandemic hospitalization estimates by 865,000/275,000 = 3.14 and 9,900,000/275,000 = 36 to model moderate and severe scenarios, while preserving the variability, spatial correlation, and temporal correlation estimated for 2009.

Results

Under the mild pandemic scenario, recommended stockpiles ranged from 200 to 400 ventilators (Figure 2, panel A). For example, if we specify the risk tolerance to be an EUD of at most 5 patients, then the recommended stockpile is 272 ventilators, including a central stockpile of 12. The PUD for this scenario, which is computed post hoc, is 30% (Figure 2, panel B). Thus, if the public health department builds the recommended central and local stockpiles, it can expect that no more than 5 patients statewide will go without ventilation, and a 70% chance exists that no demand anywhere will be unmet. As the risk tolerance decreases from an EUD of 5, the recommended stockpile grows sharply; as the EUD increases, the stockpile decreases nearly linearly (Figure 2, panel A). Ventilators are allocated primarily to local sites rather than to the central stockpile (Figure 2, panel C).

The optimal stockpile allocations under moderate and severe pandemic scenarios are qualitatively, but not quantitatively, similar (Figure 3). With an EUD tolerance of 5 patients, the recommended stockpiles increase to 1,172 and 15,697 ventilators for moderate and severe scenarios,

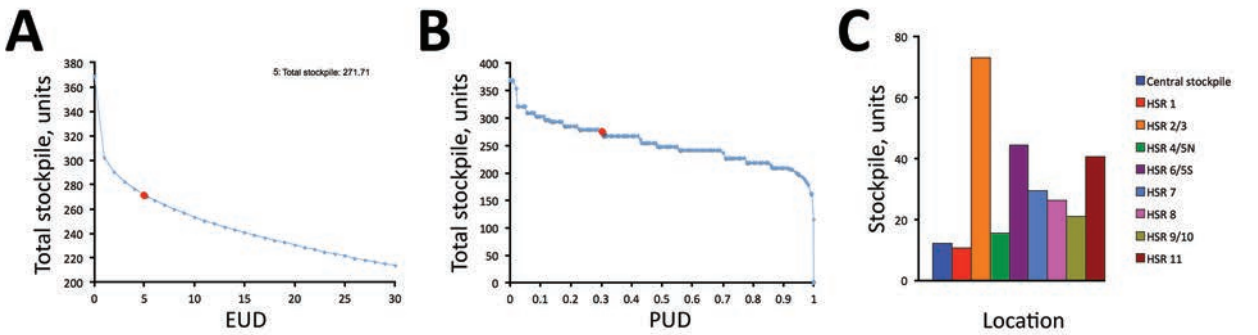

Figure 2. Optimal ventilator stockpiles for a mild pandemic scenario, Texas, USA. The total size of the optimal stockpile, summed across the central and 8 HSR stockpiles, decreases as risk tolerance increases. Risk for unmet demand for ventilators is quantified as the expected number of hospitalized influenza patients statewide not receiving necessary ventilation (EUD) (A) and the probability of at least 1 hospitalized patient in Texas not receiving necessary ventilation (PUD) (B). We optimized directly for EUD and calculated PUD post hoc. Red circles indicate EUD/PUD of 5 patients. C) Optimal allocation among central and regional sites when EUD is set to 5 patients, equivalent to a stockpile of 272 ventilators. EUD, expected unmet demand; PUD, probability of unmet demand; HSR, health service region.

respectively. These stockpiles scale roughly according to our assumptions that moderate and severe pandemics have hospitalization rates of 3.14 and 36 times higher than the mild pandemic, respectively, and that the fraction of hospitalized patients requiring ICU admission increases from 20% in the mild scenario to 25% in the other scenarios. Specifically, peak ventilator demand increases by factors of $(0.25/0.20) \times 3.14 = 3.93$ and $(0.25/0.20) \times 36 = 45$ from the mild to moderate and severe scenarios, respectively. This scaling would exactly predict how stockpiles would grow if we increased the risk tolerance by factors of 3.93 and 45. However, we fixed the EUD limit to 5 patients, so stockpile growth exceeds these scaling factors.

Sensitivity Analysis

We assessed the sensitivity of the recommended stockpiling strategies to several factors. For a fixed risk tolerance (EUD), increasing the proportions of hospitalized patients requiring ICU admission and ventilation results in comparable increases in the recommended stockpiles. However, increasing the proportion of patients requiring 2 weeks of ventilation (rather than just 1) produces a slightly more complicated effect. Because the demand at peak week will depend on both established and newly admitted patients, increasing the 2-week proportion from 0 to 1 might not exactly double the demand. Based on 2009 pandemic hospitalization data, peak-week mean demand across Texas is expected to increase by a factor of 1.42 when the 2-week proportion increases from 0.4 to 1. The recommended stockpile grows accordingly. Under the mild pandemic scenario, the stockpile grows by a factor of 1.38 for an EUD near 0 ventilators and 1.42 for an EUD close to 5 ventilators.

We also varied the wastage rate for centrally held ventilators and the region-to-region correlation in peak demand. The baseline wastage of 0.2 means that 1 in 5 ventilators distributed from the central stockpile is not used effectively. This wastage contributes to relatively small recommended central stockpiles (e.g., just 4.4% of the total stockpile under the mild scenario with an EUD of 5 ventilators). As the wastage rate decreases, the central allocation slowly increases (Table 2; online Technical Appendix Figure 2). The benefit of risk pooling through a central stockpile also grows as the region-to-region correlation in peak demand shrinks (Table 2; online Technical Appendix Figure 3).

Retrospective Analysis of 2009 Pandemic

During the 2009 pandemic, hospitals across Texas held an estimated 3,730 ventilators. When aggregated by region, the 8 HSRs had stockpiles ranging from 151 to 1,233 ventilators (online Technical Appendix Table 1). Under mild and moderate pandemic scenarios, we projected expected statewide demands for 230 and 903 ventilators, respectively, with each HSR holding a stockpile at least 6 SD above the forecasted mean demand. Given this ample regional surge capacity, there would have been no need for central stockpiling. Under the severe scenario, however, the projected statewide demand is 10,333 ventilators, far exceeding 2009 stockpiles.

Discussion

Central stockpiles can save costs but are advisable only when spatial correlation in peak demand is sufficiently low and stockpile deployment is sufficiently reliable. Data from Texas suggest that influenza peaks strongly correlate across regions. Such synchrony undercuts the risk-pooling benefits of central stockpiles. Furthermore, successful deployment requires not only central maintenance and physical transportation of ventilators to patients in need, but also healthcare facilities and clinicians trained to administer and troubleshoot available ventilator models, which

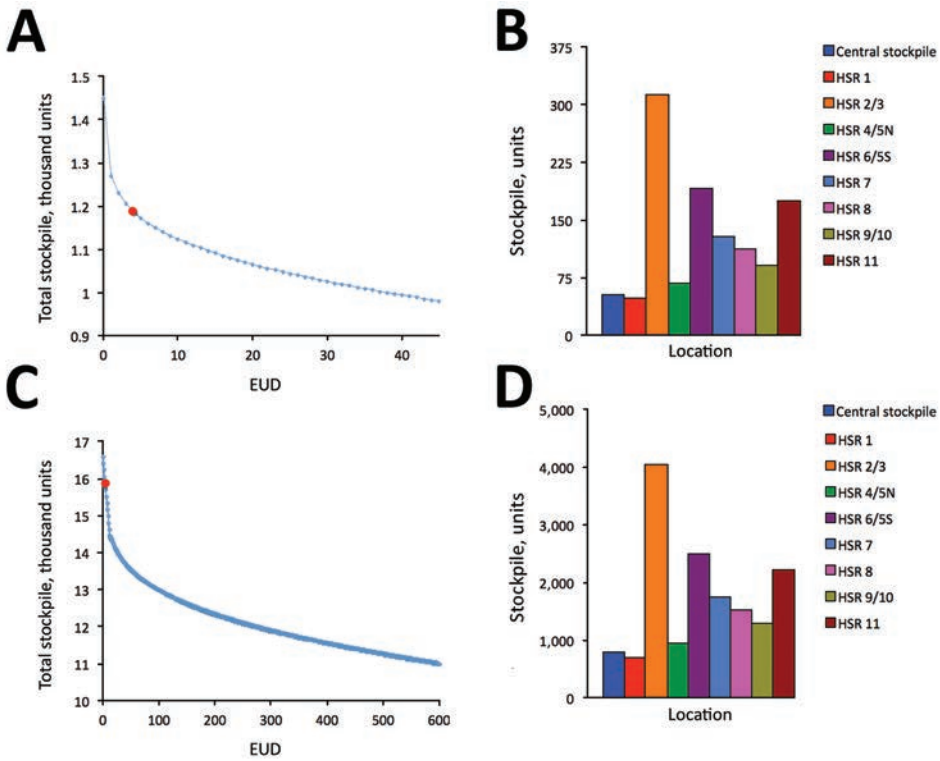

Figure 3. Optimal ventilator stockpiles for moderate and severe pandemic scenarios, Texas, USA. The total size of the required stockpile, summed across the central and 8 HSR stockpiles, decreases as risk tolerance (EUD) increases, for both moderate (A) and severe (C) pandemic scenarios. For an EUD of 5 patients (red circles), total stockpiles would be 1,172 (A) and 15,697 (C); optimal allocations to central and regional stockpiles are shown for moderate (B) and severe (D) scenarios. EUD, expected unmet demand; PUD, probability of unmet demand; HSR, health service region.

might differ from those held locally. Pandemic-related staff absenteeism might exacerbate this challenge. Our model incorporates this limitation by assuming that fraction of stockpiled ventilators are wasted. When we considered a plausible wastage parameter of 20% (based on discussions with Texas DSHS about likely impediments to successful deployment), the model recommended that <10% of ventilators be held centrally.

The recommended allocations among central and local stockpiles hinge critically on the relative efficiencies of a local versus central stockpile, which are largely unknown and perhaps changing to favor central stockpiles as delivery technology continues to improve. We made the simplifying assumption that locally held ventilators are perfectly matched to patients, and we considered a range of potential wastage rates for centrally held ventilators. In general, the more reliable central stockpile deployment, the more advisable a central stockpile. For example, assuming only 0.1% wastage, we found that that all ventilators should be held centrally, regardless of spatiotemporal correlations in peak demand (Table 2). Thus, as deployment and local capacities continue to improve, distance will become less of an issue, and the advantages of central stockpiles might outweigh their shortcomings.

Our surprisingly small central allocation stems from 2 additional factors. First, the uncertainty in our estimates of peak hospitalizations, based on 2009 pandemic data, is relatively low. Across Texas' 8 HSRs, the coefficient of variation (measuring the level of uncertainty) in peak demand for ventilators ranged from 0.17 to 0.36 and averaged 0.24 (online Technical Appendix Table 4). When we increase these coefficients governing uncertainty 3-fold, the

Table 2. Central stockpile size, as a percentage of total stockpile, as a function of wastage and region-to-region correlation in peak ventilator demand during an influenza pandemic, Texas, USA*

	Central stockpile, %		
Wastage, %	Region-to-region correlation = 0.55	Region-to-region correlation = 0.70	Region-to-region correlation = 0.85
40	2.8	1.5	0.2
30	4.7	2.9	0.9
20	7.0	**4.4**	2.0
10	9.8	6.7	3.5
1	18.0	13.5	10.1
0.5	25.4	20.6	17.0
0.3	32.8	27.4	22.7
0.2	48.2	43.9	39.3
0.1	100	100	100

*The results in this table are based on a mild pandemic scenario and a limit on expected unmet demand of 5 patients. Bold indicates the baseline value.

recommended central stockpile increases only from 4.4% to 10% of the total, assuming a mild pandemic and a risk tolerance (EUD) of 5 untreated patients. Second, the small central allocation depends on the risk tolerance. As the risk tolerance shrinks from an EUD of 5 patients, both the number of ventilators in the total stockpile and the percentage held centrally grow (online Technical Appendix Figure 3). Still, even at tighter risk tolerances and a smaller region-to-region correlation in peak demand of 0.55, the central stockpile is <10%.

Our retrospective analysis of the 2009 influenza A(H1N1) pandemic in Texas suggests that hospitals had enough ventilators on hand to treat all patients requiring mechanical ventilation throughout the pandemic. Although these quantities are expected to suffice for a moderate (1957- and 1968-like) pandemic, in which hospitalization rates roughly triple, they would fall far short in a severe (1918-like) pandemic. If we optimistically assume perfect deployment, that is, 0 wastage, by assuming timely delivery, adequately trained and available staff (respiratory therapists, nurses, and physicians), sufficient space to care for a potentially large number of patients, and requisite ancillary equipment and supplies, then even a central stockpile of 8,900 ventilators in Texas—the total number of SNS ventilators in 2010 (*9*)—would fall short, with an expected unmet demand of 576 patients.

This study was supported by the National Institutes of Health (Models of Infectious Disease Agent Study grant U01 GM087719-01) and CDC (Public Health Emergency Preparedness).

Dr. Huang is a senior data scientist at Precima, LoyaltyOne US, Inc., Chicago, Illinois, USA. He conducted this research while a PhD student in the Graduate Program in Operations Research and Industrial Engineering at the University of Texas at Austin. His research interests include optimization, public health, and supply chain management.

References

1. US Department of Health and Human Services. Pandemic flu history. 2016 [cited 2016 Jun 16]. http://www.flu.gov/pandemic/history/index.html
2. US Department of Health and Human Services. HHS pandemic influenza plan. 2005 [cited 2016 Jun 16]. http://www.flu.gov/planning-preparedness/federal/hhspandemicinfluenzaplan.pdf
3. Sutton J, Tierney K. Disaster preparedness: concepts, guidance, and research. Fritz Institute Assessing Disaster Preparedness Conference; 2006 Nov 3–4; Sebastopol, CA, USA; 2006 [cited 2016 Jun 16]. http://www.fritzinstitute.org/pdfs/whitepaper/disasterpreparedness-concepts.pdf
4. Smetanin P, Stiff D, Kumar A, Kobak P, Zarychanski R, Simonsen N, et al. Potential intensive care unit ventilator demand/capacity mismatch due to novel swine-origin H1N1 in Canada. Can J Infect Dis Med Microbiol. 2009;20:e115–23. http://dx.doi.org/10.1155/2009/808209
5. Stiff D, Kumar A, Kissoon N, Fowler R, Jouvet P, Skippen P, et al. Potential pediatric intensive care unit demand/capacity mismatch due to novel pH1N1 in Canada. Pediatr Crit Care Med. 2011;12:e51–7. http://dx.doi.org/10.1097/PCC.0b013e3181e2a4fe
6. Ercole A, Taylor BL, Rhodes A, Menon DK. Modelling the impact of an influenza A/H1N1 pandemic on critical care demand from early pathogenicity data: the case for sentinel reporting. Anaesthesia. 2009;64:937–41. http://dx.doi.org/10.1111/j.1365-2044.2009.06070.x
7. Centers for Disease Control and Prevention. Strategic National Stockpile. 2015 [cited 2016 Jun 16]. http://www.cdc.gov/phpr/stockpile/stockpile.htm
8. Malatino EM. Strategic National Stockpile: overview and ventilator assets. Respir Care. 2008;53:91–5, discussion 95.
9. Jamieson DB, Biddison ELD. Disaster planning for the intensive care unit: a critical framework. In: Scales DC, Rubenfeld GD, editors. The organization of critical care. New York: Springer; 2014. p. 261–75.
10. American Association for Respiratory Care. Guidelines for acquisition of ventilators to meet demands for pandemic flu and mass casualty incidents. 2008 [cited 2016 Jun 16]. https://c.aarc.org/resources/vent_guidelines_08.pdf
11. American Association for Respiratory Care. The Strategic National Stockpile ventilator training program. 2016 [cited 2016 Jun 16]. https://www.aarc.org/resources/clinical-resources/strategic-national-stockpile-ventilator-training-program/
12. Meltzer MI, Patel A, Ajao A, Nystrom SV, Koonin LM. Estimates of the demand for mechanical ventilation in the United States during an influenza pandemic. Clin Infect Dis. 2015;60(Suppl 1):S52–7. http://dx.doi.org/10.1093/cid/civ089
13. Ajao A, Nystrom SV, Koonin LM, Patel A, Howell DR, Baccam P, et al. Assessing the capacity of the US health care system to use additional mechanical ventilators during a large-scale public health emergency. Disaster Med Public Health Prep. 2015;9:634–41. http://dx.doi.org/10.1017/dmp.2015.105
14. Zaza S, Koonin LM, Ajao A, Nystrom SV, Branson R, Patel A, et al. A conceptual framework for allocation of federally stockpiled ventilators during large-scale public health emergencies. Health Secur. 2016;14:1–6. http://dx.doi.org/10.1089/hs.2015.0043
15. Timbie JW, Ringel JS, Fox DS, Pillemer F, Waxman DA, Moore M, et al. Systematic review of strategies to manage and allocate scarce resources during mass casualty events. Ann Emerg Med. 2013;61:677–689.e101. http://dx.doi.org/10.1016/j.annemergmed.2013.02.005
16. Wilgis J. Strategies for providing mechanical ventilation in a mass casualty incident: distribution versus stockpiling. Respir Care. 2008;53:96–100, discussion 100–3.
17. Texas Department of State Health Services and The University of Texas at Austin. Texas pandemic flu toolkit. 2013 [cited 2016 Jun 16]. http://flu.tacc.utexas.edu
18. Centers for Disease Control and Prevention. CDC estimates of 2009 H1N1 influenza cases, hospitalizations and deaths in the United States, April 2009 through January 16, 2010 by age group. 2010 [cited 2016 Jun 16]. http://www.cdc.gov/h1n1flu/estimates/April_January_16.htm
19. Texas Department of State Health Services. Texas aggregate surveillance summary—novel influenza A H1N1, week ending 12/26/09. 2009 [cited 2016 Jun 16]. http://www.dshs.state.tx.us/txflu/TX-cumulative-age-archive.shtm
20. Petris G, Petrone S, Campagnoli P. Dynamic linear models with R. New York: Springer; 2009.
21. US Homeland Security Council. National planning scenarios version 21.3 final draft. 2006 [cited 2016 Jun 16]. http://publicintelligence.net/national-planning-scenarios-version-21-3-2006-final-draft
22. Zhang X, Meltzer MI, Wortley PM. FluSurge 2.0: a manual to assist state and local public health officials and hospital

administrators in estimating the impact of an influenza pandemic on hospital surge capacity (beta test version). 2005 [cited 2016 Jun 16]. https://www.cdc.gov/flu/pandemic-resources/tools/downloads/flusurge2.0_manual_060705.pdf

23. Zhang X, Meltzer MI, Wortley PM. FluSurge—a tool to estimate demand for hospital services during the next pandemic influenza. Med Decis Making. 2006;26:617–23. http://dx.doi.org/10.1177/0272989X06295359

24. Reed C, Biggerstaff M, Finelli L, Koonin LM, Beauvais D, Uzicanin A, et al. Novel framework for assessing epidemiologic effects of influenza epidemics and pandemics. Emerg Infect Dis. 2013;19:85–91. http://dx.doi.org/10.3201/eid1901.120124

Address for correspondence: Hsin-Chan Huang, Operations Research and Industrial Engineering, The University of Texas at Austin, Austin, TX 78712, USA; email: neo.huang@utexas.edu

February 2015: **Complicated Datasets**

- Entry Screening for Infectious Diseases in Humans
- Timing of Influenza A(H5N1) in Poultry and Humans and Seasonal Influenza Activity Worldwide, 2004–2013

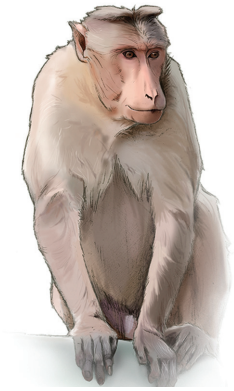

- Quantifying Reporting Timeliness to Improve Outbreak Control
- Tickborne Relapsing Fever, Bitterroot Valley, Montana, USA
- Simulation Study of the Effect of Influenza and Influenza Vaccination on Risk of Acquiring Guillain-Barré Syndrome
- *Lagenidium giganteum* Pathogenicity in Mammals
- Optimizing Distribution of Pandemic Influenza Antiviral Drugs
- Murine Typhus, Reunion, France, 2011–2013
- Evidence for *Elizabethkingia anophelis* Transmission from Mother to Infant, Hong Kong
- Microbiota that Affect Risk for Shigellosis in Children in Low-Income Countries
- pH Level as a Marker for Predicting Death among Patients with *Vibrio vulnificus* Infection, South Korea, 2000–2011
- Refining Historical Limits Method to Improve Disease Cluster Detection, New York City, New York, USA
- Naturally Acquired Antibodies against *Haemophilus influenzae* Type a in Aboriginal Adults, Canada
- Infectious Causes of Encephalitis and Meningoencephalitis in Thailand, 2003–2005

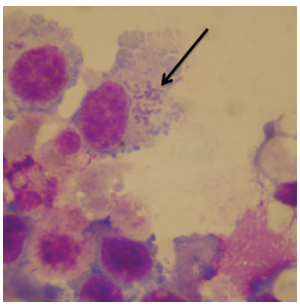

- Novel Reassortant Influenza A(H5N8) Viruses among Inoculated Domestic and Wild Ducks, South Korea, 2014
- Vesicular Stomatitis Virus–Based Vaccines against Lassa and Ebola Viruses

- Use of Insecticide-Treated House Screens to Reduce Infestations of Dengue Virus Vectors, Mexico
- Comparative Analysis of African Swine Fever Virus Genotypes and Serogroups
- Awareness and Support of Release of Genetically Modified "Sterile" Mosquitoes, Key West, Florida, USA
- Novel *Candidatus Rickettsia* Species Detected in Nostril Tick from Human, Gabon, 2014
- Outbreak of Henipavirus Infection, Philippines, 2014
- Close Relationship between West Nile Virus from Turkey and Lineage 1 Strain from Central African Republic
- Ascariasis in Humans and Pigs on Small-Scale Farms, Maine, USA, 2010–2013
- Potentially Novel *Ehrlichia* Species in Horses, Nicaragua
- *Neisseria meningitidis* ST-11 Clonal Complex, Chile 2012
- Molecular Diagnosis of Cause of Anisakiasis in Humans, South Korea
- *Streptococcus suis* Infection in Hospitalized Patients, Nakhon Phanom Province, Thailand
- Exposure-Based Screening for Nipah Virus Encephalitis, Bangladesh

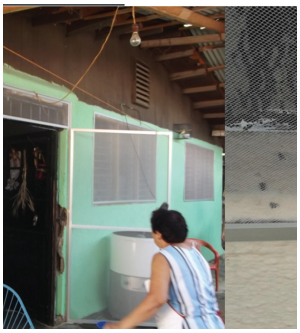

EMERGING INFECTIOUS DISEASES

https://wwwnc.cdc.gov/eid/content/21/2/contents.htm

Invasive Serotype 35B Pneumococci Including an Expanding Serotype Switch Lineage, United States, 2015–2016

Sopio Chochua, Benjamin J. Metcalf, Zhongya Li, Hollis Walker, Theresa Tran, Lesley McGee, Bernard Beall

We used whole-genome sequencing to characterize 199 nonvaccine serotype 35B pneumococcal strains that caused invasive pneumococcal disease (IPD) in the United States during 2015–2016 and related these findings to previous serotype 35B IPD data obtained by Active Bacterial Core surveillance. Penicillin-nonsusceptible 35B IPD increased during post–pneumococcal 7-valent conjugate vaccine years (2001–2009) and increased further after implementation of pneumococcal 13-valent conjugate vaccine in 2010. This increase was caused primarily by the 35B/sequence type (ST) 558 lineage. 35B/ST558 and vaccine serotype 9V/ST156 lineages were implicated as *cps35B* donor and recipient, respectively, for a single capsular switch event that generated emergent 35B/ST156 progeny in 6 states during 2015–2016. Three additional capsular switch 35B variants were identified, 2 of which also involved 35B/ST558 as *cps35B* donor. Spread of 35B/ST156 is of concern in view of past global predominance of pathogenic ST156 vaccine serotype strains. Protection against serotype 35B should be considered in next-generation pneumococcal vaccines.

Although the dramatic protective effect of the pneumococcal 7-valent conjugate vaccine (PCV7) against invasive pneumococcal disease (IPD) persisted a full decade after its introduction in the United States in 2000, the emergence of 19A and other non-PCV7 serotypes reduced the overall benefit (*1*,*2*). Before PCV7 implementation, we observed only 2 different 35B lineages within Active Bacterial Core surveillance (ABCs) (*3*), a population-based, multistate program that assesses the effect of invasive bacterial infections and is part of the Emerging Infections Program network of the Centers for Disease Control and Prevention (CDC; Atlanta, GA, USA) (http://www.cdc.gov/abcs/index.html). Both lineages were relatively rare causes of IPD but were geographically widespread in the United States before and after PCV7 introduction (*3*). One 35B lineage was antimicrobial-susceptible and multilocus sequence type (MLST) 452 (35B/ST452), and the second strain was penicillin-nonsusceptible 35B/ST558. During 1995–2001, the penicillin-nonsusceptible 35B/ST558 lineage, which had resistant MICs of 0.25–2.0 μg/mL, accounted for 69% of serotype 35B ABCs isolates (*3*). During 1999–2007 in the United States, the proportion of penicillin-nonsusceptible IPD isolates within serotype 35B increased to 84%; 35B/ST558 accounted for this increase (*4*). Consistent with this observation was a 9-fold increase in carriage of 35B/ST558 in young children in the Atlanta, Georgia, area (*5*).

After introduction of the 13-valent conjugate vaccine (PCV13) in 2010, 35B became the most common serotype in ABCs, associated with MICs ≥2 μg/mL for penicillin and amoxicillin in pediatric isolates (*6*) and in the adult population (B. Beall, unpub. data). Consistent with its status as a major cause of IPD in the post-PCV13 era, the 35B/ST558 lineage is currently commonly found in disease and asymptomatic pneumococcal carriage in many countries (*7*–*11*).

We provide a whole-genome sequence (WGS) pipeline–based resolution and description of current 35B lineages within current ABCs surveillance (*6*,*12*), including an invasive 35B variant of the historically successful ST156 lineage. Recently, we identified 2 different 35B isolates recovered during 2009 and 2012 that each appeared to have arisen through a unique capsular switch event involving the same 2 parental strains. This observation was made on the basis of the penicillin-binding protein (PBP) gene types flanking the 35B biosynthetic locus (*cps35B*) in each of the variants (*6*).

Only the 35B/ST156 variant detected during 2012 has emerged and has been detected within 6 states. ST156 has a remarkable history of conjugate vaccine evasion. Formerly the primary genotype of PCV7

Author affiliation: Centers for Disease Control and Prevention, Atlanta, Georgia, USA

DOI: http://dx.doi/10.3201/eid2306.170071

serotype 9V in the United States during the preconjugate vaccine era (*13*), 9V greatly decreased after PCV7 implementation (*1*) and was partially replaced by resistant 19A/ST156 (*14*). To verify that these isolates originated from a single recombinational serotype switch event involving 35B/ST558 and 9V/ST156 parental strains, we analyzed regions flanking the *cps35B* locus during 2015–2016, 35B/ST156 progeny and the original strain detected during 2012.

Methods

Isolates

The surveillance population of ABCs is ≈32 million persons in 10 states (http://www.cdc.gov/pneumococcal/surveillance.html). Serotype 35B IPD isolates described include 132 recovered during 2015 and 67 recovered during ABCs in 2016 (Table 1, https://wwwnc.cdc.gov/EID/article/23/6/17-0071-T1.htm). The listing of 35B isolates from 2016 is incomplete because we typically receive all ABCs isolates recovered during a given year by the following summer. Relevant ST156 lineage isolates of other serotypes recovered during this and previous periods are shown in Table 2. Total numbers of ABCs 35B isolates recovered during 1999–2015 and categorized by patient age, penicillin MIC, and IPD incidence are shown in Table 3.

WGS and WGS-Based Predictions

Library construction and sequencing was performed as described (*12*). WGS accessions for all 199 serotype 35B isolates from 2015–2016, two previous 35B switch strains from previous years, and relevant strains of other serotypes of ST156 from previous years are provided (online Technical Appendix Table, https://wwwnc.cdc.gov/EID/article/23/6/17-0071-Techapp1.pdf). WGS pipeline data and quality metrics for all isolates are also provided (online Technical Appendix Table). Capsular serotypes, antimicrobial genotypes/phenotypes, MLST, sequence type (ST), and pili (presence or absence) for year 2015–2016 isolates were deduced through our bioinformatics pipeline (*6*,*12*,*15*).

Phylogeny

Paired-end fastq files were trimmed with Cutadapt version 1.8.1 (*17*), and draft genome assemblies were

Table 2. Nonserotype 35B isolates of ST156 lineage included in study of penicillin-nonsusceptible 35B pneumococcal isolates causing IPD, United States, 1998–2015*

Serotype/ MLST type (no.)†	No.	PBP type‡	Non-PBP resistance determinants§	Antimicrobial resistance phenotype, MIC, μg/mL¶										State (year isolated)
				Pen	Amo	Tax	Cft	Cfx	Mer	Ery	Cli + Tet	Cot	Fq	
9V/156 (25)	12	15:12:18	*folA*I100L, *folPins178*	4	2	1	2	>2	0.5	S	S	R	S	CA, GA, MD, MN, NY, TN (1998–1999)
	9	15:12:18	*mef, folA*I100, *folPins178*	4	2	1	2	>2	0.5	R	S	R	S	CA, CT, MD, MN, OR, TN (1998,1999, 2015)
	2	15:12:18	*ermB, tetM*, *folA*I100L, *folAins178*	4	2	1	2	>2	0.5	R	R	R	S	CA (2015)
	1	15:12:18	*mef, tetM, folA*I100L, *folPins178*	4	2	1	2	>2	0.5	R	S	R	S	CT (2015)
	1	15:12:228	*Mef, folA*I100L, *folPins178*	4	2	1	2	>2	0.5	R	S	R	S	MD (2016)
19A/156 (4)	3	29:12:26	*mef, folA*I100L, *folAins189*	4	2	8	4	>2	0.5	R	S	R	S	CA,GA (2009)
	1	8:12:36	*mef, folA*I100L, *folAins189*	1	2	0.5	0.5	2	0.25	R	S	R	S	GA (2015)
13/156 (1)	1	15:12:173	*folA*I100L, *folPins178*	1	1	0.25	0.25	1	0.5	S	S	R	S	TN (2015)
31/156 (1)	1	15:12:18	*mef*, *folA*I100L, *folPins178*	4	2	1	2	>2	0.5	R	S	R	S	MN (2015)

*All isolates were positive for pilus PI-type 1 and negative for pilus PI-type 2. IPD, invasive pneumococcal disease; MLST, multilocus sequence type; PBP, penicillin-binding protein; R, resistant; S, susceptible; ST, sequence type.
†Types that probably arose through serotype switching are indicated in bold.
‡See Li et al. (*15*) and MIC correlates for PBP types (http://www.cdc.gov/streplab/mic-tables.html).
§For a description of WGS-based bioinformatic pipeline for deduction of all features shown, see Metcalf et al. (*6,12)*. For a description of *folP* insertions (*folPins178*, *folP189*), see Figure 1 in Metcalf et al. (*12*).
¶Predicted MICs for β-lactam antimicrobial drugs were based on transpeptidase domain sequences of PBPs 1a, 2b, and 2x (http://www.cdc.gov/streplab/mic-tables.html). For penicillin (meningitis only), nonsusceptible is considered ≥0.12 μg/mL (*16*). Currently applied clinical cutoffs are also provided for the other 5 β-lactams shown (*16*). Where shown, R and S correspond to breakpoint MIC values (*16*). Amo, amoxicillin; Cft, ceftriaxone; Cfx, cefuroxime; Cli, clindamycin; Cot, cotrimoxazole; Ery, erythromycin; Fq, fluoroquinolones levofloxacin and ciprofloxacin; Mer, meropenem; Pen, penicillin; Tax, cefotaxime.

Table 3. Annual incidence and proportions of penicillin-nonsusceptible 35B pneumococcal isolates causing IPD, United States, 1999–2015*

Year	Surveillance population	% CIS	No. 35B isolates from patients by age, y		Relative incidence of 35B IPD†	Pen MIC, μg/mL			*penNS* 35B isolates/*penS* 35B isolates
			<5	≥5		≥2	0.12–1	≤0.06	
1998	17,383,935	86.1	3	18	1.40	9	5	7	2.0
1999	18,550,681	87.0	2	18	1.24	8	3	9	1.2
2000	19,821,607	86.3	4	21	1.46	7	9	9	1.8
2001	22,479,308	88.1	2	40	2.12	14	18	10	3.2
2002	25,051,246	87.6	2	34	1.64	20	8	8	3.5
2003	25,264,246	91.4	11	49	2.56	22	26	11	4.4
2004	27,419,898	87.9	15	69	3.49	44	25	15	4.6
2005	27,816,784	89.5	11	57	2.73	35	18	15	3.5
2006	28,204,455	86.7	1	65	2.70	37	15	14	3.7
2007	28,579,312	87.5	5	83	3.52	51	23	14	5.3
2008	28,856,774	86.7	12	80	3.68	62	16	14	5.6
2009	29,206,528	89.8	8	70	2.97	45	16	17	3.6
2010	29,757,552	90.2	4	67	2.65	52	14	5	13.2
2011	30,075,050	90.3	11	77	3.28	71	7	10	7.8
2012	30,356,544	90.6	13	101	4.14	94	14	6	18.0
2013	30,604,240	88.7	15	114	4.75	94	25	10	11.9
2014	31,328,211	88.2	16	116	4.78	104	22	6	21.0
2015	31,977,800	92.0	10	121	4.45	101	24	6	20.8

*CIS, case isolates serotyped; IPD, invasive pneumococcal disease.
†Estimated cases/million = total 35Bs x 100/% CIS surveillance population/1,000,000.

constructed by using VelvetOptimiser version 2.2.5 with an optimal kmer value calculated by using VelvetK (*18*). Core genome single-nucleotide polymorphism (SNP) identification and alignment were performed by using kSNP3.0 (*19*). A maximum-likelihood phylogenetic tree was generated from the core SNP alignment by using RaxML version 7.3.0 (*20*). RaxML was run with an ASC_GTRGAMMA DNA substitution model and used the Lewis method for ascertainment bias correction. Node support was assessed by using 500 bootstrap replicates.

Conventional MIC Testing and Serotyping

Serotype 35B isolates recovered during 2015 were subjected to conventional broth dilution testing for determination of antimicrobial MICs. A selection of these isolates were also subjected to conventional serotyping by using CDC typing antisera as described (*6*).

Statistical Analyses

A χ^2 test was performed to evaluate differences among groups. This test was performed by using OpenEpi Version 3.01 (http://www.openepi.com/Menu/OE_Menu.htm).

Results

Increase in Penicillin-Nonsusceptible 35B during the Conjugate Vaccine Era

During 1998–2001, penicillin-nonsusceptible 35B accounted for 67.6% (108) of serotype 35B ABCs isolates (Table 3). During 2002–2015, the proportion of penicillin-nonsusceptible IPD isolates with serotype 35B increased to 87.7% (1,237; p<0.001).

Population Snapshot of Ongoing ABCs for 35B IPD, 2015–2016

Among 2,710 IPD isolates obtained during 2015 and subjected to WGS, 132 (4.9%) were serotype 35B. Of 1,528 IPD isolates recovered from partial year 2016 IPD surveillance, 67 (4.4%) were serotype 35B. Most (168/199) of these isolates belonged to penicillin-nonsusceptible clonal complex (CC) 558 (168 isolates) and CC156 (21 isolates) (Figure 1; Table 1). Serotype 35B CC558 and CC156 isolates of all serotypes discussed were uniformly positive for the *rrgA* gene (Tables 1, 2), which encodes a pilus subunit that functions in epithelial adhesion (*22*). Ten isolates of long-standing penicillin-susceptible 35B/ST452 (*3*) were also recovered. Single 35B isolates were identified of ST1092, a lineage of conjugate vaccine serotypes 6A and 6B (http://pubmlst.org/spneumoniae/) and of ST11818 (highly related to 15A/ST63), an antimicrobial-resistant nonvaccine serotype lineage that has increased in the post-conjugate vaccine era (*4*).

CC558 (35B/CC558)

Of 168 35B/CC558 isolates obtained, 147 were ST558, 20 were single-locus variants (SLVs) of ST558 corresponding to 13 STs, and 1 was a double-locus variant (Figure 1; Table 1). Within CC558, only ST558 had SLVs, which is consistent with initial successful establishment of 35B/ST558 in its ecologic niche and subsequent rare shedding of closely related SLVs (*21*).

The increased incidence of 35B IPD during the post-PCV7 period (2.1–3.7 cases/million population during 2001–2009 vs. 1.2–1.3 cases/million population during 1998–1999) and the post-PCV13 period (3.3–4.8 cases/million

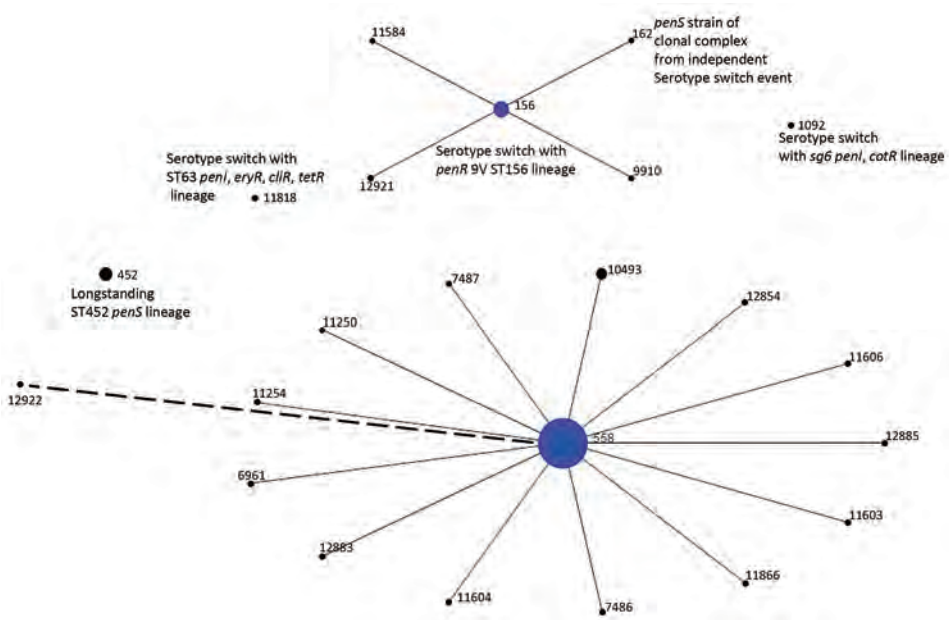

Figure 1. Population snapshot of 199 serotype 35B pneumococcal isolates obtained by ongoing Active Bacterial Core surveillance, United States, 2015–2016, configured by using eBURST (*21*). Diameters are proportional to number of isolates. Solid lines indicate single-locus variants, and the single dashed line indicates a double-locus variant of ST558. ST, sequence type.

population during 2011–2015), combined with the consistent trend of markedly increased proportions of penicillin-nonsusceptible 35B IPD isolates throughout the conjugate vaccine era (Table 2), is consistent with reported increased 35B/ST558 in IPD and carriage (*4–11*). ABCs surveillance sites increased after 2000, but 35B IPD incidence calculations did not vary whether including the expanded surveillance sites or by using only continuously participating ABCs sites during 1998–2015.

CC156 (35B/CC156)

We analyzed PBP types (*6,12,15*) of 35B/ST558 (4:7:7) and 35B/ST156 (4:12:7) isolates. These PBP amino acid sequence types are used for predicting β-lactam MICs and correspond to PBP transpeptidase domains from PBP1a, PBP2b and PBP2x, respectively. PBP genes *pbp1a* and *pbp2x* flank opposite ends of the capsular biosynthetic locus and are sometimes cotransferred during serotype switching events (*6,23–25*). The 35B/ST558 lineage has been nearly exclusively associated with PBP type 4:7:7 among isolates obtained since 1998, and the serotype 9V/ST156 lineage is similarly highly associated with PBP type 15:12:18 (*6,15*). However, 9V/ST156 is rare among IPD isolates in the post-PCV7 period.

In addition to the PBP2b-12 marker, *mef* gene, and FolA-I100L substitution, candidate *cps35B* recipient 9V/ST156 strains contain the 2-codon insertion designated *folPins178* (Table 2; Figures 2, 3). Such 1–2 codon *folP* insertions, which together with FolA-I100L confer cotrimoxazole resistance, are categorized by specific location of the insertion and specific sequence flanking the insertions (*12*). These genomic features are also found within the 35B/ST156 lineage isolates described (Table 1; Figures 2, 3), which are consistent with a 9V/ST156 (*mef*, FolA-I100L, *folPins178*) strain serving as the recipient strain for a 35B/ST558 *cps35B* donor strain (Figure 3). Another potential recipient strain present before and after PCV13 introduction was 19A/ST156 (*6,14*). However, this lineage is associated with the *folPins189* insertion (Table 2; Figure 2).

Both flanking *pbp* loci from 35B/ST558 were cotransferred with the *cps35B* locus to replace the *cps9V*, *pbp1a*-15 and *pbp2x*-18 determinants in the putative 9V/ST156 recipient, which resulted in PBP type 4:12:7 (Figure 3). This serotype switch progeny strain was obtained from a 4-year-old child during 2012 and is a potential progenitor of the current invasive 35B/CC156 lineage (isolate 2012221165) (Figures 2, 3). Antimicrobial resistance markers PBP2b-12, *mef*, FolA-I100L, and *folPins178*, combined with the close phylogenetic relatedness of the 9V/ST156 isolates (Figure 2), suggest that a member of this lineage served as the recipient parental strain for the 35B/ST156 clade isolated in ongoing ABCs during 2015–2016 (Figure 3).

Analysis of the regions flanking the *cps35B* locus for all 35B/ST156 lineage isolates obtained during 2015–2016 showed identical recombinational sites at bases 6,453 (left coordinate of progeny reference) (Figure 3) and 10,836 (right coordinate), which is clearly indicative of a single event within a 35B/ST156 ancestral strain of the 19 progeny shown (Figure 3). Thus, a double-crossover event replaced the recipient strain *cps9V* locus and flanking PBP markers (2x-18 and 1a-15) with the *cps35B* locus and its flanking PBP markers (2x-7 and 1a-4). On the basis of available strain data, the original progeny strain is predicted to have been an ST156 strain with the PBP type 4:12:7; a total of 14 of the 19 35B/ST156 lineage strains still shared these characteristics (Table 1). Five isolates are SLVs or differ in PBP2b type.

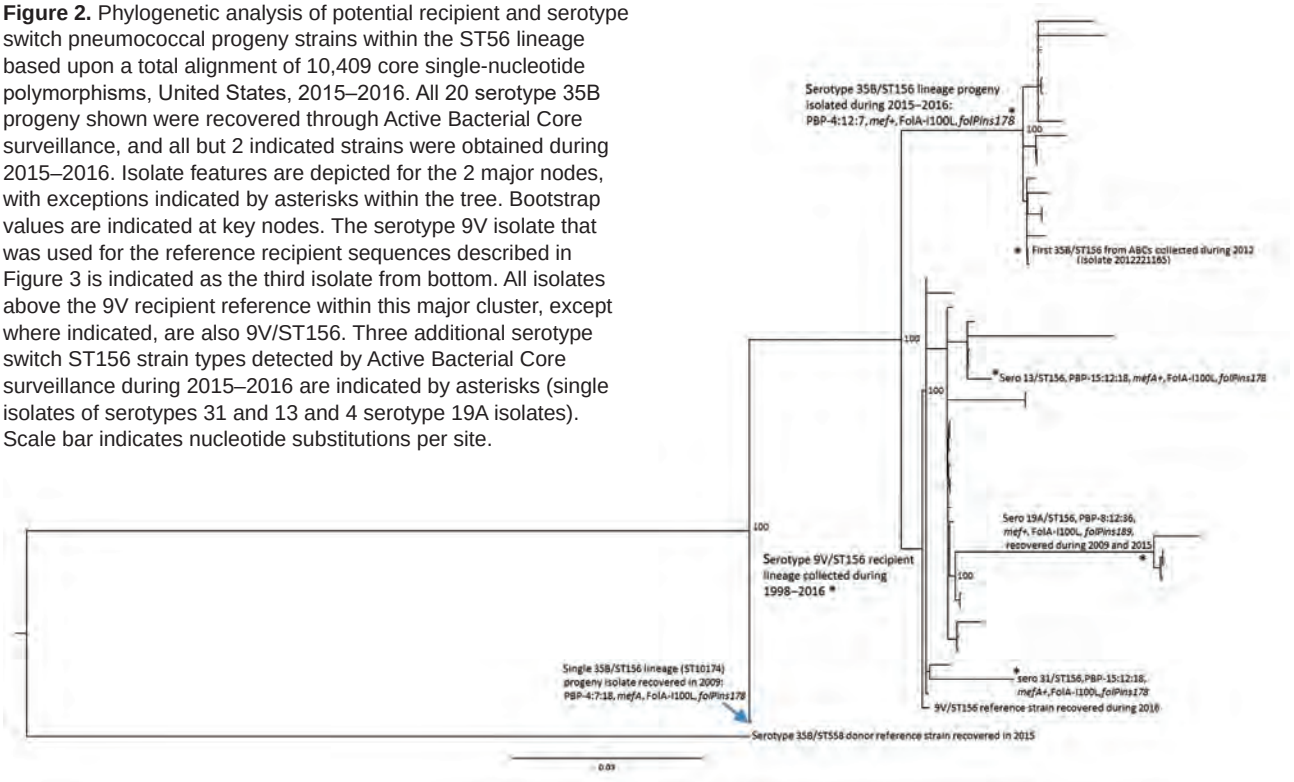

Figure 2. Phylogenetic analysis of potential recipient and serotype switch pneumococcal progeny strains within the ST56 lineage based upon a total alignment of 10,409 core single-nucleotide polymorphisms, United States, 2015–2016. All 20 serotype 35B progeny shown were recovered through Active Bacterial Core surveillance, and all but 2 indicated strains were obtained during 2015–2016. Isolate features are depicted for the 2 major nodes, with exceptions indicated by asterisks within the tree. Bootstrap values are indicated at key nodes. The serotype 9V isolate that was used for the reference recipient sequences described in Figure 3 is indicated as the third isolate from bottom. All isolates above the 9V recipient reference within this major cluster, except where indicated, are also 9V/ST156. Three additional serotype switch ST156 strain types detected by Active Bacterial Core surveillance during 2015–2016 are indicated by asterisks (single isolates of serotypes 31 and 13 and 4 serotype 19A isolates). Scale bar indicates nucleotide substitutions per site.

We detected the small (491 bp) segment (bases 11349–11839 of progeny) (Figure 3) of clearly recipient lineage origin within the left side of the major recombinational fragment. During a single–double crossover event that facilitates a serotype switch, additional independent double-crossover events appear to occur concurrently (*27*). However, these events probably do not occur simultaneously. It appears that the actual serotype switch event involved a shorter donor fragment bordering upon the right side of this small recipient lineage segment (base 11839), followed by a second double-crossover event that bordered upon the left side of the recipient lineage fragment (base 11349).

A single penicillin-susceptible 35B/ST162 (SLV of ST156) has the completely sensitive PBP type 0:0:0 (*6*,*12*) (Table 1). This strain arose through an independent serotype switch event that involved a penicillin-susceptible recipient strain.

Postserotype Switch Event Diversification of 35B/ST156 Progeny

Five of the 19 35B/ST156 lineage progeny showed indications of genetic diversification that occurred after the capsular switch event. Four of these isolates have 1 of 3 SLV MLSTs of ST156 (ST9910, ST11584, and ST12921) (Table 1). Although 18 of the 19 strains were PBP type 4:12:7, the SLV ST12921 variant had PBP type 4:11:7. For this particular strain, it is probable that recombination with a highly penicillin-resistant ST320 strain, prevalent during the post-PCV7 era and having PBP type 13:11:16 (*6*), simultaneously replaced the *pbp2b* locus and flanking *ddl* sequence to change the PBP type to 4:11:7 and the MLST type to ST12921 through transfer of *ddl* with the resistance-conferring selectable *pbp2b* allele (*28*). We also observed an increased MIC for amoxicillin for this PBP type 4:11:7 strain compared with MICs for PBP type 4:12:7 strains (Table 1).

Two isolates (20152877 and 20161763) underwent a postswitch intra–*cps35B* gene deletion event within the *wciG* gene (Figure 3), which is predicted to encode an acetyltransferase (*26*). Although these 2 isolates were serotyped as 35B by using CDC typing antisera, they differed in reactivity with serologic factor 35a compared with the other 17 isolates of this lineage (Table 4). Typing antisera factors 29b and 35c are the CDC Quellung reagents definitive for serotype 35B. The original protocol (*29*,*30*) that CDC first followed for serogroup 35 resolution also used factor 35a along with factors 29b and 35c for identification of serotype 35B. We found that the 2 *wciG* deletion strains did not react with factor 35a, but the other 17 serotype 35B strains reacted strongly with factor 35a. These preliminary data is suggestive of a new serotype within serogroup 35 because this specific factor reactivity pattern has not been observed for serogroup 35 (*31*).

Figure 3. Diagrammatic representation of *cps* loci and adjacent regions from donor, recipient and progeny strains depicting serotype switch event for pneumococcal isolates, United States, 2015–2016. Red and green lines in progeny indicate regions of sequence identity or near identity (<2 single-nucleotide polymorphisms/10,000 bp) to the above corresponding donor and recipient sequences, respectively. Rectangles indicate relative locations of PBP gene types for *pbp2x* and *pbp1a*. Below each *cps* locus, a representative reference strain is indicated along with relevant features determined through a bioinformatics pipeline (MLST, PBP type, resistance markers). Junctions between donor and recipient sequences involved in the 2 single recombinational crossovers in the gene replacement event are indicated with blue arrowheads above the progeny diagram, although a single short internal region with sequence identity to the recipient nested within the donor fragment (left coordinates 11349–11839) is also present. Below each green or red segment of the progeny, the level of sequence identity to donor and recipient is provided. The list of each progeny strain, date of isolation, and state is provided. Where MLST is not ST156, its single locus variants (ST9910, ST11584, and ST12921) are included. Two exceptions indicating flanking post-switch recombination within left coordinates 1–6453 are indicated in isolates 20152884 and 20161413 (asterisks): isolate 20152884 had only 99.3%–99.5% identity to recipient and donor over bases 1–3715, and isolate 20161413 had only 99.5%–99.7% identity to recipient and donor over bases 1–2143. Two strains on the right indicate a post-switch deletion event within the wciG putative acetyltransferase gene, which putatively contributes to the acetylation pattern of the serotype 35B polysaccharide (*26*). MLST, multilocus sequence type; PBP, penicillin-binding protein; ST, sequence type.

Further indication of chromosome-wide postswitch diversification of this single clade was shown in the left-flanking region of the *cps35B* locus. Two progeny strains showed diversification within the first 2–3.7 kb when compared with the other 17 progeny. The 6-kb region immediately to the left of base 1 in all of the progeny strains had ≤99.2% sequence identity with the most similar potential ST156 parental recipient strains that we analyzed. However, beyond this segment, progeny had sequence identity with the parental strain for ≥8 kb.

35B/ST156 Variant Lineages Arising through Separate Serotype Switch Events

The 9V/ST156 clade also appears likely to have served as the recipient for an independent serotype switch from the same 2 parental strains (Figure 3) which resulted in 35B/ST10174, an SLV of ST156 (Figure 2) obtained from an infant during 2009 (isolate 2009219987). This isolate differs in the flanking *pbp2x* marker and distal *pbp2b* marker (PBP type 4:7:18). Features of this variant have been described (*6*), and we have not obtained additional 35B isolates with these distinguishing features. A third serotype switch event involving a CC156 recipient strain is intuitive from the pipeline data, which indicate that the 35B SLV of ST162 is featured by the β-lactam–susceptible PBP type 0:0:0 (Table 1). ST162 has long been associated with penicillin-susceptible 9V strains (*13*) and more recently with PI-1 positive and penicillin-susceptible 23B, 15B, and 15C strains (*6*).

Nonserotype 35B Variants of ST156

Single ST156 isolates of serotypes 31 and 13 were obtained during 2015 (Figure 2) and showed high relatedness to different 9V subdivisions. Again, the likely recipient background for the presumed capsular switch does not appear likely to involve the 19A/ST156 lineage (Figure 2), which

Table 4. Serologic comparison of 35B/ST156 lineage strains with CDC Quellung reagents for resolution of serogroup 35B invasive serotype pneumococci including an expanding serotype switch lineage, United States, 2015–2016*

	Quellung factor				
Strain	35b	29b	35c	42a	35a
cps35B†	–	+	+	–	+
cps35B (*wciG* deletion)‡	–	+	+	–	–

*CDC, Centers for Disease Control and Prevention; ST, sequence type; –, negative; +, positive.
†Refers to 17 progeny resulting from recombination indicated in left column under progeny lineage diagram in Figure 3.
‡Refers to 2 indicated *wciG* deletion isolates in right column under progeny lineage diagram in Figure 3.

was well-represented during the 2000s after PCV7 implementation (*6*,*14*,*32*).

CCs of Remaining 35B Isolates Obtained during 2015–2016

Ten of the 12 isolates other than penicillin-nonsusceptible CC558 and CC156 (together composed of 187 isolates) were of the long-established penicillin-susceptible 35B/ST452 lineage (*3*), which decreased in proportion during the 2000s (*4*) (Figure 1; Table 3). The 2 remaining 35B isolates obtained during 2015–2016 also appear to have originated through serotype switching events involving a 35B/ST558 *cps35B* donor, as implicated by the presence of the PBP1a-4 or PBP2x-7 determinants flanking the *cps* loci of these 2 progeny strains (35B/ST11818 and 35B/ST1092) (Table 1). The 35B/ST11818 variant is an SLV of ST63 and has the same resistance features and accessory resistance genes (*ermB* and *tetM*) as the currently common 15A/ST63 clone (*4*,*6*,*32*). The 35B/ST1092 isolate is likely to have originated through serotype switching with a serogroup 6 recipient strain (*6*). The 14 remaining ST1092 isolates obtained during surveillance in 2015–2016 were serotype 6C. The 6 previously collected ST1092 IPD isolates (1999–2013) represented in our WGS collection are from serotype 6A, 6B, and 6C strains (*6*; B. Beall, unpub. data).

Discussion

An increase of penicillin-nonsusceptible serotype 35B IPD and carriage caused by 35B/ST558 has been apparent in the United States since the introduction of PCV7 in 2000, and it has shown a major increase after PCV13 implementation (*4*–*8*). This finding is of concern because even strains that are rarely detected in IPD sometimes rapidly emerge. For example, the 19A/ST320 strain was not detected during extensive characterization of pre-PCV7 ABCs isolates (*13*), yet it became the predominant invasive pneumococcal strain during 2005–2009 (*14*,*32*). We have performed comprehensive strain characterization (MLST and WGS) of pediatric (from children ≤5 years of age) ABCs isolates obtained during 1999, 2001, 2002, 2008, 2009, and 2011–2013 (*6*,*13*) and WGS-based characterization of a large sampling of isolates from all age groups during 1998–2013 (*4*,*6*,*13*; B. Beall, unpub. data).

Before 2015, we detected only 1 isolate of the 35B/ST156 lineage that was recovered during 2012 (*6*). Thus, we feel justified in describing it as newly emergent isolate. A smaller study was recently published (during peer review of this article) that described 78 invasive and 48 noninvasive serotype 35B isolates obtained during 1994–2014 from 8 hospitals in 8 states (*33*). Our data, which included a population-based sampling of 199 35B isolates obtained during 2015–2016, clearly shows the current national predominance of 35B/ST558 and does not support the observation that 35B/ST156 is the major contributor to post-PCV13 antimicrobial-resistant 35B. Both studies noted the initial appearance and emergence of 35B/ST156 in the post-PCV13 period.

This recent identification of the antimicrobial-resistant 35B/ST156 lineage and its subsequent detection within 6 ABCs sites is a cause for concern. The ST156 lineage has shown a remarkable propensity to persist through undergoing serotype-switch events (*12*,*23*,*25*,*32*). The penicillin-resistant 9V/ST156 lineage was the predominant serotype 9V cause of IPD in the United States during the pre-PCV7 era (*13*,*32*). Soon after introduction of PCV7, serotype 9V IPD became rare (*1*,*2*), and 19A became the predominant representative of the ST156 lineage within ABCs (*14*,*32*). After introduction of PCV13, 35B has become the predominant serotype of the ST156 lineage within the United States (B. Beall, unpub. data).

A distinct antimicrobial-susceptible serotype 35B SLV of ST156 (35B/ST162) is included among 35B ABCs of 35B during 2015–2016 by the β-lactam–susceptible PBP type 0:0:0. Thus, our data indicates that ≥3 independent serotype switches involving the nonvaccine type *cps35B* locus and the broad ST156 clonal complex serving as recipient strains have previously occurred. In this study, we demonstrated that all penicillin-nonsusceptible 35B/ST156 lineage isolates obtained during current ABCs (2015–2016) arose through a single ancestral recombination event. This event was facilitated through detailed analyses of crossover points and comparisons of corresponding regions of all progeny isolates with likely parental 35B/ST558 and 9V/ST156 strains. The genetic plasticity of the ST156 lineage is also highlighted in this study by detection of postserotype switch changes affecting β-lactam resistance (PBP1a type) and capsular serotype (*wciZ* deletion), which is potentially reflective of recent antimicrobial drug pressure and immunologic selection pressure.

An additional 35B variant within a vaccine serotype lineage is shown with ST1092 that is typically associated with serogroup 6 strains (Figure 1). Because these putative 35B switch variants were not detected during extensive strain surveillance before and shortly after conjugate

vaccine implementation (*3*,*4*,*13*), it is plausible that these serotype switches occurred after implementation of conjugate vaccine. The observation of a 35B variant within the antimicrobial 15A/ST63 lineage brings the number of serotype switch events generating 35B strains described in this study to 5; (35B/ST11818, 35B/ST156, 35B/ST162 from 2015–2016, and 35B/ST10174 from 2009). Except for the 35B/ST162 variant, these serotype switch events were predicted on the basis of progeny PBP type to involve the 35B/ST558 strain as the *cps35B* donor (online Technical Appendix Table).

Although conjugate vaccines have a history of providing effective and durable protection against IPD (*1*,*2*), the continued emergence and expansion of serotype 35B into different clonal complexes supports continued development of wider spectrum pneumococcal vaccines. Serotype 19A IPD, although relatively uncommon in the pre-PCV7 era, rapidly became the predominant invasive serotype in the post-PCV7 period (*14*,*32*,*34*). Serotype 35B strains have several of the same features that were found among serotype 19A strains before implementation of PCV7 in 2000. These features that could predispose for serotype 35B to continue its increasing trend as a cause of IPD include its lack of inclusion within conjugate vaccine, high carriage rates within children, antimicrobial resistance, clonal expansion, and serotype switching. An experimental 15-valent conjugate vaccine in development includes serotypes 22F and 33F (*35*), which have increased as causes of IPD in the postconjugate vaccine era. Serotypes 15A, 15B, and 23A are expressed by moderately antimicrobial-resistant clones and are not uncommon causes of IPD (*4*,*32*). Although less resistant to β-lactam antimicrobial drugs than 35B/ST558 and 35B/ST156, these strains also present a challenge to address through more encompassing pneumococcal vaccines.

Acknowledgments

We thank A. Reingold, S. Brooks, H. Randel, L. Miller, B. White, D. Aragon, M. Barnes, J. Sadlowski, S. Petit, M. Cartter, C. Marquez, M. Wilson, M. Farley, S. Thomas, A. Tunali, W. Baughman, L. Harrison, J. Benton, T. Carter, R. Hollick, K. Holmes, A. Riner, Ruth Lynfield, Anita Glennen, C. Holtzman, R. Danila, K. MacInnes, K. Scherzinger, K. Angeles, J. Bareta, L. Butler, S. Khanlian, R. Mansmann, M. Nichols, N. Bennett, S. Zansky, S. Currenti, S. McGuire, A. Thomas, M. Schmidt, J. Thompson, T. Poissant, W. Schaffner, B. Barnes, K. Leib, K. Dyer, L. McKnight, R. Gierke, O. Almendares, J. Hudson, L. McGlone, Tamara Pilishvili, G. Langley, and Cynthia Whitney for their contributions to establishment and maintenance of the ABCs system; Rebecca Gladstone, Stephen Bentley, and Paulina Hawkins for providing genome sequences through the Global Pneumococcal Sequencing Project (http://www.pneumogen.net) from isolates obtained during 1998–1999, 2009, and 2012; the Minnesota Department of Public Health laboratory for performing susceptibility testing of all isolates from Minnesota; and Robert E. Gertz, Jr for providing insights into CDC pneumococcal typing serum factors.

This study was supported by the Centers for Disease Control and Prevention and used data from the *Streptococcus pneumoniae* MLST website (http://pubmlst.org/_spneumoniae) at the University of Oxford (Oxford, UK).

Development of the *Streptococcus pneumoniae* MLST website was supported by the Wellcome Trust.

Dr. Chochua is a researcher in the Streptococcus Laboratory, National Center for Immunization and Respiratory Diseases, Centers for Disease Control and Prevention, Atlanta, GA. Her research interests are next-generation sequencing, characterization of clinical streptococcal isolates, antimicrobial resistance, genetic adaptations, and outbreak responses.

References

1. Pilishvili T, Lexau C, Farley MM, Hadler J, Harrison LH, Bennett NM, et al.; Active Bacterial Core Surveillance/Emerging Infections Program Network. Sustained reductions in invasive pneumococcal disease in the era of conjugate vaccine. J Infect Dis. 2010;201:32–41. http://dx.doi.org/10.1086/648593
2. Moore MR, Link-Gelles R, Schaffner W, Lynfield R, Lexau C, Bennett NM, et al. Effect of use of 13-valent pneumococcal conjugate vaccine in children on invasive pneumococcal disease in children and adults in the USA: analysis of multisite, population-based surveillance. Lancet Infect Dis. 2015;15:301–9. http://dx.doi.org/10.1016/S1473-3099(14)71081-3
3. Beall B, McEllistrem MC, Gertz RE Jr, Boxrud DJ, Besser JM, Harrison LH, et al.; Active Bacterial Core Surveillance/Emerging Infections Program Network. Emergence of a novel penicillin-nonsusceptible, invasive serotype 35B clone of *Streptococcus pneumoniae* within the United States. J Infect Dis. 2002;186:118–22. http://dx.doi.org/10.1086/341072
4. Gertz RE Jr, Li Z, Pimenta FC, Jackson D, Juni BA, Lynfield R, et al. Increased penicillin-nonsusceptibility of nonvaccine serotype (other than 19A and 6A) invasive pneumococci in post 7 valent conjugate vaccine era. J Infect Dis. 2010;201:770–5. http://dx.doi.org/10.1086/650496
5. Sharma D, Baughman W, Holst A, Thomas S, Jackson D, da Gloria Carvalho M, et al. Pneumococcal carriage and invasive disease in children before introduction of the 13-valent conjugate vaccine: comparison with the era before 7-valent conjugate vaccine. Pediatr Infect Dis J. 2013;32:e45–53. http://dx.doi.org/10.1097/INF.0b013e3182788fdd
6. Metcalf BJ, Gertz RE Jr, Gladstone RA, Walker H, Sherwood LK, Jackson D, et al.; Active Bacterial Core surveillance team. Strain features and distributions in pneumococci from children with invasive disease before and after 13-valent conjugate vaccine implementation in the USA. Clin Microbiol Infect. 2016;22:60.e9–29. http://dx.doi.org/10.1016/j.cmi.2015.08.027
7. Desai AP, Sharma D, Crispell EK, Baughman W, Thomas S, Tunali A, et al. Decline in pneumococcal nasopharyngeal carriage of vaccine serotypes after the introduction of the 13-valent pneumococcal conjugate vaccine in children in Atlanta, Georgia. Pediatr Infect Dis J. 2015;34:1168–74. http://dx.doi.org/10.1097/INF.0000000000000849

8. Kaur R, Casey JR, Pichichero ME. Emerging *Streptococcus pneumoniae* strains colonizing the nasopharynx in children after 13-valent pneumococcal conjugate vaccination in comparison to the 7-valent era, 2006–2015. Pediatr Infect Dis J. 2016;35:901–6. http://dx.doi.org/10.1097/INF.0000000000001206
9. Kawaguchiya M, Urushibara N, Kobayashi N. Multidrug resistance in non-PCV13 serotypes of *Streptococcus pneumoniae* in northern Japan, 2014. Microb Drug Resist. 2017;23:206–14. http://dx.doi.org/10.1089/mdr.2016.0054
10. McElligott M, Vickers I, Meehan M, Cafferkey M, Cunney R, Humphreys H. Noninvasive pneumococcal clones associated with antimicrobial nonsusceptibility isolated from children in the era of conjugate vaccines. Antimicrob Agents Chemother. 2015;59:5761–7. http://dx.doi.org/10.1128/AAC.00990-15
11. Golden AR, Adam HJ, Gilmour MW, Baxter MR, Martin I, Nichol KA, et al. Assessment of multidrug resistance, clonality and virulence in non–PCV-13 *Streptococcus pneumoniae* serotypes in Canada, 2011–13. J Antimicrob Chemother. 2015;70:1960–4.
12. Metcalf BJ, Chochua S, Gertz RE Jr, Li Z, Walker H, Tran T, et al.; Active Bacterial Core surveillance team. Using whole genome sequencing to identify resistance determinants and predict antimicrobial resistance phenotypes for year 2015 invasive pneumococcal disease isolates recovered in the United States. Clin Microbiol Infect. 2016;22:1002.e1–8. http://dx.doi.org/10.1016/j.cmi.2016.08.001
13. Beall B, McEllistrem MC, Gertz RE Jr, Wedel S, Boxrud DJ, Gonzalez AL, et al.; Active Bacterial Core Surveillance Team. Pre- and postvaccination clonal compositions of invasive pneumococcal serotypes for isolates collected in the United States in 1999, 2001, and 2002. J Clin Microbiol. 2006;44:999–1017. http://dx.doi.org/10.1128/JCM.44.3.999-1017.2006
14. Beall BW, Gertz RE, Hulkower RL, Whitney CG, Moore MR, Brueggemann AB. Shifting genetic structure of invasive serotype 19A pneumococci in the United States. J Infect Dis. 2011;203:1360–8. http://dx.doi.org/10.1093/infdis/jir052
15. Li Y, Metcalf BJ, Chochua S, Li Z, Gertz RE Jr, Walker H, et al. Penicillin-binding protein transpeptidase signatures for tracking and predicting β-lactam resistance levels in *Streptococcus pneumoniae.* MBio. 2016;7:e00756–16. http://dx.doi.org/10.1128/mBio.00756-16
16. Clinical and Laboratory Standards Institute (CLSI). Performance standards for antimicrobial susceptibility testing. Twenty-third informational supplement (M100–S22.CLSI). Wayne (PA): The Institute; 2013.
17. Martin M. Cutadapt removes adapter sequences from high-throughput sequencing reads. EMBnet. 2011;17:10–2. http://dx.doi.org/10.14806/ej.17.1.200
18. Zerbino DR, Birney E. Velvet: algorithms for de novo short read assembly using de Bruijn graphs. Genome Res. 2008;18:821–9. http://dx.doi.org/10.1101/gr.074492.107
19. Gardner SN, Slezak T, Hall BG. kSNP3.0: SNP detection and phylogenetic analysis of genomes without genome alignment or reference genome. Bioinformatics. 2015;31:2877–8. http://dx.doi.org/10.1093/bioinformatics/btv271
20. Stamatakis A. RAxML version 8: a tool for phylogenetic analysis and post-analysis of large phylogenies. Bioinformatics. 2014;30:1312–3. http://dx.doi.org/10.1093/bioinformatics/btu033
21. Feil EJ, Li BC, Aanensen DM, Hanage WP, Spratt BG. eBURST: inferring patterns of evolutionary descent among clusters of related bacterial genotypes from multilocus sequence typing data. J Bacteriol. 2004;186:1518–30. http://dx.doi.org/10.1128/JB.186.5.1518-1530.2004
22. Barocchi MA, Ries J, Zogaj X, Hemsley C, Albiger B, Kanth A, et al. A pneumococcal pilus influences virulence and host inflammatory responses. Proc Natl Acad Sci U S A. 2006;103:2857–62. http://dx.doi.org/10.1073/pnas.0511017103
23. Coffey TJ, Daniels M, Enright MC, Spratt BG. Serotype 14 variants of the Spanish penicillin-resistant serotype 9V clone of *Streptococcus pneumoniae* arose by large recombinational replacements of the *cpsA-pbp1a* region. Microbiology. 1999;145:2023–31. http://dx.doi.org/10.1099/13500872-145-8-2023
24. Brueggemann AB, Pai R, Crook DW, Beall B. Vaccine escape recombinants emerge after pneumococcal vaccination in the United States. PLoS Pathog. 2007;3:e168. http://dx.doi.org/10.1371/journal.ppat.0030168
25. Wyres KL, Lambertsen LM, Croucher NJ, McGee L, von Gottberg A, Liñares J, et al. Pneumococcal capsular switching: a historical perspective. J Infect Dis. 2013;207:439–49. http://dx.doi.org/10.1093/infdis/jis703
26. Mavroidi A, Aanensen DM, Godoy D, Skovsted IC, Kaltoft MS, Reeves PR, et al. Genetic relatedness of the *Streptococcus pneumoniae* capsular biosynthetic loci. J Bacteriol. 2007;189:7841–55. http://dx.doi.org/10.1128/JB.00836-07
27. Golubchik T, Brueggemann AB, Street T, Gertz RE Jr, Spencer CC, Ho T, et al. Pneumococcal genome sequencing tracks a vaccine escape variant formed through a multi-fragment recombination event. Nat Genet. 2012;44:352–5. http://dx.doi.org/10.1038/ng.1072
28. Enright MC, Spratt BG. Extensive variation in the *ddl* gene of penicillin-resistant *Streptococcus pneumoniae* results from a hitchhiking effect driven by the penicillin-binding protein 2b gene. Mol Biol Evol. 1999;16:1687–95. http://dx.doi.org/10.1093/oxfordjournals.molbev.a026082
29. Kauffmann F, Mørch E, Schmith K. On the serology of the pneumococcus-group. J Immunol. 1940;39:397–426.
30. Lund E. On the nomenclature of the pneumococcal types. Int J Syst Bacteriol. 1970;20:321–3. http://dx.doi.org/10.1099/00207713-20-3-321
31. Henrichsen J. Six newly recognized types of *Streptococcus pneumoniae.* J Clin Microbiol. 1995;33:2759–62.
32. Kim L, McGee L, Tomczyk S, Beall B. Biological and epidemiological features of antibiotic-resistant *Streptococcus pneumoniae* in pre- and post-conjugate vaccine eras: a United States perspective. Clin Microbiol Rev. 2016;29:525–52. http://dx.doi.org/10.1128/CMR.00058-15
33. Olarte L, Kaplan SL, Barson WJ, Romero JR, Lin PL, Tan TQ, et al. Emergence of multidrug-resistant pneumococcal serotype 35B among children in the United States. J Clin Microbiol. 2017;55:724–34. http://dx.doi.org/10.1128/JCM.01778-16
34. Moore MR, Gertz RE Jr, Woodbury RL, Barkocy-Gallagher GA, Schaffner W, Lexau C, et al. Population snapshot of emergent *Streptococcus pneumoniae* serotype 19A in the United States, 2005. J Infect Dis. 2008;197:1016–27. http://dx.doi.org/10.1086/528996
35. Sobanjo-ter Meulen A, Vesikari T, Malacaman EA, Shapiro SA, Dallas MJ, Hoover PA, et al. Safety, tolerability and immunogenicity of 15-valent pneumococcal conjugate vaccine in toddlers previously vaccinated with 7-valent pneumococcal conjugate vaccine. Pediatr Infect Dis J. 2015;34:186–94. http://dx.doi.org/10.1097/INF.0000000000000516

Address for correspondence: Bernard Beall, Centers for Disease Control and Prevention, 1600 Clifton Rd NE, Mailstop C02, Atlanta, GA 30329-4017, USA: email bbeall@cdc.gov

Serologic and Molecular Evidence of Vaccinia Virus Circulation among Small Mammals from Different Biomes, Brazil

Júlia B. Miranda, Iara A. Borges, Samantha P.S. Campos, Flávia N. Vieira, Tatiana M.F. de Ázara, Fernanda A. Marques, Galileu B. Costa, Ana Paula M.F. Luis, Jaqueline S. de Oliveira, Paulo César P. Ferreira, Cláudio Antônio Bonjardim, Silvio L.M. da Silva, Álvaro E. Eiras, Jônatas S. Abrahão, Erna G. Kroon, Betânia P. Drumond, Adriano P. Paglia, Giliane de S. Trindade

Vaccinia virus (VACV) is a zoonotic agent that causes a disease called bovine vaccinia, which is detected mainly in milking cattle and humans in close contact with these animals. Even though many aspects of VACV infection have been described, much is still unknown about its circulation in the environment and its natural hosts/reservoirs. To investigate the presence of *Orthopoxvirus* antibodies or VACV DNA, we captured small rodents and marsupials in 3 areas of Minas Gerais state, Brazil, and tested their samples in a laboratory. A total of 336 animals were tested; positivity ranged from 18.1% to 25.5% in the 3 studied regions located in different biomes, including the Atlantic Forest and the Cerrado. Analysis of nucleotide sequences indicated co-circulation of VACV groups I and II. Our findings reinforce the possible role played by rodents and marsupials in VACV maintenance and its transmission chain.

Virus species belonging to genus *Orthopoxvirus* (OPV) receive great attention because of *Variola virus* (VARV), which is associated with smallpox (*1*). Smallpox caused many deaths worldwide and was eradicated after a massive vaccination campaign developed by the World Health Organization (*2*). Because OPVs have very similar antigenic structure (*1*), cross-protection enabled the use of cowpox virus (CPXV) and later vaccinia virus (VACV) as anti-smallpox vaccine agents (*2*).

Given its widespread use, VACV has been studied for many years, and these efforts shed light on various aspects regarding virus biology. After smallpox eradication, vaccination was discontinued (*2*), and only select institutions in the United States (e.g., the military and certain public health facilities) receive the vaccine for their efforts to prevent the use of VARV as a biologic weapon. Household transmission from vaccinees and eczema vaccinatum are some of the negative aspects of vaccinating and have been responsible for severe outcomes (*3*). Although VARV is now restricted to laboratory facilities, other OPVs have been emerging as zoonotic pathogens in different geographic areas, namely CPXV in Europe, monkeypox virus (MPXV) in Africa, and VACV in Asia and South America (*4*).

In Brazil, natural infections with VACV are called bovine vaccinia (BV) and are reported in rural areas, mainly in milking cattle and in men who are in close contact with these animals. The first officially recorded reports of BV date from the early 2000s and occurred in the southeastern region of Brazil (*5*,*6*). Currently, there is evidence of virus circulation in all regions of Brazil (*7*,*8*); however, the southeast is still the epicenter of registered BV cases, with Minas Gerais state being one of the most affected. Studies have shown that mammal species in addition to bovids and humans could be naturally infected by (or at least exposed to) VACV (*9*–*19*). VACV was isolated from samples from a rodent from the Amazon region in the 1960s (*9*), and now there are other documented incidents of virus circulation in these animals (*10*–*12*,*15*,*17*). By taking into account virus detection in small rodents, the fact that CPXV (*20*) and probably MPXV have rodents as reservoirs (*21*), and the frequent reports of these animals' presence during BV outbreaks, an ecologic model was created to propose the participation of rodents in the VACV transmission chain (*12*). Because some species of native rodents could have ecologic advantages in areas with anthropic disturbance, they could work as bridges between natural and human/domestic habitats, bringing viruses from wild animals to domestic ones and vice versa (*12*). This model is reinforced by studies of virus transmission between mice and from experimental infection through contaminated

Author affiliations: Universidade Federal de Minas Gerais, Belo Horizonte, Brazil (J.B. Miranda, I.A. Borges, S.P.S. Campos, F.N. Vieira, T.M.F de Ázara, F.A. Marques, G.B. Costa, A.P.M.F. Luis, J.S. de Oliveira, P.C.P. Ferreira, C.A. Bonjardim, A.E. Eiras, J.S. Abrahão, E.G. Kroon, B.P. Drumond, A.P. Paglia, G.D.S. Trindade); Instituto Federal de Educação, Ciência e Tecnologia do Sudeste de Minas Gerais, Rio Pomba, Brazil (S.L.M. da Silva)

DOI: https://dx.doi.org/10.3201/eid2306.161643

milk (*22*). To better evaluate the circulation of VACV in small rodents, we undertook comprehensive collection campaigns in 3 areas of Minas Gerais with or without confirmed BV outbreaks. Animals were evaluated for the presence of VACV DNA and antibodies against OPV. Because marsupials were often captured and previous studies have detected OPV antibodies and VACV DNA in these animals (*17*,*19*), their samples were also tested.

Methods

Collection Sites

We collected small mammals in 3 areas of Minas Gerais. Brazil was chosen because of its history of BV outbreaks and its different biomes and conservational status (Figure 1, panel A). The 3 municipalities where collections were performed were Sabará, Serro, and Rio Pomba.

Sabará is a city located in an anthropic area situated in the transition from savannah (the Cerrado biome) to the Atlantic Forest. The study site (19°53′9″S, 43°48′45″W) was delimited on the grounds of a former educational institution in a previous study (Figure 1, panel B). Three sampling transects were demarcated: 1 in savannah vegetation with intense anthropogenic disturbance and the other 2 in forest vegetation (with 1 of the 2 having more disturbance than the other) (Figure 1, panel B). In each transect, 15 sampling points were established with 2 live traps in each, 20 m apart, where captures of small mammal took place.

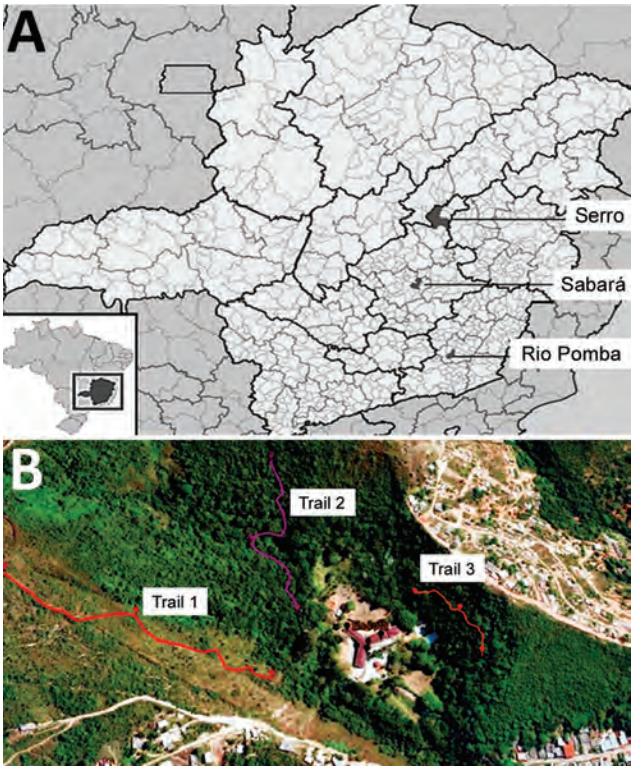

Figure 1. Locations of study areas, Minas Gerais state, Brazil. A) Locations of the 3 municipalities where collections were performed: Sabará, Serro, and Rio Pomba. Inset shows location of Minas Gerais state in southeastern Brazil. B) Identification of 3 sample transects in Sabará. Trail 1 has savannah vegetation, and trails 2 and 3 have Atlantic Forest vegetation. Sources: panel A, Scribble Maps; panel B, T.M.F. de Ázara. A color version of this figure is available online (http://wwwnc.cdc.gov/EID/article/23/6/16-1643-F1.htm).

In Rio Pomba, the field site (21°16′29″S, 43°10′45″W) has characteristic Atlantic Forest vegetation. Animal trapping was performed in the area around the Instituto Federal de Educação, Ciência e Tecnologia (Figure 2, panels A, B). Animal collections were performed in forest, pasture, and peridomicile areas (Figure 2, panels A–G). In each transect, 10 traps were placed at a distance of 10 m from each other and in alternating positions (on forest floor or on tree trunks).

Serro, a city whose economy is based on milk and cheese production, has seen many cases of BV since 2005 (*23*). The capture of small mammals was carried out in 2 farms (Figure 2, panels C, D). The study site (180°36′21.16″S, 43°23′12.89″W) is situated in the Cerrado biome and has some intersections of Atlantic Forest. Animal collections were carried out in forest, pasture, and peridomicile areas (Figure 2, panels A–G), and traps were positioned in the same manner as in Rio Pomba.

Animal Trap and Sample Collection

Captures lasted from April 2011 through May 2012 for Sabará (12 campaigns) and from September 2012 through September 2013 in Serro (5 campaigns) and Rio Pomba (6 campaigns). Small mammals were captured in size-selective live cages by using pineapple chunks and cotton balls soaked in cod liver oil as baits. Each sampling section lasted for 4 nights, and baits were replaced after 2 nights. After capture, animals were anesthetized with ketamine (70 mg/kg) and xylazine (12 mg/kg) for serum collection. Animals were weighed, measured for size, and visually evaluated for clinical signs of disease, such as skin lesions. For organ collection, animals were euthanized by intracardiac injection of 3 times the anesthetic dose according to guidelines of the American Society of Mammalogists (*24*). Collections were authorized by the Environment Ministry of Brazil through the SISBIO system (license no. 20807–2).

Biosafety

All collections were performed by trained professionals (either veterinarians or biologists) according to US Centers for Disease Control and Prevention recommendations (*25*). During animal manipulation, personal protective equipment (disposable coveralls, surgical gloves, goggles, and N98 masks) was used.

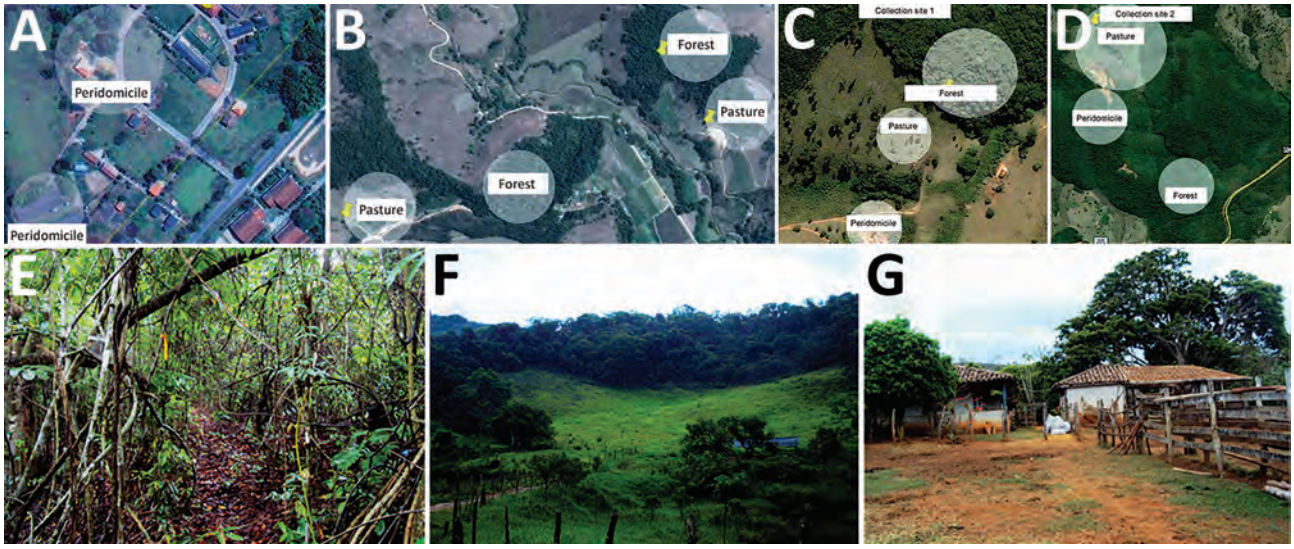

Figure 2. Location of collection sites and biomes represented in each, Minas Gerais state, Brazil. A) Collection site 1 in Serro. B) Collection site 2 in Serro. C) Peridomicile collection areas in Rio Pomba. D) Forest and pasture collection areas in Rio Pomba. E) Example of a forest area where animals were captured. F) Example of peridomicile area. G) Example of pasture area. In panels A–D, circles represent areas where transects for capture were demarcated. Sources: panels A,–D, Google Maps, modified by F.V. Nunes; panels E–G, F.V. Nunes. A color version of this figure is available online (http://wwwnc.cdc.gov/EID/article/23/6/16-1643-F2.htm).

DNA Extraction from Organs

In addition to serum, which was tested by real-time PCR (rPCR) targeting the C11R viral growth factor gene without DNA extraction, liver was the chosen organ for rPCR trials. The organs were macerated with mortar and pestle after liquid nitrogen was added, and DNA was extracted with PureLink Genomic DNA Mini Kit (Invitrogen, Carlsbad, CA, USA) as recommended by the manufacturer. The same protocol was applied for other organs tested, including intestine, bladder, heart, gonads (ovary/testicles), bone marrow, spleen, lung, diaphragm, and kidney.

Cells and Virus

A VACV Western Reserve strain was used as a positive control. BSC-40 cells were grown in Eagle's minimum essential medium (Invitrogen) supplemented with 5% fetal bovine serum (Cultilab, São Paulo, Brazil); 25 mg/mL Fungizone (amphotericin B) (Cristália, São Paulo, Brazil); 500 U/mL penicillin; and 50 mg/mL gentamicin (Schering-Plough, São Paulo, Brazil).

rPCR Assays

All rPCR experiments were performed in 48-well plates in Step One machines (Applied Biosystems, Foster City, CA, USA) by using SYBR Green Master Mix (Applied Biosystems). DNA from liver samples was diluted in water for a final use concentration of 10 ng/μL and 50 ng/μL. For serum samples, a 1:10 or 1:100 dilution was performed, and samples were tested without previous DNA extraction. For both liver and serum samples, amplification of the C11R gene was tested, and liver samples were additionally tested for amplification of the A56R hemagglutinin gene (primer sequences available upon request). For C11R, an amplicon of 82 bp and a melting temperature of 74.99°C were expected, and for A56R, a sequence of 160 bp and a melting temperature of 74.41°C were expected. All reactions had a final volume of 10 μL, and samples were tested in duplicates. Reaction steps comprised initial DNA denaturation at 95°C for 10 min, 40 cycles of denaturation (95°C for 15 s), annealing/extension (60°C for 60 s), and a melting curve (95°C for 15 s, 60°C for 60 s, and 95°C for 15 s). Samples were considered positive when melting temperature varied only up to 1°C compared with a positive control (10 ng of DNA extracted from purified VACV Western Reserve strain) and had amplification in duplicate or for >1 target. Samples with a single amplification were retested and considered equivocal when no more amplification was observed.

Nucleotide Sequencing and Sequence Analyses

Positive samples that could be reamplified (A56R-positive) or amplified by a conventional PCR targeting C11R (C11R-positive) (*26*) were chosen for sequencing. For A56R, product from the previous reaction was reamplified in a conventional PCR reaction using 1 μL of the first reaction as input and 0.2 nmol/L (A56R) rPCR primers. PCR cycling for A56R gene consisted of 10 min at 95°C for denaturation, 30 cycles of denaturation (95°C for 10 min), annealing (60°C for 60 s), extension (72°C for 60 s), and a final extension of 10 min at 72°C. Products with single bands were directly sequenced, and products with multiple bands had the target gene extracted from acrylamide gels

stained with SYBR Gold Nucleic Acid Gel Stain (Invitrogen) and had its DNA purified. Nucleotide sequencing was performed by dideoxy method in an ABI3130 platform (Applied Biosystems), and sequence quality was analyzed by using Sequence Scanner Software 1.0 (Applied Biosystems). Sequences were aligned with other reference sequences from the BLAST nucleotide database (http://blast.ncbi.nlm.nih.gov/Blast.cgi) by using MEGA 6.0; the same program was used for identity matrix construction (*27*).

Plaque-Reduction Neutralization Test

The plaque-reduction neutralization test (PRNT) protocol has been described previously by Geessien Kroon et al. (*28*). Samples were considered positive when a reduction of ≥50% in virus plaque numbers was observed.

ELISA

ELISA was performed for rodent blood samples following a protocol also described previously (*28*). For each plate, 1 positive control (serum from *Mus musculus* experimentally infected with VACV-Guarani P1) (*29*) and 3 negative controls (serum of noninfected *M. musculus*) were added. Cutoff was established as the mean of negative controls optical density units plus 3 times their SD. Samples with an optical density 10% above or below the cutoff were considered equivocal.

Interaction Networks

Interaction networks are useful to help with understanding of virus-host dynamics. Each species is represented by a vertex, and the link between 2 vertices represents the interaction between 2 different species, making it possible to analyze their interdependence (*30*). The networks also show which species have the higher number of positive samples for virus detection and the area where they were collected. By using data from VACV-positive small mammal species, we created weighted networks with the program Pajek 4.07 (*31*). Accordingly, adjacency matrices were generated for each study area in which hosts were represented by lines and VACV by columns.

Results

rPCR Amplification of VACV DNA from Free-living Small Mammals

A total of 325 animals had their samples tested by rPCR targeting the C11R gene, the A56R gene, or both. Of these animals, 21 (6.4%) tested positive (i.e., amplification in duplicates or in >1 sample/target) and 58 (17.8%) equivocal (online Technical Appendix Table 1, https://wwwnc.cdc.gov/EID/article/23/6/16-1643-Techapp1.pdf). The cycle thresholds varied from 28.42 to 39.33. From the total animals tested by rPCR, 114 had samples available for all tests (C11R targeted in liver and serum and A56R in liver). One animal was positive in the 3 tests performed, 11 in 2 tests, and 5 in only 1 test (data not shown). For the remaining positive animals, ≥1 assays could not be performed, and 1 sample type was positive in 1 test.

Of all the animals from the different collection sites in Sabará, 11/48 (22.9%) rodents and 3/76 (3.9%) marsupials were positive by rPCR. For Serro, no marsupials were positive but 4/25 (16.0%) rodents were positive. For Rio Pomba, 2/137 (1.4%) of rodents and 1/18 (5.5%) of marsupials were positive (online Technical Appendix Table 1).

Four rPCR-positive animals (2 rodents and 2 marsupials) were selected for viral DNA detection in different organs by rPCR targeting the C11R and A56R genes. Positivity was found for heart, spleen, intestines, bladder, lungs, kidneys, and gonads (online Technical Appendix Table 2). No amplification was observed in any bone marrow or diaphragm samples tested.

OPV Antibodies in Serum from Free-living Small Mammals Tested by PRNT

PRNT tests were performed in a total of 314 serum samples, and from these, 33 were considered positive, corresponding to 10.5% of the animals. The reduction percentages varied from 50.5% to 95.6%. For the Sabará collection, positivity was 9.0% (10/111), 14.3% (6/42) for rodents and 5.8% (4/69) for marsupials. For Serro, positivity was 4.2% (2/47), and only rodent samples were positive, corresponding to 8.0% (2/25) of rodents tested. For Rio Pomba, positivity was 13.4% (21/156), 14.3% (20/139) for rodents and 5.8% (1/17) for marsupials (online Technical Appendix Table 1).

OPV Antibodies in Serum from Free-living Small Mammals Tested by ELISA

ELISA tests were performed on 189 rodent serum samples; a control serum for marsupials was not available. Of the animals tested, 19/189 (10.0%) were positive and 11/189 (5.8%) equivocal (online Technical Appendix Table 1). By location, 3/35 (8.5%) animals from Sabará, 9/25 (36.0%) from Serro, and 7/129 (5.4%) from Rio Pomba were positive.

Sequencing

Two PCR amplicons, amplified from Sabará animals, were sequenced with C11R primers and resulted in sequences of 168 bp that were aligned with VACVs in Brazil and other OPVs (online Technical Appendix Figure 1). These 2 sequences had 100% similarity with each other; similarity with VACVs in Brazil ranged from 98.2% to 100% and with CPXV from 87.3% to 89.1%, whereas similarity with VARV was 94.5% and with MPXV 90.9% (data not shown). For A56R, sequencing was performed

in positive rPCR samples and resulted in 6 sequences of 102 bp. When compared with OPV sequences, 2 samples from Sabará had an 18-nt deletion shared by Brazil VACV group I, whereas the other 4 samples from Sabará, Serro, and Rio Pomba did not have that deletion, being more similar to Brazil VACV group II and other OPVs (online Technical Appendix Figure 2).

Geographic and Species Distribution of Positivity

For all areas studied, 336 animals belonging to 18 genera had their samples tested by rPCR, PRNT, and/or ELISA, and 65 (19.3%) were positive in ≥1 of these tests. Total positivity was 18.1% for Sabará, 25.5% for Serro, and 18.5% for Rio Pomba (online Technical Appendix Table 1). A higher positivity was observed for rodents (25.7%) than for marsupials (7.6%) (data not shown).

Species identified among the test-positive rodents were *Calomys* sp., *Akodon* sp., *Necromys lasiurus*, *Trinomys setosus*, *Cerradomys subflavus*, *Oligoryzomys* sp., *Nectomys squamipes*, *Mus musculus*, and *Rattus rattus*. For marsupials, the positive animals were characterized as species/genera *Didelphis* sp., and *Caluromys philander* (online Technical Appendix Table 3).

Test-positive animals were captured in all sample areas in Sabará (savannah and forest) and Serro (pasture, forest, and peridomicile areas), whereas test-positive animals in Rio Pomba were captured in pasture and forest. The interaction network for Sabará illustrates that 4 species had positive samples, with 3 of them found either in forest or savannah and the other in both areas. *N. lasiurus* (the hairy-tailed bolo mouse) had the highest number of positive samples in Sabará (Figure 3, panel A). For Serro, evidence of VACV circulation was found in 6 species; of these, 2 were captured in forest, 2 in pasture, and 2 in peridomicile areas. The species with the largest number of positive samples in Serro was *T. setosus* (the hairy Atlantic spiny rat; Figure 3, panel B). For Rio Pomba, 5 genera were positive, including *Akodon* sp. mice captured in pasture and forest, *Calomys tener* and *N. lasiurus* mice captured in forest, and *C. philander* and *Didelphis aurita* opossums captured in pasture. The species with the highest number of positive animals in Rio Pomba was *C. tener* (the delicate vesper mouse), followed by *N. lasiurus* and *Akodon* sp. mice (Figure 3, panel C).

Discussion

In our study, we analyzed different biomes in an area where BV infections are common, and the positivity rates found for VACV were 25.7% for rodents and 7.6% for marsupials. Even though VACV is known to circulate in Brazil and cause a disease that leads to economic, social, and public health effects, few studies have been conducted with the aim of clarifying the VACV transmission chain and potential natural hosts (*9*–*19*,*22*,*32*). Previous studies showed antibody positivity of 8.7%–17.9% for wild rodents captured in places with or without documented BV (*15*,*17*) and seropositivity of 8.2% for *Didelphis* spp. marsupials (*17*).

The higher positivity rate found for rodents in our study could be attributable to the use of 3 different techniques, including 2 techniques for detecting antibodies (PRNT and ELISA) and 2 targets for DNA detection (rPCR).The 3 techniques used to assess virus circulation provide distinct responses about infection stages. Whereas rPCR indicates the presence of viral DNA, the ELISA used in our study reveals the presence of IgG (indicative of previous infection) (*33*), and PRNT detects neutralizing antibodies that can be of different types, including IgG and IgM, which are produced early in the infection process (*34*). Because we found positive animals for ≥1

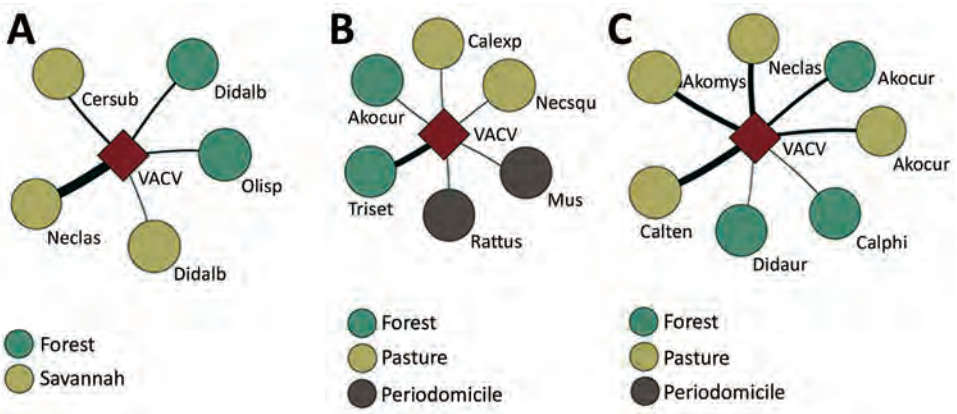

Figure 3. Interaction networks for vaccina virus among small mammals in Sabará (A), Serro (B), and Rio Pomba (C) in Minas Gerais state, Brazil. The square represents vaccinia virus. Circles represent small mammal species (labeled). The color in the circles represents the area where mammals were collected. The thickness of lines increases with the number of positive samples from a species. Acokur, *Akodon cursor* mouse; Akomys, *Akodon* cf; mystax; Calexp, *Calomys expulsus*; Calphi, *Caluromys philander*; Calten, *Calomys tener*; Cersub, *Cerradomys subflavus*; Didalb, *Didelphis albiventris*; Didaur, *Didelphis aurita*; Mus, *Mus musculus*; Neclas, *Necromys lasiurus*; Necsqui, *Nectomys squamipes*; Olisp, *Oligoryzomys* sp.; Rattus, *Rattus rattus*; Triset, *Trinomys setosus*; VACV, vaccinia virus. A color version of this figure is available online (http://wwwnc.cdc.gov/EID/article/23/6/16-1643-F3.htm).

techniques, we can speculate that an active transmission cycle is happening in all 3 study areas. Additionally, only Serro has recurrent reports of BV outbreaks (*23*,*29*), which could be a result of the presence of positive animals in the peridomicile area, where they could infect other animals, such as cows, and cause disease. Furthermore, because large-scale milk production occurs in Serro, many livestock animals, including bovines, could work as infection amplifiers.

The rPCR technique has been used for MPXV detection in rodents in Africa, where samples were considered equivocal when repeatability of results was not achieved (*21*). In our study, we made this same observation, which might be attributable to a low virus load in the samples. In turn, the low virus load could be related to the late cycle threshold in which amplification occurred and a lack of clinical signs in animals with a positive result.

Sequencing of A56R rPCR amplicons revealed the cocirculation of Brazil VACVs belonging to groups I and II, a fact that reinforces previous data on Brazil VACV virus diversity (*11*,*35*–*37*). Again, even when infected with virus belonging to group II, which were found to be virulent in a mice model (*38*), wild rodents and marsupials tested in our study did not have clinical signs detected. Also, these animals infected with VACV group I or II had viral DNA in many organs, as indicated by rPCR. It is not possible to assert that virus is replicating in these tissues, given that virus could be present in blood that circulates through these organs; however, previous in vivo infection experiments have found virus in different mice organs (*32*), probably because of systemic infection. This observation also was made in mice infected with milk (a possible route of natural infection) contaminated with VACV-Guarani P2 virus. This virus was found to be nonvirulent in a mice model; animals shed viral DNA and produced OPV antibodies but did not show clinical signs (*22*). The detection of virus DNA in intestines, bladder, and gonads could reinforce previous data suggesting that virus transmission occurs through feces (*39*) and support the hypothesis of alternative transmission through urine and sexual contact. Mariana virus has been isolated from the gonads of mice (*14*), so it could be speculated that the sexual transmission route is involved.

Among the positive rodent species, *Akodon* sp., *N. squamipes*, *Oligoryzomys* sp. (*15*,*17*), and *M. musculus* (*12*) have already been found to be positive in previous studies, reinforcing evidence of its participation in the VACV transmission cycle; however, the exact role played by these animals is not yet known. In addition to *M. musculus*, *C. subflavus*, *N. lasiurus*, *T. setosus*, *C. tener*, and *R. rattus* rodents were also found to be positive in our study, indicating the role of multiple hosts in VACV transmission in Brazil. Among the marsupials, *Didelphis* spp. opossums had already been found to be positive (*17*,*19*), and *C. philander* opossums also had positive samples.

Although only 1 virus (VACV) was analyzed for interaction network construction and no interactions between different species were observed, the networks created illustrate the participation of the small mammals for each studied area and the areas where these positive animals were collected (Figure 3). The networks also suggest an important role of *N. lasiurus* mice for the VACV transmission chain in Sabará, *T. setosus* rats in Serro, and *C. tener*, *N. lasiurus*, and *Akodon* sp. mice in Rio Pomba. Most of these species are generalist animals that can be adapted to a disturbed environment. However, the *C. philander* opossum is an arboreal species that lives in forests (*40*), which could indicate that a wild cycle is being maintained and that other animals could be transporting the virus between forests and peridomicile areas. These findings corroborate the models proposed by Abrahão et al. (*12*) in which rodents and other small mammals could work as links between natural and anthropic environments.

In conclusion, our findings reinforce evidence of participation of rodents and marsupials in the VACV transmission cycle and the possibility that these animals might work as links between natural and anthropic environments. These findings also further illustrate the multi-host characteristic of VACV infection in Brazil.

Acknowledgments

We hank Mylleus and Plataforma de Sequenciamento FIOCRUZ for sequencing. The VACV Western Reserve strain was kindly provided by C. Jungwirth of Universitat Wurzburg, Germany.

Financial support was provided by Departamento de Microbiologia, CNPq, CAPES, PRPq-UFMG, FAPEMIG, and MAPA. G.S.T., E.G.K., A.E.E., J.S.A., and A.P. are researchers from CNPq.

Ms. Miranda is graduated in biological sciences from the Universidade Federal de Minas Gerais and completed her master's degree at the same university working with emerging viral diseases. Her primary research interests are emerging diseases and viral ecology.

References

1. Moss B. Poxviridae. In: Knipe DM, Howley PM, editors. Fields virology, 6th ed. Philadelphia: Lippincott Williams & Wilkins; 2013. p. 2129–59.
2. Fenner F, Wittek R, Dumbell KR. The global spread, control and eradication of smallpox. In: The orthopoxviruses. San Diego (CA): Academic Press; 1989. p. 317–52.
3. Vora S, Damon I, Fulginiti V, Weber SG, Kahana M, Stein SL, et al. Severe eczema vaccinatum in a household contact of a smallpox vaccinee. Clin Infect Dis. 2008;46:1555–61. http://dx.doi.org/10.1086/587668

4. Essbauer S, Pfeffer M, Meyer H. Zoonotic poxviruses. Vet Microbiol. 2010;140:229–36. http://dx.doi.org/10.1016/j.vetmic.2009.08.026
5. Damaso CRA, Esposito JJ, Condit RC, Moussatché N. An emergent poxvirus from humans and cattle in Rio de Janeiro state: *Cantagalo virus* may derive from Brazilian smallpox vaccine. Virology. 2000;277:439–49. http://dx.doi.org/10.1006/viro.2000.0603
6. de Souza Trindade G, da Fonseca FG, Marques JT, Nogueira ML, Mendes LCM, Borges AS, et al. Araçatuba virus: a vaccinialike virus associated with infection in humans and cattle. Emerg Infect Dis. 2003;9:155–60. http://dx.doi.org/10.3201/eid0902.020244
7. Brum MCS, Anjos BL, Nogueira CEW, Amaral LA, Weiblen R, Flores EF. An outbreak of orthopoxvirus-associated disease in horses in southern Brazil. J Vet Diagn Invest. 2010;22:143–7. http://dx.doi.org/10.1177/104063871002200132
8. Oliveira DB, Assis FL, Ferreira PCP, Bonjardim CA, de Souza Trindade G, Kroon EG, et al. Group 1 *Vaccinia virus* zoonotic outbreak in Maranhao state, Brazil. Am J Trop Med Hyg. 2013;89:1142–5. http://dx.doi.org/10.4269/ajtmh.13-0369
9. Fonseca FG, Lanna MC, Campos MA, Kitajima EW, Peres JN, Golgher RR, et al. Morphological and molecular characterization of the poxvirus BeAn 58058. Arch Virol. 1998;143:1171–86. http://dx.doi.org/10.1007/s007050050365
10. Diniz S, Trindade GS, Fonseca FG, Kroon EG. Surto de varíola murina em camundongos suíços em biotério—Relato de caso. Arquivo Brasileiro de Medicina Veterinária e Zootecnia. 2001; 53:1–5. http://dx.doi.org/10.1590/S0102-09352001000200003
11. Trindade GS, da Fonseca FG, Marques JT, Diniz S, Leite JA, De Bodt S, et al. *Belo Horizonte virus*: a vaccinia-like virus lacking the A-type inclusion body gene isolated from infected mice. J Gen Virol. 2004;85:2015–21. http://dx.doi.org/10.1099/vir.0.79840-0
12. Abrahão JS, Guedes MICM, Trindade GS, Fonseca FG, Campos RK, Mota BF, et al. One more piece in the VACV ecological puzzle: could peridomestic rodents be the link between wildlife and bovine vaccinia outbreaks in Brazil? PLoS One. 2009;4:e7428. http://dx.doi.org/10.1371/journal.pone.0007428
13. Abrahão JS, Silva-Fernandes AT, Lima LS, Campos RK, Guedes MIMC, Cota MMG, et al. Vaccinia virus infection in monkeys, Brazilian Amazon. Emerg Infect Dis. 2010;16:976–9. http://dx.doi.org/10.3201/eid1606.091187
14. Campos RK, Brum MCS, Nogueira CEW, Drumond BP, Alves PA, Siqueira-Lima L, et al. Assessing the variability of Brazilian *Vaccinia virus* isolates from a horse exanthematic lesion: coinfection with distinct viruses. Arch Virol. 2011;156:275–83. http://dx.doi.org/10.1007/s00705-010-0857-z
15. Schatzmayr HG, Costa RVC, Gonçalves MCR, D'Andréa PS, Barth OM. Human and animal infections by vaccinia-like viruses in the state of Rio de Janeiro: a novel expanding zoonosis. Vaccine. 2011;29(Suppl 4):D65–9. http://dx.doi.org/10.1016/j.vaccine.2011.09.105
16. de Assis FL, Pereira G, Oliveira C, Rodrigues GOL, Cotta MMC, Silva-Fernandes AT, et al. Serologic evidence of orthopoxvirus infection in buffaloes, Brazil. Emerg Infect Dis. 2012;18:698–700. https://doi.org/10.3201/eid1804.111800
17. Peres MG, Bacchiega TS, Appolinário CM, Vicente AF, Allendorf SD, Antunes JMAP, et al. Serological study of vaccinia virus reservoirs in areas with and without official reports of outbreaks in cattle and humans in São Paulo, Brazil. Arch Virol. 2013;158:2433–41. http://dx.doi.org/10.1007/s00705-013-1740-5
18. Barbosa AV, Medaglia MLG, Soares HS, Quixabeira-Santos JC, Gennari SM, Damaso CR. Presence of neutralizing antibodies to *Orthopoxvirus* in capybaras (*Hydrochoerus hydrochaeris*) in Brazil. J Infect Dev Ctries. 2014;8:1646–9. http://dx.doi.org/10.3855/jidc.5216
19. Peres MG, Barros CB, Appolinário CM, Antunes JMAP, Mioni MSR, Bacchiega TS, et al. Dogs and opossums positive for vaccinia virus during outbreak affecting cattle and humans, São Paulo state, Brazil. Emerg Infect Dis. 2016;22:271–3. http://dx.doi.org/10.3201/eid2202.140747
20. McFadden G. Poxvirus tropism. Nat Rev Microbiol. 2005;3:201–13. http://dx.doi.org/10.1038/nrmicro1099
21. Reynolds MG, Carroll DS, Olson VA, Hughes C, Galley J, Likos A, et al. A silent enzootic of an orthopoxvirus in Ghana, West Africa: evidence for multi-species involvement in the absence of widespread human disease. Am J Trop Med Hyg. 2010;82:746–54. http://dx.doi.org/10.4269/ajtmh.2010.09-0716
22. Rehfeld IS, Guedes MIMC, Fraiha ALS, Costa AG, Matos ACD, Fiúza ATL, et al. *Vaccinia virus* transmission through experimentally contaminated milk using a murine model. PLoS One. 2015;10:e0127350. http://dx.doi.org/10.1371/journal.pone.0127350
23. Trindade GS, Guedes MIC, Drumond BP, Mota BEF, Abrahão JS, Lobato ZIP, et al. Zoonotic vaccinia virus: clinical and immunological characteristics in a naturally infected patient. Clin Infect Dis. 2009;48:e37–40. http://dx.doi.org/10.1086/595856
24. Sikes RS, Gannon WH; Animal Care and Use Committee of the American Society of Mammalogists. Guidelines of the American Society of Mammalogists for the use of wild mammals in research. J Mammal. 2011;92:235–53. http://dx.doi.org/10.1644/10-MAMM-F-355.1
25. Mills JN, Yates TL, Childs JE, Parmenter RR, Ksiazek TG, Rollin PE. Guidelines for working with rodents potentially infected with hantavirus. J Mammal. 1995;76:716–22. http://dx.doi.org/10.2307/1382742
26. Abrahão JS, Drumond BP, Trindade GS, da Silva-Fernandes AT, Ferreira JMS, Alves PA, et al. Rapid detection of *Orthopoxvirus* by semi-nested PCR directly from clinical specimens: a useful alternative for routine laboratories. J Med Virol. 2010;82:692–9. http://dx.doi.org/10.1002/jmv.21617
27. Tamura K, Stecher G, Peterson D, Filipski A, Kumar S. MEGA6: Molecular Evolutionary Genetics Analysis version 6.0. Mol Biol Evol. 2013;30:2725–9. http://dx.doi.org/10.1093/molbev/mst197
28. Geessien Kroon E, Santos Abrahão J, de Souza Trindade G, Pereira Oliveira G, Moreira Franco Luiz AP, Barbosa Costa G, et al. Natural *Vaccinia virus* infection: diagnosis, isolation, and characterization. Curr Protoc Microbiol. 2016;42:14A.5.1–14A.5.43. PubMed https://doi.org/10.1002/cpmc.13
29. Assis FL, Borges IA, Ferreira PCP, Bonjardim CA, Trindade GS, Lobato ZIP, et al. Group 2 vaccinia virus, Brazil. Emerg Infect Dis. 2012;18:2035–8. http://dx.doi.org/10.3201/eid1812.120145
30. Newman MEJ. The structure and function of complex networks. Society for Industrial and Applied Mathematics Review. 2003; 45:167–256.
31. Batagelj V, Mrvar A. Pajek: program for large network analysis. Connections. 1998;21:47–57.
32. Ferreira JMS, Abrahão JS, Drumond BP, Oliveira FM, Alves PA, Pascoal-Xavier MA, et al. Vaccinia virus: shedding and horizontal transmission in a murine model. J Gen Virol. 2008;89:2986–91. http://dx.doi.org/10.1099/vir.0.2008/003947-0
33. Chaudhri G, Panchanathan V, Bluethmann H, Karupiah G. Obligatory requirement for antibody in recovery from a primary poxvirus infection. J Virol. 2006;80:6339–44. http://dx.doi.org/10.1128/JVI.00116-06
34. Buller RML, Palumbo GJ. Poxvirus pathogenesis. Microbiol Rev. 1991;55:80–122.
35. Trindade GS, Lobato ZIP, Drumond BP, Leite JA, Trigueiro RC, Guedes MIMC, et al. Isolation of two vaccinia virus strains from a single bovine vaccinia outbreak in rural area from Brazil: implications on the emergence of zoonotic orthopoxviruses. Am J Trop Med Hyg. 2006;75:486–90.
36. Drumond BP, Leite JA, da Fonseca FG, Bonjardim CA, Ferreira PCP, Kroon EG. Brazilian *Vaccinia virus* strains are

genetically divergent and differ from the *Lister* vaccine strain. Microbes Infect. 2008;10:185–97. http://dx.doi.org/10.1016/j.micinf.2007.11.005

37. Oliveira G, Assis F, Almeida G, Albarnaz J, Lima M, Andrade AC, et al. From lesions to viral clones: biological and molecular diversity amongst autochthonous Brazilian *Vaccinia virus*. Viruses. 2015;7:1218–37. http://dx.doi.org/10.3390/v7031218
38. Ferreira JMS, Drumond BP, Guedes MIMC, Pascoal-Xavier MA, Almeida-Leite CM, Arantes RME, et al. Virulence in murine model shows the existence of two distinct populations of Brazilian *Vaccinia virus* strains. PLoS One. 2008;3:e3043. http://dx.doi.org/10.1371/journal.pone.0003043
39. Abrahão JS, Trindade GS, Ferreira JMS, Campos RK, Bonjardim CA, Ferreira PCP, et al. Long-lasting stability of *Vaccinia virus* strains in murine feces: implications for virus circulation and environmental maintenance. Arch Virol. 2009;154:1551–3. http://dx.doi.org/10.1007/s00705-009-0470-1
40. Paglia AP, Fonseca GAB, Rylands AB, Herrmann G, Aguiar LMS, Chiarello AG, et al. Annotated checklist of Brazilian mammals. 2nd ed. Occasional papers in conservation biology series, no. 6. Arlington (VA): Conservation International; 2012. p. 76.

Address for correspondence: Giliane de S. Trindade, Laboratório de Vírus, Instituto de Ciências Biológicas, sala 258, Universidade Federal de Minas Gerais. Avenida Antônio Carlos, 6627 - Pampulha - Belo Horizonte, Minas Gerais, Brazil, CEP 31270-901; email: gitrindade@yahoo.com.br

December 2015: **Zoonotic Infections**

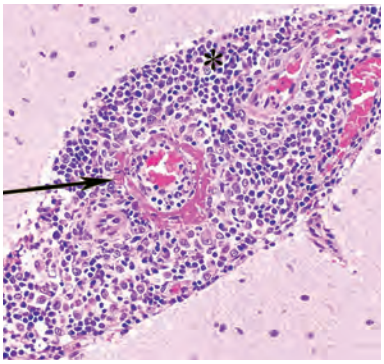

- Identifying and Reducing Remaining Stocks of Rinderpest Virus
- Opportunistic Pulmonary *Bordetella hinzii* Infection after Avian Exposure
- Zoonotic Leprosy in the Southeastern United States
- Infection Risk for Persons Exposed to Highly Pathogenic Avian Influenza A H5 Virus–Infected Birds, United States, December 2014–March 2015
- High Prevalence of Intermediate *Leptospira* spp. DNA in Febrile Humans From Urban and Rural Ecuador
- Biological Warfare Plan in the 17th Century—the Siege of Candia, 1648–1669
- Influenza A(H6N1) Virus in Dogs, Taiwan
- Methicillin-Resistant *Staphylococcus aureus* Prevalence among Captive Chimpanzees, Texas, USA, 2012
- Novel *Waddlia* Intracellular Bacterium in *Artibeus intermedius* Fruit Bats, Mexico
- Tembusu-Related Flavivirus in Ducks, Thailand

- Japanese Macaques (*Macaca fuscata*) as Natural Reservoir of *Bartonella quintana*
- *Onchocerca lupi* Nematode in a Cat, Europe

- Increased Number of Human Cases of Influenza Virus A(H5N1) Infection, Egypt, 2014–15
- Replication Capacity of Avian Influenza A(H9N2) Virus in Pet Birds, Chickens, and Mammals, Bangladesh
- Hendra Virus Infection in Dog, Australia, 2013
- No Evidence of Gouléako and Herbert Virus Infections in Pigs, Côte d'Ivoire and Ghana
- Aquatic Bird Bornavirus 1 in Wild Geese, Denmark
- Vectorborne Transmission of *Leishmania infantum* from Hounds, United States
- Porcine Deltacoronavirus in Mainland China

EMERGING INFECTIOUS DISEASES®

https://wwwnc.cdc.gov/eid/articles/issue/21/12/table-of-contents

Relative Risk for Ehrlichiosis and Lyme Disease in an Area Where Vectors for Both Are Sympatric, New Jersey, USA

Andrea Egizi, Nina H. Fefferman, Robert A. Jordan

Medscape EDUCATION ACTIVITY

JOINTLY ACCREDITED PROVIDER™
INTERPROFESSIONAL CONTINUING EDUCATION

In support of improving patient care, this activity has been planned and implemented by Medscape, LLC and Emerging Infectious Diseases. Medscape, LLC is jointly accredited by the Accreditation Council for Continuing Medical Education (ACCME), the Accreditation Council for Pharmacy Education (ACPE), and the American Nurses Credentialing Center (ANCC), to provide continuing education for the healthcare team.

Medscape, LLC designates this Journal-based CME activity for a maximum of 1.00 ***AMA PRA Category 1 Credit(s)™***. Physicians should claim only the credit commensurate with the extent of their participation in the activity.

All other clinicians completing this activity will be issued a certificate of participation. To participate in this journal CME activity: (1) review the learning objectives and author disclosures; (2) study the education content; (3) take the post-test with a 75% minimum passing score and complete the evaluation at http://www.medscape.org/journal/eid; and (4) view/print certificate. For CME questions, see page 1,056.

Release date: May 11, 2017; Expiration date: May 11, 2018

Learning Objectives

Upon completion of this activity, participants will be able to:

- Analyze the clinical presentation of ehrlichiosis.
- Compare the vectors of ehrlichiosis vs Lyme disease.
- Distinguish the ratio of ehrlichiosis to Lyme disease using a mathematical model.
- Compare predicted rates of ehrlichiosis with actual reported rates of illness.

CME Editor
Jude Rutledge, BA, Technical Writer/Editor, Emerging Infectious Diseases. *Disclosure: Jude Rutledge has disclosed no relevant financial relationships.*

CME Author
Charles P. Vega, MD, Health Sciences Clinical Professor, UC Irvine Department of Family Medicine; Associate Dean for Diversity and Inclusion, UC Irvine School of Medicine, Irvine, California, USA. *Disclosure: Charles P. Vega, MD, has disclosed the following financial relationships: served as an advisor or consultant for McNeil Consumer Healthcare; served as a speaker or a member of a speakers bureau for Shire Pharmaceuticals.*

Authors
Disclosures: ***Andrea Egizi, PhD;*** *and* ***Robert A. Jordan, PhD,*** *have disclosed no relevant financial relationships.* ***Nina H. Fefferman, PhD,*** *has disclosed the following relevant financial relationships: owns stock, stock options, or bonds from VIVUS, Inc.*

Author affiliations: Rutgers University, New Brunswick, New Jersey, USA (A. Egizi, N.H. Fefferman, R.A. Jordan); Monmouth County Mosquito Control Division, Tinton Falls, New Jersey, USA (A. Egizi, R.A. Jordan); University of Tennessee, Knoxville, Tennessee, USA (N.H. Fefferman)

DOI: http://dx.doi.org/10.3201/eid2306.160528

The lone star tick, *Amblyomma americanum*, is a vector of *Ehrlichia chaffeensis* and *E. ewingii*, causal agents of human ehrlichiosis, and has demonstrated marked geographic expansion in recent years. *A. americanum* ticks often outnumber the vector of Lyme disease, *Ixodes scapularis*, where both ticks are sympatric, yet cases of Lyme disease far exceed ehrlichiosis cases. We quantified the risk for

ehrlichiosis relative to Lyme disease by using relative tick encounter frequencies and infection rates for these 2 species in Monmouth County, New Jersey, USA. Our calculations predict ≥1 ehrlichiosis case for every 2 Lyme disease cases, >2 orders of magnitude higher than current case rates (e.g., 2 ehrlichiosis versus 439 Lyme disease cases in 2014). This result implies ehrlichiosis is grossly underreported (or misreported) or that many infections are asymptomatic. We recommend expansion of tickborne disease education in the Northeast United States to include human health risks posed by *A. americanum* ticks.

Tickborne diseases are a growing public health concern in the United States (*1*). Lyme disease, caused by the bacterium *Borrelia burgdorferi*, is the most frequently reported vectorborne illness in the Northeast (*2*) and has been the subject of widespread education campaigns aimed at preventing human encounters with its vector, *Ixodes scapularis* (the black-legged tick). Unfortunately, such campaigns focus comparatively less attention on other medically important ticks in Lyme disease–endemic areas (*3*); therefore, persons living in these areas may not fully recognize the threat posed by these species. Specifically, the much more aggressive lone star tick, *Amblyomma americanum*, transmits the agent of human monocytic ehrlichiosis and may serve as the vector for several other emerging tickborne pathogens (*3–5*). Historically found primarily in the Southeast United States but with established distributions along the Atlantic Coast and into the Midwest (*6*), *A. americanum* ticks are active concurrently with *I. scapularis* ticks; aggressively attack humans in all tick life stages (adult, nymph, and larvae); and are typically by far the more numerous of the 2 ticks where they are sympatric (*7*,*8*).

Given the abundance and aggressive host-seeking behavior of *A. americanum* ticks, it is reasonable to expect high rates of human encounters with them (*8–10*). In recent years, submissions of *A. americanum* ticks to the Monmouth County Mosquito Control Division's passive tick surveillance program (Tinton Falls, New Jersey, USA; offering free tick identification to residents since 2006) have been increasing steadily while submissions of *I. scapularis* ticks remain nearly level (Figure 1), suggesting increased human exposure to *A. americanum* ticks relative to *I. scapularis* ticks.

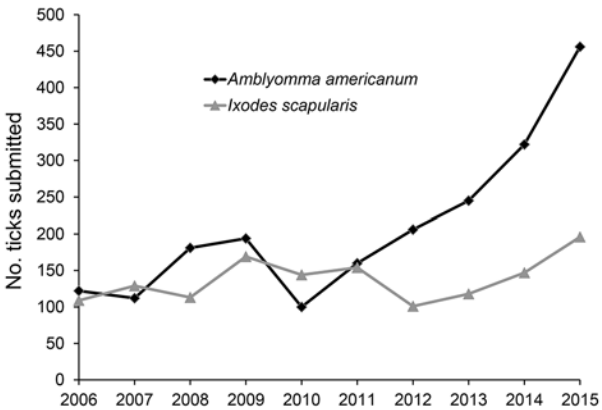

Figure 1. Number of ticks submitted each year to Monmouth County Mosquito Control Division's passive surveillance program during May–August, by year, Monmouth County, New Jersey, USA, 2006–2015.

A. americanum ticks are known vectors of ≥2 human pathogens, *Ehrlichia chaffeensis* and *E. ewingii* (*10*,*11*), which cause human ehrlichiosis, an illness often marked by an initial prodrome of undifferentiated fever, headache, myalgia, nausea, malaise, thrombocytopenia, leukopenia, and hepatic injury (elevated serum transaminase levels) (*12*). More severe complications (including toxic shock–like symptoms and meningitis or meningoencephalitis) may occur in some untreated persons (including immunocompromised patients), and death rates as high as ≈3% have been reported (*12*,*13*).

The number of ehrlichiosis cases attributable to *E. chaffeensis* that have been reported to the Centers for Disease Control and Prevention (Atlanta, GA, USA) has increased steadily since the disease became reportable, from 0.8 cases/million persons/year in 2000 to 3.0 cases/million persons/year in 2007 (*13*,*14*). However, some evidence suggests that ehrlichiosis may be substantially underreported (*12*) and even reported cases may be misclassified because of cross-reactivity between *E. chaffeensis*, *E. ewingii*, and other *Ehrlichia* and *Anaplasma* agents in widely used serologic tests (*15–17*). Health risks may be compounded if physicians are less familiar with ehrlichiosis than Lyme disease, particularly because initial symptoms may be relatively vague, resembling a viral syndrome typical of an array of tickborne diseases (*14*), which creates the potential for diagnostic confusion where *I. scapularis* and *A. americanum* ticks are sympatric (*10*). Ehrlichiosis could also be misdiagnosed as Rocky Mountain spotted fever if a patient is co-infected with *Ehrlichia* sp. and *Rickettsia amblyommatis*, (formerly *Candidatus* Rickettsia amblyommii [*18*]), a species cross-reactive in tests for rickettsial pathogens (*19*) and commonly present in ≥40% of field-collected *A. americanum* ticks (*4*).

This study quantified the risk to humans of ehrlichial infections, relative to Lyme disease risk. We used data obtained from tick surveillance programs in Monmouth County, New Jersey, an area with a high reported incidence of Lyme disease and increasing *A. americanum* tick encounter rates.

Methods

Site Description

Monmouth County (40°44′N, 74°17′W) is located in eastern-central New Jersey, a US state on the mid-Atlantic

coast. The county is 468.8 mi^2 in size and had a population of 630,380 (1,344.7 persons/mi^2) as of the 2010 census (http://www.census.gov/quickfacts/table/PST045215/34025). The geomorphologic break separating the Inner and Outer Coastal Plain physiographic provinces in New Jersey runs horizontally across the center of the county, and the resulting soil differences are reflected in vegetative differences between these 2 regions (*20*). The Outer Coastal Plain region is characterized by sandier soils that are often dry and acidic, with pine forests and cedar swamps. Previously, the distribution of *A. americanum* ticks in Monmouth County was restricted to this southern part of the county (*21*), whereas *I. scapularis* ticks were found throughout. However, recently specimens of *A. americanum* ticks have been captured in the far north and west of the county.

The county reports several hundred cases of Lyme disease annually, with a 10-year average (during 2005–2014) of 361 cases/year. By contrast, during that same period, there were on average 5.5 cases/year of *E. chaffeensis* infection and no cases of infection attributed to *E.ewingii* (*22*).

Risk Model

The relative risk for infection with a tickborne pathogen depends on multiple factors, including risk for exposure to a competent vector, risk for exposure to the pathogen from exposure to the vector, and risk for transmission from exposure to a pathogen-infected vector. To characterize the risk for human exposure to ticks, we define the parameter C_x as the relative proportion of each species (x) of tick submitted to the Monmouth County Mosquito Control Division's tick identification and testing service. This passive surveillance program, initiated in 2006, allows county residents to submit ticks they have encountered (e.g., found on their skin or clothing) for species identification. This program averages 658.9 submissions/year, although this number has increased markedly in recent years (R.A. Jordan, unpub. data). For C_x, we used the 10-year average of relative submissions data (2006–2015) during peak Lyme disease transmission season in New Jersey (May–August) (Table). Although in Monmouth *A. americanum* ticks are often 3 times as abundant as *I. scapularis* ticks in field collections (*9*), using the passive surveillance data in our model (where *A. americanum* ticks are only encountered 1.5 times as often; Table) provides a more direct measure of human exposure to ticks as well as a more conservative risk estimate.

To characterize risk for exposure to the disease from the vector, we define I_x as the prevalence of the pathogen in ticks (i.e., percentage infected), weighted by life stage. Both *I. scapularis* and *A. americanum* ticks have a 3-host life cycle, meaning that adults have had more opportunities to feed on an infected host than nymphs and consequently infection rates differ between life stages. Because transovarial transmission of either *B. burgdorferi* or *E. chaffeensis* does not occur (*23*,*24*), host-seeking larvae are not infected and therefore were not included in the calculations. Relative abundance of nymphs and adults of each species submitted to our passive tick surveillance program during May–August were reported ($C_{X,N}$ and $C_{X,D}$) and used to weight the infection prevalence of each (Table). Infection rates of *I. scapularis* ticks with *B. burgdorferi* for both life stages ($I_{IS,D}$ and $I_{IS,N}$) also were obtained from our passive surveillance program, whereby residents submitting an *I. scapularis* tick can elect to have it tested for *B. burgdorferi* through nested PCR assay (following established protocols [*8*]). Our records show that during a 10-year period of our program, 90.5% of residents submitting *I. scapularis* ticks during May–August have chosen to have them tested (R.A. Jordan, unpub. data), including 153 adults and 1,146 nymphs. However, the program does not test *A. americanum* ticks, so infection rates for this species were obtained from other sources. Rates of adult tick infection with *E. chaffeensis* and *E. ewingii* ($I_{AA,D}$) in Monmouth County were derived from Schulze et al. (*21*) and summed, yielding a total value (accounting for co-infected ticks) of 11.7% infection with human *Ehrlichia* pathogens (N = 291). Nymphal infection rates with both ehrlichia species were obtained from an unpublished dataset consisting of field-collected nymphs from 4 sites in eastern and western Monmouth County in 2014 (R.A. Jordan unpub. data). Nymphal specimens were disrupted by using a TissueLyser and DNA isolated with QIAgen DNeasy 96 well-plate blood and tissue kits (QIAGEN, Valencia, CA, USA). Specimens were tested for pathogens by using real-time PCR protocols for

Table. Parameters used in relative risk calculations for ehrlichiosis and Lyme disease, by vector, Monmouth County, New Jersey, USA*

Parameter	*Ixodes scapularis*		*Amblyomma americanum*	
Relative abundance of each species	C_{IS} = 38.32		C_{AA} = 61.68	
	Adults	Nymphs	Adults	Nymphs
Relative abundance of each life stage	$C_{IS.\,D}$ = 19.96	$C_{IS.\,N}$ = 80.04	$C_{AA.\,D}$ = 35.34	$C_{AA.\,N}$ = 64.66
Infection rates per life stage	$I_{IS.\,D}$ = 39.87	$I_{IS.\,N}$ = 23.3	$I_{AA.\,D}$ = 11.7	$I_{AA.\,N}$ = 9.04
Infection rates, weighted	I_{IS} = 26.60		I_{AA} = 9.98	

*Values are in percentages. Relative abundances (denoted by C_X) are derived from specimens submitted to the Monmouth County Mosquito Control Division's tick identification and testing service during peak Lyme disease transmission season (May–August) and during a 10-year period (2006–2015). Infection rates of *I. scapularis* ticks with *Borrelia burgdorferi* (I_{IS}) also from passive surveillance program. Infection rates of *A. americanum* ticks (I_{AA}) encompass both *Ehrlichia chaffeensis* and *E. ewingii* (accounting for co-infection).

E. chaffeensis (*25*) and *E. ewingii* (*26*). Both probes were modified slightly (shortened) to allow the use of an MGB quencher as follows (5′–3′): VIC-CGGACAATTGCT-TATAACC-MGBNFQ for *E. chaffeensis* and 6FAM-AACAATTCCTAAATAGTCTCTGAC-MGBNFQ for *E. ewingii*. Sequence detection primers and reaction conditions were as described previously (*26*). A subset of samples was compared with conventional PCR methods established by this laboratory for detection of these pathogens (*21*), and the 2 methods were found to be in agreement. The resulting infection prevalence of *Ehrlichia* pathogens in *A. americanum* nymphs ($I_{AA,N}$) (encompassing *E. chaffeensis* and *E. ewingii*, accounting for coinfection) was 9.04% (N = 752). Overall infection prevalence (I_x) in each species of tick, weighted by life stage, was calculated by multiplying the relative abundance of each life stage times its infection rate and summing across life stages (Table).

To characterize transmission risk, we defined T_X as the likelihood of successful pathogen transmission from an infected tick to a human. The general concept of vector competence includes both this direction of transmission from vector to host as well as the probability of the vector becoming infected from feeding on infected hosts, which in our calculations is already reflected in tick infection rates (I_x). Data on transmission efficiency to animals for both species is scarce because most studies feed multiple infected ticks on 1 host (so the risk imposed by a single feeding tick is unknown) and, because of the difficulty in working with large vertebrates in a laboratory setting, have very small sample sizes (*27–30*). Further, whether probabilities of transmission obtained from animal studies are applicable to humans is unknown. Therefore, although we are including the parameter T_X in the equation so that it can be applied when such data become better known, for purposes of these analyses we are setting it equal to 1 for both diseases, yielding no functional impact on the model.

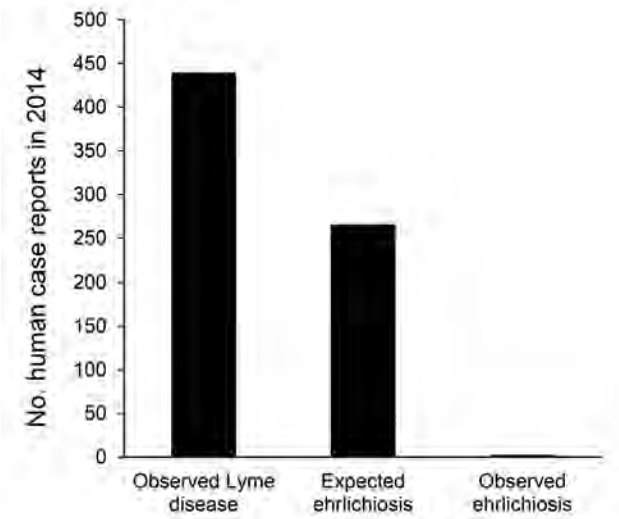

Figure 2. Number of observed versus expected ehrlichiosis cases, Monmouth County, New Jersey, USA, 2014. Expected values calculated by using number of observed Lyme disease cases as benchmark.

Calculations

Based on our definitions, we calculate the relative risk for ehrlichiosis compared to Lyme disease as risk = $(C_{AA} \times I_{AA} \times T_{AA})/(C_{IS} \times I_{IS} \times T_{IS})$. To then translate this value into expected cases of observed human infection, we move from risk to reported case numbers by using the reported number of cases of Lyme disease in Monmouth County as a benchmark. In other words, if there were *X* Lyme disease cases, then the expected number of ehrlichiosis cases would be *X* multiplied by the relative risk estimate calculated as described.

Results

The relative risk for ehrlichiosis cases compared to Lyme disease was calculated as risk = $(61.68 \times 9.98 \times 1)/(38.32 \times 26.61 \times 1) = 0.604$. These numbers mean that we should expect to see ehrlichiosis cases occur 0.604 times as often as Lyme disease cases.

In 2014, a total of 439 cases of Lyme disease were reported in Monmouth County (*22*). By using the risk estimates described, we would expect there to be ≥265 cases of ehrlichiosis, >2 orders of magnitude higher than the number of cases actually observed (Figure 2).

Discussion

We demonstrate that in Monmouth County, New Jersey, ehrlichiosis infections from *A. americanum* ticks should be occurring, at a minimum, one half as often as Lyme disease (e.g., 1 ehrlichiosis case for every 2 Lyme disease cases). This rate of occurance is clearly not the case (Figure 2), and these numbers suggest that ≈99% of potential ehrlichiosis infections are not recognized. It is possible that not all persons who become infected in Monmouth are county residents (and so their case would be recorded elsewhere) making the total number of Monmouth County–derived infections likely to be somewhat higher than the observed 2 cases. However, even if one assumes all ehrlichiosis reported for the entire state of New Jersey to originate in Monmouth County (64 cases in 2014) (*22*) these values still indicate a substantial discrepancy between numbers of observed and expected cases.

When selecting values for the parameters used in our calculations, every opportunity to be conservative was taken to avoid biasing estimates of relative risk. For example, infection (I_x) probabilities were higher for Lyme disease than ehrlichiosis (39.87% vs. 11.7% for adult ticks and 23.3% vs. 9.04% for nymphs). Although reported *B. burgdorferi* infection rates in *I. scapularis* adults frequently

range from 40% to 50% in hyperendemic areas, several studies have reported lower rates (*9*,*31*). Our weighted infection prevalence estimate of 9.98% (encompassing both *E. chaffeensis* and *E. ewingii* across adults and nymphs) is probably lower than the actual value, given that many studies have reported infection prevalence in the range of 5%–15% for *E. chaffeensis* alone and in some locations twice that rate (*3*,*32*). Last, use of passive surveillance numbers (C_x) probably underestimates the actual risk for exposure to *A. americanum* ticks; residents who recognize the tick species may be less likely to bring in *A. americanum* ticks to the passive surveillance program, because we only test *I. scapularis* (as stated on our website), and taking the 10-year average for relative abundances (2006–2015) does not account for the recent surge in *A. americanum* tick submissions from 2012 onward (Figure 1). In light of these considerations, the actual risk for *A. americanum* tick–associated ehrlichioses in Monmouth County may be much higher than we have estimated.

One caveat should be noted. Differences in PCR sensitivity between *B. burgdorferi* and *Ehrlichia* sp. assays could affect our ability to compare infection rates, although to mitigate this problem as much as possible, we relied on established primers and checked that infection rates were within ranges reported by other studies as described previously. Thus, any difference in our ability to detect pathogens between the 2 tick species is unlikely to alter our conclusions.

One possible explanation for the lower-than-expected number of reported ehrlichiosis cases is a lack of awareness about ehrlichial disease on the part of the public and physicians, leading to misdiagnosis and underreporting. The infection tends to manifest as a general influenza-like illness, and onset of a rash is rare (*12*), so persons may be less likely to visit a doctor unless more severe symptoms emerge or they are aware of a recent tick bite and the presence of tickborne diseases in the area. Awareness of non–Lyme disease tickborne illnesses is startlingly low, even in parts of the country where ehrlichiosis cases outnumber Lyme disease cases (*33*–*35*). One study found that >50% of respondents in the United States had heard of Lyme disease, whereas only 1.4% had heard of ehrlichiosis (*35*). As a consequence of these factors, when active screening for ehrlichial infections is performed, the resulting case rates are often much higher than those reported to governmental agencies (*3*,*36*,*37*). For example, Olano et al. (*37*) found that the incidence of ehrlichiosis observed when actively screening patients was as much as 2 orders of magnitude higher than the passively reported incidence.

Another explanation could be the existence of asymptomatic infections. Several studies of *E. chaffeensis* antibody seroprevalence in adults found that most of those carrying the antibodies had no recollection of a symptomatic infection (*38*–*40*). Further, a study screening blood samples from children from the Southeast United States for *E. chaffeensis* revealed that many more children had been exposed than showed clinical signs (*41*). Most documented cases of *E. chaffeensis* and *E. ewingii* infection come from older adults (*13*,*15*), so when younger adults and children become infected, they may be less likely to have symptoms or seek treatment (*41*), accounting for the large number of unreported infections. Other vectorborne diseases, such as West Nile virus, transmitted by mosquitoes, also demonstrate large numbers of asymptomatic infections and increased severity among the older population (*42*). However, because of cross-reactivity in the serologic test for *E. chaffeensis* and the lack of specific testing for *E. ewingii*, one could argue that many presumed asymptomatic cases of *E. chaffeensis* were actually incidences of infection with *E. ewingii*, which tends to be more mild (*16*). Although our study considered *E. chaffeensis* and *E. ewingii* interchangeably, if we repeat our calculations by using *E. chaffeensis* infection rates alone, we would expect Monmouth County to have seen 84 cases of *E. chaffeensis* in 2014, when only 2 were reported. Therefore, 97.6% of *E. chaffeensis* infections are potentially going unnoticed (versus 99% of ehrlichiosis infections overall), which is still a troubling discrepancy.

Across the entire United States, the number of Lyme disease cases dwarfs ehrlichiosis cases. During 2004–2013, the Centers for Disease Control and Prevention annually reported 279–528 Lyme disease cases/1 million persons (*2*). In contrast, during that same period, annual ehrlichiosis cases ranged from 3.3 to 26 cases/1 million persons (*43*). If our numbers can be extrapolated to other areas in the country, this implies that, on a national scale, potentially thousands of ehrlichiosis cases are going undiagnosed. The *A. americanum* tick appears to be expanding into geographic areas where it did not occur previously (*6*,*32*) and is becoming more abundant within its existing range (*9*,*21*,*44*). Because ehrlichiosis cases have steadily increased since becoming reportable (*13*,*15*), the spread of *A. americanum* ticks and the emergence of ehrlichiosis as a human pathogen in the United States may parallel increases in *I. scapularis* tick populations and the emergence of Lyme disease that occurred 30 years prior (*14*). Even if most unrecognized infections are mild or asymptomatic, these could still have consequences for public health; for example, blood donors who are unknowingly infected could pass the infection to immunocompromised patients (*45*), or prescription of sulfa drugs for unrelated ailments could result in worsened disease presentation (*46*).

Our findings indicate a need to increase public education efforts about the risks for acquiring tickborne diseases other than Lyme disease in the United States, and in particular, to expand prevention awareness of medically important tick species other than *I. scapularis*. Fortunately, many of these diseases, including ehrlichiosis, can be

prevented in the same manner as Lyme disease (e.g., avoidance of tick bites) and are treated similarly to Lyme disease (*12*,*47*); also, the number of ehrlichiosis cases peaks during spring and summer months, corresponding with peak Lyme disease transmission months (*13*,*15*). Consequently, refocusing existing public health education efforts to encompass the full spectrum of tickborne diseases could be accomplished without changing much of its content, although some attention should be given to the risks imposed by viruses and protozoa as well as unique characteristics of the questing behavior of *A. americanum* ticks. To better inform these educational efforts and more accurately assess tickborne disease risk, more research into diseases other than Lyme disease is required.

Humans can alter their environment in many ways that affect disease transmission, from localized changes affecting tick habitat and host abundance, to larger changes affecting the planet's climate. As these changes continue to occur, the study of vector and pathogen distributions and abundance will be critical to understanding the potential risk to humans posed by emerging pathogens. Our calculations imply that infections with *E. chaffeensis* and *E. ewingii* are underrecognized, at least in Monmouth County, New Jersey, if not throughout a larger portion of the United States where *A. americanum* ticks are abundant or becoming abundant. Additional effort is needed to determine the causes for this apparent discrepancy and to characterize the actual prevalence of ehrlichiosis in the human population, as well as to raise awareness about the risk for exposure to these pathogens in areas where *A. americanum* ticks are common.

Acknowledgments

The authors would like to acknowledge Terry L. Schulze and Holly Gaff for insightful discussions, Vivien E. Roegner for her role in laboratory analyses, and the comments of 2 anonymous reviewers that greatly improved this manuscript.

Dr. Egizi oversees a research laboratory for the Monmouth County Mosquito Control Division located in the Center for Vector Biology at Rutgers University in New Brunswick, New Jersey, USA. She is interested in using molecular tools to gain insight into the ecology and evolution of vectors and vectorborne disease in the northeastern United States.

References

1. Nadolny RM, Feldman KA, Pagac B, Stromdahl EY, Rutz H, Wee S-B, et al. Review of the Mid-Atlantic Tick Summit III: A model for regional information sharing. Ticks Tick Borne Dis. 2015;6:435–8. http://dx.doi.org/10.1016/j.ttbdis.2015.04.001
2. Centers for Disease Control and Prevention. Lyme disease data and statistics 2005–2014. 2015 [cited 2015 Dec 4]. http://www.cdc.gov/lyme/stats/index.html
3. Childs JE, Paddock CD. The ascendancy of *Amblyomma americanum* as a vector of pathogens affecting humans in the United States. Annu Rev Entomol. 2003;48:307–37. http://dx.doi.org/10.1146/annurev.ento.48.091801.112728
4. Mixson TR, Campbell SR, Gill JS, Ginsberg HS, Reichard MV, Schulze TL, et al. Prevalence of *Ehrlichia*, *Borrelia*, and Rickettsial agents in *Amblyomma americanum* (Acari: Ixodidae) collected from nine states. J Med Entomol. 2006;43:1261–8.
5. Apperson CS, Engber B, Nicholson WL, Mead DG, Engel J, Yabsley MJ, et al. Tick-borne diseases in North Carolina: is "*Rickettsia amblyommii*" a possible cause of rickettsiosis reported as Rocky Mountain spotted fever? Vector Borne Zoonotic Dis. 2008;8:597–606. http://dx.doi.org/10.1089/vbz.2007.0271
6. Springer YP, Eisen L, Beati L, James AM, Eisen RJ. Spatial distribution of counties in the continental United States with records of occurrence of *Amblyomma americanum* (Ixodida: Ixodidae). J Med Entomol. 2014;51:342–51. http://dx.doi.org/10.1603/ME13115
7. Stromdahl EY, Randolph MP, O'Brien JJ, Gutierrez AG. *Ehrlichia chaffeensis* (Rickettsiales: Ehrlichieae) infection in *Amblyomma americanum* (Acari: Ixodidae) at Aberdeen Proving Ground, Maryland. J Med Entomol. 2000;37:349–56. http://dx.doi.org/10.1093/jmedent/37.3.349
8. Schulze TL, Jordan RA, Schulze CJ, Mixson T, Papero M. Relative encounter frequencies and prevalence of selected *Borrelia*, *Ehrlichia*, and *Anaplasma* infections in *Amblyomma americanum* and *Ixodes scapularis* (Acari: Ixodidae) ticks from central New Jersey. J Med Entomol. 2005;42:450–6.
9. Schulze TL, Jordan RA, Healy SP, Roegner VE, Meddis M, Jahn MB, et al. Relative abundance and prevalence of selected *Borrelia* infections in *Ixodes scapularis* and *Amblyomma americanum* (Acari: Ixodidae) from publicly owned lands in Monmouth County, New Jersey. J Med Entomol. 2006;43:1269–75. http://dx.doi.org/10.1093/jmedent/43.6.1269
10. Stromdahl EY, Hickling GJ. Beyond Lyme: aetiology of tick-borne human diseases with emphasis on the south-eastern United States. Zoonoses Public Health. 2012;59(Suppl 2):48–64. http://dx.doi.org/10.1111/j.1863-2378.2012.01475.x
11. Goddard J, Varela-Stokes AS. Role of the lone star tick, *Amblyomma americanum* (L.), in human and animal diseases. Vet Parasitol. 2009;160:1–12. http://dx.doi.org/10.1016/j.vetpar.2008.10.089
12. Dumler JS, Madigan JE, Pusterla N, Bakken JS. Ehrlichioses in humans: epidemiology, clinical presentation, diagnosis, and treatment. Clin Infect Dis. 2007;45(Suppl 1):S45–51. http://dx.doi.org/10.1086/518146
13. Dahlgren FS, Mandel EJ, Krebs JW, Massung RF, McQuiston JH. Increasing incidence of *Ehrlichia chaffeensis* and *Anaplasma phagocytophilum* in the United States, 2000–2007. Am J Trop Med Hyg. 2011;85:124–31. http://dx.doi.org/10.4269/ajtmh.2011.10-0613
14. Paddock CD, Childs JE. *Ehrlichia chaffeensis*: a prototypical emerging pathogen. Clin Microbiol Rev. 2003;16:37–64. http://dx.doi.org/10.1128/CMR.16.1.37-64.2003
15. Nichols Heitman K, Dahlgren FS, Drexler NA, Massung RF, Behravesh CB. Increasing Incidence of ehrlichiosis in the United States: a summary of national surveillance of *Ehrlichia chaffeensis* and *Ehrlichia ewingii* infections in the United States, 2008–2012. Am J Trop Med Hyg. 2016;94:52–60. http://dx.doi.org/10.4269/ajtmh.15-0540
16. Harris RM, Couturier BA, Sample SC, Coulter KS, Casey KK, Schlaberg R. Expanded geographic distribution and clinical characteristics of *Ehrlichia ewingii* infections, United States. Emerg Infect Dis. 2016;22:862–5. http://dx.doi.org/10.3201/eid2205.152009
17. Dahlgren FS, Heitman KN, Behravesh CB. Undetermined human ehrlichiosis and anaplasmosis in the United States, 2008–2012: a catch-all for passive surveillance. Am J Trop Med Hyg. 2016;94:299–301. http://dx.doi.org/10.4269/ajtmh.15-0691
18. Karpathy SE, Slater KS, Goldsmith CS, Nicholson WL, Paddock CD. *Rickettsia amblyommatis* sp. nov., a spotted fever group *Rickettsia* associated with multiple species of *Amblyomma* ticks in North, Central and South America. Int J Syst Evol

Microbiol. 2016;66:5236–43. http://dx.doi.org/10.1099/ijsem.0.001502
19. Stromdahl EY, Jiang J, Vince M, Richards AL. Infrequency of *Rickettsia* ri*ckettsii* in *Dermacentor variabilis* removed from humans, with comments on the role of other human-biting ticks associated with spotted fever group *Rickettsiae* in the United States. Vector Borne Zoonotic Dis. 2011;11:969–77. http://dx.doi.org/10.1089/vbz.2010.0099
20. Collins BR, Anderson KH. Plant communities of New Jersey: a study in landscape diversity. New Brunswick (NJ): Rutgers University Press; 1994.
21. Schulze TL, Jordan RA, White JC, Roegner VE, Healy SP. Geographical distribution and prevalence of selected *Borrelia*, *Ehrlichia*, and *Rickettsia* infections in *Amblyomma americanum* (Acari: Ixodidae) in New Jersey. J Am Mosq Control Assoc. 2011;27:236–44. http://dx.doi.org/10.2987/11-6111.1
22. New Jersey Department of Health. 2005–2014 New Jersey Reportable Communicable Disease Reports [cited 2016 Mar 29]. https://www.nj.gov/health/cd/reportable_disease_stats.shtml
23. Rollend L, Fish D, Childs JE. Transovarial transmission of *Borrelia* spirochetes by *Ixodes scapularis*: a summary of the literature and recent observations. Ticks Tick Borne Dis. 2013;4:46–51. http://dx.doi.org/10.1016/j.ttbdis.2012.06.008
24. Long SW, Zhang X, Zhang J, Ruble RP, Teel P, Yu XJ. Evaluation of transovarial transmission and transmissibility of *Ehrlichia chaffeensis* (Rickettsiales: Anaplasmataceae) in *Amblyomma americanum* (Acari: Ixodidae). J Med Entomol. 2003;40:1000–4. http://dx.doi.org/10.1603/0022-2585-40.6.1000
25. Loftis AD, Massung RF, Levin ML. Quantitative real-time PCR assay for detection of *Ehrlichia chaffeensis.* J Clin Microbiol. 2003;41:3870–2. http://dx.doi.org/10.1128/JCM.41.8.3870-3872.2003
26. Killmaster LF, Loftis AD, Zemtsova GE, Levin ML. Detection of bacterial agents in *Amblyomma americanum* (Acari: Ixodidae) from Georgia, USA, and the use of a multiplex assay to differentiate *Ehrlichia chaffeensis* and *Ehrlichia ewingii.* J Med Entomol. 2014;51:868–72. http://dx.doi.org/10.1603/ME13225
27. Unver A, Rikihisa Y, Stich RW, Ohashi N, Felek S. The omp-1 major outer membrane multigene family of *Ehrlichia chaffeensis* is differentially expressed in canine and tick hosts. Infect Immun. 2002;70:4701–4. http://dx.doi.org/10.1128/IAI.70.8.4701-4704.2002
28. Jaworski DC, Bowen CJ, Wasala NB. A white-tailed deer/lone star tick model for studying transmission of *Ehrlichia chaffeensis.* Vector Borne Zoonotic Dis. 2013;13:193–5. http://dx.doi.org/10.1089/vbz.2011.0868
29. Starkey LA, Barrett AW, Chandrashekar R, Stillman BA, Tyrrell P, Thatcher B, et al. Development of antibodies to and PCR detection of *Ehrlichia* spp. in dogs following natural tick exposure. Vet Microbiol. 2014;173:379–84. http://dx.doi.org/10.1016/j.vetmic.2014.08.006
30. Varela-Stokes AS. Transmission of *Ehrlichia chaffeensis* from lone star ticks (*Amblyomma americanum*) to white-tailed deer (*Odocoileus virginianus*). J Wildl Dis. 2007;43:376–81. http://dx.doi.org/10.7589/0090-3558-43.3.376
31. Schulze TL, Jordan RA. The role of publicly owned properties in the transmission of Lyme disease in central New Jersey. Journal of Spirochetal and Tick-borne Diseases. 1996;3:124–9.
32. Yabsley MJ. Natural history of *Ehrlichia chaffeensis*: vertebrate hosts and tick vectors from the United States and evidence for endemic transmission in other countries. Vet Parasitol. 2010; 167:136–48. http://dx.doi.org/10.1016/j.vetpar.2009.09.015
33. Bayles BR, Evans G, Allan BF. Knowledge and prevention of tick-borne diseases vary across an urban-to-rural human land-use gradient. Ticks Tick Borne Dis. 2013;4:352–8. http://dx.doi.org/10.1016/j.ttbdis.2013.01.001
34. Armstrong PM, Brunet LR, Spielman A, Telford SR III. Risk of Lyme disease: perceptions of residents of a Lone Star tick-infested community. Bull World Health Organ. 2001;79:916–25.
35. Hook SA, Nelson CA, Mead PSUS. U.S. public's experience with ticks and tick-borne diseases: Results from national HealthStyles surveys. Ticks Tick Borne Dis. 2015;6:483–8. http://dx.doi.org/10.1016/j.ttbdis.2015.03.017
36. Walker DH. *Ehrlichia* under our noses and no one notices. In: Peters CJ, Calisher CH, editors. Infectious diseases from nature: mechanisms of viral emergence and persistence. Vienna: Springer-Verlag/Wien; 2004. p. 147–56.
37. Olano JP, Masters E, Hogrefe W, Walker DH. Human monocytotropic ehrlichiosis, Missouri. Emerg Infect Dis. 2003; 9:1579–86. http://dx.doi.org/10.3201/eid0912.020733
38. Yevich SJ, Sánchez JL, DeFraites RF, Rives CC, Dawson JE, Uhaa IJ, et al. Seroepidemiology of infections due to spotted fever group rickettsiae and *Ehrlichia* species in military personnel exposed in areas of the United States where such infections are endemic. J Infect Dis. 1995;171:1266–73. http://dx.doi.org/10.1093/infdis/171.5.1266
39. Standaert SM, Dawson JE, Schaffner W, Childs JE, Biggie KL, Singleton J Jr, et al. Ehrlichiosis in a golf-oriented retirement community. N Engl J Med. 1995;333:420–5. http://dx.doi.org/10.1056/NEJM199508173330704
40. Fritz CL, Kjemtrup AM, Conrad PA, Flores GR, Campbell GL, Schriefer ME, et al. Seroepidemiology of emerging tickborne infectious diseases in a Northern California community. J Infect Dis. 1997;175:1432–9. http://dx.doi.org/10.1086/516476
41. Marshall GS, Jacobs RF, Schutze GE, Paxton H, Buckingham SC, DeVincenzo JP, et al.; Tick-Borne Infections in Children Study Group. *Ehrlichia chaffeensis* seroprevalence among children in the southeast and south-central regions of the United States. Arch Pediatr Adolesc Med. 2002;156:166–70. http://dx.doi.org/10.1001/archpedi.156.2.166
42. Huhn GD, Sejvar JJ, Montgomery SP, Dworkin MS. West Nile virus in the United States: an update on an emerging infectious disease. Am Fam Physician. 2003;68:653–60.
43. Centers for Disease Control and Prevention. Ehrlichiosis: statistics and epidemiology, 1994–2010. 2015 [cited 2016 Jan 12]. http://www.cdc.gov/ehrlichiosis/stats
44. Ginsberg HS, Ewing CP, O'Connell AF Jr, Bosler EM, Daley JG, Sayre MW. Increased population densities of *Amblyomma americanum* (Acari: Ixodidae) on Long Island, New York. J Parasitol. 1991;77:493–5. http://dx.doi.org/10.2307/3283144
45. Regan J, Matthias J, Green-Murphy A, Stanek D, Bertholf M, Pritt BS, et al. A confirmed *Ehrlichia ewingii* infection likely acquired through platelet transfusion. Clin Infect Dis. 2013; 56:e105–7. http://dx.doi.org/10.1093/cid/cit177
46. Allen MB, Pritt BS, Sloan LM, Paddock CD, Musham CK, Ramos JM, et al. First reported case of *Ehrlichia ewingii* involving human bone marrow. J Clin Microbiol. 2014;52:4102–4. http://dx.doi.org/10.1128/JCM.01670-14
47. Centers for Disease Control and Prevention. Diagnosis and management of tickborne rickettsial diseases: Rocky Mountain spotted fever, ehrlichioses, and anaplasmosis—United States: a practical guide for physicians and other health-care and public health professionals. MMWR Morb Mortal Wkly Rep. 2006; 55(RR-4):1–29.

Address for correspondence: Andrea Egizi, Rutgers University, 180 Jones Ave, New Brunswick, NJ 08901, USA; email: andrea.egizi@co.monmouth.nj.us

Distribution and Quantitative Estimates of Variant Creutzfeldt-Jakob Disease Prions in Tissues of Clinical and Asymptomatic Patients

Jean Y. Douet, Caroline Lacroux, Naima Aron, Mark W. Head, Séverine Lugan, Cécile Tillier, Alvina Huor, Hervé Cassard, Mark Arnold, Vincent Beringue, James W. Ironside, Olivier Andréoletti

In the United-Kingdom, ≈1 of 2,000 persons could be infected with variant Creutzfeldt-Jakob disease (vCJD). Therefore, risk of transmission of vCJD by medical procedures remains a major concern for public health authorities. In this study, we used in vitro amplification of prions by protein misfolding cyclic amplification (PMCA) to estimate distribution and level of the vCJD agent in 21 tissues from 4 patients who died of clinical vCJD and from 1 asymptomatic person with vCJD. PMCA identified major levels of vCJD prions in a range of tissues, including liver, salivary gland, kidney, lung, and bone marrow. Bioassays confirmed that the quantitative estimate of levels of vCJD prion accumulation provided by PMCA are indicative of vCJD infectivity levels in tissues. Findings provide critical data for the design of measures to minimize risk for iatrogenic transmission of vCJD.

Prion diseases, or transmissible spongiform encephalopathies (TSEs), are fatal neurodegenerative disorders that occur naturally in sheep (scrapie), cattle (bovine spongiform encephalopathy [BSE]), and humans (Creutzfeldt-Jakob disease [CJD]). A key event in the pathogenesis of TSEs is the conversion of the normal cellular prion protein (PrP^{C}, encoded by the *PRNP* gene) into an abnormal disease-associated isoform (PrP^{Sc}) in tissues of infected animals. PrP^{C} is completely degraded after controlled digestion with proteinase K in the presence of nondenaturing detergents. In contrast, PrP^{Sc} is N terminally truncated under the same conditions, resulting in a proteinase K–resistant prion (PrP^{res}) (*1*).

Author affiliations: Institut National de la Recherche Agronomique, Toulouse, France (J.Y. Douet, C. Lacroux, N. Aron, S. Lugan, C. Tillier, A. Huor, H. Cassard, O. Andréoletti); University of Edinburgh, Edinburgh, Scotland, UK (M.W. Head, J.W. Ironside); Animal and Plant Health Agency, Loughborough, UK (M. Arnold); Institut National de la Recherche Agronomique, Jouy-en-Josas, France (V. Beringue)

DOI: http://dx.doi.org/10.3201/eid2306.161734

In 1996, a new form of CJD, termed variant CJD (vCJD) was identified in the United Kingdom. vCJD is believed to result from zoonotic transmission of the BSE agent, probably as a consequence of dietary exposure to BSE-contaminated meat products (*2*,*3*). The total number of clinical cases of vCJD thus far identified is limited (227 patients worldwide at the time of writing this article). However, the estimated prevalence of asymptomatic vCJD in populations exposed to the BSE agent is uncertain (*4*).

In the United Kingdom, 32,441 appendix samples collected during surgery from patients born during 1941–1985 have been tested for abnormal prion protein accumulation by using immunohistochemical analysis. This study reported a vCJD prevalence estimate of 1/2,000 in persons in these age cohorts (95% CI 1/3,500–1/1,250) (*5*). No comparable data are available concerning the prevalence of asymptomatic vCJD in other countries, although BSE exposure is known to have occurred in several countries in continental Europe, as judged by cases of vCJD that are not attributable to exposure in the United Kingdom (http://www.cjd.ed.ac.uk/documents/worldfigs.pdf).

Over the past 2 decades, several studies have reported on the distribution of the vCJD agent in tissues of infected patients (*6*–*8*). Most of these studies did not detect the vCJD agent outside the nervous system (central, peripheral, and autonomic) and lymphoid tissues. However, the sensitivity of detection techniques for PrP^{res} used in these investigations was limited.

Protein misfolding cyclic amplification (PMCA) is believed to mimic prion replication in vitro, but in an accelerated form, which enables amplification of minute amounts of PrP^{Sc} and prion infectivity (*9*). In PMCA, a PrP^{C}-containing substrate is combined with a seed that might contain otherwise undetectable amounts of PrP^{Sc}. After repeated cycles of incubation and sonication, the

amount of PrP^{Sc} increases to levels at which they can be detected by using conventional biochemical techniques. Recently, our group and others have shown that PMCA can detect endogenous vCJD agent in patient biologic fluids such as urine and blood (*10*,*11*).

In this study, we evaluated the relative sensitivity of PMCA versus that of bioassay in mice for detection of the vCJD agent. We estimated by using PMCA the level of vCJD prions in 21 tissues collected from 4 patients who died of symptomatic vCJD and from a patient with asymptomatic vCJD. We also determined whether vCJD prion levels, as estimated by using PMCA, were consistent with infectious titers, as estimated by bioassay with transgenic mice.

Methods

Ethics Statements

All animal experiments were performed in compliance with institutional and French national guidelines and in accordance with the European Community Council Directive 86/609/EEC. Animal experiments that were part of this study (national registration no. 01734.01) were approved by the local ethic committee of the Ecole Nationale Vétérinaire de Toulouse (Toulouse, France). Mouse inoculations were performed under anesthesia with isofulorane. Mice that displayed clinical signs of disease were anesthetized with isofluorane before being humanely killed by inhalation of CO_2.

Human samples were obtained from the United Kingdom National CJD Research and Surveillance Unit Brain and Tissue Bank, which is part of the Medical Research Council Edinburgh Brain Bank (Edinburgh, Scotland, UK). Tissue samples were pseudo-anonymized by using a Brain Bank reference number. All case-patients in the United Kingdom provided informed consent. Use of samples in this study was approved by the East of Scotland Research Ethics Service for the Edinburgh Brain Bank (16/ES/0084).

Table 1. Endpoint titration of reference sample from a patient with vCJD in tgBov mice expressing bovine prion protein*

	Transmission in tgBov mice	
Dilution	No. positive mice/no. tested	Mean ± SD, incubation, d
Undiluted	6/6	249 ± 2
10^{-1}	6/6	283 ± 15
10^{-2}	6/6	316 ± 21
10^{-3}	6/6	342 ± 10
10^{-4}	6/6	453 ± 66
10^{-5}	2/6	479, 495†
10^{-6}	1/6	502†
10^{-7}	0/6	>700

*A 10% (wt/vol) homogenate was prepared by using frontal cortex from a clinically affected patient with vCJD. Groups of 6 tgBov mice were inoculated intracerebrally with 20 μL of serial 10-fold dilutions of this homogenate. Mice were considered positive when abnormal prion protein deposition was detected in the brain. vCJD, variant Creutzfeldt-Jakob disease.
†Dilutions at which <50% of mice were positive.

vCJD and Control Patients

We investigated tissues from 4 clinical vCJD case-patients (vCJD-1–vCJD-4) and 1 asymptomatic person with vCJD who had received a transfusion of packed erythrocytes from a donor who subsequently died from vCJD (*12*). Tissues from 2 non–vCJD–affected patients were used as controls. For case-patients who provided appropriate consent, the entire *PRNP* gene coding sequence was established to exclude pathogenic mutations in this gene (*13*,*14*).

Mouse Bioassays

Bioassays were performed by using mice expressing bovine PrP (tgBov-tg110) as described (*15*,*16*). These mice were observed daily and their neurologic status was assessed weekly. When clinically progressive TSE symptoms were evident, or at the end of their lifespan, the animals were euthanized. Survival time was expressed as the mean ± SD days postinoculation of mice positive for PrP^{res}. For mice that showed no clinical signs, they were humanely killed at the end of their natural lifespan (600–800 days). In these instances, incubation periods are reported as >600

Table 2. Endpoint titration of PMCA seeding activity in a reference brain sample from a patient with vCJD*

	Reference vCJD 10% brain homogenate dilution series, no. of positive PMCA reactions/no. reactions conducted								
Amplification round	10^{-2}	10^{-3}	10^{-4}	10^{-5}	10^{-6}	10^{-7}	10^{-8}	10^{-9}	10^{-10}
1	6/6	6/6	0/6	0/6	0/6	0/6	0/6	0/6	0/6
2	6/6	6/6	5/6	3/6	0/6	0/6	0/6	0/6	0/6
3	6/6	6/6	6/6	6/6	3/6	0/6	0/6	0/6	0/6
4	6/6	6/6	6/6	6/6	6/6	5/6	2/6	0/6	0/6
5	6/6	6/6	6/6	6/6	6/6	5/6	2/6	0/6	0/6
6	6/6	6/6	6/6	6/6	6/6	5/6	2/6	0/6	0/6

*A 10% (wt/vol) homogenate was prepared by using frontal cortex from a symptomatic patient with vCJD (same homogenate as in Table 1). Samples were serially diluted 10-fold (10^{-2}–10^{-10}) before being used to seed PMCA reactions. Six individual replicates of each sample dilution were tested. PMCA substrate was prepared by using brains from transgenic mice overexpressing the ARQ variant of sheep prion protein. PMCAs were subjected to 6 rounds of amplification, each composed of 96 cycles (sonication for 10 s and incubation for 14.5 min at 39.5°C) in a Qsonica700 Sonicator (Qsonica LLC, Newtown, CT, USA). After each round, reaction products (1 volume) were mixed with fresh substrate (9 volumes) to seed the following round. Part of the same product was analyzed by Western blotting for abnormal PrP^{res} by using Sha31 antibody epitope YEDRYYRE. Values are number of PrP^{res} Western Blot–positive replicates corresponding to each round and each dilution. PMCA, protein misfolding cyclic amplification; PrP^{res}, proteinase K–resistant prion; vCJD, variant Creutzfeldt-Jakob disease.

days postinoculation, which corresponded to survival time observed for ≥3 of 6 mice.

Estimation of Infectious Prion Titers

We estimated infectious titer in a reference 10% (wt/vol) frontal cortex homogenate from a clinical vCJD patient by using endpoint titration (intracerebral route) in tgBov mice. Infectious titer (50% lethal dose/g intracerebral in tgBov mice) was estimated by using the Spearman method.

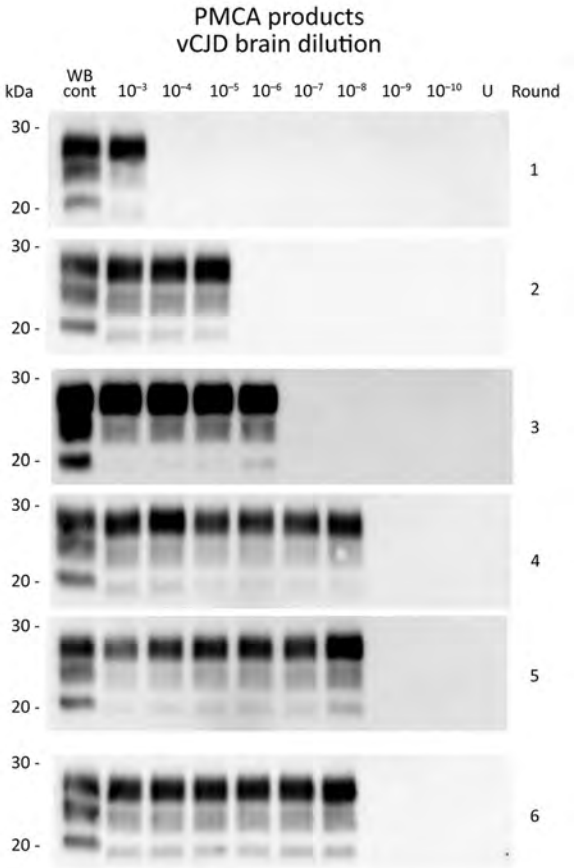

Figure 1. Western blots of variant Creutzfeldt-Jakob disease (vJCD) proteinase K–resistant prions (PrP^{res}) analyzed by protein misfolding cyclic amplification (PMCA) in tissues of clinical and asymptomatic patients. PMCAs were seeded with a 10-fold serial dilutions of a reference vCJD brain homogenate (10% wt/vol, 10^{-2}–10^{-10} dilutions). This homogenate had been endpoint titrated by bioassay in bovine prion (PrP)–expressing mice (tgBov, intracerebral route, $10^{7.7}$ 50% lethal dose/g). PMCA substrate was prepared by using brains from transgenic mice overexpressing the ARQ variant of sheep prion protein. An unseeded (lane U) reaction was included as a specificity control. PMCAs were subjected to 6 rounds of amplification, each composed of 96 cycles (sonication for 10 s and incubation for 14.5 min at 39.5°C) in a Qsonica700 Sonicator (Qsonica LLC, Newtown, CT, USA). After each round, reaction products (1 volume) were mixed with fresh substrate (9 volumes) to seed the following round. Part of the same product was analyzed by Western blotting for abnormal PrP^{res} (Sha31 antibody epitope YEDRYYRE). A sheep scrapie sample (WB cont) was included as a control on each gel. WB, Western blot.

The titer of prion infectivity in vCJD–affected patient bone marrow samples was estimated by using the method of Arnold et al. (*17*). This method uses the probability of survival (attack rate at each dilution) and the individual mouse incubation periods at each dilution to estimate infectious load and is thus able to provide more accurate estimation of titer than using either attack rate or incubation period data alone.

PMCA Reactions

A transgenic mouse line that expresses ovine $A_{136}R_{154}Q_{171}$ PrP variant PrP^{C} (tgShXI) was used to prepare the PMCA substrate as described (*18*,*19*). PMCA amplification was performed as described (*11*). Each PMCA experiment included a reference vCJD sample (10% brain homogenate) as a control for the amplification efficiency. Unseeded controls (1 unseeded control for 8 seeded reactions) were also included in each experiment. For each tested dilution of each sample, ≥4 replicates were tested in 2 independent experiments. For each sample, the highest dilution showing ≥50% of positive replicates (presence of detectable PrP^{res} in the reaction as assessed by using Western blotting) was determined.

Detection of Abnormal PrP by Western Blotting and Paraffin-Embedded Tissue Blotting

Extraction of proteinase K–resistant abnormal PrP and Western blotting were performed as described (*11*). Immunodetection was performed by using 2 PrP-specific monoclonal antibodies, Sha31 (1 μg/mL) (*20*), and 12B2 (4 μg/mL) (*21*), which recognize amino acid sequences YEDRYYRE (145–152), and WGQGG (89–93), respectively. Paraffin-embedded tissue blotting was performed as described (*22*,*23*).

Results

Sensitivity of vCJD Agent Detection by PMCA and Bioassay

To determine the relative sensitivity of PMCA, we retitrated a reference sample (10% cerebral cortex homogenate from a vCJD-affected patient) that had previously undergone endpoint titration (IC inoculation route; Table 1) in bovine PrP–expressing mice (tgBov). Amplification of a 10-fold serial dilution of this sample (6 individual replicates/dilution point) demonstrated that 4 PMCA rounds (24 hours/round, i.e., 96 h) were sufficient to reach the maximum sensitivity level of the assay. Additional PMCA rounds did not improve the analytical sensitivity of the assay or the number of positive replicates (Table 2; Figure 1). On the basis of these results, we estimated by using the Spearman method that the seeding activity of the isolate was 10^{11} 50% seeding activity/per g. Bioassay endpoint titration data for the same sample in tgBov mice

Table 3. Characteristics of 5 patients with vCJD and 2 controls in study of distribution and quantitative estimates of variant prions in tissues*

Patient identification no.	Diagnosis	Sex	Year of death	Age, y, at death	Disease duration, mo	*PRNP* gene codon 129	*PRNP* gene mutations
vCJD-1	vCJD	M	1999	33	18	MM	None detected
vCJD-2	vCJD	F	2000	17	18	MM	None detected
vCJD-4	vCJD	M	2000	26	10	MM	None detected
vCJD-3	vCJD	M	2001	26	10	MM	None detected
vCJD-A	Asymptomatic vCJD	F	2004	82	NA	MV	None detected
NC-1	No CJD (tumor, infarction, ischemia)	F	2005	85	NA	MM	No consent for sequencing
NC-2	No CJD (Alzheimer's disease, infarction, ischemia)	F	2010	80	NA	MM	None detected

*NA, not applicable; vCJD, variant Creutzfeldt-Jakob disease.

showed an infectious titer of $10^{7.7}$ LD_{50}/g. When we took into account the 4-fold lower amount of material used to seed the PMCA reaction compared with material used in mouse inoculations, we found that the PMCA protocol used was 465 times more sensitive than the bioassay of tgBov mice for detection of vCJD prions.

PMCA for Control and vCJD Patients

We complied basic demographic data for vCJD and control patients (Table 3). A 10-fold dilution series of 10% homogenates from the vCJD–affected and non–vCJD–affected control patients was prepared, and this series was subjected to 4 rounds of PMCA. Amplification products from each round were tested for PrP^{res} using by Western blotting (Table 4; Figure 2).

We found that none of the reactions seeded with tissue homogenates from non–CJD controls were positive for PrP^{res} (Table 4). In contrast, PMCA reactions seeded with tissues from the 4 symptomatic vCJD patients were positive for PrP^{res} (Table 4; Figure 2). As expected, among tested tissues, brain homogenates (temporal cortex) showed the highest seeding activity (highest PrP^{res}-positive dilution 10^{-8}). All lymphoid organs tested also showed seeding activity, but the highest PMCA-positive dilution varied

Table 4. Protein misfolding cyclic amplification reactions seeded with tissue homogenate from vCJD and control patients*

	Clinical vCJD patients, Met_{129}/Met_{129}				Preclinical vCJD patient, Met_{129}/Val_{129}	Non–vCJD controls, Met_{129}/Met_{129}	
Tissue	vCJD-1	vCJD-2	vCJD-3	vCJD-4	vCJD-A	NC-1	NC-2
Frontal cortex	10^{-8}	10^{-8}	10^{-8}	10^{-8}	–	–	–
Pituitary gland	NA	NA	NA	NA	10^{-2}	–	–
Trigeminal ganglia	NA	NA	NA	NA	–	–	–
Dorsal root ganglia	NA	NA	NA	NA	–	–	–
Cervical lymph node	10^{-5}	10^{-4}	10^{-4}	10^{-3}	10^{-4}	NA	NA
Tonsil	10^{-3}	10^{-4}	10^{-6}	10^{-3}	10^{-3}	NA	–
Appendix	10^{-4}	10^{-4}	10^{-4}	10^{-3}	10^{-2}	–	–
Distal Ileum	10^{-3}	10^{-5}	10^{-5}	10^{-2}	10^{-3}	–	–
Spleen	10^{-4}	10^{-4}	10^{-5}	10^{-4}	10^{-3}	–	–
Thymus	NA	10^{-3}	10^{-2}	10^{-2}	10^{-2}	NA	NA
Lung	10^{-2}	10^{-2}	–	–	10^{-3}	–	–
Heart	10^{-2}	10^{-2}	–	–	–	–	–
Liver	10^{-4}	10^{-2}	10^{-2}	10^{-4}	10^{-2}	–	–
Kidney	10^{-2}	10^{-3}	–	10^{-3}	–	–	–
Salivary gland	10^{-4}	10^{-3}	10^{-2}	10^{-3}	10^{-2}	–	–
Pancreas	10^{-2}	–	10^{-2}	10^{-4}	–	–	–
Thyroid	10^{-2}	–	10^{-2}	10^{-2}	–	–	–
Adrenal gland	10^{-3}	10^{-3}	10^{-3}	10^{-4}	–	–	–
Bone marrow	10^{-4}	10^{-5}	10^{-3}	10^{-4}	–	–	–
Skeletal muscle	10^{-4}	10^{-2}	–	NA	–	–	–
Testis	–	NA	–	10^{-3}	NA	NA	NA
Ovary	NA	10^{-4}	NA	NA	NA	NA	NA

*PMCA reactions were seeded with 10-fold serial dilutions of 10% tissues homogenates (10^{-2}–10^{-9}) that had been collected postmortem from 4 symptomatic vCJD patients (vCJD-1–vCJD-4) or an asymptomatic vCJD-infected person (vCJD-A). At least 4 replicates of each sample dilution were tested in 2 independent PMCA experiments. Prions from patients vCJD-1–vCJD-4 were homozygous for methionine at codon 129 of the *PRNP* gene. Prion from patient vCJD-A was heterozygous (methionine/valine) at codon 129 of the *PRNP* gene. PMCA substrate was prepared by using brains from transgenic mice overexpressing the ARQ variant of sheep prion protein. Reactions seeded with tissues from 2 non–vCJD-infected control patients (NC-1 and NC-2) were included as negative controls. PMCAs were subjected to 4 rounds of amplification, each composed of 96 cycles (sonication for 10 s and incubation for 14.5 min at 39.5°C) in a Qsonica700 Sonicator (Qsonica LLC, Newtown, CT, USA). PMCA reactions were analyzed by Western blotting for proteinase K–resistant PrP by using Sha31 antibody epitope YEDRYYRE. Values are the highest dilution that resulted in a positive Western blot result in $\geq$50% of the tested replicates after 4 PMCA amplification rounds. NA, not applicable; PMCA, protein misfolding cyclic amplification; PrP, prion protein; vCJD, variant Creutzfeldt-Jakob disease; –, negative.

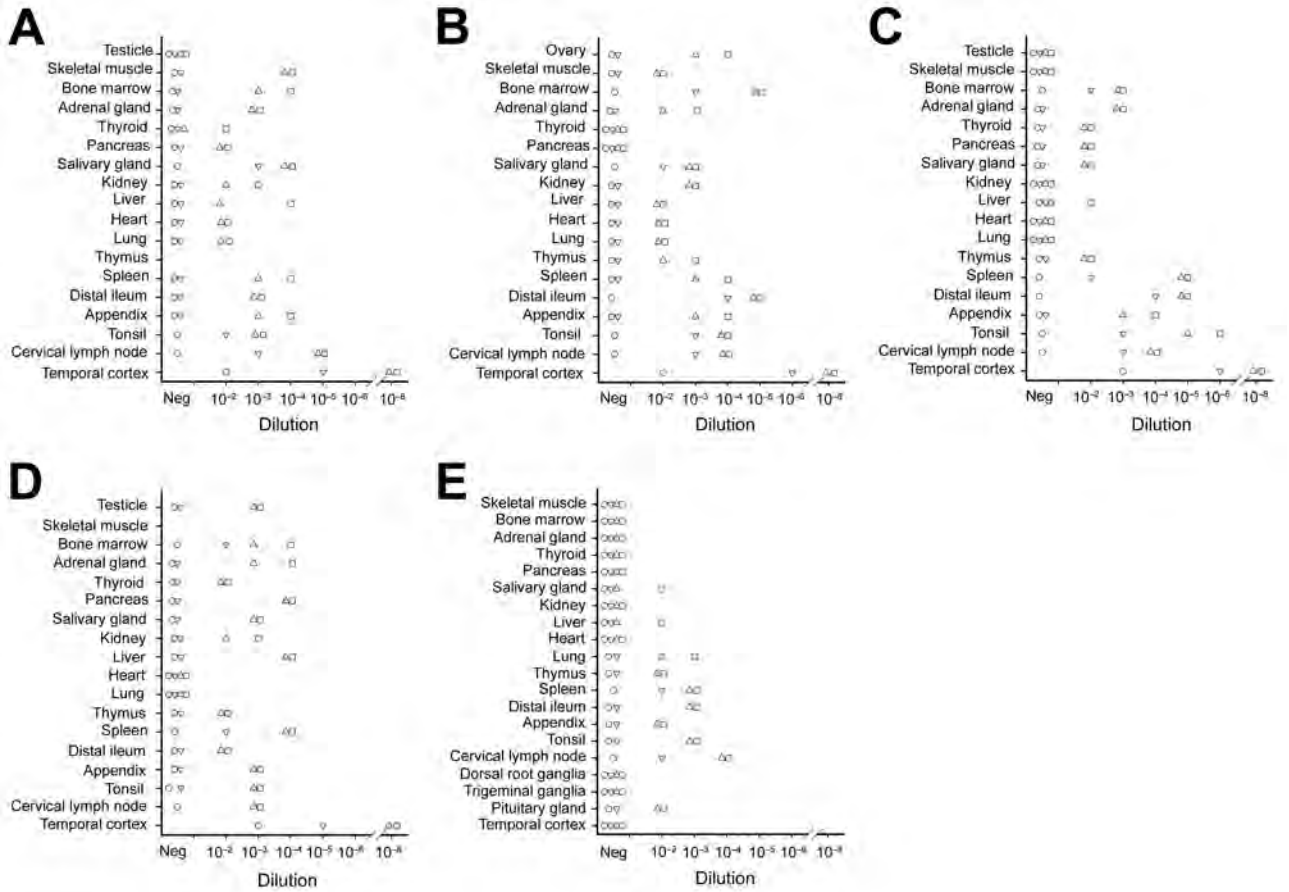

Figure 2. Protein misfolding cyclic amplification (PMCA) of peripheral tissues from patients with variant Creutzfeldt-Jakob disease (vCJD). PMCA reactions were seeded with a 10-fold dilution series of vCJD tissue homogenates (10^{-2}–10^{-9}) obtained postmortem from CJD-infected patients. At least 4 replicates of each sample dilution were tested in 2 independent PMCA experiments. Patients vCJD-1 (A), vCJD-2 (B), vCJD-3 (C), and vCJD-4 (D) died of clinical vCJD. These 4 patients were infected with prions containing methionine at codon 129 of the *PRNP* gene (homozygote). Patient vCJD-A (E) died during an asymptomatic or preclinical stage of the disease. This patient was infected with a prion containing methionine/valine at codon 129 of the *PRNP* gene (heterozygote). PMCA substrate was prepared by using brains from transgenic mice overexpressing the ARQ variant of sheep prion protein. Unseeded reactions and a reaction seeded with tissues from 2 non–vCJD-infected control patients (NC-1 and NC-2; Table 3) were included as specificity controls. PMCAs were subjected to 4 rounds of amplification, each composed of 96 cycles (sonication for 10 s and incubation for 14.5 min at 39.5°C) in a Qsonica700 Sonicator (Qsonica LLC, Newtown, CT, USA). After each round, reaction products (1 vol) were mixed with fresh substrate (9 vol) to seed the following round. Part of the same product was analyzed by Western blotting for abnormal proteinase K–resistant prions (PrP^{res}) (Sha31 antibody epitope YEDRYYRE). For each round, the highest dilution showing a positive Western blot result in at least half of the replicates tested is indicated. Circles, round 1; ∇ round 2; Δ, round 3; squares, round 4. Neg, negative.

according to the organs tested from 10^{-2} (thymus) to 10^{-6} (distal ileum and tonsil). Moreover, for a given lymphoid organ, $\leq 10^2$-fold differences was observed in seeding activity, depending on the patient and sample tested. These data indicate that for symptomatic vCJD patients, lymphoid organs contain 10^2–10^6-fold less prion seeding activity than the same amount of brain tissue (Table 4).

Salivary gland, adrenal gland, liver, and bone marrow from the 4 symptomatic vCJD patients showed positive reactions by PMCA (Figures 2, 3). Using the highest dilution to show a positive reaction as a measure of seeding activity, we found that the vCJD agent in these tissues was 10^3–10^6-fold lower than that for the brain. PrP^{res} was also detected by PMCA reactions seeded with heart, liver, kidney, skeletal muscle, several endocrine/exocrine glands (pancreas, thyroid), and gonads, from some, but not all, of the 4 clinical vCJD patients. Positive tissues contained a level of vCJD seeding activity that was equivalent to those observed in distal ileum (i.e., 10^3–10^6-fold lower than for the brain). Irrespective of the tissue used to seed the PMCA reactions, the PrP^{res} Western blot profile for positive reactions was indistinguishable from that observed in reactions seeded with the vCJD brain control (Figure 3).

Analysis of Tissues from an Asymptomatic vCJD-Infected Person

Prion seeding activity was not detected in the brain (temporal cortex) of the asymptomatic vCJD–affected patient, who was infected with a *PRNP* gene codon 129 heterozygote (Met/Val$_{129}$) prion (*12*) (Table 4; Figure 2). PMCA reactions seeded with dorsal root ganglia or trigeminal ganglia homogenates from this patient showed negative results. However, seeding activity was detected in the pituitary gland (highest PrP^{res}-positive dilution 10^{-2}). In addition, as for the symptomatic vCJD patient, PMCA amplification readily detected vCJD prions in all lymphoid organs tested from this asymptomatic person. On the basis of PMCA results, the vCJD agent load in lymphoid organs in this asymptomatic patient infected with the *PRNP* gene codon 129 Met/Val$_{129}$ prion was similar to those for patients infected with Met/Met$_{129}$ prions during the clinical stage of disease.

In addition to findings for lymphoid organs, prion seeding activity was detectable in certain peripheral tissues (salivary gland, lung, and liver) from this patient (Tables 4; Figures 2, 3). Certain tissues, such as bone marrow or adrenal gland, that contained a substantial prion seeding activity in the clinically affected patients showed negative results. Again, the PrP^{res} Western blot profile for positive reactions was indistinguishable from that observed for reactions seeded with the vCJD brain control.

vCJD Infectivity in Bone Marrow

To test whether PMCA seeding activity in peripheral tissues from vCJD patients correlated with infectivity, we inoculated bone marrow samples from the symptomatic patient into tgBov mice. Clinical TSE was observed in mice that were inoculated with each of the 4 bone marrow samples. The PrP^{res} Western blot profile and the PrP^{res} distribution pattern, as assessed by paraffin-embedded tissue blotting for brain of the bone marrow–inoculated mice, were identical to those observed in tgBov mice inoculated with the vCJD brain control sample (Figure 4).

Data obtained for mice inoculated with bone marrow samples were also used to estimate prion infectivity levels in these samples. For this purpose, we applied the method of Arnold et al. (*17*). This method combines the probability of survival (attack rate) and the individual mouse incubation period to provide an estimation of infectious titers. We used data corresponding to endpoint titration in tgBov mice for reference vCJD sample (frontal cortex from a clinical vCJD patient) (Table 1) to derive the relationship between prion titer of inoculum and the probability of infection and length of the incubation period (Figure 5). We found that bone marrow samples had an infectious titer that ranged from $10^{2.3}$ LD$_{50}$/g through $10^{4.7}$ LD$_{50}$/g in tgBov mice (Table 5).

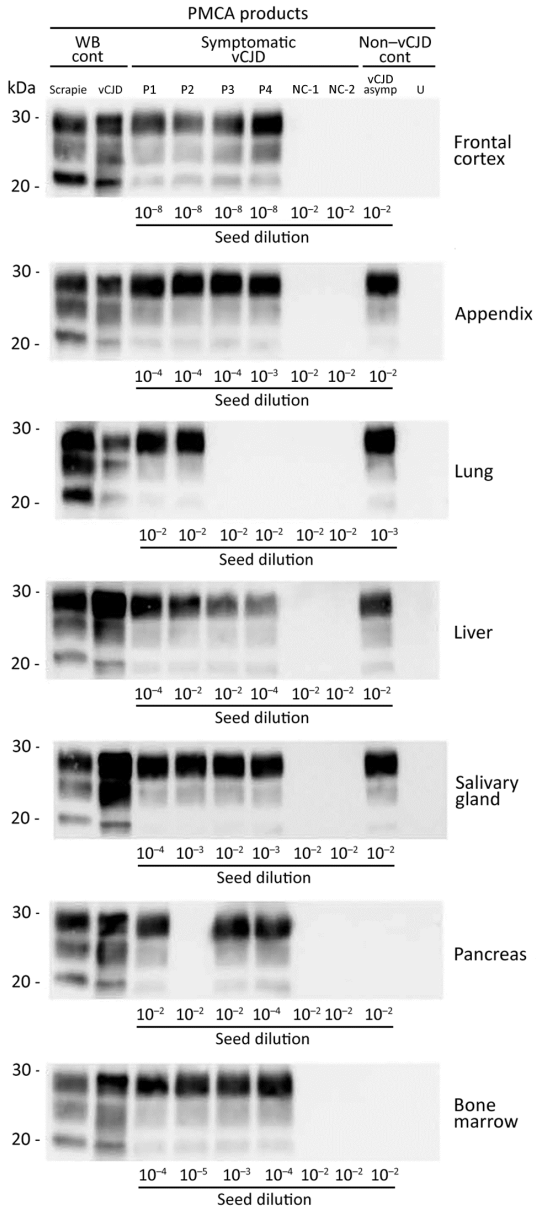

Figure 3. Western blots of proteinase K–resistant prions (PrP^{res}) in PMCA reactions seeded with peripheral tissues. PMCA reactions were seeded with a 10-fold dilution series (10^{-2}–10^{-9}) of variant Creutzfeldt-Jakob disease (vCJD) tissue homogenates that had been collected postmortem from vCJD patients during the clinical stage (symptomatic vCJD patient 1–vCJD patient 4 [P1–P4]) or at an asymptomatic or preclinical stage of the disease (vCJD asymp) (Table 2). Reactions seeded with tissues from 2 non-vCJD patients (Table 2) were used as controls, and an unseeded (lane U) reaction was included as a specificity control. Reactions were then subjected to 4 amplification rounds, each composed of 96 cycles (sonication for 10 s and incubation for 14.5 min at 39.5°C) in a Qsonica700 Sonicator (Qsonica LLC, Newtown, CT, USA). PMCA reactions were analyzed by using Western blotting for abnormal PrP^{res} (Sha31 antibody epitope YEDRYYRE). A sheep scrapie sample and a vCJD reference isolate were used as controls. For the 7 tissues tested, the dilution of tissue homogenates used to seed the PMCA reactions is indicated below the immunoblots. Cont, control; WB, Western blot.

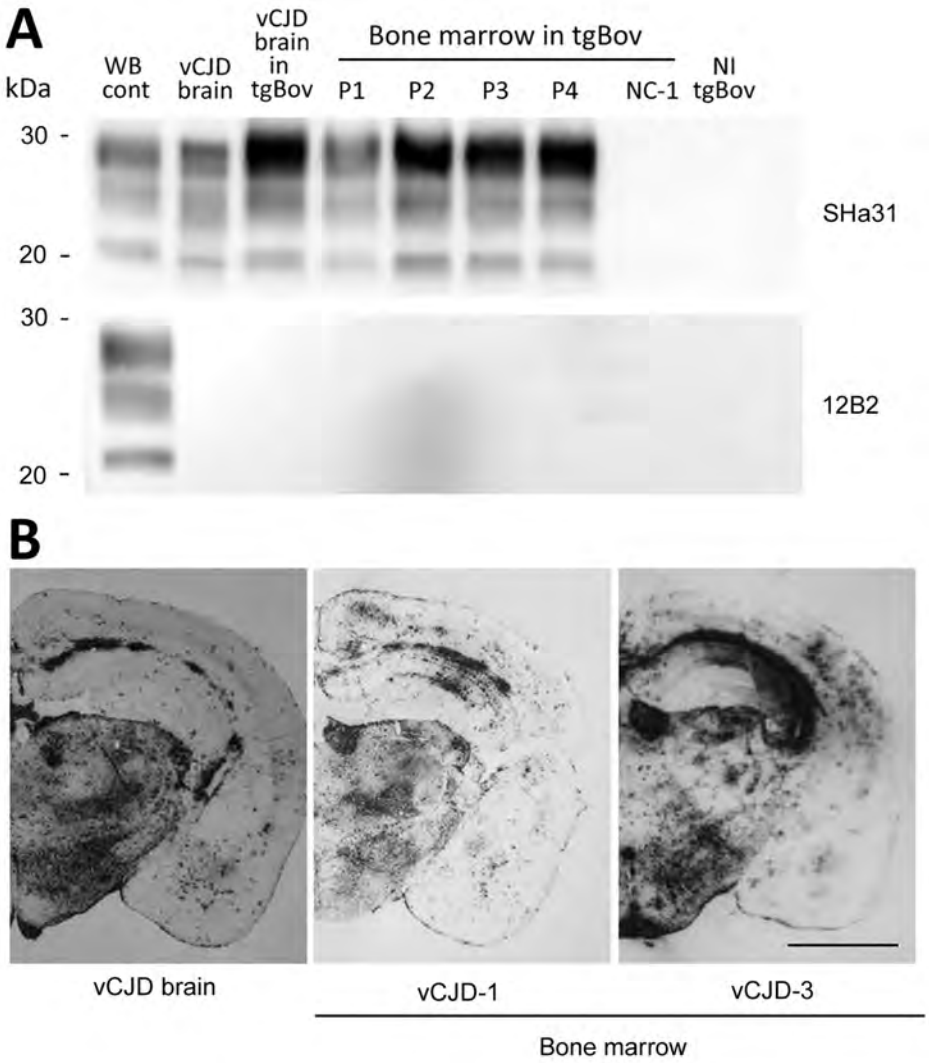

Figure 4. Detection of proteinase K–resistant prions (PrP^{res}) by using Western blotting and paraffin-embedded tissue (PET) blotting of brains of transgenic mice expressing bovine PrP (tgBov). A) PrP^{res} WB of a vCJD sample (frontal cortex), tgBov mice (brain) inoculated with the same vCJD reference isolate, bone marrow samples from vCJD-affected patients (vCJD 1–vCJD-4 [P1–P4]; Table 2), and a non–vCJD control (NC-1; Table 2). A scrapie isolate (WB cont) and a noninoculated tgBov brain (vCJD brain) homogenate were included as controls. PrP^{res} immunodetection was performed by using Sha31 monoclonal antibody (epitope $_{145}$YEDRYYRE$_{152}$) and 12B2 epitope (epitope $_{89}$WGQGG$_{93}$). B) PET blotting of PrP^{res} distribution in coronal section (thalamus level) of tgBov mice inoculated with a reference vCJD isolate (10% brain homogenate) or bone marrow (10% tissue homogenate) from 2 vCJD patients (vCJD-1 and vCJD-3; Table 2) at the clinical stage of disease. Immunodetection of PrP^{res} was performed by using Sha31 monoclonal antibody (epitope $_{145}$YEDRYYRE$_{152}$). Cont, control; NI, not inoculated; WB, Western blot. Scale bar indicates 120 μm.

These values are consistent with a 10^3–10^5 lower infectivity load in bone marrow samples than in the reference vCJD brain sample. Consistent with the PMCA results (Table 4), we found that prion load in bone marrow samples (highest PrP^{res}–positive dilution [10^{-3}–10^{-5}]) was also 10^3–10^5-fold lower than for the reference vCJD isolate (highest PrP^{res}–positive dilution [10^{-8}]). These results strongly support the idea that PMCA seeding activity provides a reliable estimate of the prion load in tissues from vCJD-infected patients.

Discussion

Most previous studies with tissue from vCJD patients have failed to identify consistent accumulation of the vCJD agent outside the nervous and lymphoreticular systems. However, data obtained in this study clearly demonstrate the presence of vCJD prions in a wide and unexpected variety of peripheral tissues.

Natural scrapie and experimental BSE in sheep are 2 models of orally transmitted prion diseases (*24*,*25*). In both diseases, the agent accumulates in the lymphoreticular system and the enteric nervous system during the early preclinical phase of the incubation period. Moreover, an early and persistent prionemia is observed in asymptomatic infected animals (*26*,*27*). These features were also observed in vCJD in humans and in view of the likely origin of vCJD (oral exposure to BSE agent), these similarities have led to a consensus that BSE and scrapie in sheep and vCJD in human have a common pathogenesis (*28*).

Although vCJD prions in a variety tissues, such as bone marrow, kidney, salivary gland, skeletal muscle, pancreas, liver, or heart, might be surprising, each of these tissue has already been demonstrated to accumulate prion infectivity or abnormal prion protein in TSE-infected sheep (*29*–*33*). Because low levels of infectivity have been reported in blood fractions from a vCJD-affected

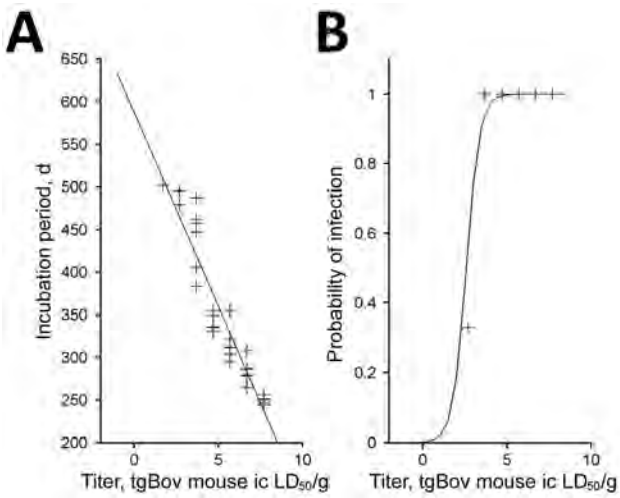

Figure 5. Dose–response relationship for A) incubation period and B) probability of infection of bovine PrP–expressing mice. Data were derived from an endpoint titration of 10% (wt/vol) frontal cortex homogenate from a patient with variant Creutzfeldt-Jakob disease. This homogenate was inoculated into tgBov mice (20 μL by intracerebral [ic] route; Table 1). This procedure was used to establish a model that estimates infectious titer in a homogenate on the basis of incubation period and the probability of infection in inoculated mice. Model plots are indicated by solid lines. +, observed value. LD_{50}, 50% lethal dose.

patient, such widespread tissue positivity might be derived from residual blood, rather than from the solid tissue in these samples (*16*). However, this proposal seems unlikely because in whole blood PMCA amplification inhibitors preclude detection of endogenous vCJD agent by this method (*11*,*34*–*36*).

The patient in our study who was infected with a prion containing *PRNP* gene codon 129 Met/Val is 1 of only 2 identified vCJD agent–infected persons known to have died of other causes before onset clinical symptoms of vCJD, and the only person who provided consent to sample autopsy tissues for research. For this patient, all previous investigations did not detect abnormal prion protein or infectivity in the brain (*12*,*37*). The negative PMCA results we obtained for cerebral cortex, dorsal root ganglia, and trigeminal ganglia tissue from this patient are consistent with a lack of central nervous system involvement at the time of death. However, PMCA seeding activity in the pituitary gland was surprising in this instance.

The presence of abnormal prion protein accumulation in the pituitary gland and other circumventricular organs before deposition of PrP^{res} in surrounding brain has been reported in TSE-infected sheep (*38*). However, this phenomenon in animals does not represent the main route for neuroinvasion and is a probable consequence of hematogenous dissemination of the TSE agent through the fenestrated capillary system of the circumventricular organs, which is substantially more permeable than the other capillaries in the brain (blood–brain barrier). Therefore, this finding might be a consequence of the hematogenous route of secondary vCJD in this person (by transfusion of packed erythrocytes from a vCJD-infected donor), in contrast to the oral route of infection in primary clinical vCJD cases (*12*).

vCJD prions were detected in certain peripheral tissues from the patients infected with a prion containing the *PRNP* gene codon 129 Met/Val. Although distribution of vCJD seeding activity in lymphoreticular tissues was similar to that observed for symptomatic vCJD patients, several tissues that were positive in clinically affected patients were negative in this heterozygous asymptomatic person. These findings suggest that involvement of some peripheral tissues might occur at a later stage in the incubation period than others, or that they could involve recirculation of the agent from the central nervous system (i.e., centrifugal spread in a late state). However, we cannot discount the possibility that that these differences in tissue distribution are caused by the hematogenous route of infection in this person (as opposed to the probable oral route in patients with clinical vCJD) or the difference between the *PRNP* gene codon 129 genotype of the asymptomatic vCJD–affected person (*PRNP* gene codon 129 Met/Val) and persons with clinical vCJD (*PRNP* gene codon 129 Met/Met).

Irrespective of the actual explanation for these differences, the presence of vCJD agent in peripheral tissues of patients during preclinical and clinical stage of the disease

Table 5. Bone marrow sample bioassay in bovine PrP–expressing mice (tgBov) for 4 patients with vCJD*

Sample	Transmission in tgBov mice		Mean infectious titer, LD_{50}/g (95% CI)
	No. positive/no. inoculated mice	Mean ± SD incubation, d	
vCJD-1	5/5	458 ± 37	$10^{3.1}$ ($10^{2.6}$–$10^{3.5}$)
vCJD-2	6/6	373 ± 35	$10^{4.7}$ ($10^{4.3}$–$0^{5.2}$)
vCJD-3	4/6	504 ± 10	$10^{2.3}$ ($10^{1.8}$–$10^{2.7}$)
vCJD-4	6/6	447 ± 91	$10^{4.0}$ ($10^{3.4}$–$0^{4.5}$)
PBS control	0/6	>600	NA

*A 10% wt/vol bone marrow homogenate prepared from 4 symptomatic vCJD patients (Table 3) was inoculated intracerebrally into 6 tgBov mice (20 μL/mouse). One mouse (inoculated with homogenate from patient vCJD-1) died within the first few days after intercerebral inoculation. Mice were euthanized when they showed clinical signs of prion infection or after 600-d postinoculation. Mice were considered prion infected when abnormal PrP deposition was detected in brain. Infectious prion titers were estimated by using the method of Arnold et al. (*17*). The method uses the probability of survival (attack rate at each dilution) and the individual mouse incubation periods at each dilution to estimate infectious load. Infectious titers are given as estimated values. LD_{50}, 50% lethal dose; NA, not applicable; PBS, phosphate-buffered saline; PrP; prion protein; vCJD, variant Creutzfeldt-Jakob disease.

indicates the potential for iatrogenic transmission of this fatal neurologic condition by surgical procedures. Furthermore, this finding shows that, for certain peripheral tissues, a level of infectivity equivalent to an end stage titer (and attendant risk) is reached at a preclinical stage.

Several hundred cases of iatrogenic CJD have been reported worldwide. These cases appear to result from transmission of sporadic CJD, and most cases have occurred in recipients of human dura mater grafts or after administration of human growth hormone extracted from cadaveric pituitaries (*39*). Although in sporadic CJD the distribution of the agent is largely restricted to the nervous system (central and peripheral), the wide distribution of the vCJD agent in the asymptomatic infected patient we report might serve to increase the range of medical procedures, including dentistry, organ transplant, and surgery involving nondisposable equipment, that might result in iatrogenic transmission of vCJD (*40–43*).

Nevertheless, >20 years after identification of the first vCJD patients, only 5 cases that are a probable consequence of iatrogenic vCJD transmission are known, all in the United Kingdom and associated with blood and blood products. These cases were caused by transfusion of non–leukocyte-depleted erythrocyte concentrates or by treatment involving large amounts of pooled plasma from the United Kingdom that were known to include donations from persons who later showed development of vCJD (*12*,*44–46*).

None of the 220 other vCJD cases identified worldwide have been linked to any other medical or dental procedure. Whereas this fact is reassuring, it would be unwise to disregard the threat that vCJD still poses for public health. Despite the relatively low number (n = 178) of vCJD clinical cases observed in the United Kingdom, the most recent epidemiologic studies indicate that ≈1 of 2,000 persons in the United Kingdom could be infected with the vCJD agent (as indicated by the presence of abnormal prion protein detected by immunohistochemical analysis of lymphoid follicles in the appendix). Each asymptomatic vCJD-infected person represents a potential source of secondary infection. The data in our report offer an opportunity for refining measures that were implemented in many countries to limit the risk for vCJD iatrogenic transmission. The apparent concordance between PMCA biochemical and infectivity bioassay data, and the higher analytical sensitivity of PMCA, suggest that future research need not rely exclusively on time-consuming and costly animal bioassay.

Our results indicate the need for vCJD screening assays. After more than a decade of effort, several vCJD blood detection tests have reached a stage in their development that could enable their evaluation as screening or confirmatory assays (*11*,*47*,*48*). In particular, there is now a strong case for use of PMCA in a highly sensitive and specific blood test for vCJD, as indicated by our previous studies (*11*,*16*) and studies by Bougard et al. (*35*) and Concha-Marambio et al. (*36*). The relationship shown here between PrP^{res} amplification by PMCA and detection of infectivity by bioassay indicates that PMCA seeding activity is a good surrogate marker of infectivity and could provide a sound basis for a vCJD blood test for use with blood or tissue donors.

This study was supported in part by the Department of Health Policy Research Programme and the Scottish Government. The National CJD Research and Surveillance Unit is supported by the Policy Research Program of the Department of Health and the Scottish Government (DH121/5061). The Edinburgh Brain Bank is supported by the Medical Research Council (MRC grant G0900580). The Unité Mixte de Recherche 1225, Ecole Nationale Vétérinaire de Toulouse was supported by the European Union FEDER/INTERREG (EFA282/13 TRANSPRION), the Institut National de la Recherche Agronomique Institut Carnot en Santé Animale, and an Agence Nationale Recherche grant (Unmasking Blood Prions; ANR-15-CE18-0028).

Dr. Douet is a research scientist and assistant lecturer in ophthalmology at the National Veterinary School of Toulouse, Toulouse, France. His primary research interests are the pathogenesis of the prion disease with special emphasis on the iatrogenic risk of transmission.

References

1. McKinley MP, Bolton DC, Prusiner SB. A protease-resistant protein is a structural component of the scrapie prion. Cell. 1983;35:57–62. http://dx.doi.org/10.1016/0092-8674(83)90207-6
2. Bruce ME, Will RG, Ironside JW, McConnell I, Drummond D, Suttie A, et al. Transmissions to mice indicate that 'new variant' CJD is caused by the BSE agent. Nature. 1997;389:498–501. http://dx.doi.org/10.1038/39057
3. Collinge J, Sidle KC, Meads J, Ironside J, Hill AF. Molecular analysis of prion strain variation and the aetiology of 'new variant' CJD. Nature. 1996;383:685–90. http://dx.doi.org/10.1038/383685a0
4. Garske T, Ghani AC. Uncertainty in the tail of the variant Creutzfeldt-Jakob disease epidemic in the UK. PLoS One. 2010;5:e15626. http://dx.doi.org/10.1371/journal.pone.0015626
5. Gill ON, Spencer Y, Richard-Loendt A, Kelly C, Dabaghian R, Boyes L, et al. Prevalent abnormal prion protein in human appendixes after bovine spongiform encephalopathy epizootic: large scale survey. BMJ. 2013;347:f5675. http://dx.doi.org/10.1136/bmj.f5675
6. Wadsworth JD, Joiner S, Hill AF, Campbell TA, Desbruslais M, Luthert PJ, et al. Tissue distribution of protease resistant prion protein in variant Creutzfeldt-Jakob disease using a highly sensitive immunoblotting assay. Lancet. 2001;358:171–80. http://dx.doi.org/10.1016/S0140-6736(01)05403-4
7. Haïk S, Faucheux BA, Sazdovitch V, Privat N, Kemeny JL, Perret-Liaudet A, et al. The sympathetic nervous system is involved in variant Creutzfeldt-Jakob disease. Nat Med. 2003;9:1121–3. http://dx.doi.org/10.1038/nm922
8. Head MW, Ritchie D, Smith N, McLoughlin V, Nailon W, Samad S, et al. Peripheral tissue involvement in sporadic, iatrogenic, and variant Creutzfeldt-Jakob disease: an

immunohistochemical, quantitative, and biochemical study. Am J Pathol. 2004;164:143–53. http://dx.doi.org/10.1016/S0002-9440(10)63105-7
9. Saborio GP, Permanne B, Soto C. Sensitive detection of pathological prion protein by cyclic amplification of protein misfolding. Nature. 2001;411:810–3. http://dx.doi.org/10.1038/35081095
10. Moda F, Gambetti P, Notari S, Concha-Marambio L, Catania M, Park KW, et al. Prions in the urine of patients with variant Creutzfeldt-Jakob disease. N Engl J Med. 2014;371:530–9. http://dx.doi.org/10.1056/NEJMoa1404401
11. Lacroux C, Comoy E, Moudjou M, Perret-Liaudet A, Lugan S, Litaise C, et al. Preclinical detection of variant CJD and BSE prions in blood. PLoS Pathog. 2014;10:e1004202. http://dx.doi.org/10.1371/journal.ppat.1004202
12. Peden AH, Head MW, Ritchie DL, Bell JE, Ironside JW. Preclinical vCJD after blood transfusion in a *PRNP* codon 129 heterozygous patient. Lancet. 2004;364:527–9. http://dx.doi.org/10.1016/S0140-6736(04)16811-6
13. Uro-Coste E, Cassard H, Simon S, Lugan S, Bilheude JM, Perret-Liaudet A, et al. Beyond PrP^{res} type 1/type 2 dichotomy in Creutzfeldt-Jakob disease. PLoS Pathog. 2008;4:e1000029. http://dx.doi.org/10.1371/journal.ppat.1000029
14. Moreno CR, Moazami-Goudarzi K, Laurent P, Cazeau G, Andreoletti O, Chadi S, et al. Which PrP haplotypes in a French sheep population are the most susceptible to atypical scrapie? Arch Virol. 2007;152:1229–32. http://dx.doi.org/10.1007/s00705-007-0956-7
15. Castilla J, Gutiérrez Adán A, Brun A, Pintado B, Ramírez MA, Parra B, et al. Early detection of PrP^{res} in BSE-infected bovine PrP transgenic mice. Arch Virol. 2003;148:677–91. http://dx.doi.org/10.1007/s00705-002-0958-4
16. Douet JY, Zafar S, Perret-Liaudet A, Lacroux C, Lugan S, Aron N, et al. Detection of infectivity in blood of persons with variant and sporadic Creutzfeldt-Jakob disease. Emerg Infect Dis. 2014;20:114–7. http://dx.doi.org/10.3201/eid2001.130353
17. Arnold ME, Hawkins SA, Green R, Dexter I, Wells GA. Pathogenesis of experimental bovine spongiform encephalopathy (BSE): estimation of tissue infectivity according to incubation period. Vet Res. 2009;40:8. http://dx.doi.org/10.1051/vetres:2008046
18. Groschup MH, Buschmann A. Rodent models for prion diseases. Vet Res. 2008;39:32. http://dx.doi.org/10.1051/vetres:2008008
19. Douet JY, Lacroux C, Corbière F, Litaise C, Simmons H, Lugan S, et al. PrP expression level and sensitivity to prion infection. J Virol. 2014;88:5870–2. http://dx.doi.org/10.1128/JVI.00369-14
20. Féraudet C, Morel N, Simon S, Volland H, Frobert Y, Créminon C, et al. Screening of 145 anti-PrP monoclonal antibodies for their capacity to inhibit PrP^{Sc} replication in infected cells. J Biol Chem. 2005;280:11247–58. http://dx.doi.org/10.1074/jbc.M407006200
21. Langeveld JP, Jacobs JG, Erkens JH, Bossers A, van Zijderveld FG, van Keulen LJ. Rapid and discriminatory diagnosis of scrapie and BSE in retro-pharyngeal lymph nodes of sheep. BMC Vet Res. 2006;2:19. http://dx.doi.org/10.1186/1746-6148-2-19
22. Cassard H, Torres JM, Lacroux C, Douet JY, Benestad SL, Lantier F, et al. Evidence for zoonotic potential of ovine scrapie prions. Nat Commun. 2014;5:5821. http://dx.doi.org/10.1038/ncomms6821
23. Lacroux C, Corbière F, Tabouret G, Lugan S, Costes P, Mathey J, et al. Dynamics and genetics of PrP^{Sc} placental accumulation in sheep. J Gen Virol. 2007;88:1056–61. http://dx.doi.org/10.1099/vir.0.82218-0
24. Andréoletti O, Berthon P, Marc D, Sarradin P, Grosclaude J, van Keulen L, et al. Early accumulation of $PrP^{(Sc)}$ in gut-associated lymphoid and nervous tissues of susceptible sheep from a Romanov flock with natural scrapie. J Gen Virol. 2000;81:3115–26. http://dx.doi.org/10.1099/0022-1317-81-12-3115
25. Foster JD, Parnham DW, Hunter N, Bruce M. Distribution of the prion protein in sheep terminally affected with BSE following experimental oral transmission. J Gen Virol. 2001;82:2319–26. http://dx.doi.org/10.1099/0022-1317-82-10-2319
26. Lacroux C, Vilette D, Fernández-Borges N, Litaise C, Lugan S, Morel N, et al. Prionemia and leukocyte-platelet–associated infectivity in sheep transmissible spongiform encephalopathy models. J Virol. 2012;86:2056–66. http://dx.doi.org/10.1128/JVI.06532-11
27. Houston F, Foster JD, Chong A, Hunter N, Bostock CJ. Transmission of BSE by blood transfusion in sheep. Lancet. 2000;356:999–1000. http://dx.doi.org/10.1016/S0140-6736(00)02719-7
28. Hilton DA. Pathogenesis and prevalence of variant Creutzfeldt-Jakob disease. J Pathol. 2006;208:134–41. http://dx.doi.org/10.1002/path.1880
29. Tamgüney G, Richt JA, Hamir AN, Greenlee JJ, Miller MW, Wolfe LL, et al. Salivary prions in sheep and deer. Prion. 2012;6:52–61. http://dx.doi.org/10.4161/pri.6.1.16984
30. Andréoletti O, Simon S, Lacroux C, Morel N, Tabouret G, Chabert A, et al. PrP^{Sc} accumulation in myocytes from sheep incubating natural scrapie. Nat Med. 2004;10:591–3. http://dx.doi.org/10.1038/nm1055
31. Chianini F, Cosseddu GM, Steele P, Hamilton S, Hawthorn J, Síso S, et al. Correlation between infectivity and disease associated prion protein in the nervous system and selected edible tissues of naturally affected scrapie sheep. PLoS One. 2015;10:e0122785. http://dx.doi.org/10.1371/journal.pone.0122785
32. Hadlow WJ, Kennedy RC, Race RE. Natural infection of Suffolk sheep with scrapie virus. J Infect Dis. 1982;146:657–64. http://dx.doi.org/10.1093/infdis/146.5.657
33. Garza MC, Monzón M, Marín B, Badiola JJ, Monleón E. Distribution of peripheral $PrP^{(Sc)}$ in sheep with naturally acquired scrapie. PLoS One. 2014;9:e97768. http://dx.doi.org/10.1371/journal.pone.0097768
34. Castilla J, Saá P, Soto C. Detection of prions in blood. Nat Med. 2005;11:982–5.
35. Bougard D, Brandel JP, Bélondrade M, Béringue V, Segarra C, Fleury H, et al. Detection of prions in the plasma of presymptomatic and symptomatic patients with variant Creutzfeldt-Jakob disease. Sci Transl Med. 2016;8:370ra182. http://dx.doi.org/10.1126/scitranslmed.aag1257
36. Concha-Marambio L, Pritzkow S, Moda F, Tagliavini F, Ironside JW, Schulz PE, et al. Detection of prions in blood from patients with variant Creutzfeldt-Jakob disease. Sci Transl Med. 2016;8:370ra183. http://dx.doi.org/10.1126/scitranslmed.aaf6188
37. Bishop MT, Diack AB, Ritchie DL, Ironside JW, Will RG, Manson JC. Prion infectivity in the spleen of a *PRNP* heterozygous individual with subclinical variant Creutzfeldt-Jakob disease. Brain. 2013;136:1139–45. http://dx.doi.org/10.1093/brain/awt032
38. Sisó S, González L, Jeffrey M. Neuroinvasion in prion diseases: the roles of ascending neural infection and blood dissemination. Interdiscip Perspect Infect Dis. 2010;2010:747892. http://dx.doi.org/10.1155/2010/747892
39. Brown P, Brandel JP, Sato T, Nakamura Y, MacKenzie J, Will RG, et al. Iatrogenic Creutzfeldt-Jakob disease, final assessment. Emerg Infect Dis. 2012;18:901–7. http://dx.doi.org/10.3201/eid1806.120116
40. Flechsig E, Hegyi I, Enari M, Schwarz P, Collinge J, Weissmann C. Transmission of scrapie by steel-surface-bound prions. Mol Med. 2001;7:679–84.
41. Taylor D. Inactivation of the BSE agent. C R Biol. 2002;325:75–6. http://dx.doi.org/10.1016/S1631-0691(02)01386-0
42. Molesworth A, Yates P, Hewitt PE, Mackenzie J, Ironside JW, Galea G, et al. Investigation of variant Creutzfeldt-Jakob disease implicated organ or tissue transplantation in the United Kingdom. Transplantation. 2014;98:585–9. http://dx.doi.org/10.1097/TP.0000000000000105

43. Jayanthi P, Thomas P, Bindhu P, Krishnapillai R. Prion diseases in humans: oral and dental implications. N Am J Med Sci. 2013;5:399–403. http://dx.doi.org/10.4103/1947-2714.115766
44. Peden A, McCardle L, Head MW, Love S, Ward HJ, Cousens SN, et al. Variant CJD infection in the spleen of a neurologically asymptomatic UK adult patient with haemophilia. Haemophilia. 2010; 16:296–304. http://dx.doi.org/10.1111/j.1365-2516.2009.02181.x
45. Llewelyn CA, Hewitt PE, Knight RS, Amar K, Cousens S, Mackenzie J, et al. Possible transmission of variant Creutzfeldt-Jakob disease by blood transfusion. Lancet. 2004;363:417–21. http://dx.doi.org/10.1016/S0140-6736(04)15486-X
46. Lefrère JJ, Hewitt P. From mad cows to sensible blood transfusion: the risk of prion transmission by labile blood components in the United Kingdom and in France. Transfusion. 2009;49:797–812. http://dx.doi.org/10.1111/j.1537-2995.2008.02044.x
47. Edgeworth JA, Farmer M, Sicilia A, Tavares P, Beck J, Campbell T, et al. Detection of prion infection in variant Creutzfeldt-Jakob disease: a blood-based assay. Lancet. 2011;377:487–93. http://dx.doi.org/10.1016/S0140-6736(10)62308-2
48. Jackson GS, Burk-Rafel J, Edgeworth JA, Sicilia A, Abdilahi S, Korteweg J, et al. A highly specific blood test for vCJD. Blood. 2014;123:452–3. http://dx.doi.org/10.1182/blood-2013-11-539239

Address for correspondence: Olivier Andréoletti, Unité Mixte de Recherche 1225, Ecole Nationale Vétérinaire de Toulouse, 23 Chemin des Cappelles, Toulouse 31076, France; email: o.andreoletti@envt.fr

etymologia

Creutzfeldt-Jakob [croyts'felt-yak"ob] Disease

Ronnie Henry, Frederick A. Murphy

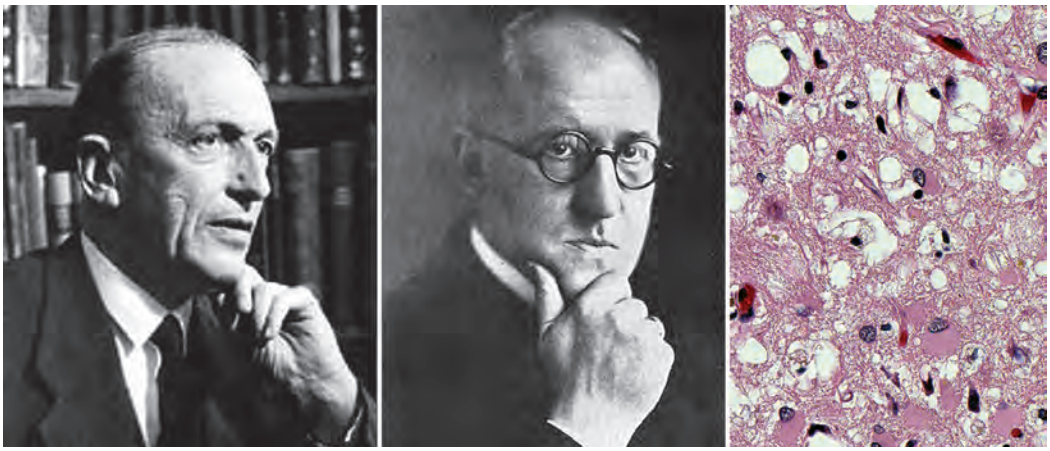

(L–R) Hans Gerhard Creutzfeldt (1885–1964); Alfons Maria Jakob (1884–1931); Creutzfeldt–Jakob disease, cerebrum hematoxylin and eosin staining showing spongiform encephalophathy. Photographs reproduced from *Foundations of Virology,* 2012, courtesy Frederick A. Murphy. Micrograph courtesy of Sherif Zaki, Centers for Disease Control and Prevention, with permission.

In 1920, German neuropathologist Alfons Maria Jakob described a series of 6 patients with spasticity and progressive dementia associated with neural degeneration. Shortly thereafter, in 1921, another German neuropathologist, Hans Gerhardt Creutzfeldt, independently published a similar case. Jakob gave credit to Creutzfeldt for describing the syndrome first, without realizing he had also uncovered the new syndrome. Walther Spielmeyer first used the term "Creutzfeldt-Jakob disease" (CJD) in 1922. CJD occurs worldwide as a rare, sporadic disease, with genetic and iatrogenic forms. A zoonotic form, variant CJD (vCJD), is caused by infection with a prion derived from bovines and occurs predominantly in the United Kingdom.

This issue of *Emerging Infectious Diseases*' long-running *Etymologia* series is dedicated to the memory of Richard T. Johnson, MD (1931–2015), the leading prion disease authority in the United States for many years and great friend of CDC's infectious disease programs, so many of which involve central nervous system disorders.

Sources

1. Brown P, Brandel JP, Sato T, Nakamura Y, MacKenzie J, Will RG, et al. Iatrogenic Creutzfeldt-Jakob disease, final assessment. Emerg Infect Dis. 2012;18:901–7. http://dx.doi.org/10.3201/eid1806.120116
2. Murphy FA. The foundations of virology: discoverers and discoveries, inventors and inventions, developers and technologies. West Conshohocken (PA): Infinity Publishing; 2012.
3. Prusiner SB. Prions. Proc Natl Acad Sci U S A. 1998;95:13363–83. http://dx.doi.org/10.1073/pnas.95.23.13363
4. Richardson EP Jr, Masters CL. The nosology of Creutzfeldt-Jakob disease and conditions related to the accumulation of PrPCJD in the nervous system. Brain Pathol. 1995;5:33–41. http://dx.doi.org/10.1111/j.1750-3639.1995.tb00575.x

Address for correspondence: Ronnie Henry, Centers for Disease Control and Prevention, 1600 Clifton Rd NE, Mailstop E03, Atlanta, GA 30329-4027, USA; email: boq3@cdc.gov

DOI: http://dx.doi.org/10.3201/eid2306.ET2306

Outbreak-Related Disease Burden Associated with Consumption of Unpasteurized Cow's Milk and Cheese, United States, 2009–2014

Solenne Costard, Luis Espejo, Huybert Groenendaal, Francisco J. Zagmutt

The growing popularity of unpasteurized milk in the United States raises public health concerns. We estimated outbreak-related illnesses and hospitalizations caused by the consumption of cow's milk and cheese contaminated with Shiga toxin–producing *Escherichia coli*, *Salmonella* spp., *Listeria monocytogenes*, and *Campylobacter* spp. using a model relying on publicly available outbreak data. In the United States, outbreaks associated with dairy consumption cause, on average, 760 illnesses/year and 22 hospitalizations/year, mostly from *Salmonella* spp. and *Campylobacter* spp. Unpasteurized milk, consumed by only 3.2% of the population, and cheese, consumed by only 1.6% of the population, caused 96% of illnesses caused by contaminated dairy products. Unpasteurized dairy products thus cause 840 (95% CrI 611–1,158) times more illnesses and 45 (95% CrI 34–59) times more hospitalizations than pasteurized products. As consumption of unpasteurized dairy products grows, illnesses will increase steadily; a doubling in the consumption of unpasteurized milk or cheese could increase outbreak-related illnesses by 96%.

Consumer demand for organic and natural foods (i.e., minimally processed foods) has been on the rise (*1*). However, in contrast to some perceptions (*2*), natural food products are not necessarily safer than conventional ones, as evidenced by higher rates of foodborne illnesses associated with unpasteurized dairy products (*3*–*6*). Pasteurization has greatly reduced the number of foodborne illnesses attributed to dairy products, and continuous efforts to reduce milk contamination pre- and post-pasteurization are further decreasing the disease burden (*3*). Yet, despite a decrease in dairy consumption in the United States (*7*), recent studies (*3*,*6*) suggest that over the past 15 years the number of outbreaks associated with unpasteurized dairy products has increased. In parallel with this increase, an easing of regulations has facilitated greater access of consumers to unpasteurized milk (e.g., through farm sales or cow share programs). The number of states where the sale of unpasteurized milk is prohibited decreased to 20 in 2011 from 29 in 2004 (*8*–*10*). This trend toward increased availability of unpasteurized dairy products raises public health concerns, especially because raw milk consumers include children (*2*,*4*,*6*).

Our study aimed at estimating the outbreak-related disease burden associated with the consumption of fluid cow's milk and cheese made from cow's milk (herein also referred to as milk and cheese or dairy products) that are unpasteurized and contaminated with *Campylobacter* spp., *Salmonella* spp., Shiga toxin–producing *Escherichia coli* (STEC), and *Listeria monocytogenes*. We also assessed how hypothetical increases in unpasteurized dairy consumption would affect this outbreak-related disease burden.

Methods

Data Sources

We used outbreak data from the National Outbreak Reporting System (NORS) (*11*) to estimate the incidence rates of illnesses and hospitalizations. NORS is a web-based platform that stores data on all foodborne disease outbreaks reported by local, state, and territorial health departments in the United States that have occurred since 2009. We included all outbreaks that occurred during 2009–2014 in which the confirmed etiologic agents were any of the 4 pathogens of interest (*Campylobacter* spp., *Salmonella* spp., STEC, and *L. monocytogenes*) and the implicated food vehicle or contaminated ingredient was milk or cheese (Figure 1). Outbreaks associated with multiple products; processed dairy products other than milk and cheese (e.g., cream, butter, yogurt, and kefir); milk produced by species other than cows; and cheese originating from species other than cows were excluded from the analysis (online Technical Appendix 1, https://wwwnc.cdc.gov/EID/article/23/6/15-1603-Techapp1.xlsx).

Author affiliations: EpiX Analytics, Boulder, Colorado, USA (S. Costard, H. Groenendaal, F.J. Zagmutt); Consultant, St. Augustine, Florida, USA (L. Espejo)

DOI: https://dx.doi.org/10.3201/eid2306.151603

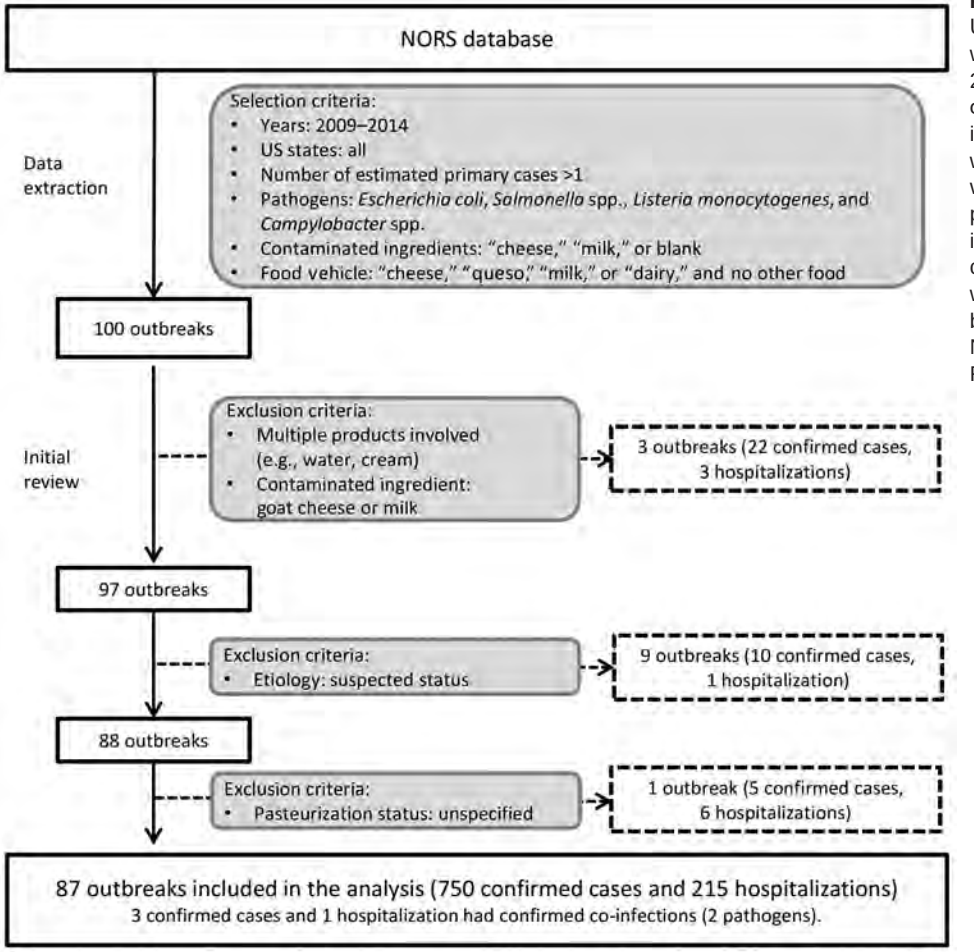

Figure 1. Process for selecting US outbreaks associated with cow's milk and cheese, 2009–2014. Laboratory-confirmed cases are cases with illness in which a specimen was collected and a laboratory was able to confirm the pathogen(s) or agent(s) causing illness. Hospitalizations are cases in which the patient was hospitalized as a result of becoming ill during the outbreak. NORS, National Outbreak Reporting System.

In addition, outbreaks with a suspected etiology status or associated with a dairy product with an unknown pasteurization status were excluded.

The stochastic model (Figure 2) was developed to estimate the following: the incidence rates of illness and hospitalization for pasteurized and unpasteurized dairy products, the excess risk associated with unpasteurized milk and cheese consumption, and the effect potential increases in consumption of unpasteurized dairy products would have on the outbreak-related disease burden (online Technical Appendix 2 Tables 1–5, https://wwwnc.cdc.gov/EID/article/23/6/15-1603-Techapp2.pdf). Inputs (other than the outbreak data) used in the stochastic model were derived from readily available sources of information (online Technical Appendix 2). Dairy consumption estimates were derived from the Foodborne Active Surveillance Network (FoodNet) Population Survey (*12*).

Estimation of the Incidence of Outbreak-Related Illnesses and Hospitalizations

We modeled the uncertainty of the pathogen-specific and pasteurization status–specific incidence rates of illness and hospitalization (λ) in the United States per serving of dairy product using a conjugate gamma distribution (*13*). The number of hospitalizations and laboratory-confirmed cases occurring during the study period (2009–2014) that were caused by a given pathogen after consumption of milk or cheese of a certain pasteurization status was obtained from the NORS database. For laboratory-confirmed cases, this number was adjusted for underreporting, under testing (only a proportion of suspected cases were sampled and tested), and underdiagnosis (based on diagnostic test sensitivity), in order to estimate illnesses for 2009–2014. These pathogen-specific factors were assumed to be independent of the product consumed and its pasteurization status, and constant for the years considered. The analysis did not include adjustment factors for potential misclassification in terms of etiology or pasteurization status. These 2 outbreak characteristics were carefully reviewed, and any outbreak for which the information could not be verified was excluded. It was thus assumed that etiology and pasteurization status misclassifications were negligible in this analysis.

Because NORS is a passive surveillance system, the inherent underreporting associated with it needed to be accounted for. We estimated an underreporting factor by

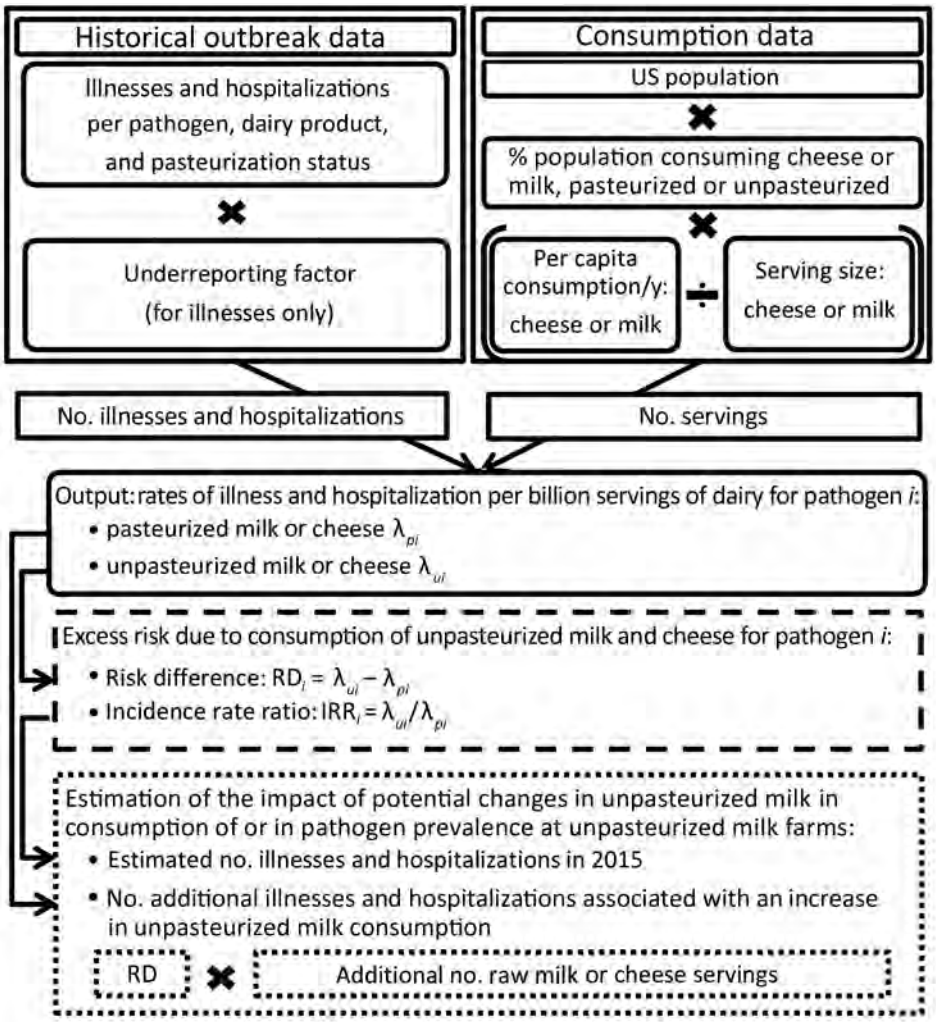

Figure 2. Stochastic model used to estimate the excess risk of outbreak-related illnesses and hospitalization due to unpasteurized dairy product consumption in the United States, 2009–2014. Model contains 3 main components: estimation of the incidence rates of illness and hospitalization for pasteurized and unpasteurized dairy products (elements in the boxes with solid lines), estimation of the excess risk associated with unpasteurized milk or cheese consumption (elements in box with dashed lines), and evaluation of the impact of hypothetical changes in consumption of unpasteurized dairy products (elements in boxes with dotted lines).

using FoodNet data, which is an active surveillance system assumed to include virtually all identified cases (online Technical Appendix 2). First, we extrapolated the total number of laboratory-confirmed cases in the US population during 2009–2013 using the incidence rates reported by FoodNet and considering the proportions of the US population included in FoodNet surveillance sites (*14*). Second, we estimated the total number of outbreak-related cases using the fraction of the US laboratory-confirmed cases that were outbreak-related (*15*). Third, we extracted the proportion of outbreak-related illnesses attributable to dairy (*16*). Fourth, we calculated the ratio of the number of outbreak-related, laboratory-confirmed cases linked to dairy consumption derived from the previously described calculations and the number of dairy-related, laboratory-confirmed cases reported through NORS to use as the underreporting factor in the analysis (online Technical Appendix 2). When estimating the underreporting factor, we assumed that the FoodNet surveillance population and reporting practices were representative of the entire United States and that the food source attribution pertaining to the illnesses from confirmed and suspected outbreaks (*16*) were equally relevant to laboratory-confirmed cases from outbreaks of confirmed status only. We used the sensitivity of the diagnostic tests as described in Scallan et al. (*15*) to estimate the proportion of false-negative, laboratory-confirmed cases from NORS (underdiagnosis factor). Finally, we derived the under-testing factor by using the ratio of laboratory-confirmed primary cases to the estimated total number of primary illnesses reported to NORS (*17*).

The annual number of servings of milk or cheese of a given pasteurization status was calculated as the product of the number of servings of milk or cheese per person for a certain year, the resident population in the United States for that year (*18*) and the percentage of the population of dairy consumers that consume milk or cheese of a particular pasteurization status. The annual per capita consumption of a given dairy product (*19*) was divided by its average serving size (i.e., the amount of milk or cheese that is generally served) (*7*,*20*,*21*) to estimate the annual per capita number

of servings of milk and cheese. These totals were then summed across the years of the study period. The per capita consumption data (*19*) were assumed to include both pasteurized and unpasteurized dairy products. Because unpasteurized dairy products constitute a small percentage of the total consumption, this assumption (if inaccurate) would likely have only a small effect on results. We also hypothesized that the serving sizes (*7*,*20*,*21*) were the same for pasteurized and unpasteurized dairy products.

The estimates of the proportion of dairy consumers that consume milk or cheese of a given pasteurization status were derived from the FoodNet Atlas of Exposure (*12*). Answers from this FoodNet survey are provided as aggregates per survey site, rather than per respondent. Therefore, answers regarding milk and cheese consumption were treated as independent. In addition, we assumed that respondents who reported consumption of unpasteurized milk or cheese did not consume pasteurized milk or cheese. Because the information to calculate the overall proportion of the US population consuming any type of cheese was unavailable, we assumed it to be equal to the proportion of the population reporting consumption of any cheese sold as or cut from solid blocks (i.e., the type of cheese consumed most commonly). We further assumed the proportion of the US population consuming unpasteurized cheese to be equal to the proportion reporting exposure to any cheese made from unpasteurized milk in the previous 7 days.

Estimation of the Excess Risks Attributed to the Consumption of Unpasteurized Milk and Cheese

We estimated the additional risks for illness and hospitalization for consumers of unpasteurized dairy products compared with consumers of pasteurized ones. We calculated excess risk using 1) risk difference (RD), which measures the absolute difference in the observed risks for illness and hospitalization between consumers of unpasteurized dairy products and consumers of pasteurized ones, and 2) incidence rate ratio (IRR), which provides a relative comparison of the risks for illness and hospitalization between the 2 exposure groups (*22*).

Effects of Hypothetical Changes in Consumption of Unpasteurized Milk or Cheese

We assessed the potential public health effects of hypothetical changes in unpasteurized milk consumption. We determined the number of illnesses in 2015 in the United States using the pathogen-specific rates of illnesses and hospitalizations per serving of dairy product. The number of hospitalizations was calculated as pathogen-specific fractions of these illnesses. The pathogen-specific probabilities of hospitalization in cases of illness were assumed unconditional on the pasteurization status of the dairy product involved, but rather dependent on the severity of illness (*23*,*24*).

We estimated the additional illnesses and the additional hospitalizations for each pathogen if a hypothetical increase in consumption of unpasteurized milk or cheese occurred using 1) the change in the proportion of the population consuming unpasteurized milk or cheese, 2) the number of servings of milk or cheese for 2015, and 3) the risk difference in illnesses per serving of dairy for that pathogen. We assumed that the overall proportion of the US population consuming milk or cheese did not change; therefore, the increase in the proportion of the US population consuming unpasteurized milk or cheese corresponded to a shift of dairy consumers from pasteurized to unpasteurized. Six hypothetical scenarios were considered: 10%, 20%, 50%, 100%, 200%, and 500% increases in the proportion of the US population consuming unpasteurized milk or cheese.

Scenario and Sensitivity Analyses

We performed a sensitivity analysis to identify the parameters that most influenced our estimates. The sensitivity of the estimates to the input parameter uncertainties was calculated by using conditional means as implemented in @RISK 6.1.2 (Palisade Corporation, Ithaca, NY, USA). In addition, we assessed the robustness of our sensitivity analysis with a scenario analysis in which we calculated our estimates with different sets of outbreak data. For the main analysis, the model was run on outbreaks of confirmed etiology and pasteurization status. In the scenario analysis, the model was then re-run with either of the 2 following sets of outbreaks added to the main data set: outbreaks of suspected etiology status (*17*) and outbreaks involving dairy products of unspecified pasteurization status assumed to be caused by pasteurized dairy products.

Model Implementation

The model was developed in Excel 2010 (Microsoft Corporation, Redmond, WA, USA) with the Monte-Carlo simulation add-in @RISK 6.1.2. Results are expressed as means and 95% credibility intervals (CrIs, a Bayesian equivalent to the confidence interval) or prediction intervals (PIs, which provides uncertainty bounds for predictions), unless stated otherwise.

Results

Incidence Rates and Increased Risks Associated with the Consumption of Unpasteurized Milk and Cheese

We used a total of 87 outbreaks causing 750 laboratory-confirmed illnesses and 215 hospitalizations in this analysis (Table 1). The incidence rates of STEC, *Salmonella* spp., and *Campylobacter* spp. illnesses and hospitalizations per 1 billion servings were higher for unpasteurized dairy product consumers than for pasteurized dairy product consumers. Illnesses and hospitalizations caused by *L. monocytogenes*

Table 1. Dairy-related illnesses and hospitalizations from 87 outbreaks, National Outbreak Reporting System, United States, 2009–2014*

	Outbreaks associated with milk and cheese consumption, N = 87†					
	Pasteurized			Unpasteurized		
Pathogen	Outbreaks	Illnesses	Hospitalizations	Outbreaks	Illnesses	Hospitalizations
STEC	0	0	0	14‡	99	42
Salmonella spp.	0	0	0	8§	83	29
Listeria monocytogenes	10	100	87	1	1	1
Campylobacter spp.	1	2	0	53‡§	465	56
Overall	11	102	87	76	648	128

*Illnesses and hospitalizations had confirmed etiologies and were associated with the consumption of milk or cheese of known pasteurization status. STEC, Shiga toxin–producing *Escherichia coli*.
†Out of the 87 outbreaks, 10 outbreaks reported a total of 17 deaths, 16 of them were linked to *L. monocytogenes* and 1 to *Campylobacter* spp.
‡One outbreak (38 illnesses and 10 hospitalizations) had 3 cases with confirmed coinfection (STEC and *Campylobacter* spp.). These 3 cases were duplicated because they were assigned to each pathogen.
§One outbreak (4 illnesses and 1 hospitalization) involved 2 pathogens: 3 Illnesses and 1 hospitalization were linked to *Campylobacter* spp. and 1 illness and 0 hospitalizations were linked to *Salmonella* spp.

infections were more often attributed to the consumption of pasteurized cheese than unpasteurized cheese (Table 2). Assuming no change in the consumption of unpasteurized dairy, dairy products contaminated with STEC, *Salmonella* spp., *L. monocytogenes*, and *Campylobacter* spp. were predicted to cause 761 (95% PI 598–994) outbreak-related illnesses and 22 (PI 13–32) hospitalizations in 2015. Unpasteurized dairy products caused 96% (PI 94%–98%) of these illnesses.

We calculated the excess risk attributable to the consumption of unpasteurized milk and cheese (Table 2; Figure 3). Because no reported illnesses were caused by *Salmonella* spp. and STEC during 2009–2014 and no hospitalizations were caused by *Campylobacter* spp., the corresponding incidence rates were extremely low (Table 2). Therefore, only RDs (and not IRRs) were reported for these pathogens. If all milk and cheese consumed were pasteurized, an average of 732 (95% PI 570–966) illnesses and 21 (95% PI 12–32) hospitalizations would be prevented per year in the United States. Of these prevented cases, 54% would be salmonellosis and 43% campylobacteriosis. The mean IRR of illnesses was 838.8 (95% CrI 611.0–1,158.0) overall from all 4 pathogens of interest (Figure 3), with 0.4 (95% CrI 0–1.2) from *L. monocytogenes* and 7,601 (95% CrI 3,711–15,346) from *Campylobacter* spp. The rate of hospitalization was higher for unpasteurized dairy consumers than for pasteurized dairy consumers (mean IRR 45.1, 95% CrI 33.7–59.2), with an IRR of 0.5 (95% CrI 0–1.7) for *L. monocytogenes*.

Effects of Hypothetical Scenarios

If the percentage of unpasteurized milk consumers in the United States were to increase to 3.8% and unpasteurized cheese consumers to 1.9% (i.e., an increase of 20%), the number of illnesses per year would increase by an average of 19% and the number of hospitalizations by 21%. If the percentages of unpasteurized milk and cheese consumers were to double, the number of illnesses would increase by an average of 96%, and the number of hospitalizations would increase by 104%, resulting in an additional 733 (95% PI 571–966) illnesses/year and 22 (95% PI 13–32) hospitalizations/year, which corresponds to a total of 1,493 (95% PI 1,180–1,955) illnesses/year (Figure 4), most caused by *Salmonella* spp. and *Campylobacter* spp.

Scenario and Sensitivity Analyses

The following conditional means sensitivity analysis reports the change in the output mean if the input variable is set to its 5th and 95th percentiles while other inputs are sampled at random. The rates of illnesses (λ) caused by the

Table 2. Incidence rates and risk differences for illness and hospitalization per 1 billion servings of milk or cheese, by pasteurization status and pathogen, United States, 2009–2014*

	Illnesses			Hospitalizations		
Pathogen	Unpasteurized	Pasteurized	Risk difference†	Unpasteurized	Pasteurized	Risk difference†
STEC	3.5 (2.7–4.5)	3.4×10^{-4} (3.1×10^{-7} to 1.7×10^{-3})	3.5 (2.7 to 4.5)	0.9 (0.6 to 1.2)	3.4×10^{-4} (3.0×10^{-7} to 1.7×10^{-3})	0.9 (0.6 to 1.2)
Salmonella spp.	49.1 (32.7–76.7)	3.4×10^{-4} (3.3×10^{-7} to 1.7×10^{-3})	49.1 (32.7 to 76.7)	0.6 (0.4 to 0.9)	3.5×10^{-4} (3.4×10^{-7} to 1.7×10^{-3})	0.6 (0.4 to 0.9)
Listeria monocytogenes	0.04 (0.003–0.100)	0.1 (0.08 to 0.12)	−0.06 (−0.11 to 0.02)	0.03 (2.2×10^{-3} to 0.1)	0.06 (0.05 to 0.07)	−0.03 (−0.06 to 0.04)
Campylobacter spp.	39.0 (30.8–48.3)	5.8×10^{-3} (2.4×10^{-3} to 1.1×10^{-2})	39.0 (30.8 to 48.3)	1.2 (0.9 to 1.5)	3.5×10^{-4} (3.5×10^{-7} to 1.7×10^{-3})	1.2 (0.9 to 1.5)
Overall	91.7 (71.8–120.9)	0.11 (0.09 to 0.13)	91.6 (71.7 to 120.8)	2.7 (2.2 to 3.3)	6.1×10^{-2} (4.9×10^{-2} to 7.5×10^{-2})	2.7 (2.2 to 3.2)

*Values are shown as mean incidence (95% credibility interval). STEC, Shiga toxin–producing *Escherichia coli*.
†Excess risk is attributable to unpasteurized dairy.

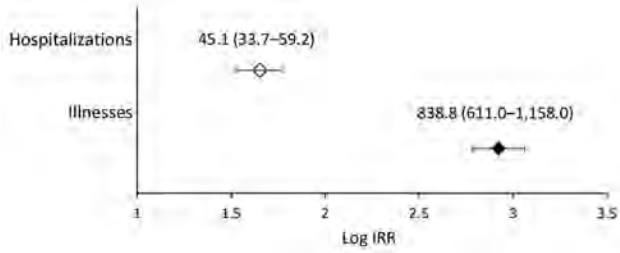

Figure 3. Forest plot showing, on a logarithmic scale, the excess risk for outbreak-related illnesses and hospitalizations caused by consumption of pasteurized and unpasteurized milk and cheese, United States, 2009–2014. Markers indicate mean log IRR of outbreak-related illnesses and hospitalizations caused by the food pathogens *Campylobacter* spp., *Listeria monocytogenes*, *Salmonella* spp., and Shiga toxin–producing *Escherichia coli* per 1 billion servings of unpasteurized milk or cheese relative to pasteurized products. Error bars indicate 95% credibility interval (CrI). Numbers above markers and bars are the IRR (not in log scale) and 95% CrI. log (IRR) = 0 indicates no difference in incidence rates between unpasteurized and pasteurized milk and cheese. IRR, incidence rate ratio.

consumption of unpasteurized milk and cheese were most sensitive to the underreporting factors (γ) for *Salmonella* spp. (mean range λ 34.9–72.5), *Campylobacter* spp. (mean range λ 33.1–45.3), and STEC (mean range λ 3.1–4.1), and at a secondary level to the undertesting (ρ) and underdiagnosis (μ) factors (results not shown). The overall IRR of illnesses was most sensitive to the underreporting factor for *Salmonella* spp. (mean range IRR 710.1–1,049.6). The number of illnesses per year caused by the consumption of milk or cheese was most sensitive to the rates of illnesses caused by *Salmonella* spp. and *Campylobacter* spp., as the main uncertainties apply to the incidence calculations for all pathogens (results not shown). Including the 9 outbreaks with a suspected-etiology status or the outbreak of unspecified pasteurization status (Figure 1) into the main analysis did not change the IRRs or the predicted number of illnesses or hospitalizations per year (results not shown).

Discussion

Unpasteurized dairy products are responsible for almost all of the 761 illnesses and 22 hospitalizations in the United States that occur annually because of dairy-related outbreaks caused by STEC, *Salmonella* spp., *L. monocytogenes*, and *Campylobacter* spp. More than 95% of these illnesses are salmonellosis and campylobacteriosis. Consumers of unpasteurized milk and cheese are a small proportion of the US population (3.2% and 1.6%, respectively), but compared with consumers of pasteurized dairy products, they are 838.8 times more likely to experience an illness and 45.1 times more likely to be hospitalized. Illnesses caused by *L. monocytogenes*, however, were found to be more often associated with the consumption of pasteurized cheese, albeit only causing 1 additional outbreak-related illness per year on average.

An easing of regulations has allowed greater access to unpasteurized milk in recent years (*8–10*), and this study shows that illnesses and hospitalizations will rise as consumption of unpasteurized dairy products increases. If such consumption were to double, the mean number of outbreak-related illnesses that occur every year would increase by 96%. Most unpasteurized dairy–related outbreaks are caused by pathogen contamination at the dairy farm (versus postpasteurization contamination for pasteurized products) (*3*); thus, one could assume that decreasing pathogen prevalence in bulk milk tanks on raw milk farms would help reduce illnesses. STEC has been found in 2.5% (95% CrI 0.1%–9.1%), *Salmonella* spp. in 4.6% (3.7%–5.6%), *L. monocytogenes* in 2.5% (0.1%–9.0%), and *Campylobacter* spp. in 4.7% (2.8%–7.0%) of bulk milk tanks on US raw milk farms (*25–29*). Given these low prevalences, strategies for further reduction are limited and involve multiple aspects of unpasteurized milk production (*30*). Boiling of milk before consumption seems to be a more realistic mitigation strategy, but this practice is unlikely to be implemented by unpasteurized dairy product advocates because it would affect the perceived benefits.

This study focused on the outbreak-related illnesses, which is only a fraction of all dairy-related illnesses in the United States. Two studies have documented the fraction of outbreak-related cases among FoodNet laboratory-confirmed cases (*15*,*31*); the fraction ranges from 0.5% for *Campylobacter* spp. to 19.0% for STEC according to Ebel et al. (*31*). These data suggest that the number of sporadic illnesses caused by contaminated dairy products in the United States might be much larger than that for outbreak-related illnesses. However, because of the lack of information on the characteristics of sporadic illnesses (such as food source attribution), we restricted the scope of this analysis to outbreak-related disease burden.

Our analysis relied on outbreak data from NORS (*11*), which is a passive reporting system affected by underreporting. We used dairy-related outbreak cases from FoodNet (*14–16*) as a comparison to estimate underreporting; therefore, any potential bias of this comparison was carried over to our estimation of outbreak-related illnesses. By extrapolating incidence rates of cases from the FoodNet catchment areas to the overall United States, we assumed that the FoodNet surveillance population and reporting practices were representative of the entire United States. However, the FoodNet catchment population represents only 15% of the US population from 10 nonrandom sites. Also, a recent study (*31*) suggested state-to-state variations in reporting practices; these variations might be even greater between FoodNet and non-FoodNet states. This difference might influence state-specific incidence rates or underreporting

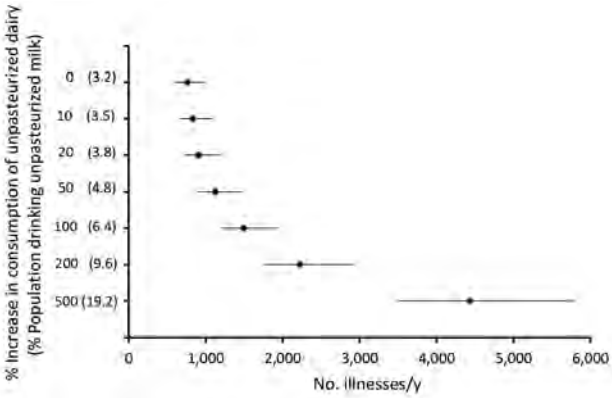

Figure 4. Number of dairy-related outbreak illnesses predicted per year in the United States if unpasteurized cow's milk and cheese consumption increases 0%, 10%, 20%, 50%, 100%, 200%, and 500%. Numbers in parentheses indicate percentage of total population consuming unpasteurized cow's milk. The illnesses graphed are those from outbreaks associated with cow's milk or cheese contaminated with Shiga toxin–producing *Escherichia coli*, *Salmonella* spp., *Listeria monocytogenes*, and *Campylobacter* spp. Markers indicate means; bars indicate 95% prediction intervals. The consumption estimates were based on the year 2015, and a 0% increase corresponds to the current proportion of the US population consuming unpasteurized dairy products.

ratios, as well as other characteristics of the reported cases. For example, if a state reported the incriminated food source as the food item (e.g., homemade yogurt), it would not have been selected for inclusion in this analysis, but if they reported the ingredient used for preparation (e.g., in the case of homemade yogurt, fluid milk), it would have been included in our analysis. However, the size and direction of such biases and uncertainties associated with these complex surveillance systems (NORS and FoodNet) are difficult to quantify because of the paucity of data.

The rates of illnesses were most sensitive to the estimated underreporting factors, which were assumed to be associated with the severity of symptoms (*23*,*24*) and other factors, such as state health department resources, and thus independent of the pasteurization status. Also, because this analysis only considered outbreaks involving milk and cheese (and no other dairy products), we are probably underestimating the incidence of illnesses and hospitalizations. However, milk and cheese are the most commonly consumed dairy sources and cause the most outbreaks (milk and cheese caused 99% of dairy-related outbreaks reported to NORS during the study period), so the underestimation is likely limited. Nonetheless, the overall comparison of risk between consumers of pasteurized and unpasteurized products should remain valid.

Estimates of the proportion of the population consuming dairy products were derived from the FoodNet population survey (*12*). We assumed that respondents who reported consumption of unpasteurized milk or cheese were not consuming pasteurized dairy. However, if unpasteurized milk or cheese only represented a fraction of their dairy consumption, the number of servings of unpasteurized dairy products could have been overestimated, and thus the risk for consumers of unpasteurized dairy products might have been underestimated. Also, the FoodNet population survey is based on a relatively small convenience sample and might therefore not be accurate. For example, the self-reported estimates of consumption of unpasteurized milk and cheese (3.2% and 1.6%, respectively) (*12*) might be underestimates or overestimates, potentially caused by consumers confusing the terms raw, organic, and natural (or other reasons). In addition, consumption might have changed since the 2007 FoodNet population survey (*12*), which might have resulted in an under- or overestimation of the risk from unpasteurized milk products. However, because the proportion of dairy consumers using unpasteurized products remains small, and the IRRs are very large, this overestimation is likely limited, and the trend for additional illnesses as unpasteurized dairy consumption grows remains valid. Similarly, estimates of the consumption of pasteurized cheese are underestimates: data available only provide estimates of the highest exposure to a single type of cheese, rather than to any type of cheese (*12*), potentially resulting in a risk overestimation for consumers of pasteurized dairy products. This is a limitation, notably for outbreaks linked to queso fresco and other Mexican-style soft cheeses. Despite these limitations, to the authors' knowledge, this study is based on the best available data and builds upon other well accepted risk attribution methods (*15*,*16*,*32*).

In conclusion, outbreaks linked to the consumption of cow's milk and cheese were estimated to cause on average 761 illnesses and 22 hospitalizations per year in the United States. Unpasteurized products are consumed by a small percentage of the US dairy consumers but cause 95% of illnesses; the risk for illness was found to be >800 times higher for consumers of unpasteurized milk or cheese than for consumers of pasteurized dairy products. Therefore, outbreak-related illnesses will increase steadily as unpasteurized dairy consumption grows, likely driven largely by salmonellosis and campylobacteriosis.

Acknowledgments

The authors thank collaborators E. Hovingh, D.R. Wolfgang, and H. Lysczek for their valuable input on milk production and consumption. We also thank the anonymous reviewers for their helpful suggestions.

This work was supported in part by a United States Department of Agriculture Special Research Grant (no. 2010-34163-21179) and the Pennsylvania Agricultural Experiment Station.

Dr. Costard is an epidemiologist working as a senior consultant at EpiX Analytics in Boulder, Colorado. Her general research interests include risk analysis, simulation modeling, and

quantitative decision support tools; she has special interests in health risk management strategies and food safety.

References

1. Food Marketing Institute. Natural and organic foods. Arlington (VA): Food Marketing Institute; 2008 [cited 2015 Sep 29]. https://www.fda.gov/ohrms/dockets/dockets/06p0094/06p-0094-cp00001-05-Tab-04-Food-Marketing-Institute-vol1.pdf
2. Katafiasz AR, Bartlett P. Motivation for unpasteurized milk consumption in Michigan, 2011. Food Prot Trends. 2012; 32:124–8.
3. Langer AJ, Ayers T, Grass J, Lynch M, Angulo FJ, Mahon BE. Nonpasteurized dairy products, disease outbreaks, and state laws—United States, 1993–2006. Emerg Infect Dis. 2012;18:385–91. http://dx.doi.org/10.3201/eid1803.111370
4. Robinson TJ, Scheftel JM, Smith KE. Raw milk consumption among patients with non–outbreak-related enteric infections, Minnesota, USA, 2001–2010. Emerg Infect Dis. 2014;20:38–44. http://dx.doi.org/10.3201/eid2001.120920
5. Claeys WL, Cardoen S, Daube G, De Block J, Dewettinck K, Dierick K, et al. Raw or heated cow milk consumption: review of risks and benefits. Food Control. 2013;31:251–62. http://dx.doi.org/10.1016/j.foodcont.2012.09.035
6. Mungai EA, Behravesh CB, Gould LH. Increased outbreaks associated with nonpasteurized milk, United States, 2007–2012. Emerg Infect Dis. 2015;21:119–22. http://dx.doi.org/10.3201/eid2101.140447
7. Stewart H, Dong D, Carlson A. Why are Americans consuming less fluid milk? A look at generational differences in intake frequency, ERR-149. 2013 May [cited 2015 Sep 29]. https://www.ers.usda.gov/webdocs/publications/err149/37651_err149.pdf?v=41423
8. National Association of State Departments of Agriculture. Raw milk survey, November, 2004 [cited 2016 Apr 29]. http://www.nasda.org/File.aspx?id=1582
9. National Association of State Departments of Agriculture. NASDA releases raw milk survey. 2008 Apr 21 [cited 2016 Apr 29]. https://view.officeapps.live.com/op/view.aspx?src=http%3A%2F%2Fwww.nasda.org%2FFile.aspx%3Fid%3D2149
10. National Association of State Departments of Agriculture. NASDA releases raw milk survey. 2011 Jul 19 [cited 2016 Apr 29]. http://www.nasda.org/file.aspx?id=3916
11. Centers for Disease Control and Prevention. National Outbreak Reporting System (NORS). Atlanta (GA): Centers for Disease Control and Prevention; 2009 [cited 2016 Apr 29]. https://www.cdc.gov/nors/index.html
12. Centers for Disease Control and Prevention. Foodborne Diseases Active Surveillance Network (FoodNet) population survey atlas of exposures, 2006-2007. Atlanta (GA): Department of Health and Human Services, Centers for Disease Control and Prevention [cited 2016 Sept 29]. https://www.cdc.gov/foodnet/surveys/FoodNetExposureAtlas0607_508.pdf
13. Gelman A, Carlin JB, Stern HS, Dunson DB, Vehtari A, Rubin DB. Bayesian data analysis. 3rd ed. London: CRC Press, Taylor & Francis Group; 2013.
14. Centers for Disease Control and Prevention. Foodborne Diseases Active Surveillance Network (FoodNet). Atlanta (GA): Centers for Disease Control and Prevention. 2014 [cited 2016 Apr 29]. https://www.cdc.gov/foodnet/index.html
15. Scallan E, Hoekstra RM, Angulo FJ, Tauxe RV, Widdowson MA, Roy SL, et al. Foodborne illness acquired in the United States—major pathogens. Emerg Infect Dis. 2011;17:7–15. http://dx.doi.org/10.3201/eid1701.P11101
16. Painter JA, Hoekstra RM, Ayers T, Tauxe RV, Braden CR, Angulo FJ, et al. Attribution of foodborne illnesses, hospitalizations, and deaths to food commodities by using outbreak data, United States, 1998–2008. Emerg Infect Dis. 2013;19:407–15. http://dx.doi.org/10.3201/eid1903.111866
17. Centers for Disease Control and Prevention. NORS: National Outbreak Reporting System guidance. Atlanta (GA): Centers for Disease Control and Prevention; 2012 [cited 2016 Apr 29]. https://www.cdc.gov/nors/pdf/NORS_Guidance_5213-508c.pdf
18. United States Census Bureau. Population estimates. 2016 [cited 2016 Apr 29]. https://www.census.gov/programs-surveys/popest.html
19. United States Department of Agriculture, Economic Research Service. Dairy data. 2014 [cited 2016 Apr 29]. http://www.ers.usda.gov/data-products/dairy-data.aspx#.UqJ_meJrfYh
20. Sebastian RS, Goldman JD, Enns CW, LaComb RP. Fluid milk consumption in the United States: what we eat in America, NHANES 2005–2006. 2010 Sep [cited 2016 Sept 29]. https://www.ars.usda.gov/ARSUserFiles/80400530/pdf/DBrief/3_milk_consumption_0506.pdf
21. Innovation Center for US Dairy. Diary's role in the diet: Cheese. 2013 [cited 2017 Apr 05]. http://www.usdairy.com/DairyResearchInstitute/NHanes/Pages/Cheese.aspx
22. Gordis L. Epidemiology. 2nd ed. Philadelphia: W.B. Saunders; 2000.
23. Haas CN, Rose JB, Gerba CP. Quantitative microbial risk assessment. New York: John Wiley & Sons; 1999.
24. Interagency Microbiological Risk Assessment Guideline workgroup. Microbial risk assessment guideline: pathogenic organisms with focus on food and water. United States Department of Agriculture, Food Safety and Inspection Service; Environmental Protection Agency; 2012 [cited 2015 Sept 29]. https://www.epa.gov/sites/production/files/2013-09/documents/mra-guideline-final.pdf
25. Jayarao BM, Henning DR. Prevalence of foodborne pathogens in bulk tank milk. J Dairy Sci. 2001;84:2157–62. http://dx.doi.org/10.3168/jds.S0022-0302(01)74661-9
26. Jayarao BM, Donaldson SC, Straley BA, Sawant AA, Hegde NV, Brown JL. A survey of foodborne pathogens in bulk tank milk and raw milk consumption among farm families in Pennsylvania. J Dairy Sci. 2006;89:2451–8. http://dx.doi.org/10.3168/jds.S0022-0302(06)72318-9
27. Van Kessel JS, Karns JS, Gorski L, McCluskey BJ, Perdue ML. Prevalence of salmonellae, *Listeria monocytogenes*, and fecal coliforms in bulk tank milk on US dairies. J Dairy Sci. 2004;87:2822–30. http://dx.doi.org/10.3168/jds.S0022-0302(04)73410-4
28. Van Kessel JA, Karns JS, Lombard JE, Kopral CA. Prevalence of *Salmonella enterica*, *Listeria monocytogenes*, and *Escherichia coli* virulence factors in bulk tank milk and in-line filters from U.S. dairies. J Food Prot. 2011;74:759–68. http://dx.doi.org/10.4315/0362-028X.JFP-10-423
29. Jayarao BM, Hovingh. Raw milk–is it safe? In: American Dairy Science Association, American Society of Animal Science, Canadian Society of Animal Science. 2014 Joint Annual Meeting abstracts. J Anim Sci. 2014;92(E-Suppl 2):147; J Dairy Sci. 2014;97(E-Suppl 1):147.
30. Hoenig DE. Raw milk production: guidelines for Maine licensed dealers. 2014 Sep 4 [cited 2015 Sep 29]. http://umaine.edu/publications/1030e/
31. Ebel ED, Williams MS, Cole D, Travis CC, Klontz KC, Golden NJ, et al. Comparing characteristics of sporadic and outbreak-associated foodborne illnesses, United States, 2004–2011. Emerg Infect Dis. 2016;22:1193–200. http://dx.doi.org/10.3201/eid2207.150833
32. Williams MS, Ebel ED, Vose D. Framework for microbial food-safety risk assessments amenable to Bayesian modeling. Risk Anal. 2011;31:548–65. http://dx.doi.org/10.1111/j.1539-6924.2010.01532.x

Address for correspondence: Solenne Costard, EpiX Analytics, 1643 Spruce St, Boulder, CO 80302, USA; email: scostard@epixanalytics.com

Sustainability of High-Level Isolation Capabilities among US Ebola Treatment Centers

Jocelyn J. Herstein, Paul D. Biddinger, Shawn G. Gibbs, Aurora B. Le, Katelyn C. Jelden, Angela L. Hewlett, John J. Lowe

To identify barriers to maintaining and applying capabilities of US high-level isolation units (HLIUs) used during the Ebola virus disease outbreak, during 2016 we surveyed HLIUs. HLIUs identified sustainability challenges and reported the highly infectious diseases they would treat. HLIUs expended substantial resources in development but must strategize models of sustainability to maintain readiness.

During the 2014–2016 West Africa Ebola virus disease (EVD) outbreak, 56 hospitals in the United States were designated by the Centers for Disease Control and Prevention as Ebola treatment centers (ETCs). ETCs added national capacity to care for patients with highly infectious diseases (HIDs); that is, hazardous, easily transmissible, life-threatening illnesses with limited treatment options, such as EVD and severe acute respiratory syndrome coronavirus (*1*). ETCs were equipped with the clinical care resources, specialized infrastructure, and trained staff to safely manage and treat a person suspected or confirmed to have EVD (*2*). After the initial designation, 1 ETC in each US Department of Health and Human Services region was selected as a Regional Ebola and Other Special Pathogens Treatment Center (RESPTC) capable of managing HIDs for extended periods (*3*).

In 2009, a consensus group of infectious disease experts in Europe defined high-level isolation units (HLIUs) as facilities providing optimal infection containment and procedures specifically designed for HID care and released specifications for such units (*1*). A 2015 pilot survey of US HLIUs described the actions taken to establish high-level isolation capabilities and identified the costs of those efforts (*4*–*6*). The survey revealed that 45 of the US hospitals spent a cumulative total of $53.9 million (nearly $1.2 million per facility) to stand up their specialized isolation units (*4*).

Because of the substantial expenses and operational challenges of maintaining readiness, how HLIUs can continue these efforts has been questioned (*7*). The EVD outbreak revealed vulnerabilities within the US healthcare and public health infrastructure to address HIDs. We aimed to identify barriers to maintenance of recently developed isolation and care capabilities, how those capabilities might be applied to outbreaks other than EVD, and further infrastructure and resources HLIUs would add if additional funding were available.

Author affiliations: University of Nebraska Medical Center, Omaha, Nebraska, USA (J.J. Herstein, K.C. Jelden, A.L. Hewlett, J.J. Lowe); Harvard Medical School, Boston, Massachusetts, USA (P.D. Biddinger); Indiana University School of Public Health, Bloomington, Indiana, USA (S.G. Gibbs, A.B. Le)

DOI: https://dx.doi.org/10.3201/eid2306.170062

The Study

In early 2016, we sent a 70-question survey to the original 56 designated US HLIUs, including the 10 RESPTCs. The survey queried challenges and concerns about the maintenance of capabilities. Results were collected through Adobe Acrobat Pro (https://acrobat.adobe.com/us/en/acrobat/acrobat-pro.html) and analyzed by using descriptive statistics. The University of Nebraska Medical Center Institutional Review Board declared the study exempt (#172–16X).

Thirty-six (64%) hospitals responded. Of the 33 that completed the full survey, 3 reported they no longer maintained their HLIU capabilities. The 2 that provided qualitative information about their decision to close reported needing HLIU resources for other, more pressing areas and cited close proximity to at least 1 other HLIU as reasons for closing.

Nineteen (58%) hospitals reported using their HLIU for non-HID patients when not activated; the other 14 (42%) use the unit exclusively for patients with HIDs or for training (Table 1). When the 19 hospitals with adaptive isolation units (i.e., units otherwise used for normal hospital care) are activated, an average of 6.31 beds (median 6, range 2–12) must be taken offline when caring for 1 patient with an HID and an average of 6.97 beds (median 7.75, range 2–12) for 2 patients. Ten (53%) HLIUs with adaptive units stated preference for a unit dedicated to care for patients with HIDs; however, when asked the estimated costs of developing a unit for 2 HID patients, estimates ranged from $1 million to $12 million. Perceived benefits of a dedicated unit included minimizing disruption of other patients (4 hospitals), a constant state of readiness (3 hospitals), and an ability to train in the unit (4 hospitals).

Our initial 2015 survey reported that hospitals designated as ETCs incurred an average per hospital of $1,197,993 (*4*). Since that time, 25 (76%) of those original facilities reported receiving some degree of federal reimbursement, and 8 (24%) had not received any reimbursement. A cumulative total of $28,146,558 in federal funding (average $1,407,328, range $33,650–$6,000,000) was reported by the 20 (60%) reporting HLIUs. After we excluded federally funded RESPTCs

Table 1. Activation of HLIUs and management of PUIs, United States*

Variable	Facilities, no./N (%)
Activation of HLIU	
HLIU can be activated 24/7 throughout the year†	32/33 (97)
Standing protocol exists to contact team members 24/7	31/33 (94)
Involve local/state public health officials in managing public concerns	32/33 (97)
PUIs	
Plan to provide care for PUIs and persons with confirmed cases	32/33 (97)
Staff used to care for PUI	
Use only HLIU staff to care for a PUI	28/32 (88)
Use other staff before disease is confirmed	4/32 (13)
Placement of PUI	
Place PUI exclusively in the HLIU while being assessed	14/32 (44)
Place PUI in either HLIU or hospital ED	12/32 (38)
Place PUI in ED until confirmed diagnosis	4/32 (13)
Other‡	2/32 (6)

*ED, emergency department; HLIU, high-level isolation unit; PUI, patient under investigation.
†Average time necessary to activate HLIU after notification of pending patient transfer is 4.58 h (median 4 h, range 1.24 h).
‡One facility sends a mobile response team to a PUI's home for evaluation, and another plans to use a mobile treatment unit (i.e., tent) for PUI placement.

and HLIUs that did not report initial investments in the pilot survey, the remaining 14 HLIUs reported a gap in reimbursement of $9,113,072.50 (mean $650,933.75 per HLIU).

Although 1 HLIU reported lacking specific protocols or an ability to care for patients with an HID other than EVD, all other HLIUs (97%) reported being prepared to care for patients with HIDs other than EVD (Figure 1). Our survey also queried HLIUs about the challenges they experienced and challenges they foresee in maintaining the capabilities and capacity needed for HID care (Figure 2). Sustainability concerns was the most cited challenge in establishing and maintaining a HLIU. HLIUs also detailed facility modifications and/or capabilities they would add if additional hypothetical funding were available (Table 2).

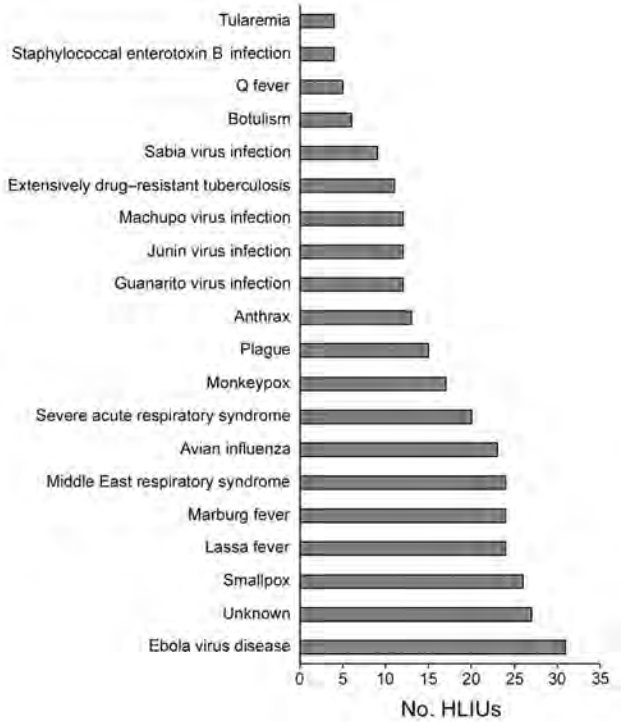

Figure 1. Diseases that 31 high-level isolation units (HLIUs) reported they would treat, United States, 2016.

Conclusions

Developed during the height of the West Africa Ebola outbreak, most newly established US HLIUs invested immense resources and effort into preparing for patients with EVD. However, no formal network of HLIUs has been established in the United States, except for the 10 RESPTCs, and at least 3 former HLIUs no longer maintain HLIU capabilities. Moreover, 14 HLIUs not designated as RESPTCs reported having spent $9.1 million more than they have been reimbursed to initially develop HLIU capabilities. As a result, these hospitals reported struggling to fund ongoing operations and sustain readiness.

Although many facilities have created adaptable-use HLIUs because they lack the capital funds, space, or both to create a dedicated unit, such units have major disadvantages

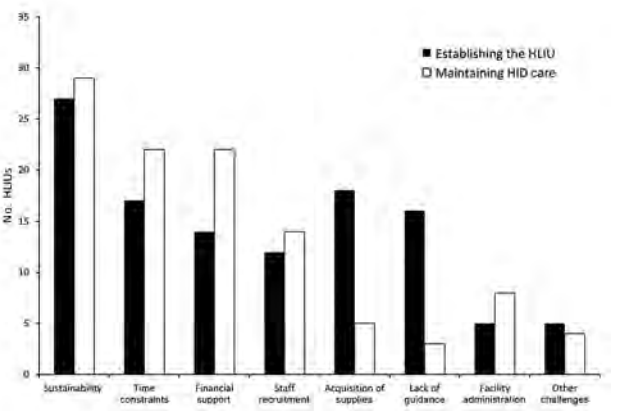

Figure 2. Challenges to establishing an HLIU and to maintaining HID care reported by survey respondents, United States, 2016 (n = 32 HLIUs). Other challenges include external support, lack of dedicated unit space, competing priorities, staffing needs, and decreasing hospital capacities. HLID, high-level isolation unit; HID, highly infectious disease.

Table 2. Operational capabilities HLIUs reported they would add or construct if funding were available, United States*

Funding amount	Capability	No. HLIUs
$100,000	Additional training/drills (e.g., for other diseases, purchase of simulation equipment)	6
	Broad supplies/equipment (e.g., beds, ventilators, family support technology/equipment)	4
	Laboratory capability and capacity (e.g., reduced transport of materials, lab hood in unit, purchase of new decontamination equipment)	4
$500,000	On-site waste disposal	4
	Expanded and updated patient rooms	3
	Enhanced laboratory capabilities (e.g., additional laboratory tests, larger lab space)	3
	Expanded isolation unit (e.g., increase capacity of negative-pressure rooms)	2
$1,000,000	Renovated/expanded isolation unit	4
	Separate, permanent isolation unit	3
	Expanded training (e.g., increased frequency)	2

*Individual HLIDs self-reported data through an electronically administered survey administered in 2016. HLIU, high-level isolation unit.

because healthcare workers are unable to train in the unit, existing patients must be relocated when the unit is activated for an HID patient, and multiple additional rooms must be taken off-line for the care of 1 patient with an HID (*8*). Thus, more than half of US HLIUs that routinely care for non-HID patients would build an HID-dedicated unit if funds were available. However, because future funding sources for non-RESPTCs are unclear, lessons on sustainability might be learned from flexible-use HLIUs in Italy and the Netherlands, which offer levels of containment based on a patient's condition and offset costs by routine use (*1*).

Our study had several limitations. The data were self-reported and not validated by external sources. The current status of HLIUs that did not participate in the follow-up survey is unknown. A decrease in participation from the initial survey to the follow-up could also be due to the longer, more detailed follow-up and could indicate the lack of attention to this area now that the EVD outbreak is over. The study population was based solely on a list published by the Centers for Disease Control and Prevention (*9*) and does not include data from other hospitals that similarly tried to strengthen their ability to treat HID patients.

In conclusion, a network of hospitals capable of treating patients with HIDs was rapidly constructed in response to the recent EVD outbreak. However, without the impending threat of EVD or another HID on the immediate horizon, public attention on HID preparedness tends to waver, and governments tend to prioritize and shift funding elsewhere. Additional external funding sources remain generally uncertain for US HLIUs not designated as RESPTCs; therefore, these HLIUs must strategize methods and models of sustainability if they are to maintain capabilities and readiness.

Acknowledgment

We gratefully acknowledge Philip Smith for his expertise and insight in developing the follow-up survey.

Ms. Herstein is a PhD student at the University of Nebraska Medical Center and a graduate research assistant for the Nebraska Biocontainment Unit and Department of Environmental, Occupational, and Agricultural Health in the College of Public Health. Her research interests include highly infectious diseases, global high-level isolation units, infectious disease response and preparedness, and infection control training of non–healthcare workers.

References

1. Bannister B, Puro V, Fusco FM, Heptonstall J, Ippolito G; EUNID Working Group. Framework for the design and operation of high-level isolation units: consensus of the European Network of Infectious Diseases. Lancet Infect Dis. 2009;9:45–56. http://dx.doi.org/10.1016/S1473-3099(08)70304-9
2. Centers for Disease Control and Prevention. Interim guidance for U.S. hospital preparedness for patients under investigation (PUIs) or with confirmed Ebola virus disease (EVD): a framework for a tiered approach [cited 2016 October 12]. http://www.cdc.gov/vhf/ebola/healthcare-us/preparing/hospitals.html
3. US Department of Health and Human Services. HHS selects regional Ebola treatment center for southwestern U.S. [cited 2016 Oct 15]. https://www.hhs.gov/about/news/2016/06/14/hhs-selects-regional-ebola-treatment-center-southwestern-us.html
4. Herstein JJ, Biddinger PD, Kraft CS, Saiman L, Gibbs SG, Smith PW, et al. Initial costs of Ebola treatment centers in the United States. Emerg Infect Dis. 2016;22:350–2. http://dx.doi.org/10.3201/eid2202.151431
5. Herstein JJ, Biddinger PD, Kraft CS, Saiman L, Gibbs SG, Le AB, et al. Current capabilities and capacity of Ebola treatment centers in the United States. Infect Control Hosp Epidemiol. 2016;37:313–8. http://dx.doi.org/10.1017/ice.2015.300
6. Jelden KC, Iwen PC, Herstein JJ, Biddinger PD, Kraft CS, Saiman L, et al. US Ebola treatment center clinical laboratory support. J Clin Microbiol. 2016;54:1031–5. http://dx.doi.org/10.1128/JCM.02905-15
7. Dzau VJ, Sands P. Beyond the Ebola battle—winning the war against future epidemics. N Engl J Med. 2016;375:203–4. http://dx.doi.org/10.1056/NEJMp1605847
8. Schilling S, Fusco FM, De Iaco G, Bannister B, Maltezou HC, Carson G, et al.; European Network for Highly Infectious Diseases project members. Isolation facilities for highly infectious diseases in Europe—a cross-sectional analysis in 16 countries. PLoS One. 2014;9:e100401. http://dx.doi.org/10.1371/journal.pone.0100401
9. Centers for Disease Control and Prevention. Current Ebola treatment centers [cited 2016 Oct 12]. https://www.cdc.gov/vhf/ebola/healthcare-us/preparing/current-treatment-centers.html

Address for correspondence: Jocelyn J. Herstein, College of Public Health, University of Nebraska Medical Center, 984388 Nebraska Medical Center, Omaha, NE 68198, USA; email: jocelyn.herstein@unmc.edu

Clinical and Molecular Characteristics of Human Rotavirus G8P[8] Outbreak Strain, Japan, 2014

Kenji Kondo, Takeshi Tsugawa, Mayumi Ono, Toshio Ohara, Shinsuke Fujibayashi, Yasuo Tahara, Noriaki Kubo, Shuji Nakata, Yoshihito Higashidate, Yoshiki Fujii, Kazuhiko Katayama, Yuko Yoto, Hiroyuki Tsutsumi

During March–July 2014, rotavirus G8P[8] emerged as the predominant cause of rotavirus gastroenteritis among children in Hokkaido Prefecture, Japan. Clinical characteristics were similar for infections caused by G8 and non-G8 strains. Sequence and phylogenetic analyses suggest the strains were generated by multiple reassortment events between DS-1–like P[8] strains and bovine strains from Asia.

Rotaviruses, the leading cause of acute gastroenteritis in children worldwide, are classified into G and P genotypes on the basis of 2 outer capsid proteins, viral protein (VP) 7 and VP4. A recently established extended rotavirus genotyping system based on the sequence of all 11 genome segments (*1*) grouped most human rotaviruses into 2 genotype constellations: Wa-like (G1/3/4/9-P[8]-I1-R1-C1-M1-A1-N1-T1-E1-H1) and DS-1–like (G2-P[4]-I2-R2-C2-M2-A2-N2-T2-E2-H2) strains.

In industrialized countries, rotavirus genotype G8 infection is common in bovines but rarely occurs in humans; however, the G8 strains are highly prevalent among humans in some countries in Africa (*2*). We investigated the clinical and molecular features of G8P[8] rotavirus, which, we unexpectedly found to be the predominant genotype in southwestern Hokkaido Prefecture, Japan, in 2014.

The Study

During March–July 2014, we obtained rotavirus-positive fecal samples from 165 children in Hokkaido with acute gastroenteritis. The children were receiving care as inpatients or outpatients at 1 of 6 medical facilities (4 hospitals and 2 clinics) in the cities of Sapporo, Tomakomai, Muroran, and Urakawa (Figure 1).

For each fecal sample, we prepared a 10% fecal suspension, from which we extracted viral RNA. We performed reverse transcription PCR on the RNA by using the SuperScript II Reverse Transcriptase (Invitrogen, Carlsbad, CA, USA); PrimeSTAR GXL DNA polymerase (Takara, Shiga, Japan); and previously described primers (*3*,*4*). We used the BigDye Terminator v.3.1 Cycle Sequencing Reaction Kit (Applied Biosystems, Foster City, CA, USA) to sequence PCR amplicons. For some of the rotavirus samples, next-generation sequencing was performed at the National Institute of Infectious Diseases in Tokyo, Japan, as described previously (*5*). Sequences of the rotaviruses used in this study were submitted to the DDBJ under accession numbers LC102884–LC103134 and LC105000–LC105532.

We successfully determined G and P genotypes for 148 of the 165 rotavirus samples by using the RotaC rotavirus genotyping tool (http://rotac.regatools.be/). The most common genotype was G8P[8], which was identified in 58 samples (39.2%), followed by G1P[8] (25.7%), G9P[8] (20.3%), and G2P[4] (12.8%) (Table 1; online Technical Appendix, https://wwwnc.cdc.gov/EID/article/23/6/16-0038-Techapp1.pdf).

We obtained clinical data for all 84 patients who sought care at the hospital or clinic in Tomakomai. Demographic and clinical characteristics (e.g., age, sex, history of rotavirus vaccination, duration of fever, and duration and frequency of diarrhea and vomiting) were not substantially different between 42 patients with G8P[8] rotavirus infection and 42 patients with non-G8P[8] rotavirus infection. The proportion of patients admitted to hospitals was also similar in the 2 groups (Table 1).

We selected 15 G8P[8] strains for whole-genome analysis. All strains had the same genotype constellation, G8-P[8]-I2-R2-C2-M2-A2-N2-T2-E2-H2, indicating a genomic backbone of the DS-1 genotype constellation. The genomes of these G8P[8] strains shared >99.6% nt identity with each other (Table 2; online Technical Appendix). All 11 genome segments of strain To14-0 (the representative G8P[8] strain in this study) exhibited the highest nucleotide identity to human G8P[8] strains isolated in Southeast Asia in 2014 (represented by strain RVN1149 from Vietnam [>99.4% nt identity] and NP-130 from Thailand [>99.5% nt identity]) (*6*,*7*) (Table 2). This finding suggests that the strains share a common G8P[8] origin.

Author affiliations: Sapporo Medical University School of Medicine, Sapporo, Japan (K. Kondo, T. Tsugawa, M. Ono, Y. Yoto, H. Tsutsumi); Tomakomai City Hospital, Tomakomai, Japan (T. Ohara); Tomakomai Children's Clinic, Tomakomai (S. Fujibayashi); Steel Memorial Muroran Hospital, Muroran, Japan (Y. Tahara); Japanese Red Cross Urakawa Hospital, Urakawa, Japan (N. Kubo); Nakata Pediatric Clinic, Sapporo (S. Nakata); Sapporo Hokushin Hospital, Sapporo (Y. Higashidate); National Institute of Infectious Diseases, Tokyo, Japan (Y. Fujii, K. Katayama)

DOI: https://dx.doi.org/10.3201/eid2306.160038

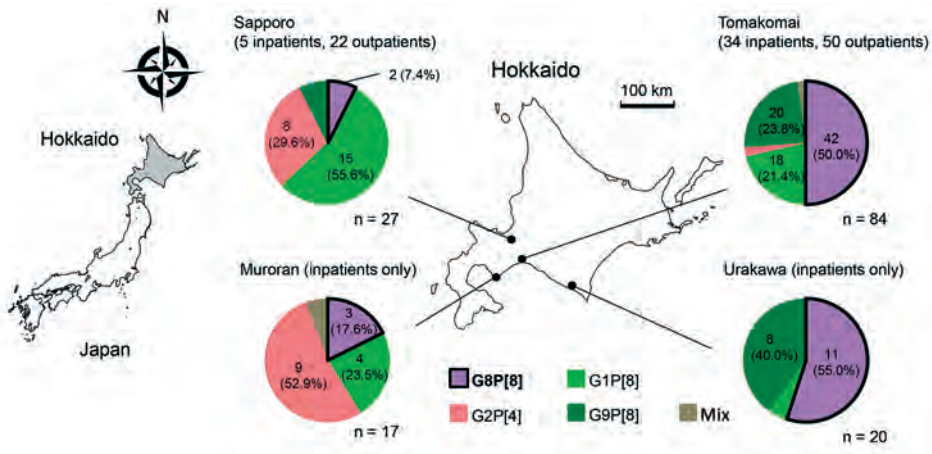

Figure 1. Distribution of rotavirus samples and their G/P genotypes in Hokkaido Prefecture (center map), Japan, 2014. The 4 locations from which the fecal samples were collected are shown on the map. Four hospitals (Tomakomai City Hospital, Japanese Red Cross Urakawa Hospital, Steel Memorial Muroran Hospital, and Sapporo Hokushin Hospital), and 2 clinics (Nakata Pediatric Clinic [Sapporo] and Tomakomai Children's Clinic) participated in the study. Map at left shows location of Hokkaido in Japan (gray shading).

The VP7 gene of rotavirus strain To14-0 shared the highest nucleotide identity with the VP7 genes of human G8P[8] strains from Southeast Asia, including strains RVN1149 and NP-130 (99.4% and 99.7% identity, respectively), and it shared slightly lower identity to the VP7 gene of human strain 04-97s379 (97.8%) from Taiwan, which is speculated to be of bovine origin (*8*) (Figure 2). The VP7 genes of other G8 strains isolated in Japan were more distantly related to the To14-0 VP7 gene (e.g., human AU109 and bovine strains shared 89.5% and 81.9%–85.1%, respectively, with To14-0) (*9*). The VP7 genes of the human G8 strains prevailing in Africa were also distantly related (<90% nt identity) to the VP7 gene of To14-0.

Among the 11 To14-0 genome segments, 8 (VP2–VP4, VP6, nonstructural protein [NSP] 1–3, and NSP5) were highly similar to those of the human DS-1–like P[8] strains that have been isolated in Asia since 2012 (e.g., SKT-109, NT004, and LS-04) (*10–12*), including the strains isolated in this study (e.g., To14-41) (Table 2; online Technical Appendix Figure, panels B–H, J). In addition, the VP6 and NSP5 genes of the strains isolated in this study were also highly similar to those of human G2P[4] strains circulating in South Korea (strain CAU15-11) and Thailand (strain NP-M51) (*12*).

In contrast, the VP1 and NSP4 genes of To14-0 were only distantly related to those of the DS-1–like P[8] strains isolated in Asia (e.g., SKT-109, NT004, and LS-04), including the strains isolated in this study (e.g., To14-41) (Table 2; online Technical Appendix Figure, panels A and I). The To14-0 VP1 gene shared high nucleotide identity with the VP1 genes of human G10P[14] strain PR457 from Italy (98.1%), which are probably the result of independent zoonotic transmissions (*13*). The To14-0 NSP4 gene shared high nucleotide identity with the NSP4 genes of human strains BSGH38 from India (96.7%) and the caprine G6P[1] strain GO34 from Bangladesh (96.0%) (*14*).

Conclusions

The clinical characteristics recorded for patients infected with G8P[8] rotaviruses and those infected with non-G8P[8] rotaviruses did not differ (Table 1). Our findings suggest that the severity of gastroenteritis caused by newly emerging G8P[8] rotaviruses could possibly be attenuated by 1) the existence of VP7/VP4 genotype cross-reactive (heterotypic) protective responses; 2) protective immunity associated with other segments, such as VP6 and NSP4 (*3,15*); or 3) both of these factors combined.

Table 1. Characteristics of patients infected with (G8P[8] and non-G8P[8] rotavirus, Tomakomai, Hokkaido Prefecture, Japan, 2014

Patient characteristic	Patients infected with rotavirus		p value*
	G8P[8], n = 42	Non-G8P[8], n = 42	
Sex, no.			1.0
M	24	24	
F	18	18	
Median age, y	1.8	2.0	0.50
Vaccinated, no (%)	2 (4.8)	1 (2.4)	0.56
Clinical symptoms, mean ± SD			
Duration of fever, d	1.3 ± 1.2	1.7 ± 1.4	0.13
Duration of diarrhea, d	2.4 ± 1.6	2.5 ± 3.2	0.51
Diarrhea episode in 24 h, maximum no.	3.6 ± 3.2	4.3 ± 4.2	0.69
Duration of vomiting, d	1.4 ± 1.2	1.8 ± 2.9	0.79
Vomiting episodes in 24 h, maximum no.	3.6 ± 3.8	3.7 ± 3.5	0.98
Admitted to hospital, no. (%)	18 (42.9%)	16 (38.1%)	0.66

*Categorical data were analyzed by using χ^2 tests; continuous data were analyzed by using Student's *t*-tests or Mann-Whitney U tests.

Table 2. Genotype constellations and nucleotide identities of strains closely related to To14-0, the representative G8P[8] rotavirus strain used in a study of the clinical and molecular features of a G8P[8] rotavirus outbreak strain, Hokkaido Prefecture, Japan, 2014

Strain (genotype representative from study/country)	Genotype constellations and nucleotide identities (%), by gene*										
	VP7	VP4	VP6	VP1	VP2	VP3	NSP1	NSP2	NSP3	NSP4	NSP5
Human/To14-0 (G8P[8] in study)	G8 (**100**)	P[8] (**100**)	I2 (**100**)	R2 (**100**)	C2 (**100**)	M2 (**100**)	A2 (**100**)	N2 (**100**)	T2 (**100**)	E2 (**100**)	H2 (**100**)
Human/VNM/RVN1149/2014/G8P[8] (G8P[8] in Vietnam)	G8 (**99.4**)	P[8] (**99.8**)	I2 (**99.8**)	R2 (**99.6**)	C2 (**99.6**)	M2 (**99.8**)	A2 (**100**)	N2 (**99.9**)	T2 (**99.5**)	E2 (**99.9**)	H2 (**99.5**)
Human/THA/NP-130/2014/G8P[8] (G8P[8] in Thailand)	G8 (**99.7**)	P[8] (**99.9**)	I2 (**99.9**)	R2 (**99.9**)	C2 (**99.8**)	M2 (**99.9**)	A2 (**99.9**)	N2 (**99.7**)	T2 (**99.8**)	E2 (**99.7**)	H2 (**99.5**)
Human/THA/KKL-17/2013/G8P[8] (G8P[8] in Thailand)	G8 (**99.5**)	P[8] (**99.8**)	I2 (91.5)	R2 (**99.9**)	C2 (**99.9**)	M2 (**99.9**)	A2 (**99.9**)	N2 (**99.8**)	T2 (**99.9**)	E2 (**99.7**)	H2 (**99.2**)
Human/THA/LS-04/2013/G2P[8] (DS-1–like G2P[8] in Thailand)	G2 (–)	P[8] (**99.8**)	I2 (**99.5**)	R2 (86.0)	C2 (**99.8**)	M2 (97.4)	A2 (**99.9**)	N2 (**99.8**)	T2 (98.6)	E2 (95.5)	H2 (**99.7**)
Human/THA/SKT-109/2013/G1P[8] (DS-1–like G1P[8] in Thailand)	G1 (–)	P[8] (**99.7**)	I2 (**98.7**)	R2 (86.1)	C2 (**99.9**)	M2 (**99.8**)	A2 (**99.8**)	N2 (85.8)	T2 (**99.8**)	E2 (94.5)	H2 (**99.2**)
Human/To14-41 (DS-1–like G1P[8] in study)	G1 (–)	P[8] (98.8)	I2 (98.3)	R2 (86.3)	C2 (**99.4**)	M2 (**99.4**)	A2 (**99.5**)	N2 (85.5)	T2 (**99.6**)	E2 (93.5)	H2 (98.8)
Human/JPN/NT004/2012/G1P[8] (DS-1–like G1P[8] in Japan)	G1 (–)	P[8] (**99.0**)	I2 (98.4)	R2 (86.3)	C2 (**99.7**)	M2 (**99.5**)	A2 (**99.5**)	N2 (85.6)	T2 (**99.6**)	E2 (94.5)	H2 (**99.2**)
Human/THA/NP-M51/2013/G2P[4] (G2P[4] in Thailand)	G2 (–)	P[4] (–)	I2 (**99.5**)	R2 (86.0)	C2 (**99.1**)	M2 (97.5)	A2 (**99.0**)	N2 (85.4)	T2 (98.7)	E2 (95.5)	H2 (**99.7**)
Human/KOR/CAU15–11/2015/G2P[4] (G2P[4] in South Korea)	G2 (–)	P[4] (–)	I2 (**99.5**)	R2 (85.9)	C2 (**99.2**)	M2 (97.4)	A2 (94.0)	N2 (84.8)	T2 (98.1)	E2 (95.3)	H2 (98.6)
Human/MU14114 (G2P[4] in study)	G2 (–)	P[4] (–)	I2 (97.0)	R2 (85.3)	C2 (96.9)	M2 (86.4)	A2 (95.8)	N2 (85.5)	T2 (96.7)	E2 (95.6)	H2 (98.3)
Human/ITA/PR457/2009/G10P[14]	G10 (–)	P[14] (–)	I2 (93.0)	R2 (98.1)	C2 (82.3)	M2 (86.6)	A11 (–)	N2 (86.4)	T6 (–)	E2 (94.3)	H3 (–)
Caprine/BGL/GO34/1999/G6P[1]	G6 (–)	P[1] (–)	I2 (94.9)	R2 (86.3)	C2 (83.4)	M2 (86.8)	A11 (–)	N2 (86.6)	T6 (–)	E2 (96.0)	H3 (–)
Human/COD/DRC88/2003/G8P[8] (G8P[8] in Africa)	G8 (86.0)	P[8] (98.3)	I2 (96.3)	R2 (85.6)	C2 (97.4)	M2 (97.0)	A2 (96.4)	N2 (85.8)	T2 (97.1)	E2 (90.1)	H2 (97.4)
Human/MWI/QEC287/2006/G8P[8] (G8P[8] in Africa)	G8 (85.5)	P[8] (98.3)	I2 (96.3)	R2 (85.6)	C2 (97.8)	M2 (96.0)	A2 (96.5)	N2 (86.9)	T2 (96.6)	E2 (89.2)	H2 (97.6)
Human/MWI/QEC289/2006/G8P[8] (G8P[8] in Africa)	G8 (85.5)	P[8] (97.5)	I2 (96.3)	R2 (85.5)	C2 (97.8)	M2 (95.9)	A2 (96.5)	N2 (86.9)	T2 (96.6)	E2 (89.2)	H2 (97.6)

*Purple indicates G8 genotype; green indicates Wa-like genome segments; red indicates DS-1–like genome segments; bold indicates nucleotide identities >99.0%; – indicates percentages not calculated because the genotype was different that for To14-0.

The VP7 genes of the human G8P[8] strains isolated in this study and in Southeast Asia appear to have a close relationship with bovine strains from Asia but not from Japan, and the VP7 gene of human G8 or bovine G8 strains previously isolated in Japan are distantly related to them. Therefore, the VP7 genes in the G8P[8] strains from this study may have originated from a bovine strain from Asia. As with the VP7 genes, the VP1 and NSP4 genes are also assumed to have been derived from artiodactyl strains.

Eight genome segments (VP2–VP4, VP6, NSP1–NSP3, and NSP5) of the human G8P[8] strains isolated in this study and from Southeast Asia are closely related to those of the DS-1–like P[8] strains that have emerged and spread in Japan and other countries of Asia since 2012 (Table 2). Therefore, these 8 genome segments of the G8P[8] strains from this study may be derived from the DS-1–like P[8] strains in Asia.

For the reasons we have stated, the G8P[8] strains isolated in this study were speculated to be formed outside of Japan by multiple reassortment events between the DS-1–like P[8] strains and bovine strains in Asia. The resulting strain was probably recently introduced into Japan.

The predominance of novel DS-1–like G8P[8] strains noted in this study indicates that these strains are sufficiently adapted to humans to sustain human-to-human transmission in an industrialized country. This finding suggests that these G8P[8] rotavirus strains could spread to other regions in the near future. Continuing surveillance is required to monitor the circulating wild-type strains, and rotavirus genotype constellations and clinical information must be analyzed to understand rotavirus virulence in humans.

This study was supported in part by a Japan Society for the Promotion of Science Grant-in-Aid for Scientific Research C (grant no. 15K09693); a commissioned project for Research on Emerging and Re-emerging Infectious Diseases from the Japanese Ministry of Health, Labor and Welfare (to K.K.); and Japan Agency for Medical Research and Development (to K.K.).

Dr. Kondo is a pediatrician in Department of Pediatrics, Sapporo Medical University School of Medicine. His primary research interests are molecular biology and the epidemiology of rotaviruses.

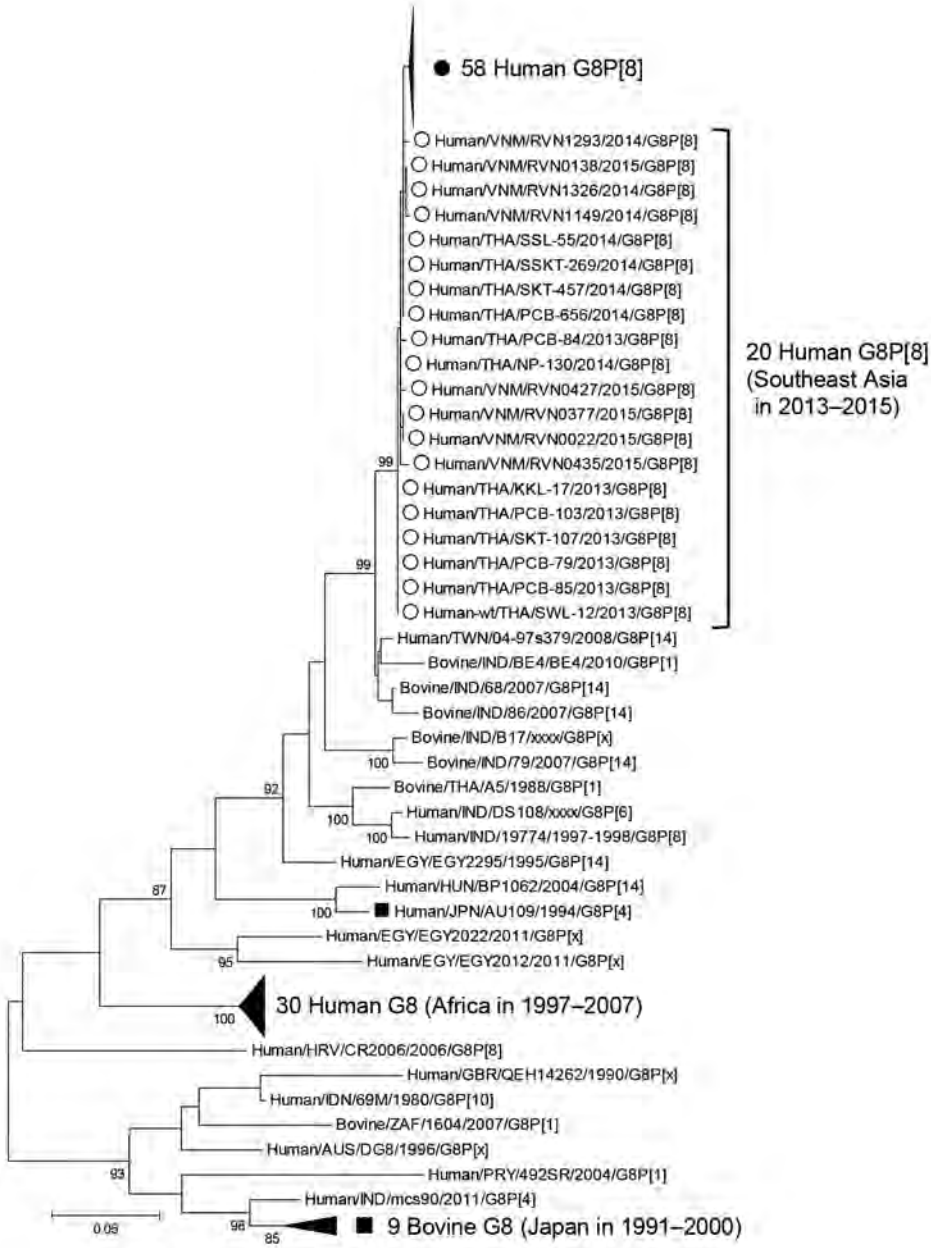

Figure 2. Phylogenetic analysis of the viral protein 7 gene of G8 rotavirus strains used in a study of the clinical and molecular features of a G8P[8] rotavirus outbreak strain, Hokkaido Prefecture, Japan, 2014. Closed circle indicates the G8P[8] rotavirus strain from Hokkaido; open circles indicate human G8P[8] strains from Southeast Asia; and closed boxes indicate other strains from Japan. A Tamura 3-parameter model was used for the maximum-likelihood method. Bootstrap values are shown at the branch nodes (values of <80% are not shown). Scale bar indicates nucleotide substitutions per site.

References

1. Matthijnssens J, Ciarlet M, McDonald SM, Attoui H, Bányai K, Brister JR, et al. Uniformity of rotavirus strain nomenclature proposed by the Rotavirus Classification Working Group (RCWG). Arch Virol. 2011;156:1397–413. http://dx.doi.org/10.1007/s00705-011-1006-z
2. Nakagomi T, Doan YH, Dove W, Ngwira B, Iturriza-Gómara M, Nakagomi O, et al. G8 rotaviruses with conserved genotype constellations detected in Malawi over 10 years (1997–2007) display frequent gene reassortment among strains co-circulating in humans. J Gen Virol. 2013;94:1273–95. http://dx.doi.org/10.1099/vir.0.050625-0
3. Fujii Y, Shimoike T, Takagi H, Murakami K, Todaka-Takai R, Park Y, et al. Amplification of all 11 RNA segments of group A rotaviruses based on reverse transcription polymerase chain reaction. Microbiol Immunol. 2012;56:630–8. http://dx.doi.org/10.1111/j.1348-0421.2012.00479.x
4. Tsugawa T, Tatsumi M, Tsutsumi H. Virulence-associated genome mutations of murine rotavirus identified by alternating serial passages in mice and cell cultures. J Virol. 2014;88:5543–58. http://dx.doi.org/10.1128/JVI.00041-14
5. Masuda T, Nagai M, Yamasato H, Tsuchiaka S, Okazaki S, Katayama Y, et al. Identification of novel bovine group A rotavirus G15P[14] strain from epizootic diarrhea of adult cows by de novo sequencing using a next-generation sequencer. Vet Microbiol. 2014;171:66–73. http://dx.doi.org/10.1016/j.vetmic.2014.03.009
6. Hoa-Tran TN, Nakagomi T, Vu HM, Do LP, Gauchan P, Agbemabiese CA, et al. Abrupt emergence and predominance in Vietnam of rotavirus A strains possessing a bovine-like G8 on a DS-1–like background. Arch Virol. 2016;161:479–82. http://dx.doi.org/10.1007/s00705-015-2682-x
7. Tacharoenmuang R, Komoto S, Guntapong R, Ide T, Sinchai P, Upachai S, et al. Full genome characterization of novel DS-1–like

G8P[8] rotavirus strains that have emerged in Thailand: reassortment of bovine and human rotavirus gene segments in emerging DS-1–like intergenogroup reassortant strains. PLoS One. 2016;11:e0165826. http://dx.doi.org/10.1371/journal.pone.0165826
8. Wu FT, Bányai K, Wu HS, Yang DC, Lin JS, Hsiung CA, et al. Identification of a G8P[14] rotavirus isolate obtained from a Taiwanese child: evidence for a relationship with bovine rotaviruses. Jpn J Infect Dis. 2012;65:455–7. http://dx.doi.org/10.7883/yoken.65.455
9. Agbemabiese CA, Nakagomi T, Doan YH, Nakagomi O. Whole genomic constellation of the first human G8 rotavirus strain detected in Japan. Infect Genet Evol. 2015;35:184–93. http://dx.doi.org/10.1016/j.meegid.2015.07.033
10. Komoto S, Tacharoenmuang R, Guntapong R, Ide T, Haga K, Katayama K, et al. Emergence and characterization of unusual DS-1–like G1P[8] rotavirus strains in children with diarrhea in Thailand. PLoS One. 2015;10:e0141739. http://dx.doi.org/10.1371/journal.pone.0141739
11. Fujii Y, Nakagomi T, Nishimura N, Noguchi A, Miura S, Ito H, et al. Spread and predominance in Japan of novel G1P[8] double-reassortant rotavirus strains possessing a DS-1–like | genotype constellation typical of G2P[4] strains. Infect Genet Evol. 2014;28:426–33. http://dx.doi.org/10.1016/j.meegid.2014.08.001
12. Komoto S, Tacharoenmuang R, Guntapong R, Ide T, Tsuji T, Yoshikawa T, et al. Reassortment of human and animal rotavirus gene segments in emerging DS-1–like G1P[8] rotavirus strains. PLoS One. 2016;11:e0148416. http://dx.doi.org/10.1371/journal.pone.0148416
13. Medici MC, Tummolo F, Bonica MB, Heylen E, Zeller M, Calderaro A, et al. Genetic diversity in three bovine-like human G8P[14] and G10P[14] rotaviruses suggests independent interspecies transmission events. J Gen Virol. 2015;96:1161–8. http://dx.doi.org/10.1099/vir.0.000055
14. Ghosh S, Alam MM, Ahmed MU, Talukdar RI, Paul SK, Kobayashi N. Complete genome constellation of a caprine group A rotavirus strain reveals common evolution with ruminant and human rotavirus strains. J Gen Virol. 2010;91:2367–73. http://dx.doi.org/10.1099/vir.0.022244-0
15. Burns JW, Siadat-Pajouh M, Krishnaney AA, Greenberg HB. Protective effect of rotavirus VP6-specific IgA monoclonal antibodies that lack neutralizing activity. Science. 1996;272:104–7. http://dx.doi.org/10.1126/science.272.5258.104

Address for correspondence: Takeshi Tsugawa, Department of Pediatrics, Sapporo Medical University School of Medicine, Minami 1-jo, Nishi 16-chome, Chuo-ku, Sapporo, Hokkaido 060-8543, Japan; email: tsugawat@sapmed.ac.jp

April 2015: **Emerging Viruses**

- Reappearance of Chikungunya, Formerly Called Dengue, in the Americas
- Hantavirus Pulmonary Syndrome, Southern Chile, 1995–2012

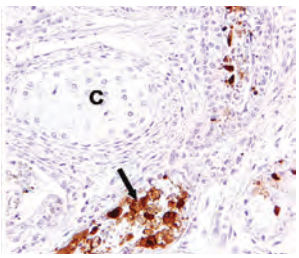

- Animal-Associated Exposure to Rabies Virus among Travelers, 1997–2012
- Evolution of Ebola Virus Disease from Exotic Infection to Global Health Priority, Liberia, Mid-2014
- Influenza A(H7N9) Virus Transmission between Finches and Poultry
- Population Structure and Antimicrobial Resistance of Invasive Serotype IV Group B *Streptococcus*, Toronto, Ontario, Canada
- Norovirus Genotype Profiles Associated with Foodborne Transmission, 1999–2012
- Sequence Variability and Geographic Distribution of Lassa Virus, Sierra Leone
- Highly Pathogenic Avian Influenza A(H5N1) Virus Infection among Workers at Live Bird Markets, Bangladesh, 2009–2010
- Deaths Associated with Respiratory Syncytial and Influenza Viruses among Persons >5 Years of Age in HIV-Prevalent Area, South Africa
- Nairobi Sheep Disease Virus RNA in Ixodid Ticks, China
- Increased Risk for Group B Streptococcus Sepsis in Young Infants Exposed to HIV, Soweto, South Africa, 2004–2008
- Bat Coronavirus in Brazil Related to Appalachian Ridge and Porcine Epidemic Diarrhea Viruses
- Tandem Repeat Insertion in African Swine Fever Virus, Russia, 2012
- Norovirus GII.21 in Children with Diarrhea, Bhutan

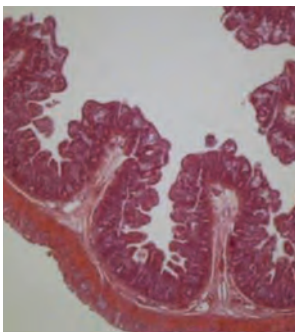

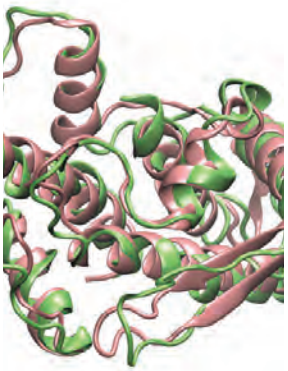

- Enterovirus D68 Infection, Chile, Spring 2014
- Zika Virus Infection, Philippines, 2012
- Chikungunya Outbreak, French Polynesia, 2014
- Avian Influenza A(H10N7) Virus–Associated Mass Deaths among Harbor Seals
- Hepatitis E Epidemic, Biratnagar, Nepal, 2014

EMERGING INFECTIOUS DISEASES

https://wwwnc.cdc.gov/eid/articles/issue/21/4/table-of-contents

Seoul Virus Infection in Humans, France, 2014–2016

Jean-Marc Reynes, Damien Carli, Jean-Baptiste Bour, Samir Boudjeltia, Anny Dewilde, Guillaume Gerbier, Timothée Nussbaumer, Véronique Jacomo, Marie-Pierre Rapt, Pierre E. Rollin, Alexandra Septfons

We report detection of Seoul virus in 3 patients in France over a 2-year period. These patients accounted for 3 of the 4 Seoul virus infections among 434 hantavirus infections (1.7%) reported during this time. More attention should be given to this virus in Europe where surveillance has been focused mostly on Puumala and Dobrava-Belgrade hantaviruses.

Seoul virus (SEOV), a hantavirus and the etiologic agent of a mild-to-moderate hemorrhagic fever with a renal syndrome, is associated worldwide with brown rats (*Rattus norvegicus*), a commensal rodent that is found in all human-inhabited locations (*1*). In Russia, South Korea, and China, a wide range (few tens to few thousands) of human infections with SEOV are reported annually (with potential serologic cross-reactivity with co-circulating Hantaan virus); otherwise, only a few countries have reported rare sporadic cases, mostly serologically confirmed (*1–4*). Four human cases were recently described in the United Kingdom and France (*4–6*). We report 3 patients in France, whose SEOV infections were confirmed by using molecular techniques, and identified through systematic surveillance within a 24-month period.

The Study

Case-patient 1 was a 27-year-old man from Dijon, France, who was hospitalized 3 days after onset of symptoms during February 2014. His clinical and biologic characteristics were fever, mild renal syndrome, thrombocytopenia, and increased levels of liver enzymes (Table 1). Hantavirus IgM and IgG were detected in an admission serum sample by using commercial ELISAs at a private clinical laboratory. Presence of IgM was confirmed at the French National Reference Center for Hantavirus (NRC; Lyon, France) by using reference ELISA and indirect fluorescent antibody assays (*5*) (Table 2).

Virus was detected by using molecular techniques as described (*5*). A partial SEOV small RNA sequence (GenBank accession no. KX064269) was isolated from an admission sample by conducting a BLAST (https://blast.ncbi.nlm.nih.gov/Blast.cgi) search. Exposure to the virus was suspected to have occurred during building restoration work (Figure 1).

Case-patient 2 was a 22-year-old man from Erize-Saint-Dizier, France (Figure 1), who was hospitalized 4 days after onset of symptoms during September 2014. His clinical and biologic characteristics were fever, thrombocytopenia, and liver function disorders (Table 1). Hantavirus IgM and IgG were detected in an admission serum sample by using commercial ELISAs at a public hospital clinical laboratory. Results were confirmed at the NRC (Table 2).

Virus was detected by using molecular techniques. A partial SEOV small RNA sequence was obtained from a serum sample, as shown by a BLAST search.

The pet rat (*Rattus norvegicus*) of case-patient 2, bought ≈1 month before onset of symptoms, was considered the presumptive source of the virus. The animal was euthanized after consent of the patient was obtained. An identical partial SEOV small RNA sequence was obtained from the liver of the animal.

Case-patient 3 was a 32-year-old man from Turckheim, France (Figure 1), who was hospitalized 4 days after onset of symptoms during January 2016. His clinical characteristics were severe fever, thrombocytopenia, liver disorders, myopericarditis, and renal syndrome that require hemodialysis (Table 1). Hantavirus IgM and IgG were detected 6 days after symptom onset by using commercial assays in a private clinical laboratory. Results were confirmed at the NRC (Table 2).

Virus was detected by using molecular techniques reported by Klempa et al. (*7*). A partial SEOV large RNA sequence (GenBank accession no. KX064268) was obtained from an admission serum sample, as demonstrated by a BLAST search.

This case-patient raised brown rats as a food source for his snakes and routinely captured and killed wild brown rats that invaded his hen house. His breeding unit was the

Author affiliations: Institut Pasteur, Lyon, France (J.-M. Reynes, D. Carli); Centre Hospitalier Universitaire Dijon-Bourgogne, Dijon, France (J.-B. Bour, S. Boudjeltia); Centre Hospitalier Universitaire Lille, Lille, France (A. Dewilde); Direction Départementale de la Cohésion Sociale et de la Protection des Populations, Colmar, France (G. Gerber); Hôpitaux Civils de Colmar, Colmar (T. Nussbaumer); Biomnis, Lyon (V. Jacomo); Centre Hospitalier, Bar-le-Duc, France (M.-P. Rapt); Centers for Disease Control and Prevention, Atlanta, Georgia, USA (P.E. Rollin); Santé Publique France, Saint-Maurice, France (A. Septfons)

DOI: http://dx.doi.org/10.3201/eid2306.160927

Table 1. Characteristics of 3 patients infected with Seoul virus, France, 2014–2016*

Characteristic†	Patient 1	Patient 2	Patient 3
Signs and symptoms			
Fever	Yes	Yes	Yes
Weakness	Yes	No	Yes
Headache	Yes	Yes	Yes
Muscle or join pain	No	No	Yes
Chest pain	No	No	Yes
Abdominal pain	No	No	Yes
Nausea	Yes	No	Yes
Vomiting	Yes	No	Yes
Anorexia	No	No	Yes
Cough	Yes	No	No
Dyspnea	No	No	Yes
Anuria	No	No	Yes
Confusion	Yes	No	Yes
Laboratory results (reference range or value)			
Leukocytes, × 10^9 cells/L (4.0–10.0 × 10^9 cells/L)	Reference	Reference e	D6: 19.4
Platelets, × 10^9/L (150–450 × 10^9/L)	D4: 52	D4: 59	D4: 21
Hemoglobin, g/dL (13.0–17.0 g/dL)	D6: 11.9	Reference e	D13: 9.8
C-reactive protein, mg/L (<3.2 mg/L)	D3: 82.0	D4: 26.0	D4: 155.0
LDH, IU/L (120–228 IU/L)	D3: 999‡	NA	D4: 876
AST, IU/L (15-37 IU/L)	D3: 440	D5: 183	D4: 439
ALT, IU/L (21–72 IU/L)	D9: 278	D5: 210	D4: 390
GGT, IU/L (15–85 IU/L)	Reference	D5: 87	D9: 722
Creatinine, mg/L (6–11 mg/L)	D3: 16.4	Reference	D8: 75.0
Microscopic hematuria	NA	No	Yes
Proteinuria, g/24 h (<0.3 g/24 h)	NA	NA	D8: 3.82

*ALT, alanine aminotransferase; AST, aspartate aminotransferase; D, day after symptom onset; GGT γ-glutamyl transferase; LDH, lactate dehydrogenase; NA, not available;
†Dysphagia, diarrhea, jaundice, sore throat, rash, bleeding manifestation, and loss of consciousness were not observed for these patients.
‡Patient 1 also had posttraumatic rhabdomyolysis: myoglobin level 869.5 μg/mL at D3 (reference range 16.0–116.0 μg/mL) and creatine kinase level 9,444 μg/mL at D5 (reference range 39–308 μg/mL).

likely source of human infection. Organs from 10 rats sampled at this unit were positive for SEOV by nested reverse transcription PCR (*7*). A partial large RNA sequence obtained from a rat was identical to that obtained from the case-patient. Only 1 wild rat caught near the hen house was sampled; results were negative for SEOV.

We obtained complete small RNA coding domain sequences (GenBank accession nos. KX064270–KX064275) from specimens from case-patients 2 and 3 (samples were not available for case-patient 1); specimens from the pet brown rat and raised brown rats suspected to be sources of infection for case-patients 1 and 2; and specimens from 2 wild brown rats suspected to sources of infection for a serologically confirmed human infection with SEOV detected in 2014 (*6*). Using MEGA version 5.1 (*8*) and a generalized time-reversible model with a gamma distribution and 5 rate categories (according to the best fit substitution model proposed), we performed phylogenetic analysis of the small RNA coding sequence. This analysis confirmed that all virus strains detected were SEOV (Figure 2).

Conclusions

Four hantaviruses (Puumala [PUUV], SEOV, Tula, and Nova viruses), have been detected in France; the first 3 viruses were associated with humans, and most human infections were with PUUV (*9*). Human SEOV infection in Europe was initially reported in 2013 (*5*); however, human

Table 2. Serologic results for hantaviruses for 3 patients with virologically confirmed infections with Seoul virus, France, 2014–2016*

Patient no.	Day of sampling†	First-line diagnostic test, commercial ELISA (index value)		Diagnostic confirmation at NRC: ELISA IgM		ELISA IgG		IFA Ig		Additional test at NRC‡ IgM
		IgM	IgG	SEOV	PUUV	SEOV	PUUV	SEOV	PUUV	PUUV
1	3	+§ (4.3)	+§ (1.9)	+	–	–	–	–	–	–
2	5	+¶ (7.9)	+¶ (>200)	+	–	E	–	+	E	–
	29	ND	ND	+	E	+	E	+	–	ND
3	4	+§ (11.8)	+§ (9.8)	+	+	E	–	+	–	–
	80	ND	ND	+	–	+	+	+	+	ND

*E, equivocal; IFA, indirect fluorescent antibody; ND, not done; NRC, National Reference Center for Hantavirus (Lyon, France); PUUV, Puumala virus, SEOV, Seoul virus; +, positive; –, negative.
†No. days after symptom onset.
‡Reascan Rapid Test (Reagena, Toivala, Finland).
§Hantavirus IgG DxSelect and Hantavirus IgM DxSelect (Focus Diagnostics, Cypress, CA, USA).
¶Hantavirus Pool 1 Eurasia IgG and IgM (Euroimmun AG, Lübeck, Germany).

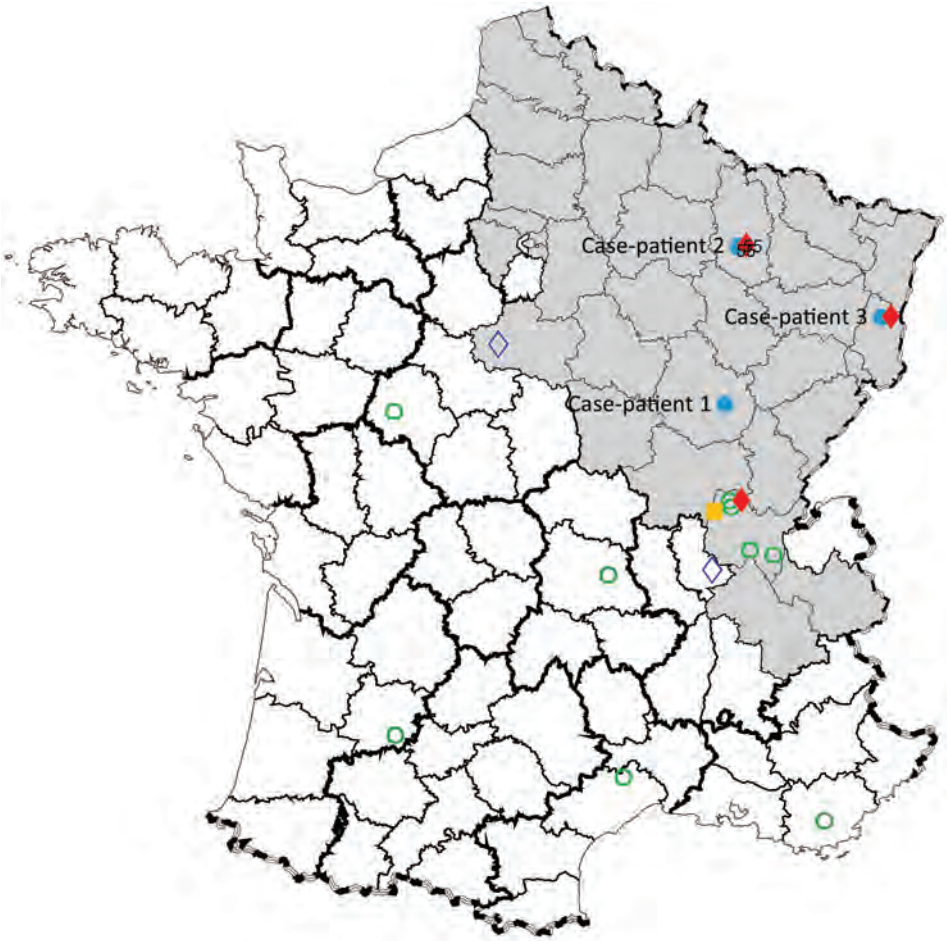

Figure 1. Geographic distribution of Seoul virus (SEOV) infections among human and rats, France 2016. Gray shading area indicates area of France to which Puumala virus is endemic. Open green circles indicate SEOV serologically confirmed human infections with SEOV reported by Ragnaud et al. (*10*), Le Guenno (*11*), and Bour et al. (*6*); solid blue circles indicate virologically confirmed human infections with SEOV reported in this study (patients 1, 2, and 3); solid yellow square indicates virologically confirmed human infection with SEOV reported by Macé al. (*5*); solid red diamonds indicate virologically confirmed SEOV infections in brown rats reported in this study; and open blue diamonds indicate virologically confirmed SEOV infections in brown rats reported by Heyman et al. (*12*) and Dupinay et al. (*13*).

SEOV infections were previously suspected by serologic analysis in France (6 cases were reported during 1977–1996). SEOV was also detected in rodents from several areas in France (Figure 1) (*10–13*).

Detection of SEOV in 3 case-patients in our study and a recent report of a human infected with SEOV (*6*) within a 2-year period indicate that SEOV infections in humans are not uncommon in France. These infections accounted for 4 (1.7%) of 234 cases of hantavirus infection, mostly with PUUV, detected serologically or virologically during the same period in France. Detection of such cases might be caused by improvements in detection of SEOV infections, rather than by emergence of SEOV infections (SEOV antigen in serologic assays and molecular detection have been used at NRC since 2012).

Some infections with SEOV are probably missed in France. Commercials kits are used for hantavirus serologic diagnosis by 15 public hospital or private clinical laboratories in France. Eleven of these hospitals used a POC Puumala IgM rapid test (Reagena, Toivala, Finland). Four other hospitals used IgM and IgG ELISA kits with mixtures of recombinant antigens, including those from SEOV or Hantaan virus strains.

Most (83.4%) diagnostic tests in 2014 were requested for patients in the area of France to which PUUV is endemic. Consequently, some SEOV infections might have been be missed because hantavirus infection is rarely suspected outside this area. Samples with positive results for SEOV are sent to NRC for diagnostic confirmation and surveillance purposes. The 3 case-patients we report initially showed positive results by ELISA at local laboratories but then showed negative results by a ReaScan Puumala IgM test (Reagena) at NRC (Table 2). Therefore, SEOV infections were probably not detected initially by the 11 local laboratories who used the PUUV IgM Rapid Test, which led to underestimation of SEOV infections in humans in France.

This negative result could have also occurred in other countries in Europe that used the same test. Consequently, use of a pan hantavirus serologic assay is preferred. Furthermore, PUUV was detected by molecular techniques for most PUUV-infected patients during the acute phase of the disease (*14*). Thus, although there are no similar data for SEOV, to avoid misdiagnosis, we suggest using molecular diagnostic tests to more specifically detect hantavirus infections.

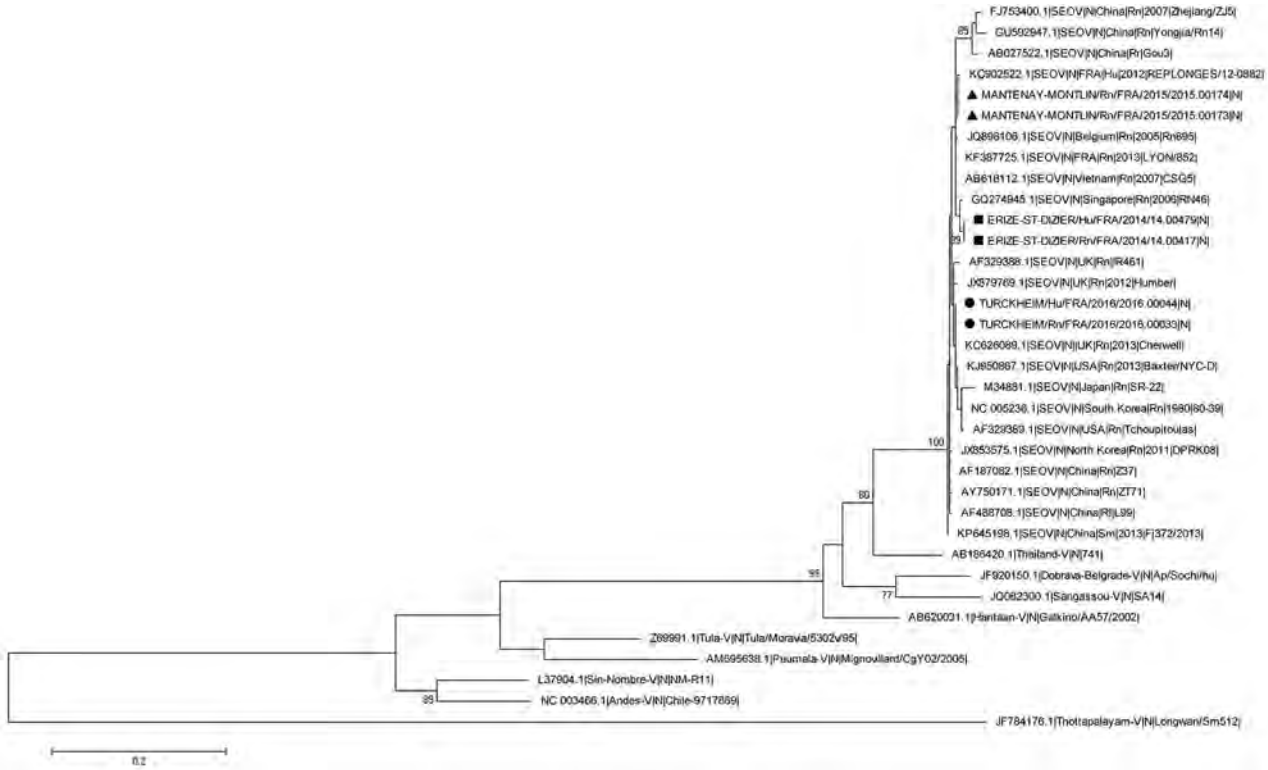

Figure 2. Phylogenetic tree based on the complete small RNA nucleotide coding sequences of Seoul virus (SEOV) strains isolated from 3 patients and rodents in contact with the patients infected with SEOV, France 2014–2016, and representative strains of SEOV and other hantavirus species. Triangles indicate sequences of strains detected in wild brown rats (this study) associated with a serologically confirmed human infection reported by Bour A et al. (*6*); squares indicate sequences of strains detected in case-patient 2 and in his pet brown rat; and circles indicate sequences of strains detected in case-patient 3 and 1 of his farmed brown rats. Bootstrap percentages ≥70% (from 500 resamplings) are indicated at each node; GenBank accession numbers are indicated for reference strains.Scale bar indicates nucleotide substitutions per site.

Furthermore, epidemiologic investigations showed that several animal traders in Europe sold pet rats or food rats to case-patients 2 and 3. These investigations also identified weak traceability of rat batches, absence of health-monitoring data for rats, and no information for the 3 case-patients on zoonotic risks for infection. Awareness of rat owners, traceability, and health monitoring of these animals, as performed for laboratory rats (*15*), should be improved.

Acknowledgments

We thank Christine Manson and David Reveille for sampling brown rats.

The Centre National de Référence des Hantavirus was supported by Santé Publique France.

Dr. Reynes is a veterinarian and a medical virologist at the Institut Pasteur, Lyon, France. His research interests focus on zoonotic infectious diseases.

References

1. Clement J, Heyman P, McKenna P, Colson P, Avsic-Zupanc T. The hantaviruses of Europe: from the bedside to the bench. Emerg Infect Dis. 1997;3:205–11. http://dx.doi.org/10.3201/eid0302.970218
2. Kariwa H, Yoshimatsu K, Arikawa J. Hantavirus infection in East Asia. Comp Immunol Microbiol Infect Dis. 2007;30:341–56. http://dx.doi.org/10.1016/j.cimid.2007.05.011
3. Knust B, Rollin PE. Twenty-year summary of surveillance for human hantavirus infections, United States. Emerg Infect Dis. 2013;19:1934–7. http://dx.doi.org/10.3201/eid1912.131217
4. Jameson LJ, Taori SK, Atkinson B, Levick P, Featherstone CA, van der Burgt G, et al. Pet rats as a source of hantavirus in England and Wales, 2013. Euro Surveill. 2013;18:20415.
5. Macé G, Feyeux C, Mollard N, Chantegret C, Audia S, Rebibou JM, et al. Severe Seoul hantavirus infection in a pregnant woman, France, October 2012. Euro Surveill. 2013;18:20464.
6. Bour A, Reynes JM, Plaisancie X, Dufour JF. Seoul hantavirus infection-associated hemorrhagic fever with renal syndrome in France: a case report [in French]. Rev Med Interne. 2016;37:493–6. http://dx.doi.org/10.1016/j.revmed.2015.10.343
7. Klempa B, Fichet-Calvet E, Lecompte E, Auste B, Aniskin V, Meisel H, et al. Hantavirus in African wood mouse, Guinea. Emerg Infect Dis. 2006;12:838–40. http://dx.doi.org/10.3201/eid1205.051487
8. Tamura K, Peterson D, Peterson N, Stecher G, Nei M, Kumar S. MEGA5: molecular evolutionary genetics analysis using maximum likelihood, evolutionary distance, and maximum parsimony methods. Mol Biol Evol. 2011;28:2731–9. http://dx.doi.org/10.1093/molbev/msr121

9. Centre National de Reference Hantavirus, Institut Pasteur. Annual activity report, 2015 [in French] [cited 2017 Feb 27]. https://www.pasteur.fr/fr/sante-publique/CNR/les-cnr/hantavirus/rapports-d-activite
10. Ragnaud JM, Lamouliatte H, Paix MA, Fleury H, Roy J, Magnol R. Hemorrhagic fever with renal syndrome: a case with jaundice [in French]. Gastroenterol Clin Biol. 1986;10:686.
11. Le Guenno B. Hantaviruses [in French]. Médecine et Maladies Infectieuses. 1997;27:703–10. http://dx.doi.org/10.1016/S0399-077X(97)80179-5
12. Heyman P, Plyusnina A, Berny P, Cochez C, Artois M, Zizi M, et al. Seoul hantavirus in Europe: first demonstration of the virus genome in wild *Rattus norvegicus* captured in France. Eur J Clin Microbiol Infect Dis. 2004;23:711–7. http://dx.doi.org/10.1007/s10096-004-1196-3
13. Dupinay T, Pounder KC, Ayral F, Laaberki MH, Marston DA, Lacôte S, et al. Detection and genetic characterization of Seoul virus from commensal brown rats in France. Virol J. 2014;11:32. http://dx.doi.org/10.1186/1743-422X-11-32
14. Lagerqvist N, Hagström Å, Lundahl M, Nilsson E, Juremalm M, Larsson I, et al. Molecular diagnosis of Puumala virus-caused hemorrhagic fever with renal syndrome. J Clin Microbiol. 2016;54:1335–9. http://dx.doi.org/10.1128/JCM.00113-16
15. Mähler Convenor M, Berard M, Feinstein R, Gallagher A, Illgen-Wilcke B, Pritchett-Corning K, et al.; FELASA working group on revision of guidelines for health monitoring of rodents and rabbits. FELASA recommendations for the health monitoring of mouse, rat, hamster, guinea pig and rabbit colonies in breeding and experimental units. Lab Anim. 2014;48:178–92. http://dx.doi.org/10.1177/0023677213516312

Address for correspondence: Jean-Marc Reynes, Centre National de Référence des Hantavirus, Unité de Biologie des Infections Virales Emergentes, Institut Pasteur, Centre International de Recherche en Infectiologie, 21 Ave Tony Garnier, 69 365 Lyon CEDEX 7, France; email: jean-marc.reynes@pasteur.fr

April 2017: Emerging Viruses

- Biologic Evidence Required for Zika Disease Enhancements by Dengue Antibodies Neurologic Complications of Influenza B Virus Infection in Adults, Romania
- Implementation and Initial Analysis of a Laboratory-Based Weekly Biosurveillance System, Provence-Alpes-Côte d'Azur, France
- Transmission of Hepatitis A Virus through Combined Liver–Small Intestine–Pancreas Transplantation
- Influence of Referral Pathway on Ebola Virus Disease Case-Fatality Rate and Effect of Survival Selection Bias
- *Plasmodium malariae* Prevalence and *csp* Gene Diversity, Kenya, 2014 and 2015
- Presence and Persistence of Zika Virus RNA in Semen, United Kingdom, 2016
- Three Divergent Subpopulations of the Malaria Parasite *Plasmodium knowlesi*
- Variation in *Aedes aegypti* Mosquito Competence for Zika Virus Transmission

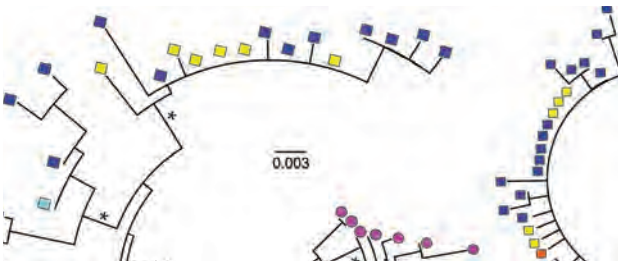

- Outbreaks among Wild Birds and Domestic Poultry Caused by Reassorted Influenza A(H5N8) Clade 2.3.4.4 Viruses, Germany, 2016
- Highly Pathogenic Avian Influenza A(H5N8) Virus in Wild Migratory Birds, Qinghai Lake, China
- Design Strategies for Efficient Arbovirus Surveillance
- Typhus Group Rickettsiosis, Texas, 2003–2013
- Detection and Molecular Characterization of Zoonotic Poxviruses Circulating in the Amazon Region of Colombia, 2014

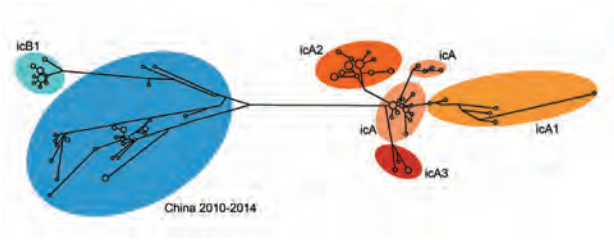

- Reassortment of Influenza A Viruses in Wild Birds in Alaska before H5 Clade 2.3.4.4 Outbreaks Incidence and Characteristics of Scarlet Fever, South Korea, 2008–2015
- Markers of Disease Severity in Patients with Spanish Influenza in the Japanese Armed Forces, 1919–1920
- Molecular Identification of *Spirometra erinaceieuropaei* in Cases of Human Sparganosis, Hong Kong
- Zika Virus Seroprevalence, French Polynesia, 2014–2015
- * Persistent Arthralgia Associated with Chikungunya Virus Outbreak, US Virgin Islands, December 2014–February 2016
- Assessing Sensitivity and Specificity of Surveillance Case Definitions for Zika Virus Disease
- Detection of Zika Virus in Desiccated Mosquitoes by Real-Time Reverse Transcription PCR and Plaque Assay
- Surveillance and Testing for Middle East Respiratory Syndrome Coronavirus, Saudi Arabia, April 2015–February 2016
- Antiviral Drug-Resistant Influenza B Viruses Carrying H134N Substitution in Neuraminidase, Laos, February 2016
- Characterization of Highly Pathogenic Avian Influenza Virus A(H5N6), Japan, November 2016
- Severe Thrombocytopenia After Zika Virus Infection, Guadeloupe, 2016
- Significant Decrease in Pertactin-Deficient *Bordetella pertussis* Isolates, Japan

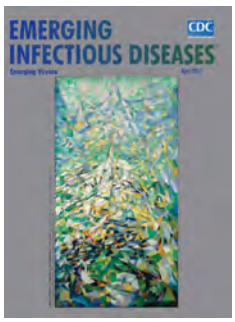

EMERGING INFECTIOUS DISEASES https://wwwnc.cdc.gov/eid/articles/issue/23/4/table-of-contents

Central Nervous System Brucellosis Granuloma and White Matter Disease in Immunocompromised Patient

Mohammed Alqwaifly, Fahad S. Al-Ajlan, Hindi Al-Hindi, Abdulaziz Al Semari

Brucellosis is a multisystem zoonotic disease. We report an unusual case of neurobrucellosis with seizures in an immunocompromised patient in Saudi Arabia who underwent renal transplantation. Magnetic resonance imaging of the brain showed diffuse white matter lesions. Serum and cerebrospinal fluid were positive for Brucella sp. Granuloma was detected in a brain biopsy specimen.

Human brucellosis is a major zoonotic disease in Saudi Arabia (*1*). This disease is caused by Brucella spp., gram-negative bacteria usually transmitted through consumption of raw meat or unpasteurized dairy products (*2*). Brucellosis is endemic to the Arabian Peninsula and countries bordering the Mediterranean Sea (*3*).

Neurobrucellosis occurs in 5%–10% of patients with brucellosis (*4*). The most frequent clinical manifestation is meningoencephalitis (*5*). Mass lesions in the brain are uncommon (*4*). Intracerebral granuloma associated with brucellosis had been reported in a community-acquired infection (*6*). We report an unusual case of neurobrucellosis and seizures in an immunocompromised patient.

The Study

The patient was a 46-year-old Saudi woman who had chronic hepatitis C, end-stage renal disease of undetermined etiology, and a renal transplant in 1993. She reported a 5-month history of headaches and seizures. Seizures were usually preceded by epigastric pain and a sensation of nausea for few seconds, followed by left arm posturing and loss of consciousness. She did not have fever, weight loss, or joint pain. She lived in a rural area, was involved in animal husbandry, and consumed unpasteurized milk products. Her husband had been treated for brucellosis. Her medications included mycophenolate mofetil (500 mg 2×/d since 1993), prednisone (5 mg 1×/d since 1993), levetiracetam (500 mg 2×/d for 5 mo), and phenytoin (200 mg every night for 1 mo).

Neurologic examination showed left homonymous hemianopia, increased deep tendon reflexes in the left hemibody, and the Babinski sign on the left hallux. Initial laboratory test results, including those for complete blood count, erythrocyte sedimentation rate, C-reactive protein, and liver and renal profiles, were within references ranges. Results of serologic analysis for HIV and hepatitis B virus were negative.

A standard agglutination tube (SAT) test result for *Brucella* spp. was positive (titer 1:320), and a 2-mercaptoethanol test result for *Brucella* spp. agglutination was positive (titer 1:160). An ELISA showed antibodies against *Brucella* spp. in serum (titer 1:5,120). Cerebrospinal fluid (CSF) had a leukocyte count of 21 (90% lymphocytes). Levels of protein, glucose, and lactate dehydrogenase in CSF were within references ranges.

Gram staining of a CSF sample and cultures for bacteria, virus, fungi, and acid-fast bacilli (AFB) showed negative results. Results of PCRs for AFB, cytomegalovirus, and JC polyomavirus were negative.

Serologic analysis of CSF showed *Brucella* IgG (titer <1:20) and antibodies against *Brucella* (titer 1:320). Test results were negative for antibodies against *Aspergillus*, *Aspergillus* galactomannan, *Blastomyces*, *Borrelia*, *Coccidia*, *Cryptococcus*, *Histoplasma*, and *Toxoplasma*.

An electroencephalogram showed sharp waves over the right temporal region and continuous slow activity over the right temporooccipital region. Magnetic resonance imaging (MRI) of the brain showed diffuse T2/fluid-attenuated inversion recovery hyperintense white matter lesions involving the right frontal, parietal and temporal lobes (Figure 1). No appreciable mass effect or enhancement after administration of gadolinium was observed. Positive emission tomography of the brain showed hypometabolic cerebral activity involving a large area of right cerebral hemisphere. Magnetic resonance spectroscopy shows a low peak of N-acetyl aspartate (2.2 ppm).

A brain biopsy specimen of cerebral cortex and superficial white matter showed a moderate lymphoplasmacytic and focally histiocytic infiltrate that involved deep cortex, white matter, and leptomeninges. The histiocytic component formed small epithelioid granulomas that were nonnecrotizing. The inflammatory reaction, including

Author affiliations: Qassim University College of Medicine, Qassim, Saudi Arabia (M. Alqwaifly); King Faisal Specialist Hospital and Research Center, Riyadh, Saudi Arabia (F.S. Al-Ajlan, H. Al-Hindi, A. Al Semari)

DOI: http://dx.doi.org/10.3201/eid2306.161173

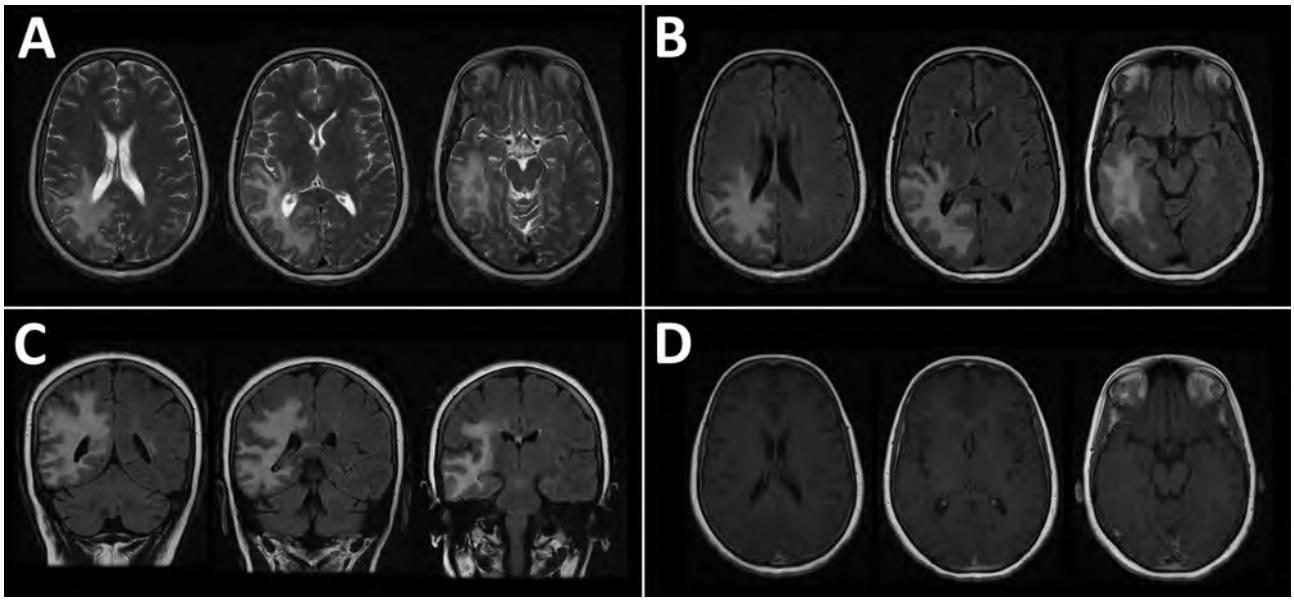

Figure 1. Magnetic resonance imaging of the brain of a 46-year-old immunocompromised woman with central nervous system brucellosis granuloma and white matter disease, Saudi Arabia. A) Axial T2 images showing hyperintensity in the right frontoparietal lobe and right temporal lobe. B) Axial fluid-attenuated inversion recovery (FLAIR) and C) coronal FLAIR images showing that hypersensitivity extends to U-fibers without involvement of the cortex. D) Gadolinium-enhanced image showing that no appreciable mass effect and no central or peripheral enhancement after administration of gadolinium were observed. Each image within each panel shows involvement in different levels of frontal, parietal, and temporal lobes.

granulomas, was mainly perivascular with some angiocentric patterns and focal parenchymal involvement. The white matter portion was heavily infiltrated by macrophages. Reactive astrogliosis was prominent. There were no morphologic signs of a specific etiology: no viral inclusions, and staining results microorganisms (AFB, fungi, Epstein-Barr virus, and JC polyomavirus) were negative (Figure 2).

A gram stain was initially negative for bacteria. At day 5, *Brucella* spp. were isolated from brain biopsy specimens. An antibiogram showed that the *Brucella* sp. was sensitive to gentamicin, streptomycin, tetracycline, trimethoprim/sulfamethoxazole, and rifampin.

The patient received intravenous ceftriaxone (2 g every 12 h), oral doxycycline (100 mg every 12 h), oral rifampin (600 mg 1×/d), and trimethoprim/sulfamethoxazole (1 tablet [160 mg/800 mg] every 12 h) for 2 wk. After discharge, she was receiving oral doxycycline (100 mg every 12 h), rifampin (600 mg, 1×/d), trimethoprim/sulfamethoxazole (1 tablet every 12 h), and ciprofloxacin (500 mg every 12 h) for 6 mo: she was also receiving levitiracetam (750 mg 2×/d), carbamazepine (200 mg 2×/d), mycophenolate mofetil (500 mg 2×/d), and prednisone (5 mg 1×/d).

Three months later, repeat MRI of the brain showed decreased T2 hyperintensity associated with volume loss

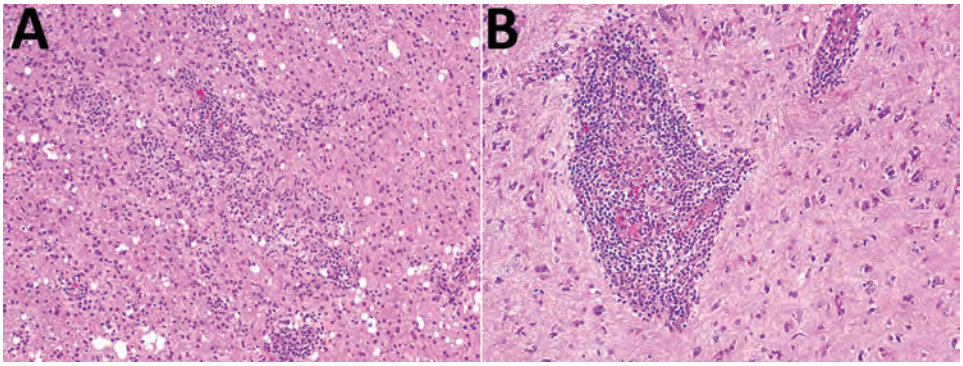

Figure 2. Histologic analysis of a brain biopsy specimen from a 46-year-old immunocompromised woman with central nervous system brucellosis granuloma and white matter disease, Saudi Arabia. A) Low magnification view of cerebral cortex showing infiltration by perivascular lymphocytes and histiocytes. Histiocytes form small nonnecrotizing granuloma (center) (original magnification ×100). B) High magnification view showing an angiocentric epithelioid granuloma cuffed by mature lymphocytes (original magnification ×200). Hemotoxylin and eosin stain.

and ex vacuo dilatation of the subjacent right lateral ventricle. We did not observe any appreciable new lesions.

After 6 months of follow-up, her headaches had resolved. However, she continued to have auras without major seizures.

Conclusions

Neurobrucellosis can affect the central or peripheral nervous systems and lead to diverse clinical syndromes (*4*). Diagnosis of neurobrucellosis depends on clinical manifestations, CSF findings suggestive of pinocytosis, high protein levels, low or standard glucose levels, and a positive antibody titer for *Brucella* spp. Although the patient had mild pleocytosis with a predominance of lymphocytes and high antibody titers against *Brucella* spp. in CSF, the CSF protein level was within the reference range. Antibodies against *Brucella* spp. in CSF are usually an indication of neurobrucellosis. However, low levels of antibodies might not be detected by SAT. In suspicious cases in which the SAT result is negative, SAT and a Coombs test, ELISA, and PCR are helpful in making a diagnosis.

77The clinical–radiologic correlation for neurobrucellosis ranges from uneventful results for imaging studies, despite positive clinical findings, to imaging abnormalities (*3*). Neurobrucellosis with a focal brain mass has been rarely observed in imaging studies (*7*,*8*).

Radiologic results in this case suggested an infectious disease, autoimmune disease, or malignancy in an immunocompromised patient. Because we deemed it necessary to exclude other conditions, such as progressive multifocal leukoencephalopathy or lymphoma, we performed a brain biopsy. The diagnosis was established by detecting antibodies against a *Brucella* sp. in serum and CSF and confirmed by isolation of a *Brucella* sp. from brain tissue.

We found that the patient had epilepsy and extensive white matter changes secondary to brucellosis. She continued to have auras without major seizures. MRI of the brain showed abnormal results (prominent white matter disease and focal encephalomalacia). Inflammation can cause permanent cellular biochemical dysfunction, which can lead to electrically irritable tissue and parenchymal damage despite successful treatment. This finding might explain the persistency of brain lesion. Appropriate antimicrobial therapy can eliminate the infection.

Longitudinal studies of white matter hyperintensities caused by vascular, noninfectious, infectious, and inflammatory conditions showed white matter hyperintensities over time despite effective treatment. Fincham et al. reported that white matter changes in neurobrucellosis were sequelae of demyelination, as confirmed by the pathologic analysis (*9*). We believe that unresolved white matter hyperintensities in this patient were a sequela of the inflammatory process. A case report documented similar clinical features in a patient with seizures caused by chronic neurobrucellosis for 2.5 years (*10*).

Granuloma is a pathogenesis of epilepsy (*11*). Solitary cysticercus granuloma and calcified lesion are 2 common neuroimaging abnormalities in patients with epilepsy. Treatment for underlying cysticercosis does not cure epilepsy (*12*). Seizures associated with central nervous system tuberculomas are often resolved after successful treatment (*13*). The underlying pathogenesis for relapsing epilepsy in neurocysticercosis is probably related to abnormal neurons and their arrangement within calcified nodules (*13*). The epilepsy prognosis for neurobrucellosis is probably similar to that for central nervous system neurocysticercosis (*13*).

A perivascular nonnecrotizing granuloma is a histopathologic feature of neurobrucellosis. Neurocellosis granuloma is a pathogenesis of refractory epilepsy. Our findings indicate the need for suspecting neurobrucellosis as a cause of epilepsy and white matter disease in immunocompromised patients in disease-endemic areas.

Dr. Alqwaifly is an assistant professor of neurology at Qassim University College of Medicine, Qassim, Saudi Arabia. His research interests are central nervous system infections, neuropathy, and movement disorders.

References

1. Kiel FW, Khan MY. Brucellosis in Saudi Arabia. Soc Sci Med. 1989;29:999–1001. http://dx.doi.org/10.1016/0277-9536(89)90056-7
2. Adams LG. The pathology of brucellosis reflects the outcome of the battle between the host genome and the *Brucella* genome. Vet Microbiol. 2002;90:553–61. http://dx.doi.org/10.1016/S0378-1135(02)00235-3
3. Al-Sous MW, Bohlega S, Al-Kawi MZ, Alwatban J, McLean DR. Neurobrucellosis: clinical and neuroimaging correlation. AJNR Am J Neuroradiol. 2004;25:395–401.
4. Shakir RA. Neurobrucellosis. Postgrad Med J. 1986;62:1077–9. http://dx.doi.org/10.1136/pgmj.62.734.1077
5. Türel O, Sanli K, Hatipoğlu N, Aydoğmuş C, Hatipoğlu H, Siraneci R. Acute meningoencephalitis due to *Brucella*: case report and review of neurobrucellosis in children. Turk J Pediatr. 2010;52:426–9.
6. Sohn AH, Probert WS, Glaser CA, Gupta N, Bollen AW, Wong JD, et al. Human neurobrucellosis with intracerebral granuloma caused by a marine mammal *Brucella* spp. Emerg Infect Dis. 2003;9:485–8. http://dx.doi.org/10.3201/eid0904.020576
7. Martínez-Chamorro E, Muñoz A, Esparza J, Muñoz MJ, Giangaspro E. Focal cerebral involvement by neurobrucellosis: pathological and MRI findings. Eur J Radiol. 2002;43:28–30. http://dx.doi.org/10.1016/S0720-048X(01)00390-4
8. Erdem M, Namiduru M, Karaoglan I, Kecik VB, Aydin A, Tanriverdi M. Unusual presentation of neurobrucellosis: a solitary intracranial mass lesion mimicking a cerebral tumor: a case of encephalitis caused by *Brucella melitensis*. J Infect Chemother. 2012;18:767–70. http://dx.doi.org/10.1007/s10156-011-0365-4
9. Fincham RW, Sahs AL, Joynt RJ. Protean manifestation of nervous system brucellosis. JAMA. 1963;184:269–76. http://dx.doi.org/10.1001/jama.1963.03700170061009
10. Yilmaz M, Ozaras R, Ozturk R, Mert A, Tabak F, Aktuglu Y. Epileptic seizure: an atypical presentation in an adolescent boy

with neurobrucellosis. Scand J Infect Dis. 2002;34:623–5. http://dx.doi.org/10.1080/00365540210147561
11. Sotelo-Morales J, García-Cuevas E, Rubio-Donnadieu F. Granuloma in cerebral parenchyma. A human model for the study of epilepsy [in Spanish]. Gac Med Mex. 1989;125:31–5, discussion 36.
12. Sharma LN, Garg RK, Verma R, Singh MK, Malhotra HS. Seizure recurrence in patients with solitary cystic granuloma or single parenchymal cerebral calcification: a comparative evaluation. Seizure. 2013;22:840–5. http://dx.doi.org/10.1016/j.seizure.2013.07.001
13. AlSemari A, Baz S, Alrabiah F, Al-Khairallah T, Qadi N, Kareem A, et al. Natural course of epilepsy concomitant with CNS tuberculomas. Epilepsy Res. 2012;99:107–11. http://dx.doi.org/10.1016/j.eplepsyres.2011.10.032

Address for correspondence: Mohammed Alqwaifly, Qassim University College of Medicine, Qassim 51391, Saudi Arabia: email: dr.qwaifly@hotmail.com

July 2016: **Zoonoses**

- Turtle-Associated Salmonellosis, United States, 2006–2014
- Pregnancy, Labor, and Delivery after Ebola Virus Disease and Implications for Infection Control in Obstetric Services, United States, 2015
- Response to Middle East Respiratory Syndrome Coronavirus, Abu Dhabi, United Arab Emirates, 2013–2014
- Current Guidelines, Common Clinical Pitfalls, and Future Directions for Laboratory Diagnosis of Lyme Disease, United
- *Tropheryma whipplei* as a Cause of Epidemic Fever, Senegal, 2010–2012
- Two Linked Enteroinvasive *Escherichia coli* Outbreaks, Nottingham, United Kingdom, June 2014
- Porcine Bocavirus Infection Associated with Encephalomyelitis in a Pig, Germany
- African Swine Fever Epidemic, Poland, 2014–2015
- Hepatitis E Virus in Dromedaries, North and East Africa, United Arab Emirates and Pakistan, 1983–2015
- Heatwave-Associated Vibriosis, Sweden and Finland, 2014
- Vesicular Disease in 9-Week-Old Pigs Experimentally Infected with Senecavirus A

- High Incidence of Chikungunya Virus and Frequency of Viremic Blood Donations during Epidemic, Puerto Rico, USA, 2014
- Outbreak of *Vibrio parahaemolyticus* Sequence Type 120, Peru, 2009
- Clinical Manifestations of Senecavirus A Infection in Neonatal Pigs, Brazil, 2015

- Infection with Possible Novel Parapoxvirus in Horse, Finland, 2013
- Travel-Associated Rabies in Pets and Residual Rabies Risk, Western Europe

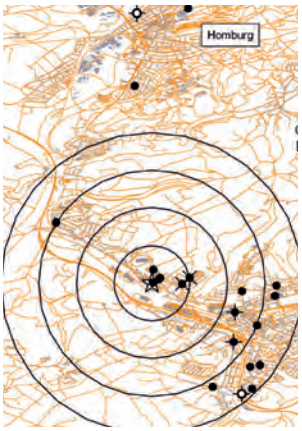

- Surveillance for Highly Pathogenic Avian Influenza Virus in Wild Birds during Outbreaks in Domestic Poultry, Minnesota, 2015
- Highly Pathogenic Avian Influenza Viruses and Generation of Novel Reassortants, United States, 2014–2015
- Naturally Circulating Hepatitis A Virus in Olive Baboons, Uganda
- Detection and Genomic Characterization of Senecavirus A, Ohio, USA, 2015
- Red Fox as a Sentinel for *Blastomyces dermatitidis*, Ontario, Canada
- Senecavirus A in Pigs, United States, 2015

EMERGING INFECTIOUS DISEASES

https://wwwnc.cdc.gov/eid/articles/issue/22/7/table-of-contents

Severe Neurologic Disorders in 2 Fetuses with Zika Virus Infection, Colombia

Jorge Acosta-Reyes, Edgar Navarro, Maria José Herrera, Eloina Goenaga, Martha L. Ospina, Edgar Parra, Marcela Mercado, Pablo Chaparro, Mauricio Beltran, Maria Luz Gunturiz, Lissethe Pardo, Catalina Valencia, Sandra Huertas, Jorge Rodríguez, Germán Ruiz, Diana Valencia, Lisa B. Haddad, Sarah C. Tinker, Cynthia A. Moore, Hernando Baquero

We report the results of pathologic examinations of 2 fetuses from women in Colombia with Zika virus infection during pregnancy that revealed severe central nervous system defects and potential associated abnormalities of the eye, spleen, and placenta. Amniotic fluid and tissues from multiple fetal organs tested positive for Zika virus.

In October 2015, Colombia confirmed its first case of autochthonous Zika virus infection (*1*). As of November 2016, ≈105,000 cases of symptomatic Zika virus disease have been reported, including 19,499 cases among pregnant women. Although Zika virus infections typically lead to comparatively benign symptoms relative to those of other arboviruses (*2*), in May 2016, the US Centers for Disease Control and Prevention concluded that congenital Zika virus infection was the cause of the severe central nervous system (CNS) defects observed in fetuses and newborns of women infected with Zika virus during pregnancy (*3*). Although the full spectrum of fetal effects of congenital Zika virus infection is not known, Zika virus has been shown to cross the placental barrier, grow in brain tissue of fetuses, infect progenitor neural cells, and increase neural cell death or attenuate their growth (*4*,*5*). Observed CNS abnormalities include microcephaly, ventriculomegaly, cerebral calcifications, absent corpus callosum, and atrophy of the cerebellum and brainstem in fetuses with congenital Zika virus infection (*6*). This report describes 2 fetuses examined after pregnancy termination who had severe CNS defects attributed to maternal Zika virus infection.

Author affiliations: Universidad del Norte, Barranquilla, Colombia (J. Acosta-Reyes, E. Navarro, M.J. Herrera, H. Baquero); Secretaría de Salud de Barranquilla, Barranquilla (E. Goenaga); Instituto Nacional de Salud, Bogotá, Colombia (M.L. Ospina, E. Parra, M. Mercado, P. Chaparro, M. Beltrán, M.L. Gunturiz, L. Pardo); Clínica Colsanitas, Clínica Reina Sofía, Bogotá (C. Valencia, S. Huertas, J. Rodríguez, G. Ruiz); Centers for Disease Control and Prevention, Atlanta, Georgia, USA (D. Valencia, S.C. Tinker, C.A. Moore); Emory University School of Medicine, Atlanta (L.B. Haddad).

DOI: http://dx.doi.org/10.3201/eid2306.161702

The Cases

Case 1 involved a 24-year-old pregnant resident of the city of Barranquilla who had symptoms compatible with Zika virus disease, including fever and generalized rash for 2 days, followed by edema and joint pain for 2 weeks, with onset occurring at 5–6 weeks of gestation. Her medical history was notable because of a prior pregnancy complicated by a stillbirth with Potter syndrome, delivered 2 months before conception of the current pregnancy. Obstetric ultrasounds at 8 and 12 weeks of gestation showed a singleton fetus with no abnormalities; an ultrasound at 15 weeks of gestation demonstrated absence of the cranial vault (exencephaly) with brain tissue loss, including absence of cerebral hemispheres (anencephaly sequence). Amniotic fluid sampled at 17 weeks was positive for Zika virus by real-time reverse transcription PCR (rRT-PCR). The fetus was at 20 weeks of gestation when evaluated.

Case 2 involved a 15-year-old pregnant resident of Bogotá who reported symptoms compatible with Zika virus disease, including generalized rash for 2 days and myalgia, after travel to a municipality with prevalent Zika virus infections, with onset occurring at 16–20 weeks of gestation. She had an uncomplicated obstetric history with 1 prior live birth. Prenatal care started in week 26; an ultrasound at that time showed a fetus with abnormal clefts in the cerebral hemispheres of the brain (schizencephaly), with cleft walls separated and filled with cerebrospinal fluid (open lip). Follow-up ultrasound indicated large regions of parietal and temporal brain parenchymal loss. The fetus was evaluated and Zika virus diagnosis confirmed at 27 weeks of gestation.

Autopsies of fetal organs and placenta with anatomic pathology and microscopic evaluation were performed for both fetuses. Tissue samples were fixed in 10% neutral-buffered formalin and fixed in paraffin; 4-μm-thick cuts were stained with hematoxylin and eosin for morphologic analysis with light microscopy. RNA was extracted from fresh tissue by using a TRIzol plus RNA purification kit (Thermo Fisher Scientific, Waltham, MA, USA). We used

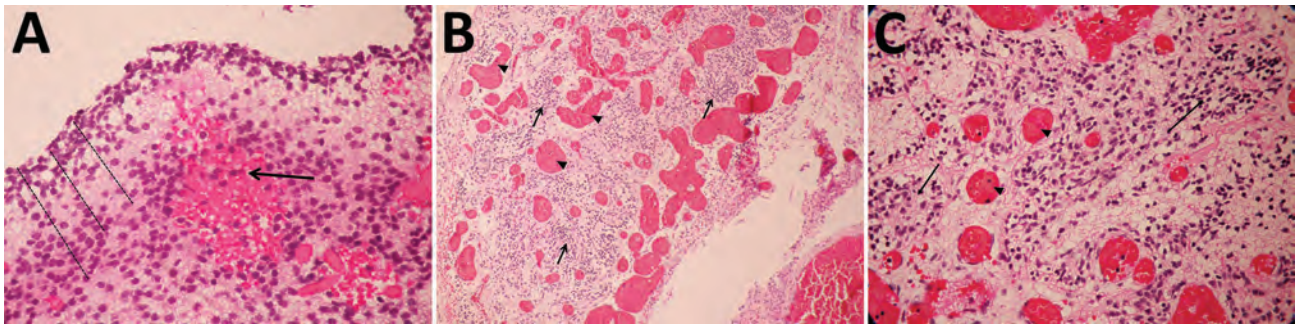

Figure 1. Pathology findings for case 1, involving a fetus examined after pregnancy termination who had severe neurologic defects attributed to maternal Zika virus infection, Colombia. A) Remnant tissue of cerebral cortex showing a reduced neuroblast layer (dotted lines) and hemorrhagic foci (arrow). Hematoxylin and eosin (H&E) staining; original magnification ×40. B) Glial leptomeningeal heterotopy showing congestive blood vessels (arrowhead) and foci of glial heterotopia (arrows). H&E staining; original magnification ×10. C) Glial leptomeningeal heterotopy showing congestive blood vessels (arrowhead) and foci of glial heterotopia (arrows). H&E staining; original magnification ×40.

rRT-PCR for the detection of Zika virus (NS5) and 1-step RT-PCR for the detection of the envelope protein–coding region (360 bp) were performed as previously described (*7*,*8*). Immunohistochemical markers were used in tissue from both fetuses. Molecular testing for syphilis, toxoplasmosis, rubella, and cytomegalovirus was performed following techniques described previously (*9*,*10*); 500-band resolution karyotype was also performed for both fetuses, and ELISA testing for HIV was performed on maternal serum samples.

We documented notable abnormalities in the CNS, eye, spleen, and placenta for 1 or both fetuses (Table, https://wwwnc.cdc.gov/EID/article/23/1/16-1702-T1.htm). All tissues tested and amniotic fluid were positive for Zika virus except eye and placenta from the fetus in case 2. Immunohistochemical markers were negative. For both cases, all tissue samples were negative for other congenital infections (i.e., syphilis, toxoplasmosis, rubella, and cytomegalovirus), high-resolution karyotype was normal, and maternal serum was HIV-negative.

For case 1, microscopic examination demonstrated evidence of recent bleeding in the residual tissues of the cerebrum and brain stem, with no microcalcifications, inclusion bodies, or inflammatory infiltrate (Figure 1). For case 2, we observed microcalcifications in areas of neurologic degeneration; a spinal cord slice showed neuropil disruption with multiple calcifications, reactive gliosis, and loss of the ascending and descending spinal cord tracts (Figure 2).

These 2 cases of fetal Zika virus infection involved severe brain tissue damage and expand the spectrum of CNS defects that might result from congenital Zika virus infection (*11*). Multiple tissues tested positive for Zika virus in both cases, providing strong evidence of vertical transmission. For case 2, the observed pattern of arrest in neuronal migration and decrease in the pattern of maturation of the CNS is consistent with the potential effects of Zika virus infection noted in previous reports (*5*). For case 1, although Zika virus was demonstrated in multiple tissues of the fetus, the birth defect identified (anencephaly) is not on the recognized spectrum of congenital infection. The timing of exposure and primary affected tissue type potentially implicate Zika virus in disruption of neural tube closure in this case. However, the pathology evaluation

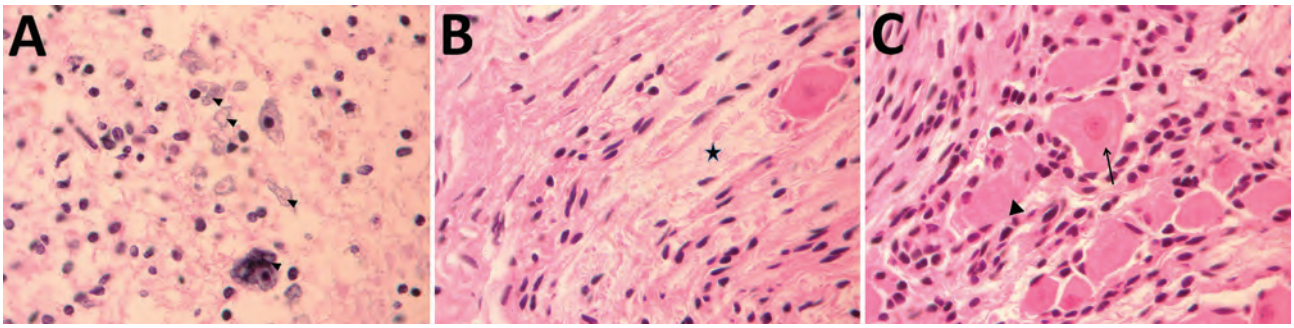

Figure 2. Pathology findings for case 2, involving a fetus examined after pregnancy termination who had severe neurologic defects attributed to maternal Zika virus infection, Colombia. A) Spinal cord slice showing neuropil disruption with multiple calcifications (arrowheads). B) Nerve showing disruptive changes of axons (Wallerian degeneration) (black star). C) Dorsal root ganglion showing spinal ganglion with satellitosis (arrow) and neuronophagia of ganglion cells (arrowhead). Hematoxylin and eosin staining; original magnification ×100.

was consistent with expected findings in any fetus with anencephaly; therefore, congenital Zika virus might have been coincidental in a fetus already predestined by other factors to have anencephaly.

The identification of virus in tissues outside of the brain suggests the need to consider other organs as targets for the virus. To improve knowledge of the spectrum of outcomes among pregnancies affected by congenital Zika virus and to identify interventions that might reduce illness among affected newborns, such as hearing and visual screening, it will be necessary to look for damage in organs other than the brain among newborns of mothers with Zika virus infection during pregnancy. The mothers of the fetuses in these 2 cases reported Zika virus disease symptoms at different times during the pregnancy (early first trimester and early second trimester), which highlights the potentially long window of vulnerability to adverse outcomes among pregnant women with Zika virus infection.

Persistent viremia in maternal serum has been previously reported (*12*–*14*); we observed positive results for Zika virus molecular tests performed on fetal tissues and amniotic fluid 15 week (case 1) and 10 weeks (case 2) after symptoms of acute infection in the pregnant women. Although we did not test for replication-competent virus, the virus probably persists in different fetal tissues after primary infection because of replication in those tissues. The virus might also replicate in placental tissue (*12*,*15*), although it is probably not the only location for viral replication in the 2 cases described in this report, given that Zika virus was identified in the placenta for only 1 of the cases.

Given the epidemic levels of Zika virus disease being reported in Colombia and the severe outcomes associated with congenital infection, we call attention to the importance of healthcare providers reporting cases of Zika virus disease for adequate public health surveillance. Recommendations might include enhanced surveillance of acute cases among pregnant women and stillbirths and abortions related to Zika virus disease during pregnancy, as well as adverse outcomes among live births. Collecting information on congenital Zika virus infection is important to helping public health authorities effectively address this new health threat and make evidence-based decisions, which will benefit Colombia and other countries throughout the world.

Dr. Acosta-Reyes is a clinical epidemiologist and currently is the Director of the Department of Public Health in the School of Medicine at Universidad del Norte, Barranquilla, Colombia. His research interests include the epidemiology, immunology, diagnosis, and prevention of arboviruses and maternal and child health.

References

1. Pacheco O, Beltrán M, Nelson CA, Valencia D, Tolosa N, Farr SL, et al. Zika virus disease in Colombia—preliminary report. N Engl J Med. 2016;NEJMoa1604037. http://dx.doi.org/10.1056/NEJMoa1604037
2. Petersen LR, Jamieson DJ, Honein MA. Zika virus. N Engl J Med. 2016;375:294–5. https://dx.doi.org/10.1056/NEJMc1606769
3. Rasmussen SA, Jamieson DJ, Honein MA, Petersen LR. Zika virus and birth defects—reviewing the evidence for causality. N Engl J Med. 2016;374:1981–7. http://dx.doi.org/10.1056/NEJMsr1604338
4. Mlakar J, Korva M, Tul N, Popović M, Poljšak-Prijatelj M, Mraz J, et al. Zika virus associated with microcephaly. N Engl J Med. 2016;374:951–8. http://dx.doi.org/10.1056/NEJMoa1600651
5. Tang H, Hammack C, Ogden SC, Wen Z, Qian X, Li Y, et al. Zika virus infects human cortical neural progenitors and attenuates their growth. Cell Stem Cell. 2016;18:587–90. http://dx.doi.org/10.1016/j.stem.2016.02.016
6. Moore CA, Staples JE, Dobyns WB, Pessoa A, Ventura CV, Fonseca EB, et al. Characterizing the pattern of anomalies in congenital Zika syndrome for pediatric clinicians. JAMA Pediatr. 2016; Nov 3 [Epub ahead of print]. http://dx.doi.org/10.1001/jamapediatrics.2016.3982
7. Faye O, Faye O, Diallo D, Diallo M, Weidmann M, Sall AA. Quantitative real-time PCR detection of Zika virus and evaluation with field-caught mosquitoes. Virol J. 2013;10:311. http://dx.doi.org/10.1186/1743-422X-10-311
8. Faye O, Faye O, Dupressoir A, Weidmann M, Ndiaye M, Alpha Sall A. One-step RT-PCR for detection of Zika virus. J Clin Virol. 2008;43:96–101. http://dx.doi.org/10.1016/j.jcv.2008.05.005
9. Bosma TJ, Corbett KM, O'Shea S, Banatvala JE, Best JM. PCR for detection of rubella virus RNA in clinical samples. J Clin Microbiol. 1995;33:1075–9.
10. Cortés LJ, Duque S, López MC, Moncada D, Molina D, Gómez-Marín JE, et al. [Gene polymorphisms in the dihydrofolate reductase (dhfr) and dihydropteroate synthase (dhps) genes and structural modelling of the dhps gene in Colombian isolates of Toxoplasma gondii [in Spanish]. Biomedica. 2014;34:556–66. http://dx.doi.org/10.7705/biomedica.v34i4.2132
11. Martines RB, Bhatnagar J, de Oliveira Ramos AM, Davi HP, Iglezias SD, Kanamura CT, et al. Pathology of congenital Zika syndrome in Brazil: a case series. Lancet. 2016;388:898–904. http://dx.doi.org/10.1016/S0140-6736(16)30883-2
12. Driggers RW, Ho CY, Korhonen EM, Kuivanen S, Jääskeläinen AJ, Smura T, et al. Zika virus infection with prolonged maternal viremia and fetal brain abnormalities. N Engl J Med. 2016;374:2142–51. http://dx.doi.org/10.1056/NEJMoa1601824
13. Bhatnagar J, Rabeneck DB, Martines RB, Reagan-Steiner S, Ermias Y, Estetter LB, et al. Zika virus RNA replication and persistence in brain and placental tissue. Emerg Infect Dis. 2017;23:405–14. http://dx.doi.org/10.3201/eid2303.161499
14. Jurado KA, Simoni MK, Tang Z, Uraki R, Hwang J, Householder S, et al. Zika virus productively infects primary human placenta-specific macrophages. JCI Insight. 2016; 1:pii:e88461. https://dx.doi.org/10.1172/jci.insight.88461
15. Meaney-Delman D, Oduyebo T, Polen KN, White JL, Bingham AM, Slavinski SA, et al. Prolonged detection of Zika virus RNA in pregnant women. Obstet Gynecol. 2016;128:724–30. http://dx.doi.org/10.1097/AOG.0000000000001625

Address for correspondence: Jorge Acosta-Reyes, Universidad del Norte, Km 5 Vía Puerto Colombia, Barranquilla, Colombia; email: acostajl@uninorte.edu.co

Domestic Pig Unlikely Reservoir for MERS-CoV

Emmie de Wit, Friederike Feldmann, Eva Horne, Cynthia Martellaro, Elaine Haddock, Trenton Bushmaker, Kyle Rosenke, Atsushi Okumura, Rebecca Rosenke, Greg Saturday, Dana Scott, Heinz Feldmann

We tested the suitability of the domestic pig as a model for Middle East respiratory syndrome coronavirus (MERS-CoV) infection. Inoculation did not cause disease, but a low level of virus replication, shedding, and seroconversion were observed. Pigs do not recapitulate human MERS-CoV and are unlikely to constitute a reservoir in nature.

As of March 10, 2017, a total of 1,917 cases of Middle East respiratory syndrome coronavirus (MERS-CoV) infection and 684 fatalities have occurred (*1*). Despite the relatively large number of cases, little is known about the disease pathology of MERS in humans (*2*). Our current understanding of the pathogenesis of MERS-CoV is therefore mostly based on data derived from studies in animal models. Although the first animal model used to study MERS-CoV pathogenesis and test potential countermeasures became available shortly after the discovery of MERS-CoV (*3*), all the animal models that have been developed so far have drawbacks (*4*). Because of the host restriction conferred by the binding of the MERS-CoV spike protein to its receptor, dipeptidyl peptidase 4 (DPP4), small animal models that are routinely used to conduct infectious disease research are not naturally susceptible to MERS-CoV infection. Although human DPP4-transgenic mouse models have been developed, these do not completely recapitulate the disease pathology observed in humans. Nonhuman primate models recapitulate mild and moderate human disease pathology; however, practical and ethical constraints limit work with these models.

The domestic pig (*Sus domesticus*) is used in infectious disease research because of similarities between human and pig anatomy, genetics, and physiology (*5*). MERS-CoV was previously shown to replicate in porcine kidney cells, albeit less efficiently than in human kidney cells (*6*). In an effort to develop a MERS-CoV animal model that recapitulates human disease better than small animal models without the constraints associated with nonhuman primate studies, we explored the possibility of using the domestic pig as an animal model of MERS-CoV infection.

Author affiliations: National Institutes of Health, Hamilton, Montana, USA (E. de Wit, F. Feldmann, E. Horne, C. Martellaro, E. Haddock, T. Bushmaker, K. Rosenke, R. Rosenke, G. Saturday, D. Scott, H. Feldmann); Columbia University, New York, New York, USA (A. Okumura)

DOI: http://dx.doi.org/10.3201/eid2306.170096

The Study

Comparison of the DPP4 nucleotide sequences of humans, dromedary camels, and domestic pigs showed that the porcine DPP4 is identical to the dromedary camel DPP4 at the 14 aa positions that have been shown to determine species tropism (Table) (*8*,*9*). We investigated whether DPP4 is expressed in the pig respiratory tract by performing immunohistochemical staining on the nasal mucosa and lung tissue obtained from healthy pigs using an antibody against DPP4 (mouse monoclonal anti-DPP4 [CD26], clone OTI11D7, 1:2,500; Origene Technologies, Inc., Rockville, MD, USA). DPP4 expression was not observed in the nasal mucosa of healthy domestic pigs (Figure 1, panel A); in the lungs, abundant DPP4 expression was observed in type I and type II pneumocytes and submucosal glands (Figure 1, panel B), suggesting MERS-CoV infection would be supported.

We inoculated 2 groups of four 4–5-week-old farm pigs (Yorkshire cross; S&S Farms, Ramona, CA, USA) intranasally (1 mL/nostril) and intratracheally (5 mL) with a total dose of 10^6 tissue culture infectious dose 50 ($TCID_{50}$) of the hCoV-EMC/2012 isolate of MERS-CoV. A group of 3 control pigs was mock inoculated with Dulbecco's modified Eagle medium (DMEM); these pigs were housed in a separate room from the MERS-CoV–inoculated pigs to prevent cross-contamination. Animal experiments were approved by the Institutional Animal Care and Use Committee of the Rocky Mountain Laboratories and conducted by certified staff in an Association for Assessment and Accreditation of Laboratory Animal Care International–accredited facility according to the institution's guidelines for animal use; staff followed the guidelines and basic principles in the US Public Health Service Policy on Humane Care and Use of Laboratory Animals and the Guide for the Care and Use of Laboratory Animals.

After inoculation with MERS-CoV, none of the pigs showed clinical signs of disease, such as increased body temperature or increased respiration, and bodyweight gain was similar between MERS-CoV–inoculated and mock-inoculated pigs (Figure 2, panel A). We collected nose and throat swabs during clinical exams and analyzed them for the presence of viral RNA by quantitative reverse transcription PCR (qRT-PCR) as described (*10*). Shedding of viral RNA from the nose and the throat increased from 1 day postinoculation (dpi) to 3 dpi in all MERS-CoV–inoculated animals, a sign that active replication occurred;

Table. Comparison of the amino acid residues shown to be essential in binding of Middle East respiratory syndrome coronavirus spike protein to DPP4 of human, dromedary camel, and domestic pig*

	DPP4, aa position													
Species	229	267	286	288	291	294	295	298	317	322	336	341	344	346
Human†	N	K	Q	T	A	L	I	H	R	Y	R	V	Q	I
Dromedary camel‡	–	–	–	V	–	–	–	–	–	–	–	–	–	–
Domestic pig§	–	–	–	V	–	–	–	–	–	–	–	–	–	–
Mouse¶	–	–	–	P	–	A	R	–	–	–	T	S	–	V

*DPP4, dipeptidyl peptidase 4; –, no change from human DPP4.
†GenBank accession no. AB451339.
‡GenBank accession no. KF574263.
§GenBank accession no. NM214257.
¶Taken from previous publication (*7*).

shedding was higher in the nose than in the throat (Figure 2, panel B). After 3 dpi, shedding of viral RNA decreased; all nose swabs were negative by 11 dpi and all throat swabs by 7 dpi.

We attempted virus propagation by inoculating VeroE6 cells with the media used to resuspend nasal and throat swab particulates and checking for the development of MERS-CoV cytopathic effect. Infectious MERS-CoV was not recovered at any time postinoculation from any swab sample.

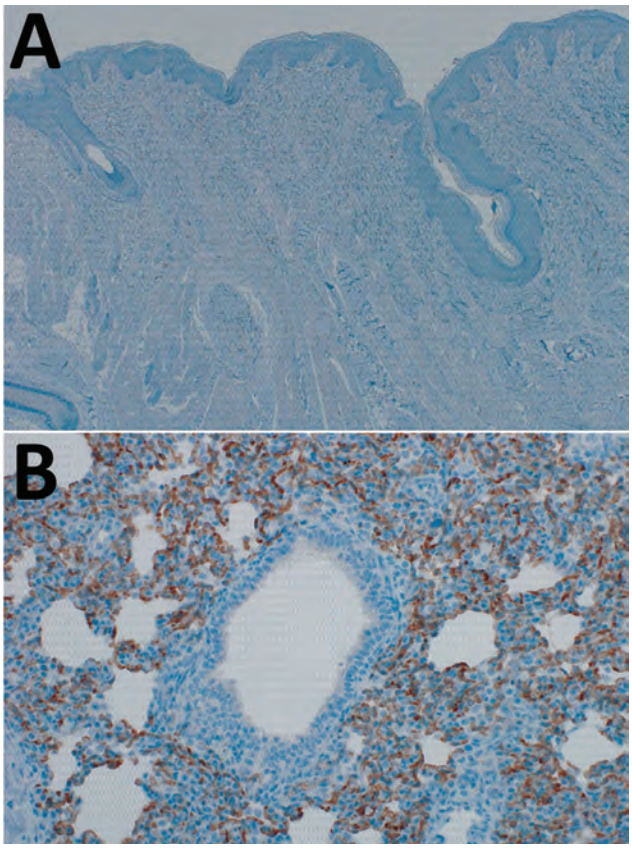

Figure 1. Dipeptidyl peptidase (DPP) 4 expression in the domestic pig respiratory tract. Tissues were stained by using a cross-reactive mouse monoclonal antibody against DPP4 (CD26, clone OTI11D7, 1:2,500; Origene Technologies, Inc., Rockville, MD, USA). DPP4 expression was absent in the nasal mucosa (A) but present in lung tissue (B) of healthy domestic pigs. Original magnification: nasal mucosa ×40; lung ×200.

On 4 and 11 dpi, we euthanized 4 MERS-CoV–inoculated pigs and collected their tissues for virologic and histologic analysis. Viral RNA could be detected by qRT-PCR in ≥1 respiratory tract tissue samples of all 4 MERS-CoV–inoculated pigs. However, viral loads were low; infectious MERS-CoV could not be isolated from any tissues positive by qRT-PCR, and the distribution of viral RNA among tissues was inconsistent from pig to pig (Figure 2 panel C). By 11 dpi, viral RNA could only be detected in the bronchial lymph node of 1 MERS-CoV–inoculated pig (Figure 2 panel C); all the tissues examined from other MERS-CoV–inoculated pigs were negative by this time. Viral RNA could not be detected in any of the extrarespiratory tissues tested, such as heart, liver, spleen, kidney, adrenal gland, duodenum, ileum, transverse colon, or urinary bladder, on 4 dpi or 11 dpi (data not shown). Histologic analysis did not reveal any lesions consistent with MERS-CoV infection in any of the collected tissues, including those of the respiratory tract. We performed immunohistochemical staining with an antibody specific for MERS-CoV on tonsil, trachea, bronchial lymph node, and right and left lower lung lobe of all pigs, as well as other tissues that tested positive for viral RNA by qRT-PCR. MERS-CoV antigen could not be detected in any of these tissues.

Serum samples collected on the day of euthanasia were tested for the presence of antibodies against MERS-CoV spike protein 1 (S1) by ELISA. By 11 dpi, antibodies directed against MERS-CoV S1 could be detected in all 4 pigs (Figure 2, panel D).

Conclusions

Recently, Vergara-Alert et al. showed MERS-CoV shedding in pigs inoculated with 10^7 $TCID_{50}$ of MERS-CoV and suggested that pigs could play a role as a reservoir for the circulation of MERS-CoV (*12*). In our hands, pigs inoculated with a 10-fold lower infectious dose of MERS-CoV were also successfully infected, but the low amount of virus replication in and shedding from the respiratory tract implies that the pig is unlikely to play a profound role as an intermediate host for MERS-CoV in nature.

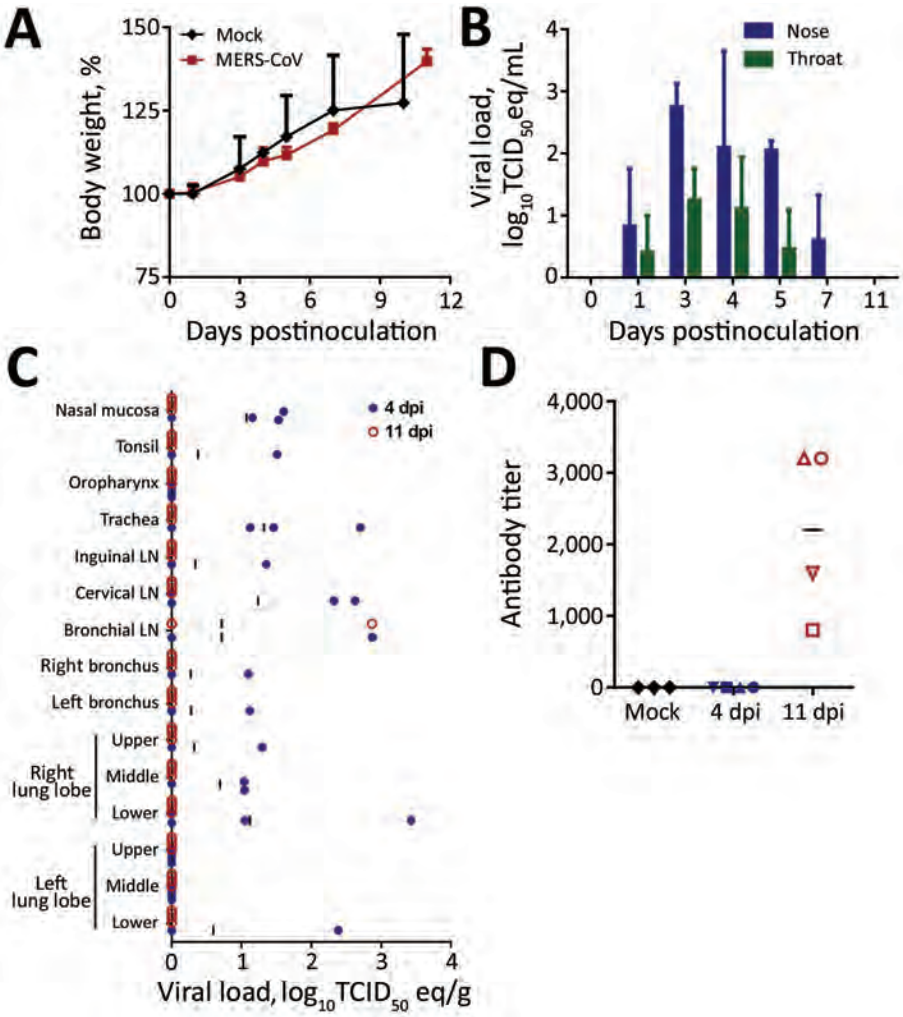

Figure 2. Propagation of Middle East respiratory syndrome coronavirus (MERS-CoV) in domestic pigs. We inoculated pigs intranasally and intratracheally with 10^6 tissue culture infectious dose 50 ($TCID_{50}$) of MERS-CoV isolate hCoV-EMC/2012 or, for controls (mock-inoculated), with Dulbecco's modified Eagle medium. A) Mean bodyweight gain comparison between mock-inoculated and MERS-CoV–inoculated animals over time. Error bars indicate SDs. B) Mean viral loads shed from the nose and throat determined at the time points indicated by quantifying virus on nasal and throat swabs collected from MERS-CoV–inoculated animals using quantitative reverse transcription PCR (*11*); in each run, standard dilutions of a titered virus stock were run in parallel to calculate $TCID_{50}$ equivalents. Error bars indicate SDs. C) Viral loads in tissues collected from MERS-CoV–inoculated animals on days 4 (closed blue circles) and 11 (open red circles) postinoculation. Viral loads were determined as in panel B. Vertical bars indicate means. D) Serum samples collected from pigs at the time of euthanasia (days 4 and 11 postinoculation) and tested for MERS-CoV antibodies by using an ELISA for MERS-CoV spike 1 protein. Antibody titers are plotted as the reciprocal of the last serum dilution positive by ELISA. Horizontal bars indicate means. LN, lymph node.

Taken together, our data indicate that MERS-CoV can infect pigs, leading to a low level of replication in the pig respiratory tract, but does not cause clinical signs of disease. Furthermore, viral shedding from mucosal membranes of the upper respiratory tract was rather limited with no infectious virus measurable at any time postinoculation. Thus, the pig is not a suitable animal disease model for MERS-CoV infection.

Acknowledgments

The authors thank the Rocky Mountain Veterinary Branch staff for the care and handling of the animals, Anita Mora for help with figure preparation, and Juergen Richt for helpful advice.

This work was supported by the Intramural Research Program of the National Institute of Allergy and Infectious Diseases of the National Institutes of Health.

Dr. de Wit is a staff scientist in the Disease Modeling and Transmission section of the Laboratory of Virology. Her research interests are in the pathogenesis and transmission of emerging viruses.

References

1. World Health Organization. Middle East respiratory syndrome coronavirus (MERS-CoV)–Saudi Arabia. Disease outbreak news. 2017 Mar 10 [cited 2017 Mar 15]. http://www.who.int/csr/don/10-march-2017-mers-saudi-arabia/en/
2. Ng DL, Al Hosani F, Keating MK, Gerber SI, Jones TL, Metcalfe MG, et al. Clinicopathologic, immunohistochemical, and ultrastructural findings of a fatal case of Middle East respiratory syndrome coronavirus infection in the United Arab Emirates, April 2014. Am J Pathol. 2016;186:652–8. http://dx.doi.org/10.1016/j.ajpath.2015.10.024
3. Munster VJ, de Wit E, Feldmann H. Pneumonia from human coronavirus in a macaque model. N Engl J Med. 2013;368:1560–2. http://dx.doi.org/10.1056/NEJMc1215691
4. Baseler L, de Wit E, Feldmann H. A comparative review of animal models of Middle East respiratory syndrome coronavirus infection. Vet Pathol. 2016;53:521–31. http://dx.doi.org/ 10.1177/0300985815620845
5. Meurens F, Summerfield A, Nauwynck H, Saif L, Gerdts V. The pig: a model for human infectious diseases. Trends Microbiol. 2012;20:50–7. http://dx.doi.org/10.1016/j.tim.2011.11.002
6. Müller MA, Raj VS, Muth D, Meyer B, Kallies S, Smits SL, et al. Human coronavirus EMC does not require the SARS-coronavirus receptor and maintains broad replicative capability in mammalian cell lines. MBio. 2012;3:e00515-12. http://dx.doi.org/10.1128/mBio.00515-12

7. van Doremalen N, Munster VJ. Animal models of Middle East respiratory syndrome coronavirus infection. Antiviral Res. 2015;122:28–38. http://dx.doi.org/10.1016/j.antiviral.2015.07.005
8. Lu G, Hu Y, Wang Q, Qi J, Gao F, Li Y, et al. Molecular basis of binding between novel human coronavirus MERS-CoV and its receptor CD26. Nature. 2013;500:227–31. http://dx.doi.org/10.1038/nature12328
9. Wang N, Shi X, Jiang L, Zhang S, Wang D, Tong P, et al. Structure of MERS-CoV spike receptor-binding domain complexed with human receptor DPP4. Cell Res. 2013;23:986–93. http://dx.doi.org/10.1038/cr.2013.92
10. Corman VM, Eckerle I, Bleicker T, Zaki A, Landt O, Eschbach-Bludau M, et al. Detection of a novel human coronavirus by real-time reverse-transcription polymerase chain reaction. Euro Surveill. 2012;17:20285.
11. de Wit E, Rasmussen AL, Falzarano D, Bushmaker T, Feldmann F, Brining DL, et al. Middle East respiratory syndrome coronavirus (MERS-CoV) causes transient lower respiratory tract infection in rhesus macaques. Proc Natl Acad Sci U S A. 2013;110:16598–603. http://dx.doi.org/10.1073/pnas.1310744110
12. Vergara-Alert J, van den Brand JM, Widagdo W, Muñoz M, Raj S, Schipper D, et al. Livestock susceptibility to infection with Middle East respiratory syndrome coronavirus. Emerg Infect Dis. 2017;23:232–40. http://dx.doi.org/10.3201/eid2302.161239

Address for correspondence: Heinz Feldmann, Laboratory of Virology, Division of Intramural Research, National Institute of Allergy and Infectious Diseases, National Institutes of Health, Rocky Mountain Laboratories, 903 S 4th St, Hamilton, MT 59840, USA; email: feldmannh@niaid.nih.gov

December 2011: **Zoonotic Infections**

- Risk for Rabies Importation from North Africa
- Continuing Threat of Influenza (H5N1) Virus Circulation in Egypt
- Worldwide Occurrence and Impact of Human Trichinellosis, 1986–2009
- Sealpox Virus in Marine Mammal Rehabilitation Facilities, North America, 2007–2009
- Transmission of Guanarito and Pirital Viruses among Wild Rodents, Venezuela
- Hepatitis E Virus in Rats, Los Angeles, California
- Enterovirus Co-infections and Onychomadesis after Hand, Foot, and Mouth Disease, Spain
- Experimental Infection of Horses with Hendra Virus/Australia/Horse/2008/Redlands
- West Nile Virus Infection of Birds, Mexico
- Lineage and Virulence of *Streptococcus suis* Serotype 2 Isolates from North America
- Isolation of Prion with BSE Properties from Farmed Goat
- Candidate Cell Substrates, Vaccine Production, and Transmissible Spongiform Encephalopathies
- Molecular Epidemiology of Rift Valley Fever Virus
- Novel Multiplexed HIV/Simian Immunodeficiency Virus Antibody Detection Assay
- Astroviruses in Rabbits
- Host Genetic Variants and Influenza-associated Mortality among Children and Young Adults
- Severe Human Bocavirus Infection, Germany
- Hepatitis E Virus Antibodies in Blood Donors, France
- Human Cardioviruses, Meningitis, and Sudden Infant Death Syndrome in Children

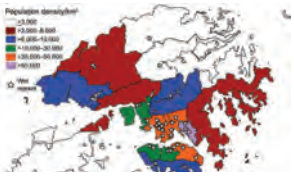

- Seroprevalence of Alkhurma and Other Hemorrhagic Fever Viruses, Saudi Arabia
- Knowledge of Avian Influenza (H5N1) among Poultry Workers, Hong Kong, China
- Risk for Human African Trypanosomiasis, Central Africa, 2000–2009

- Animal Diseases Caused by Orbiviruses, Algeria
- Genogroup I and II Picobirnaviruses in Respiratory Tracts of Pigs
- Human Liver Infection by *Amphimerus* spp. Flukes, Ecuador
- Q Fever in Woolsorters, Belgium
- *Aedes aegypti* Mosquitoes Imported into the Netherlands, 2010

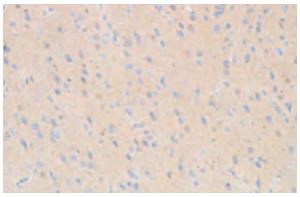

- Fatal Outbreak of *Mycoplasma capricolum* Pneumonia in Endangered Markhors
- African Swine Fever Virus Caucasus Isolate in European Wild Boars
- Novel Sylvatic Rabies Virus Variant in Endangered Golden Palm Civet, Sri Lanka
- Rickettsia parkeri in *Amblyomma maculatum* Ticks, North Carolina, 2009–2010
- Japanese Encephalitis Virus Genotype Replacement, Taiwan, 2009–2010
- Altitude-dependent *Bartonella quintana* Genotype C in Head Lice, Ethiopia
- Proximity to Goat Farms and *Coxiella burnetii* Seroprevalence among Pregnant Women
- Hemoptysis Associated with Leptospirosis Acquired in Hawaii

EMERGING INFECTIOUS DISEASES®

https://wwwnc.cdc.gov/eid/articles/issue/17/12/table-of-contents

High Rates of Neutralizing Antibodies to Toscana and Sandfly Fever Sicilian Viruses in Livestock, Kosovo

Nazli Ayhan, Kurtesh Sherifi,[1] Arber Taraku, Kristaq Bërxholi, Rémi N. Charrel[1]

Toscana and sandfly fever Sicilian viruses (TOSV and SFSV, respectively), both transmitted by sand flies, are prominent human pathogens in the Old World. Of 1,086 serum samples collected from cattle and sheep during 2013 in various regions of Kosovo (Balkan Peninsula), 4.7% and 53.4% had neutralizing antibodies against TOSV and SFSV, respectively.

Phleboviruses (family *Bunyaviridae*, genus *Phlebovirus*) are negative-sense tri-segmented RNA viruses for which mosquitoes, ticks, and sand flies are vectors. In the Old World, phleboviruses transmitted by sand flies (phlebotomines) are expanding in the Mediterranean basin, where an increasing number of new viruses have been identified (*1*). There, sand fly–borne phleboviruses are divided into 3 groups in accordance with their antigenic relationships. Two groups correspond to recognized species: *Sandfly fever Naples virus* (including sandfly fever Naples [SFNV], Massilia, Tehran, and Toscana [TOSV] viruses) and *Salehabad* virus (including Salehabad and Arbia viruses). The third group comprises 2 viruses classified as tentative species: *Sandfly fever Sicilian virus* (SFSV) and *Corfou virus* (*2*). Several are historic human pathogens, such as SFSV and SFNV, which cause sandfly fever syndrome, a self-limited but severely incapacitating febrile illness (*1*); TOSV can cause central and peripheral nervous system infections, such as meningitis and encephalitis (*3*).

Although first data on sandfly fever were acquired from the Balkan region, few studies were published specifically about the situation in Kosovo (*4*): in 1976, a total of 9.6% of human serum samples contained neutralizing antibodies against SFSV (*5*) (the exact region of Kosovo was not mentioned), and in 2011, <1% of human serum samples collected in the Pejë region contained TOSV neutralizing antibodies (*6*). Neutralizing antibody–based seroprevalence studies using animal serum proved interesting regarding the global circulation of corresponding viruses, as recently described in Portugal, Tunisia, and Greece (*7*–*9*). To improve understanding of the circulation of TOSV and SFSV in Kosovo, we tested serum samples collected in cattle and sheep through neutralizing assay and field-trapped sand flies for viral RNA.

Author affiliations: Aix-Marseille University, Marseille, France (N. Ayhan, R.N. Charrel); Fondation Mediterranee Infection Public Hospitals of Marseille, Marseille (N. Ayhan, R.N. Charrel); University of Hasan Prishtina, Prishtina, Kosovo (K. Sherifi); Agriculture University of Tirana, Triana, Albania (A. Taraku, K. Bërxholi)

DOI: http://dx.doi.org/10.3201/eid2306.161929

The Study

In 2013, serum from domestic animals was collected from 12 different regions of Kosovo. Samples were collected from 933 cattle and 153 sheep from 9 and 5 different regions, respectively, in Kosovo; the information (location, specimen, date) were recorded. Ten milliliters of blood was taken from jugular venipuncture, and serum was separated by centrifugation. All samples were stored at –20°C.

We tested cattle and sheep serum for neutralizing antibodies using the virus microneutralization assay, described for phleboviruses (*7*) in parallel with TOSV strain MRS2010-4319501 and SFSV strain Sabin. Serum samples were diluted from 1:10 to 1:80 into 96-well plates with a volume of 50 μL. Except for controls, we added a 1,000 50% tissue culture infective dose in a 50-μL volume. For controls, we added 50 μL of Eagle's minimum essential medium enriched with 5% fetal bovine serum, 1% penicillin–streptomycin, 1% L-glutamine 200 mmol/L, 1% kanamycin, and 3% fungizone. The plates were incubated at 37°C. After 1 h, a 100 μL suspension of 2×10^5 Vero cells/mL was added and incubated at 37°C in the presence of 5% CO_2. The microplates were read under an inverted microscope after 5 days for TOSV and 6 days for SFSV, and the presence (neutralization titer at 10, 20, 40, and 80) or absence (no neutralization) of cytopathic effect was noted. Cutoff value for positivity was set at titer $\geq$20 (*8*).

In 2014, a total of 267 sand flies were trapped and identified. We tested these sand flies for phleboviruses using previously described protocols (*9*).

Global rates of TOSV neutralizing antibodies were in the same magnitude in cattle (5.14%) and sheep (1.96%) in Kosovo (Table; Figure). Results observed in Pejë were congruent with recent findings obtained with human

[1]These authors contributed equally to this article.

Table. Neutralizing antibodies against SFSV and TOSV in serum from cattle and sheep, and sandflies trapped in Kosovo, 2013*

Serum source, region	SFSV		TOSV		No. sand flies	Sand fly species (%)
	Total ≥20	Positive ≥20, %	Total ≥20	Positive ≥20, %		
Cattle, n = 933	546	58.5	48	5.1		
Prizeren, n = 48	20	41.7	5	10.4	75	*Phlebotomus major* (70), *P. simici* (13), *P. tobbi* (8), *P. papatasi* (4), others (5)
Pejë, n = 50	12	24.0	0	0	0	
Rahovec, n = 198	101	51.0	15	7.6	2	*P. major* (100)
Malishevë, n = 165	129	78.2	13	7.9	0	
Glogovac, n = 50	35	70.0	0	0	0	
Klinë, n = 50	39	78.0	5	10.0	0	
Suharekë, n = 245	133	54.3	8	3.3	132	*P. major* (99), P. tobbi (1)
Gjakovë, n = 50	35	70.0	2	4.0	0	
Deçan, n = 77	42	54.6	0	0	0	
Sheep, n = 153	34	22.2	3	2.0		
Junik, n = 28	6	21.4	0	0	58	*P. major* (57), *P. tobbi* (38), others (5)
Hani i Elezit, n = 50	7	14.0	2	4.0	0	
Dragash, n = 30	17	56.7	1	3.3	0	
Pejë, n = 8	3	37.5	0	0	0	
Gjakovë, n = 37	1	2.7	0	0	0	
Total, N = 1,086	580	53.4	51	4.7	267	

*SFSV, sandfly fever Sicilian virus; TOSV, Toscana virus.

serum; in both cases, TOSV circulation appears limited (*6*). Although SFNV and TOSV belong to the same serocomplex, they can be distinguished by using neutralization; therefore, the high rate (27.9%) of SFNV neutralizing antibodies in humans reported in the 1970s (*5*) most likely reflects circulation of SFNV rather than TOSV, a finding that did not differ from our results and recent results reported by others (*6*). Rates of TOSV neutralizing

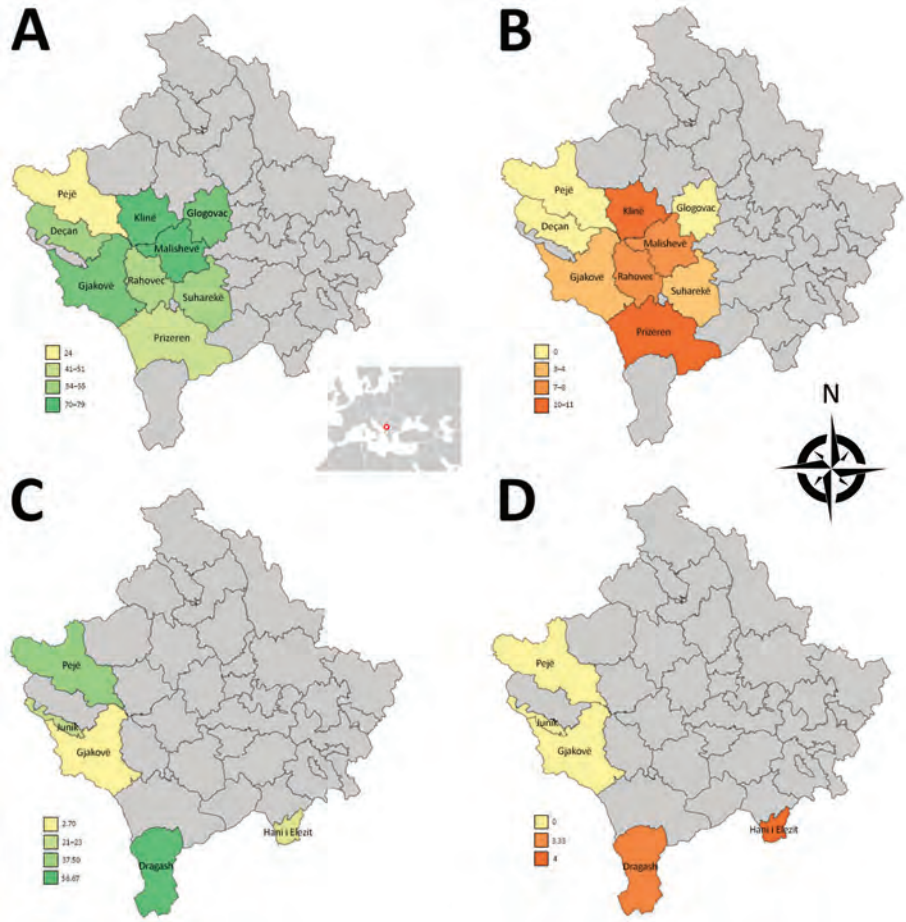

Figure. Geographic distribution of rates of neutralizing antibodies against SFSV and TOSV in cattle and sheep, Kosovo, 2013. A) SFSV neutralizing antibodies in cattle. B) TOSV neutralizing antibodies in cattle. C) SFSV neutralizing antibodies in sheep. D) TOSV neutralizing antibodies in sheep. Inset in panel A shows location of Kosovo in Europe. SFSV, sandfly fever Sicilian virus; TOSV, Toscana virus.

antibodies were highest in southwestern regions of Kosovo, whereas negative results were obtained in the Pejë area (Pejë, Deçan, Junik). Although we did not detect viral RNA in the 267 tested sand flies, TOSV was reported in Croatia and Greece (*10*,), and a new phlebovirus was described in Albania, Croatia, and Bosnia-Herzegovina (*9*; N. Ayhan et al., unpub. data).

Rates of SFSV neutralizing antibodies were much higher than those for TOSV. Results for cattle ranged from 24.0% to 78.2% (mean 58.5%); results for sheep were lower, ranging from 2.7% to 56.7% (mean 22.2%). For sheep, 4 of the 5 regions had rates of 14.0%–56.7%; the rate was much lower (2.7%) in Gjakovë.

Few data are available for comparison; 9.6% of tested human serum contained SFSV neutralizing antibodies in the 1970s (*5*). Although no direct evidence (molecular detection of viral RNA or virus isolation) exists of SFSV or another SFSV-like virus in Kosovo or neighboring countries, our results imply the presence of either SFSV or an SFSV-related virus in Kosovo. We consider it valid to use SFSV as a surrogate for all SFSV-related viruses (sandfly fever Turkey virus, sandfly fever Cyprus virus) because amino acid distances observed between the proteins that elicit neutralizing antibodies (Gn and Gc) are well within the acceptable range, (i.e., <5% different for SFSV and SFSV-related viruses) (*7*). Thus, neutralizing antibodies are unlikely to discriminate between closely related SFSV isolates.

Recent seroprevalence studies showed high seroprevalence rates for SFSV neutralizing antibodies in dogs in Portugal (50.8%) (*7*), Tunisia (38.1%–59.2% depending on the region) (*8*), and Greece (71.9%) and Cyprus (60.2%) (*11)*. Our results are congruent with data from continental Greece, with rates in the same order of magnitude (*12*). All these findings verify the high prevalence of SFSV in the Mediterranean basin. Because of the nature of this study, the serum was collected and stored under conditions that prevented attempts to detect viral RNA and isolate viral strains. SFSV remains an important human pathogen, as recently highlighted in Africa and Turkey (*12,13*).

Published data about the distribution of sand flies and species identification are old and scarce; *Phlebotomus papatasi*, *P. perfiliewi*, *P. neglectus*, and *P. tobbi* sand flies have been documented in Kosovo and neighboring countries with similar environmental and climatic conditions (*14,15*). In our study, *P. major* sand flies dominated (81%), followed by *P. tobbi* (11.2%), *P. simici* (3.7%), *P. papatasi* (1%), and other species (3.1%).

SFSV positivity varied among the regions for cattle and sheep. The regional prevalence differences might have resulted from geographic and climatic characteristics of the region that could affect the vector sand fly species distribution and population size.

Conclusions

Our results confirm that TOSV and SFSV, or an SFSV-like virus, are circulating in several regions of Kosovo, which indicates that humans are exposed to these viruses. This finding merits confirmation through seroprevalence studies and initiation of systematic testing for TOSV and SFSV real-time reverse transcription PCR for febrile illness and central nervous system infections during the warm season.

This work was supported in part by the European Virus Archive Goes Global project, which has received funding from the European Union's Horizon 2020 research and innovation program under grant agreement no. 653316; the EDENext FP7-no. 261504 European Union project and this paper is catalogued by the EDENext Steering Committee as EDENext469 (http://www.edenext.eu). The work of N.A. and R.N.C. was conducted under the frame of EurNegVec COST Action TD1303. N.A. is supported by the Fondation Mediterranee Infection.

Ms. Ayhan is a PhD student at Aix Marseille University. Her research interests include phleboviruses transmitted by sand flies in the Old World.

References

1. Alkan C, Bichaud L, de Lamballerie X, Alten B, Gould EA, Charrel RN. Sandfly-borne phleboviruses of Eurasia and Africa: epidemiology, genetic diversity, geographic range, control measures. Antiviral Res. 2013;100:54–74. http://dx.doi.org/10.1016/j.antiviral.2013.07.005
2. Plyusnin A, Beaty BJ, Elliott RM, Goldbach R, Kormelink R, Lundkvist A, et al. Bunyaviridae. In: King AMQ, Adams MJ, Carstens EB, Lefkowitz EJ, editors. Virus taxonomy: classification and nomenclature of viruses. Ninth report of the International Committee on Taxonomy of Viruses. San Diego (CA): Elsevier; 2011. p. 693–709.
3. Charrel RN, Gallian P, Navarro-Mari JM, Nicoletti L, Papa A, Sánchez-Seco MP, et al. Emergence of Toscana virus in Europe. Emerg Infect Dis. 2005;11:1657–63. http://dx.doi.org/10.3201/eid1111.050869
4. Pick A. Zur pathologie und therapie einer eigenthumlichen endemischen Krankheitsform. Wien Med Wochenschr. 1886; 33:1141–5.
5. Tesh RB, Saidi S, Gajdamovič SJA, Rodhain F, Vesenjak-Hirjan J. Serological studies on the epidemiology of sandfly fever in the Old World. Bull World Health Organ. 1976;54:663–74.
6. Venturi G, Marchi A, Fiorentini C, Ramadani N, Quaglio G, Kalaveshi A, et al. Prevalence of antibodies to phleboviruses and flaviviruses in Peja, Kosovo. Clin Microbiol Infect. 2011;17:1180–2. http://dx.doi.org/10.1111/j.1469-0691.2010.03445.x
7. Alwassouf S, Maia C, Ayhan N, Coimbra M, Cristovao JM, Richet H, et al. Neutralization-based seroprevalence of Toscana virus and sandfly fever Sicilian virus in dogs and cats from Portugal. J Gen Virol. 2016;97:2816–23. http://dx.doi.org/10.1099/jgv.0.000592
8. Sakhria S, Alwassouf S, Fares W, Bichaud L, Dachraoui K, Alkan C, et al. Presence of sandfly-borne phleboviruses of two antigenic complexes (sandfly fever Naples virus and sandfly fever Sicilian virus) in two different bio-geographical regions of Tunisia demonstrated by a microneutralisation-based seroprevalence study in dogs. Parasit Vectors. 2014;7:476. http://dx.doi.org/10.1186/s13071-014-0476-8

9. Ayhan N, Velo E, de Lamballerie X, Kota M, Kadriaj P, Ozbel Y, et al. Detection of *Leishmania infantum* and a novel phlebovirus (Balkan virus) from sand flies in Albania. Vector Borne Zoonotic Dis. 2016;16:802–6. http://dx.doi.org/10.1089/vbz.2016.2002
10. Papa A, Paraforou T, Papakonstantinou I, Pagdatoglou K, Kontana A, Koukoubani T. Severe encephalitis caused by Toscana virus, Greece. Emerg Infect Dis. 2014;20:1417–9. http://dx.doi.org/10.3201/eid2008.140248
11. Alwassouf S, Christodoulou V, Bichaud L, Ntais P, Mazeris A, Antoniou M, et al. Seroprevalence of sandfly-borne phleboviruses belonging to three serocomplexes (sandfly fever Naples, sandfly fever Sicilian and Salehabad) in dogs from Greece and Cyprus using neutralization test. PLoS Negl Trop Dis. 2016;10:e0005063. http://dx.doi.org/10.1371/journal.pntd.0005063
12. Ergunay K, Ayhan N, Charrel RN. Novel and emergent sandfly-borne phleboviruses in Asia Minor: a systematic review. Rev Med Virol. 2017; 27:e1898. http://dx.doi.org/10.1002/rmv.1898
13. Woyessa AB, Omballa V, Wang D, Lambert A, Waiboci L, Ayele W, et al. An outbreak of acute febrile illness caused by sandfly fever Sicilian virus in the Afar region of Ethiopia, 2011. Am J Trop Med Hyg. 2014;91:1250–3. http://dx.doi.org/10.4269/ajtmh.14-0299
14. Simitch T, Zivkovitch V. Phlebotome fauna in Yugoslavia and their role in the epidemiology of pappataci fever, kala-azar and cutaneous leishmaniasis [in French]. Arch Inst Pasteur Alger. 1956;34:380–7.
15. Živković V. Faunistic and ecological investigation of sandflies (Diptera, Phlebotomidae) in Serbia. Acta Vet (Beogr). 1980; 30:67–88.

Address for correspondence: Rémi N. Charrel, Aix Marseille University, UMR_D 190 Emergence des Pathologies Virales, Faculty of Medicine, 27 blvd Jean Moulin, Marseille 13385, France; email: remi.charrel@univ-amu.fr

May 2016: **Vectorborne Diseases**

- An Operational Framework for Insecticide Resistance Management Planning
- *Plasmodium falciparum* K76T pfcrt Gene Mutations and Parasite Population Structure, Haiti, 2006–2009
- Outbreak of Middle East Respiratory Syndrome at Tertiary Care Hospital, Jeddah, Saudi Arabia, 2014
- Differences in Genotype, Clinical Features, and Inflammatory Potential of *Borrelia burgdorferi* sensu stricto Strains from Europe and and the United States
- Acute Human Inkoo and Chatanga Virus Infections, Finland
- Expansion of Shiga Toxin–Producing *Escherichia coli* by Use of Bovine Antibiotic Growth Promoters
- Projecting Month of Birth for At-Risk Infants after Zika Virus Disease Outbreaks
- Genetic Characterization of Archived Bunyaviruses and Their Potential for Emergence in Australia
- *Rickettsia parkeri* Rickettsiosis, Arizona, USA

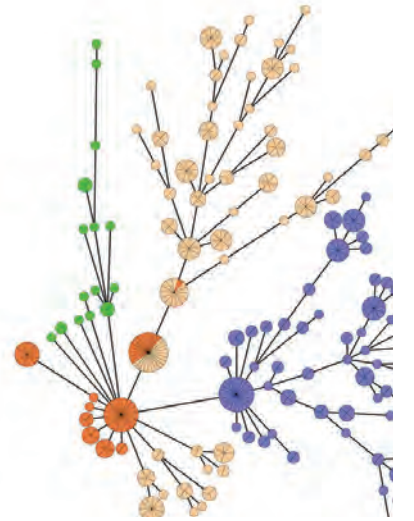

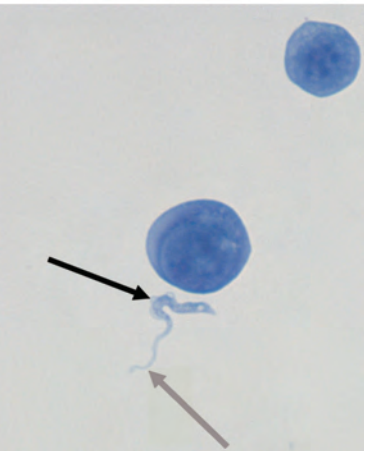

- *Plasmodium falciparum* In Vitro Resistance to Monodesethylamodiaquine, Dakar, Senegal, 2014
- Astrovirus MLB2, a New Gastroenteric Virus Associated with Meningitis and Disseminated Infection
- Spectrum of Viral Pathogens in Blood of Malaria-Free Ill Travelers Returning to Canada
- Expanded Geographic Distribution and Clinical Characteristics of *Ehrlichia ewingii* Infections, United States

EMERGING INFECTIOUS DISEASES

https://wwwnc.cdc.gov/eid/articles/issue/22/5/table-of-contents

Congenital Malformations of Calves Infected with Shamonda Virus, Southern Japan

Yoshimasa Hirashima, Shoei Kitahara, Tomoko Kato, Hiroaki Shirafuji, Shogo Tanaka, Tohru Yanase

In 2015 and 2016, we observed 15 malformed calves that were exposed to intrauterine infection with Shamonda virus, a Simbu serogroup orthobunyavirus, in Japan. Characteristic manifestations were arthrogryposis and gross lesions in the central nervous system. Our results indicate that this arbovirus should be considered a teratogenic virus in ruminants.

The Simbu virus serogroup is composed of ≥25 serologically related viruses in the family *Bunyaviridae*, genus *Orthobunyavirus* (*1*), which are transmitted mainly by *Culicoides* biting midges. Several of these viruses, such as Akabane virus, Aino virus, and Schmallenberg virus, are arboviruses associated with abortion, premature birth, stillbirth, and congenital malformations in ruminants (*2–4*).

The emergence and spread of Schmallenberg virus has had large socioeconomic effects in countries in Europe (*4,5*). Frequent epizootics of Akabane virus and Aino virus in Japan have caused many cases of congenital malformations in calves (*6*). However, the etiologic diagnosis for malformed calves associated with other arboviruses has not been established because of a lack of knowledge and sensitive diagnostic systems. Attempts to isolate viruses from sentinel cattle and *Culicoides* biting midges have contributed to knowledge about arboviruses circulating in nature and have, in some instances, helped predict the etiologic agents responsible for malformations (*7*).

Three Simbu serogroup viruses, Peaton virus, Sathuperi virus, and Shamonda virus (SHAV), were identified in Japan during the past 2 decades and have been suspected of being involved in congenital defects in calves (*8*). During December 2015–April 2016 in southern Japan, SHAV infections were identified in 15 malformed calves that had no antibodies against other teratogenic viruses. Of the 3 segments of the RNA genome of SHAV, the small and large segments have high genetic similarity with those of Schmallenberg virus, which implies the teratogenicity of SHAV in the ruminant fetus (*8*). Because there is no detailed description of an association between SHAV and malformations, we report details of these 15 clinical cases of malformations in calves suspected to be caused by SHAV infection.

Author affiliations: Kagoshima Central Livestock Hygiene Service Center, Hioki, Japan (Y. Hirashima, S. Kitahara); National Agriculture and Food Research Organization, Kagoshima, Japan (T. Kato, H. Shirafuji, S. Tanaka, T. Yanase)

DOI: http://dx.doi.org/10.3201/eid2306.161946

The Study

To obtain data on arboviruses circulating in 2015, we attempted to isolate viruses on BHK-21 and HmLu-1 cells inoculated with blood samples obtained from 60 sentinel cattle maintained on 30 farms and from pools of *Culicoides* biting midges collected by using suction light traps on 2 cattle farms in Kagoshima Prefecture in southern Japan. Two viruses (KS-1/P/15 and KS-2/P/15) were isolated from cattle blood collected during August and September 2015, and another virus (KSB-1/C/15) was isolated from a pool of *C. tainanus* midges sampled during September 2015.

We performed reverse transcription PCR (RT-PCR) with primer pairs (AKAI206F; 5′-CACAACCAAgTgTCgATCTTA-3′; and SimbuS637–656; 5′-gAgAATCCAgATTTAgCCCA-3′) specific for small RNA segment of Simbu serogroup viruses and the One Step RT-PCR Kit (QIAGEN, Hilden, Germany). We generated a product of the expected size from RNA samples of the isolated viruses. Preliminary sequence analysis for the RT-PCR product (443-nt) showed that the viruses were highly similar to SHAV. We sequenced and analyzed complete small and medium RNA segments and a partial region of the large RNA segment by using primers specific for SHAV (*8*). Sequences determined in this study were deposited in the International Nucleotide Sequence Database under accession nos. LC198185–93.

Neighbor-joining analysis available in MEGA7 (*9*) was used for phylogenetic analysis on the basis of the 3 RNA segments of the Simbu serogroup viruses. Sequences determined showed high nucleotide identities with known sequences of SHAV (98.3%–99.5% for the RNA small segment, 89.0%–97.9% for the medium RNA segment, and 91.5%–98.0% for the large RNA segment). Three phylogenetic trees showed that isolated viruses densely clustered with Japanese SHAV isolates obtained in 2002 and 2007 (Figure 1).

We performed virus neutralization tests (VNTs) on virus-infected HmLu-1 cells by using an established method (*2*). Antibodies to SHAV (titer range 1:2–1:64) were detected in serum samples from 15 malformed calves by VNTs during December 2015–April 2016 (Table). Serum

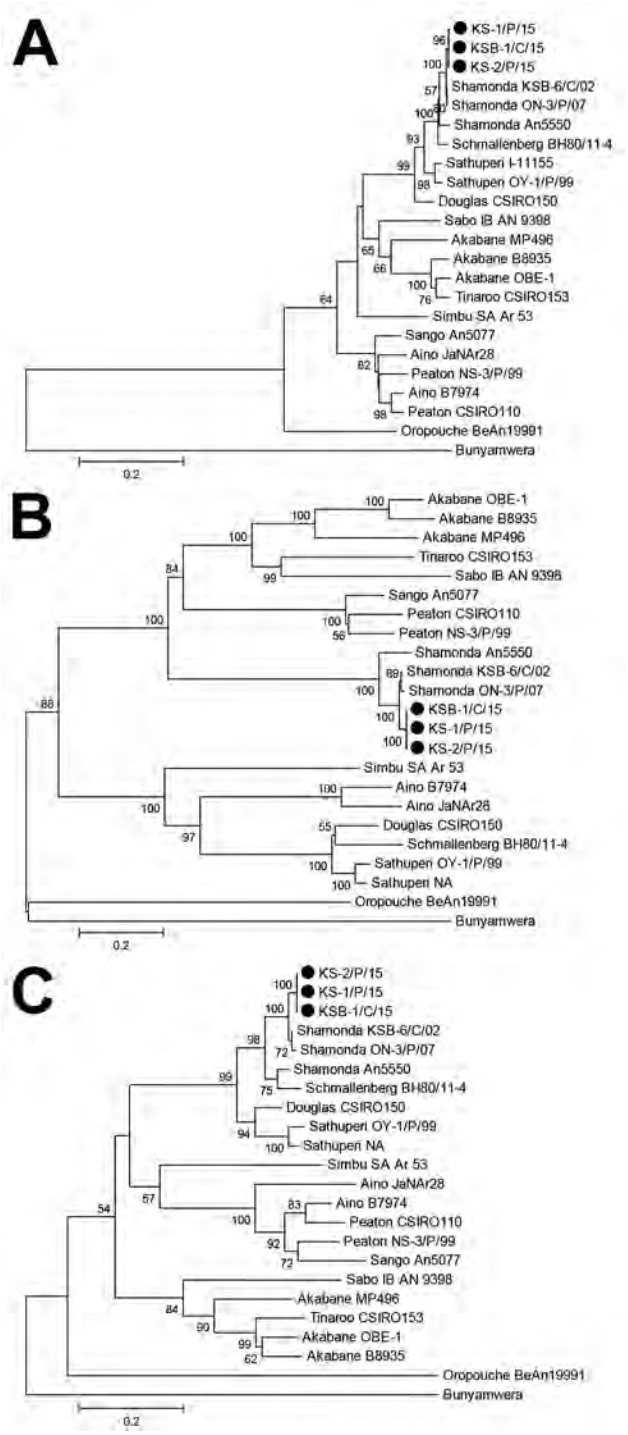

Figure 1. Neighbor-joining phylogenetic trees based on protein-coding sequences of A) small, B) medium, and C) large partial RNA segments for Simbu serogroup viruses, southern Japan, 2015–2016. Black circles indicate Shamonda viruses isolated in this study. Values along branches are percentages (≥50%) of bootstrap support of 1,000 pseudoreplicates. The 3 segmented RNAs of Bunyamwera virus were used as outgroups to root the trees. Scale bars indicate nucleotide substitutions per site. NA, details not available.

samples obtained from sentinel cattle in June, August, September, October, and November 2015 showed that seroconversion for SHAV had occurred widely in Kagoshima Prefecture during August–October.

Although 2 calves ingested colostrum substitute containing immunoglobulins, all calves tested were deprived of colostrum produced by their mothers. SHAV had not been detected in mainland Japan for ≈10 years until we identified new cases of infection in 2015. It is highly improbable that the colostrum substitute contained antibodies against SHAV. Malformed calves were delivered at or beyond term (gestation periods range 275–299 days), but 6 calves were born dead.

The small RNA–specific RT-PCR showed positive results for samples from the central nervous system (cerebrum, brainstem, or spinal cord) of 7 deformed calves. Sequences obtained were identical (except for 1 of 2 nt substitutions) with relevant sequence of SHAVs isolated in 2015.

Torticollis (10/15) or arthrogryposis (12/15) were often observed among affected calves (Figure 2). Head deformity (6/15) or spinal curvature (11/15) were also characteristic. Discoloration of skeletal muscles was observed in one third of the calves. Cerebral hemispheres appeared normal among the calves, but lateral ventricular enlargement was found in 2 calves, and cerebellar hypoplasia was found in 1 calf.

Histopathologic analysis identified calcification of nerve cells (11/15), perivascular infiltration of mononuclear cells (6/15), and gliosis (5/15), which were often observed in the cerebrum and brainstem (Figure 2). Severe degenerative changes in the ventral horn of the spinal cord were identified in 10 of the malformed calves. Fatty replacement (12/15), atrophy (9/15), and myositis (9/15) were major observations in the skeletal muscle and often correlated with muscle discolorations.

VNTs did not detect neutralizing antibodies against teratogenic arboviruses, such as Chuzan virus, Akabane virus, Aino virus, or Peaton virus in serum samples from affected calves. All tested dams of affected newborns were positive for SHAV antibodies in VNTs (titer range 1:16–≥1:256).

Conclusions

Our findings support an association between SHAV and congenital deformities in calves infected in utero. Manifestations and macroscopic and microscopic observations in the malformed calves were similar to those of calves infected with Schmallenberg virus (*10,11*). In comparison with cases attributed to Akabane virus and Aino virus, congenital lesions in the brain were relatively mild (i.e., no hydranencephaly and few lateral ventricular enlargements appeared in malformed calves). However, nonsuppurative encephalitis or nerve cell death often occurred in cerebrums and brainstems that otherwise seemed normal.

Twelve of the dams of the malformed calves in this report were vaccinated with a trivalent inactivated vaccine

Table. Characteristics of 15 malformed calves infected with Shamonda virus, southern Japan, December 2015–April 2016*

Characteristic	Calf no. 1	2	3	4	5	6	7	8	9	10	11	12	13	14	15	Total
Gestational age, d	281	275	280	278	285	291	281	280	293	279	290	287	287	276	299	NA
Euthanasia	+	+	+	–	+	+	+	+	+	–	–	–	+	–	–	9
Stillbirth	–	–	–	+	–	–	–	–	–	+	+	+	–	+	+	6
RT-PCR result	+	–	–	+	+	+	–	–	–	+	–	+	–	–	+	7
Antibody titer	1:8	1:32	1:32	1:64	1:2	1:32	1:32	1:16	1:8	1:16	1:4	1:16	1:16	1:4	1:64	NA
Clinical finding																
Torticollis	+	–	+	+	+	–	+	+	–	+	–	+	–	+	+	10
Arthrogryposis	–	–	–	+	+	+	+	+	+	+	+	+	+	+	+	12
Macroscopic finding																
Head deformity																
Brachygnathism	+	+	+	–	–	–	–	–	–	–	–	–	+	–	–	4
Asymmetry of skull	+	–	+	–	–	–	–	–	–	–	+	+	–	–	–	4
LVE	–	–	–	–	–	–	–	–	–	+	–	+	–	–	–	2
Cerebellar hypoplasia	–	–	–	–	–	–	+	–	–	–	–	–	–	–	–	1
Spinal curvature	+	–	+	+	+	–	+	+	–	+	+	+	–	+	+	11
Muscle discoloration	–	–	–	–	+	+	–	–	+	+	+	–	–	–	–	5
Histopathologic finding																
Cerebrum																
Calcification of nerve cells	–	+	+	–	+	–	+	–	–	–	–	+	–	–	–	5
Brainstem																
Calcification of nerve cells	–	–	+	+	–	+	–	+	–	+	–	+	–	+	+	8
Perivascular infiltration	–	+	–	–	–	+	+	+	+	+	–	–	–	–	–	6
Gliosis	–	–	+	+	–	+	–	–	–	+	–	–	–	+	–	5
Spinal cord																
Decrease/disappearance of ventral horn cells	–	–	–	+	–	+	+	–	+	+	+	+	+	+	+	10
Skeletal muscles																
Fatty replacement	+	–	+	–	+	+	+	–	+	+	+	+	+	+	+	12
Atrophy	+	–	+	–	+	+	+	–	+	–	+	–	–	+	+	9
Myositis	+	–	+	–	+	+	+	–	+	–	+	–	–	+	+	9

*LVE, lateral ventricular enlargement; NA, not applicable; RT-PCR, reverse transcription PCR; +, positive; –, negative.

containing Akabane, Aino, and Chuzan viruses. To our knowledge, no effective preventive measure for infection with SHAV is available. Previous surveillance in Africa, the Middle East, and Asia (*12–14*) enabled us to postulate the wide geographic distribution of SHAV. The potential risk for SHAV spreading in livestock should be considered, even in previously unaffected areas, because long-distance dispersal and accidental transportation of infected vectors from epizootic areas can introduce the virus. Also, recent outbreaks of infection with Schmallenberg virus and SHAV suggest that many Simbu serogroup viruses can affect livestock. More detailed study of this virus serogroup is warranted.

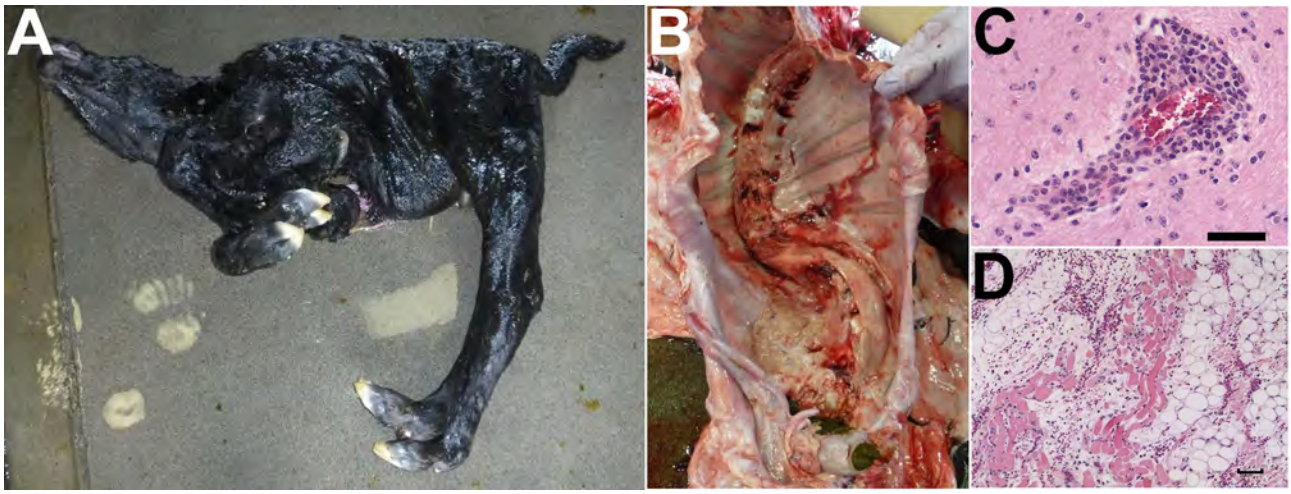

Figure 2. Characteristic observations in Shamonda virus–positive malformed calves, southern Japan, 2015–2016. A) Torticollis and arthrogryposis in calf 3. B) Spinal curvature (scoliosis) in calf 7. C) Perivascular infiltration in the midbrain of calf 7. D) Fatty replacement and atrophy in skeletal muscle of calf 3. For histopathologic analysis, thin sections prepared from paraffin-embedded tissues were stained with hematoxylin and eosin. Scale bars indicate 50 μm.

Acknowledgments

We thank veterinary officers at Kagoshima Prefectural livestock hygiene service centers and technical staff at Kyushu Research Station, National Institute of Animal Health, for excellent technical support and sampling.

Mr. Hirashima is a veterinary officer at the Kagoshima Central Livestock Hygiene Service Center, Hioki, Japan. His research interests include ruminant arboviruses associated with abnormal births and febrile diseases in southern Japan.

References

1. Elliott RM, Blakqori G. Molecular biology of orthobunyaviruses. In: Plyusnin A, Elliott RM, editors. *Bunyaviridae*: molecular and cellular biology. Norfolk (UK): Caister Academic Press; 2011. p. 1–39.
2. Tsuda T, Yoshida K, Ohashi S, Yanase T, Sueyoshi M, Kamimura S, et al. Arthrogryposis, hydranencephaly and cerebellar hypoplasia syndrome in neonatal calves resulting from intrauterine infection with Aino virus. Vet Res. 2004;35:531–8. http://dx.doi.org/10.1051/vetres:2004029
3. Kirkland PD. Akabane virus infection. Rev Sci Tech. 2015;34:403–10. http://dx.doi.org/10.20506/rst.34.2.2366
4. Afonso A, Abrahantes JC, Conraths F, Veldhuis A, Elbers A, Roberts H, et al. The Schmallenberg virus epidemic in Europe—2011–2013. Prev Vet Med. 2014;116:391–403. http://dx.doi.org/10.1016/j.prevetmed.2014.02.012
5. Hoffmann B, Scheuch M, Höper D, Jungblut R, Holsteg M, Schirrmeier H, et al. Novel orthobunyavirus in cattle, Europe, 2011. Emerg Infect Dis. 2012;18:469–72. http://dx.doi.org/10.3201/eid1803.111905
6. Forman S, Hungerford N, Yamakawa M, Yanase T, Tsai HJ, Joo YS, et al. Climate change impacts and risks for animal health in Asia. Rev Sci Tech. 2008;27:581–97. http://dx.doi.org/10.20506/rst.27.2.1814
7. Kato T, Shirafuji H, Tanaka S, Sato M, Yamakawa M, Tsuda T, et al. Bovine arboviruses in *Culicoides* biting midges and sentinel cattle in southern Japan from 2003 to 2013. Transbound Emerg Dis. 2016;63:e160–72. http://dx.doi.org/10.1111/tbed.12324
8. Yanase T, Kato T, Aizawa M, Shuto Y, Shirafuji H, Yamakawa M, et al. Genetic reassortment between Sathuperi and Shamonda viruses of the genus *Orthobunyavirus* in nature: implications for their genetic relationship to Schmallenberg virus. Arch Virol. 2012;157:1611–6. http://dx.doi.org/10.1007/s00705-012-1341-8
9. Kumar S, Stecher G, Tamura K. MEGA7: Molecular Evolutionary Genetics Analysis version 7.0 for bigger datasets. Mol Biol Evol. 2016;33:1870–4. http://dx.doi.org/10.1093/molbev/msw054
10. Bayrou C, Garigliany MM, Sarlet M, Sartelet A, Cassart D, Desmecht D. Natural intrauterine infection with Schmallenberg virus in malformed newborn calves. Emerg Infect Dis. 2014;20:1327–30. http://dx.doi.org/10.3201/eid2008.121890
11. Peperkamp NH, Luttikholt SJ, Dijkman R, Vos JH, Junker K, Greijdanus S, et al. Ovine and bovine congenital abnormalities associated with intrauterine infection with Schmallenberg virus. Vet Pathol. 2015;52:1057–66. http://dx.doi.org/10.1177/0300985814560231
12. Yanase T, Maeda K, Kato T, Nyuta S, Kamata H, Yamakawa M, et al. The resurgence of Shamonda virus, an African Simbu group virus of the genus *Orthobunyavirus*, in Japan. Arch Virol. 2005;150:361–9. http://dx.doi.org/10.1007/s00705-004-0419-3
13. Causey OR, Kemp GE, Causey CE, Lee VH. Isolations of Simbu-group viruses in Ibadan, Nigeria 1964-69, including the new types Sango, Shamonda, Sabo and Shuni. Ann Trop Med Parasitol. 1972;66:357–62. http://dx.doi.org/10.1080/00034983.1972.11686835
14. Brenner J. Preliminary report of serosurvey for circulation of viruses of the Simbu serogroup in dairy cattle in Israel, 2014. ProMed. 2016 Apr 17 [cited 2016 Dec 1]. http://www.promedmail.org, archive no. 20160417.4165684.

Address for correspondence: Tohru Yanase, Kyushu Research Station, National Institute of Animal Health, National Agriculture and Food Research Organization, 2702 Chuzan, Kagoshima 891-0105, Japan; email: tyanase@affrc.go.jp

EID Adds Advanced Search Features for Articles

Emerging Infectious Diseases now has an advanced search feature that makes it easier to find articles by using keywords, names of authors, and specified date ranges. You can sort and refine search results by manuscript number, volume or issue number, or article type. A quick start guide and expandable help section show you how to optimize your searches.

https://wwwnc.cdc.gov/eid/AdvancedSearch

EID's new mapping feature allows you to search for articles from specific countries by using a map or table to locate countries. You can refine search results by article type, volume and issue, and date, and bookmark your search results.

https://wwwnc.cdc.gov/eid/ArticleMap

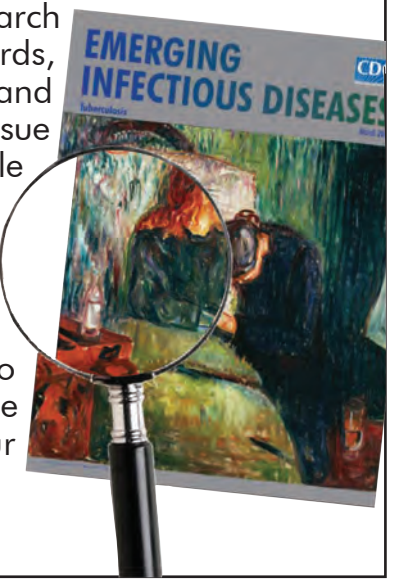

Brucella neotomae Infection in Humans, Costa Rica

Marcela Suárez-Esquivel, Nazareth Ruiz-Villalobos, César Jiménez-Rojas, Elías Barquero-Calvo, Carlos Chacón-Díaz, Eunice Víquez-Ruiz, Norman Rojas-Campos, Kate S. Baker,[1] Gerardo Oviedo-Sánchez, Ernesto Amuy, Esteban Chaves-Olarte, Nicholas R. Thomson, Edgardo Moreno, Caterina Guzmán-Verri

Several species of *Brucella* are known to be zoonotic, but *B. neotomae* infection has been thought to be limited to wood rats. In 2008 and 2011, however, *B. neotomae* was isolated from cerebrospinal fluid of 2 men with neurobrucellosis. The nonzoonotic status of *B. neotomae* should be reassessed.

Members of the genus *Brucella* are the infectious agents of brucellosis, a neglected disease responsible for economic losses resulting from abortion and low performance in production animals (*1*). The 4 species mainly responsible for this widespread bacterial zoonosis are *B. melitensis*, *B. abortus*, *B. suis*, and to a lesser extent *B. canis*. Underdiagnosis and limited awareness of the disease among healthcare practitioners is common in many countries (*1*).

B. neotomae, isolated in 1957 from wood rats (*Neotoma lepida*) in North America (*2*), has been considered nonzoonotic (*3*). It has been isolated from target organs of experimentally infected mice and guinea pigs (*4*,*5*). We report the isolation of *B. neotomae* from cerebrospinal fluid samples from 2 human patients with neurobrucellosis.

The Study

In 2008, a *Brucella* sp. isolate was submitted to the Tropical Diseases Research Center at the Universidad de Costa Rica. This isolate (denoted strain bneohCR2) was cultured from a cerebrospinal fluid sample obtained from a 64-year-old male patient at one of the main hospitals in San José, Costa Rica. In 2011, another isolate (denoted strain bneohCR1) was recovered from a cerebrospinal fluid sample from a 51-year-old male patient at a regional hospital in Costa Rica. As is common for other patients with brucellosis, the blood leukocyte count for each patient was almost within the reference range, and C-reactive protein level was within reference range. Both patients showed clinical signs compatible with neurobrucellosis (*6*), had positive Rose Bengal test results, and recovered after receiving 1 month of streptomycin (750 mg/d) and 3 months of doxycycline (100 mg/12 h).

Further bacteriologic analysis (*7*,*8*) confirmed that the isolates were a *Brucella* sp. (Table). Real-time PCR high-resolution melting analysis (*9*) confirmed genus designation but was inconclusive regarding species designation. Bruce-ladder multiplex PCR (*10*) and multiple loci variable number of tandem repeats–16-loci panel analysis (http://mlva.u-psud.fr/brucella/; Figure 1) indicated that the profiles for both DNA isolates corresponded to profiles for *B. neotomae*. Analysis of bneohCR2 by multiplex single-nucleotide polymorphism (SNP) primer extension assay (*11*) and by matrix-assisted laser desorption/ionization time-of-flight mass spectrometry of protein extracts (*12*) (online Technical Appendix Table 1, https://wwwnc.cdc.gov/EID/article/23/6/16-2018-Techapp1.pdf) confirmed that the isolate was *B. neotomae*.

We performed whole-genome sequencing of bneohCR1 and bneohCR2 and resequencing of reference strain *B. neotomae* 5K33. Sequencing data were deposited at the European Nucleotide Archive (http://www.ebi.ac.uk/ena/) under accession codes ERS1563929 (bneohCR1), ERS1563928 (bneohCR2), and ERS1624467 (SK33). To place the bneohCR1 and bneohCR2 in a phylogenetic context, publicly available reads from 51 *Brucella* whole-genome sequences (online Technical Appendix Table 2) were aligned and then mapped to *B. suis* 1330 by using SMALT version 0.5.8 (ftp://ftp.sanger.ac.uk/pub/resources/software/smalt/). Reads from bneohCR1 and bneohCR2 genomes mapped to 98.6% of the *B. suis* 1330 genome. SNPs were called from the alignment by use of Samtools (http://samtools.sourceforge.net/), and 34,307 variable sites across all isolates were extracted by using SNP sites (*13*). The resulting alignment of SNPs

Author affiliations: Universidad Nacional, Heredia, Costa Rica (M. Suárez-Esquivel, N. Ruiz-Villalobos, C. Jiménez-Rojas, E. Barquero-Calvo, E. Víquez-Ruiz, E. Moreno, C. Guzmán-Verri); Universidad de Costa Rica, San José, Costa Rica (E. Barquero-Calvo, C. Chacón-Díaz, N. Rojas-Campos, G. Oviedo-Sánchez, E. Chaves-Olarte, E. Moreno, C. Guzmán-Verri); Wellcome Trust Sanger Institute, Hinxton, UK (K.S. Baker, N.R. Thomson); Caja Costarricense del Seguro Social, Puntarenas, Costa Rica (E. Amuy)

DOI: http://dx.doi.org/10.3201/eid2306.162018

[1]Current affiliation: University of Liverpool, Liverpool, UK.

Table. Differential biochemical profile of *Brucella* isolates from 2 men with neurobrucellosis, Costa Rica, 2008 and 2011

Analysis	bneohCR1	bneohCR2
Biochemical tests		
Oxidase	-	–
Citrate utilization	–	–
Nitrate reduction	+	+
CO_2 required	–	–
H_2S production	+	+
Urease activity, h	0–0.5+	0–0.5+
Growth in presence of dyes		
Thionin 20 μg/mL	–	–
Basic fuchsin 20 μg/mL	–	–
A	+	+
M	–	–

was used for maximum-likelihood phylogenetic reconstruction by use of RAxML version 7.0.4 (https://github.com/stamatak/standard-RAxML). The generated phylogenetic tree confirmed that the bneohCR isolates clustered together with *B. neotomae* reference strain 5K33 (ENA accession no. JMSC01, assembly accession no. GCA_00742255.1) (Figure 2). Isolates bneohCR1 and bneohCR2 differed from the reference genome by 174 and 160 SNPs, respectively. This number of SNPs is smaller than that between *B. abortus* 9–941 and *B. abortus* 2308 (214 SNPs), which are 2 well-recognized strains of the same *Brucella* species.

Analysis of 23 previously reported genomic islands or anomalous genomic loci (*14*) was performed for both bneohCR genomes. For this analysis, a "genomic-island pseudomolecule" was constructed by concatenation of 23 genomic regions obtained from different *Brucella* genomes. BLAST (https://github.com/sanger-pathogens/Farm_blast) comparison of this pseudo-molecule and the bneohCR draft genomes, generated by assembly with Velvet (*15*), showed that the genomic loci known as 26.5 kb, 12 kb, and GI-6 that are absent in *B. neotomae* (*14*) are also absent in the queried genomes.

Conclusions

This report of *B. neotomae* as a cause of zoonotic disease raises questions about possible underrepresentation of reported cases. This study also has implications for brucellosis diagnosis. Specifically, the differences among *B. neotomae* and the other *Brucella* species at the biochemical level are subtle. The major difference between *B. neotomae* and *B. abortus*, the main cause of human brucellosis in Costa Rica, is the presence of oxidase activity in *B. abortus*, which is assessed subjectively (*7*,*8*). Because *B. neotomae* has not, until now, been considered zoonotic, some cases of brucellosis reported as being caused by atypical zoonotic classical *Brucella* might have been misdiagnosed cases of *B. neotomae* infection. The introduction of whole-genome sequencing into the clinical field will thus improve diagnosis.

A lack of epidemiologic information with regard to the 2 patients reported here precluded the investigation of exposure or contact with hosts known to harbor *B. neotomae*. Further studies are needed to establish which animals may act as reservoirs for *B. neotomae* in Costa Rica.

In summary, *B. neotomae* should be considered a zoonosis risk for infection in humans. Incorporation of molecular techniques for diagnosis will help resolve the

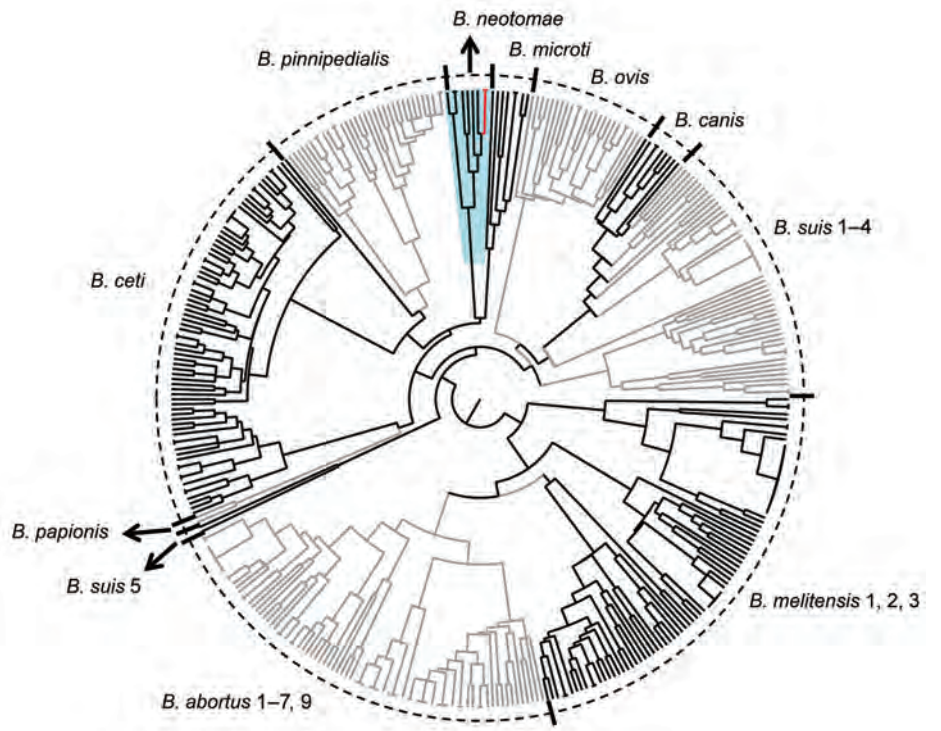

Figure 1. Dendrogram based on multiple locus variable number of tandem repeats–16-loci panel analysis of *Brucella* spp. (http://mlva.u-psud.fr/brucella/) and clinical isolates from human cerebrospinal fluid samples from 2 patients with brucellosis. The isolates bneohCR1 and bneohCR2 (red branches) showed a pattern consistent with previously reported profiles for *Brucella neotomae* (blue shading). Black, gray, and tic marks are used to differentiate between adjacent species. Arrows separate small neighboring clusters and indicate the *B. neotomae* cluster.

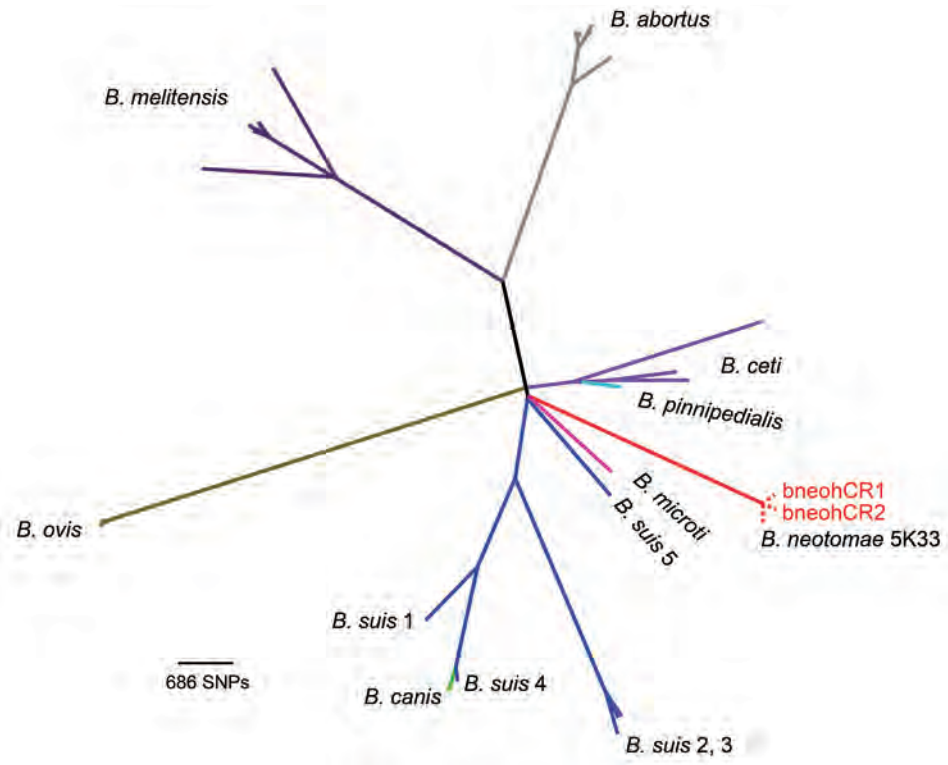

Figure 2. Phylogenetic tree based on 34,307 single-nucleotide polymorphisms (SNPs) found among 51 *Brucella* genome sequences. The clinical isolates bneohCR1 and bneohCR2 cluster with *B. neotomae* 5K33 and differ by 164 SNPs. A different color is used to represent each *Brucella* species. Dotted red lines denote the 3 *B. neotomae* isolates, which overlap at the tip of the branch because of the high identity among them.

Brucella genus homogeneity obtained when only biochemical assays are used.

Acknowledgments

We are grateful to Heilyn Estrada-Murillo for isolate information, Daphnne Garita for technical assistance, Gabriela Hernandez-Mora for provision of serotype-specific antiserum, and Gordon Dougan for helpful discussions.

This work was funded by Fondos del Sistema del Consejo Nacional de Rectores, Costa Rica, and Wellcome Trust. N.R.-V. and C.J.-R. were partially sponsored by University of Costa Rica scholarships. K.S.B. is funded by Wellcome Trust Fellowship 106690/A/14/Z. K.S.B. and N.R.T. were funded by Wellcome Trust grant no. 098051.

All procedures involving live *Brucella* were carried out according to the "Reglamento de Bioseguridad de la CCSS39975-0," year 2012, after "Decreto Ejecutivo no. 0965-S," year 2002 and protocol approved by SIA0434-14 Universidad Nacional, Costa Rica. These genetic resources were accessed in Costa Rica according to the Biodiversity Law no. 7788 and the Convention on Biological Diversity, under the terms of respect to equal and fair distribution of benefits among those who provided such resources.

Miss Suárez-Esquivel is a PhD student at Programa de Doctorado en Ciencias as Universidad de Costa Rica, working at Programa de Investigación en Enfermedades Tropicales at Universidad Nacional. Her primary research interest is the evolution of Brucella species and their host specificity.

References

1. World Health Organization. The control of neglected zoonotic diseases. In: NZD4 Organising Committee, editor. WHO conference report. Geneva: WHO Press; 2014. p. 23–35.
2. Stoenner HG, Lackman DB. A new species of *Brucella* isolated from the desert wood rat, *Neotoma lepida* Thomas. Am J Vet Res. 1957;18:947–51.
3. Moreno E. Retrospective and prospective perspectives on zoonotic brucellosis. Front Microbiol. 2014;5:213. http://dx.doi.org/10.3389/fmicb.2014.00213
4. Stoenner HG. The behavior of *Brucella neotomae* and *Brucella suis* in reciprocal superinfection experiments in mice and guinea pigs. Am J Vet Res. 1963;24:376–80.
5. Gibby IW, Gibby AM. Host–parasite relationships with *Brucella neotomae*. J Bacteriol. 1965;89:9–16.
6. Ceran N, Turkoglu R, Erdem I, Inan A, Engin D, Tireli H, et al. Neurobrucellosis: clinical, diagnostic, therapeutic features and outcome. Unusual clinical presentations in an endemic region. Braz J Infect Dis. 2011;15:52–9. http://dx.doi.org/10.1016/S1413-8670(11)70140-4
7. Alton GG, Jones LM, Angus RD, Verger JM. Techniques for the brucellosis laboratory. Paris: Institut National de la Recherche Agronomique; 1988. p. 39–41.
8. Weyant R, Popovic T, Bragg S. Basic laboratory protocols for the presumptive identification of *Brucella* species. Atlanta: Centers for Disease Control and Prevention; 2001. p. 1–16.
9. Winchell JM, Wolff BJ, Tiller R, Bowen MD, Hoffmaster AR. Rapid identification and discrimination of *Brucella* isolates by use of real-time PCR and high-resolution melt analysis. J Clin Microbiol. 2010;48:697–702. http://dx.doi.org/10.1128/JCM.02021-09
10. García-Yoldi D, Marín CM, de Miguel M-J, Muñoz PM, Vizmanos JL, López-Goñi I. Multiplex PCR assay for the identification and differentiation of all *Brucella* species and the vaccine strains *Brucella abortus* S19 and RB51 and *Brucella*

melitensis Rev1. Clin Chem. 2006;52:779–81. http://dx.doi.org/10.1373/clinchem.2005.062596
11. Scott JC, Koylass MS, Stubberfield MR, Whatmore AM. Multiplex assay based on single-nucleotide polymorphisms for rapid identification of *Brucella* isolates at the species level. Appl Environ Microbiol. 2007;73:7331–7. http://dx.doi.org/10.1128/AEM.00976-07
12. Isidoro-Ayza M, Ruiz-Villalobos N, Pérez L, Guzmán-Verri C, Muñoz PM, Alegre F, et al. *Brucella ceti* infection in dolphins from the western Mediterranean Sea. BMC Vet Res. 2014;10:206. http://dx.doi.org/10.1186/s12917-014-0206-7
13. Page AJ, Taylor B, Delaney AJ, Soares J, Seemann T, Keane JA, et al. SNP-sites: rapid efficient extraction of SNPs from multi-FASTA alignments. Microb Genomics. 2016 Apr 29. http://dx.doi.org/10.1099/mgen.0.000056
14. Mancilla M. The *Brucella* genomic islands. In: López-Goñi I, O'Callaghan D, editors. *Brucella*: Molecular Microbiology and Genomics. Poole (UK): Caister Academic Press; 2012. p. 36–57.
15. Page AJ, De Silva N, Hunt M, Quail MA, Parkhill J, Harris SR, et al. Robust high-throughput prokaryote de novo assembly and improvement pipeline for Illumina data. Microb Genomics. Microbiology Society; 2016 Aug 25. http://dx.doi.org/10.1099/mgen.0.000083

Address for correspondence: Caterina Guzmán-Verri, Programa de Investigación en Enfermedades Tropicales, Escuela de Medicina Veterinaria, Campus Benjamín Núñez, Universidad Nacional, Heredia Aptdo 304, 3000 Costa Rica; email catguz@una.cr

EID journal

Follow the EID journal on Twitter and get the most current information from *Emerging Infectious Diseases*.

Isolated Case of Marburg Virus Disease, Kampala, Uganda, 2014

Luke Nyakarahuka, Joseph Ojwang, Alex Tumusiime, Stephen Balinandi, Shannon Whitmer, Simon Kyazze, Sam Kasozi, Milton Wetaka, Issa Makumbi, Melissa Dahlke, Jeff Borchert, Julius Lutwama, Ute Ströher, Pierre E. Rollin, Stuart T. Nichol, Trevor R. Shoemaker

In September 2014, a single fatal case of Marburg virus was identified in a healthcare worker in Kampala, Uganda. The source of infection was not identified, and no secondary cases were identified. We describe the rapid identification, laboratory diagnosis, and case investigation of the third Marburg virus outbreak in Uganda.

Marburg virus disease (MVD) is caused by Marburg virus (MARV; family *Filoviridae*, which also includes Ebola viruses). The disease was first discovered in 1967 in Marburg and Frankfurt, Germany, after laboratory workers were infected from monkeys imported from Uganda (*1*). Thereafter, sporadic cases and outbreaks of MVD have been documented in South Africa, Kenya, the Democratic Republic of the Congo, Angola, Uganda, the Netherlands, and the United States (*2*). MVD remains of great public health importance because of the case-fatality rate, which can be as high as 90%, and documented human-to-human transmission, with associated socioeconomic consequences.

Uganda has experienced previous outbreaks of MVD, resulting in fatalities and socioeconomic effects from loss of tourism. The first recorded outbreak in Uganda occurred in the Kamwenge district in 2007, where 4 MVD cases were confirmed in miners at the Kitaka mine (*3*). A second, larger outbreak occurred in the western Uganda districts of Kabale, Ibanda, and Kamwenge in 2012 (*4*) and was also linked to mining activity in the Ibanda district. In addition, tourists from the United States and the Netherlands were infected with MARV in western Uganda when they visited Python Cave in Queen Elizabeth National Park in 2008 (*5*,*6*). Both Python Cave and the Kitaka mine are inhabited by Egyptian fruit bats (*Rousettus aegyptiacus*), the host reservoir of MARV (*7*).

In 2014, a fatal case of MVD occurred in Uganda. We report here on the field and laboratory investigation of this case, including possible sources of infection.

Author affiliations: Uganda Virus Research Institute, Entebbe, Uganda (L. Nyakarahuka, J. Lutwama); US Centers for Disease Control and Prevention, Entebbe (J. Ojwang, A. Tumusiime, S. Balinandi, J. Borchert, T.R. Shoemaker); Centers for Disease Control and Prevention, Atlanta, Georgia, USA (S. Whitmer, U. Ströher, P.E. Rollin, S.T. Nichol); Public Health Emergency Operations Center, Kampala, Uganda (S. Kyazze, S. Kasozi, M. Wetaka, I. Makumbi, M. Dahlke)

DOI: https://dx.doi.org/10.3201/eid2306.170047

The Study

On September 23, 2014, a healthcare worker was admitted to Mengo Hospital in Kampala, Uganda, with a febrile illness suspected to be viral hemorrhagic fever (VHF) infection. The patient, a 30-year-old man, was a radiographer who worked at Mengo Hospital and part-time at Mpigi Health Center IV in the Mpigi district, ≈30 km south of Kampala (Figure 1). His symptoms began on September 17, 2014. A rapid diagnostic test result was positive for malaria, and the patient was given intravenous ceftriaxone, 5% dextrose, and artesunate. However, his condition continued to deteriorate.

On September 26, he began to display hemorrhagic signs, notably profuse bleeding from body orifices. Clinical findings included fever (temperature 38.4°C), nausea, vomiting, diarrhea, musculoskeletal pain, abdominal pain, headache, sore throat, difficulty swallowing, difficulty breathing, anorexia, bleeding from the nose, bloody stools, vomiting blood, and upper gastrointestinal tract bleeding. He died on September 28.

Whole blood and serum samples collected on September 28 were sent to the Uganda Virus Research Institute (UVRI)/US Centers for Disease Control and Prevention (CDC) VHF laboratory in Entebbe for testing on September 30. We performed diagnostic testing by real-time reverse transcription PCR (RT-PCR), antigen detection, and MARV IgM ELISA on the suspected sample as described (*8*). We detected MARV by RT-PCR, but antigen detection and IgM serologic results were negative.

We obtained independent confirmation from duplicate whole blood and serum samples by using RT-PCR primers and probes targeting MARV VP40 gene and a commercial filovirus PCR screening assay (Altona Diagnostics, Hamburg, Germany) (*9*) (Table). On the basis of the positive RT-PCR results, we confirmed MVD in this patient. We shipped specimens to the CDC Viral Special Pathogens Branch, Division of High-Consequence Pathogens and Pathology, National Center for Emerging and Zoonotic Infectious Diseases (Atlanta, GA, USA), for further testing, including virus isolation and sequencing. A virus isolate

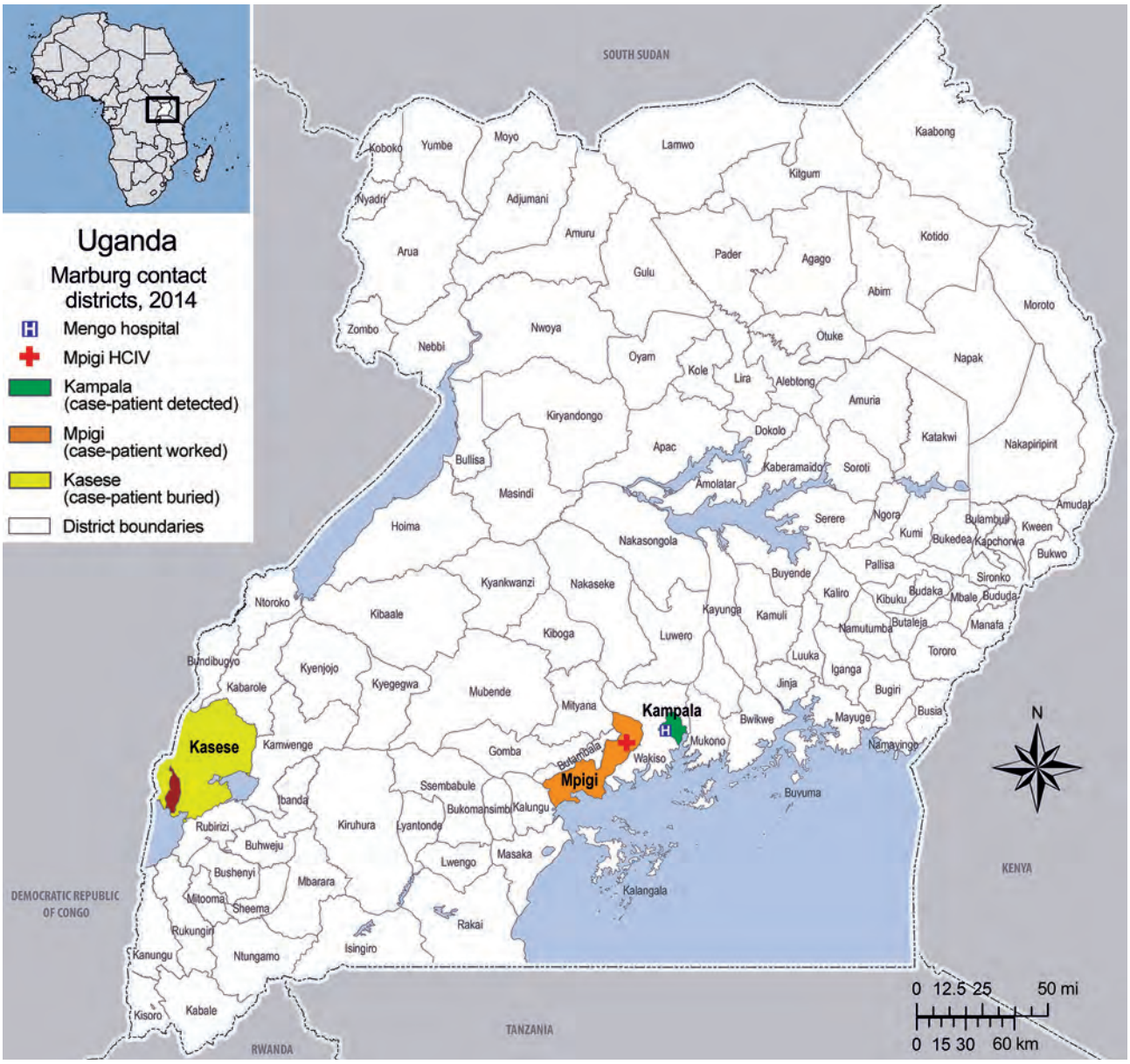

Figure 1. Locations where patient with confirmed Marburg virus disease lived, worked, and was buried, Kampala, Uganda, 2014. Inset map shows location of Uganda in Africa.

(812601) was generated from the clinical specimen after a single passage in cell culture (Vero E6).

After laboratory confirmation, a multidisciplinary team from UVRI and CDC-Uganda performed the initial outbreak investigations at Mengo Hospital and Mpigi Health Center IV. The investigation team provided the outbreak case definition, and details of case contacts were obtained from both health facilities. An investigation was also performed in Kasese District, where the health worker was taken for burial. In addition, an ecologic investigation was conducted to identify roosting sites nearby for the potential presence of *R. aegyptiacus* bats.

We created an outbreak database using the Epi Info Viral Hemorrhagic Fever outbreak management application (*10*). All case and contact data were managed by the Uganda Ministry of Health Public Health Emergency Operations Center. We identified 197 close contacts, who were followed for 21 days. During the course of follow-up, 33 (16.2%) of the 197 contacts converted to suspected case-patients by exhibiting clinically compatible signs or symptoms matching the outbreak case definition. Blood samples from suspected case-patients were tested at the UVRI/CDC laboratory in Entebbe; all were negative for MARV by RT-PCR and serologic analysis.

Table. Primers used to generate Marburg virus-specific cDNA fragments for whole-genome sequencing of isolates from Uganda

Genome fragment	Primer set	Primer sequence, 5'→3'	Region amplified	Region size, kbp
1	63F MARB-4997R	TGA CAT TGA GAC TTG TCA GTC GCT TGA TTT CCT TCA CGC	64-4998	4.9
2	3005F 6426R	AAG TCA GCG AGG GGT TGA TGA CTG GAA AAG TGC TAT GTT CCC TTC AGT GAA GAC	2970-6438	3.5
3	6101F 9405R	AGA AAA CAG AAG ACG TCC ATC TGA TG ACT TAA TGC TGC ACG AAG TGA TG	6065-9405	3.3
4	7567F 10571R	TGG CCC TGG AAT IGA AGG ACT C AGC ATA TGA ACA ATA GAT C	7548-10571	3.0
5	36F 57R	GTA CCT CTA AGG AAA ATC ATG AAG GTT GAT ATA ATT GCA CGT GTA GAT	9979-15442	5.4
6	12006F 15516R	TTG CCA GAA GGA TAA AAG GAC AAA GAG ATT TTG GAA GAT TAT ATT ACT ATC	11953-15486	3.5
7	15519F 19155R	TGG ACG ATA GGA AAT CGA GCA C TGG ACA CAC TAA AAA GAT G	15108-19111	4.0

Conclusions

We describe the second single-case filovirus outbreak detected in Uganda; a case of infection with *Sudan ebolavirus* was reported in Luwero District in 2011 (*11*). The investigation was unable to identify a conclusive source of infection, including evidence of the natural reservoir host near where the infected patient was working or residing or potential cases in persons who visited health centers before this case was confirmed. No secondary cases arose from contact with the initial case-patient.

The patient tested positive for malaria but later tested positive for MARV by RT-PCR and serologic analysis. These findings indicate that co-infection of viral hemorrhagic fever (VHF) and other tropical infectious diseases can confound diagnosis and delay early detection, potentially resulting in large outbreaks that are much harder to control, as was seen during the 2014–2015 Ebola virus outbreak in West Africa (*12*). This finding emphasizes the need for continued surveillance and awareness even when other, more common pathogens are initially suspected.

The finding of no secondary cases in this investigation can be attributed, in part, to use of infection control practices and personal protective equipment when first encountering a suspected VHF case. Because Uganda has experienced 10 VHF outbreaks since 2011, increased awareness and use of personal protective equipment and infection control practices have greatly limited secondary transmission, especially in the healthcare setting. Routine use of gloves, protective gowns, and chlorine is now more common in lower-level healthcare facilities in Uganda; these

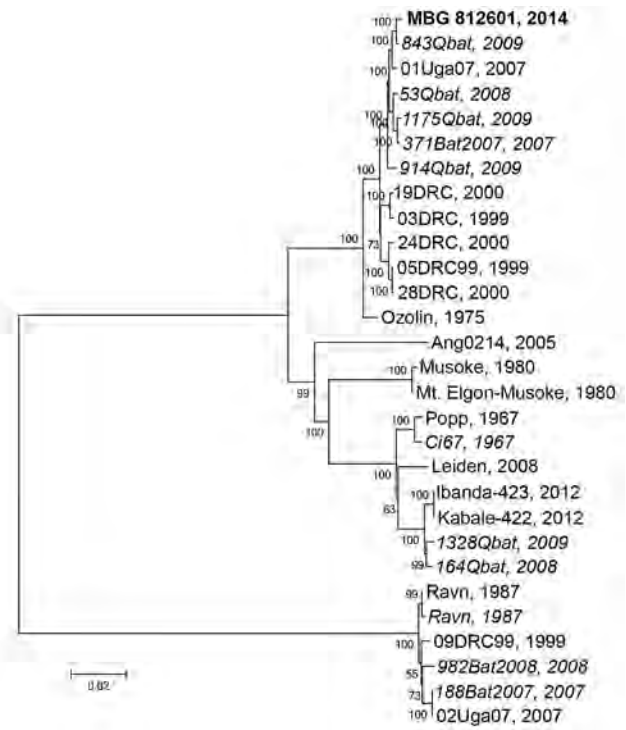

Figure 2. Phylogenetic tree comparing complete or nearly complete Marburg virus (MARV) genomes sequenced from bat and human sources in Uganda. A consensus whole-genome sequence was assembled by mapping reads to the reference MARV sequence NC_001608 using CLC Genomics Workbench (Waltham, MA, USA). A phylogenetic tree was constructed using MEGA6.06 (http://www.megasoftware.net). Viral sequences acquired from human sources are in standard type, and viral sequences acquired from bats are italicized; the sequence from the human case-patient described in this study, MBG 812601 2014, is in bold. Evolutionary history was inferred using the maximum-likelihood method based on the Tamura-Nei model with MEGA6.06. The tree is drawn to scale, with branch lengths measured in the number of substitutions per site. Values at nodes represent bootstrap values following 1,000 replicates. Scale bar represents substitutions per site. GenBank accession numbers used in this tree are KP985768, JX458855.1, FJ750957.1, JX458852.1, JX458854.1, FJ750958.1, JX458856.1, JX458828.1, JX458826.1, JX458834.1, DQ447651.1, JX458846.1, AY358025.2, DQ447657.1, Z12132.1, NC_001608.3, Z29337.1, EF446132.1, JN408064.1, KC545388.1, KC545387.1, DQ447649.1, EF446131.1, DQ447652.1, FJ750956.1, FJ750955.1, and FJ750953.1.

protective products were used at both Mengo Hospital and Mpigi Health Center IV.

The full genomic sequence of this MARV isolate (812601; Genbank accession no. KP985768) falls into a cluster that consists mostly of MARV sequences isolated from bats. The closest related sequence was obtained from MARV isolated from a juvenile male *R. aegyptiacus* bat (Q843) captured in August 2009 in Python Cave, Queen Elizabeth National Park (Figure 2). Other viral sequences from bat specimens in this clade were from bats collected from either Python Cave or the Kitaka mine during 2007–2009. The most closely related human sequence (01Uga07) was from a miner who worked in the Kitaka mine in July 2007 (*3*,*7*). Because of the wide genetic diversity of MARVs, there is no definitive way to identify where this patient may have become infected.

We do not know why the patient did not transmit MARV to any of his close contacts. We can assume that none of the contacts had substantial exposure to the patient while he was infectious. The relatively small size of this and previous filovirus outbreaks in Uganda can be attributed to enhanced VHF surveillance, rapid case identification, laboratory testing, and investments from the global health security agenda in rapid sample transportation to the national VHF reference laboratory for diagnostic testing (*13*). VHF surveillance continues to be a top priority for Uganda, and the VHF surveillance program continues to play a crucial role in detecting, responding to, and helping to control these outbreaks.

Acknowledgments

We thank the staff at Mengo Hospital, Kampala, and Mpigi Health Center IV; the initial investigation team, which included members from UVRI and CDC-Uganda for field and laboratory investigation of the outbreak; the Ministry of Health National Task Force on Epidemic Preparedness and Response; World Health Organization; Kampala City Council Authority; Kasese and Mpigi local governments; CDC Uganda, CDC, and UVRI Motorpool for transportation; and Médecins Sans Frontières for establishing an isolation ward at Mulago Hospital. We especially thank UVRI for its support of the VHF surveillance program and diagnostics laboratory. We also thank the United States Agency for International Development, African Field Epidemiology Network, and the United Nations Children's Fund, which all participated and contributed to the Marburg outbreak response and provided support to the Uganda Ministry of Health.

Dr. Nyakarahuka is a zoonotic disease epidemiologist at the Uganda Virus Research Institute in Entebbe, Uganda, with a background in veterinary medicine and public health. His work specifically focuses on the surveillance, detection and investigation of viral hemorrhagic fevers, including Ebola and Marburg viruses, and he specializes in characterizing the natural ecology of hemorrhagic fever viruses.

References

1. Siegert R, Shu HL, Slenczka W. Isolation and identification of the "Marburg virus" [in German]. Dtsch Med Wochenschr. 1968;93:604–12. http://dx.doi.org/10.1055/s-0028-1105103
2. Centers for Disease Control and Prevention. Chronology of Marburg hemorrhagic fever outbreaks; known cases and outbreaks of Marburg hemorrhagic fever, in chronological order [cited 2014 Oct 29]. http://www.cdc.gov/vhf/marburg/resources/outbreak-table.html
3. Adjemian J, Farnon EC, Tschioko F, Wamala JF, Byaruhanga E, Bwire GS, et al. Outbreak of Marburg hemorrhagic fever among miners in Kamwenge and Ibanda Districts, Uganda, 2007. J Infect Dis. 2011;204(Suppl 3):S796–9. http://dx.doi.org/10.1093/infdis/jir312
4. Knust B, Schafer IJ, Wamala J, Nyakarahuka L, Okot C, Shoemaker T, et al. Multidistrict outbreak of Marburg virus disease—Uganda, 2012. J Infect Dis. 2015;212(Suppl 2):S119–28. http://dx.doi.org/10.1093/infdis/jiv351
5. Centers for Disease Control and Prevention (CDC). Imported case of Marburg hemorrhagic fever—Colorado, 2008. MMWR Morb Mortal Wkly Rep. 2009;58:1377–81.
6. Timen A, Koopmans MP, Vossen AC, van Doornum GJ, Günther S, van den Berkmortel F, et al. Response to imported case of Marburg hemorrhagic fever, the Netherlands. Emerg Infect Dis. 2009;15:1171–5. http://dx.doi.org/10.3201/eid1508.090015
7. Towner JS, Amman BR, Sealy TK, Carroll SA, Comer JA, Kemp A, et al. Isolation of genetically diverse Marburg viruses from Egyptian fruit bats. PLoS Pathog. 2009;5:e1000536. http://dx.doi.org/10.1371/journal.ppat.1000536
8. Ksiazek TG, West CP, Rollin PE, Jahrling PB, Peters CJ. ELISA for the detection of antibodies to Ebola viruses. J Infect Dis. 1999;179(Suppl 1):S192–8. http://dx.doi.org/10.1086/514313
9. Diagnostics A. RealStar Filovirus Screen RT-PCR Kit 1.0, 2014 [cited 2016 Jun 9]. http://www.altona-diagnostics.com/tl_files/website/downloads/RealStar_Filovirus Screen RT-PCR Kit 10_CE_WEB_2014-08-29.pdf
10. Schafer IJ, Knudsen E, McNamara LA, Agnihotri S, Rollin PE, Islam A. The Epi Info Viral Hemorrhagic Fever (VHF) application: a resource for outbreak data management and contact tracing in the 2014–2016 West Africa Ebola epidemic. J Infect Dis. 2016;214(suppl3):S122–36. http://dx.doi.org/10.1093.infdis/jiw272
11. Shoemaker T, MacNeil A, Balinandi S, Campbell S, Wamala JF, McMullan LK, et al. Reemerging Sudan Ebola virus disease in Uganda, 2011. Emerg Infect Dis. 2012;18:1480–3. http://dx.doi.org/10.3201/eid1809.111536
12. The Lancet. 1 year on—lessons from the Ebola outbreak for WHO. Lancet. 2015;385:1152. http://dx.doi.org/10.1016/S0140-6736(15)60619-5
13. Borchert JN, Tappero JW, Downing R, Shoemaker T, Behumbiize P, Aceng J, et al.; Centers for Disease Control and Prevention (CDC). Rapidly building global health security capacity—Uganda demonstration project, 2013. MMWR Morb Mortal Wkly Rep. 2014;63:73–6.

Address for correspondence: Trevor R. Shoemaker, Centers for Disease Control and Prevention, P.O. Box 7007, Plot 1577 Ggaba Road, Kampala, Uganda; email: tis8@cdc.gov

Crimean-Congo Hemorrhagic Fever in Migrant Worker Returning from Oman to India, 2016

Pragya D. Yadav, Sachin Thacker, Deepak Y. Patil, Rajlaxmi Jain, Devendra T. Mourya

In January 2016, a migrant worker who returned home to India after becoming ill in Oman was confirmed to have Crimean-Congo hemorrhagic fever (CCHF). Physicians should include CCHF in the differential diagnosis for patients with hemorrhagic signs and a history of recent travel to any area where CCHF is endemic or prevalent.

Increased international travel has led to the global spread of numerous diseases (*1*). One of these diseases, Crimean-Congo hemorrhagic fever (CCHF), has affected persons in >20 countries in Africa, Asia, southeastern Europe, and the Middle East (*2*). Transmission of CCHF virus (CCHFV) to humans primarily occurs via *Hyalomma* spp. ticks and livestock. Large numbers of nosocomial and sporadic CCHF outbreaks have been reported in humans worldwide, including in India, where information about travel-associated CCHF cases is lacking (*3*). We report on a case of CCHF in a man who returned home to India after becoming ill in Oman.

The Study

On January 24, 2016, a 33-year-old migrant worker from India became ill while working in Muscat, Oman. He experienced abdominal pain, occasional dysuria, anorexia, nausea, and vomiting. The man, a supervisor on an animal farm, had occasional contact with animals, including cows, goats, horses, and camels. On January 26, he was admitted to a hospital in Muscat and diagnosed with severe thrombocytopenia and acalculous cholecystitis; he was discharged with a referral to the government hospital for further care. On January 27, instead of visiting the government hospital, he traveled to his residence in Gujarat State, India. On January 28, he was admitted to a hospital in Kutch District, Gujarat, with fever; hemorrhagic signs (melena, epistaxis, and hematuria); vomiting; loss of appetite; and altered sensorium. He had a platelet count of 33×10^9/L (reference range 130–400 $\times 10^9$/L); hemoglobin level of 6.8 g/dL (reference range 14.0–17.4 g/dL); aspartate and alanine aminotransaminase levels of 130 U/L (reference range 0–35 U/L) and 240 U/L (reference range 3–36 U/L), respectively; and prothrombin time of 17.9 sec (reference range 10–13 sec). Results for brain multidetector computed tomography scanning were normal. The patient was administered intravenous ceftriaxone, pantoprazole, somazina citicoline, and cerebroprotein hydrolysate and oral ribavirin.

On illness day 5, the physician sent a clinical sample to the National Institute of Virology in Pune, India, for testing. Results were negative for dengue NS1 antigen and IgM. However, using real-time reverse transcription PCR and IgM ELISA as previously described (*4*), the Institute detected CCHF viral RNA (9.0×10^2 copies/5 μL) and IgM.

After confirming CCHFV infection in the patient, the hospital placed him in quarantine and implemented strict barrier nursing practices; no secondary cases occurred. Contacts in India were closely monitored for 15 days; all remained asymptomatic. The patient was discharged 13 days after illness onset. A clinical sample tested 15 days after discharge was positive for CCHFV IgG and IgM and negative for viral RNA.

We attempted to isolate CCHFV by inoculating infant CD-1 mice with 20 μL of serum or blood collected from the patient on illness day 5. The mice showed no clinical signs by postinoculation day 7, when we euthanized the mice, harvested brains, made a brain suspension in 1.25% bovine serum albumin in phosphate-buffered saline, and used it to inoculate infant mice. Beginning on postinoculation day 5, these mice began showing neurologic signs, (e.g., hind limb paralysis, circling movement); 1 mouse died. We also attempted to isolate CCHFV by inoculating the brain suspension into Vero CCL-81 cells. We detected high virus loads in the mouse brain suspensions (1.2×10^4 copies/5 μL) and tissue culture fluid (2.3×10^4 copies/5 μL) (*4*).

Using the cell culture–grown virus and previously established protocols (*5*), we sequenced the complete genome (small [S], large [L], and medium [M] segments) of the virus. We used Sequencher 5.4.5 DNA Sequence Analysis Software (Gene Codes Corporation, Ann Arbor, MI, USA) to align sequences and submitted them to GenBank (accession nos. KY213714 [S gene], KY213712 [L gene], KY213713 [M gene]). We used a neighbor-joining algorithm in MEGA6 (http://www.megasoftware.net/) to perform phylogenetic analyses, and we constructed a phylogenetic tree using the sequences of the 3 segments and previously identified representative CCHFV strains.

Authors affiliations: National Institute of Virology, Pune, India (P.D. Yadav, D.Y. Patil, R. Jain, D.T. Mourya); JK Hospital, Bhuj, India (S. Thacker)

DOI: https://dx.doi.org/10.3201/eid2306.161950

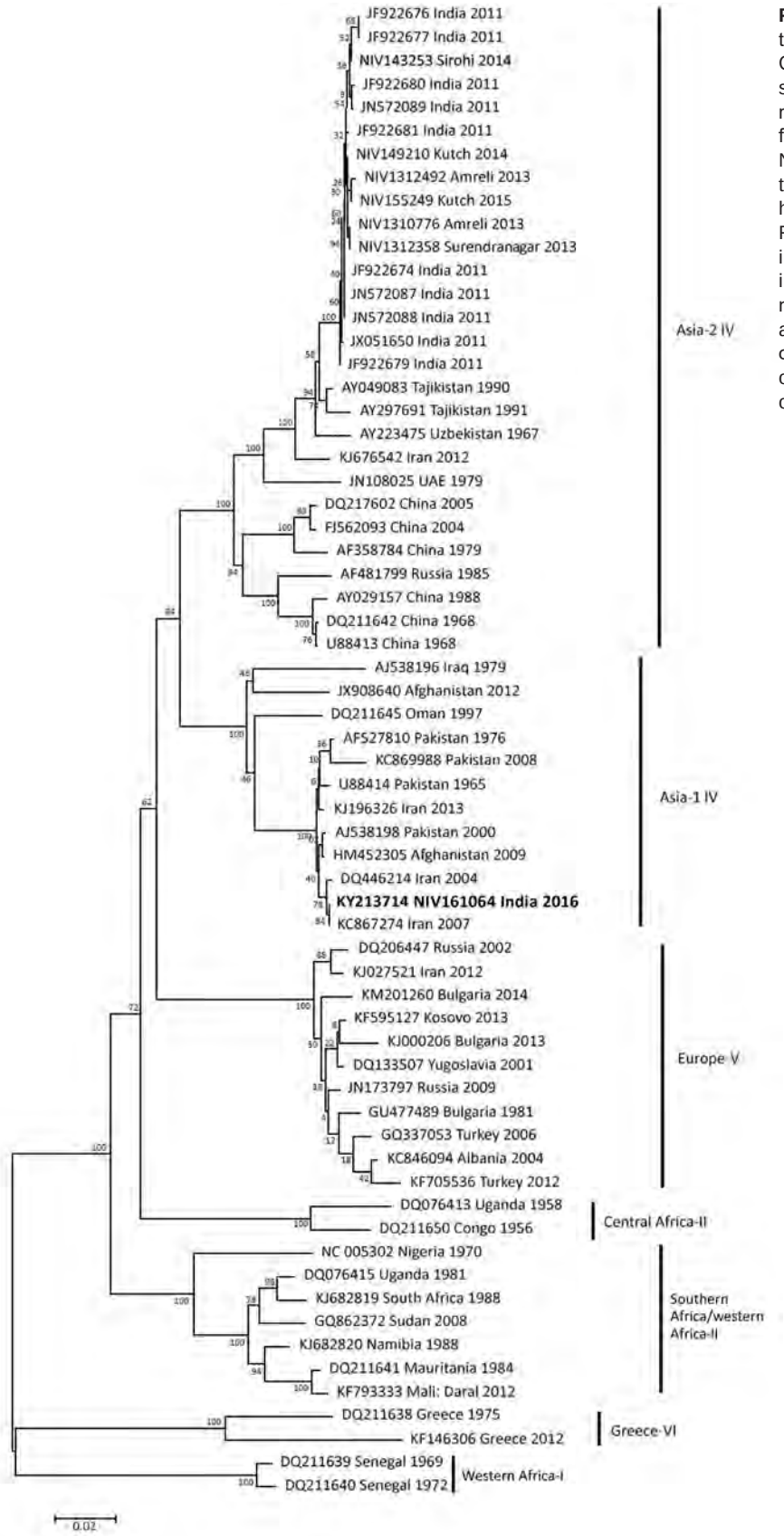

Figure 1. Phylogenetic tree comparing the small gene segment of Crimean-Congo hemorrhagic fever virus (CCHFV) strain isolated in India (bold) with reference CCHFV strains obtained from GenBank. The strain from India, NIV161064, was isolated in 2016 from the serum of a patient who had returned home to India after becoming ill in Oman. Representative reference strains were inferred by the neighbor-joining algorithm in MEGA6 (http://www.megasoftware.net/). Strains are identified by GenBank accession number and location and year of isolation. CCHFV groups are shown on the right. Scale bar indicates number of nucleotide substitutions per site.

By analyzing the S segment, we demonstrated that this CCHFV strain belongs to the Middle East Asia group IV (Asia-1) of CCHFVs, along with strains from Iran, Afghanistan, Pakistan, and Oman (Figure 1); the S segment was closest to those of strains isolated in 2007 in Zehedan, Iran (GenBank accession no. KC867274). The L segment also belongs to the Asia-IV group, along with strains from Afghanistan, Tajikistan, Iraq, and Oman and strains isolated in India in 2011 (Figure 2, panel A); the L segment was closest to that of a strain isolated in 2012 in Afghanistan (GenBank accession no. KC344855). The M segment belongs to type M2 and was closest to the M segment of strains isolated during 2004–2007 in Iran (GenBank accession nos. DQ446216, DQ446215, and KC867273) (Figure 2, panel B).

Conclusion

During 2011–2016, many CCHF cases were reported from India, especially from Gujarat State, where the virus has been endemic since 2011, and adjoining Rajsthan State, where a few sporadic cases have occurred (*4,6–11*). Furthermore, we previously conducted a countrywide, cross-sectional serosurvey that showed CCHFV is prevalent among livestock in 22 states and a union territory of India (*9*).

Our findings show that the S segment of the CCHFV isolated in this study shared maximum relatedness with the Middle East Asia group IV isolates, and the M segment belongs to the M2 group, which also includes strains from countries in the Middle East. Thus, the strain isolated from the migrant worker is a combination of the S gene of Asia-I (S–Asia-1) and M2 strains. We also observed parallel clustering of the S and L segments with Asia-IV group viruses. Like the strain in this study, most CCHFVs circulating in the Middle East are a combination of S–Asia-1 and M2 strains (*12,13*). However, CCHFV strains reported from different districts of Gujarat during 2011–2015 were a combination of S–Asia-2 and Far East M2 viruses that had different parental origins in the S (from Tajikistan strain TADJ/HU8966) and L and M (from Afghanistan strain Afg09-2990) segments, suggesting that an intragenotypic reassortant sequence entered into India. CCHF cases have been reported from Oman since 1995 (*14,15*). However, because sequences have not

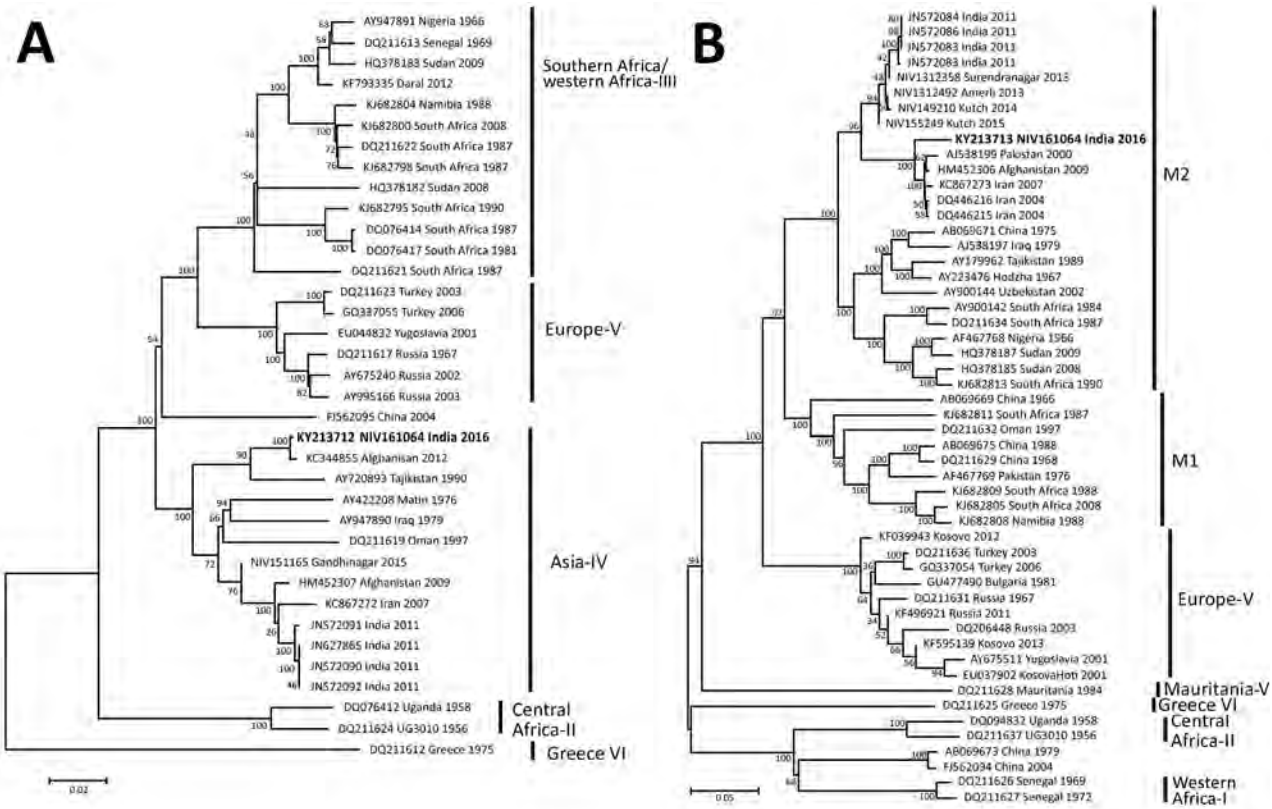

Figure 2. Phylogenetic trees comparing the large (A) and medium (B) gene segments of Crimean-Congo hemorrhagic fever virus (CCHFV) strain isolated in India (bold) with reference CCHFV strains obtained from GenBank. The strain from India, NIV161064, was isolated in 2016 from the serum of a patient who had returned home to India after becoming ill in Oman. Representative reference strains were inferred by the neighbor-joining algorithm in MEGA6 (http://www.megasoftware.net/). Strains are identified by GenBank accession number and location and year of isolation. CCHFV groups are shown on the right. Scale bars indicate number of nucleotide substitutions per site.

been reported for recent strains, we could not conduct a more robust phylogenetic analysis. Overall, our phylogenetic analyses substantiate that the case-patient in Gujarat was infected with a CCHFV strain from the Middle East while working in Oman.

The case-patient we report became ill while in Oman and traveled to Gujarat within the incubation period for CCHFV (6–7 days). On illness day 5, the case-patient was hospitalized in Gujarat and confirmed to be infected with CCHFV. Results of serologic testing for IgM corroborate that the patient acquired the infection while in Oman.

Many reports have been made around the world of travelers inadvertently importing diseases from one country to another. Thus, travelers should be made aware of communicable diseases present in countries they visit, and patients should inform doctors if they have a recent travel history. In addition, physicians should consider CCHF in the differential diagnosis of patients who have hemorrhagic signs and have recently returned from any area where CCHFV is endemic or prevalent. Increased international travel will result in further importations of infectious diseases, highlighting the need for worldwide disease surveillance and for implementation of the World Health Organization International Health Regulations (http://www.who.int/topics/international_health_regulations/en/).

Acknowledgment

We thank JK Hospital, Bhuj, Gujarat, India, for sharing clinical samples. We also thank Anita Shete, Vimal Kumar, Rajen Lakra, Prasad Sarkale, Divya Bhattad, Pravin Kore, Kumar Bagmare, and Shital Dalal for technical support; and we are sincerely grateful to Sarah Cherian for sharing her expertise on genome analysis.

Financial support was provided by the National Institute of Virology, Pune, India.

Dr. Yadav is a group leader for the maximum containment laboratory, National Institute of Virology, Pune, India. Her research interest is zoonotic diseases of high risk group viruses including CCHF, Kyasanur Forest disease, and Nipah virus.

References

1. Tatem AJ, Rogers DJ, Hay SI. Global transport networks and infectious disease spread. Adv Parasitol. 2006;62:293–343. http://dx.doi.org/10.1016/S0065-308X(05)62009-X
2. Ince Y, Yasa C, Metin M, Sonmez M, Meram E, Benkli B, et al. Crimean-Congo hemorrhagic fever infections reported by ProMED. Int J Infect Dis. 2014;26:44–6. http://dx.doi.org/10.1016/j.ijid.2014.04.005
3. Leblebicioglu H, Ozaras R, Fletcher TE, Beeching NJ; ESCMID Study Group for Infections in Travellers and Migrants (ESGITM). Crimean-Congo haemorrhagic fever in travellers: a systematic review. Travel Med Infect Dis. 2016;14:73–80. http://dx.doi.org/10.1016/j.tmaid.2016.03.002
4. Mourya DT, Yadav PD, Shete AM, Gurav YK, Raut CG, Jadi RS, et al. Detection, isolation and confirmation of Crimean-Congo hemorrhagic fever virus in human, ticks and animals in Ahmadabad, India, 2010–2011. PLoS Negl Trop Dis. 2012;6:e1653. http://dx.doi.org/10.1371/journal.pntd.0001653
5. Yadav PD, Cherian SS, Zawar D, Kokate P, Gunjikar R, Jadhav S, et al. Genetic characterization and molecular clock analyses of the Crimean-Congo hemorrhagic fever virus from human and ticks in India, 2010–2011. Infect Genet Evol. 2013;14:223–31. http://dx.doi.org/10.1016/j.meegid.2012.10.005
6. Yadav PD, Raut CG, Mourya DT. Re-occurrence of Crimean-Congo haemorrhagic fever in Ahmedabad, Gujarat, India (2012): a fatal case report. Indian J Med Res. 2013;138:1027–8.
7. Yadav PD, Gurav YK, Mistry M, Shete AM, Sarkale P, Deoshatwar AR, et al. Emergence of Crimean-Congo hemorrhagic fever in Amreli District of Gujarat State, India, June to July 2013. Int J Infect Dis. 2014;18:97–100. http://dx.doi.org/10.1016/j.ijid.2013.09.019
8. Mourya DT, Yadav PD, Shete A, Majumdar TD, Kanani A, Kapadia D, et al. Serosurvey of Crimean-Congo hemorrhagic fever virus in domestic animals, Gujarat, India, 2013. Vector Borne Zoonotic Dis. 2014;14:690–2. http://dx.doi.org/10.1089/vbz.2014.1586
9. Mourya DT, Yadav PD, Shete AM, Sathe PS, Sarkale PC, Pattnaik B, et al. Cross-sectional serosurvey of Crimean-Congo hemorrhagic fever virus IgG in livestock, India, 2013–2014. Emerg Infect Dis. 2015;21:1837–9. http://dx.doi.org/10.3201/eid2110.141961
10. Makwana D, Yadav PD, Kelaiya A, Mourya DT. First confirmed case of Crimean-Congo haemorrhagic fever from Sirohi district in Rajasthan State, India. Indian J Med Res. 2015;142:489–91. http://dx.doi.org/10.4103/0971-5916.169221
11. Yadav PD, Patil DY, Shete AM, Kokate P, Goyal P, Jadhav S, et al. Nosocomial infection of CCHF among health care workers in Rajasthan, India. BMC Infect Dis. 2016;16:624. http://dx.doi.org/10.1186/s12879-016-1971-7
12. Deyde VM, Khristova ML, Rollin PE, Ksiazek TG, Nichol ST. Crimean-Congo hemorrhagic fever virus genomics and global diversity. J Virol. 2006;80:8834–42. http://dx.doi.org/10.1128/JVI.00752-06
13. Lukashev AN. Evidence for recombination in Crimean-Congo hemorrhagic fever virus. J Gen Virol. 2005;86:2333–8. http://dx.doi.org/10.1099/vir.0.80974-0
14. Schwarz TF, Nitschko H, Jäger G, Nsanze H, Longson M, Pugh RN, et al. Crimean-Congo haemorrhagic fever in Oman. Lancet. 1995;346:1230. http://dx.doi.org/10.1016/S0140-6736(95)92936-3
15. Body MHH, Abdulmajeed HA, Hammad MH, Mohamed SA, Saif SA, AL-Maklady S, et al. Cross-sectional survey of Crimean-Congo hemorrhagic fever virus in the sultanate of Oman. Journal of Veterinary Medicine and Animal Health. 2016;8:44–9. http://dx.doi.org/10.5897/JVMAH2016.0472

Address for correspondence: Devendra T. Mourya, National Institute of Virology, 20-A, Dr. Ambedkar Rd, Pune, 411 001, India; email: dtmourya@gmail.com or directorniv@gmail.com

Rise in Group W Meningococcal Carriage in University Students, United Kingdom

Neil J. Oldfield, Caroline Cayrou, Mahab A.K. AlJannat, Ali A.A. Al-Rubaiawi, Luke R. Green, Shehzan Dada, Oliver D. Steels, Christopher Stirrup, Joe Wanford, Banan A.Y. Atwah, Christopher D. Bayliss, David P.J. Turner

MenACWY conjugate vaccination was recently introduced in the United Kingdom for adolescents and young adults to reduce disease from infection by *Neisseria meningitidis* group W. We conducted a cross-sectional meningococcal carriage study in first-year UK university students. Despite 71% MenACWY vaccine coverage, carriage of group W increased substantially.

Neisseria meningitidis causes severe sepsis and meningitis. The main reservoir in most populations is asymptomatic pharyngeal carriage in older adolescents and young adults (*1*). High carriage rates are particularly evident in semiclosed communities of young adults, such as university student populations, where persons live, work, and socialize together (*2*).

Meningococcal carriage was previously assessed in university students in the United Kingdom during 2009–10 at the University of Nottingham (UoN) when a high prevalence of capsular group Y (MenY) meningococcal carriage was detected (*3*). This high level of MenY carriage was concomitant with a rise in disease caused by MenY strains in the United Kingdom (*4*). Since 2009, although MenY disease has plateaued, capsular group W (MenW) disease has steadily increased because of the rapid expansion of hypervirulent strains belonging to the sequence type 11 clonal complex (MenW:ST-11) (*5*).

Analysis of whole-genome sequence data has shown that isolates from the same MenW:ST-11 lineage, termed the South American/UK strain, are also endemic to Chile, Brazil, and Argentina (*6*) and were recently reported in Australia (*7*). In response, Public Health England introduced the MenACWY vaccine in the routine adolescent school program for 14- and 15-year-olds and first-year university students (*8*). A catch-up campaign was used to offer MenACWY vaccine to all 14–18-year-old persons, with persons who left school in 2015 (17–18 years of age) given priority.

The rationale for targeting the vaccine to older adolescents and young adults stems from carriage studies showing that this demographic represents the principal reservoir of meningococcal carriage, as well as experience with other polysaccharide conjugate vaccines. Introduction of the MenC monovalent conjugate vaccines previously reduced carriage acquisition of MenC strains in adolescents and young adults (*9*). There is evidence, albeit limited, to suggest that the quadrivalent vaccine may have a similar effect on carriage of MenCWY strains (*10*,*11*). Reduced carriage in this population should lead to indirect protection of other age groups through herd immunity, thus enhancing the public health effect and cost-effectiveness of this approach.

The Study

To assess trends in meningococcal strain carriage, and to determine the immediate effect of the MenACWY vaccine on carriage of MenW/Y strains, we conducted a cross-sectional study in first-year students at the UoN from registration during September 2015 through March 2016. MenACWY vaccination coverage in this student population increased from 31% (preregistration) to ≈70% (immediately postregistration) as a result of a campus-based vaccination campaign targeting freshmen (*12*).

The study was approved by the Research Ethics Committee at the UoN, and written informed consent was obtained from all participants. We recruited convenience samples of first-year students in September and November 2015 and March 2016. In September, students were recruited during registration; in November and March, students were recruited in 5 dormitories (A–E) with single-occupancy rooms. We searched the UoN Health Service registration database (EMIS Web software; EMIS Health, Leeds, UK) to determine vaccination status in registered first-year students on arrival at the UoN and after the campus-based vaccination campaign.

In September, we obtained pharyngeal swab specimens from eligible students immediately before they received the MenACWY vaccine. We immediately inoculated all pharyngeal swabs onto GC selective agar (Oxoid, Basingstoke, UK) and incubated them at 37°C in air containing 5% CO_2. After 24 and 48 hours, we

Author affiliations: University of Nottingham, Nottingham, UK (N.J. Oldfield, M.A.K. AlJannat, O.D. Steels, C. Stirrup, B.A.Y. Atwah, D.P.J. Turner); University of Leicester, Leicester, UK (C. Cayrou, A.A.A. Al-Rubaiawi, L.R. Green, S. Dada, J. Wanford, C.D. Bayliss)

DOI: http://dx.doi.org/10.3201/eid2306.161768

selected oxidase-positive colonies suggestive of *Neisseria* spp. and confirmed their identity by amplification of the meningococcal gene *crgA* plus *ctrA* and/or *porA*, as described previously (*13*).

We performed PCR-based genogrouping as described previously (*13*,*14*). The Meningococcal Reference Unit, Public Health England, Manchester, UK, performed serogrouping and serotyping of MenW isolates using dot-blot enzyme immunoassay. Sequence data derived from amplified *porA* and factor H–binding protein alleles was queried against the PubMLST/Neisseria database (http://pubmlst.org/neisseria). We performed χ^2 tests for significance by using STATCALC (Epi Info version 7.2.0.1; Centers for Disease Control and Prevention, Atlanta, GA, USA).

The September sample of 769 first-year students represented 10.9% of the 7,049 first-year students registered in 2015. Carriage rates among this group increased from 14% in late September 2015 to 39% by mid-November 2015 and 46% in March 2016 (online Technical Appendix Table 1, http://wwwnc.cdc.gov/EID/article/23/6/16-1768-Techapp1.pdf). The characteristics of enrolled students and behavioral risk factors for carriage were similar at the 3 time points. The initial carriage rate of 14% was much lower for first-year students in September 2015 than in September 2009 (23.2%; $\chi^2 = 34$, df = 1; p<0.00001) (*3*), suggesting a reduction in meningococcal carriage in adolescents in the United Kingdom, possibly attributable to an alteration in risk factors for carriage. The MenY carriage rate for incoming students (1.8%) was also lower than that detected in 2009 (2.9%; $\chi^2 = 2.0$, df = 1; p = 0.15) (*3*).

In September 2015, carriage rates were 4.2% for genogroup capsule null locus (cnl), 3.3% for B, 1.8% for Y, and 0.7% for W strains. A substantial part of the increase in carriage from September 2015 through March 2016 was the result of a notable increase (0.7% to 8.0%) in carriage of MenW strains (online Technical Appendix Table 1). No change in the carriage of MenY strains was detected (online Technical Appendix Table 1). Of the 50 students colonized with MenW, 36 (72%) had received MenACWY vaccine either before or during registration, which is consistent with the overall MenACWY coverage in our first-year student cohort. Students colonized with MenW at the second and third sampling times were distributed across all 5 dormitories, suggesting widespread dissemination, and 21 (91%) of the MenW carriers in the last time point (March 2016) had been vaccinated at least 5 months before sampling (online Technical Appendix Table 2).

Analysis of the genogroup W isolates showed that 47 (90%) of 52 were serotype 2a (online Technical Appendix Table 1) and harbored alleles for factor H binding protein peptide 22 and PorA P1.5,2, identical to the corresponding alleles harbored by the MenW:ST-11 clone responsible for the increase in invasive MenW disease in the United Kingdom (*5*). We examined capsular expression by serogrouping and found 32 (62%) of the MenW isolates expressed the W capsular polysaccharide. Of the 21 MenW carriers in March 2016 who had been vaccinated at least 5 months before sampling, 15 (71%) were harboring isolates expressing the W capsule (online Technical Appendix Table 2).

Conclusions

We detected a rapid rise in carriage of MenW among first-year students in a university setting in the United Kingdom. In comparison, carriage of MenC in adolescents and young adults in the United Kingdom, including in university students, was rare before the introduction of MenC monovalent conjugate vaccines (*9*). The rise in MenW carriage is most likely due to acquisition within student dormitories or social spaces on campus but was unexpected because no such isolates were found in a similar study at the UoN in 2008–09 (*15*), and only a limited number in a multicenter carriage study involving UK universities in 2010–11 (*6*,*10*).

The increase in MenW carriage among university students merits further monitoring because it could contribute further to the sustained increase in MenW disease in the United Kingdom. Two cases of MenW disease were reported in unvaccinated students in Nottingham during 2015–16. Students attending universities exhibit high mobility and may represent an ongoing vehicle for amplification and spread of MenW into communities throughout the United Kingdom or beyond, with implications for vaccination policy and future research.

Acknowledgments

We are grateful to all participants in this study. We thank Daniel Hammersley for logistical assistance and for providing MenACWY vaccination data. We also thank Steve Gray, Anthony Carr, and Ray Borrow for serogrouping and serotyping meningococcal isolates.

This work was supported by the University of Nottingham.

Dr. Oldfield is a senior postdoctoral researcher at the School of Life Sciences, University of Nottingham, Nottingham, UK. His research interests include meningococcal carriage dynamics and pathogenesis.

References

1. Caugant DA, Maiden MCJ. Meningococcal carriage and disease—population biology and evolution. Vaccine. 2009; 27(Suppl 2):B64–70. http://dx.doi.org/10.1016/j.vaccine. 2009.04.061
2. Neal KR, Nguyen-Van-Tam JS, Jeffrey N, Slack RC, Madeley RJ, Ait-Tahar K, et al. Changing carriage rate of *Neisseria meningitidis* among university students during the first week of term: cross sectional study. BMJ. 2000;320:846–9. http://dx.doi.org/10.1136/bmj.320.7238.846

3. Ala'Aldeen DAA, Oldfield NJ, Bidmos FA, Abouseada NM, Ahmed NW, Turner DPJ, et al. Carriage of meningococci by university students, United Kingdom. Emerg Infect Dis. 2011;17:1762–3. http://dx.doi.org/10.3201/eid1709.101762
4. Ladhani SN, Lucidarme J, Newbold LS, Gray SJ, Carr AD, Findlow J, et al. Invasive meningococcal capsular group Y disease, England and Wales, 2007–2009. Emerg Infect Dis. 2012;18:63–70. http://dx.doi.org/10.3201/eid1801.110901
5. Ladhani SN, Beebeejaun K, Lucidarme J, Campbell H, Gray S, Kaczmarski E, et al. Increase in endemic *Neisseria meningitidis* capsular group W sequence type 11 complex associated with severe invasive disease in England and Wales. Clin Infect Dis. 2015;60:578–85. http://dx.doi.org/10.1093/cid/ciu881
6. Lucidarme J, Hill DMC, Bratcher HB, Gray SJ, du Plessis M, Tsang RS, et al. Genomic resolution of an aggressive, widespread, diverse and expanding meningococcal serogroup B, C and W lineage. J Infect. 2015;71:544–52. http://dx.doi.org/10.1016/j.jinf.2015.07.007
7. Carville KS, Stevens K, Sohail A, Franklin LJ, Bond KA, Brahmi A, et al. Increase in meningococcal serogroup W disease, Victoria, Australia, 2013–2015. Emerg Infect Dis. 2016;22:1785–7. http://dx.doi.org/10.3201/eid2210.151935
8. Campbell H, Saliba V, Borrow R, Ramsay M, Ladhani SN. Targeted vaccination of teenagers following continued rapid endemic expansion of a single meningococcal group W clone (sequence type 11 clonal complex), United Kingdom 2015. Euro Surveill. 2015;20:21188. http://dx.doi.org/10.2807/1560-7917.ES2015.20.28.21188
9. Maiden MCJ, Ibarz-Pavón AB, Urwin R, Gray SJ, Andrews NJ, Clarke SC, et al. Impact of meningococcal serogroup C conjugate vaccines on carriage and herd immunity. J Infect Dis. 2008; 197:737–43. http://dx.doi.org/10.1086/527401
10. Read RC, Baxter D, Chadwick DR, Faust SN, Finn A, Gordon SB, et al. Effect of a quadrivalent meningococcal ACWY glycoconjugate or a serogroup B meningococcal vaccine on meningococcal carriage: an observer-blind, phase 3 randomised clinical trial. Lancet. 2014;384:2123–31. http://dx.doi.org/10.1016/S0140-6736(14)60842-4
11. Korzeniewski K, Skoczyńska A, Guzek A, Konior M, Chciałowski A, Waśko I, et al. Effectiveness of immunoprophylaxis in suppressing carriage of *Neisseria meningitidis* in the military environment. Adv Exp Med Biol. 2014;836:19–28. http://dx.doi.org/10.1007/5584_2014_22
12. Turner DPJ, Oldfield NJ, Bayliss CD. University vaccine campaign increases meningococcal ACWY vaccine coverage. Public Health. 2017;145:1–3. http://dx.doi.org/10.1016/j.puhe.2016.12.010
13. Taha M-K, Alonso J-M, Cafferkey M, Caugant DA, Clarke SC, Diggle MA, et al. Interlaboratory comparison of PCR-based identification and genogrouping of *Neisseria meningitidis.* J Clin Microbiol. 2005;43:144–9. http://dx.doi.org/10.1128/JCM.43.1.144-149.2005
14. Claus H, Maiden MCJ, Maag R, Frosch M, Vogel U. Many carried meningococci lack the genes required for capsule synthesis and transport. Microbiology. 2002;148:1813–9. http://dx.doi.org/10.1099/00221287-148-6-1813
15. Bidmos FA, Neal KR, Oldfield NJ, Turner DPJ, Ala'Aldeen DAA, Bayliss CD. . Persistence, replacement, and rapid clonal expansion of meningococcal carriage isolates in a 2008 university student cohort. J Clin Microbiol. 2011;49:506–12. http://dx.doi.org/10.1128/JCM.01322-10

Address for correspondence: David P.J. Turner, Centre for Biomolecular Sciences, School of Life Sciences, University of Nottingham, Nottingham NG7 2RD, UK; email: david.turner@nottingham.ac.uk

EID Podcast:
Stained Glass and Flu

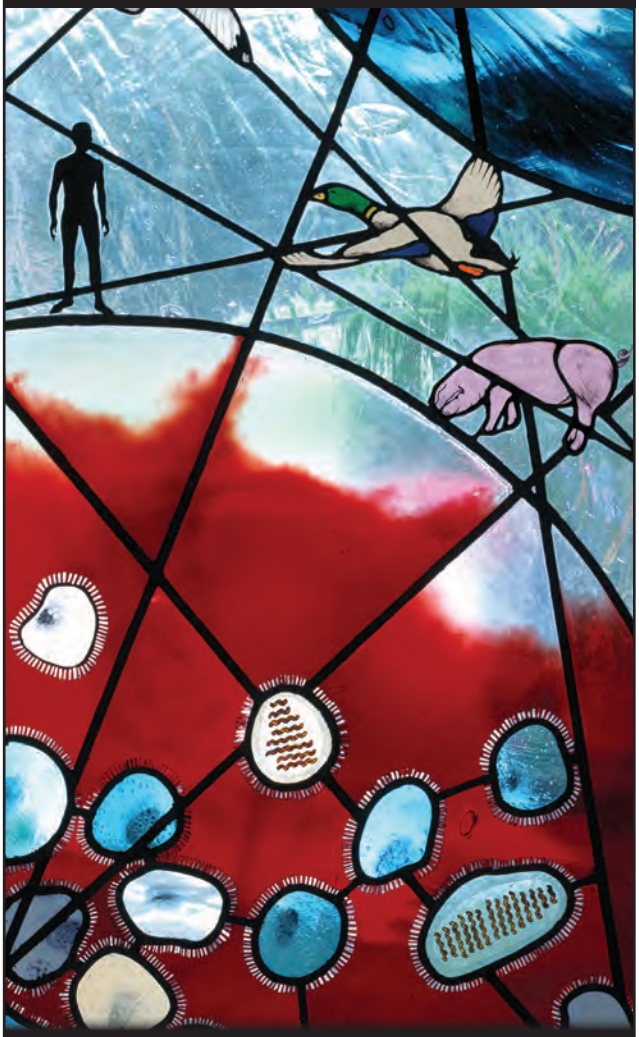

The work of art shown here depicts the interrelationship of human, animal, and environmental health.

Stained-glass windows have been appreciated for their utility and splendor for more than 1,000 years, and this engaging work of art by stained glass artist Jenny Hammond reminds us that influenza A viruses—which can be easily spread between animals and human, use various host species, and exist in many different environments—remain an enduring and global health concern.

Visit our website to listen:

EMERGING INFECTIOUS DISEASES

https://www2c.cdc.gov/podcasts/player.asp?f=8644950

Penicillin Resistance of Nonvaccine Type Pneumococcus before and after PCV13 Introduction, United States

Cheryl P. Andam,[1] Colin J. Worby,[1] Ryan Gierke, Lesley McGee, Tamara Pilishvili, William P. Hanage

Introduction of 13-valent pneumococcal conjugate vaccine in the United States was not associated with a significant change in prevalence of penicillin resistance in nonvaccine type serotypes because of the variable success of highly resistant serotypes. Differences in regional serotype distribution and serotype-specific resistance contributed to geographic heterogeneity of penicillin resistance.

Streptococcus pneumoniae (pneumococcus) causes a range of debilitating and potentially life-threatening infections, such as pneumonia, meningitis, and septicemia. To reduce illness and death caused by pneumococcal diseases, a 7-valent pneumococcal conjugate vaccine (PCV7) was introduced in 2000 and targeted serotypes 4, 6B, 9V, 14, 18C, 19F, and 23F. However, although vaccine type serotypes declined in frequency after PCV7 introduction (*1*,*2*), an increasing frequency of nonvaccine type (NVT) serotypes in samples from carriage and invasive disease was observed in subsequent years (*2*,*3*). Known as serotype replacement, this population-level change in serotype distribution, which most often involves preexisting clones and serotypes that were already in circulation before vaccine implementation (*4*), can reduce the benefits of vaccination (*5*). To address the rise in invasive pneumococcal disease associated with NVT serotypes, a second-generation conjugate vaccine was implemented in 2010 (PCV13), targeting the 7 serotypes targeted by PCV7 plus 6 additional serotypes: 1, 3, 5, 6A, 7F, and 19A (*6*).

The prevalence of penicillin-resistant pneumococcus strains varies considerably between states (*7*,*8*). Such variation might be caused by differences in serotype distribution (such that some locations have a higher prevalence of strains that are generally more resistant) or higher-than-average levels of resistance within serotypes. Before the introduction of PCV7, regional variations in the prevalence of antibiotic resistance were considered to be caused by regional differences in antibiotic use, leading to differences in the intensity of selective pressure acting on the bacterial population (*9*). The variation in the proportion of resistant isolates within individual serotypes in the United States was thought to be a reflection of this regional difference in antibiotic use and was identified as the major factor in driving geographic variation of penicillin resistance (*7*). However, post-PCV7, this factor played a diminishing role in explaining geographic heterogeneity in penicillin resistance, with variation in serotype distribution between sites being of increasing importance (*8*). Understanding the underlying causes of the geographic heterogeneity of penicillin resistance and the role of selective pressure provides important insights on the long-term dynamics of penicillin resistance in the United States.

The Study

To analyze NVT penicillin-nonsusceptible pneumococcus (PNSP) detected in patients with invasive pneumococcal disease, we used data from the Active Bacterial Core surveillance (ABCs) system, a population- and laboratory-based collaborative system between the Centers for Disease Control and Prevention and state health departments and academic institutions in 10 states (California, Colorado, Connecticut, Georgia, Maryland, Minnesota, New Mexico, New York, Oregon, and Tennessee). We considered PNSP non-PCV13 serotypes detected in patients in all age groups from 2009 (pre-PCV13, n = 285 patients) through 2012 (post-PCV13, 339 patients). Nonsusceptibility was based on the meningitis breakpoint (MIC $\geq$0.12 μg/mL), as recommended by the Clinical and Laboratory Standards Institute (*10*). Serotypes 15B, 15C, and 15B/C were grouped together as 15BC because of the reported reversible switching between the 2 serotypes, which makes the precise differentiation of these serotypes difficult (*11*).

To determine whether geographic differences in the proportions of PNSP were consistent across serotypes, we calculated the proportions of PNSP for each of the 7 most common NVT serotypes (15A, 15BC, 16F, 23A, 23B, 33F, and 35B) across the 10 sites for 2009 and 2012. We found that serotypes with the highest proportions of PNSP in 2012 already had high resistance in 2009 (Figure 1). We calculated the Spearman correlation coefficient between the proportion of PNSP for each pair of serotypes across states in 2009 (range –0.09 to 0.66) and 2012 (range 0.30–0.79)

Author affiliations: Harvard T.H. Chan School of Public Health, Boston, Massachusetts, USA (C.P. Andam, C.J. Worby, W.P. Hanage); Centers for Disease Control and Prevention, Atlanta, Georgia, USA (R. Gierke, L. McGee, T. Pilishvili)

DOI: https://dx.doi.org/10.3201/eid2306.161331

[1]These first authors contributed equally to this article.

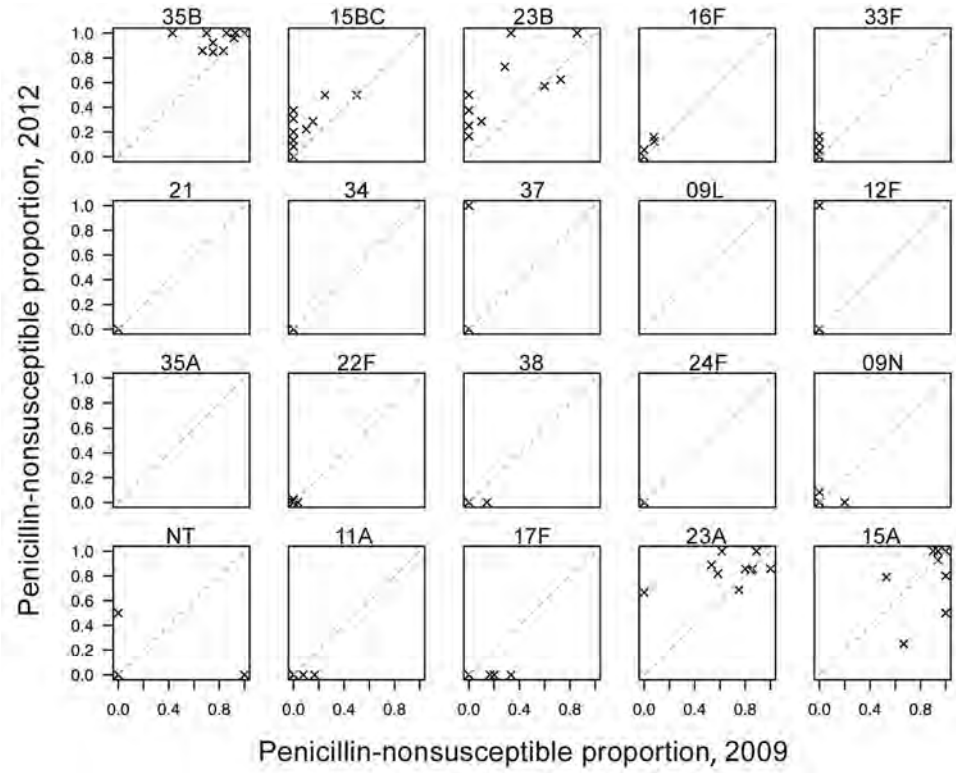

Figure 1. Comparison of proportion of nonvaccine type serotypes with penicillin resistance, by serotype, United States, 2009 and 2012. Based on Active Bacterial Core surveillance system data from 10 US states. The dashed diagonal line represents no change.

(online Technical Appendix, https://wwwnc.cdc.gov/EID/article/23/6/16-1331-Techapp1.pdf). We found significant overall correlation in 2009 and 2012 ($p<0.001$ for both years), indicating that sites with high proportions of PNSP in 1 serotype typically will also have high proportions of PNSP in other serotypes. This finding suggests that differences in selection pressure account for the geographic variation in the proportions of PNSP.

We next implemented a standardized regression approach, used previously to analyze the pneumococcal-resistance patterns pre-PCV7 (*7*) and post-PCV7 (*8*) (online Technical Appendix). To investigate the source of geographic variation in the proportion of PNSP, we tested the hypotheses that either geographic heterogeneity in serotype distribution (Std1), or serotype-specific differences in penicillin resistance (Std2) were responsible for the observed variation. These effects were quantified by regressing crude versus standardized prevalence of penicillin resistance (Figure 2; online Technical Appendix), by which a regression slope of 1 would indicate that the factor considered had zero effect. By using 2009 data, we found that regression slopes for Std1 (0.445, 95% CI –0.083 to 0.972) and Std2 (0.463, 95% CI –0.013 to 0.939) indicate that both factors played a similar intermediate role in generating this geographic variation in penicillin resistance, with neither 95% CI containing 1. In 2012, the regression coefficient for Std2 was higher (0.634, 95% CI 0.14–1.128), whereas the coefficient for Std1 decreased (0.367, 95% CI –0.025 to 0.758). Although these changes are not statistically significant relative to 2009, they might suggest shifting contributions to the observed variation in proportions of PNSP after the introduction of the PCV13 vaccine in 2010, with geographic differences in serotype distribution having an increased role and differences in serotype-specific PNSP becoming less important.

Finally, we sought to quantify the rate of change in penicillin resistance during 2009–2012 in each state. We documented the proportion of PNSP by state for the pre- and post-PCV13 periods (online Technical Appendix Table 4). No significant change in state-level resistance was observed. New Mexico, Maryland, and Georgia saw the highest increases in the proportion of PNSP during 2009–2012, whereas a slight decline was observed for Colorado, New York, and Connecticut. Although the distribution of serotypes might greatly fluctuate among geographic regions immediately after vaccine introduction, the overall proportions of NVT serotypes with penicillin resistance across the country might not vary significantly between the pre- and post-vaccine periods. Of potential importance are the small increases in the proportions of PNSP serotypes not included in either vaccine that were observed between the implementation of PCV7 and PCV13 (*12*), which might lay the foundation for changes post-PCV13.

Conclusions

The marked variation in the proportion of penicillin resistance among states highlights the potential of local

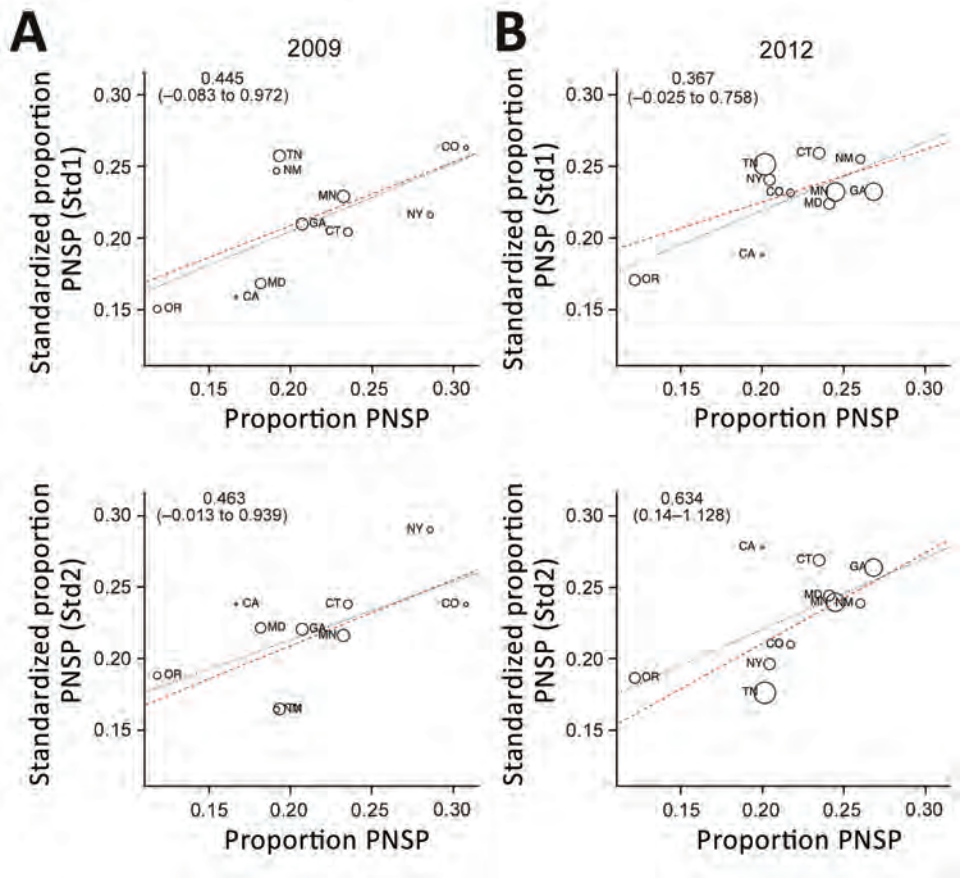

Figure 2. Crude versus standardized proportions of nonvaccine type serotypes with penicillin nonsusceptibility, by state, United States, 2009 and 2012, based on Active Bacterial Core surveillance system data from 10 US states. Std1 denotes standardization for geographic heterogeneity in serotype distribution. Std2 denotes standardization for serotype-specific differences in resistance. Regression slopes with 95% CIs are indicated in the upper left corner of each panel. Larger circles represent states with a greater number of penicillin-resistant samples. Dashed lines represent the inverse-variance weighted (red) and unweighted (gray) regression slopes. PNSP, penicillin-nonsusceptible pneumococcus.

selective pressures to favor certain serotypes and resistant strains within each serotype to increase in frequency as the population returns to equilibrium (*13*). Previous studies have already shown significant regional differences in antibiotic use and vaccination coverage across the United States (*14*,*15*). Regional rates of patient adherence to treatment regimens will also influence variations in resistance. A combination of these factors, which will likely vary between and within regions, would greatly affect proportions of resistance across the country.

In our study, we observed that the dynamics of penicillin resistance continue to shift in the wake of vaccine introduction. Our postvaccine observations were recorded shortly after the introduction of the vaccine; additional observations would be valuable to determine the stability of the postvaccine dynamics and any potential importance of the temporal changes we observed to factors contributing to variation in resistance levels. Further long-term nationwide surveillance of serotype dynamics is required to assess the multiple ecologic factors that influence antibiotic resistance in the pneumococcus in the conjugate vaccine era.

Acknowledgments

We thank the principal investigators and surveillance officers at the 10 participating ABCs sites and the ABCs Epidemiology and Streptococcal Laboratory teams at the Centers for Disease Control and Prevention.

W.P.H. was supported by the National Institute of Allergy and Infectious Diseases of the National Institutes of Health (award no. R01 AI106786-01). C.J.W. was supported by the National Institute of General Medical Sciences of the National Institutes of Health (award no. U54GM088558).

The content is solely the responsibility of the authors and does not necessarily represent the official views of the National Institutes of Health or the institutions with which the authors are affiliated. The funders had no role in study design, data collection and analysis, decision to publish, or preparation of the manuscript.

Dr. Andam is a postdoctoral fellow at the Department of Epidemiology at the Harvard T.H. Chan School of Public Health. Her research focuses on using genomic data to understand the population structure and evolution of pneumococcus.

References

1. Hsu KK, Shea KM, Stevenson AE, Pelton SI; Massachusetts Department of Public Health. Changing serotypes causing childhood invasive pneumococcal disease: Massachusetts, 2001–2007. Pediatr Infect Dis J. 2010;29:289–93. https://doi.org/10.1097/INF.0b013e3181c15471

2. Scott JR, Millar EV, Lipsitch M, Moulton LH, Weatherholtz R, Perilla MJ, et al. Impact of more than a decade of pneumococcal conjugate vaccine use on carriage and invasive potential in Native American communities. J Infect Dis. 2012;205:280–8. http://dx.doi.org/10.1093/infdis/jir730
3. Huang SS, Platt R, Rifas-Shiman SL, Pelton SI, Goldmann D, Finkelstein JA. Post-PCV7 changes in colonizing pneumococcal serotypes in 16 Massachusetts communities, 2001 and 2004. Pediatrics. 2005;116:e408–13. http://dx.doi.org/10.1542/peds.2004-2338
4. Croucher NJ, Finkelstein JA, Pelton SI, Mitchell PK, Lee GM, Parkhill J, et al. Population genomics of post-vaccine changes in pneumococcal epidemiology. Nat Genet. 2013;45:656–63. http://dx.doi.org/10.1038/ng.2625
5. Weinberger DM, Malley R, Lipsitch M. Serotype replacement in disease after pneumococcal vaccination. Lancet. 2011;378:1962–73. http://dx.doi.org/10.1016/S0140-6736(10)62225-8
6. Jefferies JMC, Macdonald E, Faust SN, Clarke SC. 13-valent pneumococcal conjugate vaccine (PCV13). Hum Vaccin. 2011;7:1012–8. http://dx.doi.org/10.4161/hv.7.10.16794
7. McCormick AW, Whitney CG, Farley MM, Lynfield R, Harrison LH, Bennett NM, et al. Geographic diversity and temporal trends of antimicrobial resistance in *Streptococcus pneumoniae* in the United States. Nat Med. 2003;9:424–30. http://dx.doi.org/10.1038/nm839
8. Link-Gelles R, Thomas A, Lynfield R, Petit S, Schaffner W, Harrison L, et al. Geographic and temporal trends in antimicrobial nonsusceptibility in *Streptococcus pneumoniae* in the post-vaccine era in the United States. J Infect Dis. 2013;208:1266–73. http://dx.doi.org/10.1093/infdis/jit315
9. Hicks LA, Chien Y-W, Taylor TH Jr, Haber M, Klugman KP; Active Bacterial Core Surveillance (ABCs) Team. Outpatient antibiotic prescribing and nonsusceptible *Streptococcus pneumoniae* in the United States, 1996–2003. Clin Infect Dis. 2011; 53:631–9. http://dx.doi.org/10.1093/cid/cir443
10. Clinical and Laboratory Standards Institute. Performance standards for antimicrobial susceptibility testing; 16th informational supplement (M100–S16). Wayne (PA): The Institute; 2008.
11. Venkateswaran PS, Stanton N, Austrian R. Type variation of strains of *Streptococcus pneumoniae* in capsular serogroup 15. J Infect Dis. 1983;147:1041–54. http://dx.doi.org/10.1093/infdis/147.6.1041
12. Gertz RE Jr, Li Z, Pimenta FC, Jackson D, Juni BA, Lynfield R, et al.; Active Bacterial Core Surveillance Team. Increased penicillin nonsusceptibility of nonvaccine-serotype invasive pneumococci other than serotypes 19A and 6A in post–7-valent conjugate vaccine era. J Infect Dis. 2010;201:770–5. http://dx.doi.org/10.1086/650496
13. Hanage WP, Bishop CJ, Lee GM, Lipsitch M, Stevenson A, Rifas-Shiman SL, et al. Clonal replacement among 19A *Streptococcus pneumoniae* in Massachusetts, prior to 13 valent conjugate vaccination. Vaccine. 2011;29:8877–81. http://dx.doi.org/10.1016/j.vaccine.2011.09.075
14. Suda KJ, Hicks LA, Roberts RM, Hunkler RJ, Taylor TH. Trends and seasonal variation in outpatient antibiotic prescription rates in the United States, 2006 to 2010. Antimicrob Agents Chemother. 2014;58:2763–6. http://dx.doi.org/10.1128/AAC.02239-13
15. Centers for Disease Control and Prevention. Invasive pneumococcal disease and 13-valent pneumococcal conjugate vaccine (PCV13) coverage among children aged ≤59 months—selected U.S. regions, 2010–2011. MMWR Morb Mortal Wkly Rep. 2011;60:1477–81.

Address for correspondence: Cheryl P. Andam, Harvard University T.H. Chan School of Public Health – Epidemiology, 677 Huntington Ave, Boston, MA 02115, USA; email: candam@hsph.harvard.edu or cheryl.andam@unh.edu

EID Podcast:
Probable Unusual Transmission of Zika Virus

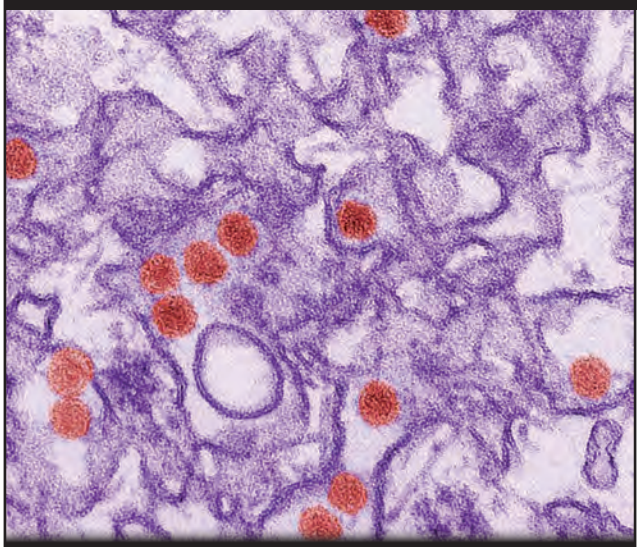

Zika virus (ZIKV), a mosquito-transmitted flavivirus, has been isolated from sentinel monkeys, mosquitoes, and sick persons in Africa and Southeast Asia. Serologic surveys indicate that ZIKV infections can be relatively common among persons in southeastern Senegal and other areas of Africa, but that ZIKV-associated disease may be underreported or misdiagnosed. In 2007, a large outbreak of ZIKV infection occurred on Yap Island in the southwestern Pacific that infected ≈70% of the island's inhabitants, which highlighted this virus as an emerging pathogen. The purpose of this study was to investigate and report 3 unusual cases of arboviral disease that occurred in Colorado in 2008

Clinical and serologic evidence indicate that two American scientists contracted Zika virus infections while working in Senegal in 2008. One of the scientists transmitted this arbovirus to his wife after his return home. Direct contact is implicated as the transmission route, most likely as a sexually transmitted infection.

Visit our website to listen:
https://www2c.cdc.gov/podcasts/player.asp?f=7106489

EMERGING INFECTIOUS DISEASES

Febrile Respiratory Illness Associated with Human Adenovirus Type 55 in South Korea Military, 2014–2016[1]

Hongseok Yoo, Se Hun Gu, Jaehun Jung, Dong Hyun Song, Changgyo Yoon, Duck Jin Hong, Eun Young Lee, Woong Seog, Il-Ung Hwang, Daesang Lee, Seong Tae Jeong,[2] Kyungmin Huh[2]

An outbreak of febrile respiratory illness associated with human adenovirus (HAdV) occurred in the South Korea military during the 2014–15 influenza season and thereafter. Molecular typing and phylogenetic analysis of patient samples identified HAdV type 55 as the causative agent. Emergence of this novel HAdV necessitates continued surveillance in military and civilian populations.

Human adenovirus (HAdV) is a common cause of respiratory infections ranging from uncomplicated upper respiratory infections to life-threatening pneumonia. Military personnel, especially new recruits, are predisposed to respiratory infections caused by HAdV (*1*). The substantial effects of HAdV infection in the military have been demonstrated by the marked increase in the incidence of febrile respiratory illness (FRI) in the US military after vaccination against the virus ended in 1999; in turn, the incidence dramatically declined after the vaccine was reintroduced (*2*).

HAdVs are a group of nonenveloped double-stranded DNA viruses comprising 7 species (A–G) and >50 types (*3*). HAdV types belonging to species B (HAdV-3, -7, -11, -16, -21) and E (HAdV-4) are commonly associated with respiratory infections in adults, particularly in military personnel (*4*). Novel types or genomic variants, such as HAdV-14 (*3*) and HAdV-7 (*5*), have been implicated in epidemics of severe infection. HAdV-55, another emerging type reported in China, Turkey, Spain, Singapore, and Israel (*5*,*6*), has been associated with severe clinical manifestations, which often lead to respiratory failure and death (*7*,*8*).

Since fall 2014, we have observed an outbreak of FRI and pneumonia in military personnel in South Korea. In addition to the increased incidence of FRI, patients experienced severe manifestations. We describe the epidemiologic, clinical, and molecular characteristics of FRI in the South Korea military during October 2014–May 2016.

Author affiliations: Armed Forces Capital Hospital, Seongnam, South Korea (H. Yoo, D.J. Hong, E.Y. Lee, K. Huh); Agency for Defense Development, Daejeon, South Korea (S.H. Gu, D.H. Song, D. Lee, S.T. Jeong); Armed Forces Medical Command, Seongnam (J. Jung, C. Yoon, W. Seog, I.-U. Hwang)

DOI: http://dx.doi.org/10.3201/eid2306.161848

The Study

We obtained data regarding temporal trends in FRI incidence from military sentinel surveillance, which has been monitoring weekly FRI rates since October 2011. Monthly numbers of patients with pneumonia (inpatients, outpatients, and emergency room patients) were extracted from a computerized data warehouse that stores data from all military hospitals. We identified pneumonia cases by using the International Classification of Diseases and Related Health Problems, 10th Revision, codes J12–J18. The influenza season, which starts in October and ends the following May, was used as a surrogate for the HAdV season in this study. More detaileds information on FRI surveillance is available in the online Technical Appendix (https://wwwnc.cdc.gov/EID/article/23/6/16-1848-Techapp1.pdf).

The trends in FRI rates showed an unusual surge during the 2014–15 influenza season (Figure 1, panel A). The FRI rate increased for 15 weeks in the 2014–15 season, compared with 10 weeks in the 2012–13 season and 5 weeks in the 2013–14 season. Peak FRI rate in the 2014–15 season (10.4%) was higher than rates in the preceding 2 seasons (4.7% and 7.5%). The numbers of pneumonia cases in 2014–15 and 2015–16 seasons were 3,140 and 3,145 patients, respectively, a 191% increase from the mean number during 3 preceding seasons.

In April 2014, a multiplex real-time PCR for identifying 15 viruses from respiratory specimens was introduced at the Armed Forces Capital Hospital, the only tertiary hospital in the South Korea military health care system (detailed methods in online Technical Appendix). A total of 1,484 nonduplicate specimens were tested by the end of May 2016 (Figure 1, panel B; online Technical Appendix Table 1, Figure). HAdV was identified in 490 (33.0%) of total specimens, and it accounted for 79.7% (282/354) and 53.2% (150/282) of positive results in the 2014–15 and 2015–16 seasons, respectively. Increased HAdV activity was observed from December until the following May.

[1]Preliminary results from this study were presented at the Annual Spring Meeting of the Korean Society for Chemotherapy, April 21–22, Seoul, South Korea.

[2]These authors contributed equally to this article.

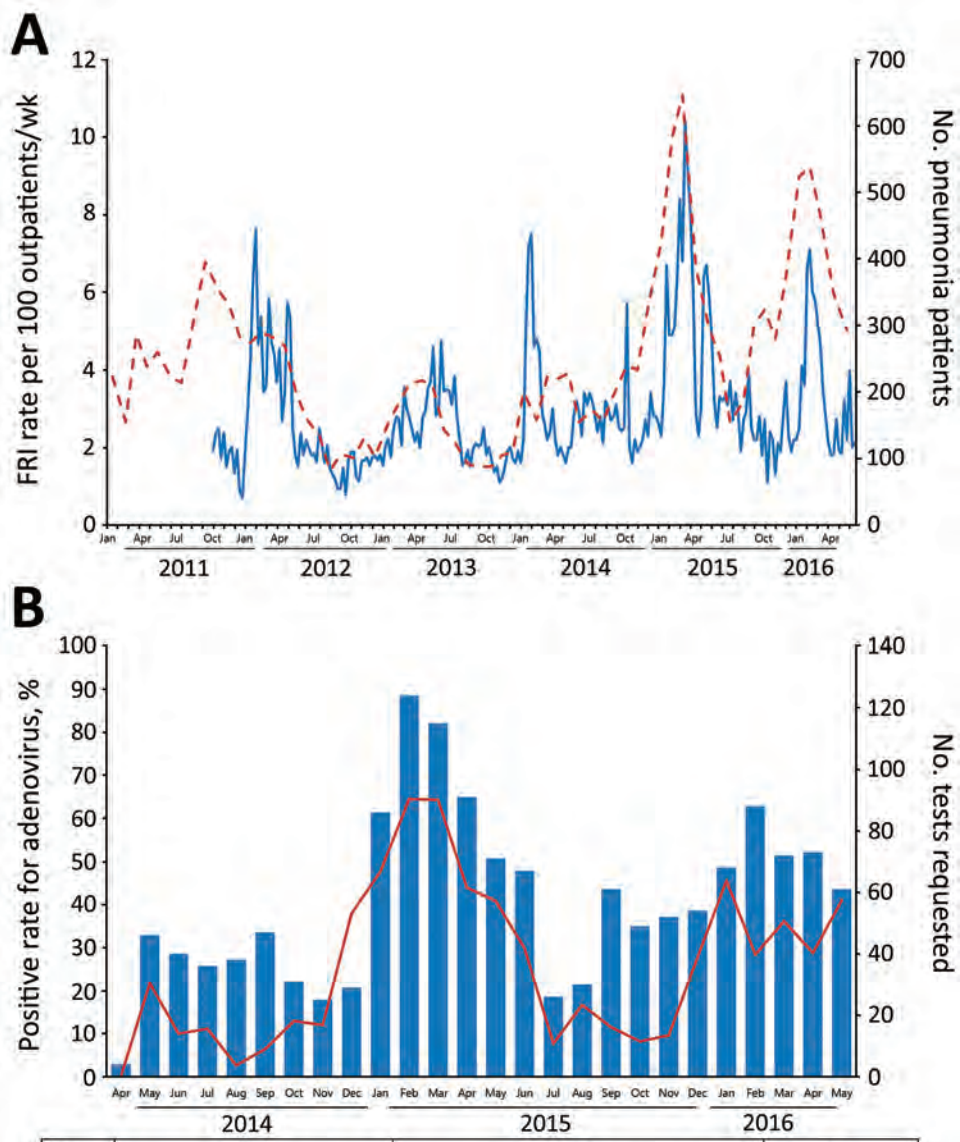

Year	2014									2015											2016				
Positive rate, %	0.0	21.7	10.0	11.1	2.6	6.4	12.9	12.0	37.9	47.7	64.5	64.3	44.0	40.8	29.9	7.7	16.7	11.5	8.2	9.6	27.8	45.6	28.4	36.1	28.8	41.0
No. tested	4	46	40	36	38	47	31	25	29	86	124	115	91	71	67	26	30	61	49	52	54	68	88	72	73	61

Figure 1. A) Weekly febrile respiratory illness (FRI) rate (solid line) and monthly number of pneumonia patients (dashed line) in the South Korea military, 2011–2016. B) Positive rate of human adenovirus from respiratory specimens (red line) and the number of respiratory virus PCR requested (blue bar) from a tertiary military hospital, South Korea, 2014–2016. The rate and number for each month are shown in the table at bottom.

We reviewed the demographic and clinical information of 878 military patients with FRI or pneumonia who were tested for respiratory viruses from October 2014 through May 2016 (Tables 1, 2). Soldiers of lower rank were markedly more likely to infected with HAdV; soldiers serving in the Air Force were less likely. Patients who had been referred from other hospitals were twice as likely to be HAdV-infected than patients who visited the Armed Forces Capital Hospital directly. Rhinorrhea, sore throat, diarrhea, and nausea/vomiting were more common in patients with HAdV infection. The proportion of patients with pneumonia and the hospitalization rate did not differ between those with and without HAdV infection. However, HAdV-infected patients had a significantly higher risk of requiring intensive care or mechanical ventilator support. In the HAdV-infected group, 8 patients required intubation and 1 died; no one in the noninfected group died or required intubation. Length of hospital stay was also significantly longer among those the HAdV-infected group than among those in the noninfected group (12.6 vs. 9.4 days).

We conducted molecular typing by the sequencing of hexon and fiber genes with 74 HAdV-positive respiratory specimens collected from March through June 2016 (methods and general characteristics of the patients are available in the online Technical Appendix Table 2). Among them, 49 samples were successfully sequenced (GenBank numbers in

Table 1. Epidemiologic characteristics of patients with or without identification of HAdV from respiratory specimens by PCR, South Korea, 2014–2016*

Epidemiologic characteristic	Patients with HAdV, n = 447	Patients with other virus PCR negative for HAdV, n = 431	OR (95% CI)	p value
Year				
Apr 2014–May 2015	274 (65.4)	145 (34.6)	3.13 (2.37–4.12)	<0.001
Jun 2015–May 2016	173 (37.7)	286 (62.3)		
Rank				
Recruit or private	251 (70.5)	105 (29.5)	3.98 (2.98–5.31)	<0.001
PFC or higher	196 (37.5)	326 (62.5)		
Service				
Army	423 (52.1)	391 (47.9)	N\A	<0.001
Navy/Marine Corps	20 (50.0)	20 (50.0)		
Air Force	1 (4.8)	20 (95.2)		
Region				
Seoul/Gyeonggi-do	376 (50.0)	376 (50.0)		0.055
Gangwon-do	46 (65.7)	24 (34.3)		
Chungcheong-do	12 (38.7)	19 (61.3)		
Gyeongsang-do	10 (58.8)	7 (41.2)		
Jeolla-do	3 (37.5)	5 (62.5)		
Route of visit				
Direct	330 (47.3)	367 (52.7)	2.03 (1.45–2.85)	<0.001
Referral	117 (64.6)	64 (35.4)		
Age, y, mean (SD)	20.8 (2.0)	22.2 (5.0)		<0.001

*Values are no. (%) except as indicated. HAdV, human adenovirus; NA, not available; OR, odds ratio; PFC, private first class.

online Technical Appendix). Phylogenetic analyses showed that all 49 HAdV strains from South Korea clustered with HAdV-55 strains from China, Singapore, Taiwan, Spain, and the United States (Figure 2).

Conclusions

We describe an outbreak of FRI associated with HAdV in the South Korea military. HAdV is a well-known major cause of FRI in the military, accounting for >50% of FRI and pneumonia cases in military recruits (*1*). Our study also confirmed the predominance of HAdV, which was identified in 49.1% of specimens from patients with FRI or pneumonia. These findings are similar to those of previous studies from South Korea and the United States (*9*,*10*).

The most notable finding of our study is the emergence of HAdV-55 in the South Korea military. HAdV-55 is a novel type that has been associated with a severe clinical course and death in healthy young adults (*7*,*8*). We also found that HAdV infection was associated with intensive care, mechanical ventilator support, and longer hospital stay. In addition, we found that the only patient who died was HAdV infected. From a molecular perspective, HAdV-55 is a novel type with a hexon gene recombination between HAdV-11 and HAdV-14 (*11*). Phylogenetic analysis by using the hexon and fiber gene sequence of 49 strains collected in our study showed that they clustered with previously reported HAdV-55 strains.

Our findings have implications beyond military settings. Spread of infection of traditionally military-associated

Table 2. Clinical characteristics of patients with or without identification of HAdV from respiratory specimens PCR, South Korea, 2014–2016*

Clinical characteristic	Patients with HAdV, n = 447	Patients with other virus or PCR negative for HAdV, n = 431	OR (95% CI)	p value
Presenting symptoms				
Cough†	423 (94.6)	395 (91.9)	1.56 (0.91–2.67)	0.102
Rhinorrhea‡	229 (51.3)	192 (44.7)	1.31 (1.00–1.71)	0.047
Sore throat§	286 (64.3)	207 (48.1)	1.94 (1.48–2.54)	<0.001
Dyspnea¶	60 (13.5)	41 (9.5)	1.48 (0.97–2.25)	0.070
Diarrhea#	125 (33.8)	60 (17.2)	2.46 (1.73–3.49)	<0.001
Nausea/vomiting**	115 (31.0)	58 (16.6)	2.25 (1.58–3.22)	<0.001
Pneumonia	231 (51.7)	250 (58.0)	0.77 (0.59–1.01)	0.060
Hospitalization	277 (62.0)	270 (62.6)	0.97 (0.74–1.28)	0.836
Intensive care	70 (25.3)	30 (11.1)	2.71 (1.70–4.31)	<0.001
Mechanical respiratory support	25 (9.0)	5 (1.9)	5.26 (1.98–13.95)	<0.001
Intubation	8 (2.9)	0	NA	0.005
Death	1 (0.4)	0	NA	0.323
Length of stay, d, mean (SD)	12.6 (9.7)	9.4 (5.0)	NA	<0.001

*Values are no. (%) except as indicated. HAdV, human adenovirus; NA, not available; OR, odds ratio. †n = 877.
‡n = 876.
§n = 875.
¶n = 876.
#n = 719.
**n = 720.

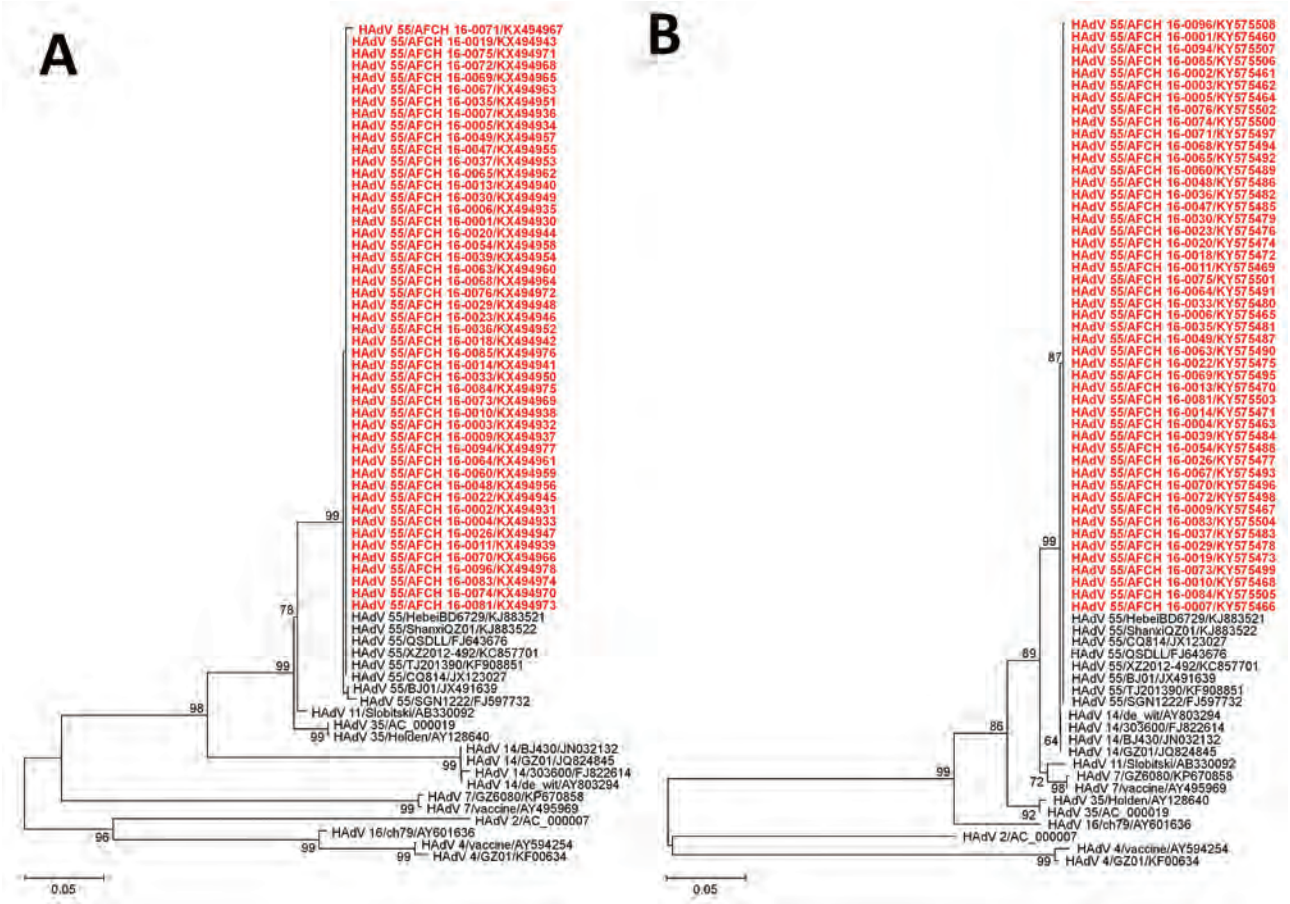

Figure 2. Phylogenetic analysis of human adenoviruses based on the partial nucleotide sequences of hexon (A) and fiber (B) genes, South Korea, 2016. Phylogenetic trees were generated by the neighbor-joining method, using the Kimura 2-parameter method. The percentage of replicate trees in which the associated taxa clustered together in the bootstrap test (1,000 replicates) are shown next to the branches. Red indicates viruses identified in this study. Scale bars denote the number of base substitutions per site.

HAdV types into civilians has been recently reported in the United States and China (*3*,*12*,*13*). Thus, surveillance of HAdV types among both military and civilian populations is warranted; such measures are being implemented by the US Centers for Disease Control and Prevention (Atlanta, GA, USA) (*12*).

Our study has some limitations. First, our findings may not be generalizable due to the retrospective nature of the study. However, the military health system in South Korea provides healthcare exclusively to all military personnel; therefore, epidemiologic information gathered from our surveillance is accurate and comprehensive. Second, we conducted molecular typing with samples collected from February 2016, which was substantially later than the onset of the epidemic. However, HAdV-55 had already been identified in a case series from our center during June 2014–May 2015 (*8*). Because evidence shows that HAdV-55 has been already circulating since early 2014, we believe we can assume that HAdV-55 was the causative agent of the outbreak described in this study. Previously, the HAdV typing study conducted in 2007 reported HAdV-7 as the most prevalent type (*14*). Lack of continuous surveillance makes it difficult to estimate exactly when this novel type was introduced into South Korea.

Further genomic analysis of the collected samples and enhanced surveillance, including of civilian populations, would provide more information on the epidemiology of HAdV infection. In addition, studies are needed on the efficacy of previous vaccines against HAdV-55.

Acknowledgments

We express our sincere gratitude to the healthcare professionals who have been involved in the care of the patients with FRI described in this study.

This work was supported by a grant from the Agency for Defense Development, Republic of Korea (UE134020ID).

Dr. Yoo is a pulmonary physician and medical officer at the Armed Forces Capital Hospital of South Korea. His research interests include pulmonary infectious diseases.

References

1. Lynch JP III, Kajon AE. Adenovirus: epidemiology, global spread of novel serotypes, and advances in treatment and prevention. Semin Respir Crit Care Med. 2016;37:586–602. http://dx.doi.org/10.1055/s-0036-1584923
2. Radin JM, Hawksworth AW, Blair PJ, Faix DJ, Raman R, Russell KL, et al. Dramatic decline of respiratory illness among US military recruits after the renewed use of adenovirus vaccines. Clin Infect Dis. 2014;59:962–8. http://dx.doi.org/10.1093/cid/ciu507
3. Kajon AE, Lu X, Erdman DD, Louie J, Schnurr D, George KS, et al. Molecular epidemiology and brief history of emerging adenovirus 14-associated respiratory disease in the United States. J Infect Dis. 2010;202:93–103. http://dx.doi.org/10.1086/653083
4. Metzgar D, Osuna M, Kajon AE, Hawksworth AW, Irvine M, Russell KL. Abrupt emergence of diverse species B adenoviruses at US military recruit training centers. J Infect Dis. 2007;196:1465–73. http://dx.doi.org/10.1086/522970
5. Lu Q-B, Tong Y-G, Wo Y, Wang H-Y, Liu E-M, Gray GC, et al. Epidemiology of human adenovirus and molecular characterization of human adenovirus 55 in China, 2009-2012. Influenza Other Respi Viruses. 2014;8:302–8. http://dx.doi.org/10.1111/irv.12232
6. Salama M, Amitai Z, Nutman A, Gottesman-Yekutieli T, Sherbany H, Drori Y, et al. Outbreak of adenovirus type 55 infection in Israel. J Clin Virol. 2016;78:31–5. http://dx.doi.org/10.1016/j.jcv.2016.03.002
7. Gu L, Qu J, Sun B, Yu X, Li H, Cao B. Sustained viremia and high viral load in respiratory tract secretions are predictors for death in immunocompetent adults with adenovirus pneumonia. PLoS One. 2016;11:e0160777. http://dx.doi.org/10.1371/journal.pone.0160777
8. Yoon H, Jhun BW, Kim SJ, Kim K. Clinical characteristics and factors predicting respiratory failure in adenovirus pneumonia. Respirology. 2016;21:1243–50. http://dx.doi.org/10.1111/resp.12828
9. Heo JY, Lee JE, Kim HK, Choe KW. Acute lower respiratory tract infections in soldiers, South Korea, April 2011–March 2012. Emerg Infect Dis. 2014;20:875–7. http://dx.doi.org/10.3201/eid2005.131692
10. Padin DS, Faix D, Brodine S, Lemus H, Hawksworth A, Putnam S, et al. Retrospective analysis of demographic and clinical factors associated with etiology of febrile respiratory illness among US military basic trainees. BMC Infect Dis. 2014;14:576. http://dx.doi.org/10.1186/s12879-014-0576-2
11. Walsh MP, Seto J, Jones MS, Chodosh J, Xu W, Seto D. Computational analysis identifies human adenovirus type 55 as a re-emergent acute respiratory disease pathogen. J Clin Microbiol. 2010;48:991–3. http://dx.doi.org/10.1128/JCM.01694-09
12. Scott MK, Chommanard C, Lu X, Appelgate D, Grenz L, Schneider E, et al. Human adenovirus associated with severe respiratory infection, Oregon, USA, 2013–2014. Emerg Infect Dis. 2016;22:1044–51. http://dx.doi.org/10.3201/eid2206.151898
13. Cao B, Huang G-H, Pu Z-H, Qu J-X, Yu X-M, Zhu Z, et al. Emergence of community-acquired adenovirus type 55 as a cause of community-onset pneumonia. Chest. 2014;145:79–86. http://dx.doi.org/10.1378/chest.13-1186
14. Jeon K, Kang CI, Yoon CH, Lee DJ, Kim CH, Chung YS, et al. High isolation rate of adenovirus serotype 7 from South Korean military recruits with mild acute respiratory disease. Eur J Clin Microbiol Infect Dis. 2007;26:481–3. http://dx.doi.org/10.1007/s10096-007-0312-6

Address for correspondence: Kyungmin Huh, Division of Infectious Diseases and Office of Infection Control, Armed Forces Capital Hospital, Seongnam, South Korea; email: kyungminhuh.id@gmail.com; Seong Tae Jeong, The 5th R&D Institute, Agency for Defense Development, Yuseong, P.O. Box 35, Daejeon, 34188, South Korea; email: seongtae@add.re.kr

June 2016: Respiratory Diseases

- Debate Regarding Oseltamivir Use for Seasonal and Pandemic Influenza
- Human Infection with Influenza A(H7N9s) Virus during 3 Major Epidemic Waves, China, 2013–2015
- Integration of Genomic and Other Epidemiologic Data to Investigate and Control a Cross-Institutional Outbreak of *Streptococcus pyogenes*
- Extended Human-to-Human Transmission during a Monkeypox Outbreak in the Democratic Republic of the Congo
- Experimental Infection and Response to Rechallenge of Alpacas with Middle East Respiratory Syndrome Coronavirus

- Use of Population Genetics to Assess the Ecology, Evolution, and Population Structure of *Coccidioides*
- Infection, Replication, and Transmission of Middle East Respiratory Syndrome Coronavirus in Alpacas
- Rapid Detection of Polymyxin Resistance in *Enterobacteriaceae*
- Human Adenovirus Associated with Severe Respiratory Infection, Oregon, 2013–2014

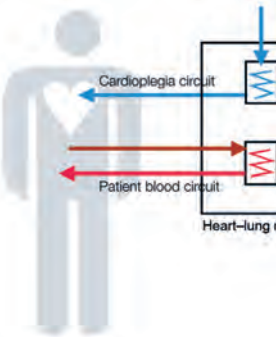

- Heterogeneous and Dynamic Prevalence of Asymptomatic Influenza Virus Infections
- Improved Global Capacity for Influenza Surveillance
- Prevalence of Nontuberculous Mycobacterial Pulmonary Disease, Germany, 2009–2014
- Antibody Response and Disease Severity in Healthcare Worker MERS Survivors
- Epidemiology of Pulmonary Nontuberculous Mycobacterial Disease, Japan
- Elevated Pertussis Reporting in Response to 2011–2012 Outbreak, New York City, New York, USA
- Hemophagocytic Lymphohistiocytosis and Progressive Disseminated Histoplasmosis
- Next-Generation Sequencing of *Mycobacterium tuberculosis*
- MERS-CoV Infection of Alpaca in a Region Where MERS-CoV is Endemic

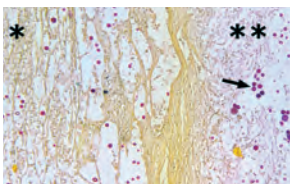

https://wwwnc.cdc.gov/eid/articles/issue/22/6/table-of-contents

EMERGING INFECTIOUS DISEASES™

Stockpiling Ventilators for Influenza Pandemics

Martin I. Meltzer, Anita Patel

For decades, public health officials have been well aware of the importance of planning and preparing for the next influenza pandemic (*1*). An open-access, spreadsheet-based tool, FluSurge 2.0, enables public health officials and hospital administrators to estimate the potential surge in demand that inevitably will occur during the next influenza pandemic. The tool provides estimates for hospital-based services, such as intensive care unit beds and mechanical ventilators (*2*,*3*). Any influenza pandemic has the potential to overwhelm existing hospital capacities, supplies, and readily available means of resupply. Thus, all capable public health services should develop and carry out plans to stockpile critical resources, such as mechanical ventilators, needed to support patients who become severely ill from pandemic influenza (*4*). A major challenge to planning is determining the amount of ventilators to stockpile and considering how to manage them so they are effectively used during the pandemic response.

In this issue (*5*), Huang et al. provide a valuable addition to public health preparedness by presenting a planning tool to help public health officials consider the optimal size of a stockpile of mechanical ventilators, compiled on the basis of data from Texas, USA. Users of their tool also can evaluate where such a stockpile should be stored: a central location, or prepositioned strategically in hospital facilities. To determine how many ventilators to stockpile and where to stockpile them, the authors explicitly include in their tool key factors such as timing of a pandemic's peak locally (not all regions will experience simultaneous peak demands for ventilators); wastage (ventilators not sent to where they are needed, when they are most needed, and/or cannot be used); and expected unmet demand for mechanical ventilators (i.e., when a hospital has more patients who need mechanical ventilation than available ventilators).

All mathematical models have limitations, and some important practical problems related to ventilator preparedness are beyond the reasonable scope of the model by Huang et al. For example, hospitals must accept responsibility for the costs and resources needed to manage and maintain an excess of ventilators that are likely to be unused in the absence of pandemic-related surges in demand for such resources. The authors mention that a potential benefit of stockpiling ventilators at hospitals is to facilitate staff training; however, only a few (1–3) ventilators would be needed to support training needs. Also, once stockpiles are established, the costs of replenishing inventory over time or replacing products to meet changing technology are not considered. The model also assumes that stockpiled ventilators will not be used for noninfluenza patients. In reality, stockpiled ventilators are likely to be simpler ventilators that can be used on more stable patients, thus freeing up other sophisticated ventilators for patients requiring greater respiratory support.

An important aspect of interpreting the results from the model of Huang et al. is the problem of expected unmet demand. There is an upper limit to the number of additional ventilators that any hospital can absorb and use to successfully help treat acutely ill patients needing mechanical ventilation. This limit is determined in large part by the number of trained staff—particularly respiratory therapists, nurses, and technicians—available to ventilate and monitor patients (*6*). That is, the number of machines is less of a constraint than is availability of trained personnel. Huang et al. allow for expected unmet needs, setting a default value of an acceptable level of 5 patients unable to receive mechanical ventilation at any given time. Assuming a moderate, 2009-type influenza pandemic, the authors estimate a 30% chance of this expected unmet need occurring. To meet this level of unmet demand in Texas, planning for a moderate or a severe pandemic requires stockpiling as few as 1,172 or as many as 15,697 ventilators, respectively. However, actually deploying and using such high volumes of mechanical ventilators would be challenging in terms of having enough hospital space and staff to support additional ventilator use. Thus, during moderate and severe pandemics, a higher level of unmet demand might need to be expected. Attending physicians will have to determine who gets access to the limited number of ventilators and who does not. Only a small number of studies describe how physicians might make such allocation decisions for critical, scarce resources (i.e., triage or prioritization) and how they would explain such decisions to the patients and their families (*7*–*9*).

Tools of the type produced by Huang et al. are essential to adequately plan and optimize the use of stockpiled resources during the next influenza pandemic. Such tools, however, are just one part of systematic planning, which should include elements such as the number to be

Author affiliation: Centers for Disease Control and Prevention, Atlanta, Georgia, USA

DOI: https://dx.doi.org/10.3201/eid2306.170434

stockpiled, how and where stockpiles should be held, maintenance of stockpiles, conditions for release, considerations for use, and what to do when stockpiles are insufficient to adequately meet surges in demand.

Dr. Meltzer is an Associate Editor of Emerging Infectious Diseases and leads the Health Economics and Modeling Unit in CDC's Division of Preparedness and Emerging Infections, National Center for Emerging and Zoonotic Infectious Diseases. His research interests include estimating the impact of influenza pandemics and the economics of controlling infectious diseases.

Dr. Patel is a senior advisor and the lead for pandemic medical care and countermeasures with CDC's Influenza Coordination Unit, Division of Viral Diseases, National Center for Immunization and Respiratory Diseases. Her research interests include developing and implementing science-based operational solutions for medical countermeasure needed to support a public health response.

References

1. Meltzer MI, Cox NJ, Fukuda K. The economic impact of pandemic influenza in the United States: priorities for intervention. Emerg Infect Dis. 1999;5:659–71. http://dx.doi.org/10.3201/eid0505.990507
2. Zhang X, Meltzer MI, Wortley PM. FluSurge—a tool to estimate demand for hospital services during the next pandemic influenza. Med Decis Making. 2006;26:617–23. http://dx.doi.org/10.1177/0272989X06295359
3. Centers for Disease Control and Prevention. FluSurge, v. 2.0 [cited 2017 Feb 20]. https://www.cdc.gov/flu/pandemic-resources/tools/flusurge.htm
4. US Department of Health and Human Services. HHS pandemic influenza plan. November 2005 [cited 2017 Feb 20]. https://www.cdc.gov/flu/pandemic-resources/pdf/hhspandemicinfluenzaplan.pdf
5. Huang HC, Araz OM, Morton DP, Johnson GP, Damien P, Clements B, et al. Stockpiling ventilators for influenza pandemics. Emerg Infect Dis. 2017;23:923–30.
6. Ajao A, Nystrom SV, Koonin LM, Patel A, Howell DR, Baccam P, et al. Assessing the capacity of the US health care system to use additional mechanical ventilators during a large-scale public health emergency. Disaster Med Public Health Prep. 2015;9:634–41. http://dx.doi.org/10.1017/dmp.2015.105
7. Christian MD, Hawryluck L, Wax RS, Cook T, Lazar NM, Herridge MS, et al. Development of a triage protocol for critical care during an influenza pandemic. CMAJ. 2006;175:1377–81.
8. Powell T, Christ KC, Birkhead GS. Allocation of ventilators in a public health disaster. Disaster Med Public Health Prep. 2008;2:20–6. http://dx.doi.org/10.1097/DMP.0b013e3181620794
9. Ventilator Document Workgroup, Ethics Subcommittee of the Advisory Committee to the Director, Centers for Disease Control and Prevention. Ethical considerations for decision making regarding allocation of mechanical ventilators during a severe influenza pandemic or other public health emergency [cited 2017 Mar 16]. https://www.cdc.gov/about/pdf/advisory/ventdocument_release.pdf

Address for correspondence: Martin I. Meltzer, Centers for Disease Control and Prevention, 1600 Clifton Rd NE, Mailstop C18, Atlanta, GA 30329-4027, USA; email: qzm4@cdc.gov

The Public Health Image Library (PHIL)

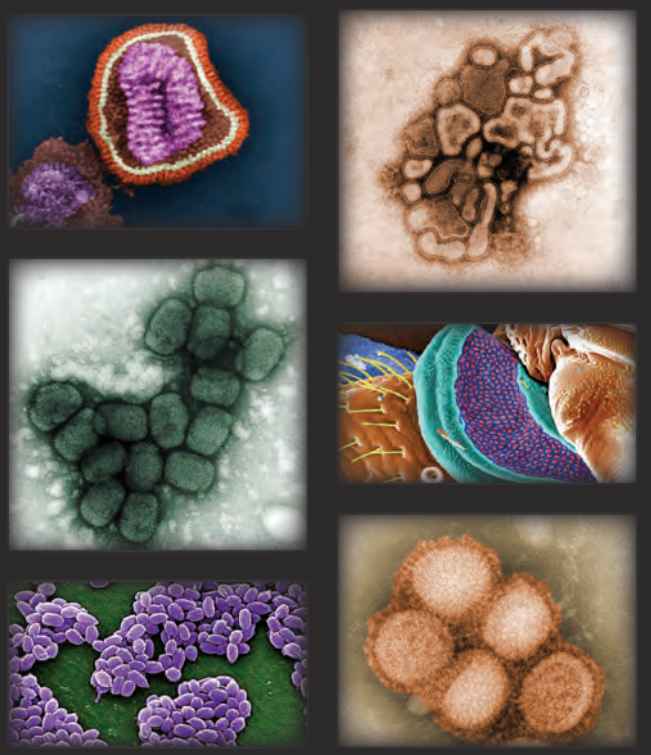

The Public Health Image Library (PHIL), Centers for Disease Control and Prevention, contains thousands of public health-related images, including high-resolution (print quality) photographs, illustrations, and videos.

PHIL collections illustrate current events and articles, supply visual content for health promotion brochures, document the effects of disease, and enhance instructional media.

PHIL images, accessible to PC and Macintosh users, are in the public domain and available without charge.

Visit PHIL at http://phil.cdc.gov/phil

Epidemiologic Survey of Japanese Encephalitis Virus Infection, Tibet, China, 2015

Hui Zhang, Mujeeb Ur Rehman, Kun Li, Houqiang Luo, Yanfang Lan, Fazul Nabi, Lihong Zhang, Muhammad Kashif Iqbal, Suolangsi Zhu, Muhammad Tariq Javed, Yangzom Chamba, Jia Kui Li

Author affiliations: Huazhong Agricultural University College of Veterinary Medicine, Wuhan, China (H. Zhang, M.U. Rehman, K. Li, H. Luo, Y. Lan, F. Nabi, L. Zhang, M.K. Iqbal, J.K. Li); Tibet Agriculture and Animal Husbandry College, Linzhi, Tibet, China (S. Zhu, Y. Chamba, J.K. Li); University of Agriculture, Faisalabad, Pakistan (M.T. Javed)

DOI: https://dx.doi.org/10.3201/eid2306.152115

We investigated Japanese encephalitis virus (JEV) prevalence in high-altitude regions of Tibet, China, by using standard assays to test mosquitoes, pigs, and humans. Results confirmed that JEV has spread to these areas. Disease prevention and control strategies should be used along with surveillance to limit spread of JEV in high-altitude regions of Tibet.

Japanese encephalitis virus (JEV) is the causative agent of a viral encephalitis that is a major public health threat in most parts of East and Southeast Asia (*1*,*2*). Tibet, China, has been considered a nonepidemic area for JEV because its mean elevation is >3,100 m, and the relatively low temperatures at the elevation do not support JEV transmission between mosquitoes, reservoirs, and amplifying hosts (*2*). However, this situation in Tibet has probably changed due to increased pig farming in the region and increased travel between Tibet and areas where JEV is endemic (*3*–*5*). To test our hypothesis, we tested for JEV in mosquitoes and measured JEV-specific IgM in swine and humans living in a high-altitude region of Tibet.

We conducted the study in Nyingchi District (elevation 3,100 m) in southeastern Tibet. The mean temperature during the study period ranged from 11.3°C to 22.4°C. Swine and humans included in the study had no history of travel to JEV-endemic areas.

To determine whether mosquitoes were infected with JEV, we collected 8,330 mosquitoes (belonging to 9 genera and 4 species) near pig sties and human residences in Nyingchi, Mainling, and Gongbo'gyamda Counties. From those 8,330 mosquitoes, we chose 2,655 JEV vector mosquitoes: 330 (3.96%) *Culex tritaeniorhynchus*, 45 (0.54%) *C. bitaeniorhynchus*, and 2,280 (27.37%) *C. pipiens* mosquitoes. To detect JEV, we used the TIANamp Virus DNA/RNA Kit (TianGen, Beijing, China) with pools of whole-body *Culex* mosquito extracts; we analyzed the samples by reverse transcription PCR (RT-PCR) amplification using the Quant One-Step RT-PCR Kit (TianGen) and primers specific for the JEV nonstructural 1 gene (*6*). Of 11 *C. tritaeniorhynchus* and 69 *C. pipiens* mosquito pools, 7 (63.6%) and 2 (2.9%), respectively, were positive for JEV by RT-PCR; the 1 *C. bitaeniorhynchus* mosquito pool was not positive for JEV (Table).

To determine the origin of JEV in pigs, we collected a total of 454 serum samples from 1- to 6-month-old pigs from local slaughterhouses. We analyzed the samples for JEV IgM by using a commercial ELISA kit as previously described (*7*). We used the χ^2 test and SPSS software (SPSS Inc., Chicago, IL, USA) to analyze all data; $p<0.05$ was considered significant.

The overall seroprevalence of JEV IgM in the pigs was 5.07%. The percentage of positive samples from Nyingchi County (3.25%) was significantly lower than that from Mainling Country (7.81%); no serum samples from Gongbo'gyamda County were JEV-positive (Table). The difference in seroprevalence of JEV in male (4.62%) and female (5.67%) pigs was not statistically significant.

To determine the prevalence of JEV infection among persons, we collected blood samples from 364 healthy human volunteers residing in the 3 counties and analyzed the samples for JEV IgM by using a commercial ELISA kit as previously described (*8*). JEV seroprevalence was11.71% for the 1- to 23-year-old age group, 13.43% for the 24- to 45-year-old age group, and 4.20% for the >45-year-old age group (Table). Seroprevalence was significantly higher among persons 1–23 or 24–45 years of age, compared with persons >45 years of age, suggesting that 1) younger persons may have greater exposure risks than persons >45 years of age, 2) JEV is a relative new introduction in the area as a result of the changing (i.e., warmer) climate, and 3) younger persons may travel more frequently than older persons to lower elevations where JEV is endemic. An IgG-based survey might identify more JEV disease, even in persons who showed no symptoms of the disease.

JEV seroprevalence was significantly higher in rural populations (6.87%) compared with urban population (3.02%). The spread of JEV may be increased by amplifying hosts (pigs); thus, the lower prevalence of JEV in urban residents may be associated with a lower number of pig farms in urban areas compared with rural villages in Nyingchi District.

In conclusion, we found that JEV infection is prevalent in a high-altitude region of Tibet that was previously considered to be free from JEV. Factors such as increased tourism (*9*), increased mean summer temperatures, increased

Table. Japanese encephalitis virus IgM–positive pigs and humans and Japanese encephalitis virus-positive *Culex* mosquitoes in Nyingchi District, Tibet, China, 2015*

Category, variable	No. IgM positive/no. tested (%)		Total no. positive/total no. tested (%)
	Male pig or person	Female pig or person	
Pigs			
County location			
Nyingchi	3/146 (2.05)	5/100 (5.00)	8/246 (3.25)
Mainling	9/105 (8.57)	6/87 (6.90)	15/192 (7.81)
Gongbo'gyamda	0/9	0/7	0/16
Total	12/260 (4.62)	11/194 (5.67)	23/454 (5.07)
Humans			
County location			
Nyingchi	6/66 (9.09)	11/93 (11.83)	17/159 (10.69)
Mainling	8/58 (13.79)	9/65 (13.85)	17/123 (13.82)
Gongbo'gyamda	1/43 (2.33)	1/39 (2.56)	2/82 (2.44)
Total	15/167 (8.98)	21/197 (10.66)	36/364 (9.89)
Age group, y			
1–23	6/57 (10.53)	7/54 (12.96)	13/111 (11.71)
24–45	7/54 (12.96)	11/80 (13.75)	18/134 (13.43)
>45	2/56 (3.57)	3/63 (4.76)	5/119 (4.20)
Total	15/167 (8.98)	21/197 (10.66)	36/364 (9.89)
Culex mosquitoes†			
C. tritaeniorhynchus	ND	ND	7/11 (0.636)‡
C. bitaeniorhynchus	ND	ND	0/1‡
C. pipiens	ND	ND	2/69 (0.029)‡

*Except as indicated, data are no. (%). ND, Not done.
†Denominator indicates no. in pool.
‡Maximum likelihood estimates (no. pools positive for JEV by reverse transcription PCR).

movement between the study area and nearby JEV-endemic regions, inadequate public health systems, increased pig farming, increased migration of water birds, and the absence of a compulsory immunization policy may contribute to emergence of this disease (*3*,*4*,*9*,*10*). Disease prevention and control strategies should be used along with surveillance to limit the spread of JEV in high-altitude regions of Tibet.

This study was supported by the Key Science Fund of the Science and Technology Agency of Tibet Autonomous Region, the Twelfth Five-Year National Science and Technology Support Project (grant no. 2012BAD3B03), and the Sustentation Fund (the serology of *Toxoplasma gondii* in Tibetan pigs) of the Huazhong Agricultural University (grant no. 52209-814121).

Mr. Zhang is a PhD scholar in the Department of Clinical Veterinary Medicine, Huazhong Agricultural University, Wuhan, China. His research has focused on the surveillance of emerging infectious diseases by molecular epidemiology analysis and the analysis of pathogenicity mechanisms.

References

1. Misra UK, Kalita J. Overview: Japanese encephalitis. Prog Neurobiol. 2010;91:108–20. http://dx.doi.org/10.1016/j.pneurobio.2010.01.008
2. Centers for Disease Control and Prevention (CDC). Japanese encephalitis surveillance and immunization—Asia and the Western Pacific, 2012. MMWR Morb Mortal Wkly Rep. 2013;62:658–62.
3. Li YX, Li MH, Fu SH, Chen WX, Liu QY, Zhang HL, et al. Japanese encephalitis, Tibet, China. Emerg Infect Dis. 2011;17:934–6. http://dx.doi.org/10.3201/eid1705.101417
4. National Bureau of Statistics of the People's Republic of China. National data. Number of hogs at year-end in Tibet from 1995 to 2014 [cited 2015 Dec 29]. http://data.stats.gov.cn/english/easyquery.htm
5. Liu Q, Cao L, Zhu XQ. Major emerging and re-emerging zoonoses in China: a matter of global health and socioeconomic development for 1.3 billion. Int J Infect Dis. 2014;25:65–72. http://dx.doi.org/10.1016/j.ijid.2014.04.003
6. Hua RH, Liu LK, Chen ZS, Li YN, Bu ZG. Comprehensive mapping antigenic epitopes of NS1 protein of Japanese encephalitis virus with monoclonal antibodies. PLoS One. 2013;8:e67553. http://dx.doi.org/10.1371/journal.pone.0067553
7. Pant GR, Lunt RA, Rootes CL, Daniels PW. Serological evidence for Japanese encephalitis and West Nile viruses in domestic animals of Nepal. Comp Immunol Microbiol Infect Dis. 2006;29:166–75. http://dx.doi.org/10.1016/j.cimid.2006.03.003
8. Moore CE, Blacksell SD, Taojaikong T, Jarman RG, Gibbons RV, Lee SJ, et al. A prospective assessment of the accuracy of commercial IgM ELISAs in diagnosis of Japanese encephalitis virus infections in patients with suspected central nervous system infections in Laos. Am J Trop Med Hyg. 2012;87:171–8. http://dx.doi.org/10.4269/ajtmh.2012.11-0729
9. Cao L, Fu S, Gao X, Li M, Cui S, Li X, et al. Low protective efficacy of the current Japanese encephalitis vaccine against the emerging genotype 5 Japanese encephalitis virus. PLoS Negl Trop Dis. 2016;10:e0004686. http://dx.doi.org/10.1371/journal.pntd.0004686
10. Prosser DJ, Cui P, Takekawa JY, Tang M, Hou Y, Collins BM, et al. Wild bird migration across the Qinghai–Tibetan plateau: a transmission route for highly pathogenic H5N1. PLoS One. 2011;6:e17622. http://dx.doi.org/10.1371/journal.pone.0017622

Address for correspondence: Jia Kui Li, Veterinary Clinical Medicine, College of Veterinary Medicine, Huazhong Agricultural University, Wuhan, Hubei 430070, China; email: lijk210@sina.com

High Frequency of Mayaro Virus IgM among Febrile Patients, Central Brazil

Sandra Brunini, Divânia Dias Silva França, Juliana Brasiel Silva, Leandro Nascimento Silva, Flúvia Pereira Amorim Silva, Mariana Spadoni, Giovanni Rezza

Author affiliations: Universidade Federal de Goiás, Goiânia, Brazil (S. Brunini); Secretaria Municipal de Saúde, Goiânia (D.D.S. França, J.B. Silva, L.N. Silva, F.P.A. Silva); Universidade Federal do Paraná, Paranà, Brazil (M. Spadoni); Istituto Superiore di Sanità, Rome, Italy (G. Rezza)

DOI: https://dx.doi.org/10.3201/eid2306.160929

Mayaro virus (MAYV), an *Aedes* mosquito–borne alphavirus, is endemic to Brazil and other South America countries. We investigated dengue- and chikungunya-negative febrile patients visiting rural areas near Goiânia, Goiás, and found a high proportion (55%) of MAYV IgM. Our findings suggest the presence of highly endemic foci of MAYV in central Brazil.

Mayaro virus (MAYV) is an *Aedes* mosquito–borne alphavirus of the New World, transmitted mainly by tree canopy–dwelling *Haemagogus* spp. mosquitoes, was discovered in Trinidad in 1954. MAYV causes a dengue-like acute febrile illness with arthralgic manifestations (*1*). Exposure to MAYV has been reported in several countries of Central and South America, and Mayaro fever has been identified in French Guiana, Suriname, Venezuela, Peru, Bolivia, and Brazil (*2*,*3*). In Brazil, Mayaro fever has been reported in the Amazon region (*2*,*4*) and in Mato Grosso (*5*,*6*).

At the end of 2014, after chikungunya virus (CHIKV) spread in South America, the Brazil Ministry of Health enhanced the surveillance system for dengue-like illness. Accordingly, febrile patients attending primary care centers are tested for dengue virus (DENV) infection by using viral antigen (NS1), virus isolation, or reverse transcription PCR (up to 5 days after symptom onset), and/or ELISA for IgM (after the sixth day). DENV-negative patients fitting the clinical and epidemiologic criteria for chikungunya set by the Ministry of Health (http://www.saude.gov.br) are notified to the Center for Strategic Information in Health Surveillance of Goiânia city for further investigation.

Blood samples collected during June 1, 2014–June 30, 2015, were stored at –20°C and sent to the Department of Arbovirology and Hemorrhagic Fevers, Instituto Evandro Chagas (Belém, Brazil), to be evaluated for CHIKV by an IgM-capture ELISA (MAC ELISA; Centers for Disease Control and Prevention, Atlanta, GA, USA). A subsample of CHIKV-negative serum collected during December 2014–June 2015 was tested by hemagglutination inhibition (HI) (*7*) against the most common arboviruses. We evaluated serum samples with monotypical or heterotypic reactivity to alphaviruses, with HI titers ≥40 using an IgM MAC ELISA for MAYV, as described by Kuno (*8*) and then modified (*9*). The results were sent to the Center for Strategic Information in Health Surveillance for further clinical and epidemiologic investigations.

We tested 75 samples from DENV-negative patients for CHIKV. Five of the 31 DENV-negative persons from whom serum was collected during June–December 2014 and none of the 44 from January–June 2015 were positive for CHIKV IgM. Two additional samples yielded indeterminate results for CHIKV.

Of 27 CHIKV-negative samples tested by HI, 16 were reactive to alphaviruses (median titer 160 [range 80–1,280]); of these, 15 (56%) were confirmed as positive by IgM MAC ELISA for MAYV, and 1 sample was borderline. The median interval between symptom onset and serum collection was 37 days (range 12–167 days).

Patients were a median of 45 years of age (range 30–70 years). Fourteen were women. Patients' educational level was high; 11 (73%) patients had >8 years' education, and 47% had >12 years' education.

All the patients with an antibody profile suggesting recent MAYV infection resided in Goiânia but had traveled to rural areas in the 15 days before symptom onset. Twelve patients had visited farms or small holdings in the forests around towns located 34 km (Hidrolandia) and 46 km (Bela Vista) from Goiânia (online Technical Appendix Figure, https://wwwnc.cdc.gov/EID/article/23/6/16-0929-Techapp1.pdf). In particular, 7 patients had been around Bela Vista and 5 in the area of Hidrolandia, whereas only 1 had been near Pontalina and 2 in Itacaja (Tocantins), which is outside the state of Goiás. Ten of these 11 patients reported engaging in recreational activities.

The high frequency of MAYV IgM detection among febrile patients in Goiânia is surprising. Identification of recent infections most likely acquired in rural areas and forests around the city of Goiânia indicates the existence of active foci where a sylvatic cycle of MAYV is established. The MAYV belt around Goiânia, where epizootics of jungle yellow fever were also reported (http://www.paho.org/hq/index.php?option=com_docman&task=doc_view&Itemid=270&gid=34247&lang=en), is represented by a wet area hosting small primates, which may play a role as virus amplifier.

Our conclusions are subject to several limitations. First, selection bias could affect findings regarding the proportion of MAYV recent infections because of the lack of systematic testing for dengue-like illness. Second, we did not conduct PCR to identify acute infections because

Table. Clinical characteristics of 15 patients positive for IgM against Mayaro virus, Goiânia, Goiás, Brazil, June 2014–June 2015

Sign or symptom	No. (%) patients
Fever	15 (100)
Arthralgia	14 (93)
Joint edema	14 (93)
Rash	14 (93)
Headache	13 (87)
Weakness	13 (87)
Myalgia	12 (80)
Eye pain	8 (53)
Icterus	4 (27)
Photophobia	3 (20)
Severe itching	3 (20)
Lymphadenopathy	2 (13)
Vomiting	2 (13)

the samples were collected after the viremic phase. Third, plaque-reduction neutralization testing was not performed, and because of the lack of convalescent serum, IgG seroconversion or titer increase were not evaluated; however, MAC ELISA is considered a valid technique for diagnosing recently acquired infection with MAYV (*10*). Finally, the frequency of rash (Table), higher than in other case series (*4*), might be overestimated because of stringent selection criteria used for MAYV testing.

In conclusion, infection with MAYV occurs more frequently than expected in central Brazil. Mayaro fever should be considered in the differential diagnosis with DENV, CHIKV, and Zika virus infections in areas characterized by arbovirus cocirculation.

Acknowledgment

We thank Lívia Carício Martins for supporting testing activities.

Dr. Brunini is an associate professor at the Faculty of Nursing, Federal University of Goiás. Her primary research interests include infectious disease epidemiology and HIV and sexually transmitted diseases.

References

1. Anderson CR, Downs WG, Wattley GH, Ahin NW, Reese AA. Mayaro virus: a new human disease agent. II. Isolation from blood of patients in Trinidad, B.W.I. Am J Trop Med Hyg. 1957;6:1012–6.
2. Azevedo RSS, Silva EVP, Carvalho VL, Rodrigues SG, Nunes-Neto JP, Monteiro H, et al. Mayaro fever virus, Brazilian Amazon. Emerg Infect Dis. 2009;15:1830–2. http://dx.doi.org/10.3201/eid1511.090461
3. Figueiredo ML, Figueiredo LTM. Emerging alphaviruses in the Americas. Rev Soc Bras Med Trop. 2014;47:677–83. http://dx.doi.org/10.1590/0037-8682-0246-2014
4. Mourão MP, Bastos Mde S, de Figueiredo RP, Gimaque JB, Galusso Edos S, Kramer VM, et al. Mayaro fever in the city of Manaus, Brazil, 2007–2008. Vector Borne Zoonotic Dis. 2012:42–6. http://dx.doi.org/10.1089/vbz.2011.0669
5. Zuchi N, Heinen LB, Santos MA, Pereira FC, Slhessarenko RD. Molecular detection of Mayaro virus during a dengue outbreak in the state of Mato Grosso, central-west Brazil. Mem Inst Oswaldo Cruz. 2014;109:820–3. http://dx.doi.org/10.1590/0074-0276140108
6. Pauvolid-Corrêa A, Juliano RS, Campos Z, Velez J, Nogueira RM, Komar N. Neutralising antibodies for Mayaro virus in Pamtanal, Brazil. Mem Inst Oswaldo Cruz. 2015;110:125–33.
7. Shope RE. The use of a microhemagglutination-inhibition test to follow antibody response after arthropod-borne virus infection in a community of forest animals. An Microbiol (Rio J). 1963;11 (Pt A):167–71.
8. Kuno G, Gómez I, Gubler DJ. Detecting artificial anti-dengue IgM immune complexes using an enzyme-linked immunosorbent assay. Am J Trop Med Hyg. 1987;36:153–9.
9. Vasconcelos PFC, Travassos Da Rosa JF, Guerreiro SC, Dégallier N, Travassos Da Rosa ES, Travassos Da Rosa AP. First register of an epidemic caused by Oropouche virus in the states of Maranhão and Goiás, Brazil [in Portuguese]. Rev Inst Med Trop Sao Paulo. 1989;31:271–8. http://dx.doi.org/10.1590/S0036-46651989000400011
10. Figueiredo LTM, Nogueira RMR, Cavalcanti SMB, Schatzmayr H, da Rosa AT. Study of two different enzyme immunoassays for the detection of Mayaro virus antibodies. Mem Inst Oswaldo Cruz. 1989;84:303–7. http://dx.doi.org/10.1590/S0074-02761989000300003

Address for correspondence: Giovanni Rezza, Department of Infectious Diseases, Istituto Superiore di Sanità, Viale Regina Elena 161, 00142 Rome, Italy; email: giovanni.rezza@iss.it

Ebola Virus Imported from Guinea to Senegal, 2014

Daye Ka,[1] Gamou Fall,[1] Viviane Cissé Diallo, Ousmane Faye, Louise Deguenonvo Fortes, Oumar Faye, Elhadji Ibrahim Bah, Kadia Mbaye Diallo, Fanny Balique, Cheikh Tidiane Ndour, Moussa Seydi,[2] Amadou Alpha Sall[2]

Author affiliations: Centre Hospitalier Universitaire de Fann, Dakar, Senegal (D. Ka, V. Cissé Diallo, L. Deguenonvo Fortes, K.M. Diallo, C.T. Ndour, M. Seydi); Institut Pasteur de Dakar, Dakar (G. Fall, Ousmane Faye, Oumar Faye, F. Balique, A.A. Sall); Hôpital National Donka, Conakry, Guinea (E.I. Bah)

DOI: https://dx.doi.org/10.3201/eid2306.161092

In March 2014, the World Health Organization declared an outbreak of Ebola virus disease in Guinea. In August 2014, a case caused by virus imported from Guinea occurred in Senegal, most likely resulting from nonsecure funerals and travel. Preparedness and surveillance in Senegal probably prevented secondary cases.

[1]These authors contributed equally to this article.

[2]These authors contributed equally to this article.

Ebola virus disease (EVD) is a hemorrhagic fever caused by Ebola virus (EBOV); the mortality rate is high (*1*,*2*). EBOV was discovered in 1976, simultaneously in Zaire (now the Democratic Republic of the Congo) and Sudan (*3*,*4*). Since then, small to large outbreaks have occurred sporadically in the Democratic Republic of the Congo, Sudan, Gabon, Uganda, Côte d'Ivoire, and Congo (*5*–*7*).

In March 2014, the World Health Organization (WHO) reported an EVD outbreak caused by Zaire EBOV in Guinea (*8*,*9*). The main feature of this outbreak was its extension into urban areas and neighboring countries (Liberia, Sierra Leone, Nigeria, Senegal, Mali). Ten countries on 3 continents were affected; 28,646 confirmed, probable, and suspected cases and 11,323 deaths were recorded.

In August 2014, Senegal was the fifth country in Africa to be affected by imported EBOV (*10*). We described this case, the patient's itinerary and epidemiologic links with confirmed case-patients in Guinea, and the evolution of the disease and the virus.

The patient was a 21-year-old man from Forecariah, Guinea, who had traveled by land to Senegal during the night of August 13–14, 2014. The date of his illness onset was August 16, 2014; symptoms were fever, vomiting, diarrhea, yellow or black feces, anorexia, and asthenia. On August 18, he visited a suburban medical center in the suburbs of Dakar, where he received treatment for malaria: quinine, antipyretic and antimicrobial medications, and intravenous rehydration. Diarrhea and vomiting stopped on day 4 after illness onset, but fever and asthenia persisted. On August 26, the patient was admitted to Fann Hospital, Dakar, with slight dehydration, fever (39.2°C), and herpetic lesions. Because no epidemiologic link with EVD was established, the patient was not isolated.

On August 27, a total of 12 members of the patient's family, all suspected of having EVD, were admitted to an Ebola treatment center in Conakry, Guinea; test results indicated EBOV positivity for 6. Epidemiologic investigation indicated that a member of this family had traveled to Dakar and was hospitalized. The Epidemic Management Committee set up by WHO in Guinea established an epidemiologic link between the patient in Fann Hospital and the confirmed case-patients in Guinea and quickly informed the health authorities in Senegal. The patient in Fann Hospital finally acknowledged that he had attended his uncle's nonsecure funeral in Guinea on August 10, before coming to Dakar (Figure).

On August 28, the man was transferred to an isolation center, and blood samples were sent to the Institut Pasteur laboratory in Dakar, a WHO-approved collaborating

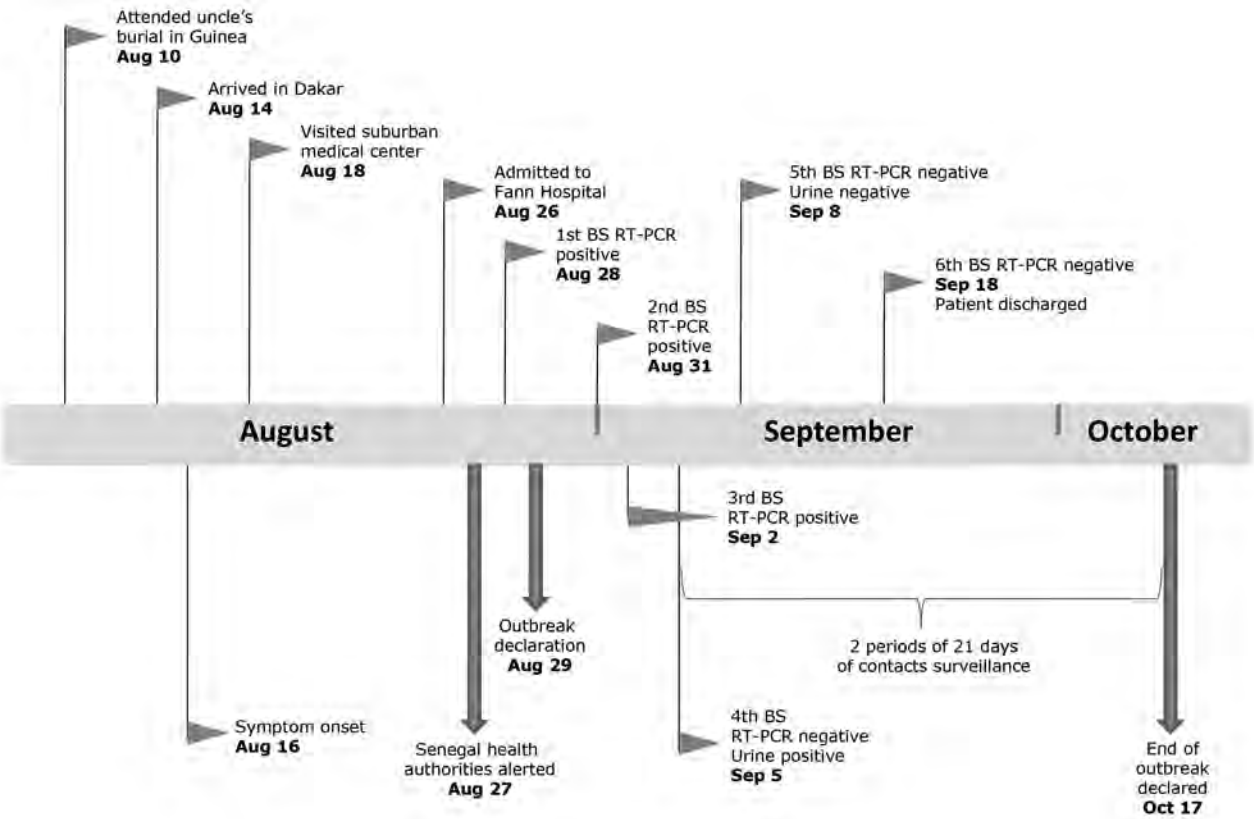

Figure. Timeline for case of Ebola virus disease imported into Senegal from Guinea, 2014. Flags indicate patient information; arrows indicate public health actions. BS, blood sample; RT-PCR, reverse transcription PCR.

Centre for EBOV diagnostics. Real-time reverse transcription PCR (RT-PCR) was positive for Zaire EBOV; viral load was 2.04×10^4 genome copies/mL. ELISA of the same sample detected Zaire EBOV–specific IgM (titer 1:400) and IgG (titer 1:3,200). This case of EVD in Senegal was reported to WHO on August 29. The patient received supportive care, and his clinical course progressed well; on August 31, he was apyrexic and his asthenia had decreased. In terms of virus evolution, a second blood sample tested on day 18 after illness onset showed diminution of viral load (4.96×10^3 genome copies/mL) and an IgG titer increase to 1:6,400. A third blood sample collected on day 20 showed a negative RT-PCR result, but a urine sample collected the same day showed a positive result with a viral load of 2.04×10^4 genome copies/mL. RT-PCRs of blood and urine collected on days 24 and 34 were negative, and serologic analyses showed a high IgG titer (1:12,800).

The patient was declared cured on September 18, 2014. Epidemiologic investigations revealed a total of 74 contacts in Senegal, including 41 healthcare workers (from the suburban medical center and Fann Hospital). Symptoms developed in 5 of these contacts, but their test results were negative for EBOV. No secondary case was detected after 42 days of monitoring, and the outbreak in Senegal was declared over on October 17, 2014, with only 1 confirmed case reported.

The case-patient's low viral load, detected during the first RT-PCR 10 days after illness onset, probably explains the absence of secondary cases in Fann Hospital. However, the absence of secondary cases in the suburban medical center that the patient had visited on days 3–4 after illness onset and among the family members in Dakar is a rare feature of EVD. The preparedness and surveillance established in Senegal after announcement of EVD in Guinea led to training of healthcare workers for proper use of protective equipment and security procedures with any patient, which probably prevented virus spread in the suburban medical center. This case of EBOV importation from Guinea to Senegal confirms the problems encountered with Ebola outbreak management, including the roles of nonsecure funerals and travel in virus spread.

Acknowledgments

We thank Moussa Dia, El Hadji Abdourahmane Faye, Ousmane Kébé, Khardiata Mbaye, Davy Evrard Kiori, and Oumar Ndiaye for their excellent technical assistance in laboratory diagnosis.

This work was supported by grants from the Institut Pasteur de Dakar, Senegal, and the Ministry of Health, Senegal.

Dr. Ka is an infectious disease physician who works in the Infectious and Tropical Diseases Clinic, Fann Hospital, Dakar, Senegal. His research interests are EVD, HIV, and hepatitis. Dr. Fall is a virologist who works at Arbovirus and Viral Hemorrhagic Fever Unit, Institut Pasteur de Dakar, Senegal. Her research interests include arbovirus–vector interactions, mechanisms of arbovirus transmission, and public health activities such as diagnosis of arboviruses and hemorrhagic fever viruses.

References

1. Cenciarelli O, Pietropaoli S, Malizia A, Carestia M, D'Amico F, Sassolini A, et al. Ebola virus disease 2013–2014 outbreak in west Africa: an analysis of the epidemic spread and response. Int J Microbiol. 2015;2015:769121. http://dx.doi.org/10.1155/2015/769121
2. Feldmann H, Klenk HD. Filoviruses. In: S. Baron, editor. Medical Microbiology, 4th ed. Galveston (TX): University of Texas Medical Branch; 1996.
3. World Health Organization. Report of an International Commission: Ebola haemorrhagic fever in Zaïre, 1976. Bull World Health Organ. 1978;56:271e93.
4. World Health Organization/International Study Team. Ebola haemorrhagic fever in Sudan, 1976. Report of a WHO/International Study Team. Bull World Health Organ. 1978;56:247–70.
5. Centers for Disease Control and Prevention. Outbreaks chronology: Ebola virus disease [cited 2015 Aug 2]. http://www.cdc.gov/vhf/ebola/outbreaks/history/chronology.html
6. World Health Organization. Ebola virus disease [cited 2015 Nov 28]. http://www.who.int/mediacentre/factsheets/fs103/en/
7. Colebunders R, Borchert M. Ebola haemorrhagic fever—a review. J Infect. 2000;40:16–20. http://dx.doi.org/10.1053/jinf.1999.0603
8. World Health Organization. Ebola virus disease in Guinea [cited 2015 Aug 18]. http://www.who.int/csr/don/2014_03_23_ebola/en
9. Baize S, Pannetier D, Oestereich L, Rieger T, Koivogui L, Magassouba N, et al. Emergence of Zaire Ebola virus disease in Guinea. N Engl J Med. 2014;371:1418–25. http://dx.doi.org/10.1056/NEJMoa1404505
10. World Health Organization. Ebola virus disease update—Senegal [cited 2014 Nov 15] http://www.who.int/csr/don/2014_08_30_ebola/en/

Address for correspondence: Ousmane Faye, Virology Pole, Institut Pasteur de Dakar, BP 220 Dakar, Senegal; email: ofaye@pasteur.sn

Tick-Borne Encephalitis Virus in Ticks and Roe Deer, the Netherlands

Setareh Jahfari, Ankje de Vries, Jolianne M. Rijks, Steven Van Gucht, Harry Vennema, Hein Sprong, Barry Rockx

Author affiliations: National Institute for Public Health and the Environment, Bilthoven, the Netherlands (S. Jahfari, A. de Vries, H. Vennema, H. Sprong, B. Rockx); Utrecht University, Utrecht, the Netherlands (J.M. Rijks); Scientific Institute of Public Health, Brussels, Belgium (S. Van Gucht)

DOI: https://dx.doi.org/10.3201/eid2306.161247

We report the presence of tick-borne encephalitis virus (TBEV) in the Netherlands. Serologic screening of roe deer found TBEV-neutralizing antibodies with a seroprevalence of 2%, and TBEV RNA was detected in 2 ticks from the same location. Enhanced surveillance and awareness among medical professionals has led to the identification of autochthonous cases.

Tick-borne encephalitis virus (TBEV) can infect humans, causing febrile illness; neurologic complications include encephalitis (*1*). TBEV is transmitted through bites of infected ticks to many animals, including deer, which serve as feeding hosts for ticks (*2*,*3*). Expansion of TBEV subtypes has been reported (*4*). Reports of TBEV-neutralizing antibodies in wildlife and cattle in Belgium prompted us to reinvestigate the presence of TBEV in the Netherlands (*5*,*6*).

During January–September 2010, hunters collected 297 blood samples from roe deer (*Capreolus capreolus*) from locations across the Netherlands. We used a commercial ELISA to detect TBEV-reactive antibodies in roe deer serum samples. Serologic screening of all 297 samples by ELISA yielded 6 positive and 8 borderline results. All positive, 7 borderline, and 3 negative serum samples were confirmed by testing in a TBEV serum neutralization test (SNT), with the Neudörfl strain as the accepted prototype TBEV-EU, formerly called central European encephalitis virus (*5*). Five of 6 ELISA positive samples and 1 of 7 borderline samples were confirmed positive by SNT. Five of the 6 SNT-confirmed roe deer were shot at or near a popular recreation area, the National Park Sallandse Heuvelrug (Figure, panel A).

In response to the serologic findings, we collected 1,160 nymph and 300 adult *Ixodes ricinus* ticks by blanket dragging in 7 locations at the national park in September 2015. We extracted RNA from pools of 5 nymphs or 2 adults (*7*) and tested for flavivirus by using a reverse transcription quantitative PCR. We detected flavivirus RNA in 1 nymph pool and 1 pool of adult female ticks.

To obtain sequences of the 2 reverse transcription quantitative PCR–positive samples, we used primers and protocols as described (*8*). Both sequences obtained from

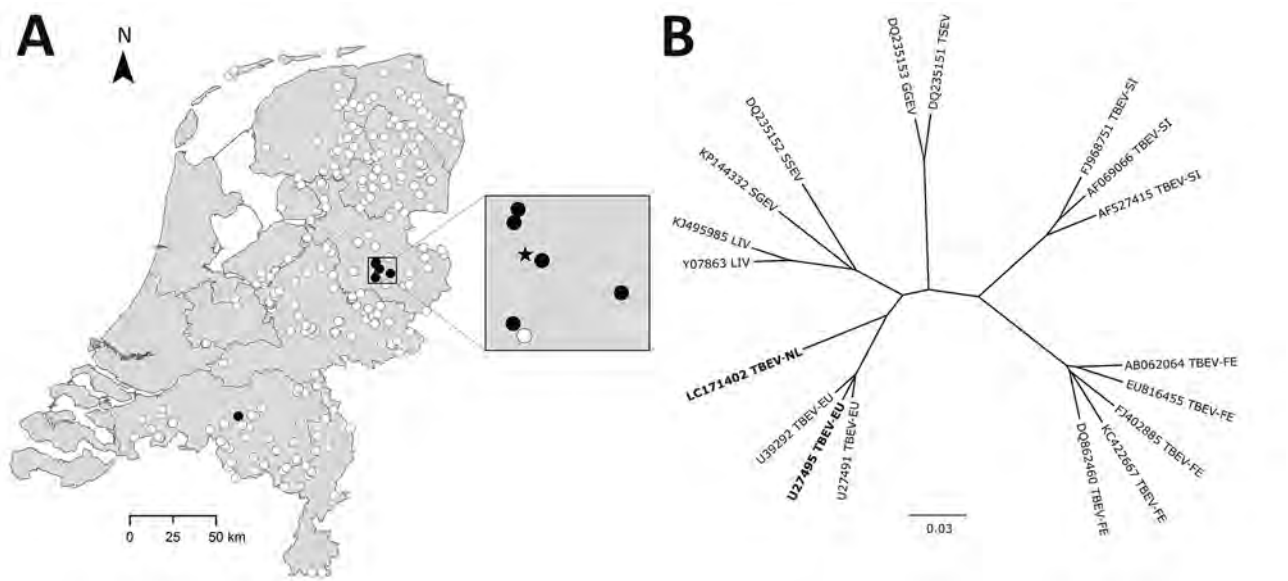

Figure. Spatial distribution of TBEV-positive roe deer and genetic cluster analysis of TBEV sequences from the Netherlands. A) Spatial distribution of serologic test results (solid black circle, SNT positive; open white circle, ELISA and/or SNT negative) for 297 serum samples from roe deer collected according to a sampling scheme designed to obtain a representative sample of the roe deer population from locations across the Netherlands. Enlargement of the National Park Sallandse Heuvelrug area indicates the locations of the TBEV serologically positive roe deer (solid black circle) in relation to the site with reverse transcription quantitative PCR–positive ticks (solid black star) from 2015. B) Genetic cluster analysis of TBEV-NL sequences obtained from tick pools in the Netherlands with other tickborne viruses (indicated by GenBank accession number). Bold indicates the TBEV-NL sequence, which consists of 10,242 nt of the genome (GenBank accession no. LC171402), and the TBEV-EU strain with which TBEV-NL clusters. Where available, representatives of the subtypes are included. We conducted distance-based analyses using Kimura 2-parameters distance estimates and constructed the trees using the neighbor-joining algorithm, implemented in Bionumerics 7.1 (Applied Math, Sint-Martens-Latem, Belgium). We calculated bootstrap proportions by analyzing 1,000 replicates for neighbor-joining trees. Scale bar indicates nucleotide substitutions per site. GGEV, Greek goat encephalomyelitis virus; LIV, Louping ill virus; SGEV, Spanish goat encephalitis virus; SSEV, Spanish sheep encephalitis virus; TBEV, tickborne encephalitis virus; TBEV-EU, TBEV European subtype; TBEV-FE, Far Eastern subtype; TBEV-NL, TBEV Netherlands subtype; TBEV-SI, TBEV Siberian subtype; TSEV, Turkish sheep encephalomyelitis virus.

the tick pools were identical. The sequences obtained in this study were designated TBEV-NL and clustered within the TBEV-EU subtype complex (Figure, panel B), with a 91% sequence identity with the currently known TBEV-EU sequences.

TBEV-EU RNA in 2 pools of ticks collected through surveillance in 1 national park confirms the presence of TBEV-EU in the Netherlands. Serologic evidence that roe deer from the same location had been infected with a flavivirus, most probably a TBEV, 5 years before the detection of TBEV RNA in ticks suggests that TBEV has been endemic to the Netherlands for at least 5 years.

The concentration of serologically positive roe deer is striking and remains unexplained. One explanation could be that this area has dense beech tree coverage, and beechnuts are a major food source for roe deer and the bank vole (*Myodes glareolus*). These host species play a pivotal role in the TBEV enzootic cycle; a habitat suitable for both may have enhanced the local establishment and spread of TBEV. In addition, the finding of a serologically positive roe deer in a southern province of the Netherlands (Figure, panel A), also known for the presence of beech trees, suggests that TBEV is distributed more widely within the Netherlands.

Dissemination of information about the occurrence of TBEV in ticks and wildlife is needed for medical professionals and the general public. In response to our findings, 2 autochthonous TBEV infections were reported in the Netherlands (*9,10*). At least 1 of these autochthonous cases was infected with a TBEV strain showing 99% homology with the Neudörfl strain, suggesting the presence of multiple TBEV-EU strains in the Netherlands. Our findings indicate that clinicians should be aware of the possibility for TBEV infection in humans in the Netherlands.

Acknowledgments

We thank Fedor Gassner, Gilian van Duijvendijk , Ryanne Jaarsma, Aleksandra Krawczyk, and Miriam Maas for performing fieldwork; Daan Vreugdenhil and Tom Klomphaar for access to the nature reserves; Natashja Buijs, Ewa Frazer, Najima Lamkaraf, and Sophie Lamoral for technical support in the laboratory; and Marion Koopmans for critically reading this manuscript.

This study was supported by the Netherlands Ministry of Health, Welfare, and Sport and performed under the frame of EurNegVec Cost Action TD1303. The collection of roe deer sera in 2010 was financed by the Netherlands Ministry of Economic Affairs (former LNV; verplichtingnummer 1400004212).

Ms. Jahfari is a PhD candidate at the Dutch National Institute for Public Health and the Environment (RIVM) and Erasmus Medical Center. Her primary research interest is tickborne diseases.

References

1. Lindquist L, Vapalahti O. Tick-borne encephalitis. Lancet. 2008; 371:1861–71. http://dx.doi.org/10.1016/S0140-6736(08)60800-4
2. Bakhvalova VN, Dobrotvorsky AK, Panov VV, Matveeva VA, Tkachev SE, Morozova OV. Natural tick-borne encephalitis virus infection among wild small mammals in the southeastern part of western Siberia, Russia. Vector Borne Zoonotic Dis. 2006;6:32–41. http://dx.doi.org/10.1089/vbz.2006.6.32
3. Gerth HJ, Grimshandl D, Stage B, Döller G, Kunz C. Roe deer as sentinels for endemicity of tick-borne encephalitis virus. Epidemiol Infect. 1995;115:355–65. http://dx.doi.org/10.1017/S0950268800058477
4. Donoso Mantke O, Schädler R, Niedrig M. A survey on cases of tick-borne encephalitis in European countries. Euro Surveill. 2008; 13:18848.
5. Roelandt S, Suin V, Van der Stede Y, Lamoral S, Marche S, Tignon M, et al. First TBEV serological screening in Flemish wild boar. Infect Ecol Epidemiol. 2016;6:31099. http://dx.doi.org/10.3402/iee.v6.31099
6. Roelandt S, Suin V, Riocreux F, Lamoral S, Van der Heyden S, Van der Stede Y, et al. Autochthonous tick-borne encephalitis virus–seropositive cattle in Belgium: a risk-based targeted serological survey. Vector Borne Zoonotic Dis. 2014;14:640–7. http://dx.doi.org/10.1089/vbz.2014.1576
7. Klaus C, Hoffmann B, Hering U, Mielke B, Sachse K, Beer M, et al. Tick-borne encephalitis (TBE) virus prevalence and virus genome characterization in field-collected ticks (*Ixodes ricinus*) from risk, non-risk and former risk areas of TBE, and in ticks removed from humans in Germany. Clin Microbiol Infect. 2010;16:238–44. http://dx.doi.org/10.1111/j.1469-0691.2009.02764.x
8. Kupča AM, Essbauer S, Zoeller G, de Mendonça PG, Brey R, Rinder M, et al. Isolation and molecular characterization of a tick-borne encephalitis virus strain from a new tick-borne encephalitis focus with severe cases in Bavaria, Germany. Ticks Tick Borne Dis. 2010;1:44–51. http://dx.doi.org/10.1016/j.ttbdis.2009.11.002
9. de Graaf JA, Reimerink JHJ, Voorn GP, bij de Vaate EA, de Vries A, Rockx B, et al. First human case of tick-borne encephalitis virus infection acquired in the Netherlands, July 2016 Euro Surveill. 2016;21:30318. http://dx.doi.org/10.2807/1560-7917.ES.2016.21.33.30318
10. Weststrate AC, Knapen D, Laverman GD, Schot B, Prick JJ, Spit SA, et al. Increasing evidence of tick-borne encephalitis (TBE) virus transmission, the Netherlands, June 2016. Euro Surveill. 2017;22:30482. http://dx.doi.org/10.2807/1560-7917.ES.2017.22.11.30482</jrn>

Address for correspondence: Hein Sprong, Center for Infectious Disease Control, National Center for Public Health and the Environment, Antonie van Leeuwenhoeklaan 9, 3721 MA, Bilthoven, the Netherlands; email: hein.sprong@rivm.nl

Outbreaks of Tilapia Lake Virus Infection, Thailand, 2015–2016

Win Surachetpong, Taveesak Janetanakit, Nutthawan Nonthabenjawan, Puntanat Tattiyapong, Kwanrawee Sirikanchana, Alongkorn Amonsin

Author affiliations:, Kasetsart University, Bangkok, Thailand (W. Surachetpong, P. Tattiyapong); Chulalongkorn University, Bangkok (T. Janetanakit, N. Nonthabenjawan, A. Amonsin); Chulabhorn Research Institute, Bangkok (K. Sirikanchana); Ministry of Education, Bangkok (K. Sirikanchana)

DOI: https://dx.doi.org/10.3201/eid2306.161278

During 2015–2016, several outbreaks of tilapia lake virus infection occurred among tilapia in Thailand. Phylogenetic analysis showed that the virus from Thailand grouped with a tilapia virus (family Orthomyxoviridae) from Israel. This emerging virus is a threat to tilapia aquaculture in Asia and worldwide.

Viral diseases are common causes of illness and death in cultured fish; such viruses include infectious salmon anemia virus, infectious hematopoietic necrosis virus, and viral hemorrhagic septicemia virus (*1*). With regard to tilapia, some viral pathogens, including betanodavirus, iridovirus, and herpes-like virus (*2*,*3*), reportedly cause severe disease. In recent years, Thailand has experienced extensive losses of tilapia; most losses occurred 1 month after transfer of fish from hatchery to grow-out cages in public rivers or reservoirs (1-month mortality syndrome). During routine investigation of this syndrome, multiple bacterial and parasitic infections were identified. However, no association was established between the outbreaks and any primary causative agent(s). Most deaths occurred within 2 weeks after the first dead fish were found. Similar observations of extensive losses of raised tilapia and wild fish in Israel and Ecuador have been reported (*4*,*5*). These outbreaks led to identification of a virus affecting tilapia, called tilapia lake virus (TiLV). The epidemiologic pattern and clinical signs for infected fish in Thailand led to suspicion of an illness of unknown etiology that was similar to TiLV infection.

During 2015–2016, we investigated 32 outbreaks involving a large number of deaths of unknown cause among Nile tilapia (*Oreochromis niloticus*) and red hybrid tilapia (*Oreochromis* spp.). The outbreaks occurred at fish farms in central, western, eastern, and northeastern Thailand (online Technical Appendix Figure 1, https://wwwnc.cdc.gov/EID/article/23/6/16-1278-Techapp1.pdf). Affected fish were commonly found within 1 month after transfer from the hatchery facility to grow-out ponds or cages. In general, clinical signs and high mortality rates were associated with fish weighing 1–50 g (online Technical Appendix Figure 2). Mortality rates among tilapia farms were 20%–90%; higher rates were associated with secondary bacterial and parasitic infections. Mortality rates peaked within 14 days after the first dead fish were found.

As part of the outbreak investigation, samples of brain tissue were taken from fish at each of the 32 outbreak locations (each with a mortality rate >1%/day for 3 consecutive days): 10–30 moribund fish and 5–10 apparently healthy fish from the same culture areas. In total, 325 samples were collected and tested for etiologic agent(s) (*4*,*6*). Samples from fish involved in 22 of the 32 outbreaks were positive for TiLV (online Technical Appendix Table 1).

For our study, we selected a field sample positive for TiLV (designated TiLV/Tilapia/Thai/TV1/2016) and processed it for whole-genome sequencing. Another 6 TiLVs were selected for sequencing of the putative polymerase basic 1 (PB1) gene (online Technical Appendix Table 2). TiLV genome sequencing was conducted by using newly designed primers based on reference TiLVs available in the GenBank database (*7*). Nucleotide sequences of 7 TiLVs from Thailand were submitted to GenBank (accession nos. KX631921–36).

Comparison of the TiLVs from Thailand with those from Israel showed high nucleotide and amino acid identities (95.18%–99.10%). Among TiLVs from Thailand, nucleotide and amino acid identities for segment 1 or the putative PB1 gene of the virus were high (99.61%–100%) (online Technical Appendix Table 3). Genetic analysis of the putative PB1 protein of TiLVs from Thailand and the viruses of the family *Orthomyxoviridae* showed that TiLVs from Thailand possessed motifs preA, A, B, C, D, and E similar to those of *Orthomyxoviridae* viruses, including influenza A, B, and C viruses; infectious salmon anemia virus; Dhori virus; and Thogoto virus (online Technical Appendix Table 4) (*8*–*10*). Phylogenetic analysis showed that TiLVs from Thailand were closely related to TiLVs from Israel and grouped with the viruses of the family *Orthomyxoviridae* but not *Arenaviridae* and *Bunyaviridae* (Figure). This result suggests that the genetic composition of this emerging virus was similar to that of orthomyxoviruses and homologous with previously published TiLV sequences.

Our PCR and whole-genome findings demonstrate genetic homology between TiLV from Thailand and the etiologic agent of a novel RNA virus infection of

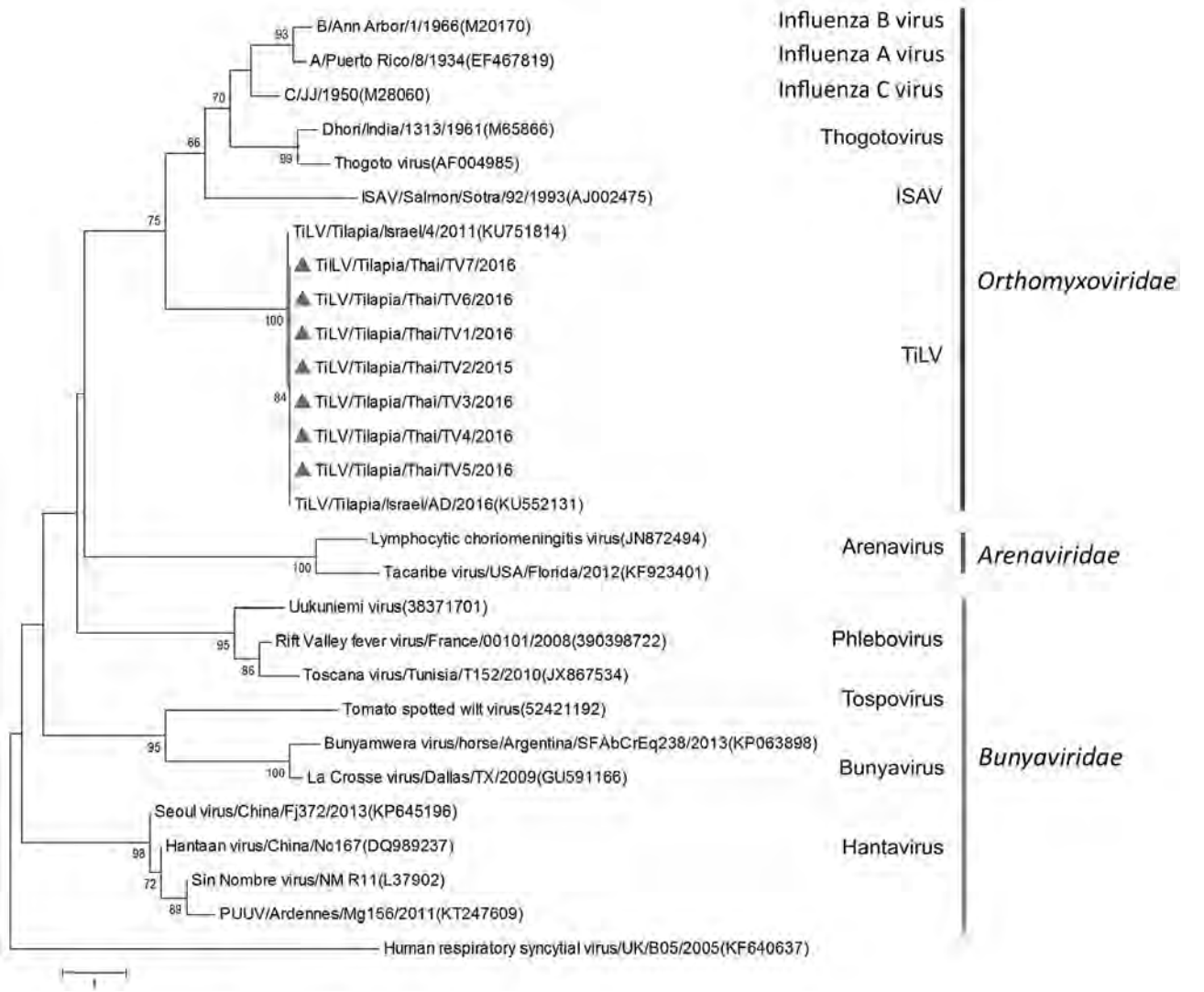

Figure. Phylogenetic analysis of the nucleotide sequences of RNA polymerase of TiLVs from Thailand (triangles) and reference viruses of the families Orthomyxoviridae, Arenaviridae, and Bunyaviridae. Genus and family groups are indicated; GenBank accession numbers are provided for reference viruses. The phylogenetic tree was constructed by using MEGA 6.0 (*10*) and applying a neighbor-joining bootstrap analysis (1,000 replications) with the Poisson model and gamma distribution. Human respiratory syncytial virus was used as an outgroup. ISAV, infectious salmon anemia virus; PUUV, Puumala virus; TiLV, tilapia lake virus. Scale bar indicates nucleotide substitutions per site.

tilapia in Israel and Ecuador (*4*,*7*). Furthermore, the clinical signs and pathological presentation of infection with TiLV from Thailand are similar to those of infection with TiLV from Israel (online Technical Appendix Figure 2). The clinical signs, gross lesions, and histopathologic lesions combined with virus identification and characterization highlight emerging TiLV in Thailand as the primary cause of the outbreaks. We also found that fish that survived massive die-offs rarely showed clinical signs, suggesting the development of specific immunity against the virus. It should be noted that the TiLVs from Thailand possessed 10 gene segments encoding 10 proteins, including segment 1 or putative PB1 protein. The pattern of protein motifs for this putative PB1 was similar to that for influenza viruses. To our knowledge, TiLV has infected tilapia only, no other aquatic or terrestrial animals.

Our results emphasize that the virus isolated from Thailand shares high sequence similarity with TiLV from Israel, suggesting that this virus spreads across continents. Given that tilapia are the main aquaculture species, control of TiLV will be improved by further efforts such as strict biosecurity, vaccine development, and selection of resistant tilapia breeds.

Acknowledgments

We thank the National Research Council of Thailand and the Agricultural Research Development Agency for financial support (PRP6005020450) and the Center for Advanced Studies for Agriculture and Food, Kasetsart University Institute for Advanced Studies. We also thank Chulalongkorn University for financial support to the Center of Excellence for Emerging and Re-emerging Infectious Diseases in Animals, the Thailand Research Fund for financial support to the Thailand Research Fund Senior Scholar (to A.A.) (RTA5780006), and the National Science and Technology Development Agency (P-15-50004).

Dr. Surachetpong is an assistant professor at the Faculty of Veterinary Medicine, Kasetsart University, Bangkok. His research interests are emerging viruses and immunology in aquatic animals.

References

1. Crane M, Hyatt A. Viruses of fish: an overview of significant pathogens. Viruses. 2011;3:2025–46. http://dx.doi.org/10.3390/v3112025
2. Keawcharoen J, Techangamsuwan S, Ponpornpisit A, Lombardini ED, Patchimasiri T, Pirarat N. Genetic characterization of a betanodavirus isolated from a clinical disease outbreak in farm-raised tilapia *Oreochromis niloticus* (L.) in Thailand. J Fish Dis. 2015;38:49–54. http://dx.doi.org/10.1111/jfd.12200
3. Shlapobersky M, Sinyakov MS, Katzenellenbogen M, Sarid R, Don J, Avtalion RR. Viral encephalitis of tilapia larvae: primary characterization of a novel herpes-like virus. Virology. 2010;399:239–47. http://dx.doi.org/10.1016/j.virol.2010.01.001
4. Eyngor M, Zamostiano R, Kembou Tsofack JE, Berkowitz A, Bercovier H, Tinman S, et al. Identification of a novel RNA virus lethal to tilapia. J Clin Microbiol. 2014;52:4137–46. http://dx.doi.org/10.1128/JCM.00827-14
5. Ferguson HW, Kabuusu R, Beltran S, Reyes E, Lince JA, del Pozo J. Syncytial hepatitis of farmed tilapia, *Oreochromis niloticus* (L.): a case report. J Fish Dis. 2014;37:583–9. http://dx.doi.org/10.1111/jfd.12142
6. Kurita J, Nakajima K, Hirono I, Aoki T. Polymerase chain reaction (PCR) amplification of DNA of red seam bream iridovirus (RSIV). Fish Pathology. 1998;33:17–23. http://dx.doi.org/10.3147/jsfp.33.17
7. Bacharach E, Mishra N, Briese T, Zody MC, Kembou Tsofack JE, Zamostiano R, et al. Characterization of a novel orthomyxo-like virus causing mass die-offs of tilapia. MBio. 2016;7:e00431–16. http://dx.doi.org/10.1128/mBio.00431-16
8. Müller R, Poch O, Delarue M, Bishop DH, Bouloy M. Rift Valley fever virus L segment: correction of the sequence and possible functional role of newly identified regions conserved in RNA-dependent polymerases. J Gen Virol. 1994;75:1345–52. http://dx.doi.org/10.1099/0022-1317-75-6-1345
9. Poch O, Sauvaget I, Delarue M, Tordo N. Identification of four conserved motifs among the RNA-dependent polymerase encoding elements. EMBO J. 1989;8:3867–74.
10. Tamura K, Stecher G, Peterson D, Filipski A, Kumar S. MEGA6: Molecular Evolutionary Genetics Analysis version 6.0. Mol Biol Evol. 2013;30:2725–9. http://dx.doi.org/10.1093/molbev/mst197

Address for correspondence: Win Surachetpong, Faculty of Veterinary Medicine, Kasetsart University, Bangkok, Thailand 10900; email: fvetwsp@ku.ac.th

Endemic Hantavirus in Field Voles, Northern England

Anna G. Thomason, Michael Begon, Janette E. Bradley, Steve Paterson, Joseph A. Jackson

DOI: https://dx.doi.org/10.3201/eid2306.161607

Author affiliations: University of Salford, Salford, UK (A.G. Thomason, J.A. Jackson); University of Liverpool, Liverpool, UK (M. Begon, S. Paterson); University of Nottingham, Nottingham, UK (J.E. Bradley)

We report a PCR survey of hantavirus infection in an extensive field vole (*Microtus agrestis*) population present in the Kielder Forest, northern England. A Tatenale virus–like lineage was frequently detected (≈17% prevalence) in liver tissue. Lineages genetically similar to Tatenale virus are likely to be endemic in northern England.

Recently a new vole-associated hantavirus (Tatenale virus) was discovered in northern England (*1*), but only from an individual *Microtus agrestis* field vole. Previously only hantaviruses from murine-associated lineages (Seoul virus [SEOV] and SEOV-like viruses) had been reported in the United Kingdom, despite the abundance of potential vole hosts in the mainland United Kingdom and the endemicity of vole-associated hantavirus lineages (Puumala virus [PUUV] and Tula virus) in mainland Europe (*2*). Here we present data suggesting that the Tatenale virus lineage is endemic in northern England.

European hantaviruses are of public health significance because they are a causative agent of hemorrhagic fever with renal syndrome (HFRS). In the United Kingdom, HFRS cases have primarily been attributed to SEOV-like viruses on the basis of serologic tests. SEOV antibodies have been detected in both humans and Norway rats (*Rattus norvegicus*) in Northern Ireland and Yorkshire (*3*,*4*), and seropositivity in humans correlates with domestic or occupational exposure to rats (*3*,*5*). However, in the United Kingdom, HFRS cases with serologic cross-reactivity to PUUV (*3*), which might share antigenic determinants with Tatenale virus, have occurred.

To investigate the endemicity of hantavirus in field voles in the United Kingdom, we surveyed the extensive field vole population in the Kielder Forest, Northumberland (≈230 km distant from the locality where Tatenale virus was discovered). All sampled sites were grassy, clear-cut areas (adjacent to forest stands) where field voles were prevalent. Fieldwork was approved by the University of Liverpool Animal Welfare Committee and conducted subject to UK home office project license PPL 70_8210. Following the

capture and processing of animals as previously described (*6*), we extracted viral RNA from 48 livers using a QIAamp Viral RNA Mini Kit (QIAGEN, Manchester, UK) and converted to cDNA using a High-Capacity RNA-to-cDNA Kit (Applied Biosystems, Warrington, UK). Hantaviruses were detected by PCR amplification of a fragment of the genomic L segment encoding RNA polymerase, following the strategy outlined by Klempa et al. (*7*).

PCR-positive results were recorded for 16.7% of voles (8/48) in total; positive voles were recorded at 3 of the 5 sampled sites and throughout the survey period, March–September 2015 (Figure, panel A; online Technical Appendix Table, https://wwwnc.cdc.gov/EID/article/23/6/16-1607-Techapp1.pdf). Three positive samples from different individual voles were sequenced (in both directions from independent replicate PCRs) by Sanger sequencing (Source BioScience, Rochdale, UK). The 380-bp sequence was identical in all 3 positive vole samples, with the exception of a single nucleotide polymorphism at position 145 (adenine, 2 voles; guanine, 1 vole; GenBank accession nos. KY751731, KY751732). The recovered sequences were similar to but divergent from Tatenale virus (86.0%–86.3% identity at the nucleotide level and 95.9%–96.7% identity at the amino acid level; online Technical Appendix Figures 1, 2). Phylogenetic analysis of the L segment demonstrated this level of divergence was comparable to the divergence among many western European lineages of PUUV (Figure, panel B; online Technical Appendix Figure 3).

Taken together with the original report, these data are sufficient to suggest that Tatenale-like hantavirus

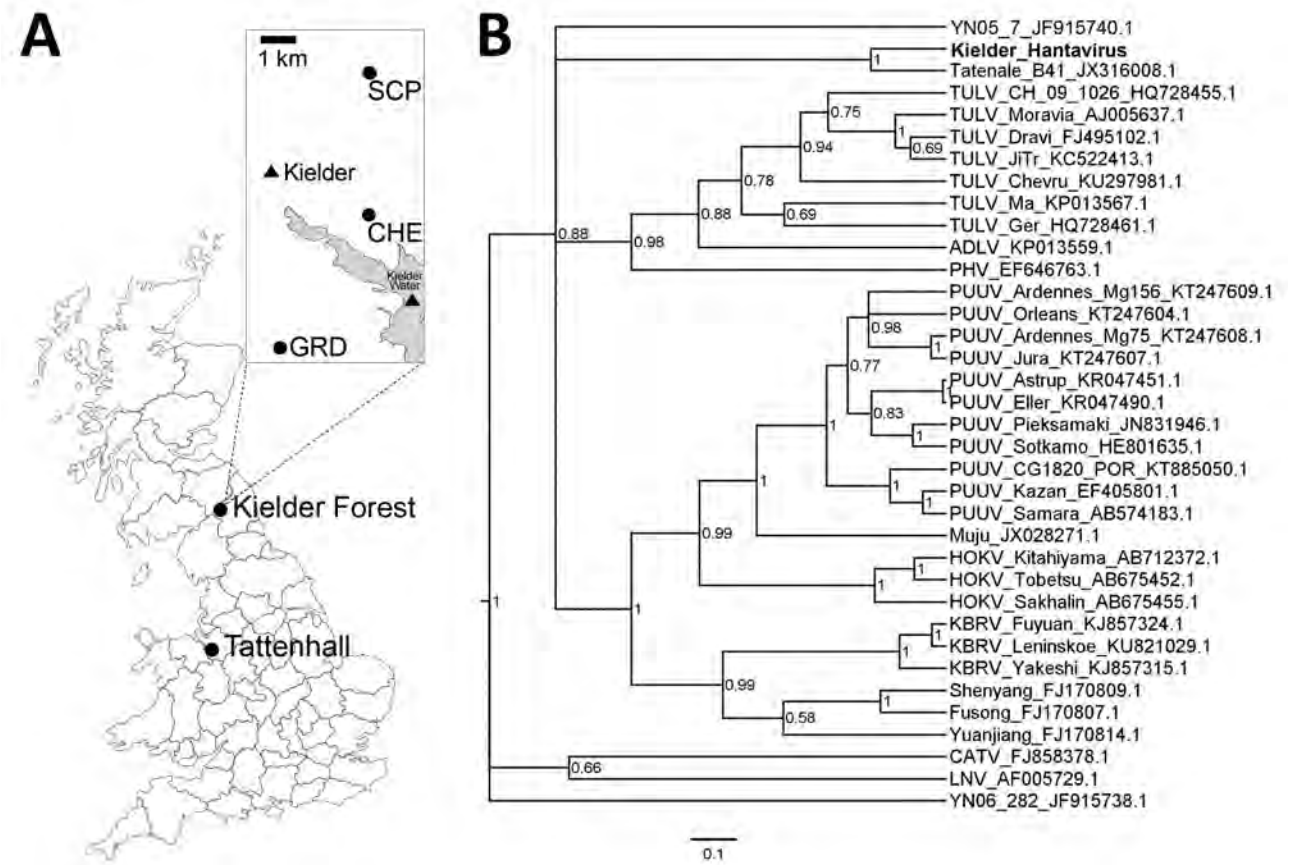

Figure. Investigation of Tatenale virus–like hantavirus lineages in the United Kingdom. A) Locations on the UK mainland where Tatenale virus–like hantavirus lineages have been found: Tattenhall, Cheshire, the site where Tatenale virus was discovered (*1*); and Kielder Forest, Northumberland. Kielder Forest sample sites are indicated in the inset (Geordies Knowe [GRD]: 55°11′1.61″N, 2°35′3.05″W; Cheese Sike [CHE]: 55°13′8.39″N, 2°32′26.50″W; Scaup [SCP]: 55°15′44.18″N, 2°32′41.05″W). B) Bayesian phylogenetic tree for the hantavirus genomic large segment (318-bp fragment with no missing data), showing relationships among Tatenale virus-like lineages and other relevant lineages. Bold represents the Tatenale virus–like lineage found in this study; either sequence reported here produces the same tree. Phylogenetic analysis was conducted by using a general time reversible plus gamma plus invariant sites model within MrBayes (*8*) software using Markov chain Monte Carlo chain lengths of 1 million and a strict clock. We estimated substitution models using MrModelTestV2 (*9*). Sequences are represented by the taxonomic names, strain (if >1 is included), and GenBank accession numbers. The tree is drawn to scale with node values representing the posterior probabilities. Scale bar represents nucleotide substitutions per site. ADLV, Adler virus; CATV, Catacamas virus; HOKV, Hokkaido virus; KBRV, Khabarovsk virus; LNV, Laguna Negra virus; PHV, Prospect Hill virus; PUUV, Puumala virus; TULV, Tula virus.

lineages are widespread and common in northern England. Furthermore, the considerable sequence divergence between samples in Cheshire and Northumberland is consistent with a long-standing endemicity in northern England. Given that PUUV has never been recorded in the United Kingdom (*2*,*10*), the possibility should be considered that a Tatenale-like virus could have been responsible for some of the HFRS cases that have occurred here. More studies are needed to confirm whether other common rodents in the United Kingdom are hosts for this virus and to further characterize its phyletic relationships and zoonotic potential. Cross-reactivity of the sera from Tatenale-like virus–infected individuals to antigens of other relevant hantaviruses should be determined to inform future serologic surveys and the diagnosis of human HFRS cases.

Acknowledgments

We thank Rebecca Barber, Lukasz Lukomski, Steve Price, and Ann Lowe for their assistance.

This work was funded by the Natural Environment Research Council, United Kingdom (research grant NE/L013517/2).

Ms. Thomason is a doctoral student at the School of Environment and Life Sciences at the University of Salford, Manchester, United Kingdom. Her interests are in the ecological dynamics of infectious disease in wildlife.

References

1. Pounder KC, Begon M, Sironen T, Henttonen H, Watts PC, Voutilainen L, et al. Novel hantavirus in wildlife, United Kingdom. Emerg Infect Dis. 2013;19:673–5. http://dx.doi.org/10.3201/eid1904.121057
2. Bennett E, Clement J, Sansom P, Hall I, Leach S, Medlock JM. Environmental and ecological potential for enzootic cycles of Puumala hantavirus in Great Britain. Epidemiol Infect. 2010;138:91–8. http://dx.doi.org/10.1017/S095026880999029X
3. Jameson LJ, Newton A, Coole L, Newman EN, Carroll MW, Beeching NJ, et al. Prevalence of antibodies against hantaviruses in serum and saliva of adults living or working on farms in Yorkshire, United Kingdom. Viruses. 2014;6:524–34. http://dx.doi.org/10.3390/v6020524
4. McKenna P, Clement J, Matthys P, Coyle PV, McCaughey C. Serological evidence of hantavirus disease in Northern Ireland. J Med Virol. 1994;43:33–8. http://dx.doi.org/10.1002/jmv.1890430107
5. Jameson LJ, Taori SK, Atkinson B, Levick P, Featherstone CA, van der Burgt G, et al. Pet rats as a source of hantavirus in England and Wales, 2013. Euro Surveill. 2013;18:18.
6. Jackson JA, Begon M, Birtles R, Paterson S, Friberg IM, Hall A, et al. The analysis of immunological profiles in wild animals: a case study on immunodynamics in the field vole, *Microtus agrestis*. Mol Ecol. 2011;20:893–909. http://dx.doi.org/10.1111/j.1365-294X.2010.04907.x
7. Klempa B, Fichet-Calvet E, Lecompte E, Auste B, Aniskin V, Meisel H, et al. Hantavirus in African wood mouse, Guinea. Emerg Infect Dis. 2006;12:838–40. http://dx.doi.org/10.3201/eid1205.051487
8. Ronquist F, Huelsenbeck JP. MrBayes 3: Bayesian phylogenetic inference under mixed models. Bioinformatics. 2003;19:1572–4. http://dx.doi.org/10.1093/bioinformatics/btg180
9. Nylander J. MrModeltest v2. Uppsala: Evolutionary Biology Centre, Uppsala University; 2004.
10. Pether JV, Lloyd G. The clinical spectrum of human hantavirus infection in Somerset, UK. Epidemiol Infect. 1993;111:171–5. http://dx.doi.org/10.1017/S095026880005679X

Address for correspondence: Joseph A. Jackson, University of Salford, School of Environment and Life Sciences, Peel Building, Salford M5 4WT, UK; email: J.A.Jackson@Salford.ac.uk

Measles Cases during Ebola Outbreak, West Africa, 2013–2106

Francesca Colavita,[1] Mirella Biava,[1] Concetta Castilletti, Serena Quartu, Francesco Vairo, Claudia Caglioti, Chiara Agrati, Eleonora Lalle, Licia Bordi, Simone Lanini, Michela Delli Guanti, Rossella Miccio, Giuseppe Ippolito, Maria R. Capobianchi, Antonino Di Caro; and the Lazzaro Spallanzani Institute for Research and Health Care Ebola Virus Disease Sierra Leone Study Group[2]

Author affiliations: Lazzaro Spallanzani Institute for Research and Health Care, Rome, Italy (F. Colavita, M. Biava, C. Castilletti, S. Quartu, F. Vairo, C. Caglioti, C. Agrati, E. Lalle, L. Bordi, S. Lanini, G. Ippolito, M.R. Capobianchi, A. Di Caro); Emergency Nongovernmental Organization, Milan, Italy (M. Delli Guanti, R. Miccio)

DOI: https://dx.doi.org/10.3201/eid2306.161682

The recent Ebola outbreak in West Africa caused breakdowns in public health systems, which might have caused outbreaks of vaccine-preventable diseases. We tested 80 patients admitted to an Ebola treatment center in Freetown, Sierra Leone, for measles. These patients were negative for Ebola virus. Measles virus IgM was detected in 13 (16%) of the patients.

The Ebola virus disease (EVD) outbreak in West Africa during 2013–2016 was one of the worst public health disasters in recent history; it caused >28,646 cases and 11,323

[1]These authors contributed equally to this article.

[2]Members of this group are listed at the end of this article.

deaths (*1*). Consequences of EVD include social instability, poor food reserves, breakdown of healthcare systems, and reduced vaccination coverage (*2*,*3*). Breakdown of healthcare systems and reduced vaccination coverage might have been the worst consequences because nearly all health resources were shifted to the EVD response. Disruptions of local health systems could lead to underreporting of other infectious diseases cases and a second crisis that could kill as many as persons as the original outbreak, if not more.

The 3 countries most affected by this outbreak (Sierra Leone, Guinea, and Liberia) have been a major part of the World Health Organization Expanded Programme on Immunization through vaccination campaigns for reducing childhood deaths from vaccine-preventable diseases, such as measles. Although there are no cures for EVD or measles, a potent measles vaccine is available, which can prevent spread of this disease. Use of this vaccine is crucial because measles is far more contagious (1 case-patient with measles can transmit infection to 12–18 persons) than EVD and might be the primary cause of major epidemics (*3*,*4*). These 3 countries reported nearly 93,685 cases of measles during 1994–2003 (although Sierra Leone did not report cases for 4 years), and during November 1, 2009–July 13, 2010, a total of 1,094 confirmed measles cases were reported in Sierra Leone. Plans for measles vaccination campaigns were implemented before the EVD outbreak because of an increase in susceptibility to measles in these 3 countries (*3*,*5*).

Historically, measles outbreaks have followed humanitarian crises, such as war (*6*), natural disasters (*7*), and political crises (*8*). Recent studies have shown that measles is one of the causative agents of secondary outbreaks during the EVD epidemics in West Africa (*9*), probably due to the disruption in vaccination campaigns, nonfunctional healthcare systems (including detection and reporting of measles cases), lack of specific treatment, and a sense of fear of contracting EVD with reluctance to approach health assistance (*10*).

Probable underreporting of and lack of data for measles cases during EVD outbreaks prompted us to investigate measles in Sierra Leone during the recent EVD outbreak. Although during the preparedness phase of the European Mobile Laboratory Project (http://www.emlab.eu), measles was to be included among diseases tested for differential diagnosis of EVD, we could not implement this approach in the field during the outbreak.

We performed a retrospective serologic study to partially investigate the role of measles in the EVD outbreak by testing serum samples negative for Ebola virus by reverse transcription PCR for measles virus IgM from persons suspected of having EVD. Samples were obtained at the Emergency Nongovernmental Organization Ebola Treatment Center (Goderich, Freetown, Sierra Leone). This study was approved by Ethical Committee of Sierra Leone.

We analyzed 80 patients, of whom 27 were ≥8 years of age and ≤25 years of age (median age 30 years) during December 2014–June 2015, who had fever (temperature ≥37.5°C) and diarrhea or vomiting. Only 1 patient had a history of rash. Measles virus IgM was detected by using an indirect immunofluorescence assay for 13 patients (16%), most (69%) of whom were in this age group ($p<0.001$). Although we could not determine whether measles IgM in these patients was caused by vaccination failures during the outbreak or failures of the Expanded Programme on Immunization, this age distribution might be indicative of noneffective immunization campaigns, especially a deficiency in the healthcare system in detecting and reporting measles cases.

The recent EVD outbreak caused breakdowns of healthcare systems in the affected countries, leading to possible secondary outbreaks (*2*,*3*). A higher risk for vaccine-preventable diseases, in particular measles, is often an early result in interruption in delivery of public health services. Recent studies have shown that the increase in measles cases during the EVD outbreak in 2013–2016 was caused by disruption of vaccination programs and underreporting of measles cases, which is probably related to effects of EVD on healthcare systems (*9*).

Our results for samples obtained from Ebola-negative patients showed a high number of measles infections during the outbreak in different age groups. Although few (n = 80) patients have been tested, our results provide useful insights into measles cases during other outbreaks in different age groups, adding new evidence from a study that focused on children (*9*).

Our findings indicate the need for correct and rapid differential diagnoses during such outbreaks to avoid spread of other infectious diseases. Furthermore, local public health systems should be strengthened in those countries that are now recovering from the EVD outbreak to reduce risks for other infectious diseases outbreaks.

Members of the Lazzaro Spallanzani Institute for Research and Health Care Ebola Virus Disease Sierra Leone Study Group: Antonella Vulcano, Francesca Colavita, Carolina Venditti, Paola Zaccaro, Antonio Mazzarelli, Concetta Castilletti, Angela Cannas, Serena Quartu, Sabrina Coen, Silvia Meschi, Claudia Minosse, Roberta Chiappini, Mirella Biava, Maria Beatrice Valli, Germana Grassi, and Daniele Lapa.

Acknowledgments

We thank Italian Ministry of Health (Ricerca Corrente and Ricerca Finalizzata) for supporting deployment of laboratory personnel; the Sierra Leone Ministry of Health and Sanitation, the Pharmacy Board of Sierra Leone, and the Sierra Leone National Laboratory Service for collaborating in overall laboratory activities implemented in the laboratory at the Princess Christian Maternity Hospital (Freetown, Sierra

Leone); staff (nurses, physicians, pharmacists, logisticians, administrators, cleaners, drivers, cooks, guards) at the Emergency Ebola Treatment Center (Goderich, Freetown, Sierra Leone) and the Emergency Surgical and Pediatric Hospital (Goderich) for their efforts and support; and the people of Goderich for their energy, optimism, cordiality, and positive attitude.

This study was supported by the Italian Ministry of Foreign Affairs (Directorate General for Development Cooperation). The Lazzaro Spallanzani Institute for Research and Health Care was supported by the European Union Horizon 2020 Research and Innovation Programme (EVIDENT, grant no. 666100); the European Union Innovative Medicine Initiative) Programme (projects EbolaMODRAD [grant no. 115843] and FILODIAG [grant no. 115844]); and the US Food and Drug Administration project (FDABAA-15-00121).

Dr. Colavita is research scientist at the Laboratory of Virology, Lazzaro Spallanzani Institute for Research and Health Care, Rome, Italy. Her research interests are infections with emerging viruses and risk group 3 and 4 pathogens, host immune responses, and host–pathogen interactions.

References

1. World Health Organization. Ebola Situation report, 2015 [cited 2017 Mar 29]. http://www.who.int/csr/disease/ebola/situation-reports/en/
2. United Nations Development Group. Socio-economic impact of Ebola virus disease in West African countries, 2015. New York: United Nations Development Programme [cited 2017 Mar 29]. http://reliefweb.int/sites/reliefweb.int/files/resources/ebola-west-africa.pdf
3. Takahashi S, Metcalf CJE, Ferrari MJ, Moss WJ, Truelove SA, Tatem AJ, et al. Reduced vaccination and the risk of measles and other childhood infections post-Ebola. Science. 2015;347:1240–2. http://dx.doi.org/10.1126/science.aaa3438
4. World Health Organization. Global vaccine action plan 2011–2020. 2013 [cited 2017 Mar 29]. http://www.who.int/immunization/global_vaccine_action_plan/en/
5. Truelove SA, Moss WJ, Lessler J. Mitigating measles outbreaks in West Africa post-Ebola. Expert Rev Anti Infect Ther. 2015; 13:1299–301. http://dx.doi.org/10.1586/14787210.2015.1085305
6. Sharara SL, Kanj SS. War and infectious diseases: challenges of the Syrian civil war. PLoS Pathog. 2014;10:e1004438. http://dx.doi.org/10.1371/journal.ppat.1004438
7. Surmieda MR, Lopez JM, Abad-Viola G, Miranda ME, Abellanosa IP, Sadang RA, et al. Surveillance in evacuation camps after the eruption of Mt. Pinatubo, Philippines. MMWR CDC Surveill Summ. 1992;41:9–12.
8. UNICEF. Sanctions: children hard hit in Haiti [cited 2017 Mar 29]. http://www.unicef.org/sowc96/dsanctns.htm
9. Suk JE, Paez Jimenez A, Kourouma M, Derrough T, Baldé M, Honomou P, et al. Post-Ebola measles outbreak in Lola, Guinea, January–June 2015. Emerg Infect Dis. 2016;22:1106–8. http://dx.doi.org/10.3201/eid2206.151652
10. Shrivastava SR, Shrivastava PS, Jegadeesh R. Legacy of Ebola outbreak: potential risk of measles outbreak in Guinea, Sierra Leone and Liberia. J Res Med Sci. 2015;20:529–30. http://dx.doi.org/10.4103/1735-1995.163982

Address for correspondence: Antonino Di Caro, Laboratory of Virology, Lazzaro Spallanzani Institute for Research and Health Care, Via Portuense 292, 00149 Rome, Italy; email: antonino.dicaro@inmi.it

Angiostrongylus cantonensis Meningitis and Myelitis, Texas, USA

Roukaya Al Hammoud, Stacy L. Nayes, James R. Murphy, Gloria P. Heresi, Ian J. Butler, Norma Pérez

Author affiliation: McGovern Medical School, University of Texas Health Science Center at Houston, Houston, Texas, USA

DOI: https://dx.doi.org/10.3201/eid2306.161683

Infection with *Angiostrongylus cantonensis* roundworms is endemic in Southeast Asia and the Pacific Basin. *A. cantonensis* meningitis and myelitis occurred in summer 2013 in a child with no history of travel outside of Texas, USA. Angiostrongyliasis is an emerging neurotropic helminthic disease in Texas and warrants increased awareness among healthcare providers.

In summer 2013, a previously healthy Caucasian 12-month-old girl was brought for treatment to a children's hospital in Houston, Texas, USA, on the 11th day of illness (day 11), manifesting intermittent fever, lethargy, and emesis. She had been evaluated by a pediatrician on day 3 and diagnosed with presumed viral infection. She attended day care, had no history of sick contacts, and apart from dogs in the house, had no notable other exposures.

At hospital admission, physical examination showed vital signs within reference ranges, mild distress, lethargy, and irritability with no focal deficits or signs of meningeal irritation. Blood test results showed leukocytosis (17,900 cells/mm^3 with 20% eosinophils). Cerebrospinal fluid (CSF) examination showed 8 erythrocytes and 568 leukocytes/mm^3 with 26% eosinophils. Results of bacterial cultures and PCR of CSF for herpes simplex virus and enterovirus were negative. She had no serologic evidence of acute infection with West Nile virus or HIV. Magnetic resonance imaging (MRI) of the brain showed normal results. She received ceftriaxone, vancomycin, and acyclovir from days 11 through 15 with no clinical improvement.

On day 16, because the child had been exposed to dogs, she was empirically treated for presumed *Toxocara* infection with albendazole and prednisone for 5 days. Her clinical

condition improved. However, 2 days after she completed the albendazole and prednisone regimen (day 23), fever and lethargy recurred, she was unable to bear weight, and CSF analysis showed increased eosinophilia (1,500 leukocytes/mm^3 with 35% eosinophils). On day 23, MRI showed diffuse leptomeningeal enhancement in the brain and spinal cord, diffuse punctate areas of cortical infarction, and intramedullary enhancement (Figure). On the same day, she was again treated with albendazole and prednisone with good response.

Results of serologic testing performed at the hospital were negative for *Trichinella*, *Toxocara*, and *Schistosoma* spp. Serum and CSF samples were sent to the Centers for Diseases Control and Prevention (Atlanta, GA, USA); PCR results showed CSF was positive for *Angiostrongylus cantonensis*, and serum was positive for *Toxocara Strongyloides stercoralis* IgG. On day 31, we diagnosed *A. cantonensis* meningitis and myelitis with cross-reactions to *S. stercoralis* and *Toxocara* spp. The patient completed 2 weeks of albendazole therapy (from day 23 through day 37) and 3 months of prednisone therapy with slow tapering. The patient's symptoms completely resolved by day 64. Lumbar punctures on days 35, 56, and 104 showed gradual return of CSF parameters to normal ranges. On day 56, results of an MRI of the brain were unremarkable.

The case was reported to the local health department, which tested snails trapped close to the patient's residence. No evidence of *A. cantonensis* roundworms was found.

In 1987, *A. cantonensis* roundworm was identified for the first time in North America in rodents. (*1*). Although a PCR-based assay did not detect *A. cantonensis* roundworm in samples of intermediate hosts (snails) in Houston, Texas, the parasite has been repeatedly identified in southeastern and Gulf states (Louisiana, Oklahoma, Mississippi, Florida) (*2*,*3*). In parallel, human infections have increased. The first reported human case of *A. cantonensis* meningitis in a nontraveler in the contiguous United States occurred in 1995 in a 10-year-old boy in New Orleans, Louisiana, who had eaten raw snails (*4*). Since the case we report, 2 additional cases in children were reported in Houston, in the spring of 2016 (*5*).

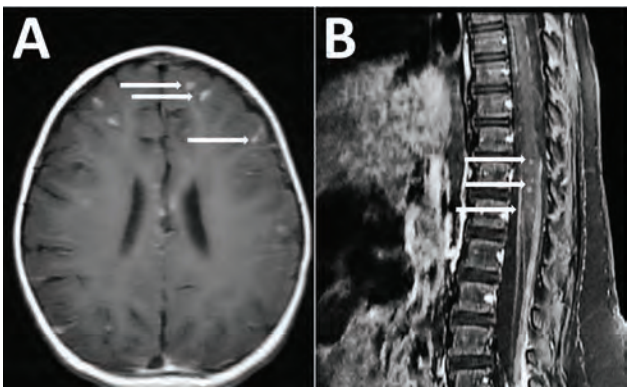

Figure. Magnetic resonance imaging (MRI) of the brain (A) and the spine (B) showing meningitis and myelitis in a 12-month-old girl with *Angiostrongylus cantonensis* infection, Houston, Texas, USA. A) Axial T1 post contrast sequences showing diffuse leptomeningeal enhancement (arrows). B) Sagittal T1 postcontrast sequences showing intramedullary enhancement in the thoracic and lumbar spinal cord T8–L5 with diffuse leptomeningeal enhancement (arrows).

The frequency of *A. cantonensis* infections in humans is likely underreported due to a combination of factors, including the frequent self-limited course of the infection, lack of awareness of the parasite, limited availability of diagnostic testing, and lack of national surveillance. Although the disease usually resolves spontaneously, case-fatality rates can reach 5% (*6*). Lack of clinical suspicion for angiostrongyliasis on the basis of signs and symptoms and delay in initiation of treatment can lead to neurologic deterioration, especially in young children, as demonstrated in our patient and another report (*7*).

In conclusion, angiostrongyliasis is an emerging neurotropic helminthic disease in Texas. Increased awareness of *A. cantonensis* infection in humans is needed among healthcare providers.

Dr. Al Hammoud is a pediatric infectious diseases fellow at University of Texas Health, McGovern Medical School. Her areas of interest include general pediatric infectious diseases, HIV-associated nephropathy, and immunization response in HIV-infected children.

References

1. Campbell BG, Little MD. The finding of *Angiostrongylus cantonensis* in rats in New Orleans. Am J Trop Med Hyg. 1988;38:568–73.
2. Teem JL, Qvarnstrom Y, Bishop HS, da Silva AJ, Carter J, White-McLean J, et al. The occurrence of the rat lungworm, *Angiostrongylus cantonensis*, in nonindigenous snails in the Gulf of Mexico region of the United States. Hawaii J Med Public Health. 2013;72(Suppl 2):11–4.
3. York EM, Creecy JP, Lord WD, Caire W. Geographic range expansion for rat lungworm in North America. Emerg Infect Dis. 2015;21:1234–6. http://dx.doi.org/10.3201/eid2107.141980
4. New D, Little MD, Cross J. *Angiostrongylus cantonensis* infection from eating raw snails. N Engl J Med. 1995;332:1105–6. http://dx.doi.org/10.1056/NEJM199504203321619
5. Foster CE, Nicholson EG, Chun AC, Gharfeh M, Anvari S, Seeborg FO, et al. *Angiostrongylus cantonensis* infection: a cause of fever of unknown origin in pediatric patients. Clin Infect Dis. 2016;63:1475–8. http://dx.doi.org/10.1093/cid/ciw606
6. Tseng YT, Tsai HC, Sy CL, Lee SS, Wann SR, Wang YH, et al. Clinical manifestations of eosinophilic meningitis caused by *Angiostrongylus cantonensis*: 18 years' experience in a medical center in southern Taiwan. J Microbiol Immunol Infect. 2011;44:382–9. http://dx.doi.org/10.1016/j.jmii.2011.01.034
7. Evans-Gilbert T, Lindo JF, Henry S, Brown P, Christie CD. Severe eosinophilic meningitis owing to *Angiostrongylus cantonensis* in young Jamaican children: case report and literature review. Paediatr Int Child Health. 2014;34:148–52. http://dx.doi.org/10.1179/2046905513Y.0000000106

Address for correspondence: Roukaya Al Hammoud, University of Texas Health, McGovern Medical School, Pediatric Infectious Diseases Division, 6431 Fannin St, Ste 3.126, Houston, TX 77030, USA; email: Roukaya.AlHammoud@uth.tmc.edu

Enterocytozoon bieneusi Microsporidiosis in Stem Cell Transplant Recipients Treated with Fumagillin[1]

Iryna Bukreyeva, Adela Angoulvant, Inès Bendib, Jean-Charles Gagnard, Jean-Henri Bourhis, Sylvie Dargère, Julie Bonhomme, Marc Thellier, Bertrand Gachot, Benjamin Wyplosz

Author affiliations: Centre Hospitalier Universitaire de Bicêtre, Le Kremlin-Bicêtre, France (I. Bukreyeva, A. Angoulvant, I. Bendib, J.-C. Gagnard, B. Wyplosz); Université Paris-Sud, Le Moulon, France (A. Angoulvant); Institut Gustave Roussy, Villejuif, France (J.-H. Bourhis, B. Gachot); Centre Hospitalier Universitaire de Caen, Caen, France (S. Dargère, J. Bonhomme); Centre Hospitalier Universitaire Pitié-Salpêtrière, Paris, France (M. Thellier); Université Pierre et Marie Curie, Paris (M. Thellier)

DOI: https://dx.doi.org/10.3201/eid2306.161825

Enterocytozoon bieneusi microsporidiosis is an emerging disease in immunocompromised patients. We report 2 cases of this disease in allogeneic hematopoietic stem cell transplant patients successfully treated with fumagillin. Thrombocytopenia occurred but without major adverse events. Modifications of immunosuppression could be avoided when *E. bieneusi* is rapidly identified and fumagillin therapy is started promptly.

Enterocytozoon bieneusi, the most common cause of microsporidiosis in humans (*1*), causes chronic diarrhea and severe wasting syndrome in immunocompromised patients (*2*). In 2002, oral fumagillin was established as an effective treatment for *E. bieneusi* microsporidiosis in HIV-infected and solid organ transplant (SOT) patients (*3*). In contrast to previous treatments that did not result in parasitologic clearance or clinical remission, fumagillin showed a cure rate of 100%, even for severely immunocompromised patients (*2*,*4*–*10*).

Thrombocytopenia is the main adverse event of fumagillin therapy, occurring in up to 33% of patients (*3*) and raising concerns about fumagillin use in patients with hematologic disorders. We report 2 cases of *E. bieneusi* microsporidiosis in allogeneic hematopoietic stem cell transplant (HSCT) recipients who were treated with fumagillin and experienced thrombocytopenia.

Patient 1 was a 50-year-old woman admitted to Centre Hospitalier Universitaire de Caen (Caen, France) after profuse watery diarrhea and abdominal discomfort for 3 weeks. She had not traveled abroad. Three years earlier, she received a genoidentical allogeneic HSCT for myeloid leukemia. She recently had cutaneous chronic graft-versus-host disease. Her immunosuppression regimen used was prednisone and mycophenolate mofetil.

At admission, the patient was dehydrated and had a weight loss of 3 kg. Laboratory analyses showed lymphocytopenia (960 lymphocytes/mm^3), reference neutrophil (5,100 cells/mm^3) and platelet (408,000 platelets/mm^3) counts, and a C-reactive protein level <5 mg/L.

Results of fecal sample analyses were negative for pathogenic bacteria and viruses. Microscopic examination of fecal smears stained with Weber-Green–modified trichrome showed microsporidia. *E. bieneusi* was identified by using monoclonal antibodies (IFA-MAbs; Bordier Affinity Products, Crissier, Switzerland).

The mycophenolate mofetil dose was reduced by 50% for 8 days but no benefit was shown. Resolution of symptoms occurred ≤5 days after initiating fumagillin therapy (60 mg/d for 14 d); fecal smears were negative for microsporidia on day 9, and transient thrombocytopenia (131,000 platelets/mm^3) was observed on day 18 (Figure). Fecal smears remained negative for *E. bieneusi* during the 6-month follow-up. No clinical relapse occurred.

Patient 2 was a 42-year-old man referred to Centre Hospitalier Universitaire de Bicêtre (Le Kremlin-Bicêtre, France) after profuse acute diarrhea for 2 weeks and a weight loss of 10 kg. He had not traveled abroad. Four years earlier, he received a genoidentical allogeneic HSCT for acute leukemia. During the follow-up period, he was given a diagnosis of chronic graft-versus-host disease. He was given extracorporeal phototherapy with mycophenolate mofetil, sirolimus, and prednisolone.

At admission, the patient was afebrile and dehydrated. Blood analyses showed severe lymphocytopenia (400 lymphocytes/mm^3), reference neutrophil (4,680 cells/mm^3) and platelet (251,000 platelets/mm^3) counts, and a C-reactive protein level <5 mg/L. Results of microbiological analyses of fecal samples were negative for viruses and pathogenic bacteria. Microscopic examination of fecal smears stained with Weber-Green–modified trichrome showed microsporidia. *E. bieneusi* was identified by using monoclonal antibodies.

The patient was treated with fumagillin (60 mg/d for 14 d) (Figure). Immunosuppressive therapy was not modified. Clinical symptoms resolved within 5 days. Platelet counts progressively decreased. Fumagillin was withdrawn on day 14, but thrombocytopenia worsened (40,000 platelets/mm^3) by day 18. However, the patient spontaneously recovered in 10 days without any bleeding. No relapses were observed. Microsporidia were not detected in fecal samples during the 6-month follow-up.

[1]Results from this study were presented at the 26th European Congress of Clinical Microbiology and Infection Diseases; April 9–12, 2016; Amsterdam, the Netherlands.

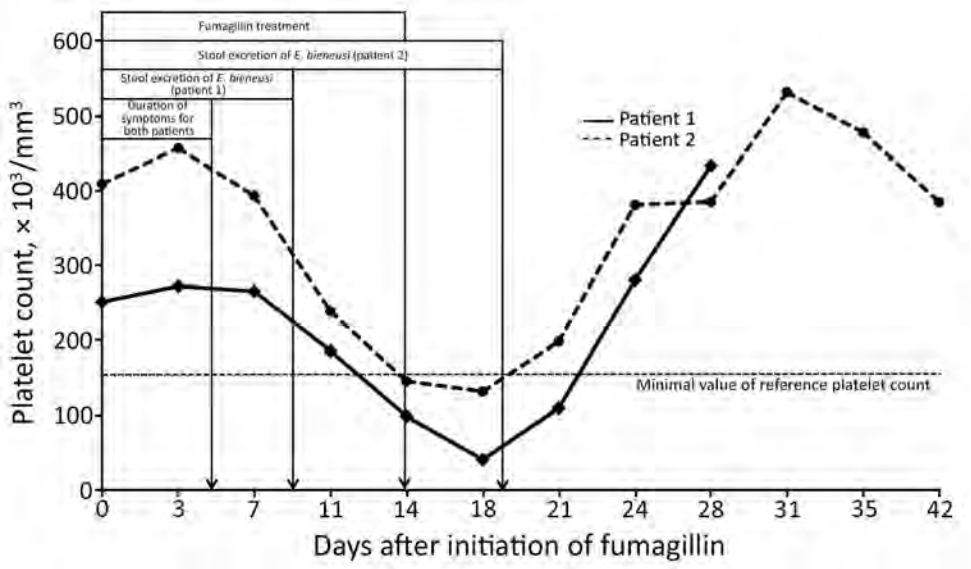

Figure. Platelet counts and clinical and parasitologic characteristics during fumagillin therapy and a 1-month follow-up of 2 allogeneic hematopoietic stem cell recipients with *Enterocytozoon bieneusi* microsporidiosis.

E. bieneusi is an emerging pathogen in immunocompromised patients (*1*). Increasing numbers of cases have been reported in SOT patients. We report 2 cases of *E. bieneusi* microsporidiosis in allogeneic HSCT recipients who were treated with fumagillin without modifying the immunosuppressive regimen for 1 recipient. In France, fumagillin can be obtained from the French National Agency for Medicines and Health Products Safety (Saint-Denis, France) after an individual patient expanded-access request is submitted.

Clinical and microbiological responses for the 2 case-patients were similar to those reported for other immunocompromised patients (*3*). No relapses were observed for 4 HIV-infected patients whose CD4 cell counts remained low, or for 2 SOT recipients who did not receive tapering immunosuppressive therapy (*3*). In other studies, 15 (70%) of 21 patients treated with fumagillin were cured without modifying immunosuppression regimens (*2*,*6*,*10*); for 6 other patients, immunosuppressive therapy was tapered (n = 4) or withdrawn (n = 2), but reasons for modifying immunosuppression were not specified. For 1 of our patients, the mycophenolate mofetil dose was reduced by 50% to decrease the immunosuppression level. However, no benefit was observed. In contrast, fumagillin led to clinical remission within 5 days.

We observed thrombocytopenia (platelet count $\leq$40,000/mm^3) in both patients but no evidence of bleeding. In other non-AIDS patients, thrombocytopenia was reported in 11 (52%) SOT patients receiving fumagillin, including 4 patients with severely low platelet counts (<25,000/mm^3) (*1*,*4*,*6*). For these patients, including those we report, thrombocytopenia occurred during the second week of treatment; a minimum value was observed a few days after completing fumagillin therapy. Spontaneous recovery occurred within 2 weeks. Bleeding, hematoma, or requirements for platelet transfusions were not reported. For both patients we report, microsporidia were not detected in fecal samples of both patients during the 6-month follow-up.

In conclusion, fumagillin was highly efficient in curing *E. bieneusi* microsporidiosis in 2 allogeneic HSCT recipients. Thrombocytopenia occurred but without major adverse events. Modifications to immunosuppression could be avoided when *E. bieneusi* is rapidly identified and fumagillin therapy is started promptly.

Dr. Bukreyeva is a physician in the Infectious and Tropical Diseases Unit at the Bicêtre University Hospital, Kremlin-Bicêtre, France. Her research interests include prevention and treatment of infections in immunocompromised patients.

References

1. Didier ES, Weiss LM. Microsporidiosis: current status. Curr Opin Infect Dis. 2006;19:485–92. http://dx.doi.org/10.1097/01.qco.0000244055.46382.23
2. Lanternier F, Boutboul D, Menotti J, Chandesris MO, Sarfati C, Mamzer Bruneel MF, et al. Microsporidiosis in solid organ transplant recipients: two *Enterocytozoon bieneusi* cases and review. Transpl Infect Dis. 2009;11:83–8. http://dx.doi.org/10.1111/j.1399-3062.2008.00347.x
3. Molina JM, Tourneur M, Sarfati C, Chevret S, de Gouvello A, Gobert JG, et al.; Agence Nationale de Recherches sur le SIDA 090 Study Group. Fumagillin treatment of intestinal microsporidiosis. N Engl J Med. 2002;346:1963–9. http://dx.doi.org/10.1056/NEJMoa012924
4. Desoubeaux G, Maakaroun-Vermesse Z, Lier C, Bailly E, Morio F, Labarthe F, et al. Successful treatment with fumagillin of the first pediatric case of digestive microsporidiosis in a liver-kidney transplant. Transpl Infect Dis. 2013;15:E250–9. http://dx.doi.org/10.1111/tid.12158
5. Pomares C, Santín M, Miegeville M, Espern A, Albano L, Marty P, et al. A new and highly divergent *Enterocytozoon bieneusi* genotype isolated from a renal transplant recipient. J Clin Microbiol. 2012;50:2176–8. http://dx.doi.org/10.1128/JCM.06791-11
6. Godron A, Accoceberry I, Couret A, Llanas B, Harambat J. Intestinal microsporidiosis due to *Enterocytozoon bieneusi* in

a pediatric kidney transplant recipient successfully treated with fumagillin. Transplantation. 2013;96:e66–7. http://dx.doi.org/10.1097/TP.0b013e3182a902e7
7. Kicia M, Wesolowska M, Jakuszko K, Kopacz Z, Sak B, Květonova D, et al. Concurrent infection of the urinary tract with *Encephalitozoon cuniculi* and *Enterocytozoon bieneusi* in a renal transplant recipient. J Clin Microbiol. 2014;52:1780–2. http://dx.doi.org/10.1128/JCM.03328-13
8. Ghoshal U, Khanduja S, Pant P, Prasad KN, Dhole TN, Sharma RK, et al. Intestinal microsporidiosis in renal transplant recipients: prevalence, predictors of occurrence and genetic characterization. Indian J Med Microbiol. 2015;33:357–63. http://dx.doi.org/10.4103/0255-0857.158551
9. Bednarska M, Bajer A, Welc-Faleciak R, Czubkowski P, Teisseyre M, Graczyk TK, et al. The first case of *Enterocytozoon bieneusi* infection in Poland. Ann Agric Environ Med. 2013; 20:287–8.
10. Champion L, Durrbach A, Lang P, Delahousse M, Chauvet C, Sarfati C, et al. Fumagillin for treatment of intestinal microsporidiosis in renal transplant recipients. Am J Transplant. 2010;10:1925–30. http://dx.doi.org/10.1111/j.1600-6143.2010.03166.x

Address for correspondence: Benjamin Wyplosz, Service de Maladies Infectieuses et Tropicales, Centre Hospitalier Universitaire de Bicêtre, 78 Rue du Général Leclerc, 94275 Le Kremlin-Bicêtre, France; email: benjamin.wyplosz@aphp.fr

Influenza A(H9N2) Virus, Myanmar, 2014–2015

Thant Nyi Lin, Nutthawan Nonthabenjawan, Supassama Chaiyawong, Napawan Bunpapong, Supanat Boonyapisitsopa, Taveesak Janetanakit, Pont Pont Mon, Hla Hla Mon, Kyaw Naing Oo, Sandi Myint Oo, Mar Mar Win, Alongkorn Amonsin

Author affiliations: Chulalongkorn University, Bangkok, Thailand (T.N. Lin, N. Nonthabenjawan, S. Chaiyawong, N. Bunpapong, S. Boonyapisitsopa, T. Janetanakit, A. Amonsin); University of Veterinary Science, Nay Pyi Taw, Myanmar (T.N. Lin, S.M Oo, M.M. Win); Ministry of Agriculture, Livestock and Irrigation, Insein, Yangon, Myanmar (P.P. Mon); Ministry of Agriculture, Livestock and Irrigation, Sintgaing, Mandalay, Myanmar (H.H. Mon); Ministry of Agriculture, Livestock and Irrigation, Nay Pyi Taw (K.N. Oo)

DOI: https://dx.doi.org/10.3201/eid2306.161902

Routine surveillance of influenza A virus was conducted in Myanmar during 2014–2015. Influenza A(H9N2) virus was isolated in Shan State, upper Myanmar. Whole-genome sequencing showed that H9N2 virus from Myanmar was closely related to H9N2 virus of clade 4.2.5 from China.

Influenza A(H9N2) virus has been found in several avian species. Despite low pathogenicity in poultry, H9N2 viruses are important to public health because of their high adaptability and frequent infection in humans. Clinical cases of H9N2 human infection have been reported in China (including Hong Kong) and Bangladesh (*1*,*2*). H9N2 viruss are constantly evolving and can reassort with other influenza A virus subtypes, resulting in novel influenza viruses. H9N2 was the likely donor of internal genes for the H5N1, H7N9, and H10N8 viruses (*3*,*4*).

During December 2014–August 2015, we conducted an influenza A surveillance program in Shan State, Myanmar. An outbreak of highly infectious avian influenza A(H5N1) in November 2007 has been the only outbreak reported in this state. For this study, we collected 648 samples from live-bird markets (LBMs) in Muse, Namkham, Laukkai, and Chinshwehaw, Shan State townships on the China–Myanmar border (online Technical Appendix 1, https://wwwnc.cdc.gov/EID/article/23/6/16-1902-Techapp1.pdf). We collected oropharygeal swab specimens from chickens (n = 273) and ducks (n = 180) as well as environmental samples (n = 195). Identification and isolation were performed at the Livestock Breeding and Veterinary Department, Yangon, Myanmar (online Technical Appendix).

Of the 648 samples subjected to virus isolation by egg inoculation, 10 were hemagglutinin (HA) positive. We further confirmed 3 samples as influenza A virus by using real-time reverse transcription PCR (RT-PCR), and we subtyped and confirmed all 3 as H9N2 (online Technical Appendix Table 1). However, the overall occurrence of H9N2 in the LBMs in this study was relatively low. The 3 H9N2 isolates, A/chicken/Myanmar/NK-2/2015(H9N2), A/chicken/Myanmar/NK-4/2015(H9N2), and A/chicken/Myanmar/NK-5/2015(H9N2), were from chickens in LBMs in Namkham Township in June 2015.

To characterize the Myanmar H9N2 virus, we performed whole-genome sequencing of these 3 isolates and submitted nucleotide sequences GenBank (accession nos. KY115364–KY115387). Although an international standard for clade nomenclature of the H9 subtype has not been well established, phylogenetic analysis showed that all 3 Myanmar H9N2 isolates were grouped into clade 4.2.5 (HA gene) and BJ94-like (neuraminidase [NA] gene) (Figure; and online Technical Appendix Figure 2) (*5*). The Myanmar H9N2 viruses clustered with avian and human H9N2 virus recovered in China in 2015. The phylogenetic analyses of internal protein genes showed similar findings; the Myanmar H9N2 viruses were also closely related to avian H9N2 viruses from China. Five internal protein genes, polymerase basic protein 2 (PB2), polymerase basic protein 1 (PB1), polymerase acidic protein (PA), nucleoprotein (NP), and membrane protein (M), were grouped with the viruses of G1 lineage, and the nonstructural (NS)

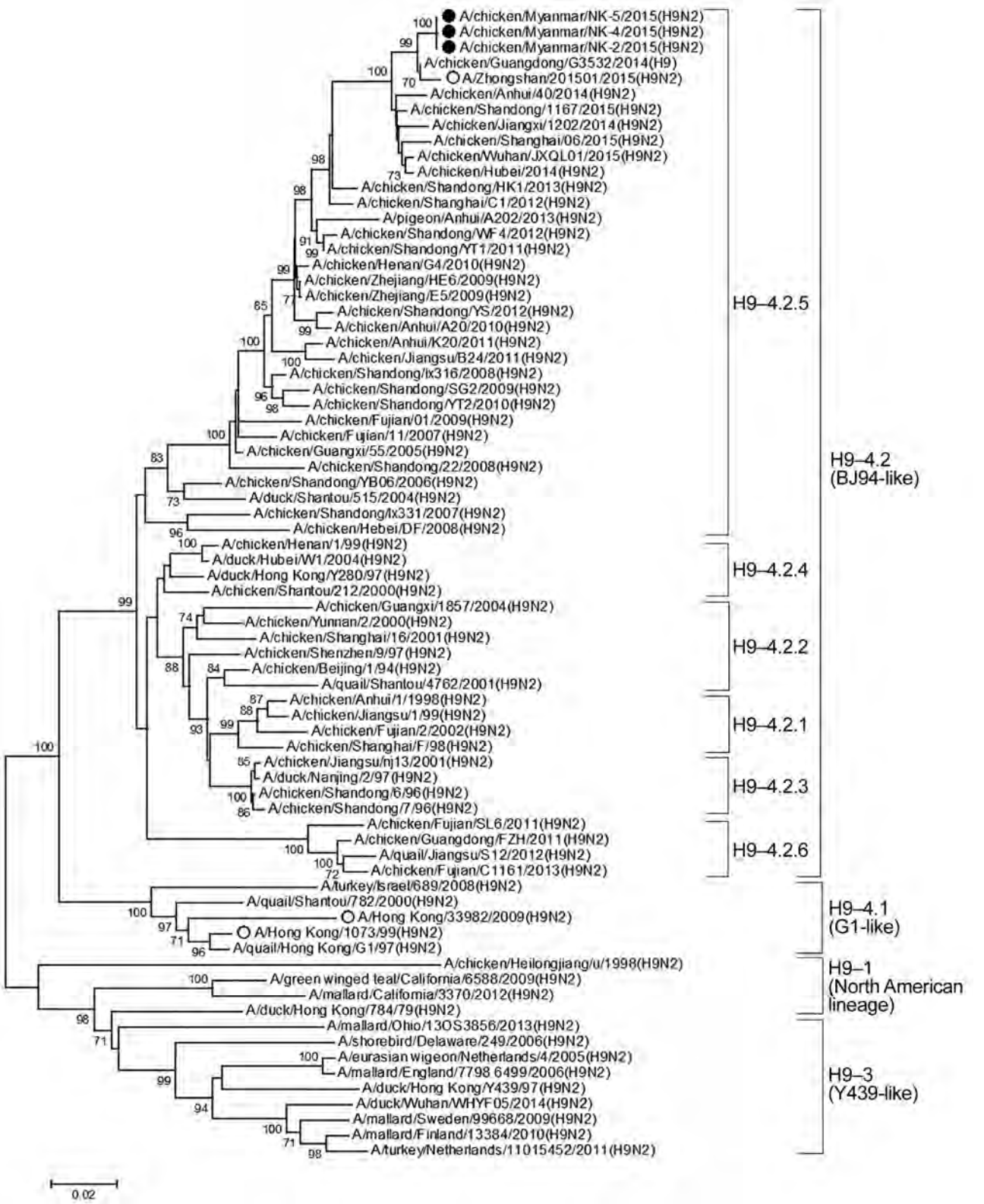

Figure. Phylogenetic tree of H9 gene of influenza A(H9N2) viruses from Myanmar and reference viruses. Phylogenetic trees were constructed by using MEGA version 6.0 (http://www.megasoftware.net/) and a neighbor-joining algorithm with the Kimura 2-parameter model and 1,000 replications of bootstrap analysis. Only bootstrap numbers >70% are shown. Black circles represent isolates from this study, and open circles represent human H9N2 isolates. Virus clades are indicated at right. Scale bar indicates nucleotide substitutions per site.

gene was grouped in BJ-94–like lineage (online Technical Appendix Figure 3). In addition, BLAST analysis (https://blast.ncbi.nlm.nih.gov/Blast.cgi) of the 8 gene segments of the Myanmar H9N2 viruses showed high percentages of nucleotide identities with H9N2 viruses from China (online Technical Appendix Table 2).

Genetic analysis showed that the Myanmar H9N2 viruses possessed R-S-S-R at the HA cleavage site, indicating low pathogenic characteristics (*6*). At the HA receptor binding sites, all Myanmar H9N2 isolates carried Q226L substitution, showing the affinity to human α-2,6-glycan receptors (*7*). The Myanmar H9N2 viruses possessed all 7 HA receptor binding sites, identical to human H9N2 virus A/Zhongshan/201501/2015 (online Technical Appendix Table 3) (*8*). For NA gene analysis, all Myanmar H9N2 viruses had a 3-aa deletion (positions 62 to 64) in the NA stalk region, suggesting virus adaptation from wild birds to poultry (*8*).

Internal protein gene analysis showed that the Myanmar H9N2 isolates possessed both avian- and human-specific amino acids. For example, no mutation was observed at E627 and D701 in PB2, retaining the avian characteristics (*9*), whereas human-specific amino acids were observed at 13P in PB1 and 409N in PA (*10*). Amino acids concerning virulence of the H9N2 viruses were also indicated. For example, the PA gene carried 672L and the NS1 gene contained 149A, relating to increased virulence of the virus (*10*). All Myanmar H9N2 viruses also possessed 31N in the M2 gene, suggesting amantadine resistance. Our results, based on the whole-genome analysis, showed that the Myanmar H9N2 viruses possessed all genetic signatures and virulence determinants similar to avian and human H9N2 viruses circulating in China in 2015 (online Technical Appendix Tables 3–5).

In conclusion, the Myanmar H9N2 viruses were considered of low pathogenicity in chickens. However, public health concerns should be raised because the viruses are closely related tom and possess virulence determinants similar to, human H9N2 reported in China in 2015. The human cases likely represent a spillover of the virus to humans from poultry (*8*). The Myanmar H9N2 viruses were obtained from healthy chickens in LBMs near the China–Myanmar border, where sources of poultry are mostly from China. Because LBMs are the major sources of several subtypes of influenza viruses, this environment provides opportunities for influenza viruses to mix, be transmitted, and exchange their gene segments. Infection and transmission in humans and poultry can frequently occur in LBM settings. Therefore, public awareness, control measures, and routine disease surveillance should be implemented.

This research was supported by the National Research University Fund (NRU59-028-HR) and the research chair grant NSTDA (P-15-50004). Chulalongkorn University provided financial support to the Center of Excellence for Emerging and Re-emerging Infectious Diseases in Animals and the graduate scholarship for Neighboring Countries to T.N.L. The Thailand Research Fund (TRF) provided financial support to the TRF Senior Scholar (RTA5780006) to A.A.

Dr. Lin, a veterinarian, is a PhD candidate at the Center of Excellence for Emerging and Re-emerging Diseases in Animals, Faculty of Veterinary Science, Chulalongkorn University, Bangkok, Thailand. His research interests are molecular epidemiology of emerging infectious diseases, especially influenza, in animals.

References

1. Butt KM, Smith GJ, Chen H, Zhang LJ, Leung YH, Xu KM, et al. Human infection with an avian H9N2 influenza A virus in Hong Kong in 2003. J Clin Microbiol. 2005;43:5760–7. http://dx.doi.org/10.1128/JCM.43.11.5760-5767.2005
2. Shanmuganatham K, Feeroz M, Jones-Engel L, Smith G, Fourment M, Walker D, et al. Antigenic and molecular characterization of avian influenza A(H9N2) viruses, Bangladesh. Emerging Infect Dis. 2013;19:1393–1402 . http://dx.doi.org/10.3201/eid1909.130336
3. Gao R, Cao B, Hu Y, Feng Z, Wang D, Hu W, et al. Human infection with a novel avian-origin influenza A (H7N9) virus. N Engl J Med. 2013;368:1888–97. http://dx.doi.org/10.1056/NEJMoa1304459
4. Zhang Y, Yin Y, Bi Y, Wang S, Xu S, Wang J, et al. Molecular and antigenic characterization of H9N2 avian influenza virus isolates from chicken flocks between 1998 and 2007 in China. Vet Microbiol. 2012;156:285–93. http://dx.doi.org/10.1016/j.vetmic.2011.11.014
5. Liu S, Ji K, Chen J, Tai D, Jiang W, Hou G, et al. Panorama phylogenetic diversity and distribution of Type A influenza virus. PLoS One. 2009;4:e5022. http://dx.doi.org/10.1371/journal.pone.0005022
6. Ge F-F, Zhou J-P, Liu J, Wang J, Zhang W-Y, Sheng L-P, et al. Genetic evolution of H9 subtype influenza viruses from live poultry markets in Shanghai, China. J Clin Microbiol. 2009;47:3294–300. Pub Med http://dx.doi.org/10.1128/JCM.00355-09
7. Matrosovich MN, Krauss S, Webster RG. H9N2 influenza A viruses from poultry in Asia have human virus-like receptor specificity. Virology. 2001;281:156–62. http://dx.doi.org/10.1006/viro.2000.0799
8. Zhao Y, Li S, Zhou Y, Song W, Tang Y, Pang Q, et al. Phylogenetic analysis of hemagglutinin genes of H9N2 avian influenza viruses isolated from chickens in Shandong, China, between 1998 and 2013. BioMed Res Int. 2015;2015:267520. http://dx.doi.org/ 10.1155/2015/267520
9. Yuan J, Xu L, Bao L, Yao Y, Deng W, Li F, et al. Characterization of an H9N2 avian influenza virus from a *Fringilla montifringilla* brambling in northern China. Virology. 2015;476:289–97. http://dx.doi.org/10.1016/j.virol.2014.12.021
10. Kandeil A, El-Shesheny R, Maatouq AM, Moatasim Y, Shehata MM, Bagato O, et al. Genetic and antigenic evolution of H9N2 avian influenza viruses circulating in Egypt between 2011 and 2013. Arch Virol. 2014;159:2861–76. http://dx.doi.org/10.1007/s00705-014-2118-z

Address for correspondence: Alongkorn Amonsin, Department of Veterinary Public Health, Faculty of Veterinary Science, Chulalongkorn University, Bangkok 10330, Thailand; email: alongkornamonsin1@gmail.com

PCR Detection of Mimivirus

Didier Raoult, Anthony Levasseur, Bernard La Scola

Author affiliation: Aix-Marseille Université, Marseille, France

DOI: https://dx.doi.org/10.3201/eid2306.161896

In an epidemiological study, mimivirus was reported as an unlikely cause of human respiratory infections in China. Our analysis revealed the nonsensitivity of the PCR method, which detected less than 10% of the current known mimivirus. We conclude that epidemiologic studies must use accurate and sensitive laboratory test methods.

The article by Zhang et al. (*1*) reporting the failure to detect mimivirus (*Acanthamoeba polyphaga* mimivirus) in patients with acute respiratory symptoms was flawed in 2 ways. First, a single mimivirus was detected by PCR but was dismissed by the authors as colonization. Second, and of greater concern, the PCR used by the authors would not detect most known mimiviruses because of primer/probe mismatches. In fact, PCRs used in most mimivirus prevalence studies would fail to detect most mimiviruses, given the extensive genome sequence diversity of these viruses (*2*).

We evaluated the PCR primers/probes used by Zhang et al. (*1*) for sequence similarity with 51 mimivirus genomes available in the public domain since March 2016, the date on which the article by Zhang et al. was submitted (*3*). Our in silico analysis found that none of the 25 genomes available from lineage A and 7 genomes from lineage B were complementary with their primers and probes, and only 5 of 19 lineage C genomes showed sufficient sequence similarity to permit successful amplification (Table). Overall, the PCR used by these authors would be predicted to detect only ≈26% of lineage C mimiviruses and <10% of published mimivirus genomes overall.

As proposed by Ngounga et al. (*4*), the great variability across the 3 lineages of mimivirus genomes requires the design of lineage-specific primers to improve PCR sensitivity (*4*). Until PCRs are improved, mimiviruses might be best detected by metagenomic approaches that have recently seen success in terms of mimivirus detection. For example, mimivirus-like reads have been identified by metagenomics in 1 (8%) of 12 fecal samples from children with acute diarrhea (*5*); 5 (27%) of 18 prostatic secretion samples from persons with prostatitis (*6*); all DNA libraries tested from the plasma of patients with hepatitis (*7*); 0.0018% of total viral reads from nasopharyngeal samples from 210 patients with respiratory tract symptoms (*8*); and all tested fecal, mid-vaginal, buccal mucosal, and retroauricular crease samples, with a predominance of mimiviruses in fecal samples reaching ≈33% of the total viral reads (*9*).

In metagenomics approaches, the number of reads detected and the distribution along the whole viral genome

Table. Mimivirus genomes in the public domain screened to determine whether the genomes were complementary with their primers/probes*

Lineage A (GenBank accession no.)	Lineage B (GenBank accession no.)	Lineage C (GenBank accession no.)
Mimivirus fauteuil (CWKE00000000)	Moumouvirus ochan (CXPE00000000)	Megavirus shan (CWIL00000000)
Mimivirus longchamps (CXOV00000000)	Moumouvirus istres (PRJEB9189)	Megavirus montpellier3 (CWIA00000000)
Mimivirus marais (PRJEB9199)	Moumouvirus battle49 (CXOS00000000)	Megavirus mont1 (CWIO00000000)
Mimivirus lactours (CXOL00000000)	Moumouvirus saoudian (CXOQ00000000)	Megavirus avenue9 (CWHN00000000)
Mimivirus PointeRouge1 (CXOW00000000)	Moumouvirus boug1 (PRJEB9190)	Megavirus balcon (PRJEB9194)
Mimivirus PointeRouge2 (CXOU00000000)	Moumouvirus goulette (KC008572)	Megavirus ursino (CWJY00000000)
Mimivirus T3 (CXOR00000000)	Moumouvirus Monve (JN885994–JN886001)	Megavirus T1 (CWIB00000000)
Mimivirus huitre A06 (CWJT00000000)		Megavirus battle43 (CWHV00000000)
Mimivirus amazonia (CWHO00000000)		Megavirus T4 (CWJR00000000)
Mimivirus battle7 (CWJW00000000)		Megavirus J3 (CWIN00000000)
Mimivirus battle19 (CWJX00000000)		Megavirus T6 (CWJQ00000000)
Mimivirus battle27 (CWJS00000000)		**Megavirus chilensis (NC_016072)**
Mimivirus battle57 (CWJZ00000000)		**Megavirus courdo11 (JX975216)**
Mimivirus battle66 (CWKA00000000)		**Megavirus lba† (JX885207)**
Mimivirus battle83 (CWKG00000000)		Powai lake megavirus (KU877344)
Mimivirus battle86 (CWKD00000000)		**Megavirus terra1 (KF527229)**
Mimivirus T2 (CXOT00000000)		Megavirus courdo5 (CWID00000000)
Mimivirus battle6 (CWJU00000000)		Megavirus bus (CWIQ00000000)
Mimivirus dakar4 (CWKF00000000)		**Megavirus courdo7 (JN885990–JN885993)**
Mimivirus (AY653733)		
Mimivirus Bombay (KU761889)		
Mimivirus terra 2 (PRJNA240235)		
Samba virus (KF959826)		
Mimivirus lentille (AFYC00000000)		
Mimivirus urine†		

*Bold indicates genomes that would be predicted to be successfully amplified using the PCR primers and probes in the article by Zhang et al. (*1*).
†Mimiviruses isolated from human samples.

are essential parameters for viral detection. In practice, the search for mimivirus is complicated by the great genetic variability of the virus and the restricted availability of mimivirus culture systems to a few research laboratories (*10*). The deficiencies we found in the report by Zhang et al. highlight the need for carefully designed epidemiologic studies using sensitive laboratory test methods to accurately assess mimivirus prevalence and the potential role of mimivirus in human disease.

Dr. Raoult is an Associate Editor of *Emerging Infectious Diseases* and professor of microbiology at the School of Medicine, Aix-Marseille University, Marseille, France, and is head of the University Hospital Institute Méditerranée Infection in Marseille.

References

1. Zhang XA, Zhu T, Zhang PH, Li H, Li Y, Liu EM, et al. Lack of mimivirus detection in patients with respiratory disease, China. Emerg Infect Dis. 2016;22:2011–2. http://dx.doi.org/10.3201/eid2211.160687
2. Colson P, Aherfi S, La Scola B, Raoult D. The role of giant viruses of amoebas in humans. Curr Opin Microbiol. 2016;31:199–208. http://dx.doi.org/10.1016/j.mib.2016.04.012
3. Levasseur A, Bekliz M, Chabrière E, Pontarotti P, La Scola B, Raoult D. MIMIVIRE is a defence system in mimivirus that confers resistance to virophage. Nature. 2016;531:249–52. http://dx.doi.org/10.1038/nature17146
4. Ngounga T, Pagnier I, Reteno DG, Raoult D, La Scola B, Colson P. Real-time PCR systems targeting giant viruses of amoebae and their virophages. Intervirology. 2013;56:413–23. http://dx.doi.org/10.1159/000354563
5. Finkbeiner SR, Allred AF, Tarr PI, Klein EJ, Kirkwood CD, Wang D. Metagenomic analysis of human diarrhea: viral detection and discovery. PLoS Pathog. 2008;4:e1000011. http://dx.doi.org/10.1371/journal.ppat.1000011
6. Smelov V, Bzhalava D, Arroyo Mühr LS, Eklund C, Komyakov B, Gorelov A, et al. Detection of DNA viruses in prostate cancer. Sci Rep. 2016;6:25235. http://dx.doi.org/10.1038/srep25235
7. Law J, Jovel J, Patterson J, Ford G, O'Keefe S, Wang W, et al. Identification of hepatotropic viruses from plasma using deep sequencing: a next generation diagnostic tool. PLoS One. 2013;8:e60595. http://dx.doi.org/10.1371/journal.pone.0060595
8. Lysholm F, Wetterbom A, Lindau C, Darban H, Bjerkner A, Fahlander K, et al. Characterization of the viral microbiome in patients with severe lower respiratory tract infections, using metagenomic sequencing. PLoS One. 2012;7:e30875. http://dx.doi.org/10.1371/journal.pone.0030875
9. Rampelli S, Soverini M, Turroni S, Quercia S, Biagi E, Brigidi P, et al. ViromeScan: a new tool for metagenomic viral community profiling. BMC Genomics. 2016;17:165. http://dx.doi.org/10.1186/s12864-016-2446-3
10. Saadi H, Pagnier I, Colson P, Cherif JK, Beji M, Boughalmi M, et al. First isolation of mimivirus in a patient with pneumonia. Clin Infect Dis. 2013;57:e127–34. http://dx.doi.org/10.1093/cid/cit354

Address for correspondence: Didier Raoult, Faculté de Médecine, Université de la Méditerranée, URMITE UMR CNRS 6236 IRD 198, Centre National de Référence, 27 Blvd Jean Moulin, Marseille 13005 CEDEX 05, France; email: didier.raoult@gmail.com

Autochthonous Case of Eosinophilic Meningitis Caused by *Angiostrongylus cantonensis*, France, 2016

Yann Nguyen, Benjamin Rossi, Nicolas Argy, Catherine Baker, Beatrice Nickel, Hanspeter Marti, Virginie Zarrouk, Sandrine Houzé, Bruno Fantin, Agnès Lefort

Author affiliations: Hôpital Beaujon, Clichy, France (Y. Nguyen, B. Rossi, C. Baker, V. Zarrouk, B. Fantin, A. Lefort); Hôpital Bichat, Paris, France (N. Argy, S. Houzé); Swiss Tropical and Public Health Institute, Basel, Switzerland (B. Nickel, H. Marti); University of Basel, Basel (B. Nickel, H. Marti)

DOI: https://dx.doi.org/10.3201/eid2306.161999

We report a case of a 54-year-old Moroccan woman living in France diagnosed with eosinophilic meningitis caused by *Angiostrongylus cantonensis.* Diagnosis was based on clinical symptoms and confirmed by testing of serum and cerebrospinal fluid samples. Physicians should consider the risk for *A. cantonensis* infection outside of endemic areas.

Angiostrongylus cantonensis is a rat lungworm that has long been recognized as a cause of eosinophilic meningitis in Southeast Asia, the Pacific Islands, and the Caribbean, where it is endemic (*1*). Although sporadic imported cases have been described in European travelers (*2–5*), no autochthonous case of eosinophilic meningitis caused by *A. cantonensis* worms has been reported previously in metropolitan France.

A 54-year-old Moroccan woman was admitted to an emergency ward in Paris in 2016 because of fever and headache lasting 2 weeks. She had a history of type 2 diabetes treated with metformin and did not receive any other medication before the onset of symptoms. She was a pesco-vegetarian and worked as a cleaning woman in an office in Paris. She had taken up residence near Paris in the 1980s and had not traveled out of France since, except for Morocco over 2 years ago.

At admission, her blood pressure was 126/68 mm Hg, and her pulse was regular at 79 beats/min. The physical examination revealed meningeal signs with neck stiffness and photophobia without neurologic localization signs. No other clinical abnormality could be evidenced. Laboratory testing of serum showed a leukocyte count of 12.1 × 10^9 cells/L (reference range 4.5–11.0 × 10^9/L) with 18% (2.2 × 10^9 cells/L) eosinophils and a C-reactive protein of 73 mg/dL (reference range 0.08–3.1 mg/L). Cerebrospinal fluid (CSF) analysis showed a leukocyte count of 950 cells/µL with 56% eosinophils, a glucose concentration within reference range at 0.4 g/L, and an elevated protein level

of 0.9 g/L. CSF pressure was 16 cm H_2O (0.16 kPa). CSF PCR tests for viral diseases (including Epstein-Barr virus and herpes simplex viruses 1 and 2); Gram stains and cultures for bacteria, mycobacteria, and fungi; and a search for malignant cells were all negative. Serologic tests specific for HIV and human T-lymphotrophic viruses 1 and 2 were negative. Parasitologic examinations of stool samples did not reveal any ova, cysts, or Charcot-Leyden crystals. Serologic tests of peripheral blood samples for *Toxocara* spp., *Trichinella* spp., *Schistosoma* spp., *Taenia solium* cysticercosis, *Gnathostoma* spp., and *Fasciola hepatica*, as well as serologic tests of CSF samples for *Gnathostoma*, were all negative. In contrast, antibodies directed toward the *A. cantonensis* 31-kDa antigen were detected by Western blot both in serum and CSF samples. Computed tomography (CT) and magnetic resonance imaging of the brain showed normal findings. Thoracic and abdominal CT showed a liver hypodensity without signs of malignancy. The patient was treated by evacuation of the CSF, prednisone (1 mg/kg equivalents for 1 wk), and albendazole (800 mg/d for 5 d), which lead to the complete regression of symptoms.

Eosinophilic meningitis is defined as a CSF eosinophil count above 10% of the total cell count, or exceeding 10 eosinophils/µL. The main etiologies of eosinophilic meningitis are parasitic infectious diseases (among which *A. cantonensis* and *Gnathostoma* spp. infections are the most frequent), hematologic or neoplastic disorders, adverse drug reactions, and primary eosinophilic meningitis (*6*). In this case, diagnosis of angiostrongyliasis was confirmed by Western blot. According to the literature, detection of the 31-kDa band by immunoblot shows a high sensitivity and specificity (>99% for both) for the diagnosis of *A. cantonensis* infections (*7*).

Human infection by *A. cantonensis* lungworm results from the ingestion of uncooked paratenic hosts (freshwater shrimps, crabs, and frogs); intermediate hosts (snails and slugs); or poorly cleaned contaminated vegetables that have been in contact with these hosts (*8*). After passage through the gastrointestinal tract, the larvae cross into systemic circulation and migrate to the central nervous system. The incubation period of this disease varies from 7 to 35 days (*1*). Although angiostrongyliasis is mainly a tropical disease, this infection has become an emerging infection in Southeast Asia, the Pacific Islands, and the Caribbean Islands and in travelers who return home from endemic areas (*9*). Some authors have suggested that global warming, changes in dietary habits, increased global transportation of food products, increased international trade, and traveling could explain this expansion (*10*).

Because the patient we describe had not left the Paris area for 2 years, an infection by consumption of contaminated food in Morocco can be excluded; *A. cantonensis* larvae do not survive longer than a few weeks to a few months in the human body (*8*). She might have acquired the infection in France by consuming imported contaminated food, but she did not declare any consumption of imported snails or freshwater shrimp. She only declared eating vegetables and fish bought in a local supermarket. We failed to identify the source of infection or risky behaviors. Because of global food trade, physicians should be aware of the risk for *A. cantonensis* infection even in patients who do not report recent travel to endemic areas.

Acknowledgments

We thank Michèle Felce for assisting with the study and Karin Stoll-Rudin for expert technical assistance.

Dr. Nguyen is a resident in internal medicine at the Assistance Publique–Hôpitaux de Paris. His primary research interests are immunology and infectious diseases.

References

1. Wang Q-P, Lai D-H, Zhu X-Q, Chen X-G, Lun Z-R. Human angiostrongyliasis. Lancet Infect Dis. 2008;8:621–30. http://dx.doi.org/10.1016/S1473-3099(08)70229-9
2. Ali AB, Van den Enden E, Van Gompel A, Van Esbroeck M. Eosinophilic meningitis due to *Angiostrongylus cantonensis* in a Belgian traveller. Travel Med Infect Dis. 2008;6:41–4. http://dx.doi.org/10.1016/j.tmaid.2007.09.001
3. Luessi F, Sollors J, Torzewski M, Müller HD, Siegel E, Blum J, et al. Eosinophilic meningitis due to *Angiostrongylus cantonensis* in Germany. J Travel Med. 2009;16:292–4. http://dx.doi.org/10.1111/j.1708-8305.2009.00337.x
4. Bärtschi E, Bordmann G, Blum J, Rothen M. Eosinophilic meningitis due to *Angiostrongylus cantonensis* in Switzerland. Infection. 2004;32:116–8. http://dx.doi.org/10.1007/s15010-004-3028-x
5. Malvy D, Ezzedine K, Receveur M-C, Pistone T, Crevon L, Lemardeley P, et al. Cluster of eosinophilic meningitis attributable to *Angiostrongylus cantonensis* infection in French policemen troop returning from the Pacific Islands. Travel Med Infect Dis. 2008;6:301–4. http://dx.doi.org/10.1016/j.tmaid.2008.06.003
6. Lo Re V III, Gluckman SJ. Eosinophilic meningitis. Am J Med. 2003;114:217–23. http://dx.doi.org/10.1016/S0002-9343(02)01495-X
7. Eamsobhana P, Gan XX, Ma A, Wang Y, Wanachiwanawin D, Yong HS. Dot immunogold filtration assay (DIGFA) for the rapid detection of specific antibodies against the rat lungworm *Angiostrongylus cantonensis* (Nematoda: *Metastrongyloidea*) using purified 31-kDa antigen. J Helminthol. 2014;88:396–401. http://dx.doi.org/10.1017/S0022149X13000321
8. Ramirez-Avila L, Slome S, Schuster FL, Gavali S, Schantz PM, Sejvar J, et al. Eosinophilic meningitis due to *Angiostrongylus* and *Gnathostoma* species. Clin Infect Dis. 2009;48:322–7. http://dx.doi.org/10.1086/595852
9. Cowie RH, Hollyer JR, da Silva AJ, Hollingsworth RG, Dixon MC, Eamsobhana P, et al. Workshop on research priorities for management and treatment of angiostrongyliasis. Emerg Infect Dis. 2012;18:e1. http://dx.doi.org/10.3201/eid1812.120499
10. Eamsobhana P. Eosinophilic meningitis caused by *Angiostrongylus cantonensis*—a neglected disease with escalating importance. Trop Biomed. 2014;31:569–78.

Address for correspondence: Yann Nguyen, Department of Internal Medicine, Hôpital Beaujon, Assistance Publique – Hôpitaux de Paris, 100 boulevard du Général Leclerc, 92110 Clichy, France; email: yann.nguyen01@gmail.com

Zika Virus–Associated Cognitive Impairment in Adolescent, 2016

Jason Zucker, Natalie Neu, Claudia A. Chiriboga, Veronica J. Hinton, Marc Leonardo, Arif Sheikh, Kiran Thakur

Author affiliations: Columbia University Medical Center, New York, New York, USA (J. Zucker, N. Neu, C.A. Chiriboga, V.J. Hinton, A. Sheikh, K. Thakur); Child, Adolescent, and Adult Psychiatry private practice, New York (M. Leonardo)

DOI: https://dx.doi.org/10.3201/eid2306.162029

Incidence of neurologic manifestations associated with Zika virus infection has been increasing. In 2016, neuropsychological and cognitive changes developed in an adolescent after travel to a Zika virus–endemic area. Single-photon emission computed tomography and neuropsychological testing raised the possibility that Zika virus infection may lead to neuropsychiatric and cognitive symptoms.

Although the full clinical spectrum of complications associated with Zika virus disease remains unclear, evidence of an association between Zika virus infection and diseases of the nervous system is growing (*1*). Increased incidence of neurologic manifestations has been reported, including cerebral birth abnormalities (*2*), Guillain-Barré Syndrome (*3*), meningoencephalitis (*4*), and memory loss (*5*). We describe a case of probable central nervous system (CNS) infection with Zika virus associated with the onset of neuropsychological and cognitive changes in an adolescent.

In summer 2016, an adolescent traveled to a Zika virus–endemic island in the southern Caribbean, where many insect bites occurred. Before the trip, the patient's medical history included mild depression treated with a selective serotonin reuptake inhibitor. Assessment after return to the United States indicated that mental and physical health were the same as before travel. One week after return, the patient experienced sore throat, headache, diffuse scarlatiniform rash (online Technical Appendix Figure 1, https://wwwnc.cdc.gov/EID/article/23/6/16-2029-Techapp1.pdf), joint pain, confusion, and short-term memory loss; no fever or eye inflammation were noted.

Three days after symptom onset, the patient received care from a pediatrician; extensive laboratory testing revealed urine reverse transcription PCR (RT-PCR) results positive for Zika virus. Serologic results were positive for Epstein-Barr virus, consistent with the patient's history of infection 15 months earlier (online Technical Appendix Table 1). Five days after symptom onset, the sore throat, headache, rash and joint pain resolved; however, 8 days after symptom onset, the neuropsychiatric symptoms worsened and included excessive energy, decreased sleep, rapid and tangential speech, grandiose thinking, impulsivity, decreased inhibition, and behavioral regression suggestive of hypomania. The patient's psychiatrist prescribed an antipsychotic medication. An ambulatory and 24-hour electroencephalogram and magnetic resonance imaging of the brain without contrast showed no abnormalities.

Symptoms failed to improve, and 13 days after symptom onset, the patient was hospitalized for further work-up. Fourteen days after symptom onset, magnetic resonance imaging of the brain with contrast showed no abnormalities. Serum was positive for dengue virus IgG and IgM (online Technical Appendix Table 2). Repeat Zika virus testing was not performed because of the prior positivity of urine RT-PCR. Fifteen days after symptom onset, cerebrospinal fluid (CSF) obtained by lumbar puncture contained 8 leukocytes/μL, 1,000 erythrocytes/μL, 55 mg/dL glucose, and 30 mg/dL protein. CSF testing for Zika virus, performed at the Wadsworth Laboratory, New York City Department of Mental Health and Hygiene (New York, NY, USA), was positive for IgM but negative by RT-PCR.

After discharge, the patient's symptoms of regression, disinhibition, and cognitive impairment persisted. Seven weeks after symptom onset, single-photon emission computed tomography revealed mildly heterogeneous cerebral cortical perfusion, with focal moderate-to-severe hypoperfusion in the inferior left frontal region (online Technical Appendix Figure 2); neuropsychological testing demonstrated evidence of superior intellectual ability (Wechsler Intelligence Scale for Children–fourth edition, General Ability Index), probably reflecting function before illness (online Technical Appendix Table 3). Processing speed was significantly slowed relative to other skills; the Processing Speed Index score was >2 SDs lower than the General Ability Index score. Performance on most memory tests and tests of executive function was within normal limits yet lower than expected given reported performance before illness. Immediate and delayed visual recall of the Rey complex figure was poor, reflecting primary difficulty encoding new visual information. On a standardized behavioral questionnaire, the patient self-reported psychiatric symptoms including anxiety, racing thoughts, and an inability to turn off thoughts. The patient had not experienced racing thoughts before the Zika virus infection, and the anxiety symptoms had worsened since the infection. In addition, the patient reported significant and functionally limiting fatigue. Nine weeks after onset, symptoms were better but not resolved; because of concerns that these symptoms were triggered by a postinfectious immune-mediated process, a trial of intravenous immunoglobulin was administered. Fifteen

weeks after symptom onset, the patient's symptoms were better but not fully resolved.

Although we cannot entirely rule out Epstein-Barr virus as a possible trigger, the length of time between previous infection and onset of neuropsychological symptoms would be unusual. In addition, although it is impossible to exclude contributions of coinfection from other mosquitoborne viruses (e.g., dengue and chikungunya), given the Zika virus positivity on RT-PCR, the patient's condition met criteria for definitive Zika virus infection and the CSF IgM titer was consistent with CNS involvement of Zika virus. The changes on single-photon emission computed tomographs and neuropsychological test scores raise the possibility that Zika virus infection may trigger neuropsychiatric and cognitive symptoms. Although we cannot prove that the patient's symptoms were related to Zika virus, clinicians should be aware of this potential association and the value of closely monitoring patients with Zika virus infection.

K.T., who helped edit the manuscript, is a World Health Organization consultant on neurologic manifestations in the context of the Zika virus outbreak, receives an honorarium as chief consult editor on Zika virus for Medscape consults, and participates in Zika research through the Neuroviruses Emerging in the Americas Study. K.T. receives funding support from the National Institutes of Health, and J.Z. receives funding support from a National Institutes of Health training grant (T32 AI007531).

Dr. Zucker is a postdoctoral fellow in adult and pediatric infectious diseases at Columbia University Medical Center. His research interests include improving prevention and treatment for adolescents and young adults living with, or at risk for, HIV infection, hepatitis C, and sexually transmitted diseases.

References

1. Araujo AQ, Silva MT, Araujo AP. Zika virus-associated neurological disorders: a review. Brain. 2016;139:2122–30. http://dx.doi.org/10.1093/brain/aww158
2. Mlakar J, Korva M, Tul N, Popović M, Poljšak-Prijatelj M, Mraz J, et al. Zika virus associated with microcephaly. N Engl J Med. 2016;374:951–8. http://dx.doi.org/10.1056/NEJMoa1600651
3. dos Santos T, Rodriguez A, Almiron M, Sanhueza A, Ramon P, de Oliveira WK, et al. Zika virus and the Guillain-Barré Syndrome—case series from seven countries. N Engl J Med. 2016;375:1598–601. http://dx.doi.org/10.1056/NEJMc1609015
4. Carteaux G, Maquart M, Bedet A, Contou D, Brugières P, Fourati S, et al. Zika virus associated with meningoencephalitis. N Engl J Med. 2016:374:1595–6. http://dx.doi.org/10.1056/NEJMc1602964
5. Nicastri E, Castilletti C, Balestra P, Galgani S, Ippolito G. Zika virus infection in the central nervous system and female genital tract. Emerg Infect Dis. 2016;22:2228–30. http://dx.doi.org/10.3201/eid2212.161280

Address for correspondence: Jason Zucker, Columbia University Medical Center, 622 West 168th St, PH4 West–474, New York, NY 10032, USA; email: jz2700@cumc.columbia.edu

Highly Pathogenic Avian Influenza Virus (H5N8) Clade 2.3.4.4 Infection in Migratory Birds, Egypt

Abdullah A. Selim, Ahmed M. Erfan, Naglaa Hagag, Ali Zanaty, Abdel-Hafez Samir, Mohamed Samy, Ahmed Abdelhalim, Abdel-Satar A. Arafa, Mohamed A. Soliman, Momtaz Shaheen, Essam M. Ibraheem, Ibrahim Mahrous, Mohamed K. Hassan, Mahmoud M. Naguib

Author affiliations: National Laboratory for Veterinary Quality Control on Poultry Production, Animal Health Research Institute, Giza, Egypt (A.A. Selim, A.M. Erfan, N. Hagag, A. Zanaty, A.-H. Samir, M. Samy, A. Abdelhalim, A.-S.A. Arafa, M.A. Soliman, M. Shaheen, E.M. Ibraheem, M.K. Hassan, M.M. Naguib); General Organization for Veterinary Services, Giza (I. Mahrous); Friedrich-Loeffler-Institut, Federal Research Institute for Animal Health, Insel-Riems, Germany (M.M. Naguib)

DOI: https://dx.doi.org/10.3201/eid2306.162056

We isolated highly pathogenic avian influenza virus (H5N8) of clade 2.3.4.4 from the common coot (*Fulica atra*) in Egypt, documenting its introduction into Africa through migratory birds. This virus has a close genetic relationship with subtype H5N8 viruses circulating in Europe. Enhanced surveillance to detect newly emerging viruses is warranted.

Avian influenza is a highly contagious disease of poultry that continues to spread across the globe in bird populations. Occasionally, transmission of a highly pathogenic avian influenza virus (HPAIV) from infected poultry to humans results in a severe public health crisis (*1*).

In 2010, strains of HPAIV (H5N8) of clade 2.3.4.4 were first detected among wild birds in Asia and later spread to domestic birds across China, South Korea, and Japan (*2*,*3*). Most recently, a novel reassortant virus of subtype H5N8 clade 2.3.4.4 was reported in Russia and further spread to many countries in Europe, Asia, and the Middle East (*4*,*5*). The spread of HPAIV (H5N8) strains has been linked to the overlapping flyways of migratory wild birds that come from different continents; this mingling of wild birds poses a major concern worldwide (*4*,*6*).

Egypt is one of the most notable migration spots for migratory birds crossing Europe, Asia, and Africa. In early winter each year, thousands of migrating waterfowl use Egypt as a resting stop before they continue their journey southward through the African continent through the East Africa/East Asia and Mediterranean/Black Sea migratory

Figure. Structural and phylogenetic modeling of highly pathogenic avian influenza virus (H5N8), EG-CA285, from migratory birds, Egypt, 2016. A) Three-dimensional structural homology model for the hemagglutinin protein of EG-CA285 created by using the ancestral virus of clade 2.3.4.4b (A/duck/Zhejiang/6D18/2013 [H5N8]) as a template. Amino acids distinguishing the EG-CA285 sequence from the modeling template are shown in red; green depicts unique mutations distinguishing this virus from the virus detected in summer 2016 in Russia, A/great crested grebe/Uvs-Nuur-Lake/341/2016. B) Phylogenetic tree of the nucleotide sequences of avian influenza virus hemagglutinin genes. Maximum-likelihood calculations were done with IQ-TREE software (http://iqtree.cibiv.univie.ac.at/) under the best-fit model according to the Akaike criterion (general time reversible plus gamma plus G4 model). Bold indicates strains from Egypt; gray shading indicates strains currently circulating in Europe. Scale bar indicates nucleotide substitutions per site.

flyways. Lake Manzala in northern Egypt is a source of fish and a major refuge for many migratory birds (online Technical Appendix Figure 1, http://wwwnc.cdc.gov/EID/article/23/6/16-2056-Techapp1.pdf1).

During a targeted surveillance for avian influenza viruses (AIVs) conducted in migratory birds by Community Animal Health Outreach (CAHO) program on November 24, 2016, we collected 19 oropharyngeal and cloacal swab samples from diseased (mild depression) and dead migratory birds (common coot, *Fulica atra*; pintail ducks, *Anas acuta*; and Garganey ducks, *A. querquedula*) in a live bird and fish market in the Damietta Governorate in Egypt. (Hunted migratory birds are commonly sold for food in markets in this region.) Two samples from 2 common coots were confirmed positive for AIV and were subtyped as H5N8 by using specific real-time reverse transcription quantitative PCR (RT-qPCR) (online Technical Appendix). On November 30, 2016, the identification of HPAIV (H5N8) from 2 common coots was reported to the World Organisation for Animal Health. Notably, this newly emerged HPAIV (H5N8) was detected in Egypt in the same place, Damietta Governorate, where HPAIV (H5N1) was first identified in 2006 during the global spread of HPAIV (H5N1) viruses of clade 2.2 (*7*). Immediately thereafter, active targeted surveillance for AIV was conducted around Lake Manzala and the surroundings areas for AIV that included wild birds and domestic poultry; however, no more positive cases were detected.

We successfully isolated and characterized 1 HPAIV (H5N8) strain by nucleotide sequencing and phylogenetic analyses on the basis of its hemagglutinin (HA) and neuraminidase (NA) gene segments. The isolate was named A/common coot/Egypt/CA285/2016 (EG-CA285).

The amino acid sequence of the protease cleavage site of EG-CA285 HA protein revealed multiple basic amino acids, PLREKRRKR/GLF, which is characteristic of HPAIV. The receptor-binding pocket of EG-CA285 HA protein showed markers of avian receptor–specific binding: Q222 and G224. We observed 3 amino acid assignment differences in the HA protein, namely, R22K, E268G, and D487Y, which distinguished EG-CA285 from the recent HPAIV (H5N8) clade 2.3.4.4b strain isolated in Russia (A/great-crested-grebe/Uvs-Nuur-Lake/341/2016; GISAID accession no EPI_ISL_224580) (Figure, panel A). In the NA protein, we observed 4 substitution mutations (V8A, V31L, G126E, I407T) that distinguished the EG-CA285 from the subtype found in Russia. Phylogenetic analysis of HA and NA gene sequences revealed that EG-CA285 virus is clustered with clade 2.3.4.4b, along with the recent viruses widely distributed throughout Europe (Figure, panel B; online Technical Appendix Figure 2). Even though the unavailability of a full-length genomic sequence of this virus is a limitation in this study, the genetic and phylogenetic features of the HA and NA gene segments confirm the intercontinental dissemination of HPAIV (H5N8) through wild birds and its introduction into Egypt.

During the evolution of subtype H5Nx viruses of clade 2.3.4.4, frequent reassortment has been noted with other co-circulating HPAIVs and low pathogenicity AIVs in different countries in Europe, North America, and East Asia (*8*). Strains of HPAIV (H5N8) have been involved in multiple independent reassortment events with other AIV subtypes found in wild birds in China, South Korea, the United States, and recently in Russia (*5*,*9*). The probable introduction of HPAIV (H5N8) to poultry populations in Egypt will further complicate disease control and prevention, especially if HPAIV (H5N1) of clade 2.2.1.2 and low pathogenicity AIV (H9N2) strains of G1 lineage are enzootic in poultry (*10*).

In addition, the threat of emergence of a novel reassortants with unpredictable gene constellations of HPAIV (H5N8) strains with enzootic strains of AIV is a public health concern. Therefore, we recommend enhanced surveillance to quickly detect newly emerged viruses. Commercial and backyard poultry owners must follow the recommended biosecurity measures. The detection and immediate reporting of novel HPAIV (H5N8) strains in Egypt will help increase AIV surveillance, detection, and prevention preparedness in other countries of continental Africa.

Acknowledgments

We acknowledge Timm Harder and Anandan Paldurai for their fruitful discussions and helpful comments on this written work. We thank the colleagues in the National Laboratory for Veterinary Quality Control on Poultry Production, General Organizations for Veterinary Services, and Community Animal Healt=h Outreach team for their valuable support. We are grateful to those who submitted sequence data to the GISAID database (online Technical Appendix Table 1).

Dr. Selim is the technical manager of the National Laboratory for Quality Control on Poultry Production, Animal Health Research Institute, Egypt. His research interest includes diagnosis and molecular epidemiology of avian influenza viruses.

References

1. Alexander DJ, Brown IH. History of highly pathogenic avian influenza. Rev Sci Tech. 2009;28:19–38. http://dx.doi.org/10.20506/rst.28.1.1856.
2. Wu H, Peng X, Xu L, Jin C, Cheng L, Lu X, et al. Novel reassortant influenza A(H5N8) viruses in domestic ducks, eastern China. Emerg Infect Dis. 2014;20:1315. http://dx.doi.org/10.3201/eid2008.140339.
3. Lee Y-J, Kang H-M, Lee E-K, Song B-M, Jeong J, Kwon Y-K, et al. Novel reassortant influenza A(H5N8) viruses, South Korea, 2014. Emerg Infect Dis. 2014;20:1087–9 and http://dx.doi.org/10.3201/eid2006.140233.

4. European Centre for Disease Prevention and Control. Outbreak of highly pathogenic avian influenza A(H5N8) in Europe—18 November 2016. Stockholm: The Centre; 2016.
5. Lee DH, Sharshov K, Swayne DE, Kurskaya O, Sobolev I, Kabilov M, et al. Novel reassortant clade 2.3.4.4 avian influenza A(H5N8) virus in wild aquatic birds, Russia, 2016. Emerg Infect Dis. 2017;23:359–60. http://dx.doi.org/10.3201/eid2302.161252.
6. Lee DH, Torchetti MK, Winker K, Ip HS, Song CS, Swayne DE. Intercontinental spread of Asian-origin H5N8 to North America through Beringia by migratory birds. J Virol. 2015;89:6521–4. http://dx.doi.org/10.1128/JVI.00728-15.
7. Saad MD, Ahmed LS, Gamal-Eldein MA, Fouda MK, Khalil F, Yingst SL, et al. Possible avian influenza (H5N1) from migratory bird, Egypt. Emerg Infect Dis. 2007;13:1120–1 and http://dx.doi.org/10.3201/eid1307.061222.
8. Lee DH, Bahl J, Torchetti MK, Killian ML, Ip HS, DeLiberto TJ, et al. Highly pathogenic avian influenza viruses and generation of novel reassortants, United States, 2014–2015. Emerg Infect Dis. 2016;22:1283–5. http://dx.doi.org/10.3201/eid2207.160048.
9. Dalby A. Complete analysis of the H5 hemagglutinin and N8 neuraminidase phylogenetic trees reveals that the H5N8 subtype has been produced by multiple reassortment events [version 1; referees: 1 approved with reservations]. [cited 2017 Apr 4]. https://f1000research.com/articles/5-2463/v1
10. Naguib MM, Arafa AS, El-Kady MF, Selim AA, Gunalan V, Maurer-Stroh S, et al. Evolutionary trajectories and diagnostic challenges of potentially zoonotic avian influenza viruses H5N1 and H9N2 co-circulating in Egypt. J Mol Epidemiol Evol Gen Infect Dis. 2015;34:278–91. http://dx.doi.org/10.1016/j.meegid.2015.06.004.

Address for correspondence: Mahmoud M. Naguib, Friedrich-Loeffler-Institut Bundesforschungsinstitut fur Tiergesundheit Südufer 10, Greifswald–Insel Riems 17493, Germany; email: Mahmoud.naguib@fli.de

October 2016: **Disease Patterns**

- Outbreaks of Human *Salmonella* Infections Associated with Live Poultry, USA, 1990–2014
- Vaccine-Derived Polioviruses and Children with Primary Immunodeficiency, Iran, 1995–2014
- Infection-Related Deaths from Refractory Juvenile Idiopathic Arthritis
- Accuracy of Diagnosis of Human Granulocytic Anaplasmosis in China
- Population-Level Effects of Human Papillomavirus Vaccination Programs on Infection with Nonvaccine Human Papillomavirus Genotypes
- Cat-Scratch Disease in the United States, 2005–2013
- Community- and Healthcare-Associated *Clostridium difficile* Infections, Finland, 2008–2013
- Carbapenem Resistance in Clonally Distinct Clinical Strains of *Vibrio fluvialis* Isolated from Diarrheal Samples
- Whole-Genome Characterization of Epidemic *Neisseria meningitidis* Serogroup C and Resurgence of Serogroup W in Niger, 2015

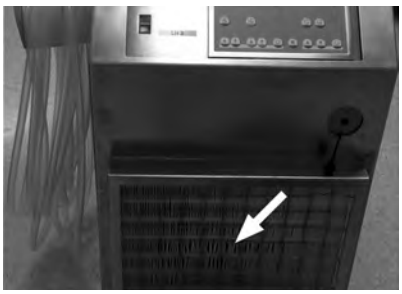

- Ebola Virus Disease in Children, Sierra Leone, 2014–2015
- Systematic Review and Meta-Analysis of the Treatment Efficacy of Doxycycline for Rectal Lymphogranuloma Venereum in Men who have Sex with Men
- Increase in Meningococcal Serogroup W Disease, Victoria, Australia, 2013–2015
- Distinct Zika Virus Lineage in Salvador, Bahia, Brazil
- *Streptococcus suis* Serotype 2 Capsule In Vivo
- Estimation of Severe MERS-CoV Cases in the Middle East, 2012–2016
- Hypervirulent Clone of Group B *Streptococcus* Serotype III Sequence Type 283, Hong Kong, 1993–2012

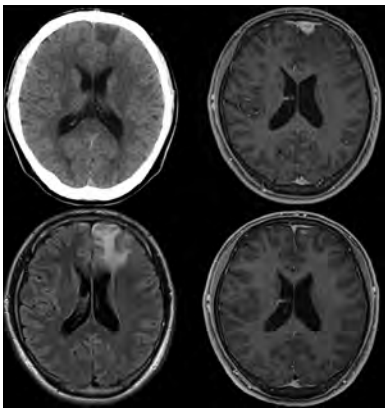

- Chikungunya Virus in Febrile Humans and *Aedes aegypti* Mosquitoes, Yucatan, Mexico
- Daily Reportable Disease Spatiotemporal Cluster Detection, New York, New York, USA, 2014–2015

EMERGING INFECTIOUS DISEASES

https://wwwnc.cdc.gov/eid/articles/issue/22/10/table-of-contents

Ramón y Cajal (1852–1934), Calyx of Held (3676) (detail), circa 1920. Pencil, India ink, ink washes on cardboard or paper. Digital image courtesy of the Cajal Institute-CSIC, Madrid, Spain.

"Unexplored Continents and Great Stretches of Unknown Territory"

Byron Breedlove

This month's cover art could be, at first glance, an image conjured by the vision of a surrealist painter in the 1920s or an intricate detail lifted from a textile designed by British artist William Morris in the 1870s. It borrows facets from both but is neither. Rather, this striking image is one among the thousands of scientific images created by Santiago Ramón y Cajal, one of the most influential neuroscientists of all time.

Cajal was born in Petilla de Aragón, a small village in northeastern Spain. He is well known for many key contributions to our knowledge of the structure of the nervous system and especially of the brain and spinal cord. Cajal's career as a researcher, teacher, and mentor spanned more than 50 years, and he published numerous groundbreaking books and more than 100 articles in French and Spanish scientific periodicals. He was

Author affiliation: Centers for Disease Control and Prevention, Atlanta, Georgia, USA

DOI: https://dx.doi.org/10.3201/eid2306.AC2306

also an artist, photographer, bodybuilder, chess player, and publisher.

A eureka moment in Cajal's career occurred in Madrid in 1887 when another scientist showed him the Golgi stain that made microscopic structures in brain tissue samples appear black against an amber background. Although Golgi's process was imprecise and inconsistent, Cajal realized that this method could be his pathway to studying microscopic details of the nervous system. After he refined and stabilized the black reaction, he logged long hours at his microscope painstakingly scrutinizing central nervous system tissues from animals and humans. Cajal eventually made more than 3,000 exquisitely detailed sketches of these images, and scientists and educators are still using them.

EID's cover art is Cajal's drawing of the calyces of Held—so named because Hans Held described the structure's resemblance to floral calyces in his 1893 article—which is one of the largest synapses in the human brain stem and is integral to the ability to detect and localize high-frequency sounds. Cajal portrayed the calyces as individual cells, encircled by thick black lines that show the axons. From this perspective, the calyces resemble flowers or seedpods intertwined about a central stalk.

Each dot, dash, or line, and the precise patterns, tones, and density in the image are in keeping with Cajal's credo that "A graphic representation of the object observed guarantees the exactness of the observation itself." (Note that the handwritten "Manzano number" in the upper left encircled by the stamped words "Museo Cajal Madrid" is a cataloguing convention added by the librarian who inventoried Cajal's archive in the 1940s.)

In *The Beautiful Brain: The Drawings of Santiago Ramón y Cajal,* Lyndel King and Eric Himmel describe how Cajal developed his sketches: "He preferred to work freehand, rarely resorting to a camera lucida, a device that projects the image from a microscope onto paper where it can be traced. He might start a drawing in pencil, and then later go over it in India ink, adding ink washes or watercolors for tonal areas."

Cajal's many distinctions include winning, along with the Italian histologist Camillo Golgi, the Nobel Prize in Physiology or Medicine in 1906. His legacy endures through the continued work and influence of the Spanish school of neurology in Madrid, which developed from his work and vision. King and Himmel offered this assessment of Cajal's scientific sketches: "When we look at his drawings today, we see not diagrams or arguments, but the first clear pictures of that remote frontier, drawn by the man who traveled farthest into its endless reaches."

Cajal's detailed work studying and documenting the complexities of the central nervous system and its myriad pathways, connections, and function remains essential to current research focused on understanding and treating infections of the central nervous system. This system may be either the main target or a secondary target for infections that can result in result in lethal, catastrophic, and debilitating illness.

The catalog of bacteria, viruses, fungi, parasites, and prions responsible for central nervous system disorders spans the alphabet from *Angiostrongylus* to Zika virus. Though we have learned a great deal about how to detect and treat central nervous system infections, the global burden of death and illness underscores the value of public health efforts to prevent, diagnose, and treat them. As Cajal said, "The brain is a world consisting of a number of unexplored continents and great stretches of unknown territory."

Acknowledgment

We gratefully recognize the Instituto Cajal (CSIC) which generously permitted the reproduction of the Cajal original drawing that forms part of the Cajal Legacy, ©CSIC.

Bibliography

1. Andres-Barquin PJ. Santiago Ramón y Cajal and the Spanish school of neurology. Lancet Neurol. 2002;1:445–52. http://dx.doi.org/10.1016/S1474-4422(02)00192-8
2. Garcia-Lopez P, Garcia-Marin V, Freire M. The histological slides and drawings of Cajal. Front Neuroanat. 2010;4:9.
3. Gibson WC. Ramón y Cajal and his school: personal recollections. J Hist Med Allied Sci. 1994;49:546–64. http://dx.doi.org/10.1093/jhmas/49.4.546
4. Hamilton J. Art exhibition celebrates drawings by the founder of modern neuroscience [cited 2017 Apr 12] http://www.npr.org/sections/health-shots/2017/01/26/511455876/art-exhibition-celebrates-drawings-by-the-founder-of-modern-neuroscience
5. Held H. The central auditory system [in German]. Arch Anat Physiol Anat Abt. 1893;17:201–48.
6. John CC, Carabin H, Montano SM, Bangirana P, Zunt JR, Peterson PK. Global research priorities for infections that affect the nervous system. Nature. 2015;527:S178–86. http://dx.doi.org/10.1038/nature16033
7. Nobel Prize. Santiago Ramón y Cajal – Biographical [cited 2017 Apr 12] http://www.nobelprize.org/nobel_prizes/medicine/laureates/1906/cajal-bio.html
8. Parikh V, Tucci V, Galwankar S. Infections of the nervous system. Int J Crit Illn Inj Sci. 2012;2:82–97. http://dx.doi.org/10.4103/2229-5151.97273
9. Swanson L, King L, Himmel E, editors. The beautiful brain: the drawings of Santiago Ramón y Cajal. New York: Abrams; 2017. p 11–18, 21–28, 34, 84, 104–105, 193.

Address for correspondence: Byron Breedlove, EID Journal, Centers for Disease Control and Prevention, 1600 Clifton Rd NE, Mailstop C19, Atlanta, GA 30329-4027, USA; email: wbb1@cdc.gov

EMERGING INFECTIOUS DISEASES®

Upcoming Issue

- Risk Factors for *Legionella longbeachae* Legionnaires' Disease, New Zealand
- Novel Retinal Lesion in Ebola Survivors, Sierra Leone, 2016
- Case–Control Study of Risk Factors for Meningococcal Disease in Chile
- Phylogeography of *Burkholderia pseudomallei* Isolates, Western Hemisphere
- Effects of Zika Virus Strain and *Aedes* Mosquito Species on Vector Competence
- Clonal Clusters and Virulence Factors of Group C and G Streptococci Causing Severe Infections, Manitoba, Canada, 2012–2014
- Attributable Fraction of Influenza Virus Detection to Illness in HIV-Infected and HIV-Uninfected Patients, South Africa, 2012–2016
- Competence of *Aedes aegypti*, *Ae. albopictus*, and *Culex quinquefasciatus* Mosquitoes as Zika Virus Vectors, China
- One-Year Follow-Up Antibody Responses in Patients Infected with MERS-CoV, South Korea, 2015
- Concurrent Infection with Hepatitis C Virus and *Streptococcus pneumoniae*, Alberta, Canada
- Emergency Meningococcal ACWY Vaccination Program for Teenagers to Control Group W Meningococcal Disease, England, 2015–2016
- *Francisella tularensis* ssp. *holarctica* in Australian Ringtail Possums
- Environmental Factors as Key Determinants for Visceral Leishmaniasis in Solid Organ Transplant Recipients, Madrid, Spain
- Rabbit Hepatitis E Virus Infections in Humans, France
- Detection and Genetic Characterization of Human Adenovirus 14 Strain in Students with Influenza-Like Illness, New York, 2014–2015
- Norovirus GII.P16/GII.2–Associated Gastroenteritis, China, 2016
- Association of GII.P16-GII.2 Recombinant Norovirus Strain with Increased Norovirus Outbreaks, Guangdong, China, 2016
- *Escherichia coli* Isolates with mcr-1 Gene, Australia, 2011 and 2013
- Live Cell Therapy as Potential Risk Factor for Q Fever
- *Mycobacterium gordonae* in Patient with Facial Ulcer, Nosebleeds, and Positive T-SPOT.TB Test, China
- *Rickettsia sibirica mongolitimonae* Infection, Turkey, 2016

Complete list of articles in the July issue at http://www.cdc.gov/eid/upcoming.htm

Upcoming Infectious Disease Activities

June 1–5, 2017
ASM
American Society for Microbiology
New Orleans, LA, USA
http://www.showsbee.com/fairs/25161-ASM-Microbe-2017.html

June 4–8, 2017
Council of State and Territorial Epidemiologists
2017 Annual Conference
Boise, ID, USA
http://www.csteconference.org/2017/

June 19–21, 2017
Transmission of Respiratory Viruses
Harbour Grand Hong Kong
Hong Kong, China
https://transmission2017.med.hku.hk/mass_email.html

June 20–21, 2017
SHEA/CDC ORTP Regional Training Program
Sonesta Philadelphia Rittenhouse Square
Philadelphia, PA, USA
http://ortp.shea-online.org/

December 5–8, 2017
6th National Congress of Tropical Medicine and International Symposium on HIV/aids Infection
9th National Congress of Microbiology and Parasitology
80th Anniversary of the Institute of Tropical Medicine Pedro Kourí
Havana, Cuba
http://microbiologia2017.sld.cu/index.php/microbiologia/2017

February 1–3, 2018
8th Advances in Aspergillosis
Lisbon, Portugal
www.AAA2018.org

March 1–4, 2018
18th International Congress on Infectious Diseases (ICID)
Buenos Aires, Argentina
http://www.isid.org/icid/

Announcements

To submit an announcement, send an email message to EIDEditor (eideditor@cdc.gov). Include the date of the event, the location, the sponsoring organization(s), and a website that readers may visit or a telephone number or email address that readers may contact for more information.

Announcements may be posted on the journal Web page only, depending on the event date.

Earning CME Credit

To obtain credit, you should first read the journal article. After reading the article, you should be able to answer the following, related, multiple-choice questions. To complete the questions (with a minimum 75% passing score) and earn continuing medical education (CME) credit, please go to http://www.medscape.org/journal/eid. Credit cannot be obtained for tests completed on paper, although you may use the worksheet below to keep a record of your answers.

You must be a registered user on http://www.medscape.org. If you are not registered on http://www.medscape.org, please click on the "Register" link on the right hand side of the website.

Only one answer is correct for each question. Once you successfully answer all post-test questions, you will be able to view and/or print your certificate. For questions regarding this activity, contact the accredited provider, CME@medscape.net. For technical assistance, contact CME@medscape.net. American Medical Association's Physician's Recognition Award (AMA PRA) credits are accepted in the US as evidence of participation in CME activities. For further information on this award, please go to https://www.ama-assn.org. The AMA has determined that physicians not licensed in the US who participate in this CME activity are eligible for AMA PRA Category 1 Credits™. Through agreements that the AMA has made with agencies in some countries, AMA PRA credit may be acceptable as evidence of participation in CME activities. If you are not licensed in the US, please complete the questions online, print the AMA PRA CME credit certificate, and present it to your national medical association for review.

Article Title

Sporadic Creutzfeldt-Jakob Disease in 2 Plasma Product Recipients, United Kingdom

CME Questions

1. Your patient is a 62-year-old woman with a long history of clotting disorder and recent onset of rapidly progressive dementia with prominent motor features. According to the case reports by Urwin and colleagues, which of the following statements about the clinical features of 2 cases of sporadic Creutzfeldt-Jakob disease (sCJD) reported in patients with clotting disorders treated with fractionated plasma products is most accurate?

A. Course was rapidly progressive with symptoms including incoordination, shuffling gait, seizure, daytime hypersomnolence, myoclonus, emotional lability, dysphasia, and limb rigidity
B. Vision was unaffected
C. One patient had a history of potential iatrogenic exposure, and the other had a family history of CJD
D. Survival duration from time of onset was roughly 1 year

2. According to the case reports by Urwin and colleagues, which of the following statements about the laboratory and pathology findings of 2 cases of sCJD reported in patients with clotting disorders treated with fractionated plasma products is correct?

A. Cerebrospinal fluid real-time quaking-induced conversion (CSF RT-QuIC) was positive in only 1 patient
B. Neuropathology was typical for sCJD in both patients, and neither had evidence of peripheral pathogenesis on immunostaining of lymphoreticular tissues as is seen in variant CJD (vCJD)
C. Both patients had an MM genotype at codon 129 of PRNP, proving the diagnosis of sCJD
D. Only 1 patient had a type 1A isoform PrPSc on Western blot

3. According to the case reports by Urwin and colleagues, which of the following statements about the clinical implications of 2 cases of sCJD reported in patients with clotting disorders treated with fractionated plasma products is correct?

A. The study proves that treatment with plasma products causes sCJD
B. Look-back studies in the United States and United Kingdom have shown transfusion-transmission of sCJD
C. Plasma-derived products pose no risk for sCJD transmission
D. It is essential to continue to search for cases of transfusion-transmission of sCJD through CJD surveillance programs

Earning CME Credit

To obtain credit, you should first read the journal article. After reading the article, you should be able to answer the following, related, multiple-choice questions. To complete the questions (with a minimum 75% passing score) and earn continuing medical education (CME) credit, please go to http://www.medscape.org/journal/eid. Credit cannot be obtained for tests completed on paper, although you may use the worksheet below to keep a record of your answers.

You must be a registered user on http://www.medscape.org. If you are not registered on http://www.medscape.org, please click on the "Register" link on the right hand side of the website.

Only one answer is correct for each question. Once you successfully answer all post-test questions, you will be able to view and/or print your certificate. For questions regarding this activity, contact the accredited provider, CME@medscape.net. For technical assistance, contact CME@medscape.net. American Medical Association's Physician's Recognition Award (AMA PRA) credits are accepted in the US as evidence of participation in CME activities. For further information on this award, please go to https://www.ama-assn.org. The AMA has determined that physicians not licensed in the US who participate in this CME activity are eligible for AMA PRA Category 1 Credits™. Through agreements that the AMA has made with agencies in some countries, AMA PRA credit may be acceptable as evidence of participation in CME activities. If you are not licensed in the US, please complete the questions online, print the AMA PRA CME credit certificate, and present it to your national medical association for review.

Article Title

Relative Risk for Ehrlichiosis and Lyme Disease in an Area Where Vectors for Both Are Sympatric, New Jersey, USA

CME Questions

1. You are seeing a 23-year-old previously healthy woman for a 2-day history of fever and headache. She spent last week hiking in the mountains, and you are concerned that she may have a tick-borne illness. Which of the following statements regarding the clinical presentation and prognosis of ehrlichiosis is most accurate?

A. It frequently presents with more general symptoms such as fever and headache
B. Rash is necessary to make the clinical diagnosis of ehrlichiosis
C. Ehrlichiosis is not associated with any organ damage
D. Mortality rates associated with ehrlichiosis may be as high as 20%

2. You obtain a more thorough history of tick exposures from this patient. What should you consider regarding the vectors for ehrlichiosis and Lyme disease?

A. *Ixodes scapularis* can transmit both *Borrelia burgdorferi* and *Ehrlichia chaffeensis*
B. *I. scapularis* is much more aggressive than *Amblyomma americanum*
C. *A. americanum* has historically been found in the southeastern United States
D. Samples of *A. americanum* have been declining in New Jersey

3. Ehrlichiosis is in your differential diagnosis for this patient. What was the predicted ratio of ehrlichiosis to Lyme disease in the current study?

A. 0.05
B. 0.6
C. 1.0
D. 2.3

4. How did the actual rate of reported ehrlichiosis compare with that in the statistical model in the current study?

A. The actual rate of ehrlichiosis was approximately 100% lower than that in the model
B. The actual rate of ehrlichiosis was approximately 20% lower than that in the model
C. The actual rate of ehrlichiosis was approximately the same as that in the model
D. The actual rate of ehrlichiosis was approximately 50% higher than that in the model

Emerging Infectious Diseases is a peer-reviewed journal established expressly to promote the recognition of new and reemerging infectious diseases around the world and improve the understanding of factors involved in disease emergence, prevention, and elimination.

The journal is intended for professionals in infectious diseases and related sciences. We welcome contributions from infectious disease specialists in academia, industry, clinical practice, and public health, as well as from specialists in economics, social sciences, and other disciplines. Manuscripts in all categories should explain the contents in public health terms. For information on manuscript categories and suitability of proposed articles, see below and visit http://wwwnc.cdc.gov/eid/pages/author-resource-center.htm.

Summary of Authors' Instructions

Author's Instructions. For a complete list of EID's manuscript guidelines, see the author resource page: http://wwwnc.cdc.gov/eid/page/author-resource-center.

Manuscript Submission. To submit a manuscript, access Manuscript Central from the Emerging Infectious Diseases web page (www.cdc.gov/eid). Include a cover letter indicating the proposed category of the article (e.g., Research, Dispatch), verifying the word and reference counts, and confirming that the final manuscript has been seen and approved by all authors. Complete provided Authors Checklist.

Manuscript Preparation. For word processing, use MS Word. Set the document to show continuous line numbers. List the following information in this order: title page, article summary line, keywords, abstract, text, acknowledgments, biographical sketch, references, tables, and figure legends. Appendix materials and figures should be in separate files.

Title Page. Give complete information about each author (i.e., full name, graduate degree(s), affiliation, and the name of the institution in which the work was done). Clearly identify the corresponding author and provide that author's mailing address (include phone number, fax number, and email address). Include separate word counts for abstract and text.

Keywords. Use terms as listed in the National Library of Medicine Medical Subject Headings index (www.ncbi.nlm.nih.gov/mesh).

Text. Double-space everything, including the title page, abstract, references, tables, and figure legends. Indent paragraphs; leave no extra space between paragraphs. After a period, leave only one space before beginning the next sentence. Use 12-point Times New Roman font and format with ragged right margins (left align). Italicize (rather than underline) scientific names when needed.

Biographical Sketch. Include a short biographical sketch of the first author—both authors if only two. Include affiliations and the author's primary research interests.

References. Follow Uniform Requirements (www.icmje.org/index.html). Do not use endnotes for references. Place reference numbers in parentheses, not superscripts. Number citations in order of appearance (including in text, figures, and tables). Cite personal communications, unpublished data, and manuscripts in preparation or submitted for publication in parentheses in text. Consult List of Journals Indexed in Index Medicus for accepted journal abbreviations; if a journal is not listed, spell out the journal title. List the first six authors followed by "et al." Do not cite references in the abstract.

Tables. Provide tables within the manuscript file, not as separate files. Use the MS Word table tool, no columns, tabs, spaces, or other programs. Footnote any use of boldface. Tables should be no wider than 17 cm. Condense or divide larger tables. Extensive tables may be made available online only.

Figures. Submit editable figures as separate files (e.g., Microsoft Excel, PowerPoint). Photographs should be submitted as high-resolution (600 dpi) .tif or .jpeg files. Do not embed figures in the manuscript file. Use Arial 10 pt. or 12 pt. font for lettering so that figures, symbols, lettering, and numbering can remain legible when reduced to print size. Place figure keys within the figure. Figure legends should be placed at the end of the manuscript file.

Videos. Submit as AVI, MOV, MPG, MPEG, or WMV. Videos should not exceed 5 minutes and should include an audio description and complete captioning. If audio is not available, provide a description of the action in the video as a separate Word file. Published or copyrighted material (e.g., music) is discouraged and must be accompanied by written release. If video is part of a manuscript, files must be uploaded with manuscript submission. When uploading, choose "Video" file. Include a brief video legend in the manuscript file.

Types of Articles

Perspectives. Articles should not exceed 3,500 words and 50 references. Use of subheadings in the main body of the text is recommended. Photographs and illustrations are encouraged. Provide a short abstract (150 words), 1-sentence summary, and biographical sketch. Articles should provide insightful analysis and commentary about new and reemerging infectious diseases and related issues. Perspectives may address factors known to influence the emergence of diseases, including microbial adaptation and change, human demographics and behavior, technology and industry, economic development and land use, international travel and commerce, and the breakdown of public health measures.

Synopses. Articles should not exceed 3,500 words in the main body of the text or include more than 50 references. Use of subheadings in the main body of the text is recommended. Photographs and illustrations are encouraged. Provide a short abstract (not to exceed 150 words), a 1-line summary of the conclusions, and a brief biographical sketch of first author or of both authors if only 2 authors. This section comprises case series papers and concise reviews of infectious diseases or closely related topics. Preference is given to reviews of new and emerging diseases; however, timely updates of other diseases or topics are also welcome. If detailed methods are included, a separate section on experimental procedures should immediately follow the body of the text.

Research. Articles should not exceed 3,500 words and 50 references. Use of subheadings in the main body of the text is recommended. Photographs and illustrations are encouraged. Provide a short abstract (150 words), 1-sentence summary, and biographical sketch. Report laboratory and epidemiologic results within a public health perspective. Explain the value of the research in public health terms and place the findings in a larger perspective (i.e., "Here is what we found, and here is what the findings mean").

Policy and Historical Reviews. Articles should not exceed 3,500 words and 50 references. Use of subheadings in the main body of the text is recommended. Photographs and illustrations are encouraged. Provide a short abstract (150 words), 1-sentence summary, and biographical sketch. Articles in this section include public health policy or historical reports that are based on research and analysis of emerging disease issues.

Dispatches. Articles should be no more than 1,200 words and need not be divided into sections. If subheadings are used, they should be general, e.g., "The Study" and "Conclusions." Provide a brief abstract (50 words); references (not to exceed 15); figures or illustrations (not to exceed 2); tables (not to exceed 2); and biographical sketch. Dispatches are updates on infectious disease trends and research that include descriptions of new methods for detecting, characterizing, or subtyping new or reemerging pathogens. Developments in antimicrobial drugs, vaccines, or infectious disease prevention or elimination programs are appropriate. Case reports are also welcome.

Another Dimension. Thoughtful essays, short stories, or poems on philosophical issues related to science, medical practice, and human health. Topics may include science and the human condition, the unanticipated side of epidemic investigations, or how people perceive and cope with infection and illness. This section is intended to evoke compassion for human suffering and to expand the science reader's literary scope. Manuscripts are selected for publication as much for their content (the experiences they describe) as for their literary merit. Include biographical sketch.

Research Letters Reporting Cases, Outbreaks, or Original Research. EID publishes letters that report cases, outbreaks, or original research as Research Letters. Authors should provide a short abstract (50-word maximum), references (not to exceed 10), and a short biographical sketch. These letters should not exceed 800 words in the main body of the text and may include either 1 figure or 1 table. Do not divide Research Letters into sections.

Letters Commenting on Articles. Letters commenting on articles should contain a maximum of 300 words and 5 references; they are more likely to be published if submitted within 4 weeks of the original article's publication.

Commentaries. Thoughtful discussions (500–1,000 words) of current topics. Commentaries may contain references (not to exceed 15) but no abstract, figures, or tables. Include biographical sketch.

Books, Other Media. Reviews (250–500 words) of new books or other media on emerging disease issues are welcome. Title, author(s), publisher, number of pages, and other pertinent details should be included.

Conference Summaries. Summaries of emerging infectious disease conference activities (500–1,000 words) are published online only. They should be submitted no later than 6 months after the conference and focus on content rather than process. Provide illustrations, references, and links to full reports of conference activities.

Online Reports. Reports on consensus group meetings, workshops, and other activities in which suggestions for diagnostic, treatment, or reporting methods related to infectious disease topics are formulated may be published online only. These should not exceed 3,500 words and should be authored by the group. We do not publish official guidelines or policy recommendations.

Photo Quiz. The photo quiz (1,200 words) highlights a person who made notable contributions to public health and medicine. Provide a photo of the subject, a brief clue to the person's identity, and five possible answers, followed by an essay describing the person's life and his or her significance to public health, science, and infectious disease.

Etymologia. Etymologia (100 words, 5 references). We welcome thoroughly researched derivations of emerging disease terms. Historical and other context could be included.

Announcements. We welcome brief announcements of timely events of interest to our readers. Announcements may be posted online only, depending on the event date. Email to eideditor@cdc.gov.

In This Issue

Synopsis

Sporadic Creutzfeldt-Jakob Disease in 2 Plasma Product Recipients, United Kingdom 893

Research

Hospital Outbreaks of Middle East Respiratory Syndrome, Daejeon, South Korea, 2015 898
Genomic Analysis of *Salmonella enterica* Serovar Typhimurium DT160 Associated with a 14-Year Outbreak, New Zealand, 1998–2012 906
Stockpiling Ventilators for Influenza Pandemics 914
Invasive Serotype 35B Pneumococci Including an Expanding Serotype Switch Lineage, United States, 2015–2016 922
Serologic and Molecular Evidence of Vaccinia Virus Circulation among Small Mammals from Different Biomes, Brazil 931
Relative Risk for Ehrlichiosis and Lyme Disease in an Area Where Vectors for Both Are Sympatric, New Jersey, USA 939
Distribution and Quantitative Estimates of Variant Creutzfeldt-Jakob Disease Prions in Tissues of Clinical and Asymptomatic Patients 946
Outbreak-Related Disease Burden Associated with Consumption of Unpasteurized Cow's Milk and Cheese, United States, 2009–2014 957

Dispatches

Sustainability of High-Level Isolation Capabilities among US Ebola Treatment Centers 965
Clinical and Molecular Characteristics of Human Rotavirus G8P[8] Outbreak Strain, Japan, 2014 968
Seoul Virus Infection In Humans, France, 2014–2016 973
Central Nervous System Brucellosis Granuloma and White Matter Disease in Immunocompromised Patient 978
Severe Neurologic Disorders in 2 Fetuses with Zika Virus Infection, Colombia 982
Domestic Pig Unlikely Reservoir for MERS-CoV 985
High Rates of Neutralizing Antibodies to Toscana and Sandfly Fever Sicilian Viruses in Livestock, Kosovo 989
Congenital Malformations of Calves Infected with Shamonda Virus, Southern Japan 993
Brucella neotomae Infection in Humans, Costa Rica 997
Isolated Case of Marburg Virus Disease, Kampala, Uganda, 2014 1001
Crimean-Congo Hemorrhagic Fever in Migrant Worker Returning from Oman to India, 2016 1005
Rise in Group W Meningococcal Carriage in University Students, United Kingdom 1009
Penicillin Resistance of Nonvaccine Type Pneumococcus before and after PCV13 Introduction, United States 1012
Febrile Respiratory Illness Associated with Human Adenovirus Type 55 in South Korean Military, 2014–2016 1016

Commentary

Stockpiling Ventilators for Influenza Pandemics 1021

Vol 23, No 6, June 2017
EMERGING INFECTIOUS DISEASES
Pages 893–1056

DEPARTMENT OF HEALTH & HUMAN SERVICES
Public Health Service
Centers for Disease Control and Prevention (CDC)
Mailstop D61, Atlanta, GA 30329-4027

Official Business
Penalty for Private Use $300
Return Service Requested

MEDIA MAIL
POSTAGE & FEES PAID
PHS/CDC
Permit No. G 284